ПУБЛИКАЦИЈЕ АСТРОНОМСКЕ ОПСЕРВАТОРИЈЕ У БЕОГРАДУ
PUBLICATIONS OF THE ASTRONOMICAL OBSERVATORY OF BELGRADE

Св. 100 No. 100

PROCEEDINGS

of the XIX Serbian Astronomical Conference

Belgrade, October 13 – 17, 2020

ЗБОРНИК РАДОВА

XIX Српске астрономске конференције

Београд, 13 – 17. октобар 2020.

Edited by Anđelka Kovačević, Jelena Kovačević Dojčinović,
Dušan Marčeta and Dušan Onić

Б Е О Г Р А Д
2021

PUBL. ASTRON. OBS. BELGRADE No. 100, 1-414 BELGRADE, JUNE 2021

PUBLICATIONS OF THE ASTRONOMICAL OBSERVATORY OF BELGRADE

FOUNDED IN 1947

EDITORIAL BOARD:

Dr. Srdjan SAMUROVIĆ, Editor-in-Chief (Astronomical Observatory, Belgrade)

Dr. Rade PAVLOVIĆ (Astronomical Observatory, Belgrade)
Dr. Miroslav MIĆIĆ (Astronomical Observatory, Belgrade)
Dr. Branislav VUKOTIĆ (Astronomical Observatory, Belgrade)

All papers in this Publication are peer reviewed.

Published and copyright © by Astronomical Observatory, Volgina 7, 11060 Belgrade 38, Serbia

Director of the Astronomical Observatory: Dr. Gojko Djurašević

Typesetting: Tatjana Milovanov

Internet address `http://www.aob.rs`

ISSN 0373-3742

ISBN 978-86-80019-96-3

Number of copies / тираж: 150

Production: Donat Graf d.o.o. offset & digital, Vučka Milićevića 29, Grocka

ПУБЛИКАЦИЈЕ АСТРОНОМСКЕ ОПСЕРВАТОРИЈЕ У БЕОГРАДУ
PUBLICATIONS OF THE ASTRONOMICAL OBSERVATORY OF BELGRADE

Св. 100 No. 100

PROCEEDINGS

of the XIX Serbian Astronomical Conference

Belgrade, October 13 – 17, 2020

ЗБОРНИК РАДОВА

XIX Српске астрономске конференције

Београд, 13 – 17. октобар 2020.

Edited by Anđelka Kovačević, Jelena Kovačević Dojčinović,
Dušan Marčeta and Dušan Onić

Б Е О Г Р А Д
2021

PUBL. ASTRON. OBS. BELGRADE No. 100, 1-414 BELGRADE, JUNE 2021

XIX SERBIAN ASTRONOMICAL CONFERENCE
October 13 - 17, 2020, Belgrade, Serbia

Scientific Organizing Committee:

Anđelka Kovačević (co-chair, Faculty of Mathematics, Belgrade)
Jelena Kovačević Dojčinović (co-chair, Astronomical Observatory, Belgrade)

Olga Atanacković (Faculty of Mathematics, Belgrade)
Dejan Urošević (Faculty of Mathematics, Belgrade)
Bojan Arbutina (Faculty of Mathematics, Belgrade)
Goran Damljanović (Astronomical Observatory, Belgrade)
Edi Bon (Astronomical Observatory, Belgrade)
Miroslav Mićić (Astronomical Observatory, Belgrade)
Jelena Petrović (Astronomical Observatory, Belgrade)

Local Organizing Committee:

Dušan Marčeta (co-chair, Faculty of Mathematics, Belgrade)
Dušan Onić (co-chair, Faculty of Mathematics, Belgrade)

Viktor Radović (Faculty of Mathematics, Belgrade)
Stanislav Milošević (Faculty of Mathematics, Belgrade)
Vladimir Đošović (Faculty of Mathematics, Belgrade)
Vladimir Zeković (Faculty of Mathematics, Belgrade)
Milica Vučetić (Faculty of Mathematics, Belgrade)
Aleksandra Ćiprijanović (Mathematical Institute of the Serbian Academy of Sciences and Arts)

XIX Serbian Astronomical Conference is sponsored by:

Министарство просвете,
науке и технолошког развоја

САНУ
СРПСКА АКАДЕМИЈА
НАУКА И УМЕТНОСТИ

UNIVERSITY OF
BELGRADE

Telekom Srbija

cost
EUROPEAN COOPERATION
IN SCIENCE & TECHNOLOGY

NoR CEL
Network of Researchers on the Chemical Evolution of Life

CONTENTS

PREFACE

The jubilar Volume 100 (2021) of the Publications of the Astronomical Observatory of Belgrade series provides a written record of the talks and posters presented at the XIXth Serbian astronomical conference which was held virtually during October 13-17, 2020, due to world-wide pandemic situation.

More than 100 scientific participants had many fruitful discussions and exchanges that contributed to the fulfillment of the conference. Participants from 23 countries made the conference truly international in scope. The 85 abstracts of oral talks and 16 abstracts of posters that were presented formed the heart of the conference and provided opportunity for discussion. Of the total number of presented abstracts, 52 of these are included in this proceedings volume. There were 6 Invited reviews lectures covering the different areas of the conference (listed in alphabetical order): Lucio Crivellari (Instituto de Astrofísica de Canarias) presented alternative strategies to solve stellar atmosphere problem, Zoran Knežević (Serbian academy of science and arts) presented survey of the positions of secular resonances in the asteroid belt, Stefanie Komossa (Max Planck Institute for Radioastronomy, Bonn) reviewed supermassive binary black holes, Debora Sijacki (University of Cambridge) presented supermassive black holes in all their guises, Jian-Min Wang (Institute of High Energy Physics Chinese Academy of Sciences) reviewed observational signatures of close binaries of supermassive black holes in active galactic nuclei, and Alexander F. Zakharov (Institute of Theoretical and Experimental Physics, Moscow) reviewed tests of gravity theories with black hole observations.

Our special thanks go to dr Mirjana Pović (Ethiopian Space Science and Technology Institute and Institute of Astrophysics of Andalusia) for her participation, and who has been awarded the Jocelyn Bell Burnell Inspiration Medal, an award which is awarded this year for the first time. Also, included among the speakers were several young scientists, namely, postdocs and students, who brought new perspectives to their fields. Particularly we thank young researchers from the Center for Theoretical Physics of Polish Academy of Sciences, dr Mary Loli Martínez-Aldama and PhD student Swayamtrupta Panda for their participation and contributions.

Praise is also deserved for the organizers and external reviewers who have invested significant time in analyzing and assessing papers, who hold and maintain a high standard of quality for this conference.

We are pleased to acknowledge the official sponsorship of the conference by the Ministry of Education, Science and Technological Development of Republic Serbia (MESTD), Serbian academy of science and arts (SASA), University of Belgrade (UB), Telekom Srbija, COST Action CA16104 - gravitational waves, black holes and fundamental physics (GWverse), and NoRCEL. Assistant Minister, dr Aleksandar Jović,

(MESTD), Academician Zoran Kneževićc, General Secretary of SASA, prof. dr Zoran Rakić, Dean of Faculty of Mathematics UB and Vitor Cardoso, Chair of CA16104 generously accepted an invitation to address the audience at the opening of the conference.

For the first time, the conference program included format of special sessions: The gravitational-wave Universe supported by CA16104 and Interdisciplinary studies (astrobiology, astrochemistry, geophysics, atmospheric physics, and space astronomy) and simulations, supported by NoRCEL.

The conference legacy is freely accessible on the internet http://astro.math.rs/kas19/. A special note of gratitude to the Local organizing committee and Ms Tanja Milovanov who contributed much behind the scenes for many months in preparation of the conference and in the final delivery of the book of abstracts and these proceedings.

Instead of conclusion, we look forward to seeing all of you at the jubilar XXth Serbian astronomical conference.

Coeditors

Andjelka Kovačević, Faculty of Mathematics UB
Jelena Kovačević Dojčinović, Astronomical Observatory Belgrade
Dušan Marčeta, Faculty of Mathematics UB
Dušan Onić, Faculty of Mathematics UB

Invited Reviews

Publ. Astron. Obs. Belgrade No. 100 (2021), 15 - 27 *Invited Review*

ALTERNATIVE STRATEGIES TO SOLVE THE STELLAR ATMOSPHERE PROBLEM

L. CRIVELLARI[1,2,3]

[1] *Instituto de Astrofísica de Canarias, E-38200 La Laguna, Tenerife, Spain*
E–mail: luc_ext@iac.es

[2] *INAF - Osservatorio Astronomico di Trieste, Italy*

[3] *INFN - Sezione di Perugia, Italy*

Abstract. At the heart of the computation of model atmospheres there is the so-called Stellar Atmosphere Problem, which consists of the self-consistent solution of the radiative transfer equations under specific constraints. The amazing progresses achieved in the field since the 1970s are due to both the dramatic increase of the computational facilities and the development of effective numerical algorithms. The purpose of this review is to draw attention to some methods, alternative to those that are mostly used nowadays such as the ALI methods. The improvement of the latter has been brought about by mathematical refinement, whereas the former are the result of a careful analysis of the physics of the problem. Rather than attempting an exhaustive presentation of these novel methods, which would be out of place here, the prime aim of this article is to sketch the main guidelines and to stress that it is always the physics itself that dictated the most effective algorithm.

1. INTRODUCTION

The comparison between observed and synthetic spectra is the key to the diagnostics of the physical and chemical properties of heavenly bodies. The computation of the spectral distribution of the electromagnetic radiation emitted by astrophysical objects requires the previous calculation of a model of their structure in terms of the fundamental dynamical and thermodynamic variables. This is tantamount to solve the Stellar Atmosphere Problem. As we will show, the latter is a non-local problem, owing to the transport of energy through the structure, and it is non-linear because of the coupling of all the relevant equations. To get rid of the second difficulty a straightforward approach would be to make the original system of equations linear and eventually convert it into a system of linear algebraical equations. Algorithms based on the Gauss-Seidel method can be envisaged for the numerical solution of the latter. In the practice of stellar atmosphere modelling several linearization methods have been introduced since the 1960s [1].

[1] For a basic review see Mihalas, 1978, Ch. 7. A recent general review on numerical methods in radiative transfer can be found in Atanacković, 2020, pp. 81-116.

Radiant energy is always transported in stellar atmospheres. The formal solution of the radiative transfer (RT) equation for the mean value of the specific intensity of the radiation field is given by the so-called Λ-operator. Numerical methods, based on the repeated application of the above operator (Λ-iteration methods) can be envisaged. However it is a matter of experience, justified by theoretical considerations, that the Λ-iteration is very slow (to say nothing that it may converge to a false solution). In order to speed up the convergence Accelerated Lambda Iteration (ALI) methods have been sought. Each element of the matrix representative the Λ-operator and its collocation has a precise physical meaning: it expresses the contribution to the radiation field, at a given point inside the stellar atmosphere, originating at distant points (non-local aspect of RT). The greater the optical path from the point source, the more removed from the diagonal of the matrix is the corresponding element. By taking this into account, ALI methods replace the original full matrix used in the straightforward Λ-iteration with an approximate diagonal (or n-diagonal) matrix. From the mathematical point of view ALI is the application of preconditioning to the iterative solution of a linear system of equations [2]. A review of ALI methods can be found in *Stellar Atmospheres: Beyond Classical Models* (Crivellari et al. 1991).

The improved rate of convergence brought about by ALI methods is due to mathematical improvements. In contrast, we present here alternative sequential methods, which have been designed taking into account the physics that governs the structure of a stellar atmosphere. After mentioning the algorithmic representation of physical systems in Sec. 2, we list the fundamental equations of the stellar atmosphere problem in Sec. 3. Successively in Sec. 4 we show the way they are solved sequentially within an iterative procedure, whose effectiveness is brought about by the use of iteration factors that we are going to discuss in some detail in Sec. 5. The seminal idea introduced by Eduardo Simonneau (Simonneau and Crivellari, 1988; Simonneau and Atanacković-Vukmanović, 1991) has been developed and applied by Olga Atanacković and coworkers to several line transfer problems. Their main results are presented in Sec. 5. Future applications of the foregoing strategy to the modelling of the circumstellar envelopes of AGB stars will be mentioned in Sec. 6.

2. ALGORITHMIC REPRESENTATION OF PHYSICAL SYSTEMS

This is not the place for a philosophical inquiry into the reality of the phenomenological world. All that we want here is to achieve an effective description of physical systems; in other words a representation of their structure [3]. As a necessary premise let us first introduce two definitions:

(i) By physical system we mean any arbitrary set of objects that can be identified and quantified by means of physical variables. To specify the state of the system a proper set of variables must be chosen that is necessary and sufficient to include the maximum available information required to determine both the properties of the system at a given time and its future evolution.

(ii) We define the structure of a system as the organization of the parts into which it can be ideally separated. The structure shall be shaped by the mutual interactions among these components.

[2] See Atanacković, 2020, p. 112.

[3] For more details see Crivellari (2005).

Following Bridgman's operational perspective [4] we ideally dissect a physical system into an ensemble of simpler interacting parts so that we can describe the global behaviour of the system in terms of the laws governing its elementary components. Such a process leads eventually to a *model* of the physical system that, for its own analytical nature, can be easily translated into set of equations that constitute a *mathematical model*. The exact solution of this system of equations is not possible in general. The unavoidable numerical solution can be achieved via discretization; for instance, by means of a discrete ordinates method. After that the original system of equations has been replaced by the corresponding system of discrete equations, it is matter to seek for a suitable numerical algorithm for their solution.

If each stage of the previous steps has been worked out properly, the structure of the ultimate *algorithmic model* will be akin to that of the original model. It may therefore be considered as an operative representation of the physical system under study. Joseph Fourier claimed that the relations among the mathematical functions of the physical variables and their derivatives are not just matter of calculus; they are actually present in the natural phenomena themselves [5]. According to this point of view the general scheme, required to convert the mathematical model into numerical information by means of algorithms, partakes of Nature, too. This somewhat naive form of realism, together with Henri Poincarè's statement [6] that *"La physique ne nous donne pas seulement l'ocasión de résoudre des problèmes ... Elle nous fait presentir la solution."* shall be our tenet in the quest for the optimum algorithm.

3. THE FUNDAMENTAL EQUATIONS OF THE STELLAR ATMOSPHERE PROBLEM

We will go beyond Auer's definition (Auer, 1971) and say that the *Stellar Atmosphere Problem* consists in the solution of the equations that define the structure of a stellar atmosphere under specific assumptions, i.e. constraints, initial and boundary conditions, simplifying hypotheses.

3. 1. THE EQUATIONS

The fundamental equations are listed in Table 1. From the macroscopic standpoint the constitutive equations link the variables P, ρ and $\mathbf{v}$ that shape the fluid dynamic structure. They play a protagonist role in what we call the *mechanical block*. With regard to the energetics of the system, the transport and energy equations determine its internal energy and hence the thermal structure. They constitute our *energy block*, whose protagonist variable is the temperature T.

The foregoing equations are the continuous mathematical representation of the physics that shapes the structure of a stellar atmosphere, described by the values adopted at each point by the fundamental physical variables. These values are determined by:

[4] P.W. Bridgman (1882 - 1961) American physicist, Nobel Prize for Physics in 1947. In order to get rid of the ambiguities inherent in the definition of scientific ideas, he introduced an 'operational' approach to scientific meaning, described in his book *The Logic of Modern Physics* (1927). Operationalism consists in defining physical concepts in terms of the operations, both physical and mental, involved in their measurement.

[5] J.-B. J. Fourier: 1831, *Analyse des Équations Déterminées*, (Paris: Firmin Didot fréres), p. 185.

[6] H. Poincarè: 1911, *La valeur de la Science*, (Paris: Flammarion), Ch. V, p. 153.

Table 1: The fundamental equations that shape the structure of a stellar atmosphere.

Constitutive equations:	conservation of mass and momentum equation of motion
Equation of state:	macroscopic LTE state of matter
Microscopical description of matter:	atomic occupation numbers: Boltzmann and Saha laws in LTE statistical equilibrium equations in non-LTE
Transport equations:	radiative transfer convective transport
Energy equations:	conservation of energy both for matter and the radiation field

- the relations among the variables;
- the constraints imposed by the external conditions;
- the internal energy of the system.

3. 2. A NON-LINEAR AND NON-LOCAL PROBLEM

The essential difficulty of the stellar atmosphere problem arises because all the physical variables interact throughout the whole atmosphere. The problem is therefore strongly *non-linear*. Moreover, the local variation of a variable can have an important effect on the properties at a great distance, giving rise to a *non-local* problem. In principle it could be possible to overcome the former drawback via a proper linearization technique that convert the original system of equations into the equivalent system of linear algebraical equations, but in the practice such a direct approach is often unfeasible. In the specific case of the stellar atmosphere problem the number of discrete points that warrant an adequate coverage for the behaviour with depth of the structure, as well as that required to cover the range of frequencies for radiative transfer, turns out to be exceedingly high. The dimensions of the matrix of the coefficients of the system may be therefore as large as 10^4. It is well known that the numerical inversion of large or ill-conditioned matrices is a severe problem. In a seminal paper on the numerical inversion of matrices of high order von Neumann and Goldstine (1947) consider that, in order to be suitable for numerical computation, transcendental operations and implicit definitions (e.g. the solution of algebraical equations) must be replaced by algorithms involving only those elementary operations that computers can handle directly. Consequently, they state that, when 'exact' (transcendental) arithmetic is replaced by 'approximate' arithmetic, no computing machine can perform all the operations faultlessly because of the finite number of digits available.

4. ITERATIVE SOLUTIONS OF THE STELLAR ATMOSPHERE PROBLEM

Since the 1960's a lot of iterative algorithms have been conceived in order to achieve the numerical solution of the Stellar Atmosphere Problem. In the following we are going to compare the widely used Complete Linearization Method with our own sequential approach, firstly devised by Eduardo Simonneau in the 1980's.

4. 1. COMPLETE LINEARIZATION METHOD VS. ITERATIVE SEQUENTIAL APPROACH

The basic idea of the *Complete Linearization Method* (CLM) [7] is to write the system of fundamental equations in terms of a starting approximate solution and to expand linearly the relevant variables around the values given by the former (linear perturbation). By replacing the original variables with their linear expansion one obtains a system of linear algebraical equations in which the new unknowns are the perturbations of the variables. This scheme is then iterated to convergence. At the basis of the CLM is the assumption, explicitly stated by Mihalas, that no one variable is more 'fundamental' than any other, for they all interact mutually.

Against such an 'egalitarian' treatment we shall remark that: (i) the different processes are characterized by very different scales; (ii) the strength of the coupling among the different phenomena may vary considerably case by case. A *sequential* procedure may therefore be envisaged. According to the nature of their mutual interactions, we individualize the different processes and group them into *elementary blocks* such that each of the latter contains the statement of a *self-consistent* physical problem. We may define these problems as 'atomic', in the sense that the relevant physical information cannot be further reduced. Afterwards the elementary blocks are organized into a sequence in which the atomic problems are solved one by one. Data coming from the solution of upstream blocks are of course required for the solution of the one under consideration, which will constitute the input for the downstream blocks. At the core of an effective strategy to solve the global problem is finding the proper sequence of the elementary blocks.

The equations in Table 1 are listed according to a certain order that may be considered as 'natural'. The mechanical block, which includes the constitutive equations together with the equation of state, accounts for the dynamic and thermodynamic properties of the stellar atmosphere material. It is therefore the first to be solved. However, the number of available equations is less than that of the variables involved; in the most general case 5 equations for the 3 variables T, P, ρ and the 3 components of the vector $\mathbf{v}$. The amount of energy carried on throughout the atmosphere (mainly by radiative transfer) under the constraint of energy conservation is considered in the energy block, whose protagonist variable is T, as already mentioned. The coupling of the two blocks via the microscopic description of matter allows the closure of the global system of equations.

Of course, the solution of the foregoing system requires a numerical algorithm. The above considerations dictate in a natural way the *sequential* approach, sketched in Fig. 1. If an initial guess of the run of one of the fundamental variables is given, the number of the variables is equal to that of the equations of the mechanical block, which therefore can be solved. The microscopic state of matter can then be determined,

[7] See Mihalas, 1978, pp. 230-234.

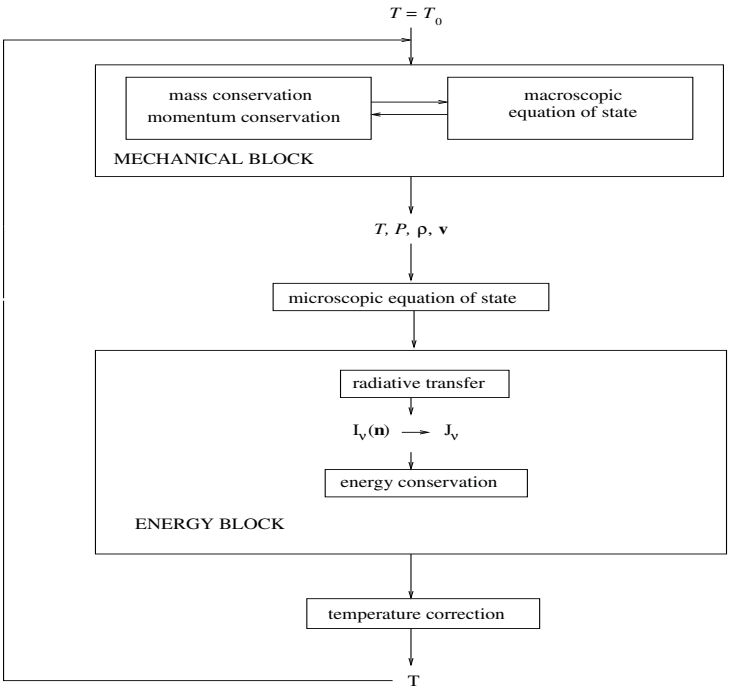

Figure 1: The 'natural' sequential procedure. In the mechanical block the constitutive equations are solved simultaneously. The correction of the current temperature distribution is achieved after the energy block. For an atmosphere in radiative equilibrium the RE constraint can be used as a transcendental equation to correct the current temperature T. Such an iterative procedure is equivalent to a Λ-iteration.

so that the emissivity η_ν and extinction $\chi_\nu = a_\nu + \sigma_\nu$ (the macroscopic transport coefficients that define the RT equations) can be computed. The solution of the system constituted by the latter yields the values of the specific intensity of the radiation field, $I_\nu(\mathbf{n})$, and its mean value J_ν. At this point the constraint of energy conservation can be checked. In general it will be not satisfied and the run of the trial variable has to be up-dated. Because the constraint of energy conservation involves the internal energy $U(T)$, T is the logical choice for the trial variable. In particular, when the simplifying hypothesis of radiative equilibrium (RE) is assumed, the corresponding energy conservation equation can be used as a transcendental equation in T to correct the current trial distribution. Then the sequential scheme is iterated until a prefixed criterion of convergence is achieved.

It is, however, a matter of experience that the foregoing 'natural' scheme does not work in the practice. The iterative solution of the coupled equations in the mechanical block is quickly obtained. But the convergence of the global procedure, namely the successive corrections of the temperature, is either infinitely slow or may even converge to a solution, which is false from the physical standpoint. This should be expected because the iterative solution inside the energy block is akin to a Λ-iteration, whose drawbacks are well known.

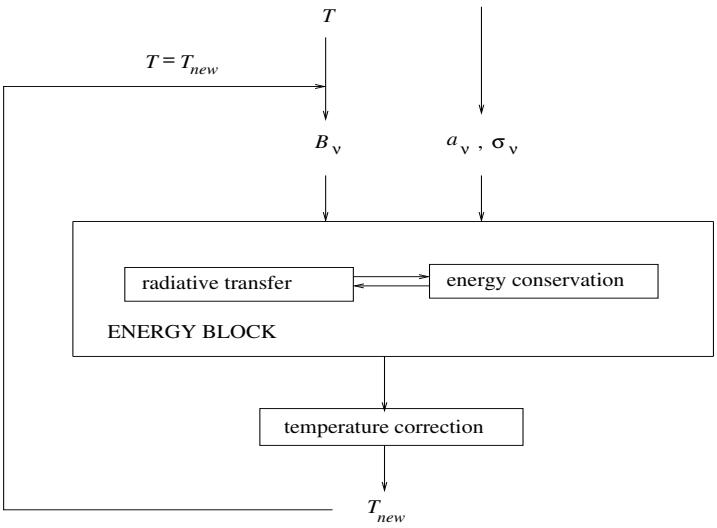

Figure 2: Simultaneous solution of radiative transfer and the RE constraint. The latter is included in the source function of each specific RT equation.

4. 2. COUPLING OF THE RT AND ENERGY CONSERVATION EQUATIONS

The sequential procedure in the energy block can be replaced by the simultaneous solution of the coupled RT and energy conservation, like the constitutive equations in the mechanical block (see Fig. 2.) For the sake of an illustrative example let us consider a stellar atmosphere in radiative equilibrium. In this case, taking into account the customary form of the source function $S_\nu \ = \ \varepsilon_\nu \ B_\nu \ + \ (1 \ - \ \varepsilon_\nu) \ J_\nu$, where $\varepsilon_\nu \ \equiv \ a_\nu \ / \ (a_\nu \ + \ \sigma_\nu)$, the equation of energy conservation reduces to

$$J_a \ \equiv \ \int_0^\infty a_\nu \ J_\nu \ d\nu \ = \ \int_0^\infty a_\nu \ B_\nu(T) \ d\nu \ , \tag{1}$$

where J_a accounts for the amount of radiant energy absorbed and $B_\nu(T)$ is the Planck function. We can linearize the latter around the value $B_\nu(T_0)$ corresponding to the trial temperature distribution, that is

$$B_\nu(T) \ = \ B_\nu(T_0) \ + \ \left(\frac{\partial B_\nu}{\partial T} \right)_0 \ (T \ - \ T_0) \ . \tag{2}$$

By taking into account eqs. 1 and 2 it follows that the correction of the temperature can be expressed as

$$T \ - \ T_0 \ = \ \left[J_a \ - \ \int_0^\infty a_\nu \ B_\nu(T_0) \ d\nu \right] \ / \int_0^\infty a_\nu \ \left(\frac{\partial B_\nu}{\partial T} \right)_0 \ d\nu \ . \tag{3}$$

Consequently, we can rewrite eq. 2 as

$$B_\nu(T) \;=\; f_1(\nu;T_0) \;+\; f_2(\nu;T_0)\; J_a \;, \tag{4}$$

where the values of f_1 and f_2 are computed with the trial value T_0 of the temperature. By substitution, the source function can be written as

$$S_\nu \;=\; \varepsilon_\nu \;[f_1(\nu;T_0) \;+\; f_2(\nu;T_0)\; J_a] \;+\; (1 \;-\; \varepsilon_\nu)\; J_\nu \;. \tag{5}$$

Recast into this form the source function of each specific RT equation includes the RE constraint. All the specific equations are coupled through the common term $J_a \;\equiv\; \int a_\nu \; J_\nu \; d\nu$. The problem is that this integral is formally akin to a diffusion integral. To solve iteratively a diffusion problem is equivalent in the practice to a Λ-iteration. The intrinsic difficulty arises from the coupling in the source function of each RT equation of all the monochromatic specific intensities, that is to say *all the individual solutions*, which are characterized by different hight scales due to the huge difference of opacity with frequency. Ostensively we can define the above one, brought about by the long-range interactions, as a *strong* coupling. In contrast the rapid iterative simultaneous solution of the equations of the mechanical block justifies labelling their coupling as *weak*.

5. THE ITERATION FACTORS METHOD

A smart strategy to soften the strong coupling between the RT equations and the RE constraint has been conceived by Eduardo Simonneau. Such an approach, the *Iteration Factors Method*, fully generalizes the idea of the Variable Eddington Factors (VEF) [8]. A first application to the iterative temperature correction in a stellar atmosphere (Simonneau and Crivellari, 1988) was succesively used for the computation of stellar atmosphere models when convective transport is taken into consideration (Crivellari and Simonneau, 1991),

5. 1. FUNDAMENTALS OF THE METHOD

As an illustrative example, we consider the particular but paradigmatic case of a plane-parallel stellar atmosphere in radiative equilibrium. The first two μ-moments of the relevant RT equations integrated over the full frequency range (bolometric) that link the bolometric μ-moments J, H and K of the specific intensity of the radiation field, are

$$\frac{dH(\tau)}{d\tau} \;=\; \frac{1}{\chi_R(\tau)} \;\left[\; \int_0^\infty a_\nu \; J_\nu \; d\nu \;-\; \int_0^\infty a_\nu \; B_\nu(T) \; d\nu \;\right] \tag{6}$$

and

$$\frac{dK(\tau)}{d\tau} \;=\; \frac{\chi_H(\tau)}{\chi_R(\tau)} \; H(\tau) \;, \tag{7}$$

where τ and χ_R are the Rosseland optical depth and mean opacity, respectively, and

[8] See Mihalas, 1978, pp. 46-47.

$$\chi_H(\tau) \equiv \int_0^\infty \chi_\nu(\tau)\ H_\nu(\tau)\ d\nu\ /\ H(\tau)\ . \tag{8}$$

In eq. 8, $\chi_\nu = a_\nu + \sigma_\nu$ is the monochromatic extinction (i.e. absorption plus scattering) coefficient. The RE constraint requires the two integrals on the RHS of eq. 6 to be equal; it holds, therefore, that $H(\tau) = H = const.$ The constant H is fixed by the luminosity of the star and is a *datum* of the problem. If we define now

$$\beta(\tau) \equiv \chi_H(\tau)\ /\ \chi_R(\tau)\ , \tag{9}$$

we can rewrite eq. 7 as

$$\frac{dK(\tau)}{d\tau} = \beta(\tau)\ H\ . \tag{10}$$

The further definition of a ratio akin to the VEF,that is

$$F(\tau) \equiv K(\tau)\ /\ J(\tau)\ , \tag{11}$$

will yield the necessary closure for the system constituted by the first two μ-moments of the bolometric RT equation. Thanks to the above factor we can recast eq. 10 in the form

$$\frac{d}{d\tau}\ [\ F(\tau)\ J(\tau)\ ] = \beta(\tau)\ H\ . \tag{12}$$

This is an RT equation for the bolometric mean specific intensity that *includes the RE constraint*.

By introducing the customary definition of the absorption mean $a_J \equiv \int a_\nu\ J_\nu\ d\nu\ /\ J$ and the Planck mean $a_P \equiv \int a_\nu\ B_\nu(T)\ d\nu\ /\ B(T)$, after defining the factor

$$\alpha(\tau) \equiv a_J(\tau)\ /\ a_P(\tau) \tag{13}$$

we can rewrite the RE constraint as

$$B(T) = \alpha(\tau)\ J(\tau)\ . \tag{14}$$

If $J(\tau)$ is known, eq. 14 gives the 'corrector' of the current temperature and the new temperature, *consistent with the RE constraint* will be

$$T(\tau) = \left[\ \frac{\pi}{\sigma_{rad}}\ \alpha(\tau)\ J(\tau)\right]^{1/4}\ , \tag{15}$$

where σ_{rad} is the Stefan-Boltzmann constant.

5. 2. ITERATION FACTORS FOR THE SOLUTION OF THE ENERGY BLOCK

The solution for $J(\tau)$ consistent with the RE constraint, as given by eq. 12, is obtained only if $\beta(\tau)$ and $F(\tau)$ are known. When dealing with the energy block in the course of the iterative sequential procedure the transport coefficients a_ν and σ_ν are external data, hence $\beta(\tau)$ is given. On the contrary, the ratio $F(\tau) = K(\tau)/J(\tau)$ depends on the previous solution of the RT equations. An operative solution can be achieved by means of a new iterative scheme inside the energy block. The first

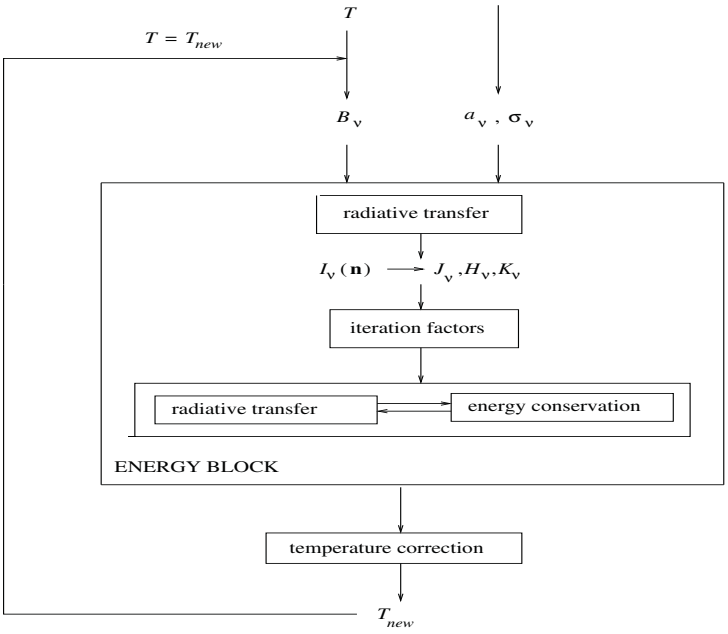

Figure 3: Simultaneous solution of the RT equation for J and the RE constraint obtained introducing proper iteration factors that convert the coupling into a 'weak' one.

step consists in the solution of the specific RT equations, whose source functions are computed with the current temperature distribution and the transport coefficients (the input to the block). The approximate closure for the system of the μ-moments of the bolometric RT equations, that is $F(\tau)$, can then be computed in order to solve eq. 12. On the other hand the factor $\alpha(\tau)$, the key to correcting the temperature via eq. 15, is computed from the values of J_ν, the solution of the specific RT equations. This scheme (see Fig. 3) is iterated with the up-to-dated temperature until a given convergence criterion is satisfied.

Experience shows that this new procedure rapidly converges to a solution that is correct from the physical standpoint, owing to the fundamental fact that the coupling between the RT equation for $J(\tau)$ and the RE constraint is now brought about by the ratio $K(\tau)/J(\tau)$ and not by the integral $J_a \equiv \int a_\nu J_\nu \, d\nu$, as in the previous scheme for the energy block. The foregoing *strong* coupling has been converted into a *weak* one. The success of the above strategy is essentially due to the introduction of the factors $\alpha(\tau)$, $\beta(\tau)$ and $F(\tau)$. Because of their intrinsic nature they carry on information optimally from a block to the successive one. As they are a ratio between homogeneous quantities, they mend the errors that affect the current values by eliminating wrong factors of scale. We call such ratios, that prove to be good *quasi-invariants* along the iterative sequential procedure, *Iteration Factors*.

5. 3. DEVELOPMENTS AND FURTHER APPLICATIONS

The convergence of some of the iterative methods currently in use can be greatly accelerated when we treat separately, within a *forth-and-back process*, the natural two-stream representation of the radiation field along each line of propagation. Integral methods based on the Λ-operator employ an *implicit* representation of the source function when computing the mean intensity of the radiation field. In contrast to the above scheme, which might be regarded as *global*, one may consider a *local* implicit scheme: the specific intensity propagating along a given direction is expressed at a given point as a linear combination of the unknown values of the source function S and its first derivative S' at that point. In contrast with other ALI methods, the FBILI method proposed here is a two-point algorithm that works by taking into account the values of S and S' on pairs of successive depth points. In the first step of an iterative procedure, the *forward-elimination* (FE), the values of the incoming specific intensities, as well as the coefficients of the linear relation above mentioned, are computed with the formal solution of the RT equation by using the known current values of S and S'. These coefficients are stored to be used in the successive *back-substitution* (BS). The FE starts at one of the end points, where the given value of the incoming specific intensity sets one of the boundary conditions, and sweeps inwards all the inner points up to the last one, where the outgoing specific intensity is given by the second boundary condition. In the BS the up-dated values of the source function are computed together with those of the outgoing intensities.

Such a simple and efficient approach, called as *Forth-and-Back Implicit Λ-Iteration* (FBILI), has been introduced by Atanacković-Vukmanović (1991) and later developed by Atanacković-Vukmanović et al. (1997). The implicit representation of the source function in the computation of the intensities within the above iterative scheme dramatically accelerates the rate of convergence of the iterative process while retaining the straightforwardness of an ordinary Λ-iteration. This is mainly because, in the FE when the coefficients of the implicit linear relation are computed, the only piece of information that the FBILI retains from the previous iteration at each depth point is the value of a single *iteration factor*, i.e. the ratio of the non-local part of the ingoing mean intensity to that of the current source function S_0. This iteration factor is used in the next step of iteration. It is worth stressing that the implementation of this new method comes from physical considerations, not from a previous analysis of the mathematical properties of the problem. Once again it is physics that dictates the optimum algorithm.

Along the foregoing guidelines, significant developments and new applications to the line formation problem have been introduced by Olga Atanacković and coworkers at the Faculty of Mathematics of the University of Belgrade. Let us quote here only the most significant results. *The Iteration Factors Method for the line formation problem*: for the paradigm problem of the Two-Level Atom line transfer Atanacković-Vukmanović (1991), Atanacković-Vukmanović and Simonneau (1994); for multi-level atom line transfer Kuzmanovska-Brandovska and Atanacković (2010). *The FBILI method for multi-level line transfer*: Kuzmanovska, Atanacković and Faurobert (2017). *The FBILI method for radiative transfer in 2D*: Milić and Atanacković (2014).

6. MODELLING AGB STARS AND THEIR CIRCUMSTELLAR ENVELOPES

Sergio Cristallo and Luciano Piersanti at the INAF - Oss. Astronomico d'Abruzzo (Italy) are conducting a research project to study giant stars on the asymptotic branch of the Hertzsprung-Russell diagram (AGB stars) and their circumstellar envelopes; it is part of the n_TOF (neutron time-of-flight) experiment at CERN. In particular, they concentrate on circumstellar envelopes. Besides the modelling of the overall structure and atmosphere of AGB stars, the subjects covered include the formation of molecules and dust grains in their neighborhood. The complex interactions among the physical processes involved require effective *ad hoc* numerical methods for the solution of the relevant non-local and non-linear problem. A first step into this direction has been the construction of the hydrodynamic code VULCAN that can follow the propagation of shocks in the circumstellar envelopes of AGB stars (Cristallo et al. in preparation). Modelling AGB stars implies to take into consideration the physical properties of both their outermost layers and the circumstellar medium, as well as the hydrodynamics of the material lost during the stellar lifetime, all of which requires proper solutions for the constitutive equations, the equation of state and the RT equations. The architecture of the Iterative Sequential Approach allows for direct control over the results of each elementary block and their quantitative effects on the structure of the atmosphere brought about by each physical process. Therefore, to adopt this strategy will greatly help the implementation of the corresponding numerical algorithms in the VULCAN code. Preliminary results have been achieved. A test model atmosphere has been computed under the simplifying hypotheses of hydrostatic and radiative equilibrium. The significant improvements introduced are: (i) the previous solution of the 1D RT has been replaced by the 3D solution obtained with the Implicit Integral Method of Simonneau and Crivellari (Simonneau and Crivellari, 1993; Gros et al., 1997) ; (ii) after the due revision of the equation of state to take into account the H_2 molecule and compute the corresponding atomic population, the contributions of selected molecules (CO, H_2O, SiO and TiO) have been included in the opacity of the stellar material; (iii) the injection of non-radiative energy in the outer layer, in order to mimic the passage of a shock, has been considered. The next steps will be the removal of the current simplifying hypothesis of hydrostatic equilibrium to allow for the correct fluid dynamics treatment, as well as the inclusion of convective transport.

Acknowledgement

This article is dedicated to my mentor and friend Eduardo Simonneau, who conceived the ideas at the basis of the algorithms and methods presented here and had a substantial part in their implementation. I am happy to thank the organizers of the XIX Serbian Astronomical Conference, and my friend Olga in particular, for the opportunity to review our longstanding collaboration and to outline future applications.

References

Atanacković-Vukmanović, O.: 1991, *PhD Thesis, Department of Astronomy, Faculty of Mathematics, University of Belgrade.*

Atanacković-Vukmanović, O., Simonneau, E.: 1994, *JQSRT*, **51**, 525.

Atanacković-Vukmanović, O., Crivellari, L., Simonneau, E.: 1997, *Astrophys. J.*, **487**, 735.
Atanacković, O.: 2020, *Numerical Methods in Radiative Transfer*, in *Radiative Transfer in Stellar and Planetary Atmospheres, L. Crivellari, S. Simón-Díaz and M.J. Arévalo eds, Cambridge – Cambridge University Press*, 81.
Auer, L. H.: 1971, *JQSRT*, **11**, 573.
Crivellari, L. and Simonneau, E.: 1991, *Astrophys. J.*, **367**, 612.
Crivellari, L.: 2005, *Algorithmic Representation of Astrophysical Structures*, in *The Role of Mathematics in Physical Sciences, G. Boniolo, P. Budinich and M. Trobok eds, Springer*, 97.
Crivellari, L., Hubeny, I., Hummer, D. G.: 1991, *Stellar Atmospheres: Beyond Classical Models, NATO ASI Series C, Vol. 341, Dordrecht – Kluwer Acad. Publishers*
Gros, M., Crivellari, L., Simonneau, E.: 1997, *Astrophys. J.*, **489**, 331.
Kuzmanovska-Barandovska, O., Atanacković, O.: 2010, *JQSRT*, **111**, 708.
Kuzmanovska O., Atanacković, O., Faurobert, M.: 2017, *JQSRT*, **196**, 230.
Mihalas, D.: 1978, *Stellar Atmospheres, 2nd ed., San Francisco – W.H. Freeman and Co.*
Milić, I., Atanacković, O.: 2014, *Adv. Space Res.*, **54**, 1297.
Simonneau, E., Crivellari, L.: 1988, *Astrophys. J.*, **330**, 415.
Simonneau, E., Crivellari, L.: 1993, *Astrophys. J.*, **409**, 830.
Simonneau, E., Atanacković-Vukmanović, O.: 1991, in *Stellar Atmospheres: Beyond Classical Models, Crivellari, L., Hubeny, I., Hummer, D.G. eds, NATO ASI Series C, Vol. 341, Dordrecht – Kluwer Acad. Publishers*, 105.
von Neumann, J., Goldstine, H. H.: 1947, *Bull. Amer. Math. Soc.*, **53 (11)**, 1021.

Publ. Astron. Obs. Belgrade No. 100 (2021), 29 - 42 *Invited Review – special session "The gravitational-wave Universe" supported by COST Action CA16104*

SUPERMASSIVE BINARY BLACK HOLES AND THE CASE OF OJ 287

S. KOMOSSA[1], S. CIPRINI[2,3], L. DEY[4], L. C. GALLO[5], J. L. GÓMEZ[6], A. GONZALEZ[5], D. GRUPE[7], A. KRAUS[1], S. J. LAINE[8], M. L. PARKER[9,10], M. J. VALTONEN[11,12], S. CHANDRA[13], A. GOPAKUMAR[4], D. HAGGARD[14,15] and M. A. NOWAK[16]

[1] *Max-Planck-Institut für Radioastronomie, Auf dem Hügel 69, 53121 Bonn, Germany*
[2] *Istituto Nazionale di Fisica Nucleare (INFN) Sezione di Roma Tor Vergata, Via della Ricerca Scientifica 1, 00133, Roma, Italy*
[3] *ASI Space Science Data Center (SSDC), Via del Politecnico, 00133, Roma, Italy*
[4] *Department of Astronomy and Astrophysics, Tata Institute of Fundamental Research, Mumbai 400005, India*
[5] *Department of Astronomy and Physics, Saint Mary's University, 923 Robie Street, Halifax, NS, B3H 3C3, Canada*
[6] *Instituto de Astrofísica de Andalucía-CSIC, Glorieta de la Astronomía s/n, E-18008 Granada, Spain*
[7] *Department of Physics, Earth Science, and Space System Engineering, Morehead State University, 235 Martindale Dr, Morehead, KY 40351, USA*
[8] *IPAC, Mail Code 314-6, Caltech, 1200 E. California Blvd., Pasadena, CA 91125, USA*
[9] *European Space Agency (ESA), European Space Astronomy Centre (ESAC), E-28691 Villanueva de la Canada, Madrid, Spain*
[10] *Institute of Astronomy, University of Cambridge, Madingley Road, Cambridge CB3 0HA, UK*
[11] *Finnish Centre for Astronomy with ESO, University of Turku, FI-20014, Turku, Finland*
[12] *Department of Physics and Astronomy, University of Turku, FI-20014, Turku, Finland*
[13] *Centre for Space Research, North-West University, Potchefstroom 2520, South Africa*
[14] *Department of Physics, McGill University, 3600 rue University, Montréal, QC H3A 2T8, Canada*
[15] *McGill Space Institute, McGill University, 3550 rue University, Montréal, QC H3A 2A7, Canada*
[16] *Department of Physics, Washington University in St. Louis, One Brookings Dr., St. Louis, MO 63130-4899, USA*

Abstract. Supermassive binary black holes (SMBBHs) are laboratories par excellence for relativistic effects, including precession effects in the Kerr metric and the emission of gravitational waves. Binaries form in the course of galaxy mergers, and are a key component in our understanding of galaxy evolution. Dedicated searches for SMBBHs in all stages of their evolution are therefore ongoing and many systems have been discovered in recent years. Here we provide a review of the status of observations with a focus on the multiwavelength detection methods and the underlying physics. Finally, we highlight our ongoing, dedicated multiwavelength program MOMO (for Multiwavelength Observations and Modelling of OJ

287). OJ 287 is one of the best candidates to date for hosting a sub-parsec SMBBH. The MOMO program carries out a dense monitoring at >13 frequencies from radio to X-rays and especially with Swift since 2015. Results so far include: (1) The detection of two major UV-X-ray outbursts with Swift in 2016/17, and 2020; exhibiting softer-when-brighter behaviour. The non-thermal nature of the outbursts was clearly established and shown to be synchrotron radiation. (2) Swift multi-band dense coverage and XMM-Newton spectroscopy during EHT campaigns caught OJ 287 at an intermediate flux level with synchrotron and IC spectral components. (3) Discovery of a remarkable, giant soft X-ray excess with XMM and NuSTAR during the 2020 outburst. (4) Spectral evidence (at 2σ) for a relativistically shifted iron absorption line in 2020. (5) The non-thermal 2020 outburst is consistent with an after-flare predicted by the SMBBH model of OJ 287. The blazar is also the target of multi-year EHT/ALMA/GMVA campaigns.

1. INTRODUCTION

SMBBHs form in galaxy mergers which happen frequently throughout the history of the universe (Volonteri et al. 2003). Coalescing binaries are the loudest sources of low-frequency gravitational waves (GWs; Centrella et al. 2010, Kelley et al. 2019). An intense electromagnetic search for wide and close binaries in all stages of their evolution is therefore ongoing. Wide pairs can be directly identified by spatially-resolved imaging spectroscopy. However, indirect methods are required for detecting the most compact, most evolved systems. These latter systems are well beyond the "final parsec" in their evolution (Begelman et al. 1980; Colpi 2014; see Fig. 1) and they are in a regime where GW emission contributes to, or even dominates, the shrinkage of their orbits.

Detecting and modelling SMBBHs in all stages of their evolution from wide to close systems allows us to address questions which are central to our understanding of the assembly history and demography of supermassive black holes (SMBHs), and of galaxy-SMBH formation and (co-)evolution across cosmic times (e.g., Komossa et al. 2016). These questions are:

- When does accretion start during a galaxy merger?
- How long does accretion last, how much feedback is triggered, and therefore how fast and how much do the SMBHs grow?
- How much do the SMBHs' spins change during accretion and merger?
- How often are both SMBHs active?
- How much accretion happens before and how much after the coalescence?
- How efficient is the loss of angular momentum due to the binary's interactions with gas and stars (final parsec problem; Fig. 1), and how fast do the two SMBHs coalesce?
- How frequent are recoiling SMBHs and therefore, how frequent are galaxies without central SMBHs?
- What is the distribution of recoil velocities and amplitudes, and how long do the SMBHs remain active after the kick?

Further, SMBBH searches will not only inform the future space-based GW missions and the pulsar-timing arrays (PTAs) on the expected coalescence rates, but will also reveal the (pre-coalescence) initial conditions in systems that will later become major GW events.

Whenever both merging galaxies harbor an SMBH, the formation of a binary is inevitable. The merger evolves in several stages (Begelman et al. 1980; our Fig. 1). The early stages of galaxy merging are driven by dynamical friction. At close separations, on the order of parsecs, the two SMBHs form a bound pair. The further shrinkage of their orbit then depends on the efficiency of interactions with stars and gas. Without any such interactions which carry away energy and angular momentum, the binary would stall and may then never coalesce within a Hubble time. This problem is known as the "final parsec problem". Recent simulations have shown that interactions with gas (like molecular clouds in the center; "massive perturbers") or with stars in asymmetric nuclear potentials and on elongated orbits, efficiently drive the binary beyond the final parsecs (e.g., review by Colpi 2014). At separations well below a parsec, emission of GWs then becomes the dominant effect that leads to efficient further orbital shrinkage, followed by the final coalescence. This GW-driven regime can be thought of as proceeding in several stages: the inspiral phase, the dynamical merger, and the final ringdown. During each stage characteristic GW radiation is emitted (Centrella et al. 2010).

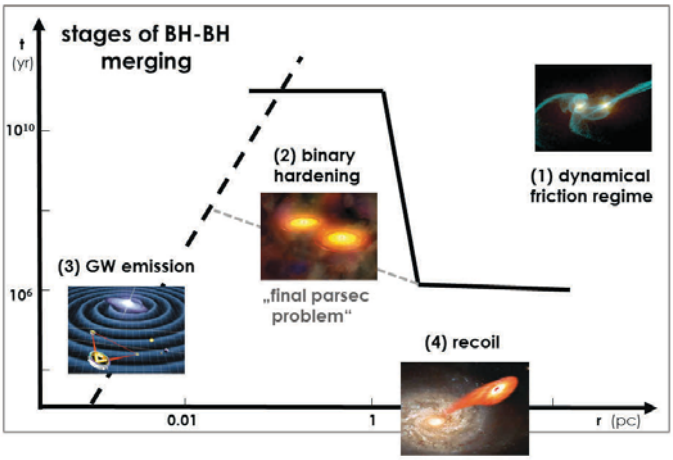

Figure 1: Sketch of the evolutionary stages of SMBBHs in galaxy mergers, following Begelman et al. (1980). After (1) the merging of the galaxies due to dynamical friction, the two SMBHs will (2) form a bound pair at separations of the order of parsecs. As the binary hardens, (3) its orbit will shrink due to the emission of GW radiation, leading to the final coalescence accompanied by a strong burst of GW emission, and followed by (4) the recoil of the newly formed single black hole. The kick velocity depends on the orbital configuration and black hole mass ratio (therefore no particular timescale or distance should be associated with it in the sketch).

Observing pairs and binaries of SMBHs in all stages of galaxy merger evolution is of great interest. Given the limited space of this review, and the large number of important observational and theoretical results which have emerged on this topic in recent years, it is impossible to give credit to all of these. We would therefore like to apologize in advance. We will focus on reviewing the major observational signatures which have been used to search for wide and close systems of SMBBHs, and we will mention some of the first-identified and best-studied representative systems.

2. WIDE PAIRS, SPATIALLY RESOLVED

During gas-rich galaxy mergers, large amounts of gas are funnelled to the center and are available for accretion onto one or both SMBHs (Mayer 2013). In the early evolutionary stages of a galaxy merger, the two SMBHs can still be spatially resolved (in X-rays, Chandra achieves $0\farcs5$ resolution, which is similar to ground-based non-AO-assisted imaging spectroscopy in the optical) and they can therefore be uniquely identified. Accreting SMBHs reveal their presence by a number of characteristic emission signatures. These include luminous X-ray emission from the accretion disk itself, bright and extended jets in radio(-loud) systems, and optical emission lines from the broad-line region (BLR) and narrow-line region (NLR) (these two systems of gas clouds reprocess the incident continuum emission from the accretion disk into emission lines; Peterson 1997).

In gas-rich mergers which have their cores heavily obscured by gas and dust, X-rays are the most powerful probe of active SMBHs, since hard X-rays can penetrate even high column densities ($N_{\rm H}$) of gas. Matter only becomes Compton-thick at $N_{\rm H} \approx 10^{24}$ cm^{-2}. Breakthroughs in the observations of galaxy pairs and mergers were made by the Chandra X-ray observatory. It was launched in 1999 and for the first time in the history of X-ray astronomy provided us with high-resolution sub-arcsecond imaging and spectroscopy.

About 15% of all active galactic nuclei (AGN) are radio-loud and drive powerful radio jets that are launched in the immediate vicinity of the SMBH. While jets often show a knotty structure, the true radio cores can be identified by their compactness, variability and especially their flat radio spectra. Binaries therefore reveal themselves by the presence of two radio cores and/or two separate jet systems.

In less heavily obscured galaxy mergers, a small fraction of photons from the accretion disk still reach the NLR, at distances of ∼10–1000 pc from the core. SMBH pairs therefore can reveal their presence by two NLRs in form of double-peaked emission lines and especially double-peaked [OIII]λ5007 that often is the brightest optical NLR line. Great progress in this field has been made since large spectroscopic sky surveys became available. Especially, the exceptional Sloan Digital Sky Survey (SDSS) has enabled the selection of large numbers of [OIII] double-peakers. At the same time, it has to be kept in mind that mechanisms other than SMBH pairs can also produce double-peaked emission lines in *single* SMBH systems. These mechanisms include two-sided outflows, two-sided jet-NLR interactions, warped galactic disks, or a single active SMBH illuminating the insterstellar media of two galaxies. Therefore, multi-wavelength follow-up observations have been employed to confirm or reject the binary nature of [OIII] double-peakers (e.g., Fu et al. 2011, Liu et al. 2018, Comerford et al. 2018, Rubinur et al. 2019). Only a small fraction (a few percent) turned out to be active SMBH pairs.

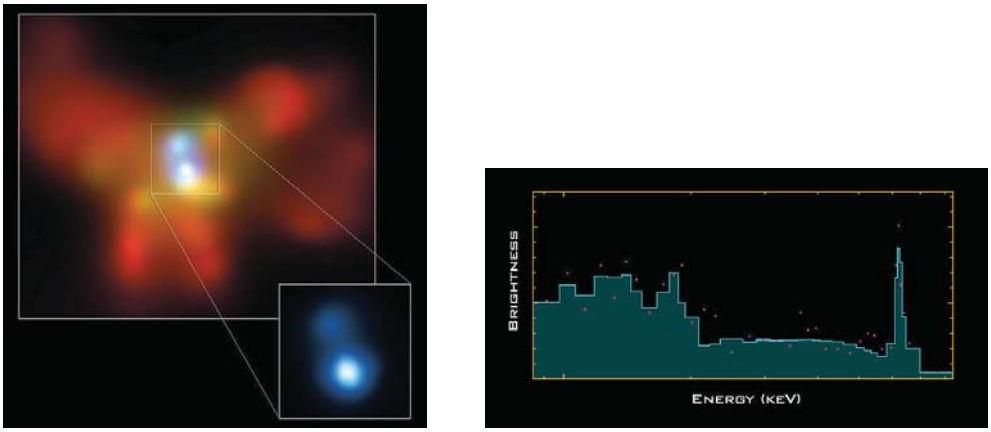

Figure 2: Pair of active SMBHs (blue) at the core of the galaxy NGC 6240 detected with Chandra imaging spectroscopy (image credit: NASA/CXC/Komossa et al. 2003). The two accreting SMBHs are identified by their luminous, hard, point-like X-ray emission and their spectra. The Chandra ACIS-S X-ray spectra of both nuclei (right panel: Southern nucleus) show the signatures of heavily obscured but intrinsically luminous AGN including the characteristic iron line near 6.4 keV.

Examples of wide systems of binary SMBHs in advanced galaxy mergers include NGC 6240 identified in X-rays with Chandra imaging spectroscopy (Komossa et al. 2003; see Fig. 2), 0402+379 (4C +37.11) identified in the radio regime with the VLBI technique (Rodriguez et al. 2006), and SDSSJ 1502+1115 in the optical with double-peaked [OIII] emission and multiwavelength confirmation (Fu et al. 2011).

3. COMPACT BINARIES, SPATIALLY UNRESOLVED

Nearly all the sub-parsec systems are spatially unresolved, and we rely on indirect methods to identify them. The most common search methods are all based on signs of semi-periodicity and are discussed in the following sections.

3. 1. SEMI-PERIODIC JET STRUCTURES

A number of AGN radio jets show semi-periodic deviations from a straight line. One way to explain these observations is involving the presence of a binary SMBH that causes either a modulation due to orbital motion of the jet-emitting SMBH around the primary SMBH, or jet precession. This method was among the first explored in the search for SMBBHs, and was motivated by the structures, bendings, and helicities observed in radio jets (Begelman et al. 1980)[1]. Radio interferometry has provided us with the highest-resolution observations of jets over decades. Mrk 501 is an early example of an AGN with helical radio jet structure, interpreted as Kelvin-Helmholtz instability driven at the origin through the orbital motion of an SMBBH (Conway &

[1]See Saslaw et al. (1974) for a discussion of SMBBH formation in three-body-interactions and radio constraints at that time.

Wrobel 1995). Hydrodynamical models favored a driving period of order 10^4 yr to explain the observed jet morphology.

Radio observations using the technique of phase-referencing allow for ultrahigh-precision measurements of changes in the spatial location of a radio source. Such observations have the great potential of directly measuring the orbital motion of a jet-emitting SMBH (Sudou et al. 2003). This remarkable technique was applied to the radio galaxy 3C66B. Semi-periodic changes in the radio VLBA core position at 2.3 GHz with a period of 1.05 yr were interpreted as orbital motion in a binary SMBH system (Sudou et al. 2003). Since the model requires a massive primary, part of the allowed parameter space was already excluded by pulsar timing array (PTA) constraints. These constraints place an upper limit of $M_{\rm BH,primary} < 1.7 \times 10^9$ M$_\odot$ (Arzoumanian et al. 2020).

3. 2. SEMI-PERIODIC LIGHT CURVES

If one of the SMBHs in a binary system is emitting a (radio) jet, then there are several processes that produce a semi-periodic light-curve signal that traces either the orbital evolution of the system or else is a sign of precession induced by the second mass. Flux changes are then either true changes of the intrinsic emission or they are artefacts of beaming due to a jet with a systematically varying angle w.r.t our line of sight.

An unavoidable consequence of the presence of compact SMBBHs therefore is the prediction that we should see semi-periodicities in light curves of at least a fraction of the whole (radio) binary population. However, there are also challenges when searching for periodicities in single light curves and/or large data bases: On the one hand, we need densely sampled light curves that cover at least several periods, since stochastic red noise variations can mimic periodicities (Vaughan et al. 2016). On the other hand, true intrinsic periodicities can be veiled by additional stochastic variability processes which we know are omnipresent in accretion and jet systems.

Because of the great importance of identifying sub-parsec SMBBHs, many dedicated searches are ongoing, and many candidates have been presented in the last few years. Here, we would like to highlight two examples; the blazar OJ 287 (Sillanpää et al. 1996) and the flat-spectrum radio quasar (FSRQ) PG1302–102 (Graham et al. 2015). OJ 287 is the best-studied and best-modelled candidate to date for hosting a compact sub-parsec binary system and will be further discussed in Sect. 4 and 5. PG1302–102 was identified in a search for periodic signals in light curves of 247000 quasars of the Catalina Transient Survey data base (Graham et al. 2015). The system triggered multiple follow-up observations and explorations of different variants of binary SMBH models (e.g., D'Orazio et al. 2015, Kovačević et al. 2019, Saade et al. 2020, and references therein; Fig. 3). Graham et al. (2015) reported a period of 5.2 yr. Their model requires jet precession in an SMBBH with <0.01 pc separation.

The majority of sources with candidate semi-periodic light curves is radio-loud. In radio-quiet systems, circumbinary disk simulations of mergers predict (X-ray) emission periodically modulated at the orbital period (e.g., d'Ascoli et al. 2018). Systems with optical continuum and line variability are further discussed in Sect. 3.4.

3. 3. TIDAL DISRUPTION EVENT (TDE) LIGHT CURVES

Stars are tidally disrupted by SMBHs once the tidal forces of the black hole exceed the self-gravity of the star. Part of the stellar material is then accreted by the

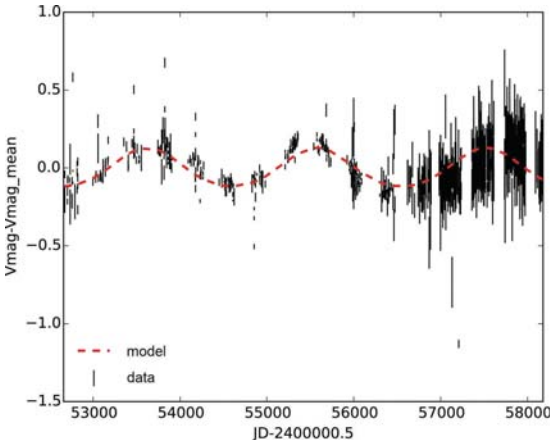

Figure 3: Light curve (V magnitude, subtracted by mean value of V) of the candidate SMBBH in PG1302–102 and best-fit sinusoidal model, adapted from Kovačević et al. 2019.

SMBH causing a luminous flare of electromagnetic radiation that declines as $t^{-5/3}$ (Rees 1990). A few dozen TDEs have now been reported (review by Komossa 2017), following their first discovery in X-rays by the ROSAT mission.

The TDE lightcurves of single and binary SMBHs are characteristically different. The binary model predicts characteristic dips and recoveries in a TDE light curve when the second SMBH perturbs the stream of the stellar material, temporarily interrupting and then restarting the accretion process (Liu et al. 2009). This method of binary detection is of special interest, as it probes the SMBBH population in *quiescent*, non-active galaxies, while most other methods require at least one, or both, SMBHs to be active (an AGN) to identify the binary system.

The first candidate SMBBH system identified from a TDE light curve is that of SDSSJ1201+3003 (Liu et al. 2014). A model with $M_{\rm BH} = 10^{6-7}$ $M_\odot$ and mass ratio $q = 0.1$ at 0.6 milli-parsec separation reproduces the light curve well.

3. 4. DOUBLE-PEAKED, BROAD BALMER LINES AND THEIR VARIABILITY

A few percent of all quasars show broad, double-peaked emission lines from the BLR. According to an early idea of Gaskell (1983), these could be the sign of the presence of a binary SMBH, with each SMBH binding its own BLR. A key prediction of the model is the Doppler-shift of each of the two line peaks as the two SMBHs orbit each other, implying a changing red/blue shift of each line peak on the timescale of years or decades. In the majority of the systems monitored, most recently selected from the SDSS spectroscopic data base, the predicted kinematic Doppler-shift was not observed, and warped disks in *single* AGN or other mechanisms are the preferred interpretation (Doan et al. 2020). A few candidate binary systems have remained. Their monitoring continues.

In a few cases, exceptional spectroscopic coverage already exists, spanning decades. A very well monitored AGN interpreted as binary because of its characteristic broad-

line and continuum variability is NGC 4151. Based on an outstanding 43 years of spectroscopic monitoring, Bon et al. (2012) reported periodic variability in flux and in radial velocity of one BLR component that they interpreted as shock waves generated by the supersonic motion of the components through surrounding ISM. Their model requires an SMBBH with an eccentric orbit and a period of 15.9 yr.

3. 5. ADDITIONAL METHODS

Many other methods have been suggested or have already been employed to identify compact binary candidates (see also the recent review by de Rosa et al. 2019). These include: UV/X-ray deficits from truncated circumbinary disks (Tanaka et al. 2012), periodic self-lensing and partial eclipses (D'Orazio & di Stefano 2018, Ingram et al. 2021), acceleration of jet precession (Liu & Chen 2007), characteristically variable and double-peaked/deformed Fe Kα lines (Yu & Lu 2001, McKernan et al. 2013), disappearance and reappearance of AGN broad Balmer lines (Wang & Bon 2020), photocenter position variability (Popović et al. 2012, Kovačević et al. 2020), astrometric orbital motion tracking in the Gaia data base (D'Orazio & Loeb 2019) or with the Event Horizon Telescope (Gómez, priv. com), magnetic field-line structure (Gold et al. 2014), (radio)-jet polarimetry (Dey et al. 2021), and electromagnetic signals contemporaneous with binary coalescence (Haiman 2017). Indirectly, the detection of recoiling SMBHs also imply binary coalescences (Lousto & Zlochower et al. 2011, Komossa et al. 2008). In recent years, PTAs have started to place constraints on the population of binaries (Sesana et al. 2018) and were first used to constrain 3C66B models (Sect. 3.1).

Table 1: Summary of the systems mentioned in this review (upper panel: spatially resolved SMBH pairs, lower panel: spatially unresolved SMBBH candidates). All of them stand out in being among the first identified and best-studied systems of their kind. Column 2 provides the classification of the host galaxy or AGN type (ULIRG stands for ultraluminous infrared galaxy; FSRQ for flat-spectrum radio quasar). In column 4, the waveband in which the system was first identified is reported. Column 5 gives the method of binary identification.

name	(AGN) type	redshift	waveband	method
NGC 6240	ULIRG	0.024	X-rays	imaging spectroscopy
0402+379	radio galaxy	0.055	radio	imaging spectroscopy
SDSS J1502+1115	Seyfert	0.39	optical	[OIII] double-peaks & radio imaging
OJ 287	BL Lac	0.306	optical	semi-periodic light curve
Mrk 501	BL Lac	0.034	radio	semi-periodic jet structure
3C66B	radio galaxy	0.021	radio	semi-periodic astrometric position
PG1302–102	FSRQ	0.3	optical	semi-periodic light curve
SDSS J1201+3003	quiescent	0.146	X-rays	TDE lightcurve
NGC 4151	Seyfert	0.003	optical	semi-periodic light curve & broad line

4. THE CASE OF OJ 287

The nearby blazar OJ 287 is the longest-studied and one of the best candidates to date for hosting a compact SMBBH (reviews by Kidger 2007 and Dey et al. 2019), in a regime where GW emission already contributes to a measurable shrinkage of the

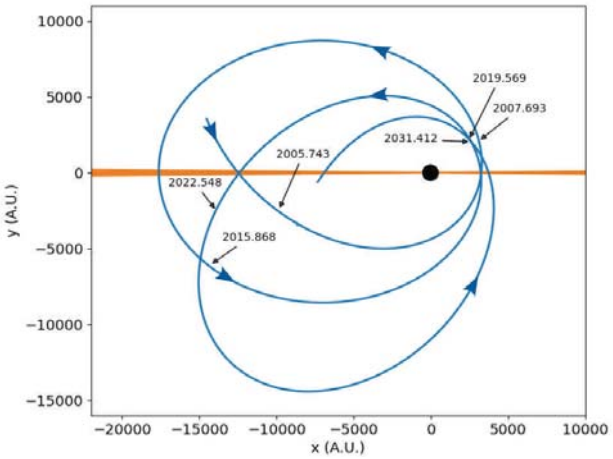

Figure 4: General-relativistic, precessing orbit of the secondary SMBH in the SMBBH model of OJ 287, adopted from Dey et al. (2018) and Laine et al. (2020). The primary SMBH is located at the origin with its accretion disk in the y = 0 plane. Flares arise due to the impacts of the secondary SMBH on the accretion disk of the primary. But there is a delay (that can be calculated from the model) between the actual impacts and the times when the flares become visible. The black arrows point to the positions of the secondary SMBH at the times when the impact flares become visible.

binary orbit (Valtonen et al. 2008, Dey et al. 2018, Laine et al. 2020). We therefore review this system in some more detail. The unique optical light curve of OJ 287 (e.g., Hudec et al. 2013) shows double-peaks every ∼12 years that have been interpreted as arising from the orbital motion of an SMBBH, with an orbital period on that order.

Different variants of binary scenarios of OJ 287 have been considered, following the discovery that major optical outbursts of OJ 287 repeat (Sillanpää et al. 1996). The best explored model by far explains the double peaks as episodes where the secondary SMBH impacts the disk around the primary twice during its ∼12 yr orbit ("impact flares" hereafter; Lehto & Valtonen 1996, Valtonen et al. 2019). The most recent 4.5 order post-Newtonian orbital modelling successfully reproduces the overall long-term light curve of OJ 287 until 2019 (Valtonen et al. 2016, Dey et al. 2018, Laine et al. 2020, and references therein). The model requires a compact SMBBH with a semi-major axis of 9300 AU with a massive primary SMBH of 1.8×10^{10} $M_\odot$ with spin 0.38, and a secondary of 1.5×10^8 $M_\odot$. Because of the strong general-relativistic orbital precession of the secondary, $\Delta\Phi$=38 deg/orbit, the impact flares are not always separated by 12 yr. Their separation varies with time and in a predictable manner (Fig. 4).

In the SMBBH model, impact flares are triggered when the secondary SMBH crosses the accretion disk twice during its orbit. The secondary's impact drives two supersonic bubbles of hot, optically thick gas from the disk. The bubbles expand and cool. Once they become optically thin, they start emitting and only then the flare becomes observable (see hydrodynamic simulations by Ivanov et al. 1998). Impact

flares were most recently reported in 2015 and 2019 (Valtonen et al. 2016, Laine et al. 2020). At such epochs, there is an additional optical-IR emission component that may extend into soft X-rays, and the total optical flux is less polarized (Valtonen et al. 2016, Ciprini et al. 2007). In addition to the impact flares, the model predicts "after-flares" when the impact disturbance reaches the inner accretion disk (Sundelius et al. 1997) and triggers new jet activity, identified most recently with the bright X-ray–UV–optical outburst in 2020 (Komossa et al. 2020).

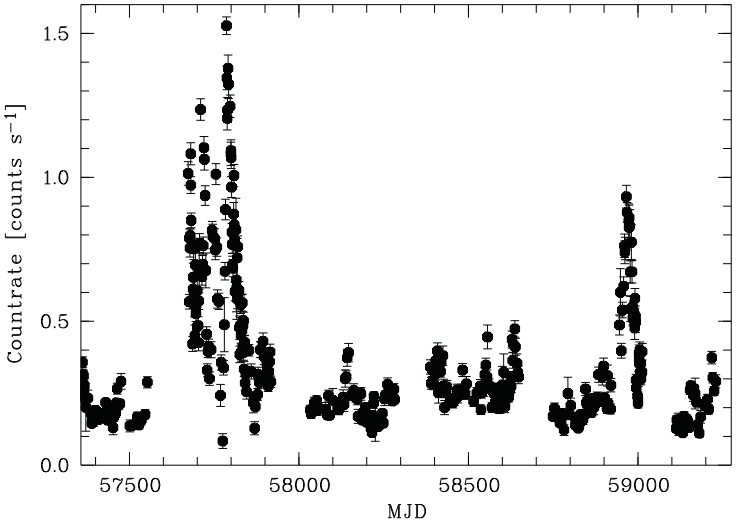

Figure 5: Swift 0.3–10 keV X-ray light curve of OJ 287 since Dec. 2015, including the two bright outbursts in 2016/17 and 2020 (Komossa et al. 2017, 2020). The majority of observations was obtained in the course of the MOMO program.

5. THE MOMO PROGRAM

The MOMO program, for "Multiwavelength Observations and Modelling of OJ 287" (Komossa et al. 2017, 2020, 2021) has an observational and a theoretical part. The observational part consists of long-term flux and spectroscopic monitoring and deep follow-up observations of OJ 287 at >13 different frequencies from the radio to the X-ray band. The Neil Gehrels Swift observatory (Swift hereafter) and the Effelsberg telescope play a central role. A few individual observations are timed with the Event Horizon Telescope (EHT; Event Horizon Telescope Collaboration 2019) to obtain quasi-simultaneous SEDs[2]. MOMO was initiated in late 2015, with >2000 data sets obtained so far. The program is the densest long-term monitoring of OJ 287

[2]Independent of the MOMO program, OJ 287 is a prime target of the EHT, and has been observed annually with ALMA and GMVA since 2017, providing radio VLBI observations of the twisted jet of OJ 287 at high resolution and sensitivity (Gómez et al. 2021, in prep.). Such observations have the potential of distinguishing between jet precession triggered by a binary or a tilted precessing accretion disk.

involving X-rays and broad-band SEDs. The theoretical part of the program aims at understanding aspects of accretion and jet physics of the blazar central engine in general, and the binary SMBH in particular. Some main findings of this ongoing project are summarized below.

(1) Our long-term Swift observations (Fig. 5; Komossa et al. 2017, 2020, 2021, and 2021b in prep.) established OJ 287 as one of the most spectrally variable blazars in the X-ray band (photon indices $\Gamma_x = 1.5,...,3$), changing between inverse Compton emission at low-states, and a strong synchrotron component at high-states.

(2) Two major X-ray–UV(–optical) outbursts were discovered with Swift in 2016/17 (Komossa et al. 2017) and in 2020 (Komossa et al. 2020)[3]. The *non-thermal* nature of the outbursts was clearly established based on multiple independent arguments: The exclusion of an accretion-disk contribution because the X-rays varied faster than the light-crossing time of the last stable orbit around the primary SMBH; the presence of a radio outburst accompanying the X-ray-optical outburst; the close correlations of fluxes in the Swift bands; and the high level of optical polarization measured in independent projects (Komossa et al. 2020, and references therein).

(3) The Swift multi-band coverage was enhanced around the dates EHT observed OJ 287 in 2017 and 2018. Selected SEDs are shown in Fig. 6. In 2018, XMM-Newton spectroscopy (Komossa et al. 2021; our Fig. 7) during the EHT campaign revealed an intermediate-low flux and spectral state well described by a combination of logarithmic parabolic power-law emission of synchrotron nature and a flat ($\Gamma_x = 1.5$) IC component.

(4) A remarkable, giant soft X-ray excess (Fig. 7) of synchrotron origin was discovered during the 2020 outburst of OJ 287 based on XMM-Newton and NuSTAR observations (Komossa et al. 2020)[4]. NuSTAR also revealed an additional and unusually soft emission component extending up to $\sim$ 70 keV of unknown nature[5]. Spectral evidence (at 2σ) for a relativistically shifted iron absorption line in 2020 was seen with XMM-Newton, however it needs independent confirmation in deeper future observations that catch OJ 287 in the same state. The 2020 X-ray–optical outburst was accompanied by a radio outburst (Fig. 7, right panel).

(5) The non-thermal 2020 outburst is consistent with an after-flare predicted by the SMBBH model, where new jet activity is launched following a change in the accretion rate as a consequence of the secondary's disk impact (Komossa et al. 2020).

The MOMO program will continue observations of OJ 287 as it nears its next impact flare predicted by the SMBBH model (Dey et al. 2018), expected in 2022.

6. SUMMARY AND OUTLOOK

Binary SMBHs in all stages of their evolution are central to SMBH demographics and galaxy evolution across cosmic times. The field has rapidly evolved in the last decade, with many systems and candidates identified through multiwavelength observations

[3]The optical outbursts were independently detected in ground-based monitoring campaigns (e.g., Zola et al. 2020)

[4]A similar soft emission component was detected with Swift during the 2016/17 outburst (Komossa et al. 2017, 2020), but we lack deeper XMM-Newton observations at that epoch.

[5]A mix of synchrotron and IC emission is a possibility; another one is a temporary accretion-disk corona contribution (even though there is no other optical–X-ray evidence for significant disk emission during the outbursts).

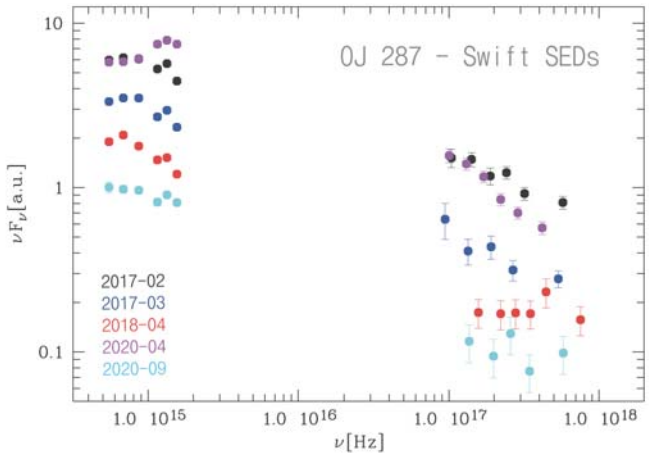

Figure 6: Observed Swift SEDs of OJ 287 at selected epochs, including the 2016/17 and 2020 outbursts at peak, the March–April 2017 and 2018 near-EHT epochs, and the 2020 low-state (Komossa et al. 2021). Optical–UV and X-ray fluxes are correlated. The X-ray spectral steepening at high-states is due to the increasing contribution of the synchrotron component(s).

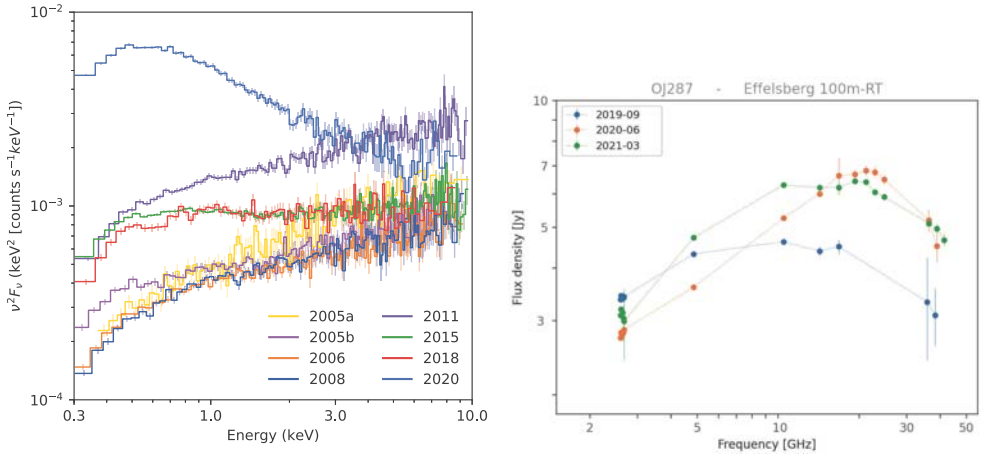

Figure 7: Left: Comparison of all XMM-Newton spectra of OJ 287. A giant soft X-ray excess is obvious in the 2020 spectrum (blue) obtained at the peak of the outburst (Komossa et al. 2020). The XMM-Newton spectrum taken quasi-simultaneous with the EHT observation in 2018, at intermediate flux level, is marked in red. Right: Selected multifrequency Effelsberg radio spectra of OJ 287 between 2.6 and 40 GHz from the MOMO program.

and orbital modelling, including candidate evolved systems well beyond the final parsec and wide pairs in the early stages of galaxy mergers. The fact that many of these systems are in nearby galaxies (Tab. 1) implies that binaries should be common throughout the universe. Binary SMBHs are most easily detectable electromagnetically, if at least one or both SMBHs are active; while an elusive population of binaries could well exist at the cores of quiescent, inactive galaxies. Stellar tidal disruption event lightcurves provide us with a unique tool of searching for such a binary population. While the last few years have seen the first direct detection of gravitational waves from stellar-mass black-hole binaries with ground-based detectors, supermassive black-hole binaries are the loudest known sources of GWs detectable with the future space-based gravitational-wave interferometer LISA. Meanwhile, pulsar-timing arrays have greatly advanced in recent years and have started to place constraints on the population of the most massive binaries known. The EHT with its unprecedented spatial resolution holds the promise of spatially resolving the small-separation SMBBH of OJ 287 for the first time. Among the population of sub-parsec binary SMBHs, the blazar OJ 287 stands out as the longest-studied and best-studied candidate which is already in a regime where gravitational-wave emission contributes measurably to the orbital shrinkage. As a bright multimessenger source, OJ 287 is the target of an ongoing, dense monitoring program, MOMO. The program has revealed high-amplitude outbursts interpreted in the context of the binary model as after-flares. MOMO observations continue as OJ 287 nears its next predicted impact flare.

Acknowledgements

SK would like to thank the organizers for their invitation to give this review at the COST workshop on "The gravitational-wave Universe" during the excellent XIX Serbian Astronomical Conference. We would like to thank A.B. Kovačević for her permission to show her figure. This review is based on published results obtained by the international community with a multitude of observing facilities and surveys world-wide. Previously unpublished data shown here for the first time were obtained with the Neil Gehrels Swift observatory and the 100-m telescope of the Max-Planck-Institut für Radioastronomie at Effelsberg.

References

Arzoumanian, Z. et al.: 2020, *Astrophys. J.*, **900**, 102.
Begelman, M. C., Blandford, R. D., Rees, M. J.: 1980, *Nature*, **287**, 307.
Bon, E. et al.: 2012, *Astrophys. J.*, **759**, 118.
Centrella, J. et al.: 2010, *Reviews of Modern Physics*, **82**, 3069.
Ciprini, S. et al.: 2007, *MmSAI*, **78**, 741.
Colpi, M.: 2014, *Space Sci. Rev.*, **183**, 189.
Comerford, J. et al.: 2018, *Astrophys. J.*, **867**, 66.
Conway, J. E., Wrobel, J. M.: 1995, *Astrophys. J.*, **439**, 98.
d'Ascoli, S. et al.: 2018, *Astrophys. J.*, **865**, 140.
de Rosa, A. et al.: 2019, *New Astron. Rev.*, **86**, 101525.
Dey, L. et al.: 2018, *Astrophys. J.*, **866**, 11.
Dey, L. et al.: 2019, *Universe*, **5**, 108.
Dey, L. et al.: 2021, *MNRAS*, **503**, 4400.

Doan, A. et al.: 2020, *MNRAS*, **491**, 1104.
D'Orazio, D. J., Haiman, Z., Schiminovich, D.: 2015, *Nature*, **525**, 351.
D'Orazio, D. J., Di Stefano, R.: 2018, *MNRAS*, **474**, 2975.
D'Orazio, D. J., Loeb, A.: 2019, *Phys. Rev. D*, **100**, 103016.
Event Horizon Telescope Collaboration, Akiyama, K. et al.: 2019, *Astrophys. J.*, **875**, L1.
Fu, H. et al.: 2011, *Astrophys. J.*, **740**, L44.
Gaskell, M.: 1983, in *Proceedings of the 24th Liege Int. Astrophys. Coll.*, 473.
Gold, R. et al.: 2014, *Phys. Rev. D*, **89**, 064060.
Graham, M. J. et al.: 2015, *Nature*, **518**, 74.
Haiman, Z.: 2017, *Phys. Rev. D*, **96**, 023004.
Hudec, R. et al.: 2013, *Astron. Astrophys.*, **559**, 20.
Ingram, A. et al.: 2021, *MNRAS*, **503**, 1703.
Ivanov, P. B., Igumenshchev, I. V., Novikov, I. D.: 1998, *Astrophys. J.*, **507**, 131.
Kelley, L. et al.: 2019, *BAAS*, **51**, 490.
Kidger, M.: 2007, *Cosmological Enigmas: Pulsars, Quasars, and Other Deep-Space Questions*, The Johns Hopkins University Press.
Komossa, S.: 2017, *Astron. Nachrichten*, **338**, 256.
Komossa, S. et al.: 2003, *Astrophys. J. Letters*, **582**, L15.
Komossa, S., Zhou, H., Lu, H.: 2008, *Astrophys. J. Letters*, **678**, L81.
Komossa, S., Baker, J. G., Liu, F. K.: 2016, *IAU Focus Meeting*, **29B**, 292.
Komossa, S. et al.: 2017, *IAUS*, **324**, 168.
Komossa, S. et al.: 2020, *MNRAS*, **498**, L35.
Komossa, S. et al.: 2021, *MNRAS*, **498**, L35.
Kovačević, A. B. et al.: 2019, *Astrophys. J.*, **871**, 32.
Kovačević, A. B. et al.: 2020, *Astron. Astrophys.*, **644**, A88.
Laine S. et al.: 2020, *Astrophys. J. Letters*, **894**, L1.
Lehto, H. J., Valtonen, M. J.: 1996, *Astrophysical Journal*, **460**, 207.
Liu, F. K., Chen, X.: 2007, *Astrophys. J.*, **671**, 1272.
Liu, F. K., Li, S., Chen, X.: 2009, *Astrophys. J. Letters*, **706**, L133.
Liu, F. K., Li, S., Komossa, S.: 2014, *Astrophys. J.*, **786**, 103.
Liu, X. et al.: 2018, *Astrophys. J.*, **854**, 169.
Lousto, C., Zlochower, Y.: 2011, *Phys. Rev. Lett.*, **107**, 231102.
Mayer, L.: 2013, *CQGra*, **30**, 244008.
McKernan, B. et al.: 2013, *MNRAS*, **432**, 1468.
Peterson, B. M.: 1997, *An Introduction to Active Galactic Nuclei*, Cambridge University Press.
Popović, L. Č. et al.: 2012, *Astron. Astrophys.*, **538**, 107.
Rees, M. J.: 1990, *Science*, **247**, 817.
Rodriguez, C. et al.: 2006, *Astrophys. J.*, **646**, 49.
Rubinur, K., Das, M., Kharb, P.: 2019, *MNRAS*, **484**, 4933.
Saade, M. L. et al.: 2020, *Astrophys. J.*, **900**, 148.
Saslaw, W. C., Valtonen, M. J., Aarseth, S. J.: 1974, *Astrophys. J.*, **190**, 253.
Sesana, A. et al.: 2018, *Astrophys. J.*, **856**, 42.
Sillanpää, A. et al.: 1996, *Astron. Astrophys.*, **305**, L17.
Sudou, H. et al.: 2003, *Science*, **300**, 1263.
Sundelius, B. et al.: 1997, *Astrophys. J.*, **484**, 180.
Tanaka, T., Menou, K., Haiman, Z.: 2012, *MNRAS*, **420**, 705.
Valtonen, M. J. et al.: 2008, *Nature*, **452**, 851.
Valtonen, M. J. et al.: 2016, *Astrophys. J. Letters*, **819**, L37.
Valtonen, M. J. et al.: 2019, *Astrophys. J.*, **882**, 88.
Vaughan, S. et al.: 2016, *MNRAS*, **461**, 3145.
Volonteri, M., Haardt, F., Madau, P.: 2003, *Astrophys. J.*, **582**, 559.
Wang, J. M., Bon, E.: 2020, *Astron. Astrophys.*, **643**, L9.
Yu, Q., Lu, Y.: 2001, *Astron. Astrophys.*, **377**, 17.
Zola, S. et al.: 2020, *Astron. Telegram*, **13637**, 1.

Publ. Astron. Obs. Belgrade No. 100 (2021), 43 - 53 *Invited Review – special session "The gravitational-wave Universe" supported by COST Action CA16104*

TESTS OF GRAVITY THEORIES WITH BLACK HOLE OBSERVATIONS

A. F. ZAKHAROV[1,2,3]

[1] *Institute of Theoretical and Experimental Physics, 117259 Moscow, Russia*
E–mail: zakharov@itep.ru

[2] *Bogoliubov Laboratory for Theoretical Physics, JINR, 141980 Dubna, Russia*

[3] *National Research Nuclear University MEPhI (Moscow Engineering Physics Institute), 115409, Moscow, Russia*

Abstract. Black holes with different masses are observed in a wide range of electromagnetic radiation frequencies. Astronomers believe that they have detected neutrinos whose sources are associated with black holes. The first detection of gravitational radiation from merging binary black holes occurred using the LIGO–Virgo gravitational wave detectors just a few years ago. After that, researchers began to talk about the fruitfulness of multi-messenger astronomy. At present, we can say that the general relativity is the best theory of gravity, however, in recent years, many alternative theories of gravity have emerged and the emergence of at least part of these theories has been associated with attempts to explain the problems of dark matter and dark energy with changes in the gravity law. We discuss the possibilities of using black hole observations to test the predictions of general relativity and obtain constraints on the parameters of alternative theories of gravity. Earlier, we discuss constraints on the theory of gravity from observations of the supermassive black holes at the Galactic Center and at the center of the galaxy M87.

1. INTRODUCTION

In 2002 I was invited to present a lecture on gravitational microlensing and dark matter problem at the XIII National Astronomical Conference in Belgrade. In 2003 my contribution for the conference proceedings was published in Publications of the Astronomical Observatory of Belgrade (Zakharov 2003) and it is a pleasure to note that this paper was cited by Weinberg (2008). Since these times I established a fruitful and pleasant collaboration with Serbian astrophysicists.

In the paper I mention prizes and their recipients working in BH physics which closely connected with our studies in the subject because it means a recognition of an importance and an interest to these fields among the wide world scientific community.

1. 1. INCREASING IMPACT OF ASTROPHYSICS AND GENERAL RELATIVITY

There are not many Nobel prize recipients who were awarded the prize for their studies in astrophysics and general relativity earlier because for many years astrophysics was not treated as a branch of contemporary physics since astrophysics was not precise

enough (a famous Russian physicist V. L. Ginzburg ironically told about the issue that "in astronomy one is equal to ten") meanwhile general relativity was checked only in a weak gravitational field limit. However, I would like to note that works of three Nobel prize winners (in 2017, 2019 and 2020) in last four years are devoted to astrophysical applications of general relativity.

Word combination "black hole" is extremely popular not only in physics and astronomy (Google counts around 924 million cases of its usage) and three Nobel prizes are connected with this astrophysical object. In 1983 Subrahmanyan Chandrasekhar[1] was awarded the Nobel prize for the discovery of limiting mass of white dwarfs (Chandrasekhar 1931, 1934) (see, an interesting discussion of the issue by Yakovlev (1994) where contributions of other authors (Frenkel 1928; Stoner 1930, 1932; Landau 1932) was discussed). Later, the conclusion about a limiting mass of neutron star was found (Gamow 1937; Oppenheimer & Volkoff 1939). I would like to mention that some time ago Yakovlev et al. (2013) revisited the Landau's contribution in a creation of the neutron star concept. I would like to note that the result about mass limits for neutron stars and white dwarfs was interpreted by Chandrasekhar as a physical reality in contrast to many other famous scientists like A. Eddington and L. Landau who noted that the conclusion about the limiting mass of white dwarfs should be incorrect if laws of quantum mechanics and quantum statistics are violated (Landau 1932). These assumptions were inspired probably by N. Bohr (who claimed that energy conservation law could be violated) since in twenties and thirties of XX century it was a period of a formation of new non-classical physics and basic physical concepts were changed and a process of trial and error to find new physical theory was in action.

In 2017 Rainer Weiss, Kip S. Thorne and Barry Barish[2] were awarded the Nobel prize in physics "for decisive contributions to the LIGO detector and the observation of gravitational waves" from binary black holes (Abbott et al. 2016). In the paper the authors discovered gravitational waves and binary black holes and in addition, they found a constraint on graviton mass. We will discuss graviton mass constraints from different type of observations below.

[1]At the same year in his fundamental book on black holes Chandrasekhar noted that "the black holes of nature are the most perfect macroscopic objects, there are in the Universe: the only elements of their construction are our concepts of space and time. And since a general theory of relativity provides a only single unique family of solutions for their descriptions are the simplest objects as well". This family of solutions is determined by only three parameters, mass, charge and spin of a black hole. Initially, this statement was formulated by J. Wheeler as the theorem on an absence of hairs for black holes. Later, the theorem was proven assuming rather natural conditions.

[2]One of the key founder LIGO project, Ronald Drever, in principle could get the Nobel prize since in 2016 he got the Breakthrough Prize, the Gruber Prize in Cosmology, the Shaw prize ("Nobel of the East"), the Kavli Prize in astrophysics, the Harvey prize in physics and technology and all these prizes he got together with Rainer Weiss and Kip S. Thorne for the development of LIGO detector and the discovery of gravitational waves from binary black holes. Unfortunately, outstanding experimentalist Ron Drever died on 7 March 2017 and cannot get the Nobel prize in 2017 but perhaps he could be a Nobel prize winner if he would still alive in fall 2017.

2. 2020 AS THE BLACK HOLE YEAR

In 2020 the black hole concept got the high recognition among a scientific community.

2. 1. ROGER BLANDFORD AND ENERGY RELEASE FROM BLACK HOLES

The Shaw Prize in Astronomy 2020 is awarded to Roger D. Blandford (USA) "for his foundational contributions to theoretical astrophysics, especially concerning the fundamental understanding of active galactic nuclei, the formation and collimation of relativistic jets, the energy extraction mechanism from black holes, and the acceleration of particles in shocks and their relevant radiation mechanisms".

R. Blandford contributed essentially in different topics of relativistic astrophysics including black hole physics and gravitational lensing. For instance, Blandford and Znajek (1977) proposed a way to extract energy from a rotating black hole in a presence of magnetic field with a special configuration. Frolov and Zelnikov (2011) provided a clear description of physical ideas which were used in the Blandford – Znajek process.

2. 2. SHAW PRIZE IN ASTRONOMY AS A PRECURSOR FOR NOBEL PRIZES

Many people got Nobel prizes after the Shaw prize, therefore, the Shaw prize recipients are highly likely pretender for the Nobel prize. We list a couple of examples. In 2004 P. James E. Peebles got the Shaw prize and in 2019 he got the Nobel prize. Geoffrey Marcy and Michel Mayor got the Shaw prize in 2005. G. Marcy was one of real candidates for searches of exoplanets with transit and Doppler shift measurements but in 2015 he was accused by the administration of his University (UC, Berkeley) in sexual harassment and after that he expressed his intention to step down from his professorship at UC Berkeley. In 2019 Michel Mayor and Didier Queloz got the Nobel prize. Saul Perlmutter, Adam Riess and Brian Schmidt got the Shaw prize in 2006 and they were awarded the Nobel prize in 2011. Reinhard Genzel got the Shaw prize in 2008 Ronald Drever (1931-2017); Kip S. Thorne and Rainer Weiss got the Shaw prize in 2016 and they were awarded the Nobel prize in 2017.

2. 3. THE CRAFOORD PRIZE IN ASTRONOMY

In 1980 Swedish economist and industrialist Holger Crafoord (1908 – 1982) and his wife Anna-Greta established the Holger Crafoord's Endowment, which was donated to the Royal Swedish Academy of Sciences for contributions in mathematics, astronomy, geosciences (particularly ecology) biosciences and rheumatology (the disciplines are complimentary to the Nobel prize ones). The Crafoord Prize has an excellent reputation among a scientific community and the Prize is awarded personally by the King of Sweden.[3]

In 2012 Reinhard Genzel and Andrea M. Ghez[4] were awarded the Crafoord Prize "for their observations of the stars orbiting the galactic centre, indicating the presence of a supermassive black hole". For the next Crafoord Prize in astronomy in 2016 Roger Blandford and Roy Patrick Kerr were selected "for fundamental work concerning rotating black holes and their astrophysical consequences". Really, in 1963 Kerr found the solution describing the metric of a rotating black hole but as I mentioned earlier

[3]https://www.crafoord.se/en/the-crafoord-foundation/the-founder-holger-crafoord/.
[4]The first woman to be awarded this prize.

Blandford (and Znajek) proposed a process where a part of a rotational energy of a black hole could be converted into energy of highly energetic jets. It means studies of black holes are the astronomical investigations with the highest priority for the the Crafoord Prize Committee.

2. 4. ANDREW FABIAN: TESTS OF STRONG GRAVITY FROM X-RAY OBSERVATIONS OF BLACK HOLES

The Norwegian Academy of Science and Letters has decided to award the Kavli Prize in Astrophysics for 2020 to Andrew Fabian (University of Cambridge, UK) "for his ground breaking research in the field of observational X-ray astronomy, covering a wide range of topics from gas flows in clusters of galaxies to supermassive black holes at the heart of galaxies." Really, Fabian et al. (1989) proposed a way to recognize that emission region for X-ray radion is located near a black hole horizon and the authors outlined an opportunity to evaluate a black hole spin. Later, Tanaka et al. (1995) discovered a specific shape of the iron K_α with observations of the Seyfert Galaxy MCG-6-30-15 with the Japanese ASCA satellite and the authors founded that emission region for the iron K_α has to be located so closely to the black hole horizon and therefore they also concluded that spin has to be very close to extreme value. Recent reviews of the subject are presented by Fabian et al. (2000), Zakharov and Repin (2006), Jovanović and Popović (2009).

2. 5. APS EINSTEIN PRIZE FOR STUDIES OF COMPACT OBJECTS

The Albert Einstein Medal is an award established by the Albert Einstein Society in Bern. First given in 1979, the award is presented to people for "scientific findings, works, or publications related to Albert Einstein each year". In 2019 C. M. Will got the medal. American Physical Society Einstein prize selected Clifford Martin Will (University of Florida) and Saul Teukolsky (Cornell University and Caltech) as recipients of Albert Einstein prize in 2021 "for outstanding contributions to observational tests of general relativity with theories of gravitational waves, astrophysical black holes, and neutron stars.".

3. NOBEL PRIZE IN 2020: THEORETICAL AND OBSERVATIONAL STUDIES OF BLACK HOLES

The Royal Swedish Academy of Sciences has decided to award the Nobel Prize in Physics 2020 to Roger Penrose[5] (University of Oxford, UK), Reinhard Genzel (Max Planck Institute for Extraterrestrial Physics, Garching, Germany and University of California, Berkeley, USA) and Andrea Ghez[6] (University of California, Los Angeles, USA). One half of the prize was given to Roger Penrose "for the discovery that black hole formation is a robust prediction of the general theory of relativity" and the other half was given jointly to Reinhard Genzel and Andrea Ghez "for the discovery of a supermassive compact object at the Centre of our Galaxy". Roger Penrose showed that the general theory of relativity leads to the formation of black holes. Reinhard

[5]In 2019 R. Penrose was awarded the Pomeranchuk prize established by the Institute of Theoretical and Experimental Physics (Moscow) and he is the only Pomeranchuk prize laureate who later got the Nobel prize.

[6]The forth woman to be awarded the Nobel prize in physics.

Genzel and Andrea Ghez discovered that an invisible and extremely heavy object governs the orbits of stars at the Galactic Center. A supermassive black hole is the most natural explanation for observations of Keck and VLT (GRAVITY) groups. "The discoveries of this year's Laureates have broken new ground in the study of compact and supermassive objects. But these exotic objects still pose many questions that beg for answers and motivate future research. Not only questions about their inner structure, but also questions about how to test our theory of gravity under the extreme conditions in the immediate vicinity of a black hole", says David Haviland, chair of the Nobel Committee for Physics. It means that a scientific community will wait for ground breaking discoveries in black hole investigations.

4. ROGER PENROSE AND THEOREMS ON SINGULARITIES

One of the first vacuum solution of Einstein equation was the Schwarzschild solution (1916) in the form,

$$ds^2 = \left(1 - \frac{\alpha}{r}\right) dt^2 - \left(1 - \frac{\alpha}{r}\right)^{-1} dr^2 - r^2(d\theta^2 + \sin^2\theta d\phi^2), \qquad (1)$$

where $r = (R^3 + \alpha^3)^{1/3}$, $\alpha = 2Gm/c^2$, while R is an ordinary radial polar coordinate. Soon after that Droste (1916) presented the solution in different coordinates, (see, Eq. (1)), but Droste (1916) interpreted r as an ordinary radial polar coordinate. These coordinates are now called Schwarzschild coordinates and such an object is called a black hole. A coordinate value $r_S = \alpha$ corresponds to a discontinuity of metric g_{rr} and it was called a singularity for many years. For instance, Regge and Wheeler (1957) investigated a stability of singularity (now we call it the event horizon). It was a long discussion about an opportunity to use the Schwarzschild solution for a real physical object. Oppenheimer and Snyder (1939) found that a black hole could be formed in a result of dust collapse. The authors used a spherically symmetric approximation to prove the claim. However, many people thought the Oppenheimer – Snyder model is too rough to describe a real astronomical object. For instance, Einstein (1939) considered an opportunity to mimic the Schwarzschild metric with moving objects and the Einstein conclusion was much more general than his analysis of his specific model and he noted that "the essential result of this investigation is a clear understanding as to why the "Schwarzschild singularities" do not exist in physical reality. Although the theory given here treats only clusters whose particles move along circular paths it does not seem to be subject to reasonable doubt that mote general cases will have analogous results. The "Schwarzschild singularity" does not appear for the reason that matter cannot be concentrated arbitrarily." It means that Einstein claimed the Schwarzschild metric has no chance to describe a real astronomical object. Einstein's assistant P. Bergman (1942) expressed a similar opinion and wrote that "in nature mass is never sufficiently concentrated to permit Schwarzschild singularity to occur in empty space. It means that Einstein and a lot of his followers thought that the Schwarzschild metric has only purely mathematical value and it is useless to model physical objects. A physical sense and a causal structure of the coordinate singularity at the event horizon started to be much more clear after studies of Finkelstein (1958) and Kruskal (1960).[7] There is a real singularity at the origin $r = 0$ for the Schwarzschild metric (and this

[7] A historical overview of the issue is given by Eisenstaedt (1982).

singularity cannot be removed with a coordinate transformation) since components of Riemann tensor for the metric tend to infinity for $r \to 0$. This circumstance leads to a publication of paper with title "Black holes 'do not exist'" (Ball, 2005). The author motivated this statement with the investigations by Chapline (2005) who claimed that at the end of stellar evolution a massive star could form so called "dark energy star" instead of black hole. It means that only around 15 years researchers discussed a useless of black hole concept for a description of a physical reality and practically they re-phrased old Einstein arguments formulated in 1939.

A formation of singularities in general relativity using natural assumptions about properties of stress-energy tensor was investigated by different researchers for many years. Using geometrical approach Roger Penrose investigated such a task without assumptions about symmetry conditions as it was done earlier. Penrose (1965) claimed that if actual physical singularities have to be occurred if inside of the collapsing object a) Positive local energy occurs; b) Einstein's equations are not violated; c) the space-time manifold is complete, d) concepts of space-time does not lose its meaning at high curvatures due to quantum phenomena. Recently, Penrose noted that the trapped surface is the key concept to prove existence of black holes.[8] Later, Hawking (1966) and Hawking and Penrose (1970) proposed different versions of the theorem. Now these statements are called Hawking – Penrose theorems on singularities (see, also Penrose (1968), Hawking and Ellis (1973), Misner, Thorne and Wheeler (1973)). One should keep in mind that we could be sure that the conclusions of the Penrose (1965) theorem are correct only in the case if its conditions occur, otherwise the theorem conclusions may be incorrect. For instance, equation of state for dark energy $p = w\rho$ and $w < -1$ and in this case a local energy may be negative (condition a) of the Penrose theorem is violated) and one could not claim for sure that physical singularities would be occurred. In principle, one could not exclude an opportunity that each of conditions (a) – d)) is violated and in the case one can not guarantee that physical singularities do exist. No doubt that the Penrose theorem (1965) played a fundamental role in a development of singularity studies in general relativity, however, we should note that conditions of the theorem (especially, a) and d)) can not be easily checked for real physical problem.

In addition to the trapped surface, Penrose introduced many important concepts in general relativity, for instance, the Hawking – Penrose theorems on singularities, the Penrose conformal diagrams, the Penrose twistors, the Newman – Penrose formalism (tetrads), the cosmic principle censorship, the Penrose process describing how to extract energy from a rotating black hole.

5. THE GALACTIC CENTER: OBSERVATIONS AND MODELS

It is generally accepted that there are supermassive black holes centers of galaxies, including our own Galaxy, see, for instance, paper by Kormendy and Ho (2013). In spite of that, theorists proposed many other alternative models (including exotic ones), for instance, a dense cluster of stars (Reid, 2009), fermion balls (Munyaneza and Viollier, 2002), boson stars (Jetzer, 1992; Torres, 2000), neutrino balls (de Paolis et al. 2001). Later, some of these models have been ruled out, or the range of parameters of these models are significantly limited with consequent observations (Reid, 2009).

[8] https://www.nobelprize.org/prizes/physics/2020/penrose/interview/.

Since the Galactic Center is the closest galactic center, the object was observed in different spectral bands, from radio to X-ray and γ. Based on results of observations it was suggested that it has to a supermassive black hole with mass not more $5\times10^6\ M_\odot$ (Rees, 1982), while Genzel and Townes (1987) and Genzel, Hollenbach and Townes (1994) claimed that observations are consistent with a supermassive black hole with mass around $10^6\ M_\odot$, while a number of people thought that black hole mass should be in the range of $10\,M_\odot$ to $100\,M_\odot$ (Ozernoy, 1987). It is amazing that based on relatively simple theoretical models and on observational results which allowed different interpretations, Rees and Genzel, Townes et al. correctly found the mass interval for the black hole at the Galactic Center (recently, R. Genzel noted that it is impossible to overestimate Townes's contribution impact in Galactic Center studies).

Shen et al. (2005), Doeleman et al. (2008), Doeleman (2017) observed Sgr A* with mm-interferometric observations and these authors found that the apparent size of the source has to be < 1 AU.

6. OBSERVATIONS OF BRIGHT STARS AND GAS CLOUDS AT THE GALACTIC CENTER

Two groups of astronomers observed motions of bright stars near the Galactic Center for almost three decades. One group of American astronomers led by A. Ghez uses Keck telescopes at Hawaii, another German – French group led by R. Genzel uses Very Large Telescopes (VLT) in Chile. Now four VLT telescopes are combined in giant interferometer which is called GRAVITY. The PI of GRAVITY collaboration is Frank Eisenhauer. The collaboration got a number of excellent results including new confirmations of GR predictions. At the end of last century almost simultaneously Eckart and Genzel (1996, 1997) and Ghez et al. (1998) found motions of bright stars at the Galactic Center. Eckart and Genzel (1996, 1997) used special equipment at the the 3.5-m New Technology Telescope (NTT) which gave them opportunity to monitor the stars for four years, while Ghez et al. (1998) used speckle interferometry at the Keck telescope.

7. ADAPTIVE OPTICS FOR GALACTIC CENTER OBSERVATIONS

The possibility of compensating astronomical seeing which is called now adaptive optics was proposed by Babcock (1953). A creation of telescopes with adaptive optics is an excellent example of a wonderful application of mathematics for a development of new technologies, however, like in this case sometimes it needs a significant time. Many years ago, famous Russian mathematician A. N. Kolmogorov (1941) proposed his phenomenological model for turbulence. These ideas were developed by Kolmogorov's student Obukhov (1941) who later was an academician of Soviet Academician and a director of Institute which is called now for Obukhov Institute of Atmospheric Physics. V. I. Tatarski (1961, who was a head of the laboratory at the Institute under Obukhov) significantly developed the Kolmogorov – Obukhov turbulence theory for propagation of electro-magnetic radiation and this stochastic approach for turbulence laid theoretical foundations for adaptive optics, see paper by Becker (1993), where first astronomical results obtained with adaptive optics systems were discussed. An obscuration by interstellar dust at the Galactic Center is very strong at visible wavelength, however, observations at near IR band (or astronomical

K-band) observations are possible. Observations and experiments showed that the Kolmogorov – Obukhov turbulence theory describes rather well atmospheric turbulence at K-band. In observations with adaptive optics astronomers used natural or artificial guide star created by laser excitation. Based on observations of guide star movable secondary mirrors correct wavefront of electromagnetic radiation toward a selected object. The Keck's group is equipped with adaptive optics for more than 20 years (Wizinowich et al., 2000) and slightly later the MPE – ESO group got a similar facilities (Rousset et al., 2003).

8. TESTING GR PREDICTIONS WITH S2

8. 1. GRAVITATIONAL REDSHIFT NEAR PERICENTER PASSAGE OF S2 STAR

The S2 star passed the its pericenter on May 19, 2018 and it is natural to expect to find relativistic effect, relativistic redshift of S2. Really, soon after the passage that the GRAVITY collaboration: Abuter et al. (2018) reported the discovery of gravitational redshift for S2. The GRAVITY collaboration: Abuter et al. (2018) represented the total redshift obtained from spectroscopical observations in the following form

$$z_{\rm tot} = z_K + f \times (z_{GR} - z_K), \tag{2}$$

where z_K is the Keplerian redshift, z_{GR} is gravitational redshift calculated taking into account the first post-Newtonian correction, $f = 0$ corresponds to Keplerian (Newtonian) fit, while $f = 1$ corresponds to the first parametric post-Newtonian fit. The GRAVITY collaboration established that $f = 0.90 \pm 0.09|_{\rm stat} \pm 0.15|_{\rm sys}$ and the authors also concluded that S2 data are inconsistent with a pure Newtonian dynamics with around 10σ confidence level.

Later, the estimate for redshift parameter has been corrected and GRAVITY collaboration: Abuter et al. (2019) found $f = 1.04 \pm 0.05$ with around 20σ confidence level and in addition the authors claimed that they evaluated the distance toward the Galactic Center with unprecendented accuracy, namely they found $R_0 = 8178 \pm 13|_{\rm stat} \pm 22|_{\rm sys}$ pc.

The Keck team (Do et al., 2019) obtained similar results namely, the authors found that $f = 0.87 \pm 0.17$ and it is consistent with GR at the 1 σ level. The Newtonian model $f = 0$ has to rejected with 5σ confidence level.

8. 2. RELATIVISTIC PRECESSION FOR S2 STAR ORBIT

To evaluate relativistic precession for S2 star the GRAVITY collaboration: Abuter et al. (2020) used the Will (2008) proposal for GR testing with observations of S2 like stars. The authors used the standard β and γ parameters for PPN approximation (Will, 2018). In general relativity, $\beta_{GR} = \gamma_{GR} = 1$. It is known that relativistic precession could expression through β and γ parameters (Will, 2008)

$$\Delta\phi_{\text{ per orbit}} = (2 + 2\gamma - \beta)\frac{\pi R_S}{a(1 - e^2)}, \tag{3}$$

where R_S is the Schwarzschild radius, a is the semi-major axis and e is the eccentricity of the orbit. For S2 star $a = 125$ mas ($R_0 = 8246.7$ pc) and $e = 0.88$. If we note $f_{SP} = (2 + 2\gamma - \beta)/3$, then in GR f_{SP} should be equal 1. From their observations

the GRAVITY collaboration: Abuter et al. (2020) found $\beta = 1.05 \pm 0.11$ and $\gamma = 1.18 \pm 0.34$ and $f_{SP} = 1.10 \pm 0.19$, therefore observations are in concordance with GR predictions and an extended mass distribution has a low impact on relativistic precession of S2 orbit.

9. CONSTRAINTS ON ALTERNATIVE THEORIES OF GRAVITY

It is clear, that there is an extended mass distribution around the supermassive black hole due to a presence of a stellar cluster and possibly a presence of dark matter. As it was shown by Rubilar and Eckart (2001), Nucita et al. (2007), Zakharov et al. (2007) an existence of an extended mass distribution leads to pericenter shift in the direction which is opposite to relativistic one.

In the last years, theorists proposed a number of alternative theories of gravity and sometimes they theories have non-Newtonian limit in a weak gravitational field approximation. Borka et al. (2013), Zakharov et al. (2016), Zakharov et al. (2018) found constraints on parameters of Yukawa gravity and graviton mass, in particular, the graviton mass constraint $m_g = 2.9 \times 10^{-21}$ eV found by Zakharov et al. (2016) is included in Particle Data Group (Tanabashi, 2018, 2019). Zakharov (2018) showed an opportunity to evaluate a tidal charge since in this case the pericenter shift could be calculated analytically. Hees et al. (2017), the GRAVITY Collaboration: A. Amorim et al.,: 2019, the GRAVITY collaboration: Abuter et al. (2020) demonstrated opportunities to improve current constraints on alternative theories of gravity.

The author thanks D. Borka, V. Borka Jovanović, P. Jovanović, L. Č. Popović for useful discussions and the organizers of the 19th Serbian Astronomical Conference for their attention to this contribution. The author thanks also an anonymous reviewer for useful remarks.

Acknowledgements

The author thanks D. Borka, V. Borka Jovanović, P. Jovanović, L. Č. Popović for useful discussions and the organizers of the 19th Serbian Astronomical Conference for their attention to this contribution. The author thanks also an anonymous reviewer for useful remarks.

References

Abbott, B. P., Abbott, R. , Abbott, T. D. et al. (LIGO Scientific Collaboration and VIRGO collaboration): 2016, *Phys. Rev. D*, **116**, 061102.
Babcock, H. W.: 1953, *Publ. Astron. Soc. Pacific*, **65**, 229.
Ball, P.: 2005, *Nature*, doi:10.1038/news050328-8.
Beckers, J. M.: 1993, *Annu. Rev. Astron. Astrophys.*, **31** 13.
Bergman, P. G.: 1942, *Introduction to the Theory of Relativity*, Dover, New York.
Blandford, R. D., Znajek, R. L.: 1977, *MNRAS*, **179**, 433.
Borka, D., Jovanović, P., Borka Jovanović, V., Zakharov, A. F.: 2013, *J. Cosm. Astropart. Phys. (JCAP)*, **11**, 050.
Chandrasekhar, S.: 1931, *MNRAS*, **91**, 456.
Chandrasekhar, S.: 1934, *Observatory*, **57**, 373.
Chandrasekhar, S.: 1983, *The Mathematical Theory of Black Holes*, Oxford University Press.
Chapline, G.: 2005, http://xxx.arxiv.org/abs/astro-ph/0503200.
De Paolis, F., Ingrosso, G., Nucita, A. A. et al., 2001, *Astron. Astrophys.*, **376**, 853.

Do, T., Hees, A., Ghez, A. et al.: 2019, *Science*, **365**, 664; arXiv:1907.10731v1 [astro-ph.GA].
Doeleman, S.: 2017, *Nat. Astron.*, **1**, 646.
Doeleman, S. S. et al.: 2008, *Nature*, **455**, 78.
Droste J.: 1917, *Koninklijke Nederlandsche Akademie van Wetenshappen Proceedings*, **19**, 197 ; Droste J.: 2002, *Gen. Relat. Grav.*, **34**, 1545 (reprinted).
Eckart, A., Genzel, R.: 1996, *Nature*, **383**, 415.
Eckart, A., Genzel, R.: 1997, *MNRAS*, **284**, 576.
Einstein, A.: 1939, *Ann. Math.*, **40**, 922.
Eisenstaedt, J.: 1982, *Arch. Hist. Exact Sci.*, **27**, 157.
Fabian, A. C., Iwasawa, K., Reynolds, C. S., Young, A. J.: *Publ. Astron. Soc. Pacific*, **112**, 1145.
Fabian, A. C., Rees, M. J., Stella, L., White, N.: 1989, *MNRAS*, **238**, 729.
Frenkel, J.: 1928, *Zeitschrift für Physik*, **50**, 234.
Frolov, V. P., Zelnikov: 2011, *Introduction to Black Hole Physics*, Oxford: Oxford University Press.
Gamow, G.: 1937, *Structure of Atomic Nuclei and Nuclear Transformations*, Oxford: Clarendon Press.
Genzel, R., Hollenbach, D., Townes, C. H.: 1994, *Reports on Progress in Phys.*, **57**, 417.
Genzel, R., Townes, C. H.: 1987, *Annu. Rev. Astron. Astrophys.*, **25**, 377.
Ghez, A. M., Klein, B. L., Morris, M., Becklin, E. E.: 1998, *Astrophys. J.*, **509**, 678.
GRAVITY Collaboration: R. Abuter et al.: 2018, *Astron. Astrophys.*, **615**, L15.
GRAVITY Collaboration: R. Abuter et al.: 2019, *Astron. Astrophys.*, **625**, L10.
GRAVITY Collaboration: R. Abuter et al.: 2020, *Astron. Astrophys.*, **636**, L5.
GRAVITY Collaboration: A. Amorim et al.: 2019, *Month. Not. R. Astron. Soc.*, **489**, 4606.
Hawking, S. W., Penrose, R.: 1970, *Proc. R. Soc. (London)*, **A294**, 511.
Hawking, S. W., Ellis G. F. R.: 1973, *The Large Scale Structure of Space-time*, Cambridge University Press.
Hawking, S. W., Penrose, R.: 1970, *Proc. R. Soc. (London)*, **A314**, 529.
Hees, A., Do, T., Ghez, A. M. et al.: 2017, *Phys. Rev. Lett.*, **118**, 211101.
Jetzer, P.: 1992, *Phys. Rep.*, **220**, 163.
Jovanović, P., Popović, L. Č.: 2009, arXiv:0903.0978.
Kolmogorov, A. N.: 1941, *DAN SSSR* **30**, 301; Kolmogorov, A. N.: 1968 *Sov. Phys. Usp.*, **10**, 734 (reprinted).
Kormendy J., Ho, L.: 2013, *Annu. Rev. Astron. Astrophys.*, **51**, 511.
Misner, C., Thorne, K. S., Wheeler, J. A.: 1973, *Gravitation*, San Francesco: W. H. Freeman and Company.
Munyaneza, F., Viollier, R. D.: 2002, *Astrophys. J.*, **564**, 274.
Nucita, A. A., De Paolis, F., Ingrosso, G. et al.: 2007, *Publ. Astron. Soc. Pacific*, **119**, 349.
Obukhov, A. M.: 1941, *DAN SSSR*, **32**, 22.
Oppenheimer, J. R., Volkoff, G. M.: 1939, *Phys. Rev.*, **55**, 374.
Oppenheimer, J. R., Snyder, H.: 1939, *Phys. Rev.*, **56**, 455.
Ozernoy, L. M.: 1987, *AIP Conference Proceedings*, **155**, 181.
Penrose, R.: 1965, *Phys. Rev. Lett.*, **14**, 579.
Penrose, R.: 1968, *Battelle Rencontres, 1967 Lectures if Physics and Mathematics, eds. C. M. de Witt and J.A. Wheeler*, p. 121, New-York: Benjamin.
Rees, M. J.: 1982, *AIP Conference Proc.*, **83**, 166.
Regge, T., Wheeler, J. A.: 1957, *Phys. Rev.*, **108**, 1063.
Reid, M.: 2009, *Intern. J. Mod. Phys.* D, **18**, 889.
Rousset, G., Lacombe, F., Puget, P. et al.: 2003, *Proc. of the SPIE*, **4839**, p. 140.
Rubilar, G. F., Eckart, A.: 2001, *Astron. Astrophys.*, **74**, 95.
Schwarzschild, K.: 1916, *Sitzungsberichte Kuniglich-Preussischen Akad. Wissenschaften*, 189; Schwarzschild, K.: 2003, *Gen. Relat. Grav,*, **35**, 951 (reprinted).
Shen, Z.-Q., Lo, K. Y., Liang, M.-C. et al.: 2005, *Nature*, **438**, 62.
Stella, L.: 1990, *Nature*, **344**, 747.
Stoner, E. C.: 1930, *Phil. Mag.*, **9**, 944.
Stoner, E. C.: 1932, *MNRAS*, **92**, 651.

Tanabashi, M. et al. (Particle Data Group): 2018 and 2019 update, *Phys. Rev.* D, **98**, 030001.
Tanaka, Y., Nandra, K., Fabian, A. C. et al.: 1995, *Nature*, **375**, 659.
Tatarski, V. I.: 1961, *Wave Propagation in a Turbulent Atmosphere*, New York: Dover.
Torres, D. F., Capozziello, S., Lambiase, G.: 2000, *Phys. Rev.* D **62**, 104012.
Weinberg, S.: 2008, *Cosmology*, Oxford: Oxford University Press.
Will, C. M.: 2008, *Astrophys. J.*, **674**, L25.
Will, C. M.: 2018, *Theory and Experiment in Gravitational Physics*, Cambridge: Cambridge University Press.
Yakovlev, D. G.: 1994, *Physics – Uspekhi*, **37**, 609.
Yakovlev, D. G., Haensel, P., Baym, G., Pethick Ch.: 2013, *Physics – Uspekhi*, **56**, 289.
Zakharov, A. F.: 2003, *Publ. Astron. Observ. Belgrade*, **75**, 27: arXiv:astro-ph/021229.
Zakharov, A. F.: 2018, *Eur. Phys. J.* C, **78**, 689.
Zakharov, A. F., Repin, S. V.: 2006, *New Astron.*, **11**, 405.
Zakharov, A. F., Jovanović, P., Borka, D., Borka Jovanović, V.: 2016, *J. Cosm. Astropart. Phys. (JCAP)*, **05**, 045.
Zakharov, A. F., Jovanović, P., Borka, D., Borka Jovanović, V.: 2018, *J. Cosm. Astropart. Phys. (JCAP)*, **04**, 050.
Zakharov, A. F., Nucita, A. A., De Paolis, F., Ingrosso, G.: 2007, *Phys. Rev.* D, **76**, 062001.

Invited Lectures

Publ. Astron. Obs. Belgrade No. 100 (2021), 57 - 65 *Invited Lecture*

SEARCHING FOR EXTREMELY ACCRETING QUASARS

N. BON[1], P. MARZIANI[2] and E. BON[1]

[1] *Astronomical Observatory, Volgina 7, 11000 Belgrade, Serbia*
E–mail: nbon@aob.bg.ac.rs
E–mail: ebon@aob.bg.ac.rs

[2] *INAF, Osservatorio Astronomico di Padova, IT 35122, Padova, Italy*
E–mail: paola.marziani@oapd.inaf.it

Abstract. Quasars are most luminous objects and therefore can be detected as far as the edge of the known Universe. As such they could be useful for measuring cosmological distances. The problem is that quasars show large diversity in their properties – their luminosity is spread over six orders of magnitudes, that makes them not suitable for conventional standard candles. A sub-group of quasars, called highly or extremely accreting quasars (xA quasars) radiate close, or even above Eddington luminosity. They are extreme in many aspects – xA quasars are among quasars with highest accretion rates, and their emitting line regions show the lowest ionization parameter and the highest electron density. We focus on low-z xAs with high host galaxy contribution and also strong FeII emission lines in their optical spectra. They share several other multi-frequency properties which can be used for their identification. Our ability to distinguish xA quasars as sources whose Eddington ratio is extreme and ideally scattering little around a well-defined value opens up the possibility to use these quasars as potential cosmological probes. We address problems that could lead to misidentification of xA quasars using optical spectra.

1. INTRODUCTION

Back in 1929 Edwin Hubble discovered the expansion of the Universe using velocity - distance relation among nearby extra-galactic nebulae - the distance modulus is increasing with the redshift. It was a discovery that scientists until nowadays try to apply to higher distances. In order to measure distance in the Universe it is crucial to choose a sample of standard candles - objects with known luminosity. For a very long period of time, type Ia supernovae and variable stars such as Cepheids have been used as standard candles with very high precision (see e.g. Kirchner 2004, Rubin et al. 2012). The problem is that supernovae can be detected only up to $z \sim 1.3$.

Quasars are objects that can be observed at all redshift scales - from our "vicinity" till the edge of the known Universe (up to $z \sim 7.6$). Besides, they are the most luminous sources in the Universe, whose bolometric luminosity can reach up to 10^{48}erg s^{-1}. Quasars are easily recognizable and numerous. Up to now, more than 750,000 quasars have been discovered (see SDSS DR 16, Lyke et al. 2020). For these reasons, there were many attempts to use quasars as standard candles or as standard rulers. But, the main problem is that - even though quasars are the most luminous

objects in the Universe, and therefore easily detectable, their luminosity is spread over six orders of magnitude, making them opposite of what standard candles by definition are. Besides, they are highly variable sources in luminosity and spectral energy distribution and their spectral properties do not show strong signs of a luminosity dependence. Moreover, quasars are anisotropic sources. So, the goal should be to find one or more parameters closely related to the intrinsic luminosity of quasars, or in other words, to isolate class of quasars with a constant characteristic, that we can use for redshift-independent estimate of luminosity.

There were several tentative experiments to use quasars in the context of distance measurements:

- "Baldwin effect" - Baldwin (1977) noticed that the equivalent width of emission line (such as CIV λ1549) decreases as the UV continuum luminosity (λ 1450) increases. It was believed that the redshift independency of flux ratio used to obtain equivalent width could be used for distance measurements, but a large dispersion in this anticorrelation (e.g., Baldwin, Wampler, & Gaskell 1989) returns distance calibrations of a low quality in comparison with other standard candles.

- BLR reverberation - The reverberation studies showed a tight relation between the delay (τ) of the emission line and the intrinsic luminosity (most frequently calculated from the flux measured at 5100 Å (F_{5100}) (e.g., Peterson et al. 1999, Kaspi et al. 2000)). Line delay can be explained as an effective radius of the BLR region, related with the luminosity as $r_{BLR} \sim L^{1/2}$ (Watson et al, 2011). The dispersion in the $r_{BLR} - L$ relation is low. Bentz et al. (2013) measured the dispersion of only 0.13 dex in clean sample. Therefore, with a larger sample and broader coverage of the redshift range this method could present a very good alternative to type Ia supernovae.

- Continuum reverberation - The observed delays between different continuum wavelengths depend on the disk's radial temperature distribution, its accretion rate, and the central black hole mass. Wavelength - dependent continuum time delays can be used to calculate the AGN distance (Collier et al. 1999), knowing the accretion disk flux, which can be obtained by taking difference spectra to isolate the variable component of AGN light.

- Dust reverberation - The dust reverberation allow us to derive the inner radius of the dust torus by measuring the lag between the flux variation of the UV/optical continuum from the accretion disk and that of the near-infrared thermal emission from the dust torus. The inner radius of the dust torus is expected to be proportional to the square-root of the accretion-disk luminosity, and that opens the possible application of the dust reverberation to the cosmological distance measurement (Kobayashi et al. 1998).

Even though reverberation methods offer promising possibilities to use quasars as standard candles, objects monitored in reverberation campaigns are most often on low z scales. Besides, monitoring is usually very time consuming.

Therefore these methods have not been until now efficient to build samples with large number of sources that could be used in cosmological studies. The following methods use single observations for cosmological studies, and hence are more appropriate for making large samples of objects of interest:

- X-ray excess variance method - La Franca et al. (2004) proposed the method to determine the absolute luminosity from the X-ray excess variance and the full width half maximum (FWHM) of Hβ emission line. The method requires a single optical spectrum of an object, but the difficulty lies in the high quality measurement of the high frequency tail of the X-ray power spectrum. Hopefully, the Athena X-ray Observatory, expected to be launched in 2028, will provide significant number of measurements.

- Super Eddington black holes - In a super-Eddington accretion regime a "thick disk" is expected to develop (Abramowicz et al. 1988). The accretion flow remains optically thick so that radiation pressure "fattens" it. When the mass accretion rate becomes super-Eddington, the emitted radiation is advected toward the black hole, so the radiative efficiency of the accretion process is expected to decrease, causing an asymptotic behavior of the luminosity as a function of the mass accretion rate (Wang et al. 2014).

- Continuum shape method - This method proposed to use the non-linear relation between X-ray and UV emission as an absolute distance indicator (Lusso & Rissality, 2015). This relation implies that quasars more luminous in the optical are relatively less luminous in the X-rays. This is the first successful method for measuring distances on a high redshifts (up to z $\sim$ 6), using quasars as standard candles.

If Eddington ratio and black hole mass can be derived from some distance-independent measure it would be possible to derive distance-independent quasar luminosities. Marziani & Sulentic (2014) succeeded to isolate a subclass of quasars -xA quasars or extreme accretors - that radiate close to the Eddington limit, and show distinct optical and UV spectral properties that can be recognized in spectra. They propose precise criteria based on the line ratios (AlIIIλ1860/SiIII]λ1892 $\geq$ 0.5, and (ii) SiIII]λ1892/CIIIλ1909 $\geq$ 1.0) which lead to a source sample with very low dispersion of $\sim$ 0.13 dex in the Eddington ratio. The major issue related to the cosmological application of the xA quasar luminosity estimates from line widths is the identification of proper emission lines whose broadening is predominantly virial over a wide range of redshift and luminosity. At lower redshift the good virial estimator is Hβ emission line, while on higher redshifts, AlIIIλ1860 can be used with the same purpose (Marziani & Sulentic 2014, Negrete et al. 2018, Dultzin et al. 2020, Marziani et al. in preparation).

Negrete et al. (2018) selected much larger sample of xA sources and provided interesting constraints on cosmological parameters. Dultzin et al. 2020 gave very interesting overview on this topic and discuss the perspective of the method based on xA quasars. In this paper we will give an overview on xA sources, and of the techiques used for their search.

2. MAIN SEQUENCES OF UNOBSCURED QUASARS

Basically according to the viewing angle and subsequently according to their fluxes, spectral characteristics - width, shifts and intensities of emission lines, quasars can be divided into two sub-groups - Type 1 or unobscured quasars and Type 2 quasars. But even in the Type 1, quasars differ according to their observational properties (emission line profiles - shifts, widths and intensities, contribution of the iron emission in the spectra, luminosity,...), and also physical characteristics (mass of central black hole, ionization parameter, dimensionless accretion rates, electron density, inclination angle...) (Sulentic et al. 2000). The first sistematization of diverse characteristics of quasars was done by Boroson & Green (1992), using a Principal Component Analysis (PCA) of 87 PG quasars. They noticed that the dominant source of variation in the observed properties is related to a parameter RFe_{II} - intensity ratio between the FeII blend at λ4570 and Hβ (RFe_{II}). The optical plane FWHM(Hβ) and RFe_{II}, can serve to classify quasars along sequence according to systematically-changing properties. This sequence is called Main Sequence of Quasars.

After that time, the number of observed quasars is dramatically increased, but the main sequence has retained its validity (Sulentic et al., 2007; Zamfir et al., 2010; Shen and Ho, 2014; Wolf et al., 2019). According to the width of broad Hβ line it is possible to separate quasars into two populations - pop. A, with FWHM(Hβ) less than 4000 km/s, and pop B. with FWHM(Hβ) higher than this limit (Sulentic et al. 2000). The limit between two populations depends on the luminosity (Marziani et al. 2009). Besides, in the plane RFe_{II}-FWHM(Hβ) data point can be separated into different bins - along RFe_{II} axis into bins, such as A1, A2, A3, etc. (the separation between bins is 0.5 RFe_{II}), and along FWHM(Hβ) axis into A1, B1+, B1++ (4000 km/s is sepation between bins). Each bin represents one spectral type. Quasars within one spectral bin are in similar dynamical and physical conditions.

3. EXTREME ACCRETORS

The subject of our interest are extremely accreting sources, that cover the very end of Main sequence. If the main driver of the quasar sequence is Eddington ratio (Marziani et al, 2001, Shen & Ho, 2014, Bon et al. 2018), it is expected that xA quasars have the strongest contribution of FeII in their optical spectra, and should be the highest radiators, as observationally confirmed. As already mentioned, Marziani & Sulentic (2014) showed that xA quasars radiate at extreme L/L_{Edd}, with very low dispersion ($\sim$ 0.13 dex in the Eddington ratio). This result is consistent with the expectation of accretion disks at very large accretion rates (Abramowicz et al., 1988). Accretion disk theory predicts low radiative efficiency at high accretion rate and that L/L_{Edd} saturates toward a limiting values (Abramowicz et al., 1988; Mineshige et al., 2000; Sadowski et al., 2014). For this reason we use to call them "Eddington standard candles".

Extreme accretors satisfy three conditions that allow us to use them as "Eddington standard candles": (i) constant Eddington ratio, (ii) virial motion of low-ionization BLR clouds, and (iii) constant ionization parameter that allows spectral invariance (more details in Dultzin et al. 2020). The condition (ii) permits to express black hole mass by the virial relation, that means that by simple measurements of FWHM of low-ionization lines, we can estimate z-independent accretion luminosity.

xA quasars are little variable in the optical band, and therefore variability is not significantly affecting measurements of Eddington ratio.

3. 1. SELECTION OF EXTREME ACCRETING QUASARS

If we select spectral types along the optical plane of main sequence, satisfying the condition $R_{FeII} \geq 1.0$ (A3, A4, etc.), selected spectra of xA quasars will be characterized with strong FeII emission and Lorentzian Balmer line profiles. They represent around 10% of quasars at low-z ($z \lesssim 0.8$). This simple selection criterion in optical band corresponds to UV selection criteria, mentioned above, based on UV line ratios, and proposed by Marziani & Sulentic (2014): (AlIIIλ1860/SiIII]λ1892 $\geq$ 0.5, and (ii) SiIII]λ1892/CIIIλ1909 $\geq$ 1.0).

To clarify some main properties of extreme accretors, Negrete et al. (2018) identified 334 SDSS quasars on redshift ≤ 0.8, that satisfy criterion $R_{FeII} \geq 1$. They found strong outflow signatures in [OIII], but also in the case of Hβ lines, as a presence of blues-shifted component in the line profile. Since FWHM of Hβ is used as a "virial broadening estimator", the effect of outflow has to be taken into account, in order to estimate a "clear" virial component of the line profile. Besides, authors emphasize a strong effect of the viewing angle on Hβ broadening, that has to be accounted for, in order to bring into agreement the virial luminosity estimates and concordance cosmology.

3. 2. PROBLEMS IN XA SELECTION

Automatic selection of xA quasars using a large databases can be coarseness, and therefore can include spurious xA sources in the set, that can dramatically increase the dispersion in the Hubble diagram of quasars. Negrete et al. (2018) noticed that 32 spectra in their sample have strong contribution of stellar population, which can affect measurements of R_{FeII}. This subsample of objects (hereafter, host galaxy sample) required a different and more carefull approach (Bon et al. 2020, hereafter, Bon20). Spectra were analyzed with the simultaneous multicomponent fit of a host galaxy spectrum, AGN continuum, FeII template and emission lines, using the technique based on ULySS - full spectrum fitting package (Koleva et al. 2009, Bon et al. 2014, Bon et al. 2016). They found that all of the 32 spectra show moderate-to-strong FeII emission and the vast majority strong absorption features in their spectra are typical of evolved stellar populations. The authors emphasized the importance of simultaneous fit in the analysis, because FeII can mimic stellar population spectra (see Figure 1). Namely, in half of the host galaxy sample the stellar population contribution is higher than 40%, and therefore prominent absorption lines of evolved stellar population do mimic FeII emission, so any analysis that does not take into account host galaxy contribution can make mistaken identification of FeII spectral features, overestimate of R_{FeII}, and hence misclassify sources as xA.

From the simultaneous fit results, Bon20 measured the line fluxes, FeII contribution, stellar host contribution, AGN continuum contribution, and some other spectral parameters. This allowed to calculate the mass of the central super-massive black hole (SMBH) using several different methods, as well as an accretion rate. The main problem that pointed out the misclassification of 32 sources was their low L/L_{Edd} (almost all sources have $\log(L/L_{Edd}) \leq$ -0.5), which is not in the agreement with expected values for xA sources.

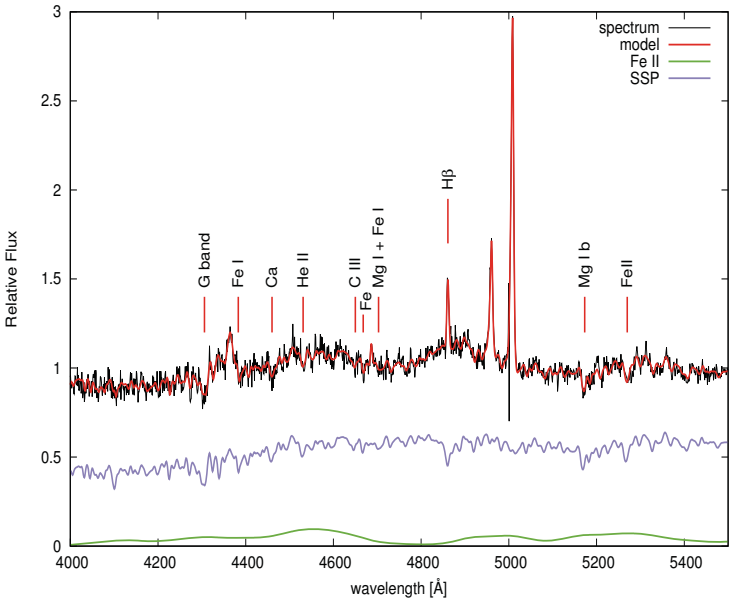

Figure 1: Quasar spectra of SDSS J113651.66+445016.4 where the host galaxy mimic strong FeII emission leading to a mistaken identification of strong FeII emitters. The panel shows (from top to bottom): the real spectra and the best fitting model; single stellar population spectrum that was used in the best fitting model; and the FeII template used in the fit. Some prominent absorption lines are marked on the plot.

The Eddington luminosity is defined by limiting requirement for accretion; the radiation pressure force per particle is equal to the gravitational force. For the case of solar metallicity this implies (see more in Netzer, 2013): $L_{\rm L}/L_{\rm Edd} = 1.5{\times}10^{38} M/M_{\odot}$ erg/s. Therefore, the key point is to determine the $M_{\rm BH}$. Following Vestergaard & Peterson (2006, hereafter, VP06) Bon calculated black hole virial masses with additional constrains for the virial factor as follows:

$$M_{\rm BH} = f\frac{r_{\rm BLR}(\delta v)^2}{G} = f_1(\dot{m}, a) f_2(\theta\,|\,\dot{m})\frac{r_{\rm BLR}(\delta v)^2}{G}, \qquad (1)$$

where $r_{\rm BLR}$ is the broad line region size, a is the parameter of a black hole spin, and the broad line virial velocity broadening δv is FWHM of the broad component of Hβ (Negrete et al. 2018). The virial form factor f was assumed to be the product of two terms, one depending on accretion rate and a black hole spin, and another one depending on orientation effects. The dependence on dimensionless accretion rate of f_1 has been parametrized by the $r_{\rm BLR}$ dependence on luminosity (Du et al. 2016). The spin parameter affects the temperature of the accretion disk and hence the SED of the ionizing continuum (Wang et al. 2014).

As the first step Bon20 calculated $M_{\rm BH}$ using Bentz et al. (2013, hereafter B13) correlation between $r_{\rm BLR}$ and optical luminosity, assuming form factor $f = 1$. These results were correlated with the masses obtained from the VP relation. No orientation effects had been considered in both cases.

Typical uncertainties for the $M_{\rm BH}$ are expected to be ≈ 0.3 dex at 1σ (VP06, Marziani et al. 2019), where the main source of uncertainty is most likely due to the combined effect of orientation and Eddington ratio.

The effect of the viewing angle on the Hβ line is assumed to depend on FWHM of the broad Hβ emission line with the relation proposed in Mejia-Restrepo et al. (2018):

$$f_2^\star = \left(\frac{\rm FWHM}{4550}\right)^{-1.17}, \tag{2}$$

In addition, we used the correction for $r_{\rm BLR}$ proposed by Martinez-Aldama et al. (2019): $\delta r_{\rm BLR} = \log\,(r_{\rm BLR}/r_{\rm BLR,B13})$, with the $f_2^\star$ dependence on FWHM. Then, the correction to $r_{\rm BLR}$ is: $\delta r_{\rm BLR} = (-0.271 \pm 0.030) \log \frac{L_{\rm bol}}{L_{\rm Edd}{}^\star} + (-0.396 \pm 0.032)$, where $L_{\rm Edd}{}^\star$ means that the Eddington luminosity has been computed with virial mass relation assuming correction $f_2^\star$ (Eq. 2).

After the corrections, only one xA candidate (SDSSJ105530.40+132117.7) is recognised as high accretor, with $L/L_{\rm Edd} \approx -0.35$, close to the lower limit for extreme accreting sources.

Another way to estimate $L/L_{\rm Edd}$ can be using the fundamental plane (FP) of accreting black holes (Du et al. 2016), which is based on a correlation between the Eddington ratio, and the observational parameters $R_{\rm FeII}$ and the ratio D between FWHM and velocity dispersion of broad Hβ line ($D = FWHM/\sigma$). The correlation can be written as: $L_{\rm L}/L_{\rm Edd} \approx a + bD + cR_{\rm FeII}$, where a, b, c are coefficients obtained from the fitting of a sample as reported by Du et al. (2016), a=0.31, b=-0.82 and c=0.8. The fundamental plane is consistent with the relations derived from the E1 approach ($L/L_{\rm Edd}$ and $\dot{\mathcal{M}}$ increase as the Hβ profile become narrower [1].).

Spectra from the host galaxy sample appeared to be mainly population B2 and B3, and the shapes of their line profiles were relatively broad, while the $R_{\rm FeII}$ appeared to be relatively high, which according to FP approach lead to overestimated values of Eddington ratio, in comparison to the values obtained by the standard definition of Eddington ratio. In order to investigate the origin of this disagreement, Bon20 reconsidered the fit obtained by Du et al. (2016), due to the possibility of a bias for low $L/L_{\rm Edd}$. The fundamental plane fit of Du et al. (2016) predicts a value of $L/L_{\rm Edd}$ objects almost one order of magnitude systematically higher with respect to the one expected by the distribution of the rest of the objects. We obtained a slightly corrected fit by fitting the residuals with a linear function ($\delta = \log L/L_{\rm Edd} - \log L/L_{\rm Edd}$). A post-correction best fitting line is consistent with $\delta(L/L_{\rm Edd}) \equiv 0$. Applying this correction to the residuals we obtain a slightly modified equation for the fundamental plane $\log L/L_{\rm Edd} = \alpha + \beta D + \gamma R_{\rm FeII} \approx 0.774 - 1.33D + 1.30R_{\rm FeII}$. Unfortunately, this new corrected law, do not solve the disagreement between the VP conventional estimates of $L/L_{\rm Edd}$ (see more in Bon20). The disagreement is so large that the highest radiating source in this sample ($L/L_{\rm Edd} \sim 2$) according to the FP has $L/L_{\rm Edd} \approx 0.04$ following VP. This leads to inconsistencies between the main sequence interpretation and spectral type assignment (see, Bon20). Even with the modified FP formula

[1] As the broad Hβ profile becomes narrower, the line shape changes from Gaussian distribution to Lorentzian, and therefore the parameter D=FWHM/σ tends to 0, since σ bacomes very large. This implies that high $R_{\rm FeII}$ leads to high L/L_{Edd}

with the parameters reported above, the modified FP brings in agreement only several points at the low-$L/L_{\rm Edd}$ end, while the rest of the data remains above the VP estimates by ≈1 dex.

In order to further investigate this discrepancies, Bon20 used the stellar velocity dispersion $\sigma_\star$ of the host, using the scaling law $M_{\rm BH} \approx 1.95 \cdot 10^8 \, (\sigma_\star/200)^{5.12}$ M$_\odot$ (McConnell et al. 2011), which is an updated formulation of the original scaling law of Ferrarese & Merritt (2000) and computed $M_{\rm BH}$. The $M_{\rm BH}$ calculated from the VP formula and $M_{\rm BH}$ from host show systematic differences, due to resolution limitations of the SDSS spectra. Bon20 obtained disagreement with measured dispersions when they were lower than twice of the resolution (for SDSS resolution is about 69 km s^{-1}), while the results of masses obtained from stellar and VP showed agreement when the host absorption line dispersion was above $\sigma_\star \geq 150$ km s^{-1} (see more in Bon et al. 2020).

Another possibility for this discrepancy is a degeneracy between effects of orientation and $M_{\rm BH}$ in the optical plane of the main sequence. Also, Bon20 could not exclude that B2 and B3 objects contain higher masses of $M_{\rm BH}$. These effects would imply a significant decrease in $L/L_{\rm Edd}$ in the transition from B2 to A2.

After all corrections end tests that Bon20 applied on host galaxy sample, they concluded that all of these objects appears to be low accreting objects, except for only one of them, which could have the value of $L/L_{\rm Edd}$ =0.3.

4. SUMMARY

Extreme accretors represent the sub-class of quasars with almost constant L/L_{Edd}, and therefore might be suitable as Eddington standard candles. The Hubble diagram for xA quasars is consistent with concordance cosmology, and provides better constrain on Ω_M (0.3 ± 0.06) than type Ia supernovae, because of the z ∼ 2 coverage (Dultzin et al. 2020).

In this paper we presented some important techniques needed in the search for high accreting quasars. Multicomponent simultaneous analysis of nebular, stellar and FeII pseudo continuum is important to decrease the possibility to inject some spurious objects that can dramatically increase the dispersion in the Hubble diagram of quasars.

The next step is to select larger sample from the latest data releases of SDSS, that can clarify the main properties of xA quasars.

Acknowledgements

N.B. and E.B. acknowledge support by the Ministry of Education, Science and of the Republic of Serbia through the contract no. 451-03-9/2021-14/200002.

References

Abramowicz, M. A., Czerny, B., Lasota, J. P., Szuszkiewicz, E.: 1988 *ApJ*, **332**, 646.
Lyke, B. W., Higley, A.N., McLane, J. N. et al.: 2020, *ApJS*, **250**, 8.
Baldwin, J. A.: 1977, *ApJ*, **214**, 679.
Baldwin, J. A., Wampler, E. Joseph, Gaskell, C. Martin: 1989, *ApJ*, **338**, 630.
Bentz, M. C., Denney, K. D., Grier, C. J. et al.: 2013, *ApJ*, **767**, 149.

Bon, N. Marziani, P. Bon, E. et al.: 2020, *A&A*, **635**, 151.
Bon, N., Marziani, P., Bon, E.: 2018, *FrASS*, 5, 3B.
Bon, N. Popović, L. Č., Bon, E.: 2014, *AdSpR*, **54**, 1389.
Bon, E., Zucker, S., Netzer, H. et al.: 2016, *ApJS*, **225**, 29.
Boroson, T. A., Green, R. F.: 1992, *ApJS*, **80**, 109.
Collier, S., Horne, K., Wanders, I., Peterson, B.: 1999, *MNRAS*, **302**, 24.
Dultzin, D., Marziani, P., Del Olmo, A. et al.: 2020, *FrASS*, **6**, 80.
Du, P. and Wang, J.-M.: 2019, *ApJ*, **886**, 42.
Du, P., 12 colleagues: 2016, *The Astrophysical Journal*, 820.
Ferrarese, L., Merritt, D.: 2000, *The Astrophysical Journal*, **539**, L9–L12.
Green, P., J., Forster, K., Kuraszkiewicz, J.: 2001, *ApJ*, **556**, 727.
Hubble, E.: 1929, *PNAS*, **15**, 168.
Kaspi, S., Smith, P. S., Netzer, H. et al.: 2000, *ApJ*, **533**, 631.
Kirshner, R. P.: 2004, *PNAS*, **101**, 8.
Kobayashi, Y., Yoshii, Y., Peterson, B. et al.: 1998, *Proceedings of the SPIE*, **3352**, 120.
Koleva, M., Prugniel, Ph., Bouchard, A., Wu, Y.: 2009, *A&A*, **501**, 1269.
Kormendy, J., Illingworth, G.: 1982, *The Astrophysical Journal*, **256**, 460.
La Franca, F, Bianchi, S, Ponti, G. et al.: 2014, *ApJL*, **787**, 12.
Marziani and Sulentic: 2014, *MNRAS*, **442**, 1211.
Marziani, P., Sulentic, J. W., Stirpe, G. M., Zamfir, S.; Calvani, M.: 2009, *A&A*, **495**, 83.
Marziani, P., Sulentic, J. W., Zwitter, T., Dultzin-Hacyan, D., and Calvani, M.: 2001, *ApJ*, 558, 553.
McLure, R. J., Dunlop, J. S.: 2001, *Monthly Notices of the Royal Astronomical Society*, **327**, 199–207.
Mejía-Restrepo, J. E., Lira, P., Netzer, H., Trakhtenbrot, B., Capellupo, D. M.: 2018, *Nature Astronomy*, **2**, 63–68.
Mineshige, S., Kawaguchi, T., Takeuchi, M., Hayashida, K.: 2000, *PASJ*, **52**, 499.
Negrete, C. A., Dultzin, D., Marziani, P. et al.: 2018, *A&A*, **620**, 118.
Netzer, H. Cambridge, UK: Cambridge University Press, 2013.
Peterson, B., Barth, A. J., Berlind, P., et al.: 1999, *ApJ*, **510**, 659.
Risaliti and Lusso: 2015, *ApJ*, **815**, 33.
Rubin, et al.: 2012, *ApJ*, **763**, 1.
Sadowski, A., Narayan, R., McKinney, J. C., Tchekhovskoy, A.: 2014, *MNRAS*, **439**, 503.
Shen, Y., and Ho, L. C.: 2014, *Nature*, **513**, 210.
Sulentic, J. W., Bachev, R., Marziani, P. et al.: *ApJ*, **666**, 757.
Sulentic, J. W., Marziani, P., Dultzin-Hacyan, D.: 2000, *ARA&A*, **38**, 521.
Wang, J. M, Du, P., Hu, C., Netzer, H. et al.: 2014, *ApJ*, **793**, 108.
Watson, D., Denney, K. D., Vestergaard, M., Davis, T. M.: 2011, *ApJL*, **740**, 49.
Wolf, J., Salvato, M., Coffey, et al.: 2020, *MNRAS*, **492**, 3580.
Zamfir, S., Sulentic, J. W., Marziani, P., Dultzin, D.: 2010, *MNRAS*, **403**, 1759.

Publ. Astron. Obs. Belgrade No. 100 (2021), 67 - 74 *Invited Lecture – special session "The gravitational-wave Universe" supported by COST Action CA16104*

A MODEL OF QUANTUM COSMOLOGY: FUZZY DE SITTER SPACE

MAJA BURIĆ

University of Belgrade, Faculty of Physics, Studentski trg 12, 11000 Belgrade, Serbia
E–mail: majab@ipb.ac.rs

Abstract. Quantization of gravity is probably the most important unsolved problem of theoretical physics today. For many years it has been approached only theoretically, but in the last decades there is a growing amount of astrophysical and cosmological data that give input and guide the further research. Present theories of quantum gravity are formulated in a variety of ways: we here describe a model of fuzzy de Sitter space obtained in the context of noncommutative geometry, and discuss some of its implications to cosmology.

1. INTRODUCTION

In many ways, gravity is unique among physical phenomena. Historically it had a distinctive role in our understanding and description of Nature, as
– observations of motion of planets and Sun established astronomy as first of the natural sciences, while attempts to systematize and explain these observations made gravity the first of fundamental forces to be theoretically described;
– efforts to understand gravity brought, in physics, fundamental ideas like Newton's laws of classical mechanics and Einstein's general relativity (GR);
– Newton's and Einstein's theories marked significant steps in the development of mathematics (differential calculus and analysis, geometry) and its relation to physics;
– finally, a unique feature of gravity is that it has not been quantized, yet. It is indeed this segment where we expect gravity to bring the next fundamental breakthrough.

Some of important GR results that form our current intuition about gravity are:
– spacetime is not an empty stage, a fixed framework (as in Newton's mechanics), but a dynamical object interacting with matter. In particular, the universe evolves;
– gravitational force can be described in purely geometric terms: physical quantities that characterize spacetime are invariants like geodesic lines or curvature invariants;
– dynamics of spacetime is described through a classical field that carries energy and momentum: Einstein equations are obtained from the principle of minimal action;
– Einstein equations are covariant under the changes of coordinates: diffeomorphism invariance can be understood as a guiding symmetry principle to formulate GR;
– solutions to Einstein equations generically have singularities, like the black hole or the big bang singularity. This result (due to Penrose and Hawking, around 1965) was awarded by the Nobel prize in 2020. To obtain it, one analyzes the real physical situations: the energy conditions on matter, boundary conditions, etc.

However, we know that matter is quantized, either as point particles (in the non-relativistic regime) or as quantum fields. This raises two important questions: how to couple classical gravity to quantum matter; further, how to quantize gravity? The standard recipe for quantization in quantum field theory (QFT) is to describe gravity as classical field theory, expand it around the minimal-energy solution (vacuum), and quantize perturbatively. Alternatively, one can generalize the quantum-mechanical approach: write the dispersion relation for gravity (Hamiltonian constraint) and quantize it, to obtain the gravitational analogue of the Schrödinger equation (Wheeler-de Witt equation). But the standard recipes do not work: they give either unphysical results (as gravity is not renormalizable) or formal answers (as there is no effective way to do calculations that include functional equations, beyond the simplest cases). Apart from heuristic reasons, gravity has to be quantized for physical and consistency reasons: if it is a fundamental force, it should be unified with other fundamental interactions and described in the same way, by quantum field theory. Furthermore, classical singularities of GR certainly are unphysical, and quantization is a way to remove them.

There is no *a priori* justification to extrapolate, to assume that spacetime on the Planck scale has the same structure as it has on the atomic, galactic or cosmological scales. Perhaps the (classical) structure of spacetime at small scales is not that of a manifold, but discrete ('quantum spacetime does not have points')? Quantum field theories on flat and curved spaces have the problem of ultraviolet (UV) divergences: the propagator between points x and x' is divergent in the coincidence limit $x \to x'$ (i.e. $p \to \infty$). This problem is solved by renormalization; but were the spacetime structure lattice-like, it would have not existed. Diverse ideas are developed along these lines. Perhaps the most physical way to give structure to the spacetime points is to develop a model that 'delocalizes' their description, as in string theory or in loop quantum gravity. Another, straightforward way, is to describe spacetime coordinates by noncommuting operators, as in quantum mechanics. An important constraint on all theories of quantum gravity is the classical, that is, macroscopic limit to GR. In principle we build from the known: we usually keep one of desirable or intuitive properties of general relativity (e.g. its field-theoretic interpretation, geometric interpretation, symmetry principle) and relax the others.

2. NONCOMMUTATIVE GEOMETRY

The framework which we use is that of noncommutative (NC) geometry. NC geometry is a very active area of research since the 1990s; some prominent names who developed it on the side of mathematics include Fields medalists Connes and Kontsevich. Many theoretical physicists, aspiring to different physical applications, have been involved in this area of research, developing notions of noncommutative space, noncommutative differential geometry and noncommutative field theory. An approach inspired by the geometric description gravity, in the sense that it generalizes the Cartan formalism of differential geometry, is Madore's noncommutative frame formalism (Madore, 1995) used here. We present a model of noncommutative or fuzzy de Sitter space developed in Buric *e*t al. 2015, 2018, 2019.

There are several noncommutative spaces whose properties are thoroughly investigated and well established, including description of classical and quantized fields on them. The best known example is NC space with constant noncommutativity

of Cartesian coordinates, or 'Moyal deformation' of the flat space: there are various applications of this model to cosmology, though one should perhaps notice that it is, by definition, anisotropic. Another paradigmatic example is the fuzzy sphere, a two-dimensional spherically symmetric NC space of constant curvature defined by the Lie algebra of rotation group. Further examples are κ-Minkowski space, fuzzy hyperboloid, fuzzy $\mathbb{CP}^n$ spaces, spaces built on different $\star$-products, etc. In order to obtain noncommutative spaces that extend basic solutions of GR (e.g. FLRW cosmologies, black holes), one should preferably keep the spherical symmetry and work in four spacetime dimensions: but this task proves to be far from straightforward (Buric and Madore, 2014). The main reason is that the algebraic structure of spacetime imposes additional constraints which are, beyond commutative geometry, rather nontrivial. We discuss here a generalization of the fuzzy sphere construction: the four-dimensional fuzzy de Sitter space, based on the algebra of the de Sitter group $SO(1,4)$ and its (unitary irreducible) representations. Although the full details are rather technical, let us at least introduce the basic elements of the description.

Noncommutative space has a structure of an algebra $\mathcal{A}$. It is generated by coordinates x^μ which are real i.e. hermitian, but in principle, non-commuting,

$$[x^\mu, x^\nu] = i\hbar J^{\mu\nu}(x)\,. \tag{1}$$

They can be ordinary commutative variables but also operators, finite matrices, etc. Dimensional parameter $\hbar$ sets the scale of noncommutativity; the formal limit $\hbar \to 0$ is the commutative or macroscopic limit mentioned above. Uncertainty relations that follow from (1) in the case when $J^{\mu\nu} \neq 0$ imply that 'there are no points' on a specific NC space, i.e. that all coordinates cannot be measured simultaneously. The structure of a NC space can be understood in terms of the spectra of its coordinates. Obviously, a change of coordinates changes their spectra, but there is an overall diffeomorphism invariance, meaning that one can transform (1) using the standard algebraic rules. Apart from the properties of coordinates, there are other ways to describe a NC space, e.g. its symmetries, its coherent states, and of course its commutative limit.

Differential-geometric structure of $\mathcal{A}$ is given by the momentum algebra, i.e. the algebra of derivatives. In the NC frame formalism, momenta p_α are functions or operators that define the free falling frame (tetrad) e_α,

$$e_\alpha f = [p_\alpha, f]. \tag{2}$$

The commutator satisfies the Leibniz rule, so e_α is a derivation. Dual to derivations e_α are differential 1-forms θ^α; the differential of a function is defined as

$$df = (e_\alpha f)\,\theta^\alpha\,. \tag{3}$$

On curved commutative manifold the moving frame is given by its components e^μ_α, $e_\alpha f = e^\mu_\alpha\,(\partial_\mu f)$, and momenta are combinations of partial derivatives,

$$p_\alpha = e^\mu_\alpha\,\partial_\mu, \qquad e^\mu_\alpha = [p_\alpha, x^\mu]\,. \tag{4}$$

In analogy, in the noncommutative case the tetrad and the metric are defined by

$$e^\mu_\alpha = [p_\alpha, x^\mu]\,, \qquad g^{\mu\nu} = e^\mu_\alpha\, e^\nu_\beta\, \eta^{\alpha\beta}\,, \tag{5}$$

with additional conditions to assure orthonormality of the moving frame. Laplacian of a scalar function is defined as

$$\Delta f = \eta^{\alpha\beta}[p_\alpha, [p_\beta, f]]\,. \tag{6}$$

It is possible, and rather straightforward, to define quantities like connection, covariant derivative, curvature and torsion, so one can achieve the full differential-geometric description. Further, one can introduce scalar, spinor and gauge fields with their classical equations of motion. Action for the classical fields can be given as well, providing that there is well defined integral/trace.

3. FUZZY DE SITTER SPACE

As a model of quantum cosmology we discuss four-dimensional fuzzy de Sitter space. In the commutative case, de Sitter space is defined as an embedding

$$-v^2 + w^2 + x^2 + y^2 + z^2 = \frac{3}{\Lambda} \tag{7}$$

in the flat 5-dimensional space

$$ds^2 = -dv^2 + dw^2 + dx^2 + dy^2 + dz^2, \tag{8}$$

where Λ is the cosmological constant. De Sitter space is a maximally symmetric space, its symmetry group is the de Sitter group $SO(1,4)$.

In order to introduce the fuzzy version of de Sitter space, it is natural to start with its symmetry algebra. This enables, on the one hand, to control symmetries of the resulting NC space; on the other hand, it allows concrete calculations as there are exact results on this Lie algebra and its representations. The $so(1,4)$ algebra has ten generators $M_{\alpha\beta}$ that satisfy

$$[M_{\alpha\beta}, M_{\gamma\delta}] = -i(\eta_{\alpha\gamma}M_{\beta\delta} - \eta_{\alpha\delta}M_{\beta\gamma} - \eta_{\beta\gamma}M_{\alpha\delta} + \eta_{\beta\delta}M_{\alpha\gamma})\,, \tag{9}$$

$\alpha, \beta, ... = 0, 1, 2, 3, 4$; our signature is $\eta_{\alpha\beta} = \mathrm{diag}(+----)$. The Casimir operators, quadratic and quartic, are

$$\mathcal{Q} = -\frac{1}{2}\, M_{\alpha\beta}M^{\alpha\beta}, \qquad \mathcal{W} = -W_\alpha W^\alpha\,, \tag{10}$$

with the 'Pauli-Lubanski' vector $W_\alpha = \frac{1}{8}\,\epsilon_{\alpha\beta\gamma\delta\eta}M^{\beta\gamma}M^{\delta\eta}$. The Casimir relation $\mathcal{W}=$ const is analogous to the embedding (7) which defines commutative de Sitter space. Therefore we introduce noncommutative coordinates as

$$x^\alpha = \ell\, W^\alpha \tag{11}$$

and define fuzzy de Sitter space as a unitary irreducible representation of the $SO(1,4)$.

There are at least two choices of momenta that give geometry (metric, curvature) of the de Sitter space in the commutative limit. We discuss the one defined by four momenta p_0, p_i,

$$ip_0 = \sqrt{\Lambda}\, M_{04}\,, \qquad ip_i = \sqrt{\Lambda}\,(M_{i4} + M_{0i}). \tag{12}$$

The line element that the noncommutative frame formalism gives is

$$ds^2 = -(\theta^0)^2 + (\theta^i)^2 = -d\tau^2 + e^{2\tau}\, dx^i dx^i \tag{13}$$

and the corresponding scalar curvature is constant. From the expression for the line element we can identify the cosmic time,

$$\frac{\hat{\tau}}{\ell} = \log \frac{x^0 + x^4}{\ell} = \log\left(W^0 + W^4\right). \tag{14}$$

It is different from the embedding time, $x^0 = \ell W^0$; the spatial coordinates are $x^i = \ell W^i,\ i = 1, 2, 3$.

Unitary irreducible representations of the de Sitter group are infinite-dimensional, labelled two quantum numbers (s, ρ). They fall into three categories (Dixmier, 1961):
∘ principal continuous series: $\rho \geq 0,\ \ s = 0, \frac{1}{2}, 1, \frac{3}{2}, \ldots$
$\mathcal{Q} = -s(s+1) + \frac{9}{4} + \rho^2, \quad \mathcal{W} = s(s+1)(\frac{1}{4} + \rho^2)$
∘ complementary continuous series: $\nu = i\rho \in \mathbb{R}, \quad |\nu| < \frac{3}{2}, \quad s = 0, 1, 2 \ldots$
$\mathcal{Q} = -s(s+1) + \frac{9}{4} - \nu^2, \quad \mathcal{W} = s(s+1)(\frac{1}{4} - \nu^2)$
∘ discrete series: $s = \frac{1}{2}, 1, \frac{3}{2}, 2 \ldots, \ \ q = \frac{1}{2} + \nu = \frac{1}{2} + i\rho = s, s-1, \ldots 0 \ \text{ or } \ \frac{1}{2}$
$\mathcal{Q} = -s(s+1) - (q+1)(q-2), \quad \mathcal{W} = -s(s+1)q(q-1).$

We would like to determine the spectra of the above-defined physical coordinates. The most effective way is to use the Hilbert space representation corresponding to one of representations given above, in which $M_{\alpha\beta}$, W_α are differential operators. Such representations exist: we will discuss the principal continuous series (ρ, $s = \frac{1}{2}$). The representation space is the space of Dirac bispinors $\psi(\vec{p})$ that satisfy the Dirac equation, with scalar product

$$(\psi, \psi) = \int \frac{d^3p}{2p_0}\, \psi^\dagger \gamma^0 \psi\,. \tag{15}$$

Using the Dirac representation of γ-matrices, we find

$$\psi(\vec{p}) = \begin{pmatrix} \varphi(\vec{p}) \\ -\dfrac{\vec{p}\cdot\vec{\sigma}}{p_0 + m}\, \varphi(\vec{p}) \end{pmatrix}, \qquad (\psi, \psi') = \int \frac{d^3p}{p_0}\, \frac{2m}{p_0 + m}\, \varphi^\dagger \varphi'\,, \tag{16}$$

where $\varphi(\vec{p})$ is a spinor and $\vec{\sigma}$ are the Pauli matrices. The group generators are

$$M_{ij} = L_{ij} + S_{ij}, \qquad S_{ij} = \frac{i}{4}\left[\gamma_i, \gamma_j\right] \tag{17}$$

$$M_{0i} = L_{0i} + S_{0i}, \qquad S_{0i} = \frac{i}{4}\left[\gamma_0, \gamma_i\right] \tag{18}$$

$$M_{40} = -\frac{\rho}{m}\, p_0 + \frac{1}{2m}\left\{p^i, M_{0i}\right\}, \tag{19}$$

$$M_{4k} = -\frac{\rho}{m}\, p_k - \frac{1}{2m}\left\{p^0, M_{0k}\right\} - \frac{1}{2m}\left\{p^i, M_{ik}\right\}, \tag{20}$$

with

$$L_{ij} = i\left(p_i \frac{\partial}{\partial p^j} - p_j \frac{\partial}{\partial p^i}\right), \qquad L_{0i} = ip_0 \frac{\partial}{\partial p^i}, \tag{21}$$

$$L_{40} = -\frac{\rho}{m} p_0 + \frac{1}{2m} \{p^i, L_{0i}\}, \tag{22}$$

$$L_{4k} = -\frac{\rho}{m} p_k - \frac{1}{2m} \{p^0, L_{0k}\} - \frac{1}{2m} \{p^i, L_{ik}\}. \tag{23}$$

Using these, we obtain the operators of coordinates in this representation,

$$\frac{x^0}{\ell} = W^0 = -\frac{1}{2m} \begin{pmatrix} (\rho - \frac{i}{2}) p_i \sigma^i + i\, p_0^2 \frac{\partial}{\partial p^i} \sigma^i & \epsilon^{ijk} p_0 p_i \frac{\partial}{\partial p^j} \sigma_k + \frac{3i}{2} p_0 \\ \epsilon^{ijk} p_0 p_i \frac{\partial}{\partial p^j} \sigma_k + \frac{3i}{2} p_0 & (\rho - \frac{i}{2}) p_i \sigma^i + i p_0^2 \frac{\partial}{\partial p^i} \sigma^i \end{pmatrix}, \tag{24}$$

$$\frac{x^4}{\ell} = W^4 = -\frac{1}{2} \begin{pmatrix} ip_0 \frac{\partial}{\partial p^i} \sigma^i & \epsilon^{ijk} p_i \frac{\partial}{\partial p^j} \sigma_k + \frac{3i}{2} \\ \epsilon^{ijk} p_i \frac{\partial}{\partial p^j} \sigma_k + \frac{3i}{2} & ip_0 \frac{\partial}{\partial p^i} \sigma^i \end{pmatrix}. \tag{25}$$

The remaining expression for the x^i is in principle of similar structure but longer.

4. COSMOLOGICAL IMPLICATIONS

We can now formulate and solve the eigenvalue equations for coordinates of the fuzzy de Sitter space and determine their spectra. W^0, W^4 and $W^0 + W^4$ commute with the angular momenta L_i, so we can choose their eigenfunctions in the form

$$\varphi(\vec{p}) = \frac{f(p)}{p} \varphi_{jm} + \frac{h(p)}{p} \chi_{jm}, \tag{26}$$

where the spinor spherical harmonics are given by

$$\varphi_{jm} = \begin{pmatrix} \sqrt{\frac{j+m}{2j}}\, Y_{j-1/2}^{m-1/2} \\ \sqrt{\frac{j-m}{2j}}\, Y_{j-1/2}^{m+1/2} \end{pmatrix}, \quad \chi_{jm} = \begin{pmatrix} \sqrt{\frac{j+1-m}{2(j+1)}}\, Y_{j+1/2}^{m-1/2} \\ -\sqrt{\frac{j+1+m}{2(j+1)}}\, Y_{j+1/2}^{m+1/2} \end{pmatrix}, \tag{27}$$

$Y_l^m(\theta, \varphi)$ are the usual spherical harmonics in momentum space, $p = |\vec{p}|$, etc. The nontrivial part for each eigenvalue problem is the radial equation for $f(p)$ and $h(p)$. Computations are long but relatively straightforward: we just review the results.

Because of the $SO(1,4)$ symmetry, the spectra of spatial coordinates W^i and of W^4 are the same. The spectrum of W^4 is continuous: the real line. Its eigenfunctions $|\lambda jm\rangle$ are normalized as

$$\langle \lambda jm | \lambda' j' m' \rangle = \delta(\lambda - \lambda')\, \delta_{jj'}\, \delta_{mm'}. \tag{28}$$

Their radial part contains the associated Legendre functions, $P_{-2i\lambda}^{-j}(p_0)$.

The spectrum of the embedding time W^0 is discrete and its eigenvalues are given by $k(k+1) - k'(k'+1)$, where $k, k' = 0, \frac{1}{2}, 1, \frac{3}{2}, \ldots$.

The radial equation for the cosmic time $e^{\hat{\tau}/\ell} = W^0 + W^4$ is the most interesting. It reduces to the Bessel equation in variable $z = \sqrt{\frac{(p_0-1)}{(p_0+1)}}$ and the solutions are given in terms of Bessel functions $J_j(2\lambda z)$. The eigenvalue $\lambda = e^{\tau/\ell}$ is continuous,$\lambda \in (0, \infty)$. This is in contradiction with the fact that, apparently, all eigenfunctions are normalizable. A careful analysis shows that, naively defined, the cosmic time $\hat{\tau}$ is not a self-adjoint operator. To obtain its self-adjoint extension one has to add specific boundary conditions, i.e. to reduce the initial Hilbert space of functions to a subspace of physical states. This reduction makes the spectrum of the cosmic time discrete, and the corresponding eigenfinctions $|\tau jm\rangle$ orthonormal,

$$\langle \tau jm | \tau' j' m' \rangle = \delta_{\tau\tau'}\, \delta_{jj'}\, \delta_{mm'}\,. \tag{29}$$

The boundary condition is of the form

$$\frac{J_{j+1}(2\lambda)}{J_j(2\lambda)} = \text{const}\,, \tag{30}$$

and it determines the allowed discrete eigenvalues, $\tau = \ell \log \lambda$. The solutions for value 1 of the given constant are given graphically below.

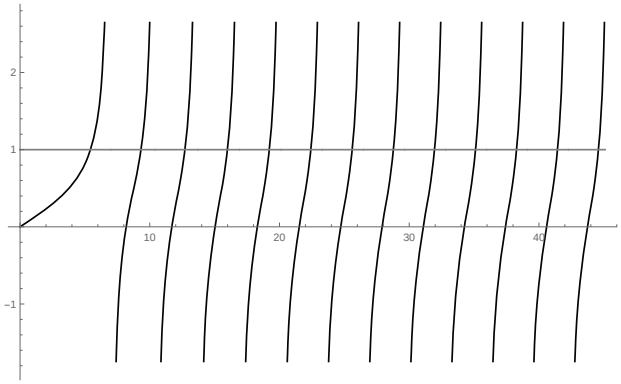

Let us summarize and discuss consequences of our results to cosmology.

The main result is that spatial coordinates of fuzzy de Sitter space are continuous, while time is discrete. If we calculate the expectation value of the radius of universe,

$$(x^i)^2 = -\ell^2\, W_i W^i \tag{31}$$

at fixed moment of time τ, we find

$$\mathcal{W} + \lambda^2 \leq \langle \tau jm | - \ell^2\, W_i W^i | \tau jm \rangle \leq \mathcal{W} + 2\lambda^2\,, \tag{32}$$

where $\mathcal{W}$ is the value of the quartic Casimir operator, $\ell\sqrt{\mathcal{W}} = \ell\sqrt{\frac{3}{16} + \frac{3\rho^2}{4}} \geq 0$. This means that the radius of the universe is bounded below by $\ell\sqrt{\mathcal{W}}$: it cannot vanish in physical states, which implies that there is no big bang singularity.

The radius of the universe grows with time exponentially: for late times we have the usual behavior

$$\sqrt{\langle \tau jm| - \ell^2 W_i W^i |\tau jm\rangle} \sim \lambda = e^{\tau/\ell}. \tag{33}$$

Discreteness of time becomes relevant only in the 'deep quantum region' $\lambda \to 0$, i.e. $\tau \to -\infty$. For values away from the Planck scale time is almost continuous: the difference between its consecutive eigenvalues is macroscopically negligible,

$$\tau_{n+1} - \tau_n \approx \ell \, \log\,(1 + \frac{1}{n}\,)\,. \tag{34}$$

Further interesting properties of our model, not discussed in details here, include symmetry. Namely, the choice of a specific self-adjoint extension breaks the initial symmetry at distances of order ℓ, i.e. near the Planck scale. This 'spontaneous symmetry breaking' can be pursued in all mathematical details; in particular, in the macroscopic limit $\ell \to 0$ the full symmetry is recovered.

There are several possible directions in which this work should be continued. In applications to cosmology, an important problem (well defined within the given formalism) is to include the scalar fied: describe its classical evolution, fluctuations and then eventually, find the implications to inflation. We expect, further, that (small) anisotropies like those observed in the CMB can be described by perturbation theory, and indeed, there are results for perturbations of the flat noncommutative spaces. Of course, for a fuller characterization of the CMB radiation one should develop a description of gauge and fermion fields on the fuzzy de Sitter background. These results would give signatures of noncommutativity, i.e. its potentially measurable effects. A more difficult problem, as we see it, is to find other 'ground states' of noncommutative geometry, NC spaces that describe relevant configurations like an arbitrary FLRW spacetime or black holes. Typically in these cases there is less symmetry, so it is not quite clear what is the algebraic structure one should start with. However, it is an important avenue of further research as, as we have seen, noncommutative geometry can provide mechanisms to solve singularity problems of general relativity while preserving the correct macroscopic limits.

References

Buric, M., Latas, D.: 2019, *Phys. Rev. D*, **100**, 024053.
Buric, M., Latas, D., Nenadovic, L.: 2018, *Eur. Phys. J. C*, **78**, 953.
Buric, M., Madore, J.: 2014, *Eur. Phys. J. C*, **74**, 2820.
Buric, M., Madore, J.: 2015, *Eur. Phys. J. C*, **75** 10, 502.
Dixmier, J.: 1961, *Bull. Soc. Math. France*, **89**, 9.
Madore, J.: 1995, "An Introduction To Noncommutative Differential Geometry And Its Physical Applications", *Lond. Math. Soc. Lect. Note Ser.*, **257**.

Publ. Astron. Obs. Belgrade No. 100 (2021), 75 - 83 *Invited Lecture*

TOWARDS GAIA DR3 AND SOME RESULTS OF COMPARISON BETWEEN GAIA DR2 AND GROUND-BASED DATA

G. DAMLJANOVIĆ
Astronomical Observatory, Volgina 7, 11060 Belgrade 38, Serbia
E–mail: gdamljanovic@aob.rs

Abstract. Gaia satellite of European Space Agency (ESA) was launched at the end of 2013, and the astronomical observations were started in mid-2014. The first Gaia data release (Gaia DR1) appeared on 14^{th} September 2016, and the second one (Gaia DR2) on 25^{th} April 2018. The next result, the third Gaia solution splits into an early Gaia EDR3 (it appeared on 3^{rd} December 2020) and Gaia DR3 (it is going to appear during the first half of 2022). The main information about Gaia DR3, and some results of comparison between the Gaia DR2 and independent ground-based data of common stars are presented, here.

1. INTRODUCTION

The Gaia result is a unique time-domain space survey, and Gaia is well into its extended mission lifetime. The plan of Gaia was to repeatedly map all sky during its 5-year lifetime (from mid-2014 to mid-2019), but the last extension was given for Gaia from 1^{st} January 2023 to 31^{st} December 2025. After the first Gaia data release – DR1 (on 14^{th} September 2016), the second one – DR2 (on 25^{th} April 2018), and the early release called Gaia early third data release – EDR3 (on 3^{rd} December 2020), the full Gaia data release – DR3 or the catalogue is planned for the first half of 2022. Both solutions (EDR3 and DR3) are based on 34 months of Gaia observations, and feature the same source list.

Before the Gaia mission of the European Space Agency (ESA) it was the Hipparcos (High Precision PARallax Collecting Satellite) ESA mission as the predecessor of Gaia (ESA 1997; van Leeuwen 2007). It means, the Gaia is another big mission of the ESA, and the next step of the European pioneering high-accuracy astrometry. The Gaia satellite was launched at the end of 2013, and the plan was to survey all objects to ≈ 20 mag in V-band for astrometry and photometry or ≈ 1 billion sources, and to ≈ 16 mag in spectroscopy or ≈ 150 million ones (Prusti 2012)), but now there are more than six years after the first astronomical observations of Gaia (in mid-2014). The mentioned releases (DR1, DR2, and EDR3) are a few important steps for the final Gaia catalogue and the Gaia reference frame. The Gaia has got an interdisciplinary character, and Gaia-based results are useful for all the relevant scientific communities. The Gaia is doing revolution in astronomy, our understanding of the Milky Way galaxy, stellar physics and the Solar System bodies.

Mainly, the Gaia EDR3 catalogue contains the improved astrometry and photometry of DR2, but the Gaia DR3 catalogue is going to contain the Gaia EDR3 and other data: mean radial velocities for stars (with atmospheric-parameter estimates), variable-star classifications with the epoch photometry, Solar-System results (some orbital solutions, epoch observations, etc.), double and multiple stars, quasars and results of extended objects, etc. The photometry for all astrometrically detected objects was done. The orbital parameters could be calculated with much higher precision for the binary and multiple stars using the Gaia high spatial resolution. About the exoplanets, it is expected to find several thousands of systems. In stellar astrophysics, the improvement in the distances will allow to obtain models of stars at different steps of evolution using the improvement of parallaxes via Gaia observations. The Gaia will be of importance in the case of faint rare objects (as brown or white dwarfs). It is detecting the Solar System objects, a few millions of galaxies (as not points, but extended objects), quasars, etc. About asteroids, there is an improvement of their ephemerides, masses, etc. About the quasars, they are of importance for reference systems and fundamental physics.

Gaia has two fields of view separated by 106.5 degrees, and rotates around itself with a period of 6^h. As a result, a sequence of measurements consists of several transits separated successively by 1^h46^m and 4^h14^m, which correspond to the times elapsed from one field to the other. The next sequence of transits appears about 1 month later, due to the rotation axis precession and the satellite orbital motion. There are from 40 to 250 measurements per observed object (Prusti 2012) during the five-year observations.

2. GAIA DR1

The Hipparcos result was the Hipparcos Catalogue with $\approx$ 118000 stars. The Hipparcos changed the astronomy at the end of the last century, but the Gaia is the cornerstone mission of ESA at the beginning of 21^{st} century. The goal of the Gaia mission was $\approx$ 1 billion stars and $\approx$ 500000 extragalactic sources (Prusti 2012), or to observe the mentioned extragalactic sources and stars in our Milky Way galaxy: astrometry, photometry, and spectroscopy. The astrometry is going from milliarcsec to microarcsec, plus the data of radial velocities V_r. Finally, to produce the Gaia Catalogue in the optical domain and in line with the International Celestial Reference Frame – ICRF (which is based on the VLBI observations). The VLBI coordinates of extragalactic sources at J2000.0 materialize the International Celestial Reference System – ICRS which is kinematically defined by: the origin of its axes (the barycentre of the Solar System), a principal plane (close to the mean equator at J2000.0), and an origin of right ascensions (close to the dynamical equinox at J2000.0).

The first release of the Gaia catalogue (DR1) is the main goal of that ESA mission and the first step of the future Gaia celestial reference frame (Gaia CRF). The Gaia CRF is going to link to the ICRF. The Gaia is determining the high accurate positions, proper motions and parallaxes (five-parameter astrometric solution) of observed objects. Plus, the G magnitudes for these objects; the Gaia G-band is the white-light photometry band. In the DR1, there are $\approx$ 2 million stars using Tycho-Gaia solution, and it is based on the first observational period ($\approx$ 14 months). Also, in that solution, only data were published about flux time-series variability detection for Cepheids and RR Lyrae, but not for AGNs and quasars. The DR1 is not an independent solution,

but it is the Tycho-Gaia astrometric solution (Lindegren et al. 2016). More about the DR1 could be found in (Lindegren et al. 2016).

3. GAIA DR2 AND EDR3

The useful data for the second Gaia solution - DR2 are from August 2014 even the start of astronomical observations was in July 2014 (the first month of Gaia observations was not included in the DR2 because the data quality is not good enough). The main part of the DR2 catalogue is five-parameter astrometric solution for ≈ 1.3 billion stars: positions (α_{ICRS} and δ_{ICRS}), parallax, and proper motions (μ_α and μ_δ). It is of importance to mention that the parallax values (given in DR2) could be less than zero, which, though meaningless, is due to the calculation procedure. Also, it was the case in the Hipparcos Catalogue for some stars. The DR2 is based on 640 days or 1.75 years of Gaia operational phase (≈ 21 months with some interruptions) or the period from 22^{nd} August 2014 to 23^{rd} May 2016. It contains results for 1.693 billion sources in the G magnitude range 3 to 21, but for 1.332 billion sources there are all mentioned five astrometric parameters. Its reference epoch is $J2015.5 = JD2457206.375$ TCB or 2^{nd} July 2015 at $21^h0^m0^s$ TCB; it is about half-way through the observational period. That epoch is 0.5 years later than the DR1 one, and there are some differences in the positional data between the DR1 and DR2 releases. The reference epoch was chosen to get minimal correlations between the positions and proper motions.

The positions (α_{ICRS}, δ_{ICRS}) and proper motions (μ_α, μ_δ) refer to the ICRS. Plus, for an additional 0.361 billion mostly faint objects, there are the approximate α_{ICRS} and δ_{ICRS} (Lindegren et al. 2018); the DR2 is available in the online Gaia Archive. In both, DR2 and DR1 cases, there are only photometric data as time-series for Cepheids and RR Lyrae, but no quasars and other objects with unstable flux.

The DR2 catalogue does not include any other astrometric data (Hipparcos or Tycho ones). It means, it is independent (in contrast to the DR1 solution). In DR1 and DR2 solutions, all sources are reduced as single stars. The main values are presented by the five astrometric parameters. In the case of unresolved binaries, the results of some binary stars refer to the photocentre or to either component for resolved ones. The main steps (of the models, algorithms, and astrometric solution) are described in Lindegren et al. (2012; 2016). By using the photometric processing of data via the blue BP and red RP photometers, the colour information in DR2 for most of the sources could be found. The median uncertainty is near 0.04 mas in parallax and position for bright sources ($G < 14$ mag) at reference epoch of DR2 ($J2015.5$), 0.1 mas for $G = 17$ mag, and 0.7 mas in the case of $G = 20$ mag. The mentioned values for proper motions (μ_α and μ_δ) are: 0.05, 0.2, and 1.2 mas/yr, respectively. In the case of binary stars and other perturbations, the non-linear motions are not included in DR2. It means, only the uniform space motion of the object relative to the Solar System barycentre was considered. In line with Lindegren et al. (2018), the mentioned motions are going to be included into the Gaia DR3 solution.

The IAU Working Group "Third Realization of ICRF" is responsible for the ICRF3 catalogue. Mignard et al. (2018) used an ICRF3 prototype with 4262 sources observed in X/S bands, and 2820 quasars matched the ICRF3 prototype. Moreover, the number of extragalactic sources was updated by Charlot et al. (2020). Currently, there are 4536 objects at S/X, 824 objects at K, 678 objects at X/Ka. In line with Lindegren et al. (2018), the optical Gaia DR2 CRF is aligned with ICRS. It is non-

rotating to within 0.15 mas/yr with respect to the quasars. Using the extragalactic objects visible in the optical and radio domains, the primary solution was linked to the ICRS; the DR2 is aligned with ICRS and non-rotating with respect to the quasars (as quasars are distant objects) and the Gaia-CRF2 is the celestial reference frame of Gaia DR2. The astrometric calibration parameters of the CCDs were determined via an astrometric solution for $\approx 1\%$ of the input data ($\approx$ 16 million selected objects). In line with Lindegren et al. (2018), the astrometric parameters were calculated for the other sources. In that way, the systematic effects in the parallaxes are less than 0.1 mas (depending on positions, magnitude and colour). The Barycentric Celestial Reference System – BCRS is the primary coordinate system; the axes are aligned with the ICRS and its origin is at the Solar System barycentre. The barycentric coordinate time – TCB is the time-like coordinate of the BCRS. A consistent theory of relativistic astronomical reference systems was used during the processing of the Gaia data in line with Soffel et al. (2003).

The third Gaia data release splits into two solutions: the early release (EDR3), and the full Gaia data release (DR3). The EDR3 consists: astrometric, photometric, and radial-velocity data (V_r), variable-star and non-single-star results, object classifications with multiple astrophysical parameters for stars, quasars, galaxies, and unresolved binaries, exo-planets, epochs and transits for all objects, etc. The five-parameter astrometric solution of the EDR3 (positions, proper motions, and parallaxes) is done for around 1.5 billion sources. The limiting G magnitude is of about 21 and a bright limit of about 3. Just positions on the sky (α and δ) or two-parameters solutions are presented for around 300 million additional objects. The G magnitudes are done for both sets of data; they are presented for around 1.8 billion sources, but G_{BP} and G_{RP} magnitudes for around 1.5 billion sources. It is necessary to be careful about G, G_{BP}, and G_{RP} bands because the EDR3 photometric system is different from the system in DR1 and DR2. There are about 1.5 million objects useful for the Gaia celestial reference frame (Gaia CRF). The source list for Gaia EDR3 is independent of DR2 and of DR1; from DR2 to EDR3 the changes impact until 5% of the sources.

4. GAIA DR3

Some data (variables, Solar System objects, astrophysical parameters) are not presented in the Gaia EDR3, but they are going to be a part of the Gaia DR3 (together with "new" V_r values). Both data sets, EDR3 and DR3, are based on the data collected between 25^{th} July 2014 and 28^{th} May 2017 (a period of 34 months). The DR2 was based on 22 months of data, and DR1 on 14 months (the first ones). The Gaia DR3 (and EDR3) reference epoch is $J2016.0$; for DR2 it was $J2015.5$ and for DR1 it was $J2015.0$. The Gaia EDR3 optical reference frame is aligned to the ICRS (it will be the case of DR3, also), and because of this the positions and proper motions are referred to the ICRS.

At the first place, the Gaia DR3 solution is going to contain the improved astrometry and photometry of DR2. Also, it will be consisting of: the epoch photometry and variable-star classifications, mean V_r velocities for stars without detected variability, BP/RP and RVS spectra for spectroscopically objects or the object classification and astrophysical parameters, preliminary orbital solutions and individual epoch observations for the Solar-System results, non-single star catalogues, etc.

Table 1: The $D = 1.4$ m telescope of ASV.

Site Telescope $D(cm)/F(cm)$	longitude - $\lambda(^o)$ latitude - $\varphi(^o)$ altitude - h (m)	CCD camera pixel array and scale $(^{''})$ pixel size (μm) and field of view - FoV $(^{'})$
ASV (AOB) Ritchey-Chrétien 140/1142	21.6 43.1 1143	1. Apogee Alta U42 (mid-2016 – mid-2018) 2048x2048, 0.24 13.5x13.5, 8.3x8.3
		2. Andor iKon-L (from mid-2018 until now) 2048x2048, 0.24 13.5x13.5, 8.3x8.3

5. SERBIAN-BULGARIAN TELESCOPES IN LINE WITH GAIA MISSION

After launching the Gaia satellite, the astrometry with ground-based optical telescopes (of small and medium size) has become very actual part of astronomical investigation. Some ground-based observations started in accordance with the Gaia ESA mission using these telescopes. Some tasks are: the photometry of Gaia Alerts objects, the astrometric monitoring of Gaia satellite, the link between radio and optical positions of quasars, the realisation of a catalogue of quasars, etc. In Table 1, the main information about the $D = 1.4$ m telescope of Astronomical Station Vidojevica – ASV (of Astronomical Observatory in Belgrade – AOB, Serbia) is presented; see Fig. 2. It is the main AOB instrument at the new ASV site.

In 2013, we established the "Serbian – Bulgarian mini-network telescopes" (using 6 telescopes) to do the observations of Gaia Alerts and other objects in accordance with the Gaia mission (Damljanović et al. 2014). Also, these activities are in line with the bilateral Serbian-Bulgarian joint research SANU-BAN project "Gaia Celestial Reference Frame (CRF) and fast variable astronomical objects" during three years period (from 2020 to 2022, the head is G. Damljanović). SANU and BAN are the Serbian Academy of Sciences and Arts and Bulgarian Academy of Sciences. The $D = 60$ cm Bulgarian telescope is at the Astronomical Observatory Belogradchik (see Fig 1.), the other three Bulgarian instruments of Gaia Alerts interest ($D = 2$ m, $D = 60$ cm and 50/70 cm Schmidt-camera) are at the Rozhen Observatory, and one $D = 60$ cm telescope is at ASV. These instruments and their CCD cameras were described in the paper (Damljanović et al. 2020; Taris et al. 2018). From 2005 there is $D = 40$ cm MEADE instrument at AOB which was moved from AOB (Belgrade city) to ASV site (near Prokuplje) during 2020; the new dome for that instrument is ready at ASV in 2020 (Fig. 3) and the first data using it are expected in 2021.

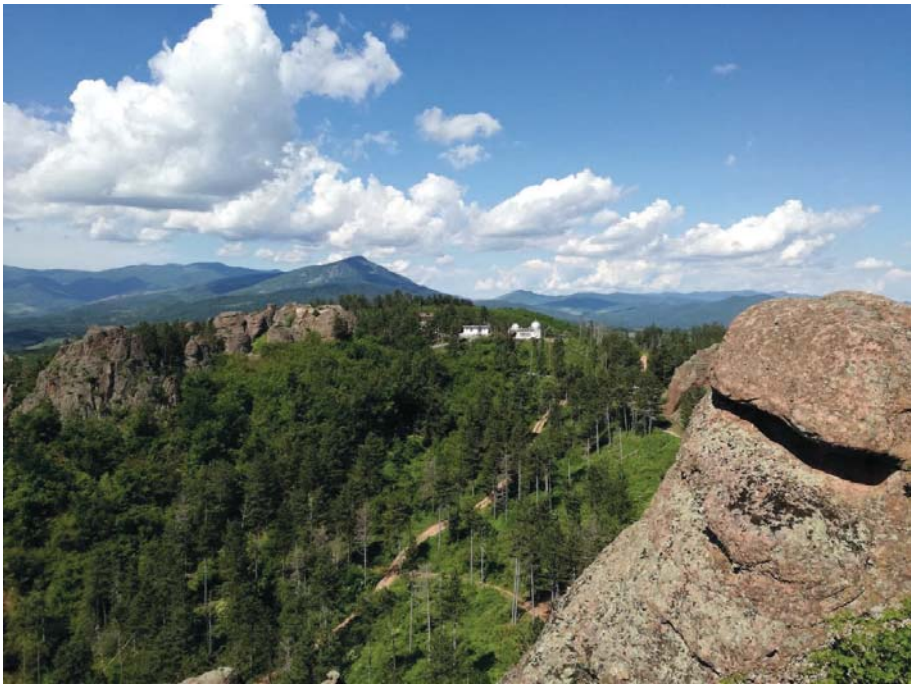

Figure 1: The Astronomical Observatory Belogradchik between famous rocks.

Figure 2: The telescope $D = 1.4$ m of Astronomical Station Vidojevica – ASV.

Figure 3: The dome for $D = 40$ cm MEADE telescope of ASV.

6. SPIN INVESTIGATION OF THE BRIGHT GAIA DR2 USING SOME INDEPENDENT GROUND-BASED DATA

About the spin (with components ω_X, ω_Y and ω_Z) investigation of the bright Gaia DR2 reference frame, the independent proper motion in declination μ_δ ground-based data were used (to determine ω_X and ω_Y). They are the μ_δ values of: 387 stars of the International Latitude Service – ILS catalogue, and 682 stars of the independent latitude stations – INDLS catalogue. Both catalogues (the ILS and INDLS) data are available in the Strasbourg astronomical Data Center: the ILS data at https://doi.org//10.26093/cds/vizier.36310145, and the INDLS data via ftp://cdsarc.u-strasbg.fr/pub/cats/J/AN/341/8. It is a contribution to a possible validation of the Gaia astrometry. Also, the new Hipparcos – NHIP (van Leeuwen 2007) values μ_δ were used for the same stars. The mean accuracy of the ILS μ_δ values is 0.21 mas/yr and of INDLS μ_δ values is 0.51 mas/yr; the stars are from 4 to 8 magnitude in V-band. An indication (Lindegren 2020) that the bright reference frame of Gaia DR2 rotates relative to the faint DR2 (of the order of 0.1 mas/yr) is supported using the ILS and INDLS data (Damljanović and Taris 2019; Damljanović 2020). The bright reference frame of Gaia DR2 is based on stars with $G \leq 13$ mag, the faint part of DR2 (quasars based one) on stars with $G \geq 16$ mag, and the faint part of DR2 is aligned with the ICRS via quasars (Lindegren et al. 2018) because these quasars with optical counterparts are visible in the optical domain mostly with $G \geq 17$ mag. Also, the DR2 stars with $G \leq 6$ mag mostly have inferior astrometry (Lindegren 2018).

The mentioned spin components ω_X and ω_Y could be calculated using μ_δ (of ILS and INDLS catalogues) and μ'_δ values (of DR2 for the same stars) via Lindegren formula (2020)

$$\mu_\delta - \mu'_\delta \approx -\omega_X \sin\alpha + \omega_Y \cos\alpha,$$

where (after the least squares method – LSM): ω_X is not significant on the 2σ level, but ω_Y is of the order of 0.1 mas/yr and it is significant on the 2σ level (Damljanović and Taris 2019; Damljanović 2020). The value ω_Z is close to zero (Lindegren 2020). The right ascension α is from the DR2 catalogue.

The ILS and INDLS data are in the Hipparcos celestial reference frame, and the calculated ω_Y value is the component of the spin between that frame (or catalogue) and the bright DR2 frame (or catalogue). A part of ω_Y belongs to the ILS and INDLS catalogues (because ω_Y is about -0.2 ± 0.08 mas/yr for μ_δ differences ILS−NHIP and INDLS−NHIP), but another one (ω_Y is about -0.5 ± 0.08 mas/yr for ILS−DR2 and INDLS−DR2) belongs to the bright DR2 frame (Damljanović 2021). For the case NHIP−DR2 and same stars, ω_Y is about -0.4 ± 0.08 mas/yr. It means, the value ω_Y is of the order of 0.1 mas/yr for DR2 stars in V-magnitude from 4 mag to 8 mag.

7. CONCLUSIONS

After the first Gaia data release (Gaia DR1) and the second one (Gaia DR2), the third Gaia solution splits into two parts: an early Gaia EDR3, and Gaia DR3. EDR3 appeared on 3^{rd} December 2020, and the final solution (Gaia DR3) is going to appear during the first half of 2022. The main information about these solutions and Serbian-Bulgarian telescopes in line with the Gaia mission is presented, here. Also, some original results about the spin investigation of the bright Gaia DR2 (stars with $G \leq 13$ mag) are achieved using the independent ILS and INDLS catalogues of μ_δ values. These results (Damljanović and Taris 2019; Damljanović 2020) support an indication that the bright reference frame of Gaia DR2 rotates relative to the faint DR2 (stars with $G \geq 16$ mag) of the order of 0.1 mas/yr (Lindegren 2020). The ILS and INDLS catalogues data are available in the Strasbourg astronomical Data Center: the ILS data at https://doi.org//10.26093/cds/vizier.36310145, and the INDLS data via ftp://cdsarc.u-strasbg.fr/pub/cats/J/AN/341/8.

Acknowledgements

The author thanks the referee for the very constructive comments, which helped substantially improve the manuscript. This research was supported by the Ministry of Education, Science and Technological Development of the Republic of Serbia (contract No 451-03-68/2020-14/200002). This work has made use of data from the European Space Agency (ESA) mission Gaia (https://www.cosmos.esa.int/gaia), processed by the DPAC (https://www.cosmos.esa.int/web/gaia/dpac/consortium , Gaia Data Processing and Analysis Consortium).

References

Charlot, P., Jacobs, C. S., Gordon, D. et al.: 2020, A&A, **644**, A159.
Damljanović, G., Vince, O., Boeva, S.: 2014, Serb. Astron. J., **188**, 85 – 93.
Damljanović, G., Taris, F.: 2019, A&A, **631**, A145.
Damljanović, G.: 2020, AN, **341**, 770 – 780.
Damljanović, G., Bachev, R., Boeva, S, et al.: 2020, Publ. Astron. Soc. "Rudjer Bošković", **20**, 15 – 22.
Damljanović, G.: 2021, AcA, in procedure.
ESA: 1997, The Hipparcos and Tycho Catalogues, ESA SP-1200.
Lindegren, L., Lammers, U., Hobbs, D. et al.: 2012, A&A, **538**, A78.
Lindegren, L., Lammers, U., Bastian, U. et al.: 2016, A&A, **595**, A4.
Lindegren, L., Hernandez, J., Bombrun, A. et al.: 2018, A&A, **616**, A2.
Lindegren, L.: 2020, A&A, **633**, A1.
Mignard, F., Klioner, S. A., Lindegren, L. et al.: 2018, A&A, **616**, A14.
Prusti, T.: 2012, AN, **333**, No. 5/6, 453.
Soffel, M., Klioner, S. A., Petit, G. et al.: 2003, AJ, **126**, 2687.
Taris, F., Damljanović, G., Andrei, A. et al.: 2018, A&A, **611**, A52.
van Leeuwen, F.: 2007, Hipparcos, the New Reduction of the Raw Data, Springer, Dordrecht.

Publ. Astron. Obs. Belgrade No. 100 (2021), 85 - 96 *Invited Lecture – special session "The gravitational-wave Universe" supported by COST Action CA16104*

NONCOMMUTATIVE $SO(2,3)$ MODEL

MARIJA DIMITRIJEVIĆ ĆIRIĆ, DRAGOLJUB GOČANIN, NIKOLA KONJIK and VOJA RADOVANOVIĆ[1]

University of Belgrade, Faculty of Physics
Studentski trg 12, 11000 Beograd, Serbia
E–mail: rvoja@ipb.ac.rs

Abstract. This is a review of some of our recent work concerning Noncommutative (NC) Field Theory based on $SO(2,3)_\star$ gauge invariance. An important feature of this theory is that gravitational field, given in terms of a vierbein (frame field), becomes manifest only after a suitable gauge fixing, and it is formally unified with other gauge fields of the theory. Starting with a model of pure NC gravity, we extend it by introducing matter and (non)Abelian gauge fields. Using the enveloping algebra approach and the Seiberg-Witten map, we construct the corresponding NC deformed actions and expand them perturbatively in powers of the canonical parameter of noncommutativity. The first non-vanishing NC correctionturns out to be linear in the NC parameter and it encodes a particular coupling of matter and gauge fields to gravity due to spacetime noncommutativity. This feature is augmented by the fact that some of these corrections pertain even in flat spacetime where they induce potentially observable NC effects. We discuss the obtained NC deformation of electron's dispersion relation in the presence of constant background magnetic field – NC Landau levels.

1. INTRODUCTION

Noncommutative (NC) Field Theory, i.e. a theory of (relativistic) fields on a noncommutative spacetime, is a candidate for an effective theory of the underlying (and yet unknown) fundamental theory of quantum gravity. The construction of a NC field theory relies on the method of deformation quantization via NC $\star$-product (a method also used in phase space quantum mechanics), developed mainly by Flato, Sternheimer and Kontsevich Bayen et al. (1978), Sternheimer (1998), Kontsevich (2013). In general, one speaks of a deformation of an object/structures whenever there is a family of similar objects/structures and a deformation parameter that measures their distortion from the original, undeformed one. In physics, this parameter appears as some fundamental constant of nature that measures a deviation from the classical (undeformed) theory. When it is zero, the classical theory is restored. To deform a continuous structure of spacetime, an abstract algebra of NC coordinates is introduced. These NC coordinates, denoted by $\hat{x}^\mu$, satisfy some non-trivial commutation

[1]Talk given by Voja Radovanović.

relations, and so, it is no longer the case that $\hat{x}^\mu \hat{x}^\nu = \hat{x}^\nu \hat{x}^\mu$. Abandoning this basic property results in various new physical effects that are not present in a field theory developed on ordinary spacetime. The simplest case of noncommutativity is the so called canonical noncommutativity, defined by

$$[\hat{x}^\mu, \hat{x}^\nu] = i\theta^{\mu\nu}, \tag{1.1}$$

where $\theta^{\mu\nu}$ are components of a constant, antisymmetric matrix.

Instead of deforming the algebra of coordinates, one can take an alternative, but equivalent approach in which noncommutativity appears in the form of NC $\star$-products of functions (fields) of ordinary commutative coordinates. Specifically, to establish canonical noncommutativity, we use the Moyal-Weyl $\star$-product

$$(\hat{f} \star \hat{g})(x) = e^{\frac{i}{2}\theta^{\mu\nu}\frac{\partial}{\partial x^\mu}\frac{\partial}{\partial y^\nu}} f(x)g(y)|_{y\to x}. \tag{1.2}$$

The first term in the expansion is the ordinary point-wise multiplication of functions. The quantities $\theta^{\mu\nu}$ are assumed to be small deformation parameters that have dimensions of $(length)^2$. They are fundamental constants, like the Planck length or the speed of light.

The subject of NC gravity has received a lot of attention and various approaches to this problem have been developed. In Chamseeddine (2001), Chamseeddine (2004), Cardella and Zanon (2003) a deformation of pure Einstein gravity via Seiberg-Witten map is proposed. Twist approach to NC gravity is explored in Aschieri et al. (2005, 2006), Ohl and Schenckel (2009), Aschieri and Castellani (2010). Some other variants are given in Yang (2009), Steinacker (2010), Burić and Madore (2008, 2014), Tomassini and Viaggiu (2014), Faizal (2013), Kobakhidze et al. (2016), Klammer and Steinacker (2009), Harikumar and Rivelles (2006), Dobrski (2017, 2011), Burić et al. (2006b, 2008). The connection to Supergravity (SUGRA) is established in Aschieri and Castellani (2009b), Castellani (2013). Finally, in Dimitrijević Ćirić et al. (2017a), Dimitrijević Ćirić et al. (2017b), Dimitrijević et al. (2012), Dimitrijević and Radovanović (2014) an approach based on canonically deformed Anti de Sitter (AdS) symmetry group, i.e. $SO(2,3)_\star$ group, is developed. In this approach NC gravity is treated as a (deformed) gauge theory, and gravity becomes manifest only after a suitable symmetry breaking (gauge fixing). The action is constructed without previously introducing the metric tensor (it is topological) and the second order NC correction to the Einstein-Hilbert action can be found explicitly. Special attention is devoted to the meaning of coordinates in the context of spacetime noncommutativity. Namely, the results suggest that coordinates in which one postulates canonical noncommutativity are the Fermi inertial coordinates, i.e. coordinates of an inertial observer along a geodesic. Commutator between arbitrary coordinates can in principle be derived from the canonical noncommutativity as demonstrated in Dimitrijević Ćirić et al. (2017a).

The success of the pure gravity model led us to consider matter and gauge fields in the $SO(2,3)_\star$ framework. Dirac spinor field and $U(1)$ gauge field coupled to gravity are introduced in Gočanin and Radovanović (2018) and Dimitrijević-Ćirić et al. (2018), respectively, and physical consequences such as NC deformation of Landau levels are analyzed. From a different perspective, the problem was also treated by

Aschieri and Castellani Aschieri and Castellani (2009a, 2012, 2013), Aschieri (2014). Here we will present the most important results concerning the $SO(2,3)_\star$ framework.

2. COMMUTATIVE MODEL AND ITS NC DEFORMATION

The first step in our analysis is to establish a well-defined commutative (undeformed) model that will subsequently be deformed by substituting ordinary point-wise field multiplication with NC Moyal-Weyl $\star$-product. We propose a commutative action built out of commutative fields on 4-dimensional Minkowski space, endowed with local $SO(2,3)$ symmetry, which can be extended to $SO(2,3) \otimes SU(N)$ if we want to include Yang-Mills fields. For electromagnetic field we use Abelian $U(1)$ group. Then, we demonstrate that, by choosing a suitable gauge (symmetry breaking), this "symmetric-phase" topological action exactly reduces to the action for classical electrodynamics in curved spacetime with the usual, undeformed $SO(1,3) \otimes U(1)$ gauge symmetry.

2. 1. ADS ALGEBRA

Generators of $SO(2,3)$ group are denoted by M_{AB} (with group indices $A, B = 0, 1, 2, 3, 5$) and they satisfy the AdS algebra,

$$[M_{AB}, M_{CD}] = i(\eta_{AD} M_{BC} + \eta_{BC} M_{AD} - \eta_{AC} M_{BD} - \eta_{BD} M_{AC}), \tag{2.3}$$

where η_{AB} is $5D$ flat metric with signature $(+,-,-,-,+)$. A realization of this algebra can be obtained from $5D$ gamma matrices Γ_A that satisfy Clifford algebra $\{\Gamma_A, \Gamma_B\} = 2\eta_{AB}$. The generators are given by $M_{AB} = \frac{i}{4}[\Gamma_A, \Gamma_B]$. One choice of $5D$ gamma matrices is $\Gamma_A = (i\gamma_a\gamma_5, \gamma_5)$, where γ_a are the usual $4D$ gamma matrices. The local Lorentz indices, $a, b, \ldots$, take values $0, 1, 2, 3$. In this particular representation, the $SO(2,3)$ generators are given by $M_{ab} = \frac{i}{4}[\gamma_a, \gamma_b] = \frac{1}{2}\sigma_{ab}$ and $M_{5a} = \frac{1}{2}\gamma_a$. The total gauge potential (master potential) Ω_μ of the $SO(2,3)\otimes U(1)$ gauge group consists of two independent parts, $\Omega_\mu = \omega_\mu + A_\mu$. The first part is the $SO(2,3)$ gauge potential that can be naturally decomposed into spin-connection $\omega_\mu{}^{ab}$ and vierbein e_μ^a,

$$\omega_\mu = \frac{1}{2}\omega_\mu{}^{AB} M_{AB} = \frac{1}{4}\omega_\mu{}^{ab}\sigma_{ab} - \frac{1}{2l} e_\mu^a \gamma_a, \tag{2.4}$$

where l is a constant length scale (AdS radius). Note that in this framework the vierbein field e_μ^a is treated as an additional gauge field, standing on equal footing with the spin-connection (which is a gauge field for the Lorentz group $SO(1,3)$). It is related to the metric tensor by $\eta_{ab} e_\mu^a e_\nu^b = g_{\mu\nu}$ and $e = \det(e_\mu^a) = \sqrt{-g}$. The second part, A_μ, is the electromagnetic field potential. The field strength associated with the full gauge potential Ω_μ is

$$\mathbb{F}_{\mu\nu} = \partial_\mu \Omega_\nu - \partial_\nu \Omega_\mu - i[\Omega_\mu, \Omega_\nu], \tag{2.5}$$

and it can be decomposed as $\mathbb{F}_{\mu\nu} = F_{\mu\nu} + \mathcal{F}_{\mu\nu}$, where the $SO(2,3)$ field strength $F_{\mu\nu}$ is given by

$$F_{\mu\nu} = \partial_\mu \omega_\nu - \partial_\nu \omega_\mu - i[\omega_\mu, \omega_\nu] = \Big(R_{\mu\nu}{}^{ab} - \frac{1}{l^2}(e_\mu^a e_\nu^b - e_\mu^b e_\nu^a)\Big)\frac{\sigma_{ab}}{4} - \frac{1}{l} T_{\mu\nu}{}^a \frac{\gamma_a}{2}, \tag{2.6}$$

where $R_{\mu\nu}{}^{ab}$ is the curvature tensor and $T_{\mu\nu}{}^{a}$ torsion. Finally, $\mathcal{F}_{\mu\nu}$ is the usual $U(1)$ field strength

$$\mathcal{F}_{\mu\nu} = \partial_\mu A_\nu - \partial_\nu A_\mu. \tag{2.7}$$

A necessary step for obtaining electrodynamics in curved spacetime from $SO(2,3) \otimes U(1)$ model is gauge fixing, i.e. symmetry breaking from $SO(2,3)$ to $SO(1,3)$. For that reason one usually introduces an auxiliary field $\phi = \phi^A \Gamma_A$ as in Stelle and West (1980), MacDowell and Mansouri (1977), Towsend (1977), Wilczek (1998). We break the symmetry by fixing the value of the auxiliary field, in particular, by setting $\phi^a = 0$ and $\phi^5 = l$. This field is a spacetime scalar and an internal-space vector and it satisfies the constraint $\phi^A \phi_A = l^2$. It transforms in the adjoint representation of $SO(2,3)$ and its covariant derivative is given by

$$D_\mu \phi = \partial_\mu \phi - i[\Omega_\mu, \phi] = \partial_\mu \phi - i[\omega_\mu, \phi]. \tag{2.8}$$

We see that $U(1)$ part of the master potential doesn't contribute at the classical level. This simplification is a peculiarity of the Abelian $U(1)$ group and it does not hold in a more general case of a non-Abelian Yang-Mills theory. After the gauge fixing, the components of $D_\mu \phi$ become $(D_\mu \phi)^a = e^a_\mu$ and $(D_\mu \phi)^5 = 0$. This is how we get gravity from the auxiliary field ϕ.

2. 2. PURE GRAVITY

In the papers of Stelle, West and Wilczek Stelle and West (1980), Wilczek (1998) a commutative action for *pure gravity* with $SO(2,3)$ gauge symmetry was constructed. Also, in the papers of Chamseddine and Mukhanov Chamseddine and Mukhanov (2013, 2010), GR is formulated by gauging $SO(1,4)$ or, more suitable for SUGRA, $SO(2,3)$ group. Proceeding within this general framework, we show that it can also accommodate fermionic matter fields, specifically, the Dirac spinor field, and electromagnetic $U(1)$ gauge field. We are going to do that by providing a model of commutative action for the Dirac spinors and $U(1)$ gauge field, invariant under ordinary (undeformed) $SO(2,3) \otimes U(1)$ gauge transformations, which exactly reproduces classical electrodynamics in curved spacetime after the symmetry breaking.

In Dimitrijević Ćirić et al. (2017b) the $SO(2,3)$ model of pure gravity action and its NC deformation are analyzed. The commutative action consists of three parts,

$$S_1 = \frac{ilc_1}{64\pi G_N} \mathrm{Tr} \int d^4x \, \epsilon^{\mu\nu\rho\sigma} F_{\mu\nu} F_{\rho\sigma} \phi, \tag{2.9}$$

$$S_2 = \frac{c_2}{128\pi G_N l} \mathrm{Tr} \int d^4x \, \epsilon^{\mu\nu\rho\sigma} F_{\mu\nu} D_\rho \phi D_\sigma \phi \phi + h.c., \tag{2.10}$$

$$S_3 = -\frac{ic_3}{128\pi G_N l} \mathrm{Tr} \int d^4x \, \epsilon^{\mu\nu\rho\sigma} D_\mu \phi D_\nu \phi D_\rho \phi D_\sigma \phi \phi. \tag{2.11}$$

Gauge fixing yields

$$S = \frac{-1}{16\pi G_N} \int d^4x \left(\frac{c_1 l^2}{16} \epsilon^{\mu\nu\rho\sigma} \epsilon_{abcd} R_{\mu\nu}{}^{ab} R_{\rho\sigma}{}^{cd} + \sqrt{-g} \left((c_1 + c_2) R - \frac{6}{l^2} (c_1 + 2c_2 + 2c_3) \right) \right). \tag{2.12}$$

For the sake of generality, three a priori undetermined dimensionless constants are introduced. They can be fixed by some consistency condition. The first part of the action is a topological Gauss-Bonnet term which has no effect on the equations of motion, and so, we can set $c_1 = 0$. The Einstein-Hilbert term requires $c_1 + c_2 = 1$, while the absence of the cosmological constant is ensured by having $c_1 + 2c_2 + 2c_3 = 0$.

After NC deformation and perturbative expansion in powers of $\theta^{\mu\nu}$, it was confirmed that the first order NC correction to the commutative action vanishes. This was an already known result, e.g. Aschieri et al. (2013). The first non-vanishing correction is quadratic in the NC parameter. In the low energy limit, equations of motion for the vierbein and the spin-connection are given by

$$\delta e^a_\mu : R_{\alpha\gamma}{}^{cd} e^\gamma_d e^\alpha_a e^\mu_c - \frac{1}{2} e^\mu_a R + \frac{3}{l^2}(1 + c_2 + 2c_3) e^\mu_a = \tau_a{}^\mu = -\frac{8\pi G_N}{e} \frac{\delta S^{(2)}_{NC}}{\delta e^a_\mu}, \quad (2.13)$$

$$\delta \omega_\mu{}^{ab} : T_{ac}{}^c e^\mu_b - T_{bc}{}^c e^\mu_a - T_{ab}{}^\mu = S_{ab}{}^\mu = -\frac{16\pi G_N}{e} \frac{\delta S^{(2)}_{NC}}{\delta \omega_\mu{}^{ab}}. \quad (2.14)$$

The effective energy-momentum tensor $\tau_a{}^\mu$ and the effective spin-tensor $S_{ab}{}^\mu$ both depend on $\theta^{\mu\nu}$, and we can conclude that noncommutativity acts as a source of curvature and torsion. From (2.13) it follows that the scalar curvature of NC Minkowski space is $R = \frac{11}{l^6}\theta^2$. Thus, in $SO(2,3)_\star$ model, there exists an NC deformation of the Minkowski space and the NC correction to the flat metric is given by

$$\begin{aligned} g_{00} &= 1 - R_{0m0n} x^m x^n, \\ g_{0i} &= -\frac{2}{3} R_{0min} x^m x^n, \;\; g_{ij} = -\delta_{ij} - \frac{1}{3} R_{imjn} x^m x^n. \end{aligned} \quad (2.15)$$

Its form suggests that the coordinates x^μ we started with are actually the Fermi normal coordinates. These are inertial coordinates of an observer moving along a geodesic and they can be introduced in a small neighborhood along the geodesic (inside a small cylinder surrounding the geodesic) Manasse and Misner (1963), Chicone and Mashoon (2006), Klein and Randles (2011). The apparent breaking of the diffeomorphism invariance due to canonical noncommutivity can be understood as a consequence of working in a preferred reference system given by the Fermi normal coordinates. A local observer moving along a geodesic measures $\theta^{\mu\nu}$ to be constant. In any other reference frame this will not be the case.

2. 3. COMMUTATIVE ACTIONS FOR MATTER FIELDS

Now we turn to the construction of $SO(2,3) \otimes U(1)$ invariant theory for matter and $U(1)$ gauge field coupled to gravity. In Dimitrijević-Ćirić et al. (2018) we proposed an action for the $U(1)$ gauge field,

$$S_A = c\, Tr \int d^4x\, \varepsilon^{\mu\nu\rho\sigma} \Big\{ f \mathbb{F}_{\mu\nu} D_\rho \phi D_\sigma \phi \phi + \frac{i}{3!} f f D_\mu \phi D_\nu \phi D_\rho \phi D_\sigma \phi \phi \Big\} + h.c. \quad (2.16)$$

It includes an additional auxiliary field $f = \frac{1}{2} f^{AB} M_{AB}$. Like ϕ, this field transforms in the adjoint representation of $SO(2,3)$ and it is invariant under $U(1)$ (i.e. not

charged). Its role is to produce the canonical kinetic term for $U(1)$ gauge field in curved spacetime in the absence of the Hodge dual operation (this operation cannot be defined without prior knowledge of the metric tensor, and we don't have one at our disposal). Note also that c is some yet undetermined constant of mass dimension 1.

After gauge fixing, the purely gravitational part of the action (2.16) vanishes and we are left with

$$S_A = -8cl \int d^4x\, e\, f^{ab} e_a^\mu e_b^\nu \mathcal{F}_{\mu\nu} - 4cl \int d^4x\, e \left(f^{ab} f_{ab} + 2 f^{a5} f_a{}^5 \right). \tag{2.17}$$

Equations of motion for the components of the auxiliary field f are

$$f_{a5} = 0, \quad f_{ab} = -e_a^\mu e_b^\nu \mathcal{F}_{\mu\nu}. \tag{2.18}$$

We use these equations to eliminate the auxiliary field in the action (2.17) and this leaves us with the action for pure $U(1)$ gauge field in curved spacetime,

$$S_A = 4cl \int d^4x\, e\, \mathcal{F}_{\mu\nu} \mathcal{F}^{\mu\nu}. \tag{2.19}$$

To obtain the canonical kinetic term we set $c = -\frac{1}{16l}$.

The Dirac spinor field ψ transforms in the fundamental representation of $SO(2,3) \otimes U(1)$ gauge group. Its covariant derivative is given by (we assume $q = -1$)

$$D_\mu \psi = \partial_\mu \psi - i\Omega_\mu \psi = \nabla_\mu \psi + \frac{i}{2l} e_\mu^a \gamma_a \psi - iA_\mu \psi = \widetilde{\nabla}_\mu \psi + \frac{i}{2l} e_\mu^a \gamma_a \psi, \tag{2.20}$$

where we introduced $\widetilde{\nabla}_\mu = \nabla_\mu - iA_\mu$ as a covariant derivative for $SO(1,3) \otimes U(1)$ gauge group.

In Gočanin and Radovanović (2018) we proposed the following fermionic action

$$S_{\psi,kin} = \frac{i}{12} \int d^4x\, \varepsilon^{\mu\nu\rho\sigma} \Big[\bar{\psi} D_\mu \phi D_\nu \phi D_\rho \phi D_\sigma \psi - D_\sigma \bar{\psi} D_\mu \phi D_\nu \phi D_\rho \phi \psi \Big]. \tag{2.21}$$

After the symmetry braking it becomes

$$S_{\psi,kin} = \frac{i}{2} \int d^4x\, e\, \left[\bar{\psi} \gamma^\sigma \widetilde{\nabla}_\sigma \psi - \widetilde{\nabla}_\sigma \bar{\psi} \gamma^\sigma \psi \right] - \frac{2}{l} \int d^4x\, e\, \bar{\psi} \psi, \tag{2.22}$$

which is exactly the Dirac action in curved spacetime for spinors with cosmological mass term $2/l$, interacting via $U(1)$ gauge field. Note that $\widetilde{\nabla}_\sigma \psi = \nabla_\sigma \psi - iA_\sigma \psi$, includes the $U(1)$ gauge field.

To obtain fermions with arbitrary mass, we have to include the following additional "mass terms" (terms of the type $\bar{\psi} \dots \psi$)

$$\begin{aligned}
S_{\psi,m}^{(1)} &= \frac{ic_1}{2} \Big(\frac{m}{l} - \frac{2}{l^2} \Big) \int d^4x\, \varepsilon^{\mu\nu\rho\sigma} \Big[\bar{\psi} D_\mu \phi D_\nu \phi D_\rho \phi D_\sigma \phi \phi \psi + \bar{\psi} \phi D_\mu \phi D_\nu \phi D_\rho \phi D_\sigma \phi \psi \Big], \\
S_{\psi,m}^{(2)} &= \frac{ic_2}{2} \Big(\frac{m}{l} - \frac{2}{l^2} \Big) \int d^4x\, \varepsilon^{\mu\nu\rho\sigma} \Big[\bar{\psi} D_\mu \phi D_\nu \phi D_\rho \phi \phi D_\sigma \phi \psi + \bar{\psi} D_\mu \phi \phi D_\nu \phi D_\rho \phi D_\sigma \phi \psi \Big], \\
S_{\psi,m}^{(3)} &= ic_3 \Big(\frac{m}{l} - \frac{2}{l^2} \Big) \int d^4x\, \varepsilon^{\mu\nu\rho\sigma}\, \bar{\psi} D_\mu \phi D_\nu \phi \phi D_\rho \phi D_\sigma \phi \psi.
\end{aligned} \tag{2.23}$$

If we demand that a priori undetermined dimensionless coefficients c_1, c_2, and c_3 satisfy the constraint $c_2 - c_1 - c_3 = -\frac{1}{24}$, after the symmetry breaking, the sum of the three terms in (2.23) becomes

$$S_{\psi,m} = -\left(m - \frac{2}{l}\right)\int d^4x\, e\, \bar{\psi}\psi, \tag{2.24}$$

and the total action, $S_\psi = S_{\psi,kin} + S_{\psi,m}$, is exactly the Dirac action for spinors of mass m in curved spacetime,

$$S_\psi = \frac{i}{2}\int d^4x\, e\, \left[\bar{\psi}\gamma^\sigma\widetilde{\nabla}_\sigma\psi - \widetilde{\nabla}_\sigma\bar{\psi}\gamma^\sigma\psi\right] - m\int d^4x\, e\, \bar{\psi}\psi. \tag{2.25}$$

Thus, by starting with a theory with $SO(2,3)\otimes U(1)$ gauge symmetry, by a suitable gauge fixing, we have obtained the standard action for electrodynamics in curved spacetime.

2. 4. SEIBERG-WITTEN MAP

Now that we have established our commutative $SO(2,3)\otimes U(1)$ model for matter and $U(1)$ gauge field coupled to gravity, we want to deform it via NC Moyal-Weyl $\star$-product. Due to noncommutativity of the $\star$-product NC fields do not belong to the Lie algebra of the gauge group, since the deformed Lie algebra commutation relations do not close in the Lie algebra itself. These fields actually belong to the enveloping algebra. The closure condition for the algebra of gauge transformation becomes a set of differential equations, which are solved by iteration, order-by-order in the NC parameter $\theta^{\alpha\beta}$. Seiberg-Witten (SW) map Jurčo et al. (2001), Seiberg and Witten (1999) provides a solution to these equations. It also ensures that no additional degrees of freedom (no new fields) are included through NC deformation. NC quantities can be represented as perturbation series in powers of the parameter of noncommutativity, with expansion coefficients built out of commutative fields. For example, NC spinor and adjoint field are represented as

$$\widehat{\psi} = \psi - \frac{1}{4}\theta^{\alpha\beta}\omega_\alpha(\partial_\beta + D_\beta)\psi + \mathcal{O}(\theta^2), \tag{2.26}$$

$$\widehat{\phi} = \phi - \frac{1}{4}\theta^{\alpha\beta}\{\omega_\alpha, (\partial_\beta + D_\beta)\phi\} + \mathcal{O}(\theta^2), \tag{2.27}$$

where ω_α is the ordinary gauge potential. We see that at the zeroth order these NC fields reduce to their undeformed counterparts. The obtained NC action possesses deformed $SO(2,3)_\star \otimes U(1)_\star$ symmetry. Assuming that deformation parameter is small, we expend the NC action in powers of $\theta^{\mu\nu}$ using the general formula

$$\begin{aligned}\left(\widehat{A}\star\widehat{B}\right)^{(1)} &= -\frac{1}{4}\theta^{\alpha\beta}\{\omega_\alpha, (\partial_\beta + D_\beta)AB\} + \frac{i}{2}\theta^{\alpha\beta}D_\alpha A D_\beta B + cov(\widehat{A}^{(1)})B \\ &\quad + A cov(\widehat{B}^{(1)}),\end{aligned} \tag{2.28}$$

where $cov(\widehat{A}^{(1)})$ is the covariant part of $A's$ first order NC correction, and $cov(\widehat{B}^{(1)})$, the covariant part of $B's$ first order NC correction. SW ensures the $SO(2,3)\otimes U(1)$

invariance of the expansion, order by order in $\theta^{\alpha\beta}$. It turns out that the leading term in the expansion does not vanish after the symmetry breaking, and we thus obtain linear NC correction to classical electrodynamics in curved spacetime. The calculation is long and tedious and we will not present the details here. Schematically, the spinorial piece is given by

$$\widehat{S}^{(1)}_{\psi} = \theta^{\alpha\beta} \int d^4x \; e \; \bar{\psi}\Big(\mathcal{A}_{\alpha\beta}{}^{\rho\sigma}\widetilde{\nabla}_{\rho}\widetilde{\nabla}_{\sigma} + \mathcal{B}_{\alpha\beta}{}^{\sigma}\widetilde{\nabla}_{\sigma} + \mathcal{C}_{\alpha}\widetilde{\nabla}_{\beta} + \mathcal{D}_{\alpha\beta}\Big)\psi. \tag{2.29}$$

Objects $\mathcal{A}, \mathcal{B}, \mathcal{C}, \mathcal{D}$ are complicated functions of geometric and $U(1)$ quantities, e.g. we have interactions of the following type, $\bar{\psi}\sigma_{\alpha}{}^{\sigma}\widetilde{\nabla}_{\beta}\widetilde{\nabla}_{\sigma}\psi$, $\bar{\psi}R_{\alpha\beta}{}^{\rho\sigma}\gamma_{\rho}\widetilde{\nabla}_{\sigma}\psi$, $\bar{\psi}T_{\alpha\beta}{}^{\sigma}\widetilde{\nabla}_{\sigma}\psi$, $\bar{\psi}\mathcal{F}_{\alpha\mu}\gamma^{\mu}\widetilde{\nabla}_{\beta}\psi$, $\bar{\psi}\mathcal{F}_{\alpha\beta}\psi$, $\bar{\psi}\sigma_{\alpha\beta}\psi$ etc. More importantly, we want to emphasize the fact that this θ-linear NC correction pertains in the limit of flat spacetime. This enables us to derive some tangible phenomenological consequences of our model that could potentially be tested experimentally in a not to far future.

3. FLAT SPACETIME NC ELECTRODYNAMICS

The action for NC electrodynamics in flat spacetime, up to first order in $\theta^{\alpha\beta}$, is given by

$$\begin{aligned}\widehat{S}_{flat} = &\int d^4x \left[\bar{\psi}(i\not{\mathcal{D}} - m)\psi - \frac{1}{4}\mathcal{F}_{\mu\nu}\mathcal{F}^{\mu\nu}\right] - \theta^{\alpha\beta}\int d^4x \;\left[\frac{1}{8}\mathcal{F}_{\alpha\beta}\mathcal{F}^{\mu\nu}\mathcal{F}_{\mu\nu} + \frac{1}{2}\mathcal{F}_{\alpha\mu}\mathcal{F}_{\beta\nu}\mathcal{F}^{\mu\nu}\right] \\ &+ \theta^{\alpha\beta}\int d^4x \;\bar{\psi}\Bigg[-\frac{1}{2l}\sigma_{\alpha}{}^{\sigma}\mathcal{D}_{\beta}\mathcal{D}_{\sigma} + \frac{7i}{24l^2}\varepsilon_{\alpha\beta}{}^{\rho\sigma}\gamma_{\rho}\gamma_5\mathcal{D}_{\sigma} - \left(\frac{m}{4l^2} + \frac{1}{6l^3}\right)\sigma_{\alpha\beta} \\ &+ \frac{3i}{4}\mathcal{F}_{\alpha\beta}\not{\mathcal{D}} - \frac{i}{2}\mathcal{F}_{\alpha\mu}\gamma^{\mu}\mathcal{D}_{\beta} - \left(\frac{3m}{4} - \frac{1}{4l}\right)\mathcal{F}_{\alpha\beta}\Bigg]\psi,\end{aligned} \tag{3.30}$$

where we introduced flat spacetime covariant derivative $\mathcal{D}_{\mu} = \partial_{\mu} - iA_{\mu}$. We notice immediately that this action is different than the actions for NC electrodynamics already present in the literature Burić and Radovanović (2002), Wulkenhaar (2002), Burić et al. (2006a). The new interaction terms between spinors and the $U(1)$ field, specific to the $SO(2,3)_{\star}$ model, appear as residuals from the gravitational interaction, and they lead to some non-trivial consequences such as the modification of the dispersion relation for electrons.

By varying the NC action (3.30) with respect to $\bar{\psi}$ we obtain deformed Dirac equation for electron coupled to some background electromagnetic field A_{μ},

$$\left(i\not{\partial} - m + \not{A} + \theta^{\alpha\beta}\mathcal{M}_{\alpha\beta}\right)\psi = 0. \tag{3.31}$$

To simplify the analysis, we assume that only two spatial dimensions are mutually incompatible, e.g. $[x^1, x^2] = i\theta^{12}$. Thus, we have $\theta^{12} = -\theta^{21} =: \theta \neq 0$ and all other components of $\theta^{\alpha\beta}$ equal to zero. We will consider the case of an electron in background magnetic field.

3. 1. ELECTRON IN BACKGROUND MAGNETIC FIELD

Using the NC deformed Dirac equation (3.31), we can see how noncommutativity modifies the energy levels of an electron in a constant background magnetic field $\boldsymbol{B} = B\boldsymbol{e}_z$. Classical (undeformed) energy levels for a relativistic electron are given by

$$E^{(0)}_{n,s} = \sqrt{p_z^2 + m^2 + (2n+s+1)B}. \tag{3.32}$$

We are looking for a linear NC correction $E^{(1)}_{n,s} \sim \theta$ of the energy levels (3.32). Working perturbatively in θ, they can be calculated by the following formula,

$$E^{(1)}_{n,s} = -\frac{\theta^{\alpha\beta} \int dy\ \bar{\psi}^{(0)}_{n,s} \mathcal{M}_{\alpha\beta} \psi^{(0)}_{n,s}}{\int dy\ \bar{\psi}^{(0)}_{n,s} \gamma^0 \psi^{(0)}_{n,s}}. \tag{3.33}$$

In particular, for $\theta^{12} = -\theta^{21} = \theta \neq 0$ we obtain

$$\begin{aligned} E^{(1)}_{n,s} = &- \frac{\theta s}{E^{(0)}_{n,s}} \left[\frac{m^2}{12l^2} - \frac{m}{3l^3} \right] - \frac{\theta B s}{E^{(0)}_{n,s}(E^{(0)}_{n,s} + m)} \left[\frac{m}{12l^2} - \frac{1}{3l^3} \right] (2n+s+1) \\ &+ \frac{\theta B^2}{2E^{(0)}_{n,s}} (2n+s+1). \end{aligned} \tag{3.34}$$

Non-relativistic limit of the NC energy levels is obtained by expanding undeformed energy function $E^{(0)}_{n,s}$ assuming $p_z^2,\ B \ll m^2$,

$$\begin{aligned} E^{(0)}_{n,s} &= \sqrt{p_z^2 + m^2 + (2n+s+1)B} \\ &\approx m \left[1 + \frac{p_z^2 + (2n+s+1)B}{2m^2} - \frac{(p_z^2 + (2n+s+1)B)^2}{8m^4} \right]. \end{aligned} \tag{3.35}$$

Expending (3.34) we obtain the NC correction to the energy levels of a non-relativistic electron,

$$\begin{aligned} E^{(1)}_{n,s} = &\left[\frac{\theta s}{3l^3} - \frac{\theta s m}{12l^2} \right] \left[1 - \frac{p_z^2}{2m^2} + \frac{3p_z^4}{8m^4} + \frac{3p_z^2(2n+s+1)B}{8m^4} \right] \\ &+ \frac{\theta B^2}{2m} (2n+s+1) \left[1 - \frac{p_z^2 + (2n+s+1)B}{2m^2} + \frac{3(p_z + (2n+s+1)B)^2}{8m^4} \right]. \end{aligned} \tag{3.36}$$

For an electron constrained to the NC x, y-plane we take $p_z = 0$ and NC energy levels reduce to

$$\begin{aligned} E_{n,s} = &\left[m - s\theta \left(\frac{m}{12l^2} - \frac{1}{3l^3} \right) \right] + \frac{2n+s+1}{2m} B_{eff} - \frac{(2n+s+1)^2}{8m^3} B_{eff}^2 \\ &+ \mathcal{O}(\theta^2), \end{aligned} \tag{3.37}$$

where we introduced $B_{eff} = (B + \theta B^2)$ as an effective magnetic field. We see that a spin-dependent shift of mass appears. If we compare this expression with the one for undeformed energy levels $E^{(0)}_{n,s}$, we see that the only effect of noncommutaivity is to modify the mass of an electron and the value of the background magnetic field.

This interpretation of constant noncommutativity is in accord with string theory. In the famous paper of Seiberg and Witten Seiberg and Witten (1999) it is argued, in the context of string theory, that coordinate functions of the endpoints of an open string constrained to a D-brane in the presence of a constant Neveu-Schwarz B-field satisfy the constant noncommutativity algebra. This implies is that a relativistic field theory on NC spacetime can be interpreted as a low energy limit of the theory of open strings.

4. FURTHER DEVELOPMENT

This newly established theory of NC Electrodynamics, both in curved and flat spacetime, paves the way for a variety of further investigation. Here we point to some of them:

(1) *Experimental verification*: The $SO(2,3)_\star \otimes U(1)_\star$ model of NC Electrodynamics predicts a potentially observable modifications of some of the basic properties of an electron. It is crucial that these corrections are linear in the noncommutativity parameter. With our growing ability to probe high energies scales, this could enable us to obtain an experimental verification.

(2) *Renormalization*: The so called minimal NC electrodynamics is not a renormalisabile theory because of the fermionic loop contributions Burić and Radovanović (2002), Wulkenhaar (2002), Burić et al. (2006). It would be interesting to analyze the renormalisability of the $SO(2,3)_\star$ model in order to theoretically determine on which scale does noncommutativity operates.

(4) *NC Standard Model*: One could incorporate scalar fields in the $SO(2,3)_\star$ framework in order to construct the full NC extension of the Standard Model of elementary particles.

(6) *NC Quantum Hall Effect*: Quantum Hall Effect is one of the most interesting phenomena in physics. Our results could be extended in a way that would allow us to see how noncommutativity modifies the behavior of electrons in some material medium. One line of investigation is to explore the Quantum Hall Effect taking into account the NC deformation of Landau levels found in our model.

References

Aschieri, P.: 2014, Extended gravity from noncommutativity, *Springer Proc. Phys.*, **145**, 151, [arXiv:1207.5060].

Aschieri, P., Castellani, L.: 2009a, Noncommutative $D = 4$ gravity coupled to fermions, *JHEP*, **0906**, 086, [arXiv:0902.3823].

Aschieri, P., Castellani, L.: 2009b, Noncommutative supergravity in $D = 3$ and $D = 4$, *JHEP*, **0906**, 087, [arXiv:0902.3823].

Aschieri, P., Castellani, L.: 2010, Noncommutative Gravity Solutions, *J. Geom. Phys.*, **60**, 375-393, [arXiv:0906.2774].

Aschieri, P., Castellani, L.: 2012, Noncommutative gravity coupled to fermions: second order expansion via Seiberg-Witten map, *JHEP*, **1207**, [arXiv:1111.4822].

Aschieri, P., Castellani, L.: 2013, Noncommutative gauge fields coupled to noncommutative gravity, *General Relativity and Gravitation*, **45**, 3, [arXiv:1205.1911v1].

Aschieri, P., Blohmann, C., Dimitrijević, M., Meyer, F., Schupp, P., Wess, J.: 2005, A Gravity Theory on Noncommutative Spaces, *Class. Quant. Grav.*, **22**, 3511, [hep-th/0504183].

Aschieri, P., Dimitrijević, M., Meyer, F., Wess, J.: 2006, Noncommutative Geometry and Gravity, *Class. Quant. Grav.*, **23**, 1883, [hep-th/0510059].

Aschieri, P., Castellani, L., Dimitrijević, M.: 2013, Noncommutative gravity at second order via Seiberg-Witten map, *Phys. Rev. D*, **87**, 024017, [arXiv:1207.4346].

Bayen, F., Flato, M., Fronsdal, C., Lichnerowicz, A., Sternheimer, D.: 1978, Deformation theory and quantization, *Ann. Phys.*, **111**, 61.

Burić, M., Madore, J.: 2008, Spherically Symmetric Noncommutative Space: $d = 4$, *Eur. Phys. J.*, **C58**, 347, [arXiv: 0807.0960].

Burić, M., Madore, J.: 2014, On noncommutative spherically symmetric spaces. *Eur. Phys. J. C*, **74**, 2820. https://doi.org/10.1140/epjc/s10052-014-2820-8.

Burić, M., Radovanović, V.: 2002, The One loop effective action for quantum electrodynamics on noncommutative space, *JHEP*, **0210**, 074, [hep-th/0208204].

Burić, M., Latas, D., Radovanović, V.: 2006a, Renormalizability of noncommutative SU(N) gauge theory, *JHEP*, **0602**, 046, [hep-th/0510133].

Burić, M., Grammatikopoulos, T., Madore, J., Zoupanos, G.: 2006b, Gravity and the Structure of Noncommutative Algebras, *JHEP*, **0604**, 054, [hep-th/0603044].

Burić, M., Madore, J., Zoupanos, G.: 2008, The Energy-momentum of a Poisson structure, *Eur. Phys. J.*, **C 55**, 489-498, [arXiv:0709.3159].

Cardella, M. A., Zanon, D.: 2003, Noncommutative deformation of four-dimensional gravity, *Class. Quant. Grav.*, **20**, L95, [hep-th/0212071].

Castellani, L.: 2013, Chern-Simons supergravities, with a twist, *JHEP*, **1307**, 133, [arXiv:1305.1566].

Chamseeddine, A. H.: 2001, Deforming Einstein's gravity, *Phys. Lett. B*, **504**, 33, [hep-th/0009153].

Chamseeddine, A. H.: 2004, $SL(2, C)$ gravity with a complex vierbein and its noncommutative extension, *Phys. Rev. D*, **69**, 024015.

Chamseddine, A. H., Mukhanov, V.: 2010, Gravity with de Sitter and Unitary Tangent Groups, *JHEP*, **1003**, 033, [arXiv:1002.0541].

Chamseddine, A. H., Mukhanov, V.: 2013, Who Ordered the Anti-de Sitter Tangent Group?, *JHEP*, **1311**, 095, [arXiv:1308.3199].

Chicone, C., Mashoon, B.: 2006, Explicit Fermi coordinates and tidal dynamics in de Sitter and Godel spacetimes, *Phys. Rev. D*, **74**, 064019, [gr-qc/0511129].

Dimitrijević, M., Radovanović, V.: 2014, Noncommutative $SO(2, 3)$ gauge theory and noncommutative gravity, *Phys. Rev. D*, **89**, 125021, [arXiv:1404.4213].

Dimitrijević, M., Radovanović, V., Štefančić, H.: 2012, AdS-inspired noncommutative gravity on the Moyal plane, *Phys. Rev. D*, **86**, 105041, [arXiv:1207.4675].

Dimitrijević Ćirić, M., Nikolić, B., Radovanović, V.: 2017a, Noncommutative gravity and the relevance of the θ-constant deformation, *Europhys. Lett.*, **118** no.2, 21002, [arXiv:1609.06469].

Dimitrijević Ćirić, M., Nikolić, B., Radovanović, V.: 2017b, NC $SO(2, 3)_\star$ gravity: noncommutativity as a source of curvature and torsion, *Phys. Rev. D*, **96**, 064029, [arXiv:1612.00768].

Dimitrijević-Ćirić, M., Gočanin, D., Konjik, N., Radovanović, V.: 2018, "Noncommutative Electrodynamics from $SO(2, 3)_\star$ Model of Noncommutative Gravity", *Eur. Phys. J. C*,

78, 548.

Dobrski, M.: 2017, Background independent noncommutative gravity from Fedosov quantization of endomorphism bundle, *Classical and Quantum Gravity*, **34**, 075004.

Dobrski, M.: 2011, On some models of geometric noncommutative general relativity, *Phys. Rev. D*, **84**, 065005, [arXiv:1011.0165].

Faizal, Mir: 2013, Noncommutative Quantum Gravity, *Mod. Phys. Lett. A*, **28**, 1350034, [arXiv:1302.5156].

Gočanin, D., Radovanović, V.: 2018, Dirac field and gravity in NC $SO(2,3)_\star$ model, *Eur. Phys. J. C*, **78**, 195.

Harikumar, E., Rivelles, V. O.: 2006,Noncommutative Gravity, *Class. Quant. Grav.*, **23**, 7551-7560, [hep-th/0607115].

Jurčo, B., Möller, L., Schraml, S., Schupp, P., Wess, J.: 2001, Construction of non-Abelian gauge theories on noncommutative spaces, *Eur. Phys. J. C*, **21**, 383, [hep-th/0104153].

Klammer, D., Steinacker, H.: 2009, Cosmological solutions of emergent noncommutative gravity, *Phys. Rev. Lett.*, **102**, 221301, [arXiv:0903.0986].

Klein, D., Randles, E.: 2011, Fermi coordinates, simultaneity, and expanding space in Robertson-Walker cosmologies, *Annales Henri Poincare*, **12**, 303-328, [arXiv:1010.0588].

Kobakhidze, A., Lagger, C., Manning, A.: 2016, Constraining noncommutative spacetime from GW150914, *Phys. Rev. D*, **94**, 064033, [arXiv:1607.03776],

Kontsevich, Maxim: 2013, Deformation quantization of Poisson manifolds, I, *Lett. Math. Phys.*, **66**, 157-216, [q-alg/9709040].

MacDowell, S. W., Mansouri, F.: 1977, Unified geometrical theory of gravity and supergravity, *Phys. Rev. Lett.*, **38**, 739.

Manasse, F. K., Misner, C. W.: 1963, Fermi Normal Coordinates and Some Basic Concepts in Differential Geometry, *J. Math. Phys.*, **4**, 735-745.

Ohl, T., Schenckel, A.: 2009, Cosmological and Black Hole Spacetimes in Twisted Noncommutative Gravity, *JHEP*, **0910**, 052, [arXiv: 0906.2730].

Seiberg, N., Witten, E.: 1999, String theory and noncommutative geometry, *JHEP*, **09**, 032, [hep-th/9908142].

Steinacker, H.: 2010, Emergent Geometry and Gravity from Matrix Models: an Introduction, *Class. Quant. Grav.*, **27**, 133001, [arXiv:1003.4134].

Stelle, K. S., West, P. C.: 1980, Spontaneously broken de Sitter symmetry and the gravitational holonomy group, *Phys. Rev D*, **21**, 1466.

Sternheimer, D.: 1998, Deformation quantization: Twenty years after, *AIP Conf. Proc.*, **453**, 107, [math.qa/9809040].

Tomassini, L., Viaggiu, S.: 2014, Building non-commutative spacetimes at the Planck length for Friedmann flat cosmologies, *Class. Quant. Grav.*, **31** 185001, [arXiv:1308.2767].

Towsend, P. K.: 1977, Small-scale structure of spacetime as the origin of the gravitation constant, *Phys. Rev. D*, **15**, 2795.

Wilczek, F.: 1998, Riemann-Einstein structure from volume and gauge symmetry, *Phys. Rev. Lett.*, **80**, 4851-4854, [hep-th/9801184].

Wulkenhaar, R.: 2002, Nonrenormalizability of theta expanded noncommutative QED, *JHEP*, **0203**, 024,[hep-th/0112248].

Yang, H. S.: 2009, Emergent gravity from noncommutative spacetime, *Int. J. Mod. Phys.*, **A24**, 4473, [hep-th/0611174].

Publ. Astron. Obs. Belgrade No. 100 (2021), 97 - 106 *Invited Lecture*

INVESTIGATION OF ACTIVE GALACTIC NUCLEI IN TIME DOMAIN ERA

D. ILIĆ[1], A. KOVAČEVIĆ[1] and L. Č. POPOVIĆ[1,2]
[1] *Department of Astronomy, Faculty of Mathematics, University of Belgrade, Studentski trg 16, Belgrade, Serbia*
E–mail: dilic@matf.bg.ac.rs
E–mail: andjelka@matf.bg.ac.rs
[2] *Astronomical Observatory, Volgina 7, Belgrade, Serbia*
E–mail: lpopovic@aob.rs

Abstract. The perfect case for time-domain investigations are active galactic nuclei (AGNs) since they are luminous objects that show strong variability. Key result from the studies of AGNs variability is the estimated mass of a supermassive black hole (SMBH), which resides in the center of an AGN. Moreover, the spectral variability of AGN can be used to study the structure and physics of the broad line region, which in general can be hardly directly observed. Here we review the current status of AGNs variability investigations in Serbia, in the perspectives of the present and future monitoring campaigns.

1. INTRODUCTION

With the advances of technology and robotization of telescopes, we have entered the era of massive astronomical time-domain observations, with several missions already running and producing amazing results (e.g. Djorgovski et al. 2016). This is the case also for the investigations of active galactic nuclei (AGNs). The Sloan Digital Sky Survey (SDSS) is one of the most famous and successful example, which is currently releasing its sixteenth data release containing images and spectra of millions of objects, as well as providing a Time Domain Spectroscopic Survey of 131,000 quasars (e.g. Ahumada et al. 2020). In the next decade, we expect to have comprehensive monitoring campaigns, out of which the Vera Rubin Observatory Legacy Survey of Space and Time (LSST) with its very high cadence 10-year photometric survey seems to be very promising for the quasar investigations (Ivezić et al. 2019). LSST will provide millions of quasar photometric light curves, which will facilitate better understanding of the physical processes that power quasars and their variability (Brandt et al., 2018). LSST will be complemented with several spectral surveys, and one promising example is the Maunakea Spectroscopic Explorer (MSE) that is an 11m aperture telescope (MSE Science Team 2019). This survey will cover both the time and spectral domain, including also the infrared band, which is important for the high-redshift quasar studies. The MSE will lead the world in multi-object spectroscopy, with its unique capability to study up to 4,000 astronomical objects at

once. It will provide spectral light curves of the largest number of quasars, which analysis will enable mapping of the inner regions in AGNs (Shen et al. 2019).

This motivates us to do investigations of AGNs using optical spectroscopy in time-domain, of which recent results we give an overview in this Proceedings. We cover topics from: i) long-term monitoring campaign of the sample of near-by AGNs, ii) studies of oscillations in AGN light curves in search for periodic signals, iii) studies of the optically extremely variable AGNs. The findings of our research project are put in the concept of applications and impact to future large surveys, especially the LSST. These investigations are done at the Astronomical Observatory in Belgrade and the Department of Astronomy of the Faculty of Mathematics, University of Belgrade, mainly through the project of "Astrophysical spectroscopy of extragalactic objects", 176001, supported by the Ministry of Education, Science and Technological Development of the Republic of Serbia, which was financed by the end of 2019. This paper is organized as follows: in Sec. 2 we shortly describe the theoretical background of AGN structure, and give the current overview of time-domain investigation of AGNs, in Sec. 3 we list some of the major results of our findings, in Sec. 4 put them in concept of future surveys, and in Sec. 5 a short summary is given.

2. OVERVIEW OF AGNs AND TIME-DOMAIN INVESTIGATIONS

2. 1. ACTIVE GALACTIC NUCLEI

AGNs are nested in the center of only a small fraction of all galaxies (Netzer 2006). However, it is widely believed that every larger galaxy has undergone a phase of activity, when its supermassive black hole (SMBH) was actively accreting matter from the surroundings. This process of accretion is responsible for the production of powerful and energetic continuum emission, which produces a variety of different phenomena, such as the production of relativistic radio-jets, disk-winds, or ionized gaseous regions (for a textbook on AGNs, see e.g. Netzer 2006). The broad optical emission lines originate in the broad line region (BLR), which is photoionized by the continuum emission from the accretion disk. The accretion disk and BLR are sometimes "hidden" within the larger dusty region, which is a dominant source of obscuration of optical emission in some type of AGN. Dust is mostly located in equatorial plane and is usually referred as a dusty "torus", but recent high-resolution observations showed that the polar dust is also present (Hönig & Kishimoto 2017, Stalevski et al. 2017, 2019).

Quasars are classified in many ways, depending on their observed properties. One division is on type 1 and type 2 AGNs (or unobscured and obscured AGNs) which is based on the presence or absence of optical broad emission lines, respectively. The main reason for this division is to be the viewing angle, i.e. the angle how the AGN axis of symmetry (i.e. the accretion disk axis) is inclined with respect to the observer. If we would be looking at the AGN closer to the AGN axis, we would be seeing inside the dusty region, thus detecting the unobscured accretion disk and BLR, i.e. broad emission lines (Antonucci & Miller 1985, Urry & Padovani 1995). When the viewing angle is larger, we would be seeing the central parts covered by the dusty region, and the continuum and broad emission lines would be obscured, as it is in the case of type 2 AGNs (Hickox & Alexander, 2018).

We are especially focused on the BLR investigations through the analysis of the optical spectroscopy. Primarily because one can estimate the SMBH mass from the dynamics of the BLR gas, which is gravitationally bound to a SMBH. For this we need to measure the BLR size, which is measured through the reverberation mapping (RM, see e.g., Blandford & McKee 1982, Gaskell & Sparke 1986). The RM measures a characteristic size of the BLR from the time lag (i.e. light echo) between variability of the continuum emission, which powers the BLR, and the delayed response of the BLR emission. The RM was applied to a limited sample of AGNs, even if the SDSS survey results are considered (e.g. Shen et al. 2019). However, it has produced the so-called "single-epoch virial BH mass estimators" (e.g., Vestergaard & Peterson 2006) that provides an empirical SMBH mass estimate using the single-epoch spectroscopy and the relation between the BLR radius and continuum luminosity (so-called radius-luminosity scaling relation, see e.g., Bentz et al. 2009). This method has been widely applied to AGNs at different redshifts and luminosities.

We still do not have a complete physical picture of the BLR which is known to be very complex (Sulentic et al. 2000), and this can directly affect the accuracy of the SMBH mass estimates (as discussed in e.g. Mejía-Restrepo et al. 2018). There are many opened question about the geometry and kinematics, e.g. is the BLR truly virialized to the SMBH (Jonić et al. 2016, Popović et al. 2019), do we have a Keplerian motion, outflows or inflows (e.g. Wang et al. 2017), what is the inclination of the moving gas (e.g. Mejía-Restrepo et al. 2018, Afanasiev et al. 2019). The physical properties (e.g. gas temperature, density, ionization parameter) of the emitting plasma in the BLR are still not well constrained (Ilić et al. 2012). Currently the BLR is not spatially resolved, except with the state-of the-art interferometry such as GRAVITY (Gravity Collaboration, Sturm et al. 2018, Amorim et al. 2020, 2021, Wang et al. 2020, Songsheng et al. 2021) or the proposed upgrade GRAVITY+ (Eisenhauer 2019)[1]. Thus the spectroscopy is still important tool to observe and study the BLR.

2. 2. TIME-DOMAIN ASTRONOMY OF AGNS

The International Astronomical Union (IAU) has very recently recognized that the time-domain investigations are an important aspect of the modern research and has founded a Working Group on Time Domain Astronomy in 2015 (see e.g. their 2019 annual report[2]). Time domain astronomy studies the transient Universe and covers objects from the near-by Solar system, through variable starts, to galaxies at cosmological distances, i.e. quasars. As already stated, this is strongly driven by current and coming large time domain surveys, such as the Catalina Real-Time Transient Survey (CRTS, Drake et al. 2009), Zwicky Transient Facility (ZTF, Ofek et al. 2020), and the coming LSST.

Quasars are in the focus of the time-domain investigations (Graham, 2019), since one of the most peculiar observational feature of quasars is its variability, which can be on the orders of hours to months, depending on the wavelength band (see e.g. Peterson, 2001). Especially, the broad emission lines can strongly change both the flux and profile. The flux variations were used for the RM studies to "resolve"

[1]https://www.mpe.mpg.de/7480772/GRAVITYplus_WhitePaper.pdf

[2]https://www.iau.org/static/science/scientific_bodies/working_groups/260/wg-tda-annual-report-2019.pdf

the BLR in time-domain and measure the size of the BLR (e.g. Peterson et al. 2004), and consequently the SMBH mass (see review Popović 2020), whereas the line profile variability can be used to constrain the geometry of the BLR (e.g. Popović et al. 2011). Particularly important aspect of time-domain photometric observation of AGNs, is the search for periodic signal which could lead to the detection of close binary SMBH systems (see e.g. with CRTS, Graham et al. 2017) and possible future targets for detection of gravitational waves (for a review see Popović 2012, and recent works Kovačević et al., 2019, 2020b). One particular class of AGNs are so-called changing-look AGNs (CL AGNs), which show extreme variability of emission line intensities and profiles, with sometimes almost complete disappearance and reappearance of the broad component in some emission lines (e.g. Denney et al. 2014, Oknyansky et al. 2017). Physical processes causing such dramatic change are still unknown (e.g. Ilić et al. 2020), but this could be also a signature of a presence of close binary SMBH (Wang & Bon 2020). So far, surveys have discovered only a small fraction of changing-look candidates (e.g., Runco et al. 2016, MacLeod et al. 2016), but future surveys like the LSST will be able to discover many or even show that this phase is not so rare.

3. RESULTS OF OUR STUDIES OF AGNs VARIABILITY

3. 1. LONG TERM REVERBERATION MAPPING (LOTERM) CAMPAIGN

The long term spectroscopic AGNs monitoring program (Long Term Reverberation Mapping - LoTeRM) was a programme initiated by late A.I. Shapovalova with the aim to study the structure of BLR and estimate the mass of the SMBH. LoTeRM has been running for the last ∼30 years collecting data from several world-wide optical telescopes (see Shapovalova et al. 2009, Ilić et al. 2017, for reviews). The LoTeRM sample included type 1 AGNs of different variability properties (e.g., low or high level of variability, in the range of 5-40%), and different spectral line profiles (e.g., double-peaked profiles or asymmetric profiles). So far the data have been published for the following sub-types: Seyfert 1 galaxies (NGC 5548, NGC 4151, NGC 7469), Narrow-line Seyfert 1 galaxy - NLSy 1 (Ark 564), double-peaked line radio loud (3C 390.3) and radio quiet (Arp 102B) galaxy, luminous quasar (E1821+643), a SMBH binary candidate, and a CL AGN (NGC 3516). Each object has been first presented and analyzed separately in a series of papers (see release paper Shapovalova et al. 2001, 2004, 2008, 2010a, 2012, 2013, 2016, 2017, 2019). Spectral data were all uniformly reduced and analyzed, creating a unique sample of homogeneous long-term light curves of different properties (Figure 1), making it a valuable set for studies of AGN variability. As a part of the Shapovalova et al. monitoring campaign, in Bon at al. (2016) additional observations of NGC 5548 covering 2003–2013 are given. In the same paper an important historical light-curve of NGC 5548 which covers more than 40 years of observations was constructed. Some of the results of LoTeRM were included in the AGNs Black Hole Mass Database (Bentz & Katz 2015)[3].

The LoTeRM project is currently expanding to include other telescope, such as the 1.4m Milankovic telescope at Astronomical Station Vidojevica, Serbia, and 1.5m telescope of the Observatory of Sierra Nevada, Granada, Spain. The Milankovic telescope is for the moment only equipped for the photometric monitoring, which

[3]http://www.astro.gsu.edu/AGNmass/

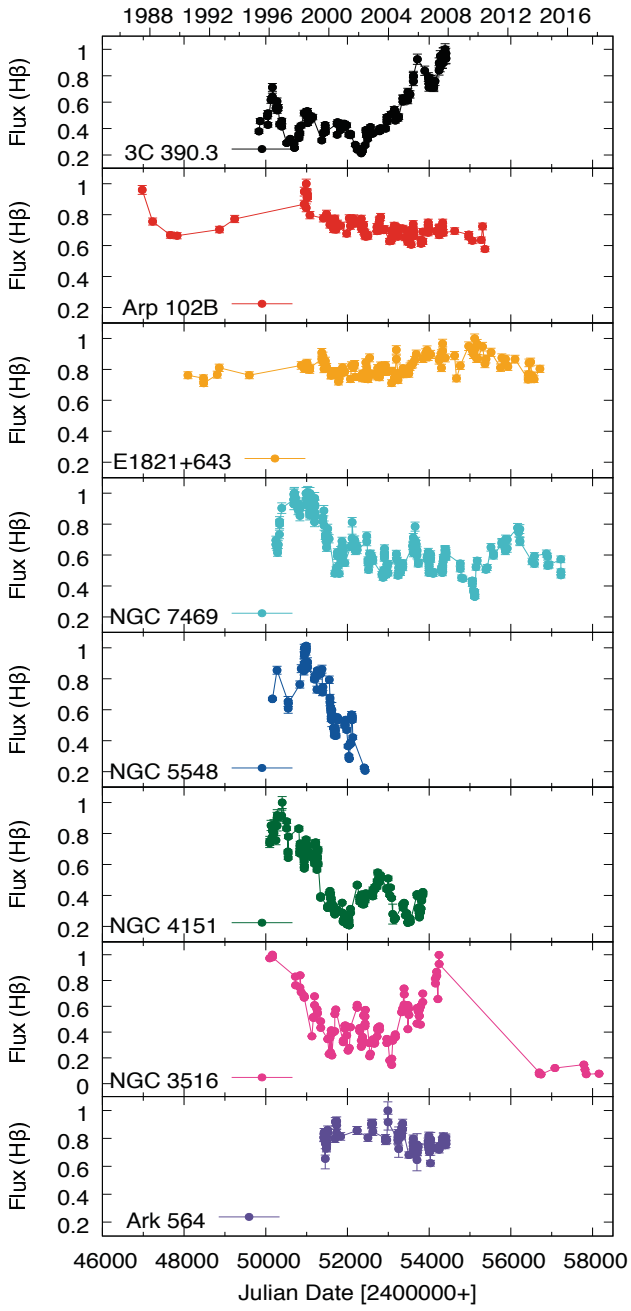

Figure 1: Hβ light curves of the sample of eight type 1 AGNs from the LoTeRM campaign (only data presented in the first data release papers are shown). Different sub-types of type 1 AGNs are shown, which exhibit different level of variability and optical spectral lines behavior. Light curves are normalized to the maximal flux.

can be used in combination with the spectral data or carefully selected narrow/mid-band filter for the RM applications (Malygin et al. 2020). This was used in case of NGC 4395, which is a bulgeless dwarf galaxy with one of the smallest SMBH of only 10,000 solar masses (Woo et al. 2019). This SMBH mass was confirmed with the international intranight RM campaign done by more than a dozen of telescope across the world including the 1.4m Milankovic telescope (Cho et al. 2020). The observed time delays of the BLR were only ∼1-2 hours, and it was important to show that this case of very low-luminosity AGN follows the radius-luminosity scaling relations (Bentz et al. 2013).

3. 2. OSCILLATORY PATTERNS IN AGN LIGHT CURVES

We used this sample of AGNs to investigate the behavior of long-term light curves, and search for periodicity or patterns which could signify different underlying dynamical processes. In case of 3C 390.3, it was shown that quasi-periodical oscillations may be present in the continuum and Hβ light curves (Shapovalova et al. 2010). Possibly, the outbursts seen in the Hβ line could be explained by successive occurrences of two bright orbiting spots in the accretion disk (Jovanović et al. 2010). Careful investigation of the repeating variability pattern in complex broad emission line profiles, resulted with a first paper on the spectroscopically discovered binary orbit of SMBH binary system candidate in NGC 4151 (Bon et al. 2012). Later it was shown that a binary SMBH system may be possibly present in another well-known object NGC 5548 (e.g. Li et al. 2016), since significant periodicity in light and radial velocity curves in NGC 5548 were detected (Bon et al. 2016).

Furthermore, a novel hybrid method to search for periodic oscillatory patterns was developed - 2DHybrid method (see Kovačević et al. 2018, for details). The 2DHybrid combines two techniques continuous wavelet transform and correlation coefficients, to analyze the Gaussian-processed AGN light curves. We have applied the 2DHybrid to our LoTeRM sample (Kovačević et al. 2018, 2020a) finding periodic variations in most of them, but of different origin. In case of the two double-peaked line objects 3C 390.3 and Arp 102B, for which we found a good evidence that they have qualitative different dynamics (Kovačević et al. 2018).

With the 2DHybrid method we probed the light curve of the famous case of a binary SMBH candidate PG1302-102, which photometric light curve showed clear periodic behaviour (Graham et al., 2015). More recent optical observations showed a disturbed light curve of PG1302-102, which lead to less significant periodicity detection (Liu et al. 2018). However, our hybrid method for periodicity detection was able to identify the periodic signal even in light curve with larger fluctuations (Kovačević et al. 2019), and proposing a model of a binary system in which a perturbation in the accretion disk of a more massive component is present (Simić & Popović 2016). This model of a binary system has been further developed to include a SMBBH system which considers that both SMBH have their accretion disc and BLR regions, and are both surrounded by a common circumbinary BLR (Popović et al. 2021).

3. 3. EXTREMELY VARIABLE AGNS

Long-term monitoring of AGNs is particularly important to understand the trend of their variability and capture possible extreme events in the optical band, such as the changing look transition, i.e. the disappearance of the broad component in some

emission lines. Moreover, it could be that the CL phenomenon is a common phase, and that it could be detected in each strongly variable AGN if constantly observed (see discussion in Oknyansky et al 2017). The CL transition could be caused by the intrinsic changes of accretion disk, obscuration of the BLR, tidal disruption events, or even presence of the close binary SMBH (Wang & Bon 2020). Therefore, understating these object could help shedding light on understanding the AGN structure and evolution.

Our sample contains several cases of extremely variable objects in the optical band (e.g. NGC 4151, NGC 5548), and the CL state for NGC 5548 was reported in Shapovalova et al. (2004). Another example of CL AGN is a Seyfert galaxy NGC 3516, for which is known to have strong optical variability and has changed its type in the past (Andrillat & Souffrin 1968). For NGC 3516, the LoTeRM campaign collected a 22 years of data, from 1996 to 2018, and we found strong variability in the continuum and broad lines (Shapovalova et al. 2019). The minimum of activity was observed in 2014, when the broad lines almost disappeared. In 2017, the object was still in the low state, but broad lines started to appear (see Figure 2 in Shapovalova et al. 2019). Recent short-term intensive optical campaign (from September 2019 to January 2020) indicate that NGC 3516 is maybe awakening (Ilić et al. 2020). The observational facts supporting this are the increase of the continuum emission, the variability of the coronal lines, and the very broad component in the Balmer lines. It is necessary to continue the intensive monitoring of this object to capture a possible transition phase. Moreover, using multiwavelength facilities (optical, UV, and X-ray) and different tools (spectroscopy, spectro-polarymetry) may be needed to finally describe the processes behind the changing-look phenomenon in AGNs.

4. IMPLICATIONS TO LARGE SURVEYS

The LSST will provide photometric light-curves of millions of AGNs, and one of its key science case is the probing of the accretion disk and BLR with the RM (Brandt et al. 2018). The key science case of MSE is the spectral RM campaign of around 5000 quasars up to the redshift of 3, providing robust estimates of time lags for the largest sample of quasars (Shen et al. 2019). In order to process such a huge amount of data, novel tools and approaches largely based on machine learning (ML) algorithms, are required.

One challenge is how to do cross-correlation analysis of realistic light curves, which usually have problems, such as e.g. gaps, nonuniform cadence, etc. One solution could be a novel ML tool (Gaussian PROcesses for TIme Delays Estimates in AGNs - GPro-TIDE) for time-delays measurements that utilizes generalized Gaussian processes to model the observed light curves used for extraction of time-delays (e.g., Kovačević et al. 2014, 2015, 2018). Another challenge is to have codes for autonomous and fast spectral fitting of multi-component and complex quasar optical spectra. For this a solution could be a FANTASY code (Fully Automated pythoN Tool for AGN Spectra analYsis), which is currently in testing fase (see Rakić et al., in this proceedings). For the classification of AGNs and studies of correlation between AGN properties in multidimesional space, more advance ML techniques based on manifold learning could be used (see Jankov et al., in this proceedings).

Finally, there is an important question about the operation strategies and survey cadences of time-domain surveys required in order to be able to extract the presented

investigations (for LSST see e.g. Jones et al. 2020). For these different statistical proxies should be developed and tested on both real observed and idealized modeled light curves (Kovačević et al. 2021). These metrics could be used for future surveys for testing the selection of operation strategies.

5. SUMMARY

Here we summarize the findings of the investigations of AGNs variability done within the project "Astrophysical spectroscopy of extragalactic objects" at the Astronomical Observatory and Department of Astronomy in Belgrade. The presented results of the LoTeRM campaign of type 1 AGNs include: i) a creation of homogeneous sample of very long (10+ years) light curves, which specific feature is that they come from type 1 AGN of different spectral properties and variability, ii) a developed 2DHybrid tool for the detection of the periodic oscillations in AGNs and analysis of the underlying dynamics, iii) a capture of the changing look transition in type 1 AGNs. These findings may have an application and impact to future large surveys, such as the LSST or MSE, which key-science projects will be the investigations of quasar variability. Our group is actively contributing to the development of the LSST and MSE as members of respective Science Collaborations. Through these investigation, many tools and techniques are being developed in preparation for these and other future vast surveys.

Acknowledgments.

This paper is devoted to Dr. Alla I. Shapovalova, Research Professor of the Special Astrophysical Observatory of the Russian Academy of Science, who sadly passed away beginning of 2019. She was a pioneer in the field of AGN spectral observation and analysis, and the great inspiration to the monitoring of AGN and studies of its variability. We acknowledge the financial support of the Ministry of Education, Science and Technological Development of the Republic of Serbia through contracts no. 451-03-68/2020-14/200104 (DI, AK, LČP) and 451-03-68/2020-14/20002 (LČP).

References

Ahumada, R., Prieto, C. A., Almeida, A. et al.: 2020, *ApJS*, **249**, 3.
Afanasiev, V. L., Popović, L. Č., Shapovalova, A. I.: 2019, *MNRAS*, 482, 4985.
Andrillat, Y., Souffrin, S.: 1968, *ApJL*, **1**, 111.
Antonucci, R. R. J., Miller, J. S.: 1985, *ApJ*, **297**, 621.
Gravity Collaboration, Amorim, A., Bauböck, M., Brandner ,W., Bolzer, M., Clénet, Y., Davies, R. et al.: 2021, arXiv, arXiv:2102.00068
Gravity Collaboration, Amorim, A., Bauböck, M., Brandner, W., Clénet, Y., Davies, R., de Zeeuw, P. T. et al.: 2020, *A&A*, **643**, A154.
Bentz, M. C., Denney, K. D., Grier, C. J. et al.: 2013, *ApJ*, **767**, 149.
Bentz, M. C., Katz, S.: 2015, *PASP*, **127**, 67.
Bentz, M. C., Peterson, B. M., Netzer, H., Pogge, R. W., Vestergaard, M.: 2009, *ApJ*, **697**, 160.
Blandford, R. D., McKee, C. F.: 1982, *ApJ*, **255**, 419.
Bon, E., Jovanović, P., Marziani, P. et al.: 2012, *ApJ*, **759**, 118.
Bon, E., Zucker, S., Netzer, H. et al.: 2016, *ApJS*, **225**, 29.
Brandt, W. N., Ni, Q., Yang, G., Anderson, S. F. et al.: 2018, arXiv181106542B
Cho, H., Woo, J.-H., Hodges-Kluck, E. et al.: 2020, *ApJ*, **892**, 93.

Denney, K. D., De Rosa, G., Croxall, K. et al.: 2014, *ApJ*, **796**, 134.
Djorgovski, S. G., Graham M. J., Donalek C., Mahabal A. A., Drake A. J., Turmon M., Fuchs T.: 2016, arXiv:1601.04385
Drake, A. J., Djorgovski, S. G., Mahabal, A. et al.: 2009, *ApJ*, **696**, 870.
Eisenhauer, F.: 2019, The Very Large Telescope in 2030, 30.
Gaskell, C. M., Sparke, L. S.: 1986, *ApJ*, **305**, 175.
Graham, M. J.: 2019, *IAUS*, **339**, 147.
Graham, M. J., Djorgovski, S. G., Drake, A. J. et al.: 2017, *MNRAS*, **470**, 4112.
Graham, M. J., Djorgovski, S. G., Stern, D. et al.: 2015, *Nature*, **518**, 74.
Hickox, R. C., Alexander D. M.: 2018, *ARA&A*, **56**, 625.
Hönig, S. F., Kishimoto, M.: 2017, *ApJL*, **838**, L20.
Ilić, D., Oknyansky, V., Popović, L. Č. et al.: 2020, *A&A*, **638**, 13.
Ilić, D., Shapovalova, A. I., Popović, L. Č. et al.: 2017, *FrASS*, **4**, 12I.
Ivezić, Ž., Kahn, S. M., Tyson, J. A. et al.: 2019, *ApJ*, **873**, 111.
Jones, L., Yoachim, P., Ivezic, Z. et al.: 2020, AAS/Division for Planetary Sciences Meeting Abstracts.
Jonić, S., Kovačević-Dojčinović, J., Ilić, D., Popović, L. Č.: 2016, *Ap&SS*, **361**, 101.
Jovanović, P., Popović, L. Č., Stalevski, M. et al.: 2010, *ApJ*, **718**, 168.
Kovačević, A., Ilić, D., Popović, L. Č. et al.: 2021, *in preparation.*
Kovačević, A. B., Pérez-Hernández, E., Popović, L. Č., Shapovalova, A. I., Kollatschny, W., Ilić, D.: 2018, *MNRAS*, **475**, 2051.
Kovačević, A. B., Popović, L. Č., Ilić, D.: 2020a, *Open astronomy*, **29**, 51.
Kovačević, A. B., Popović, L. Č., Shapovalova, A. I., Ilić, D.: 2017, *Ap&SS*, **362**, 31.
Kovačević, A. B., Popović, L. Č., Simić, S., Ilić, D.: 2019, *ApJ*, **871**, 32.
Kovačević, A. B., Popović L. Č., Shapovalova A. I., Ilić D., Burenkov A. N., Chavushyan V. H.: 2014, *AdSpR*, **54**, 1414.
Kovačević, A. B., Popović L. Č., Shapovalova A. I., Ilić D., Burenkov A. N., Chavushyan V. H.: 2015, *JApA*, **36**, 475.
Kovačević A. B., Yi T., Dai X., Yang X., Čvorović-Hajdinjak I., Popović L. Č.: 2020b, *MNRAS*, **494**, 4069.
Li, Y.-R., Wang, J.-M., Ho, L. C. et al.: 2016, *ApJ*, **822**, 4.
Liu, T., Gezari, S., Coleman Miller, M.: 2018, *ApJL*, **859**, L12.
MacLeod, C. L., Ross, N. P., Lawrence, A. et al.: 2016, *MNRAS*, **457**, 389.
Malygin, E., Uklein, R., Shablovinskaya, E., Grokhovskaya, A., Perepelitsyn, A.: 2020, *CoSka*, **50**, 328.
Mejía-Restrepo, J. E., Lira, P., Netzer, H., Trakhtenbrot, B., Capellupo, D. M.: 2018, *NatAs*, **2**, 63.
MSE Science Team: Babusiaux, C., Bergemann, M., Burgasser, A. et al.: 2019, arXiv:1904.04907
Ofek, E. O., Soumagnac, M., Nir, G., Gal-Yam, A., Nugent, P., Masci, F., Kulkarni, S. R.: 2020, *MNRAS*, **499**, 5782.
Oknyansky, V. L., Gaskell, C. M., Huseynov, N. A. et al.: 2017, *MNRAS*, **467**, 1496.
Oknyansky, V. L., Winkler, H., Tsygankov, S. S. et al.: 2019, *MNRAS*, **483**, 558.
Peterson, B. M.: 2001, *Advanced Lectures on the Starburst-AGN*, 3.
Peterson, B. M.: 2004, *IAUS*, **222**, 15.
Popović, L. Č.: 2012, *NewAR*, **56**, 74.
Popović, L. Č.: 2020, *OAst*, **29**, 1P.
Popović, L. Č., Kovačević-Dojčinović, J., Marčeta-Mandić, S.: 2019, *MNRAS*, **484**, 3180.
Popović, L. Č., Shapovalova, A. I., Ilić, D. et al.: 2011, *A&A*, **528**, 130.
Popović, L. Č., Simić, S., Kovačević, A. et al.: 2021, *MNRAS*, accepted, arXiv:2105.09061.
Runco, J. N., Cosens, M., Bennert, V. N. et al.: 2016, *ApJ*, **821**, 33.
Shapovalova, A. I., Burenkov, A. N., Carrasco, et al.: 2001, *A&A*, **376**, 775.
Shapovalova, A. I., Doroshenko, V. T., Bochkarev, et al.: 2004, *A&A*, **422**, 925.
Shapovalova, A. I., Popović, L. Č., Afanasiev, V. L.: 2019, *MNRAS*, **485**, 4790.
Shapovalova, A. I.; Popović, L. Č., Bochkarev, N. G.: 2009, *NewAR*, **53**, 191S.
Shapovalova, A. I., Popović, L. Č., Burenkov, A. N. et al.: 2010a, *A&A*, **517**, 42.
Shapovalova, A. I., Popović, L. Č., Burenkov, A. N. et al.: 2010b, *A&A*, **509**, 106.
Shapovalova, A. I., Popović, L. Č., Burenkov, A. N. et al.: 2012, *A&ASS*, **202**, 10.

Shapovalova, A. I., Popović, L. Č., Burenkov, A. N. et al.: 2013, *A&A*, **559**, 10.
Shapovalova, A. I., Popović, L. Č., Chavushyan, V. H. et al.: 2016, *ApJS*, **222**, 25.
Shapovalova, A. I., Popović, L. Č., Chavushyan, V. H. et al.: 2017, *MNRAS*, **466**, 4759.
Shapovalova, A. I., Popović, L. Č., Collin, S. et al.: 2008, *A&A*, **486**, 99.
Shen, Y., Anderson, S., Berger, E. et al.: 2019, Bulletin of the American Astronomical Society, 51, 3, 274, Science White Paper for the US Astro 2020 Decadal Survey.
Shen, Y., Grier, C. J., Horne, K., Brandt, W. N., Trump, J. R., Hall, P. B., Kinemuchi, K. et al.: 2019, *ApJL*, **883**, L14.
Simić, S., Popović, L. Č.: 2016, *Ap&SS*, **361**, 59.
Songsheng, Y.-Y., Li, Y.-R., Du, P. et al.: 2021, *ApJS*, **253**, 57.
Stalevski, M., Asmus, D., Tristram, K. R. W.: 2017, *MNRAS*, **472**, 3854.
Stalevski, M., Tristram, K. R. W., Asmus, D.: 2019, *MNRAS*, **484**, 3334.
Gravity Collaboration, Sturm, E., Dexter, J., Pfuhl, O., Stock, M. R., Davies, R. I., Lutz, D. et al.: 2018, *Nature*, **563**, 657.
Sulentic, J. W., Marziani, P., Dultzin-Hacyan, D.: 2000, *ARA&A*, **38**, 521.
Urry, C. M., Padovani, P.: 1995, *PASP*, **107**, 803.
Wang J.-M., Bon, E.: 2020, *A&A*, **643**, L9.
Wang, J.-M., Du, P., Brotherton, M. S., Hu, C., Songsheng, Y.-Y., Li, Y.-R., Shi, Y. et al.: 2017, *NatAs*, **1**, 775.
Wang, J.-M., Songsheng, Y.-Y., Li, Y.-R. et al.: 2020, *NatAs*, **4**, 517.
Woo, J.-H., Cho, H., Gallo, E., Hodges-Kluck, E., Le, H. A. N., Shin, J., Son, D. et al.: 2019, *NatAs*, **3**, 755.

Publ. Astron. Obs. Belgrade No. 100 (2021), 107 - 114 *Invited Lecture*

WIND MODELS OF MASSIVE STARS AND MASS-LOSS RATES DETERMINATION

J. KUBÁT and B. KUBÁTOVÁ
Astronomický ústav, Akademie věd České republiky, 251 65 Ondřejov, Czech Republic
E–mail: kubat@sunstel.asu.cas.cz

Abstract. Determination of mass-loss rates of massive stars is an important output of massive star analysis, which influences our understanding of stellar evolution. Stellar mass-loss rates are usually determined using wind models with a different level of sophistication. Commonly used models are based on an assumption of spherical symmetry and solve the NLTE radiative transfer consistently for a given density and velocity structure, which means that the hydrodynamic structure is held fixed. Usually, an approximate dependence of velocity on radius is being assumed (the so-called β-velocity law). Using a different approach, mass-loss rates can be predicted by hydrodynamic models, which do not solve the radiative transfer, but they describe the radiation force in a parametric way (using force multipliers). The most sophisticated wind models do not use the simplifications of the β-velocity law and the force multlipliers. Consistent NLTE wind models including both the wind dynamics and NLTE radiative transfer can be calculated.

1. INTRODUCTION

The large luminosity, short life, and final supernova explosions of massive stars make them an important source of heating and ionization of interstellar medium, as well as they provide kinetic energy via their outflows. Their importance is not diminished by the fact that they are rare, they form a small but important fraction of the stellar population visible even at large distances.

The main task of the quantitative spectroscopy of massive stars is a determination of the stellar mass M_*, stellar radius R_*, stellar luminosity L_*, chemical composition (abundances α_k for each element k) and of wind parameters, namely the terminal wind velocity v_∞ and mass-loss rate $\mathrm{d}M/\mathrm{d}t = \dot{M}$ for each studied star. The mass-loss rate is of a particular importance. Besides its direct effect of lowering the stellar mass, it is also an important input parameter for stellar evolution codes. It can not be measured directly, its determination relies on wind models, which are briefly discussed in this paper.

2. MASS-LOSS RATE DETERMINATION AND WIND MODELLING

Unlike terminal wind velocity (v_∞) measurement, which is relatively straightforward and can be done by direct measurement of the position of the blue edge of the P-Cygni line profile (see, e.g. Lamers & Cassinelli, 1999), direct mass-loss rate determination

is not possible. Wind mass-loss rate is being determined indirectly, by comparison of model predicted spectra with observed ones. If the spectra match, then the mass-loss rate used in calculation of the theoretical spectrum is attributed to the star. However, since the problem is complicated, approximations have to be used in wind model calculations and theoretical spectra predictions.

Because of high complexity of the problem, simplifying assumptions considered as 'standard' ones are being used. The winds are assumed to be stationary and spherically symmetric consisting of homogeneous spherical shells, which means that 1-D models are being solved. In addition, a core-halo approximation is often being used. This means that the wind region is considered as a shell around a star with a photospheric radiation as a lower boundary condition and with no back influence of the wind region on the stellar photosphere. The inclusion of a quasi-hydrostatic lower part of the model atmosphere improved the situation.

Wind models are calculated assuming basic stellar parameters (M_*, R_*, L_*, and Z) with the final goal to predict emergent radiation and compare it with observations. A 1-D spherically symmetric wind model can be considered as a dependence of a set of wind describing structural quantities on the radial coordinate r. These involve temperature T, mass density ρ, radial velocity v, atomic level populations (number densities) n_i (i stands for the level index), and the radiation field for each frequency, represented here by its specific intensity $I(\nu)$. In some cases, some of the radius dependences or additional parameters (e.g., $\dot{M}$) are assumed in order to simplify and speed up the process of model calculations. The final step of modelling is comparison with observations. This can be done only by comparison of emergent radiation from the model with observed radiation from the stellar source. If both match, the parameters used for calculation of a model, and both assumed and calculated structural quantities are attributed to the stellar source.

Let us describe several options used in modelling winds and mass-loss rate determination. Note that the division presented here is rough and methods that do not exactly fit to our classification categories may exist.

Formal solution of the radiative transfer equation. This is a solution of the radiative transfer equation for given opacity end emissivity (see Hubeny & Mihalas 2015). In the case of wind modelling it means that all structural quantities except the radiation field are given (i.e. assumed). This implies that also the mass-loss rate is given. The level populations are also given, either they are determined using a simple nebular model (e.g. Kraus et al. 2000) or the local thermodynamic equilibrium (LTE) is assumed. The latter assumption is used for calculation of the emergent radio flux from the outermost parts stellar winds (Panagia & Felli 1975, Wright & Barlow 1975), which can be then compared with radio observations to determine $\dot{M}$.

In optically thin media, absorption is usually considered in a simplified manner or is it neglected.

NLTE wind models. If the structure is given and LTE is not an acceptable assumption (which is always in massive star winds), we have to solve for the level populations, which have to be determined consistently with the radiation field. In this case we assume $T(r)$, $\rho(r)$, and $v(r)$ as given and seek solution for $I(\nu, r)$ and $n_i(r)$ by simultaneous solution of the radiative transfer equation and kinetic equilibrium equations. This type of model is usually referred to as the NLTE line formation problem.

In a generalized NLTE line formation problem the mass density is not assumed arbitrarily, but it is calculated from given $v(r)$ and $\dot{M}$ using the continuity equation. The velocity field is usually assumed in the form of a β-velocity law, which can be written as (β is a free parameter)

$$v(r) = v_\infty \left(1 - \frac{R_*}{r}\right)^\beta . \tag{1}$$

This implies that v_∞ has to be assumed as well. Then the equations of kinetic equilibrium together with the radiative transfer equation (the above mentioned NLTE line formation problem) have to be solved to determine the emergent radiation.

Alternatively also $T(r)$ can be determined together with the solution of the NLTE line formation problem by adding the equation of radiative equilibrium or the thermal balance equation to the set of simultaneously solved equations.

Full radiation hydrodynamics (stationary) models. The ideal case for modelling is to solve for all structural variables mentioned at the beginning of this section. This means to solve the continuity equation, equation of motion, radiative transfer equation, the kinetic (statistical) equilibrium equations, and the energy equation to obtain the structure of the mass density $\rho(r)$, velocity $v(r)$, radiation field $I(\nu, r)$, level populations $n_i(r)$, and temperature $T(r)$, ideally simultaneously. To our knowledge, there is currently no code which does such full solution without fixing any of the structural variables. However, several codes use some simplifications or iterative schemes to obtain the full stationary RHD solution, and are on their way towards the full solution. A more detailed description of these models is in the Section 6.

Hydrodynamic wind models with a parametric radiation force. The last type of models we mention here does not allow a direct comparison with observations, as the radiation field is not an output of such models, rather it is used as an input to calculate the radiation force necessary to drive the line driven wind. An option to determine the radiation force in a parametric way is frequently used. This option implicitly means that both the radiation field and level populations are assumed, and the hydrodynamic equations (continuity equation, equation of motion, and sometimes also the energy equation) are solved to detemine mass density and velocity (and sometimes the temperature structure). These models are described in the Section 3.

3. HYDRODYNAMIC WIND MODELS

The task of hydrodynamic wind modelling is to obtain a solution of stationary hydrodynamic equations for given basic stellar parameters (M_*, R_*, L_*, and α_k). Hydrodynamic models seek solution of the continuity equation (which determines the mass-density ρ)

$$\frac{\mathrm{d}\left(r^2 \rho v\right)}{\mathrm{d}r} = 0, \tag{2}$$

equation of motion (which determines the radial velocity v)

$$\rho v \frac{\mathrm{d}v}{\mathrm{d}r} = -\frac{\mathrm{d}p}{\mathrm{d}r} - \frac{GM_*\rho}{r^2} + g_{\mathrm{rad}} \tag{3}$$

(p is the gas pressure, G is the gravitational constant, and g_{rad} is the radiation force density), and sometimes also the energy equation (which determines the temperature T). Alternatively, a prescribed $T(r)$ or its constant value is used.

The key quantity in hydrodynamic equations of a radiatively driven stellar wind is the radiation force density. It is caused by radiation-matter interaction and it accelerates the stellar wind. It is given by the integral (Hubeny & Mihalas, 2015, Eq. 11.50)

$$\vec{g}_{\rm rad} = \frac{1}{c}\int_0^\infty {\rm d}\nu \oint {\rm d}\omega\, \vec{n}\,[\chi(\nu,\vec{n})I(\nu,\vec{n}) - \eta(\nu,\vec{n})]\,. \tag{4}$$

which clearly describes the fact that $\vec{g}_{\rm rad}$ may be large if both opacity and radiation flux are large. It can be split to the radiative force caused by radiation-matter interaction in continuum transitions (ionization, free-free transitions, and continuum scattering) $\vec{g}_{\rm rad,C}$, and to the radiative force caused by absorption and scattering in spectral lines $\vec{g}_{\rm rad,L}$. The latter is calculated as a sum of the radiation force caused by individual line transitions, $\vec{g}_{\rm rad,L} = \sum_{\rm lines} \vec{g}_{{\rm rad},l}$. Then

$$\vec{g}_{\rm rad} = \vec{g}_{\rm rad,C} + \sum_{\rm lines} \vec{g}_{{\rm rad},l}. \tag{5}$$

The detailed calculation of the line radiation force is quite time-consuming and complicated, since the radiation force in each line depends on corresponding atomic level populations, which have to be obtained by solution of kinetic equilibrium equations for each element considered. This is why approximations are used. The most common approximation of the line radiation force (the so-called CAK approximation) was introduced in first hydrodynamic wind models (Castor, Abbott, Klein 1975; Abbott 1982) and later modified by Gayley (1995). The radiation force in this approximation is expressed with the help of parameters (also referred to as force multipliers) k (or Q), α, and δ (for a more detailed description, see, e.g., Hubeny & Mihalas 2015, Section 20.3). These parameters offer a simple approximation of the radiation force. They can be determined by detailed calculation of the line opacity (e.g., Abbott 1982). This is usually done only for a restricted set of stellar parameters.

Using this simplified description of the influence of radiation on stellar wind, hydrodynamic wind codes calculate the model hydrodynamical structure (depth dependence of structural variables on radius). As a part of the output, they also predict values of v_∞ and $\dot{M}$. The latter quantity is usually referred to as the *predicted mass-loss rate*. Hydrodynamic wind models do not offer emergent spectrum.

Hydrodynamic wind modelling was initiated by seminal works of Castor et al. (1975), Abbott (1980), and Pauldrach et al. (1986). Later the stationary hydrodynamic codes gradually incorporated the radiative transfer solution to improve the parametric treatment of the radiative force. However, parametric description of the radiative force is still used in time dependent hydrodynamic simulations of stellar winds (e.g. Owocki 2011, and references therein).

4. NLTE WIND MODELS

NLTE wind models assume the hydrodynamic wind velocity structure, which usually has the form of the β-velocity law (1) for the radial velocity component. Note that this law with $\beta = 0.5$ was derived by Chandrasekhar (1934) assuming that the wind driving force was proportional to gravity. Knowing $v(r)$, the mass density $\rho(r)$ is calculated from the continuity equation (2) using the assumed value of the mass-loss

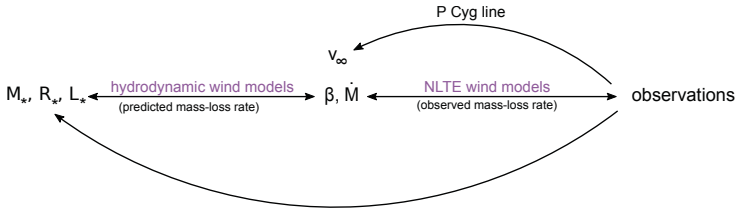

Figure 1: The scheme of stellar (M_*, R_*, L_*) and wind (v_∞, $\dot{M}$) parameters determination using independent NLTE wind models and hydrodynamic wind models.

rate $\dot{M}$. Then the equations of radiative transfer and kinetic equilibrium are solved simultaneously to obtain consistent values of level populations and radiation filed. This solution can be accompanied with a solution of an energy equation (radiative equilibrium or thermal balance) to determine temperature.

Typical representants of this modelling are codes `PoWR` (e.g. Hamann & Gräfener 2004), `FASTWIND` (e.g. Santolaya-Rey et al. 1997, Puls et al. 2005), and `CMFGEN` (e.g. Hillier & Miller 1998). In these codes, the dependence $v(r)$ is assumed, either in the form of the β-velocity law (1) or a more involved relation using two free β-like parameters (the double-β velocity law). Also the stellar mass-loss rate $\dot{M}$ is assumed. Then a full NLTE line formation problem is solved, which also predicts the emergent radiation spectrum. Note that the back influence of radiation changes on wind acceleration is typically not considered. The emergent spectrum is then compared with observations. If both spectra match with sufficient accuracy, the assumed value $\dot{M}$ is then referred to as the *observed mass-loss rate*.

5. OBSERVED AND PREDICTED MASS-LOSS RATES

The two ways of modelling mentioned in preceding sections (3 and 4) offer two values of mass-loss rates, namely the "predicted mass-loss rate" and the "observed mass-loss rate". If both values match, it is usually considered as the match of theory and observations. This situation is schematically depicted in the Fig. 1. Note that the observed mass-loss rate is in fact based on a hydrodynamically simplified model, so instead of match of observations and theory it is rather a match of the approximate hydrodynamic model with exact radiative transfer and exact hydrodynamic model with approximate radiative transfer.

6. FULL RADIATION HYDRODYNAMICS NLTE WIND MODELS

The drawbacks of the mass-loss rate determination mentioned in the preceding section are removed when full radiative hydrodynamic NLTE models are used. This means that for given M_*, L_*, R_*, Z a solution of the continuity equation, equation of motion, energy equation, radiative transfer equation, and kinetic equilibrium equations is performed to obtain $I(\nu, r)$, $n_i(r)$, $\rho(r)$, $v(r)$, and $T(r)$. This full solution gives also the values of $\dot{M}$ as the integral of the continuity equation and v_∞ as the velocity at the outermost point of the model.

In the modelling process several common additional assumptions used in hydrodynamic (Section 3) and NLTE (Section 4) wind models can be released, mainly the parametric representation of the radiative force and the division of the atmosphere model to a photosphere and wind (i.e., the core-halo approximaton).

Line radiation force. The parametric description using force multipliers (the CAK approximation) is not used any more. Instead, a detailed full description of the line radiative force (5) is used, where contributions of all transitions are taken into account separately. The need to calculate opacities for each transition causes the necessity to calculate NLTE level populatons, since LTE is not applicable in stellar winds. This is done using the kinetic equilibrium equations, which (neglecting time and advection terms) can be expressed for the level i as

$$n_i \sum_j \left[R_{ij}(I) + C_{ij}\right] = \sum_j n_j \left[R_{ji}(I) + C_{ji}\right]$$

where the dependence of radiative rates on radiation I is emphasized. Knowing n_i, the radiation force can be calculated. An equation (4) simplified for isotropic emissivity (in the comoving frame) can be used. The pioneer in construction of this type of models was A. Pauldrach, first steps were summarized in Pauldrach et al. (1994). This work was extended in Pauldrach et al. (2001) and applied to wind modeling of ζ Pup in Pauldrach et al. (2012). An independent modeling method that includes consistent calculation of radiation force was developed by Krtička & Kubát (2004), who used Sobolev approximation for line force calculation, later replaced by CMF radiation transfer (Krtička & Kubát, 2010).

Photosphere. The core-halo approximation splits the expanding stellar atmospheres to two parts, namely the hydrostatic photopshere and the wind above it. Using this assumption the photospheric radiation is considered as a lower boundary condition for the wind model. The influence of the wind part on the photosphere (wind blanketing, Abbott & Hummer, 1985) is not taken into account. As a drawback, there is usually no smooth transition from the photosphere to the wind.

Relaxing the core-halo approximation means that the almost static photosphere becomes an integral part of the model. The wind model starts already at large optical depths where the diffusion approximation is valid and the transition from the photosphere to the wind is smooth. First attempts to consistently remove the artificial splitting were done in an approximate way by Gabler at al. (1989).

Global NLTE wind models. Krtička & Kubát (2010, 2017, 2018) presented a method to solve all the above mentioned equations while relaxing the core-halo and parameterized line force assumptions. The chemical composition of the wind is arbitrary and no force multipliers are used. In their code the radiation force is calculated using actual level populations obtained by solution of kinetic equilibrium equations. The radiation field, which enters these equations is calculated in a slightly simplified way, the continuum radiative transfer is solved exactly (as it is practically the same as in the static case) and the line transfer is solved using the Sobolev approximation. The line radiation force is calculated using the radiation field obtained by a CMF solution of the radiative transfer, which improves the previously used Sobolev radiative transfer solution. The photosphere-wind transition is smooth. Application of the global wind models to stars from our Galaxy (Krtička & Kubát, 2017) and Magellanic Clouds (Krtička & Kubát, 2018) showed that the mass-loss rates obtained using global models are lower than the commonly used values of Vink et al. (2001). The latter were obtained using a detailed Monte Carlo evaluation of the driving force for given $v(r)$.

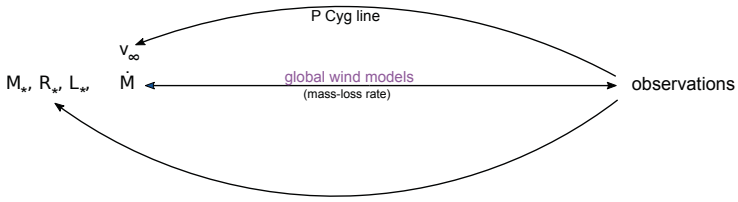

Figure 2: The scheme of stellar (M_*, R_*, L_*) and wind (v_∞, $\dot{M}$) parameters determination using full radiative hydrodynamic NLTE wind models.

Recently, NLTE wind modeling codes mentioned in the section 4 were also improved to include hydrodynamic solutions as a part of modelling (e.g. `PoWR`, Gräfener & Hamann, 2005; Sander et al., 2017; `FASTWIND`, Sundqvist et al., 2019).

Improved velocity law. An important aspect of the velocity structure obtained from the full radiation hydrodynamic NLTE wind model is that it differs from the commonly used β-velocity law (1). A more reliable analytical description of the velocity structure can be obtained using the polynomial expansion, $v(r) = \sum_{i=0}^{3} \tilde{v}_i \tilde{P}_i(1 - R_*/r)$, using Legendre polynomials $\tilde{P}_i$ and fitting coefficients $\tilde{v}_i$ (see Krtička & Kubát, 2011). A similar improved formula

$$v(r) = \sum_{i=1}^{2} \tilde{v}_i \left(1 - \gamma \frac{R_*}{r}\right)^i , \tag{6}$$

($\tilde{v}_i$ and γ are fitting parameters) was used to fit the calculated model velocity structure obtained by Krtička et al. (2021) for B supergiants.

Clumping. The big challenge in current methods for $\dot{M}$ determination are wind inhomogeneities (clumping), which is a 3-D phenomenon. However, currently existing unified (global) models are 1-D, and the only way to implement clumping in them is to use simplifying assumptions or parameterized methods (Sundqvist & Puls 2018, and references therein). The 3-D modelling of optically thick clumping was done only for limited spectral regions, but its effect on mass-loss rate determination was clearly shown (Šurlan et al. 2013).

7. SUMMARY AND CONCLUSIONS

The current commonly used method for mass-loss rate determination consists of two steps. First the NLTE wind models with a prescribed (β) velocity law are calculated and the "observed mass-loss rates" are determined. Then these values are verified by hydrodynamic calculations to match the "predicted mass-loss rates". This two-step determination should be replaced by full radiation hydrodynamic NLTE wind models, which offer the consistent mass-loss rate values directly (see Fig. 2). These models represent an improvement in massive star analysis. They offer a tool for more reliable modeling of atmospheres and winds of massive stars.

References

Abbott, D. C.: 1980, *Astrophys. J.*, **242**, 1183.
Abbott, D. C.: 1982, *Astrophys. J.*, **259**, 282.
Abbott, D. C., Hummer, D. G. : 1985, *Astrophys. J.*, **294**, 286.
Castor, J. I., Abbott, D. C., Klein, R. I.: 1975, *Astrophys. J.* **195**, 157.
Chandrasekhar, S.: 1934, *Mon. Not. Roy. Astron. Soc.*, **94**, 522.
Gabler, R., Gabler, A., Kudritzki, R. P., Puls, J., Pauldrach, A.: 1989, *Astron. Astrophys.*, **226**, 162.
Gayley, K. G.: 1995, *Astrophys. J.*, **454**, 410.
Gräfener, G., Hamann, W.-R.: 2005, *Astron. Astrophys.*, **432**, 633.
Hamann, W.-R., Gräfener, G.: 2004, *Astron. Astrophys.*, **427**, 697.
Hillier, D. J., Miller, D. L.: 1998, *Astrophys. J.*, **496**, 407.
Hubeny, I., Mihalas, D.: 2015, *Theory of Stellar Atmospheres*, Princeton University Press, Princeton.
Kraus, M., Krügel, E., Thum, C., Geballe, T. R.: 2000, *Astron. Astrophys.*, **362**, 158.
Krtička, J., Kubát, J.: 2004, *Astron. Astrophys.*, **417**, 1003.
Krtička, J., Kubát, J.: 2010, *Astron. Astrophys.*, **519**, A50.
Krtička, J., Kubát, J.: 2011, *Astron. Astrophys.*, **534**, A97.
Krtička, J., Kubát, J.: 2017, *Astron. Astrophys.*, **606**, A31.
Krtička, J., Kubát, J.: 2018, *Astron. Astrophys.*, **612**, A20.
Krtička, J., Kubát, J., Krtičková, I.: 2021, *Astron. Astrophys.*, **647**, A28.
Lamers, H. J. G. L. M., Cassinelli, J. P.: 1999, *Introduction to Stellar Winds*, Cambridge Univ. Press.
Owocki, S. P.: 2011, *Bulletin de la Société Royale des Sciences de Liège*, **80**, 16.
Panagia, N., Felli, M.: 1975, *Astron. Astrophys.*, **39**, 1.
Pauldrach, A., Puls, J., Kudritzki, R. P.: 1986, *Astron. Astrophys.*, **164**, 86.
Pauldrach, A. W. A., Kudritzki, R. P., Puls, J., Butler, K., Hunsinger, J.: 1994, *Astron. Astrophys.*, **283**, 525.
Pauldrach, A. W. A., Hoffmann, T. L., Lennon, M.: 2001, *Astron. Astrophys.*, **375**, 161.
Pauldrach, A. W. A., Vanbeveren, D., Hoffmann, T. L.: 2012, *Astron. Astrophys.*, **538**, A75.
Puls, J., Urbaneja, M. A., Venero, R., Repolust, T., Springmann, U., Jokuthy, A., Mokiem, M. R.: 2005, *Astron. Astrophys.*, **435**, 669.
Sander, A. A. C., Hamann, W.-R., Todt, H., Hainich, R., Shenar, T.: 2017, *Astron. Astrophys.*, **603**, A86.
Santolaya-Rey, A. E., Puls, J., Herrero, A.: 1997, *Astron. Astrophys.*, **323**, 488.
Sundqvist, J. O., Puls, J.: 2018, *Astron. Astrophys.*, **619**, A59.
Sundqvist, J. O., Björklund, R., Puls, J., Najarro, F.: 2019, *Astron. Astrophys.*, **632**, A126.
Šurlan, B., Hamann, W.-R., Aret, A., Kubát, J., Oskinova, L. M., Torres, A. F.: *Astron. Astrophys.*, **559**, A130.
Vink, J. S., de Koter, A., Lamers, H. J. G. L. M.: 2001, *Astron. Astrophys.*, **369**, 574.
Wright, A. E., Barlow, M. J.: 1975, *Mon. Not. Roy. Astron. Soc.*, **170**, 41.

Publ. Astron. Obs. Belgrade No. 99 (2021), 115 - 122 *Invited Lecture*

MODELS FOR MEASURING EXPLOSION ENERGIES AND ISM DENSITIES OF SUPERNOVA REMNANTS IN THE GALAXY

D. A. LEAHY

Dept. Physics and Astronomy, University of Calgary, Calgary, Alberta, Canada T2N 1N4
E–mail: leahy@ucalgary.ca

Abstract. Supernova remnant (SNR) models have been developed to explain the observed characteristics of SNRs, and thus to deduce their physical properties. One important part of modelling is use of hot plasma (X-ray) emission models to derive temperature and amount of shocked plasma and the SNR shock velocity. Coupled with a SNR evolution model, one can use the current state of a SNR to deduce fundamental properties of the supernova (SN) explosion. The general phases of SNR evolution are the ejecta-dominated phase, the adiabatic phase and the radiative phase. The transition phases between these are less-appreciated but at least as important, because the transition phases account for much of the total lifetime of a SNR. Progress in X-ray observations of SNRs has resulted in a significant sample of Galactic SNRs with measured X-ray spectra. We have developed spherically symmetric models over the past few years (Leahy and Williams 2017, Leahy et al. 2019) which allow inference of SNR explosion energy, circumstellar medium density and age. With detailed enough X-ray spectra, ejecta mass and whether the SN occurs in a uniform or stellar wind environment can also be determined. We have applied the models to observations of LMC SNRs (Leahy 2017) and of Galactic SNRs (Leahy and Ranasinghe 2018, Leahy et al. 2020). We find that the energy and density distributions can be well fit with log-normal distributions and that SNR birth-rates are consistent with SN rates.

1. INTRODUCTION

Various areas in astrophysics are impacted by the energy and mass input to the interstellar medium in galaxies by supernovae (SN) and their remnants (SNR). These areas include stellar evolution, the physical and chemical evolution of the interstellar medium (ISM, e.g. see Cox 2005 for a review) and the subsequent impact on star formation and evolution of galaxies. Studying SNRs is one of the best ways of measuring the kinetic energy input of SN into the ISM (Cox 2005).

SNRs are observed in radio, infrared, optical, X-ray and gamma-ray bands (see, e.g. Bandiera 2001 for a review). The radio emission is a tracer of relativistic electrons accelerated by the SNR shock, with these electrons containing <1% of the SN energy. The infrared emission is from shock heated dust and the optical line emission from small clouds of dense gas recombining behind the shock. The X-rays are from the plasma heated by the SNR shock, with temperature ∼1 keV and are a measure of the bulk energy of the SN explosion as most of the energy goes into shock heating of the gas. Gamma-rays are also from high energy particles, electrons and protons,

accelerated by the shock. The physics of X-ray emission is much better understood for SNRs than that of radio emission or gamma-ray emission. Infrared and optical emission are mostly sensitive to the amount of dust present and the properties of small dense clouds, respectively. Thus modelling X-ray emission, which depends mainly on the shock energy deposited in the hot gas, is most effective for determining SNR energies.

Historically, the observations of SNRs were made in radio and optical much before X-ray, infrared or gamma-ray observations. ∼300 SNRs have been observed in radio, with significantly fewer observed in other bands, including X-rays. Thus, only a small fraction of the SNRs in our Galaxy have previously been characterized well enough to determine their evolutionary state, including explosion type, explosion energy, and age. A number (∼10) historical SNRs have been observed in great detail and modeled with hydrodynamic simulations. E.g., Tycho has been modeled (Badenes et al. 2006) and used to test different models for SN Type Ia explosions.

However, most SNRs do not have comprehensive multi-band observations (imaging and spectra), so they not been the subject to detailed hydrodynamic modeling. Thus, the author has led a project to create an intermediate modelling approach (Leahy & Williams 2017, Leahy et al. 2019, Leahy et al. 2020). It is based on hydrodynamic simulations, but uses analytic and numerical fits (which we call semi-analytical) to create models which can be easily calculated and applied to SNRs. The goal is to apply this model to observationally less-constrained SNRs, to determine their bulk physical characteristics. When more detailed observations become available for any given SNR, full hydrodynamic modelling can be carried out to improve upon the results from the semi-analytical model.

Below, the basics of the SNR model are described in the Model section. The multiple stages of the model and the hydrodynamic simulations used to build the model are described. Application of the model to observations of SNRs are given in the Results section. The conclusions for explosions energies of SNRs and ISM densities are given in the Summary and Conclusions section.

2. MODEL OF SNR EVOLUTION

The basis of the model is to calculate quantities related to the observations that determine the evolutionary state of the SNR. We make the assumption of spherically symmetric evolution. The evolutionary state is determined by the initial conditions of the SNR and its age.

The main initial conditions are SN explosion energy (E_0), mass of ejected stellar envelope (M_{ej}), and circumstellar medium density (CSM) or ISM (n_0 or stellar wind parameter q). Secondary initial conditions which are next most important are: the density distribution of the stellar ejected envelope, the density distribution of the CSM or ISM. Tertiary initial conditions which also affect the evolution, e.g. for the strength of the line emission from the shocked gas and for equation of state of the plasma, are composition of the ejecta, composition of the CSM/ISM, the rate at which shocked ions and electrons come into equipartition, the CSM/ISM temperature and emissivity, and CSM/ISM turbulence velocity. The large number of input parameters makes construction of a universal model difficult. However many can be implemented by use of analytic approximations into the SNR model code.

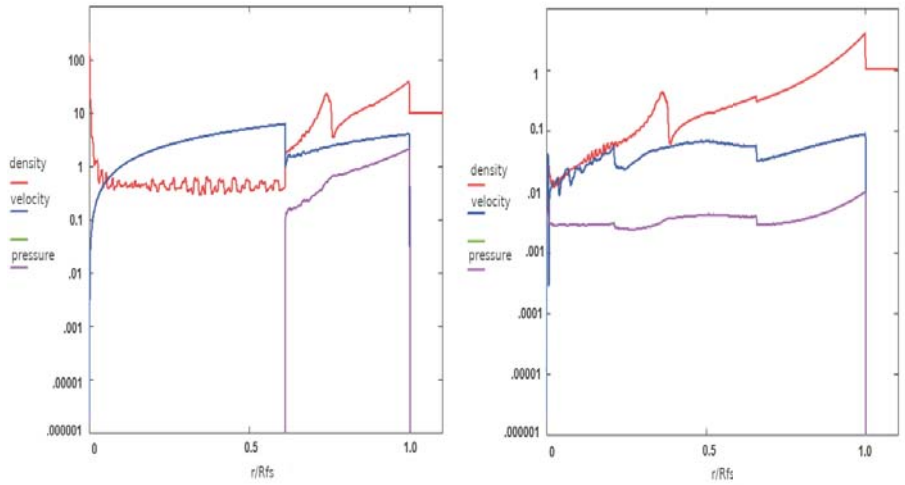

Figure 1: The interior structure of a supernova remnant for $s = 0$, $n = 8$ from hydrodynamic simulations at the characteristic times: $t/t_{\rm ch} \simeq 1$ with $R_{\rm FS}/R_{\rm ch} \simeq 1.1$ (left), and $t/t_{\rm ch} \simeq 10$ with $R_{\rm FS}/R_{\rm ch} \simeq 2.9$ (right). The density, velocity and pressure are scaled to their characteristic values, and are plotted vs. radius in units of the forward shock radius ($r/R_{\rm FS}$). The vertical axis is on log scale.

To be useful in deriving the main initial conditions (E_0, $M_{\rm ej}$, n_0 or q) and SNR age from observations, the model has to be able to predict the current observables of an SNR. These are (Leahy et al. 2019): the observed radius ($R_{\rm fs}$) of the forward shock (fs), the X-ray emission measure ($EM_{\rm fs}$) of the (fs), and the emission-measure-weighted shock temperature ($T_{\rm fs}$). In cases, in particular for young SNR, where both forward and reverse shock are observed, more information can be derived on initial and secondary initial conditions.

The early evolution, prior to radiative losses, follows a unified evolution. This is described in Truelove & McKee (1999) (hereafter TM99), where the evolution of forward and reverse shock radius and shock velocity vs. characteristic (dimensionless) time are calculated. Our models (Leahy & Williams 2017, Leahy et al. 2019, Leahy et al. 2020) all include the basic TM99 model but add calculation of EM and EM-weighted temperature of the shocked gas. Leahy & Williams (2017) calculated forward-shock (fs) emission measures ($EM_{\rm fs}$) and temperatures ($T_{\rm fs}$) for the adiabatic phase; and calculated $EM_{\rm fs}$, $T_{\rm fs}$, $EM_{\rm rs}$ and $T_{\rm rs}$ and for the early self-similar ejecta dominated (ED) phase.

Leahy et al. (2019) carried out more extensive and accurate hydrodynamic simulations than previous work. Here we show of the interior structure of the SNR in Figures 1 and 2. The emphasis here is on the late time evolution, so here we show the extension of the numerical calculations to later times, up to $t/t_{\rm ch} > 1000$. A new result found is that the reverse shock propagating through the ejecta leaves behind a peak in the density profile, where the reverse shock transitions from the ejecta envelope into the ejecta core. The peak, in contrast to expectations, expands more slowly

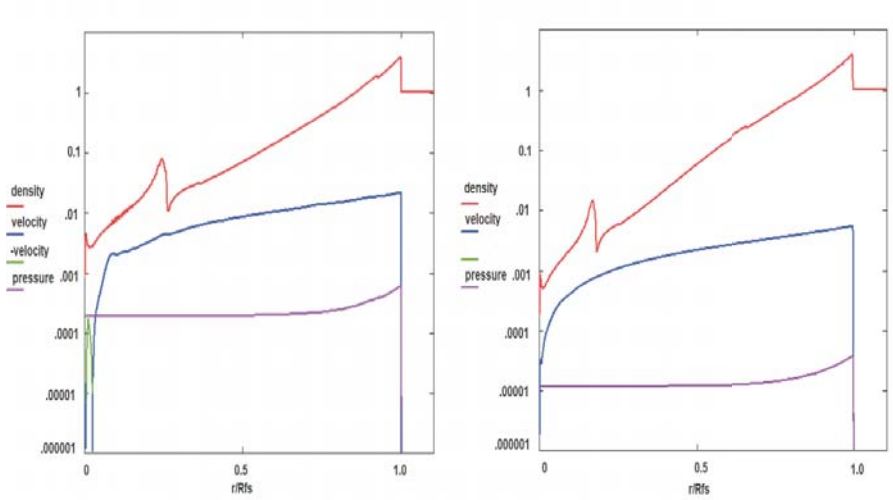

Figure 2: The interior structure of a supernova remnant for $s = 0$, $n = 8$ from hydrodynamic simulations at the characteristic times: $t/t_{\rm ch} \simeq 100$ with $R_{\rm FS}/R_{\rm ch} \simeq 7.4$ (left), and $t/t_{\rm ch} \simeq 1000$ with $R_{\rm FS}/R_{\rm ch} \simeq 19$ (right). The density, velocity and pressure are scaled to their characteristic values, and are plotted vs. radius in units of the forward shock radius ($r/R_{\rm FS}$). The vertical axis is on log scale.

than the simple prediction of homologous interior expansion. I.e. the radius of the shocked ejecta density peak, in units of the shock radius, decreases with time.

$EM_{\rm fs}$, $T_{\rm fs}$, $EM_{\rm rs}$ and $T_{\rm rs}$ were calculated by Leahy et al. (2019) directly from the hydrodynamic simulations for all SNR non-radiative stages (ED, transition ED to adiabatic, and adiabatic). E.g. Figures 6, 7 and 8 of Leahy et al. (2019) show the interior structure for the ED phase for several ejecta profiles (n= 6, 8, 10, and 12) and for constant density CSM ($s = 0$) and stellar wind profile CSM ($s = 2$). The dimensionless emission measures vs. impact parameter were shown for the above cases plus $n = 7$ and 14 in Figures 9 and 10 of Leahy et al. (2019). The complete time evolution of integrate emission measure and emission-measure-weighted temperature for both forward and reverse shocks were calculated for $s = 0$ and $s = 2$; and for each value of s all n values from 6 through 14 were calculated.

All of these results have been incorporated into the most recent release of the Python SNR modelling program SNRPy, publically available at http:\\quarknova.ca. The models include electron heating by collisions with ions, which uses the formalism of Raymond, Cox and Smith (1976).

Figures 3 and 4 here show the main panel of SNRPy, when the selected plot is radius or velocity of fs and rs vs. time. The large number of inputs available are seen on the left hand side of the graphical interface of SNRPy. Typically the rs speeds up when it enters the ejecta core, after propagating through the power-law envelope in a nearly self-similar matter. Figures 5 and 6 show EM and EM-weighted temperature of fs gas and rs gas vs. time. $EM_{\rm rs}$ decreases after the rs reaches the ejecta core, whereas $EM_{\rm fs}$ continues to increase until the SNR becomes radiative.

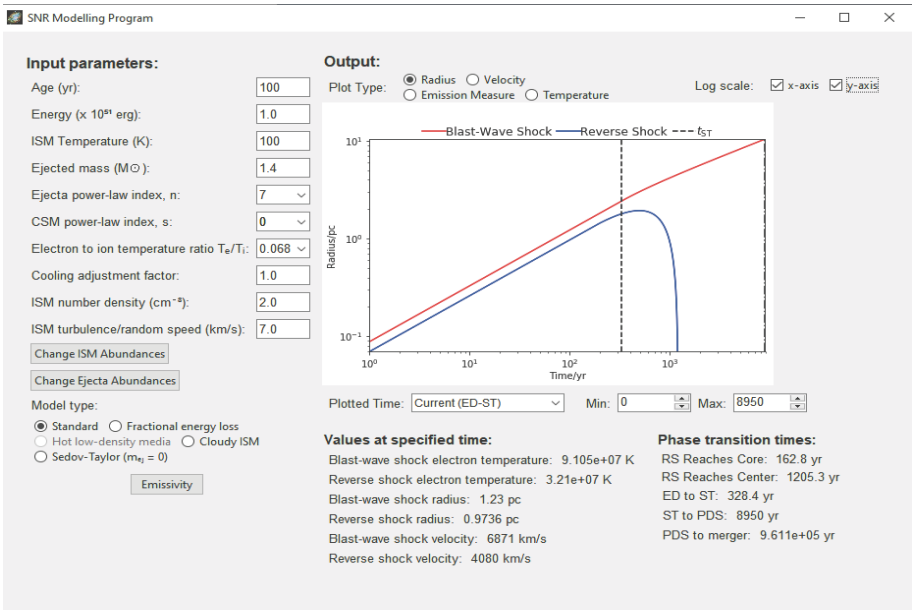

Figure 3: Screenshot of graphics interface of the SNRPy software illustrating evolution of forward and reverse shock radius vs. time. The input parameters to the model are in the left 1/3 of the panel. Output parameters are below the graph of radius vs. time.

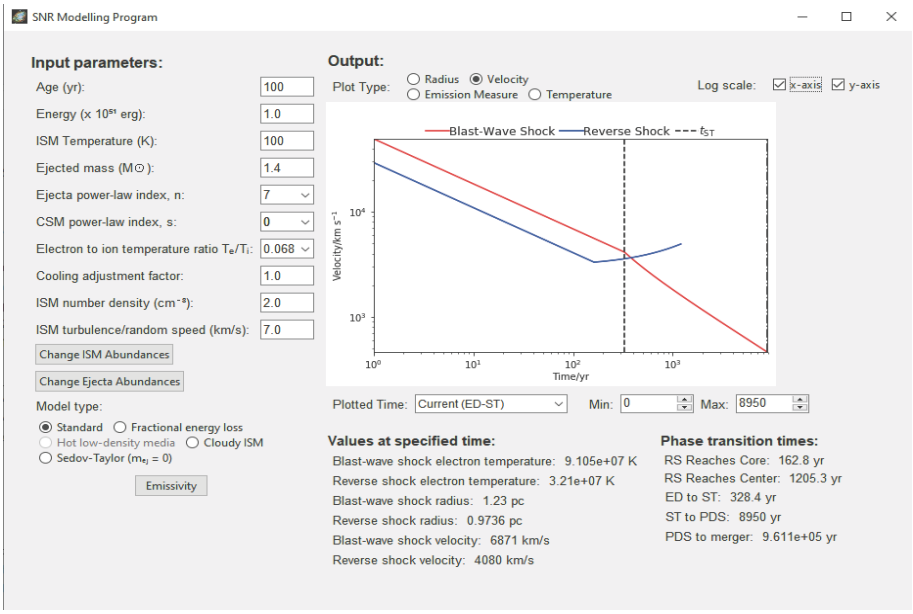

Figure 4: Screenshot of graphics interface of the SNRPy software illustrating evolution of forward and reverse shock velocity vs. time.

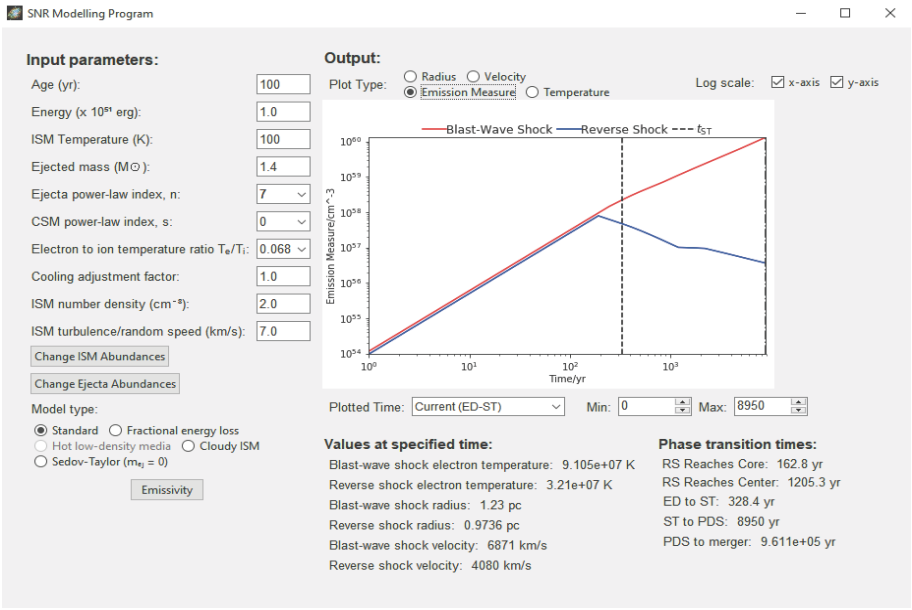

Figure 5: Screenshot of graphics interface of the SNRPy software illustrating evolution of forward and reverse shock emission measure vs. time.

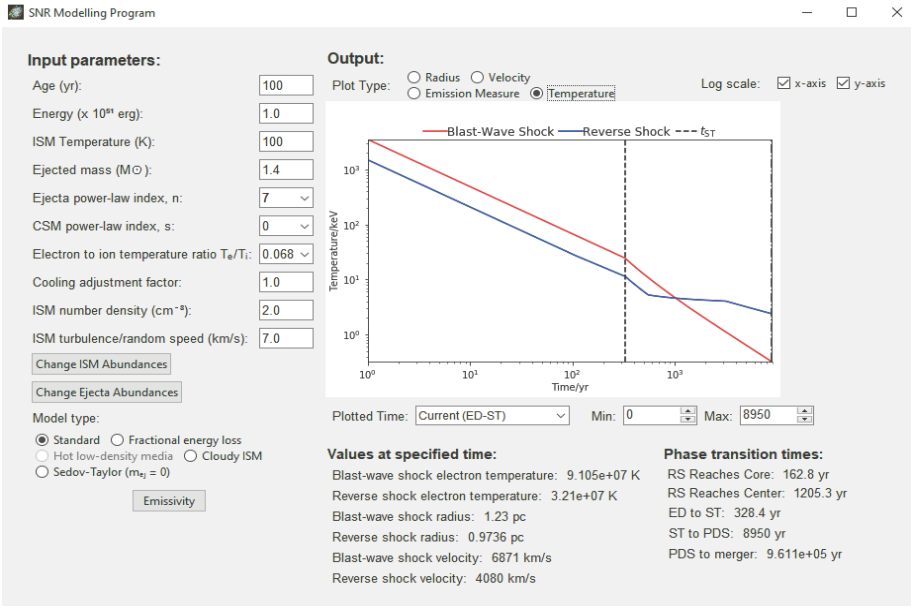

Figure 6: Screenshot of graphics interface of the SNRPy software illustrating evolution of forward and reverse shock emission-measure-weighted temperature vs. time.

3. RESULTS AND DISCUSSION

The SNR evolution model was first applied to 50 LMC SNRs with measured $R_{\rm fs}$, $EM_{\rm fs}$, $T_{\rm fs}$ (Maggi et al. 2016) by Leahy (2017). The main results were that the distribution of explosion energies (E_0) and of ISM densities (n_0) were both log-normal. A log-normal distribution is expected when a number of processes with random variables, even if each process is non-Gaussian, act in a multiplicative manner, so is not surprising in retrospect. Both the density of the ISM and the explosion process for SN are complex and involve many physical factors, with each factor have variation from location to location in the ISM, or from one SN progenitor to another. Previously it was only known that E_0 and n_0 varied from SNR to SNR. The large range of variation (about 2 orders of magnitude), the means and the shapes of the distributions for E_0, n_0) were previously unknown. The mean explosion energy was found to be 5×10^{50} erg, significantly less than the canonical explosion energy of 1×10^{51} erg, used in most simple models. This work also found the SNR birthrate for the LMC to be 1/ 500 yr, which is one of the best determinations so far.

A sample of Galactic SNRs was modelled, for the first time using emission measures and temperatures, by Leahy & Ranasinghe (2018). This work confirmed the log-normal distributions of E_0 and n_0, and that it also applied to Galactic SNRs. The mean energy and mean density for the 15 SNRs were found to be 5×10^{50} erg and 0.26 cm^{-3}, respectively. This confirmed the low mean energy of observed SNRs compared to what is usually assumed in SNR models. Table 2 of that paper also demonstrated the importance of including electron heating by ions for all derived parameters (age, E_0, and n_0).

Leahy et al. (2020) added a calculation of the inverse model, which enabled applying the rather complex model to a large number of SNRs. 43 Galactic SNRs were modelled. The sample included all SNRs, except for the historical SNRs, that had observations of the forward shock R, EM and T. These models assumed $s = 0$ and $n = 7$, in order to have the same number of output parameters (age, E_0, n_0) as input parameters. For the 7 known mixed morphology SNRs, the Cloudy ISM (White and Long 1991) model was applied as a more accurate representation, with results given in Table 3 of Leahy et al. (2020). The subset of SNRs with measurements of both forward shock and reverse shock ($R_{\rm fs}$, $EM_{\rm fs}$, $T_{\rm fs}$, $EM_{\rm rs}$ and $T_{\rm rs}$) were modelled in more detail. We note that $R_{\rm rs}$ is not measured for SNRs. In this case the extra two observed quantities constrain whether the CSM is uniform ($s = 0$) or stellar wind profile ($s = 2$) and distinguish between ejecta profiles (n). 3 of the 12 have (s, n)=(0,7), 4 have (s,n)=(2,7), and 5 have (s, n)=(2,12). Of the 12 SNRs, the 5 Type Ia all have (s, n)=(2,12), i.e. all Type Ia SNRs have occurred in a stellar wind environment.

4. SUMMARY AND CONCLUSION

Supernova remnants (SNRs) play an important role for energy and mass injection into the interstellar medium (ISM). We have developed improved models of SNRs which are readily applied to those SNRs with measured radius, forward shock (fs) emission measure ($EM_{\rm fs}$) and EM-weighted temperature ($T_{\rm fs}$) of the fs gas. These models are based on hydrodynamic simulations and cover the stages of evolution including' early ejecta-dominated (ED) phase, the non-radiative ISM dominated phase, and the long transition between the two. The forward shock radius, $EM_{\rm fs}$ and $T_{\rm fs}$ for forward-

shocked (shocked ISM) gas, and $EM_{\rm rs}$ and $T_{\rm rs}$ for reverse-shocked (rs) gas (shocked ejecta) are calculated for the full evolution.

The model allows a wide range of input parameters relevant to SN explosions. These are SN energy, ejected mass, elemental abundances of the ejecta, ejecta envelope power-law index (n), ISM power-law index (s), ISM temperature, ISM abundances, ISM turbulence velocity, and SNR age. Electron heating by Coulomb collisions is automatically included, but $T_{\rm e}/T_{\rm ion}$ can also be specified by hand. A simple prescription is used to determine when radiative losses set in (following Cioffi et al. 1988). The subsequent radiative phases are calculated according to the prescriptions in Cioffi et al. (1988), with the difference that we smoothly join the start of the radiative evolution onto the end of the adiabatic evolution by matching appropriate boundary conditions.

With the new models, we have studied 3 samples of SNRs. These are 50 SNRs in the LMC with X-ray observations (Leahy, 2017), 15 SNRs in the inner Galaxy with X-ray observations and distance determinations (Leahy & Ranasinghe 2018), and the available set at all Galactic longitudes (excluding the inner Galaxy set of Leahy & Ranasinghe 2018) of 43 Galactic SNRs with distances and X-ray observationis (Leahy et al. 2020). The results of all three analyses are compatible, although the accuracy of the SNR models has been improved between the first study (using the Leahy & Williams 2017 version) and the latest study (using the Leahy et al. 2019 version).

Generally, the explosion energy distribution follows a log-normal distribution, with mean energy $\sim 5 \times 10^{50}$ erg, and the ISM density distribution follows a log-normal distribution, with mean density depending on the SNR sample (highest for the inner Galaxy SNR sample, similar for the LMC and larger Galaxy samples). For the whole Galaxy sample (43 SNRs from Leahy et al. 2020 plus 15 SNRs from Leahy & Ranasinghe 2018) we derive a birthrate, corrected for incompleteness, of $\sim$1/35yr, which is consistent with the Galactic SN rate (Tammann et al. 1994). Future work will expand the samples which are modelled and further improve the SNR models.

Acknowledgement

This work was supported by a grant from the Natural Science and Engineering Research Council of Canada.

References

Bandiera, R.: 2001, 225 *Frontier Objects in Astrophysics and Particle Physics, eds. F. Giovannelli & G. Mannocchi*, 225.
Cioffi, D. F., McKee, C. F., Bertschinger, E.: 1988, *The Astrophysical Journal*, **334**, 252.
Cox, D. P.: 2005, *Annual Reviews of Astronomy & Astrophysics*, **43**, 337.
Leahy, D. A.: 2017, *The Astrophysical Journal*, **837**, 36.
Leahy, D. A., Williams, J. E.: 2017, *The Astronomical Journal*, **153**, 239.
Leahy, D.A., Ranasinghe, S.: 2018, *The Astrophysical Journal*, **866**, 9.
Leahy, D., Wang, Y., Lawton, B. et al.: 2019, *The Astronomical Journal*, **158**, 149.
Leahy, D. A., Ranasinghe, S., Gelowitz, M.: 2020, *The Astrophysical Journal Supplement*, **248**, 16.
Maggi, P., Haberl, F., Kavanagh, P. J. et al.: 2016, *Astronomy & Astrophysics*, 585, A162.
Raymond, J. C., Cox, D. P., Smith, B. W.: 1976, *The Astrophysical Journal*, **204**, 290.
Tammann, G. A., Loeffler, W., Schroeder, A.: 1994, *The Astrophysical Journal Supplement*, **92**, 487.
Truelove, J. K., McKee, C. F.: 1999, *The Astrophysical Journal Supplement*, **120**, 299.
White, R. L., Long, K. S.: 1991, *The Astrophysical Journal*, **373**, 543.

Publ. Astron. Obs. Belgrade No. 100 (2021), 123 - 130 *Invited Lecture – special session "The gravitational-wave Universe" supported by COST Action CA16104*

SUPERMASSIVE BLACK HOLE GROWTH AND GRAVITATIONAL WAVE RADIATION

M. MICIC

Astronomical Observatory, Volgina 7, 11000 Belgrade, Serbia
E–mail: micic@aob.rs

Abstract. Supermassive black holes (SMBH) with masses $10^6 - 10^{10} M_\odot$ exist at the centres of all massive galaxies (both late and early type). They form through mergers and gas accretion very early. Mostly at redshift z $\sim$ 2 - 3. But some of them form short after the formation of the first galaxies as early as z $\sim$ 7. The time available for their formation is so short that we still do not know about the properties of the seed black holes from which SMBH forms. Two competing theories are: formation from the mergers of POP III remnants, $\sim 10^2 - 10^3 M_\odot$ BHs, or, formation of the massive BHs directly collapsed from the gas cloud into $\sim 10^4 - 10^5 M_\odot$ BHs. Both theories assume gas accretion episodes between and after BH mergers. While POP III seeds model struggles to find mechanism behind the necessary super Eddington accretion, collapse model has a problem with explaining accretion at Eddington ratio for hundreds of millions of years. Since merger histories of black holes in these two models are very different, gravitational wave radiation from BHs mergers will be a powerful method for distinguishing between these two SMBH formation models. Here we review the latest results from the works on both theories and the results on the gravitational wave radiation from BH mergers expected to be detected by Laser Interferometer Space Antenna (LISA).

1. INTRODUCTION

The subject of supermassive black hole (SMBH) growth has been very controversial and the proposed scenarios are many. Two of them stand out and they have been the most popular ones for the last two decades. However, even the most popular models face a lot of problems. That is why Laser Interferometer Space Antenna (LISA, www.lisamission.org) will be crucial to distinguish between these growth models.

1. 1. SMBH GROWTH SCENARIOS

Figure 1 is taken from Smith & Bromm 2019, and it shows two most popular competing scenarios, SMBH grows from stellar remnant black holes, or through the direct collapse of the gas cloud into a supermassive black hole. Another popular model is runaway mergers in stellar cluster but this can be viewed as a subclass of the direct collapse model, where instead of collapsing entire gas cloud into a supermassive star, it fragments first, and then stars merge to form a supermassive star. So what are these scenarios competing for?

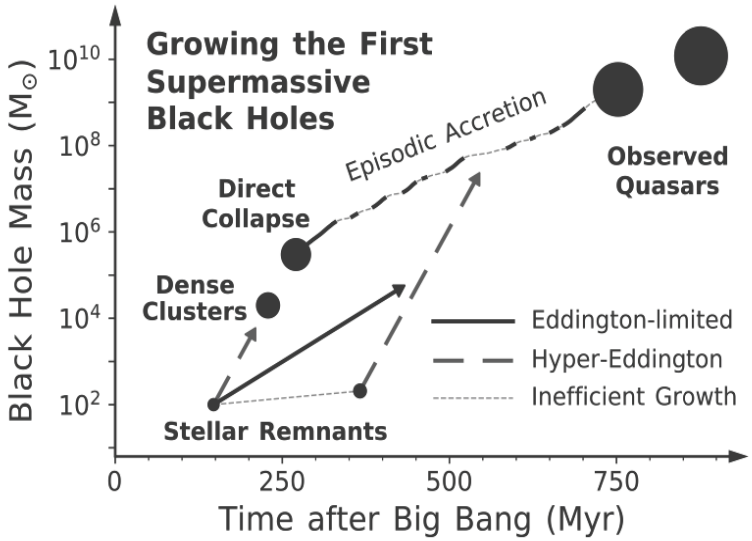

Figure 1: Black hole mass as a function of time after Big Bang. Plot shows three black hole growth models. Stellar remnant model where black holes grow through episodes of Hyper Eddington and Eddington limited gas accretion; Direct collapse model where black hole grows through episodes of Eddington limited gas accretion; and runaway mergers in stellar clusters. Taken from Smith & Bromm 2019.

They are competing to explain how to form a billion $M_\odot$ black hole at redshift z=7. This is so early in the formation of the Universe that special conditions are required no matter which growth scenario is considered. In essence, there is simply not enough time for black hole to grow. If we assume Eddington limited accretion (accretion at the rate of Eddington ratio of 1), then it would take hundreds of millions of years to sustain this kind of accretion to reach supermassive range for black holes. This is unlikely, considering the violent environment of the first galaxies. If we assume so called super-Eddington accretion with Eddington ratio between 1 and 10, then the amount of time necessary for a black hole to accrete, reduces. And even more in the case of hyper-Eddington accretion at Eddington ratio larger than 10, for which we do not know how realistic it is.

1. 2. STELLAR REMNANT BLACK HOLES SCENARIO (SRBH)

The most popular model ten years ago, for the formation of supermassive black holes was from the black hole seeds formed from the first stars. These black holes are remnants of Population III stars (Bromm & Yoshida 2011, Heger & Woosley 2002) which form at very high redshift, as high as redshift z = [20, 30]. Population III stars form from metal free gas clouds which cool and fragment through molecular hydrogen lines. This process of cooling is not efficient, so first stars form very massive (hundreds of solar masses). And being so massive they live only couple of millions of years. Their remnants are 10 - 100 $M_\odot$ black holes. But since they form in low density environments of mini halos, they can not accrete efficiently.

As halos merge, these first black holes sink to the centres of gas rich atomic cooling halos (ACHs), where they can, in one of the models, accrete gas in numerous episodes with greater than 3 - 4 Eddington ratio gas accretion, combined with BH mergers. Smole et al. 2015 posed a question if we go through dark matter halo merger trees in the early Universe, what would be the required accretion rate, on average, for the first black holes to grow to supermassive values. They did not impose condition that accretion rate has to be alway the same in every episode. Accretion can be at the Eddington limit or even hyper-Eddington, but the important accretion rate is the average one over all accretion episodes that a particular black hole goes through. And it turned out that one does not have to go to hyper-Eddington accretion values, but that a more moderate rate of just 3 to 4 times above Eddington limit should be enough. In some other models, Inayoshi et al. 2016 found that in a very special set of circumstances, for example, if gas around the black hole is very dense, then black holes can accrete rapidly, in one go, with Eddington ratio larger than 10.

1. 3. DIRECT COLLAPSE BLACK HOLES (DCBH)

Second scenario (model) is direct collapse black holes which form in gas rich high redshift galaxies. Assuming that gas does not cool efficiently, it will collapse into supermassive star, which then collapses into a massive black hole with $\sim$ 100,000 $M_{\odot}$. There is plenty of work on this subject since direct collapse model is the one community is betting on (Begelman et al. 2006, Dijkstra et al. 2008, Regan & Haehnelt 2009, Choi et al. 2013, Agarwal et al. 2012, Visbal et al. 2015, Regan et al. 2017). And since thats the case we will discuss this model in more detail.

The large amount of work in the field is focused on showing, in both large and small scale simulations, that a very special set of circumstances for the formation of supermassive black hole can be achieved. These are exactly the opposite conditions from those required in stellar remnant model. Here the idea is to prevent gas fragmentation. One of the necessary mechanisms is Lyman Werner radiation from the first stars required to destroy molecular hydrogen, or this can be done through collisional dissociation. Another requirement which helps setting up the environment is keeping the gas worm. This can be achieved if dark matter halo mergers are so frequent, that gas is constantly stirred and cooling interrupted.

If all of the mentioned mechanisms work, then a massive halo with gas at around 8000K and no molecular hydrogen would form. Next step would be to inefficiently cool the gas cloud through Lyman Alpa radiation, while avoiding fragmentation, until the gas becomes optically thick gas. Optically thick gas cloud constitutes a protostar. Newly formed protostar continues to accrete the gas rapidly, ignites nuclear reactions, and if it avoids UV feedback, it becomes a supermassive star. Soon enough, supermassive star collapses to form a supermassive black hole.

1. 4. PROBLEMS IN BOTH MODELS

The goal in both scenarios is to produce black holes massive enough so that the rest of their growth can be achieved via Eddington limited gas accretion.

However, many problems arise in both models. First problem in the case of stellar remnant black holes model is gravitational wave recoil (Campanelli et al. 2007). As these black holes form with similar masses, if they merge, then the recoil that follows would eject the new black hole from its host halo (Micic et al. 2011). Masses of the

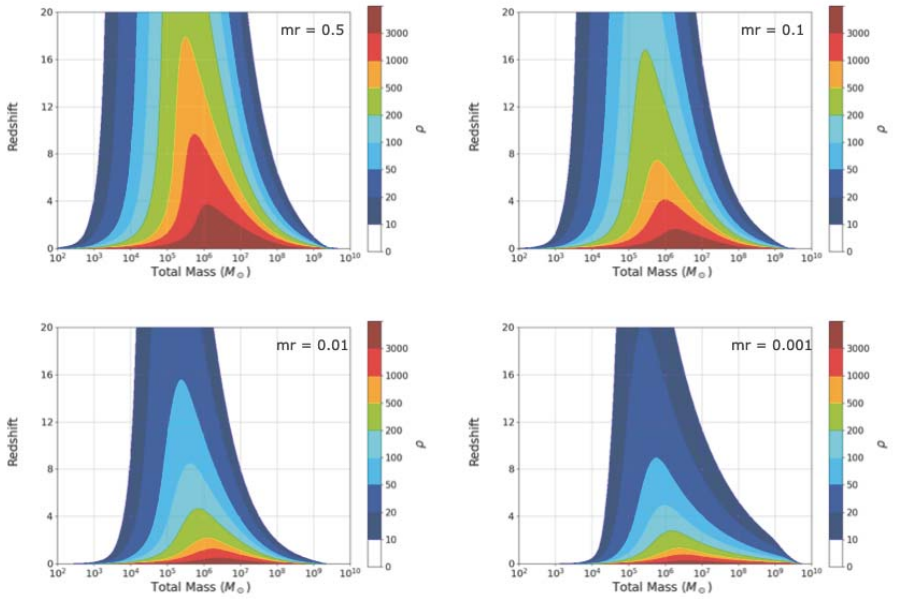

Figure 2: Redshift of the black hole merger as a function of combined mass of merging black holes. Four waterfall panels show signal to noise map for black hole mergers for four mass ratios of merging black holes [0.5, 0.1, 0.01, 0.001). Code available at https://github.com/mikekatz04/BOWIE

first black holes would be similar because they form in a vary narrow mass range with not a lot of gas to accrete. They merge in small mass halos with small gravitational potential which means low escape velocity.

Second problem is that atomic cooling halos with pristine gas are rare at high redshift (Chon et al. 2016). Next is the photo-heating feedback (Pacucci et al. 2015) which must be avoided in order to achieve hyper Eddington accretion. Simulations show that this is possible but we don't know how realistic this is.

At the end there is a question of how long the hyper Eddington accretion can be maintained in the violent environment of the first galaxies. For the direct collapse black hole model, a very specific set of conditions is required. As already mentioned in the previous section, it is very hard to prevent cooling because of the presence of molecular hydrogen, metals and dust.

Whatever the outcome is going to be in the future research, these two models should lead to the SMBH formation by redshift z = [6 - 7], so the merger history that follows at low redshift should be similar. But before SMBH formation, at high redshift, BH merger histories in these models should be quite different.

While in stellar remnant model we expect to see plenty of high mass ratio mergers of 100 to 10,000 $M_\odot$ black holes, in the direct collapse model, these mergers would be rare, or none, since we build SMBH in one go.

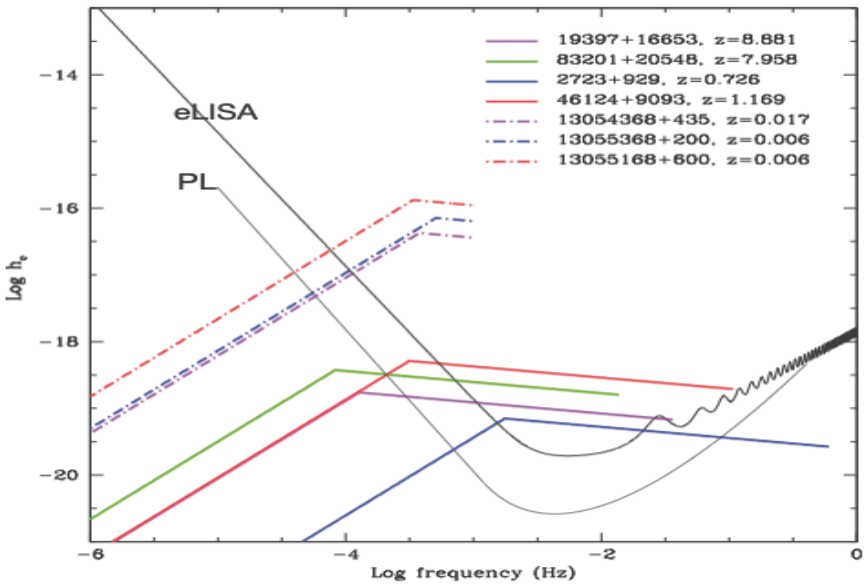

Figure 3: Characteristic strain as a function of observed frequency. Inspiral and coalescence for four high redshift mergers presented with thick lines, and for three low redshift EMRI's presented with dashed lines. Label shows masses of the merging black holes and the merger redshift. Overplotted are sensitivity curves for eLISA and for proposed LISA (PL).

2. OBSERVATIONS WITH LISA

This is where LISA will be crucial, since these are exactly types of mergers that LISA will be able to observe.

LISA will trail Earth's orbit by 50 million km. The original arm length was suppose to be 5 million km, later eLISA was proposed with arm length of 1 million km, and eventually, 2.5 million km was approved in 2017. Longer arm length is preferable since strength of the signal is directly proportional: $h_c = \Delta L \ / \ L$, where h_c is the characteristic strain amplitude, ΔL is the arm length, and L is distance from Earth to LISA.

LISA will measure change in the arm length caused by the passage of gravitational wave radiation. One can think of this value as the strength of the received signal which is called characteristic strain. Most important thing here to remember is that LISA will be perfect for the detection of black hole mergers.

Figure 2 shows signal to noise ratio map for the proposed LISA. Redshift of the black hole merger is on the y-axis, and the combined mass of the merging black holes on x-axis. This plot is called waterfall plot and we decided to focus on the waterfall plots for the proposed LISA only. For classic LISA this waterfall would be a little bit wider, while for eLISA it would be a little bit narrower. We used BOWIE package (Katz & Larson 2019) to produce it. The entire package can be cloned at the github (https://github.com/mikekatz04/BOWIE).

The top left of Figure 2 shows signal to noise ratio map for black hole mergers with mass ratio of 0.5. As we decrease the mass ratio of merging black holes, signal to noise reduces. Top right in the Figure 2 shows waterfall plot for mass ratio of 0.1. Bottom left for mass ratio 0.01, and bottom right for mass ratio of 10^{-3}. One can notice that as mass ratio of merging black holes decreases, so does the signal to noise ratio. As the result, LISA will preferably see high mass ratio mergers. The important note to take is that LISA sweet spot is for SMBHs between 10^6 and 10^7 $M_\odot$.

3. REALISTIC BLACK HOLE MERGERS

What happens when we look at the real bh mergers in cosmological simulations? Where do we expect black hole mergers to place themselves in our waterfall plots?

When we look at the merger history of massive elliptical galaxies or even clusters of galaxies, there are numerous SMBHs with a large number of mergers in their history. But if we consider spiral galaxies in the field, then we are looking at the low density regions of the Universe where mergers are sparse. This further means that once a spiral galaxy in the field, and its SMBH, are formed, there are no more major mergers.

As the result, in the case of the direct collapse model, SMBH is directly created. Its mass is $\sim 10^5$ - 10^6 $M_\odot$ and it can continue growing through gas accretion if there is gas in its vicinity. This kind of bh will have a number of extreme mass ratio mergers at lower redshifts. While in the case of the stellar remnant model, black hole first goes through episodes of high mass ratio bh mergers followed by gas accretion. Sure, once SMBH is formed, it also will have low redshift extreme mass ratio mergers similar to the direct collapse model. This is exactly what merger trees extracted from cosmological simulations show.

Figure 3 shows extracted bh mergers visible by LISA, from the merger tree of a galaxy similar to Andromeda galaxy (Holley-Bockelmann et al. 2010), for the stellar remnant model. The plot shows characteristic strain for the selected classes of resolvable black hole mergers in the simulation, as a function of observed frequency. Presented are the last days of the black hole inspiral and the merger. Overplotted are sensitivity curves for PL and eLISA. The merger redshift and pre-merger masses of the black hole binary are labeled. LISA will be able to observe all mergers with characteristic strain above the sensitivity curve.

Figure 3 distinguishes between two types of mergers. High redshift black hole mergers with mass ratios larger than 0.1 are placed in the bottom part of the sensitivity curve. These are lower mass black holes that form in stellar remnant model only. They have similar masses and their mergers are always at high redshift. The second group of mergers are the low redshift extreme mass ratio mergers in the upper part of the sensitivity curve. After SMBH has formed, disregarding the model, it is likely to merge with much smaller black holes at low redshift.

We can look at this in our waterfall plot. Figure 4 shows four waterfall panels for the four high redshift mergers from the previous figure. One can see that these are high redshift mergers with a decent signal to noise ratio between 100 and 500. Low redshift extreme mass ratio mergers are not presented since all of them are in the LISA sweet spot at 10^7 $M_\odot$ black holes at redshift zero, where signal to noise is highest.

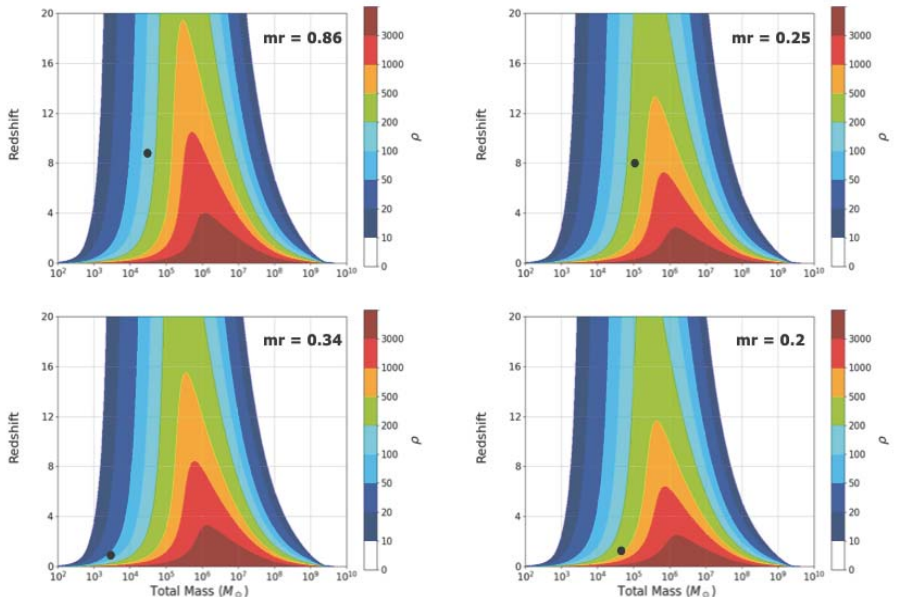

Figure 4: Waterfall panels with the same nomenclature as in Figure 2. Black dotes represent four high redshift mergers for four different mass ratios of merging black holes.

4. CONCLUSIONS

In conclusion, how do we distinguish between Stellar Remnant and Direct Collapse scenarios? Both models predict extreme mass ratio mergers at low redshift, but only stellar remnant model predicts high redshift, high mass ratio, mergers. As mentioned before and also seen in Figure 3, these two types of mergers separate in the characteristic strain plot above the LISA sensitivity curve. So LISA detecting smaller number of these, similar mass, high redshift, black hole mergers, would point toward direct collapse black hole model. However, if LISA detects a large number of mergers of similar mass black holes early in the Universe, then the stellar remnant model is likely to win.

Since LISA will not be launched any time soon (probably 20 years from now), we should already know a lot about the properties of the first stars and first galaxies from James Web Space Telescope (JWST). Although that is not going to be that easy. JWST will certainly be able to detect Population III Supernovae (Kasen et al. 2011), which should give us statistics for stellar remnant black hole model. Problem is that it is going to be hard to distinguish these supernovae from AGNs or high redshift galaxies (Hartwig et al. 2018). It should also detect black hole accretion that follows (Natarajan et al. 2017), but the problem will be distinguishing stellar from massive black holes (Valiante et al. 2018). So we will certainly learn more with JWST, but it seems that we will need LISA to disentangle SMBH growth models, and decide which one is the correct one.

Acknowledgements

The authors acknowledge financial support from the Ministry of Education, Science and Technological Development of the Republic of Serbia through the project #ON176021 "Visible and invisible matter in nearby galaxies: theory and observations ". This work was supported by the Ministry of Education, Science and Technological Development of the Republic of Serbia (MESTDRS) through the contract no. 451-03-68/2020/14/200002 made with the Astronomical Observatory of Belgrade.

References

Agarwal, B., Khochfar, S., Johnson, J. L., Neistein, E., Dalla Vecchia, C., Livio, M.: 2012, *Monthly Notices of the Royal Astronomical Society*, **425**, 2854.
Begelman, M. C., Volonteri, M., Rees, M. J.: 2006, *Monthly Notices of the Royal Astronomical Society*, **370**, 289.
Bromm, V., Yoshida, N.: 2011, *Annual Review of Astronomy and Astrophysics*, **49**, 373.
Campanelli, M., Lousto, C. O., Zlochower, Y., Merritt, D.: 2007, *Physical Review Letters*, **98**, 231102
Choi, J. H., Shlosman, I., Begelman, M. C.: 2013, *The Astrophysical Journal*, **774**, 149.
Chon, S., Hirano, S., Hosokawa,T., Yoshida, N.: 2016, *The Astrophysical Journal*, **832**, 134.
Dijkstra, M., Haiman, Z., Mesinger, A., Wyithe, J. S. B.: 2008, *Monthly Notices of the Royal Astronomical Society*, **391**, 1961.
Hartwig, T., Bromm, V., Loeb, A.: 2018, *Monthly Notices of the Royal Astronomical Society*, **479**, 2202.
Heger, A., Woosley, S. E.: 2002, *The Astrophysical Journal*, **567**, 532.
Holley-Bockelmann, K., Micic, M., Sigurdsson, S., Rubbo, L. J.: 2010, *The Astrophysical Journal*, **713**, 1016.
Inayoshi, K., Haiman, Z., Ostriker, J. P.: 2016, *Monthly Notices of the Royal Astronomical Society*, **459**, 3738.
Kasen, D., Woosley, S. E., Heger, A.: 2011, *The Astrophysical Journal*, **734**, 102.
Katz, M. L., Larson, S. L.: 2019, *Monthly Notices of the Royal Astronomical Society*, **483**, 3108.
Micic, M., Holley-Bockelmann, K., Sigurdsson, S.: 2011, *Monthly Notices of the Royal Astronomical Society*, **414**, 1127.
Natarajan, P., Pacucci, F., Ferrara, A., Agarwal, B., Ricarte, A.: 2017, *The Astrophysical Journal*, **838**, 117.
Pacucci, F., Volonteri, M., Ferrara, A.: 2015, *Monthly Notices of the Royal Astronomical Society*, **452**, 1922.
Regan, J. A., Haehnelt, M. G.: 2009, journalMonthly Notices of the Royal Astronomical Society, **396**, 343.
Regan, J. A., Visbal, E., Wise, J. H., Haiman, Z., Johansson, P. H., Bryan, G. L.: 2017, *Nature Astronomy*, **1**, 0075.
Smith, A., Bromm, V.: 2019, *Contemporary Physics*, **60**, 111.
Smole, M., Micic, M., Martinovic, N.: 2015, *Monthly Notices of the Royal Astronomical Society*, **451**, 1964.
Valiante, R., Schneider, R., Zappacosta, L., Graziani, L., Pezzulli, E., Volonteri, M.: 2018, *Monthly Notices of the Royal Astronomical Society*, **476**, 407.
Visbal, E., Haiman, Z., Bryan, G. L.: 2015, *Monthly Notices of the Royal Astronomical Society*, **453**, 4456.

Publ. Astron. Obs. Belgrade No. 100 (2021), 131 - 136 *Invited Lecture*

MONITORING OF LOWER IONOSPHERE: POSSIBLE EARTHQUAKE PRECURSORS AND APPLICATION IN EARTH OBSERVATIONS BY SATELLITE

A. NINA

Institute of Physics Belgrade, University of Belgrade,
Pregravica 118, 11080 Belgrade, Serbia
E–mail: sandrast@ipb.ac.rs

Abstract. Ionospheric observations can be used for indirect detection of various processes in the outer space and Earth. In addition, the ionosphere affects the propagation of electromagnetic signals used in numerous practical applications. Here, we present the latest research based on the observation of the low ionosphere by very low frequency radio signals recorded in Belgrade related to a possible new type of earthquake precursor, and the impact of the perturbed ionospheric D-region on the propagation of satellite signals used in Earth's observations.

1. INTRODUCTION

Research of the ionosphere is of great importance for both science (first of all for geosciences) and modern technologies based on the use of satellite and ground based electromagnetic signals. Practical applications of these studies are important for many contemporary area of human life including telecommunications, GPS positioning and Earth observations. Namely, disturbances of the ionosphere can strongly affect propagation of these electromagnetic waves and induce significant errors in measurements and modelling of different parameters (Nina et al., 2020b). In addition, there are many studies which indicate connections between ionospheric disturbances and natural disasters (Nina et al., 2017; Pulinets and Boyarchuk, 2004; NaitAmor et al.,2018; Kumar et al. 2016). Some of these ionospheric perturbations are recorded before events which are following by large catastrophes (Maekawa et al., 2006; Maurya etal.,2016; Molchanov et al, Yamauchi et al., 2007) and for this reason their investigation is of high priority.

The lower ionosphere can be monitored by several techniques including those based on propagation of very low/low frequency (VLF/LF) radio signals in the Earth-ionosphere waveguide. The advantages of this method in analysis of the atmospheric layer between 50 km and 90 km are (1) continuous monitoring of signals with time resolution that is usually better than 1 s, and (2) observation of large part of the lower ionosphere which is provided by numerous worldwide located transmitters and receivers.

In this paper we present recent investigation based on data collected by the Belgrade VLF/LF receiver station located at the Institute of Physics Belgrade. We pay attention to two studies related to disturbances in periods around earthquake (EQ) events (Nina et al., 2020a) and during a solar X-ray flare influence (Nina et al., 2020b). In first study attention is focused on analysis of possible connections between an earthquake and changes in electrical properties of the lower ionosphere. In the second study we analysed influence of the intensive perturbed ionospheric D-region by a solar X-ray flare on satellite signals.

2. OBSERVATIONS, DATA PROCESSING AND MODELLING

In our research we use data obtained in the lower ionosphere observation by VLF signals emitted by the ICV, GQD and DHO transmitters located in Italy, the UK and Germany (see Table 1) and recorded by Belgrade receiver station. The propagation paths od these signals are shown in map given in Fig. 1.

Table 1: Transmitter locations and frequencies for the considered VLF signals.

	Transmitter location	Frequency (kHz)
ICV	Isola di Tavolara, Italy	20.27
GQD	Rhauderfehn, Germany	22.1
DHO	Anthorn, the UK	23.4

We analyse data recorded by the Absolute Phase and Amplitude Logger (AbsPAL) and Atmospheric Weather Electromagnetic System for Observation Modeling and Education (AWESOME) receivers in the first and second analysis, respectively. We analyse data sets for all three signals with time sampling of 0.1 s and for DHO signlal with time sampling of 1 s, respectively.

2. 1. NOISE AMPLITUDE REDUCTION AS POSSIBLE EARTHQUAKE PRECURSOR

There are many studies which indicate relationships between EQ events and ionospheric disturbances (see, for example, Biagi et al., 2001; Nina et al. 2020a; Pulinets and Boyarchuk, 2004). These studies are primarily based on the comparison of variations detected during different days. In Nina et al., 2020a, variations in natural short period noise amplitude are analysed for time period around the Kraljevo EQ (Mw=5.4) occurred on 3 November, 2010. We analysed data recorded by the 0.1-s time resolution in order to investigate signal changes several hours before and after the considered EQ event.

In addition, three EQs with magnitudes 4.3, 4.4 and 4.5 are analysed. One of them (Mw=4.4) occurred at location that was very close to the epicentre of the main EQ, while the epicentres of other events were at longer distance from the signal propagation paths than in the first two cases. For all of these events it is common that magnitudes were greater than 4 and that they occurred in the night-time period.

In this analysis, three signals emitted in Italy (ICV), the UK (GQD) and Germany (DHO) and recorded in Belgrade are analysed. The noise amplitude is calculated from the amplitude deviation from smoothed curve during the considered time periods.

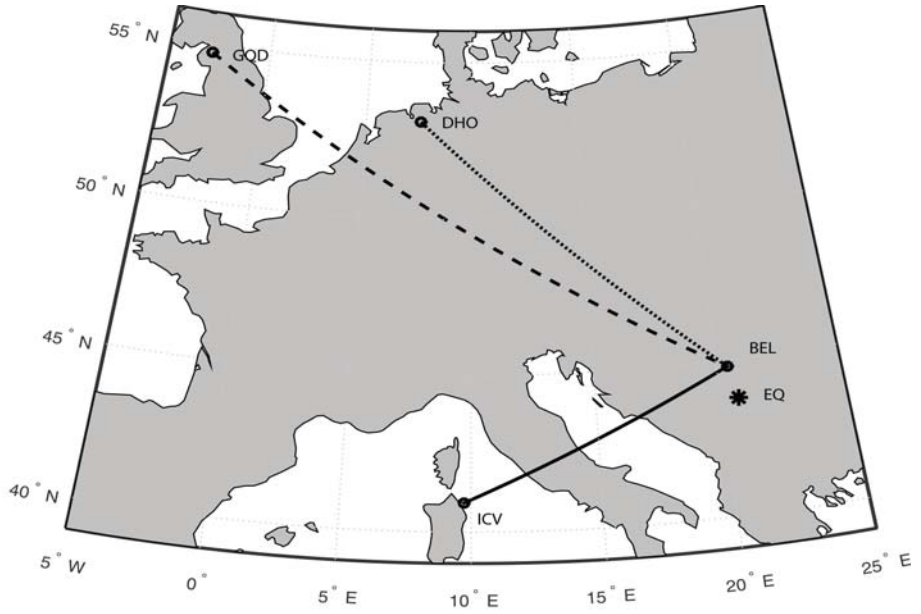

Figure 1: Propagation paths of the VLF signals recorded by the Belgrade receiver station (BEL) in Serbia and emitted by the transmitters ICV in Italy (solid line), GQD in the UK (dashed line), and DHO in Germany (dotted line). Locations of the Kraljevo earthquake is shown as stars.

2. 2. INFLUENCE OF THE D-REGION ON SATELLITE SIGNAL PROPAGATION

There are numerous models that are used in calculations of the ionospheric contribution in the signal delay, so called ionospheric delay, (Nava et al., 2008; Zhao and Zhou, 2018). Mostly, they use observational data as input and use analytical expressions for modelling of the ionospheric delay. If the observational data relates to one or more altitudes, a particular model is single or multiple layer model, respectively. In both cases these altitudes are above 100 km because upper areas has larger influences on signal propagation due to larger electron density. For this reason, calculations of the total electron content (TEC), which is required for modelling of the signal delay, are based on approximations that electron density vertical distribution can be obtained from the observational data at fixed altitudes and used expressions. Because of the fact that ionospheric parameters can be significantly changed in a localized area during some time interval, two questions should be considered: (1) Are the used expressions applicable during intensive disturbances? and (2) Can local disturbances below 100 km be important?

In Nina et al., 2020b influence of a solar X-ray flare which primarily disturbs the D-region (50 km- 90 km) on GNSS and Synthetic Aperture Radar (SAR) signal delay is considered. Error in modelling of the signal delay $P_{\mathrm{D}} = C \cdot TEC_{\mathrm{D}}/f^2$ if the D-region is not included in consideration depends on the total electron content in D-region, TEC_{D}, which is given by expression:

$$\mathrm{TEC_D} = \delta H_\mathrm{D} \sum_{i=1}^{N_\mathrm{D}} N_\mathrm{ei} n_\mathrm{i} [{n_\mathrm{i}}^2 - (n_0 \sin(\Theta_0))^2]^{-0.5}. \quad (1)$$

where δH_D is the thickness of horizontally uniform layers in the D-region, N_ei and n_i are the electron density and refractive index in layer i, respectively, and Θ_0 is the wave propagation angle in the D-region.

3. RESULTS

3. 1. NOISE AMPLITUDE REDUCTION AS POSSIBLE EARTHQUAKE PRECURSOR

Significant reduction of the noise amplitude is recorded for ICV signal emitted in Italy whose propagation path lies the closest to the EQ epicentre. The beginning of this reduction is before the EQ which indicates possibility that this type of variation can be consider as EQ preqursor. Variations in the noise amplitude are also recorded for other two signals but they are not specific for the considered night and they can not be connected with EQ event.

To examine influences of the epicentre distance from the signal propagation path and to examine noise amplitude reduction recorded in the other time periods additional analyses of the ICV signal amplitude are performed. They were related to:

- Time evolution of the amplitude noise in periods around three EQs of magnitudes 4.4 (the same epicetre location like for the main EQ event), and magnitudes 4.3 and 4.5 (epicentres at larger distance than in the first two cases);
- Time evolutions of the noise amplitude during hole three days.

The noise reduction is also recorded for EQ with epicentre near the epicentre of Kraljevo EQ. In the other two cases these reductions are not recorded which indicates importance od epicentre distance from the signal propagation path.

To examine the regular daily variations in the noise amplitude (this analysis is important for the extraction of the sudden from periodic variations) the short-period noise amplitude is analysed during three whole days: 3 and 4 November when two EQs near Kraljevo occurred, and 9 November when significant reduction of the noise amplitude is also recorded in analysis of two months in periods of 1 hour around time of Kraljevo EQ (0:56:54.4 ± 0:30 UT). During these day, 46 EQs (excluding 29 that occurred in a few hours after Kraljevo EQ when extraction of their influence is not possible) were detected with epicentres not far from the ICV signal propagation path (`http://www.emsc-csem.org/Earthquake/`). The most intensive were two EQs with Mw>5 (near Kraljevo (Mw=5.4) and in Tyrrhenian Sea (Mw=5.1)) and two EQs with Mw>4 (near Kraljevo (Mw=4.3) and in Western Mediterranean Sea (Mw=4.3)). Only 13 of these EQ events had the magnitude greater than 3. Analysis of the noise amplitude during these three days shown:

- The short-period amplitude reduction starting before the EQ event is recorded for all 4 detected EQs with magnitude greater than 4.
- 8 of 10 EQs near Kraljevo (i.e. 80%) with magnitude greater than 2.5 are connected with the noise amplitude reduction.

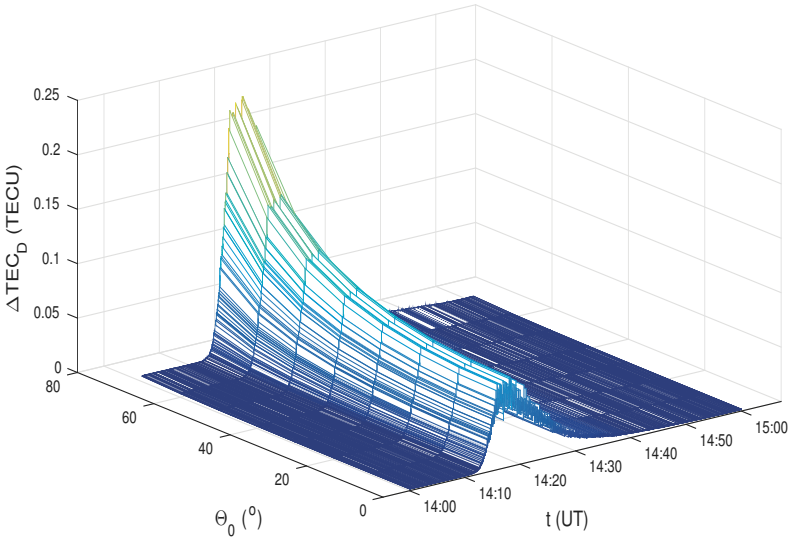

Figure 2: Time evolution of changes in the total electron density within D-region, $\Delta\mathrm{TEC_D}$, for different incident angles, Θ of signal in this area during influence of a solar X-ray flare occurred on 1 May 2013.

- Thirteen out of a total of 15 (or 87%) decreases of the short-period noise amplitude can be related to EQ events.

In addition, it is very important to point out that reductions of the short-period noise amplitude are recorded in all day periods.

3. 2. INFLUENCE OF THE D-REGION ON SATELLITE SIGNAL PROPAGATION

As one can see in Fig. 2, changes in $\mathrm{TEC_D}$ can be intensive. Results presented in Nina et al., 2020b show that, for more intensive flares, the D-region can provide the signal delay of more than 1 m for large incident angles. Keeping in mind that delays of 1 cm are included in signal propagation modelling it can be concluded that, although quiet D-region does not affect satellite signal propagations, its influence cannot be ignored in periods of intensive disturbances because errors in modelling can be important.

4. SUMMARY

In this work we present review of the recent results obtained in the lower ionosphere investigation based on data obtained by VLF/LF receiver station in Belgrade. We present analyses of (1) possible new type of earthquake precursor visualized as reduction of the signal noise amplitude before the earthquake event, and (2) influence of the ionospheric D-region which is disturbed by a solar X-ray flare on delay of satellite signals.

The main results of these studies indicate that:

- Reduction of VLF signal noise amplitude is recorded before several earthquakes and that confirmation of connection of these changes with earthquake events requires more detailed statistical analysis.
- Influence of the significantly disturbed D-region on propagation of satellite signals can be important and its contribution in signal delay should be involved in modelling.

These studies open many questions important for practical application of ionospheric research and they will be in focus forthcoming studies.

Acknowledgements

The author acknowledges funding provided by the Institute of Physics Belgrade, through the grant by the Ministry of Education, Science, and Technological Development of the Republic of Serbia.

References

Biagi, P. F., Piccolo, R., Ermini, A., Martellucci, S., Bellecci, C., Hayakawa, M., Kingsley, S. P.: 2001, *Ann. Geophys.*, **44**, 5.

Kumar, S., Kumar, A., Maurya, A. K., Singh, R.: 2016, *J. Geophys. Res. Space*, **121**, 5930.

Maekawa, S., Horie, T., Yamauchi, T., Sawaya, T., Ishikawa, M., Hayakawa, M., Sasaki, H.: 2006, *Ann. Geophys.*, **24**, 2219.

Maurya, A. K., Venkatesham, K., Tiwari, P., Vijaykumar, K., Singh, R., Singh, A. K., Ramesh, D. S.: 2016, *J. Geophys. Res. Space*, **121**, 10403.

Molchanov, O., Hayakawa, M., Oudoh, T., Kawai, E.: 1998, *Phys. Earth Planet. Inter.*, **105**, 239.

NaitAmor, S., Cohen, M. B., Kumar, S., Chanrion, O., Neubert, T.: 2018, *Geophys. Res. Lett.*, **45**, 10185.

Nava, B., Cosson, P., Radicella, S.: 2008, *J. Atmos. Solar-Terr. Phy.*, **70**, 1856.

Nina, A., Radovanović, M., Milovanović, B., Kovačević, A., Bajčetić, J., Popović, L. Č.: 2017, *Adv. Space Res.*, **60**, 1866.

Nina, A., Pulinets, S., Biagi, P. F., Nico, G., Mitrović, S., Radovanović, M., Popović, L. Č.: 2020a, *Sci. Total Env.*, **710**, 136406.

Nina, A., Nico, G., Odalović, O., Čadež, V., Drakul, M. T., Radovanović, M., Popović, L. Č.: 2020b, *IEEE Geosci. Remote Sens. Lett.*, **17**(7), 1198.

Pulinets, S., Boyarchuk, K.: 2004. *Ionospheric Precursor of Earthquakes*, Springer, Heidelberg, Germany.

Yamauchi, T., Maekawa, S., Horie, T., Hayakawa, M., Soloviev, O.: 2007, *J. Atmos. Sol.-Terr. Phys.*, **69**, 793.

Zhao J., Zhou, C.: 2018, *GPS Solut.*, **22**, 48.

Publ. Astron. Obs. Belgrade No. 100 (2021), 137 - 144 *Invited Lecture*

SUN AND SOLAR ACTIVITY: OPPORTUNITIES FOR OBSERVATIONS AND DEVELOPMENT

N. PETROV

Institute of Astronomy and National Astronomical Observatory, Bulgarian Academy of Sciences, 72 Tsarigradsko shose blvd., 1784 Sofia, Bulgaria
E–mail: nick@astro.bas.bg

Abstract. The fast technological development and the new possibilities for observations allowed solving some of the theoretical issues in modern heliophysics and astronomy in general. But there are still unresolved questions regarding the physical processes of solar activity and space weather. We use the potential of both ground-based and space-based astronomical observatories to analyze the present results and understandings in the field of heliophysics. We show the current observational possibilities and perspectives for development in the research of the solar activity in Bulgaria.

1. INTRODUCTION

For thousand years, as history shows, scientific advances happen in stages. One observes years of dynamic and fast growth or relatively quiet periods in appearance of new scientific ideas. Of course, the new scientific proposals precede the technical applications, it is hardly possible otherwise, except when a random and unexpected experimental result happens. It is not easy to show constant development of new concepts and ideas as well as qualitative change of well-established scientific models. It looks like during the last 60 years the new approaches in science are in a quiet period. On the other hand, during the last two-three decades we witness the highest rate of development of the human civilization, in terms of new technological and engineering achievements and their applications. These achievements offer to us, astronomers, new opportunities for highly detailed research of a multitude of yet unanswered questions.

Still debatable are the questions related to: appearance, evolution, and periodicity of solar magnetic field; the processes which cause the heating of the solar corona and the acceleration of the solar wind; the causes for solar flare; processes of accretion of interplanetary material. The answers of questions related to the nature and physics of these phenomena are directly connected to constant monitoring of solar activities such as sunspots, prominences, solar flares and coronal mass ejections. Real cosmic observatories were launched on different orbits such as SOHO[1], STEREO[2],

[1]https://sohowww.nascom.nasa.gov/
[2]https://stereo.gsfc.nasa.gov/

SDO[3], Ulysses[4], GOES[5], RHESSI[6], Hinode[7], etc. It is possible today to perform solar observations in large range of the electromagnetic spectrum – gamma rays, X-rays, ultraviolet (UV), visible and infrared, radio waves. All these observations are aimed at increasing our understanding of the physics of the Sun.

Frequently we refer to the year 2020 as a new era in solar astronomy. We have a new generation of ground- and space-based observatories, which were impossible to construct up to now. We have the first images of the granulation of the solar photosphere by Daniel K. Inouye Solar Telescope, which were used for the first light press release in January 2020 and received broad coverage in the international press (Rimmele et al., 2020). Its 4-m aperture provides the highest-resolution observations of the Sun ever achieved. The telescope's field of view (FOV) using the Visual Broadband Imager is 55 arcsec×55 arcsec and the resolution is close to the diffraction limit at the wavelength of 789 nm (0.04 arcsec). A newly developed data center located at the NSO Headquarters in Boulder will initially serve fully calibrated data to the international users community. Higher-level data products, such as physical parameters obtained from inversions of spectro-polarimetric data will be added as resources allow.

We need to mention also the new space-based missions ESA/NASA Solar Orbiter and NASA Parker Solar Probe. Both missions will have the opportunity to research the solar atmosphere primarily in the UV range of the electromagnetic spectrum – which is impossible for telescopes based on the Earth's surface.

Solar Orbiter, a mission of international collaboration between ESA and NASA, will explore the Sun and heliosphere from close up and out of the ecliptic plane. Understanding the coupling between the Sun and the heliosphere is of fundamental importance to understanding how the Solar System works and is driven by solar activity. To address this and other fundamental questions of solar and heliospheric physics, Solar Orbiter will combine in-situ measurements as close as 0.28 AU to the Sun with simultaneous high-resolution imaging and spectroscopic observations. These will be acquired in and out of the ecliptic plane, and Solar Orbiter will be the first mission ever to make remote-sensing observations of the Sun's polar regions (Albert et al. 2020).

Parker Solar Probe (PSP) will be the first spacecraft to fly into the low solar corona. PSP's main science goal is to determine the structure and dynamics of the Sun's coronal magnetic field, understand how the solar corona and wind are heated and accelerated, and determine what processes accelerate energetic particles (Fox et al. 2016).

In addition to delivering ground-breaking science in its own right, Solar Orbiter has important synergies with NASA's Parker Solar Probe mission, as well as other space- and ground-based observatories.

The above-mentioned three grand projects are targeted mainly at studying the minor structures of the Sun, while also including solar activity phenomena at a global aspect, related to the whole Solar System. These observations are supported by ground-based telescopes with more modest dimensions, appropriate for large-scale

[3]https://sdo.gsfc.nasa.gov/
[4]http://www.esa.int/Science_Exploration/Space_Science/Ulysses_overview
[5]https://www.goes-r.gov/
[6]https://hesperia.gsfc.nasa.gov/rhessi3/
[7]https://hinode.msfc.nasa.gov/

structures studies. Observations of total solar eclipses is still a main and powerful method for research of solar corona in the range of 1 – 10 solar radii. A comprehensive observational network, which includes space- and ground-based facilities, appears to be the most suitable form of research of the manifestations of solar activity, completed together by scientists from all over the globe.

In this paper we show our new project for observation and research of solar chromosphere through commissioning of a new 30-cm chromosphere telescope in Bulgaria. We present our intentions to develop our observational capabilities with regards to the monitoring of active manifestations of solar activity at different layers of solar atmosphere.

2. RESEARCH IN THE FIELD OF HELIOPHYSICS FROM BULGARIA AND THE INSTITUTE OF ASTRONOMY WITH NATIONAL ASTRONOMICAL OBSERVATORY AT THE BULGARIAN ACADEMY OF SCIENCES

At different layers of solar atmosphere (photosphere, chromosphere, transition region and corona) sporadic interactions between solar plasma and magnetic field of different space and time scales, as well as with different balance of mass and energy, happen. This complex of events is known as solar activity. There is a large number of solar activity phenomena, but the main ones, which have substantial geoeffective potential, are sunspots, prominences, solar flares, and coronal mass ejections.

Naturally at the end of the XX and the beginning of the XXI century, the space sciences and heliophysics in particular, established the term "space weather", which includes the physical conditions in the solar atmosphere, the solar wind, magnetosphere, ionosphere and thermosphere of the Earth, which could create unfavorable conditions for the normal operations of space- and ground-based technological systems or could negatively influence human health (Bonadonna et al. 2016). The Sun is major source and engine of the space weather, setting its parameters at every moment in accordance with the level and type of solar activity.

Historically, the development of Bulgarian astronomy naturally leads to the development of solar research. We owe its historical roots to the activity of Prof. Marin Bachevarov – Dean of the Faculty of Physics and Mathematics of Sofia University, Rector of the University and a pioneer for the construction of the first modern observational astronomical instrument in Bulgaria – a 6-inch refractor. From 1899 to 1905 Prof. Bachevarov, together with a group of students, began regular observations of sunspots from the Observatory in Sofia (Petrov et al. 2018, Tsvetkov and Petrov 2020). Years later, in 1961, the first research expedition to observe a total solar eclipse on February 15 was organized in Bulgaria (Dermendjiev et al. 1999).

In the very beginning of 1990s the foundations of modern observational solar physics were laid in Bulgaria by Prof. Vladimir Dermendzhiev, who built solar tower with 15-cm refractor for white-light observations of active processes. It was the first important step to the realization of the idea of own observational base in the Institute of Astronomy and National Astronomical Observatory (IANAO). Sun and Space Weather project was established by scientists from Department "Sun" at IANAO.

Since then the research done by the scientists from Bulgarian solar group relies both on ground- and space-based observations. We determined the time profiles,

dynamic parameters (speed and acceleration) and the horizontal shifting of the "footpoints" of plenty of eruptive prominences observed by the telescope of the Astronomical Institute at the University of Wroclaw in Poland, SOHO, and SDO, as well as their connection to solar flares and/or CME (Duchlev et al. 2010; Tsvetkov and Petrov 2018, 2020; Tsvetkov 2020).

Research of eruptive prominences observed in UV by SDO and STEREO were performed during the last several years. A reconstruction of the coronal magnetic fields in the surroundings of prominences and a comparison of the kinematic properties of the prominences during eruption with spatial distribution of the rate of decrease of magnetic field with height was shown. This allows determining the mechanism of formation of the prominences and demonstrates the possibilities for prediction of appearance of instabilities leading to eruptions by tracking the values of the index, characterizing the decrease of the magnetic field in strength when reaching critical levels (Myshyakov and Tsvetkov 2020).

The team of the Sun and Space Weather project in IANAO has experience in processing observations of solar energetic particles (protons), their association with solar eruptive processes (flares, coronal mass ejections, prominences, radio emission), detailed analysis of particular events, as well as compiling numerous catalogues (Miteva et al. 2013, 2018) necessary for statistical studies covering almost two solar cycles (Miteva and Tsvetkov 2019; Bogomolov et al. 2018; Tsvetkov et al. 2018).

Observations and research of the solar corona at total solar eclipses are part of the activities of our team. Our main priority tasks are related to investigation of the fine structure of solar corona in white light, prominences and their surroundings (Myshyakov and Tsvetkov 2020); sublimation of dust particles in solar corona up to 10 solar radii (Gulyaev and Petrov 2003); polarization of solar corona in white light (Merzlyakov et al. 2019); as well as phenomena in the Earth's atmosphere during total solar eclipse (Tsvetkov et al. 2019).

As a result of engineering efforts, a solar coronagraph was built in the solar tower of National Astronomical Observatory (NAO) Rozhen in 2005 (Petrov et al. 2018). The renovation and progress of solar observational infrastructure in Bulgaria continued in 2019 with laying the foundations of building the first chromospheric telescope in Bulgaria.

3. NEW 30-CM CHROMOSPHERE TELESCOPE IN ROZHEN OBSERVATORY

Our new telescope should be designed so as to be adapted to new scientific challenges. The new 30-cm solar telescope to be installed in NAO Rozhen can be described in terms of requirements of modern solar and solar-terrestrial physics. Nowadays ground-based imaging of the Sun can be used as a complement monitoring of the solar activity. Its main advantages in the era of space-borne instruments are the relatively low cost of implementation and the ability to access the received data immediately.

We plan a new beginning for H_α solar observations to reveal the active nature of the solar atmosphere. The interaction between the convective motions in the photosphere and the dynamics in the hot corona happen in the chromosphere – an intermediate layer where the kinetic energy of the plasma gradually becomes weaker than the energy of the magnetic field and the plasma parameter β shifts from $\beta > 1$ (photosphere) to $\beta \leq 1$ (Rodriguez Gomez et al. 2019) before reaching low-beta values

in the corona and in the active region chromosphere (β <<1) (Sakurai 2017). The chromosphere is also a region from solar atmosphere where the temperature rises in height as it is situated right above the temperature minimum layer.

Prominences/filaments, fibrils, Ellerman bombs, flares, etc. are only part of the phenomena observable in H_α. One of the main scientific purposes of the new solar telescope is dedicated to make regular observations of various manifestations of solar activity. A free-access online database is going to be established and updated as soon as the daily observations begin.

A network with amplified magnetic field situated above the photospheric network is visible in the chromosphere during H_α observations. It is called chromospheric network and is outlining the supergranulation cells. A downward flow of material with typical velocity of about 1-2 km s^{-1} marks their boundaries (Rieutord and Rincon 2010). Bright streams of luminous gas about 10000 km high, called spicules originate from the chromospheric network (Sterling 2000). They are one of the smallest quiet-Sun structures available for observations. The surface of the spicules is assumed as the actual boundary between the chromospheric and coronal material.

Our telescope is currently under construction although it has already received its first light. It is designed as Schmidt–Cassegrain reflector with diameter of the main mirror $D = 305$ mm and a focal length $F = 3050$ mm (Figure 1), which determines the telescope ratio – $F/10$. It is equipped with Hinode solar guider and a flat K8 glass filter with a bandwidth 6560±500 Å that provides reflection of at least 94% of the light in non-working areas of the spectrum to prevent overheating.

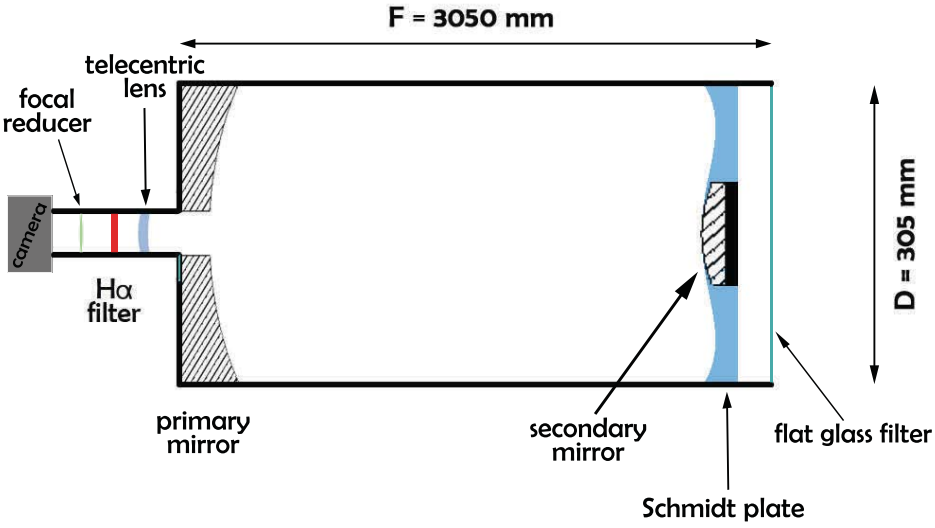

Figure 1: Optical scheme of the Schmidt–Cassegrain telescope.

The DayStar H_α filter that the telescope uses, works best for parallel beam of light. The larger its divergence when reaching the H_α filter is, the larger the bandpass width becomes. This means that at large focus distances we get better approximation of the falling light to parallel beam, resulting in higher resolution of the image.

A system of telecentric lens (up to 5x) provides the opportunity for correction of the focal length. The effective focal length F_{eff} will vary in range 3050 to 15250 mm and, respectively, the field of view will change between 2.5×2.5 arcmin and 10×10 arcmin.

With this telescope, we will be able to obtain observational material from active regions in the solar chromosphere with a line-of-sight velocity resolution between 0 and 10 km s^{-1}. At the end of the tube will be placed a H_α filter (λ=6562.801 Å) with a bandwidth ∼0.3 Å (central area of the filter) and a possibility for displacement of the center of the bandpass at ±0.5 Å by 0.1 Å step. The telescope was planned to receive its first light from the territory of NAO Rozhen in the first half of 2020, but now the deadline is indefinitely extended due to the pandemic situation.

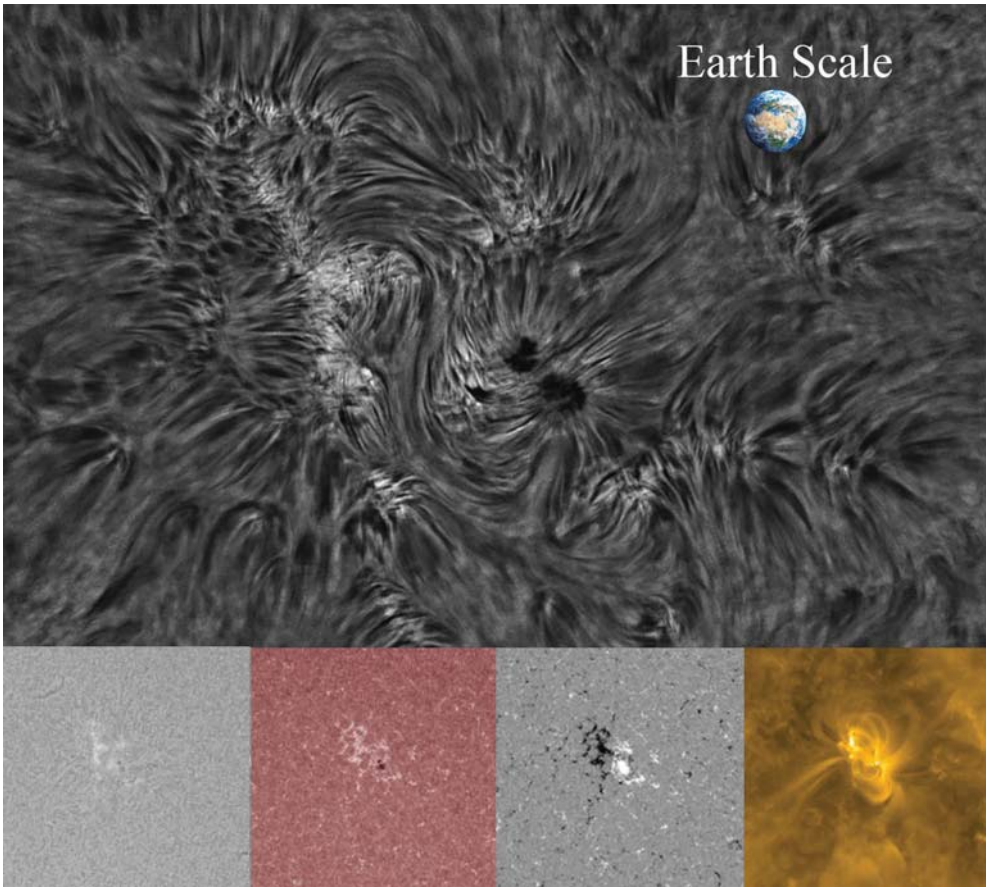

Figure 2: Upper image: A preliminary image of the telescope, taken on 2020 August 10, showing the active region 12770. Lower images: The same active region as captured by Kanzelhoehe H_α telescope, SDO/AIA 1700 Å, SDO/HMI magnetogram and SDO/AIA 171 Å, respectively.

Nevertheless, the optical part of the telescope is already constructed and the first calibration test image, taken at the factory is now released (Figure 2). It is captured

when to the telescope $F = 3050$ mm is attached a telecentric focal extender 4.3× equal to $F = 13115$ mm. Immediately after the H_α filter we have optics system for reducing of the total focus distance and for forming of the final image. This focal reducer increases the FOV, increases the ratio and reduces the exposure time.

The reduction coefficient of the focal reducer is 0.65× that, finally, makes $F = 8525$ mm. The digital camera in use is Basler ace acA1920-155um, with pixel dimensions 5.86 μm×5.86μm. The scale of the image is 0.13 arcsec/px in unfavorable weather conditions with high seeing.

Apart from the operational software for telescope control, for the analysis of the observational data, a new software product founded on existing procedures in the IDL-based software product SolarSoftware will be developed. Precise data processing is the basis for quality scientific production, which necessitates the development of a specific algorithm that will facilitate and universalize the preliminary data analysis. Processed data will be provided through a specially designed website.

Upon its completion, the telescope will serve same tasks, both in regular solar observations and in the effective training, qualification and educational activities related to heliophysics and astronomy.

4. CONCLUSIONS

We present an overview of the capabilities and technical specifications of the new 30-cm solar telescope that is going to receive its first light from the territory of NAO Rozhen in 2021. The telescope suggests a H_α view to the structures and dynamics of solar chromosphere in precise detail. Unlike most of the H_α telescopes used nowadays it is not going to capture full disk images of the Sun. The changeable field of view that varies between 2.5×2.5 arcmin and 10×10 arcmin will offer observations of particular separate chromospheric parts. A database with free access that is going to archive daily observations is currently under construction.

Acknowledgements

This study is supported by the National Science Fund of Bulgaria with contract No. KP-06-H28/4 and the joint project of cooperation between IANAO, Bulgarian Academy of Sciences and the Department of Astronomy, Faculty of Mathematics, University of Belgrade, Serbian Academy of Sciences and Arts P-04/04.02.2020.

References

Albert, K., Hirzberger, J., Kolleck, M. et al.: 2020, *A&A*, **642**, id.A1, 31 pp.
Bogomolov, A. V., Myagkova, I. N., Myshyakov, I., Tsvetkov, Ts., Kashapova, L., Miteva, R.: 2018, *JASTP*, **179**, 517.
Bonadonna, M., Lanzerotti, L., Stailey, J.: 2016, *Space Weather*, **15**.
Dermendjiev, V. N., Mishev, D., Koleva, K.: 1999, *Solar eclipses*, Prof. Marin Drinov Academic Publishing House, Sofia, Bulgaria.
Duchlev, P., Koleva, K., Dechev, M., Petrov, N., Kokotanekova, J., Rompolt, B., Rudawy, P.: 2010, *BAJ*, **13**, 47.
Fox, N. J., Velli, M. C., Bale, S. D. et al.: 2016, *Space Science Reviews*, **204**, Issue 1-4, 7.
Gulyaev, R. A., Petrov, N. I.: 2003, *AApTr*, **22**, Issue 4-5, 617.
Merzlyakov, V. L., Tsvetkov, Ts., Starkova, L. I., Miteva, R.: 2019, *Serb. Astron. J.*, **199**, 83.

Miteva, R., Tsvetkov, Ts.: 2019, *AIP Conference Proceedings*, **2075**, Issue 1, id.090014.
Miteva, R., Klein, K.-L., Malandraki, O., Dorrian, G.: 2013, *Sol Phys*, **282**, Issue 2, 579.
Miteva, R., Samwel, S. W., Costa-Duarte, M. V.: 2018, *Sol Phys*, **293**, Issue 2, 44.
Myshyakov, I., Tsvetkov, Ts.: 2020, *ApJ*, **889**, Issue 1, 7.
Petrov, N., Kjurkchieva, D., Tsvetkov, Ts.: 2018, *AApTr*, **30**, Issue 4, 441.
Rieutord, M., Rincon, F.: 2010, *Living Rev. Sol. Phys.*, **7**, article number: 2.
Rimmele, T. R., Warner, M., Keil, St. L. et al.: 2020, *Sol Phys*, **295**, Issue 12, article id.172.
Rodriguez Gomez, J. M., Palacios, J., Vieira, L. E. A., Dal Lago, A.: 2019, *ApJ*, **884**, Issue 1, 7.
Sakurai, T.: 2017, *Proceedings of the Japan Academy, Series B Physical and Biological Sciences*, **93(2)**, 87.
Sterling, A. C.: 2000, *Sol Phys*, **196**, 79.
Tsvetkov, Ts., Petrov, N.: 2018, *JASTP*, **177**, 29.
Tsvetkov, Ts., Petrov, N.: 2020, *ApJ*, **893**, Issue 1, 7.
Tsvetkov, Ts.: 2020, *BAJ*, **33**, 117.
Tsvetkov, Ts., Petrov, N.: 2020, *Proceedings of the Twelfth Workshop "Solar Influences on the Magnetosphere, Ionosphere and Atmosphere"*, 36.
Tsvetkov, Ts, Miteva, R., Petrov, N.: 2018*JASTP*, **179**, 1.
Tsvetkov, Ts., Miteva, R., Ivanov, E., Popov, V., Nakeva, Y., Bojevski, L., Damm, T., Petrov, N.: 2019, *Proceedings of the Fifteenth International Scientific conference "Space, Ecology, Safety - SES2019"*, held 6-8 November 2018 in Sofia, Bulgaria. Edited by P. Getsov, G. Mardirossian and Ts. Srebrova, 52.

Publ. Astron. Obs. Belgrade No. 100 (2021), 145 - 152 *Invited Lecture*

THE CENTENARY OF THE JEANS EQUATIONS: DARK MATTER IN MASSIVE EARLY-TYPE GALAXIES

S. SAMUROVIĆ
Astronomical Observatory, Volgina 7, 11060 Belgrade, Serbia
E–mail: srdjan@aob.bg.ac.rs

Abstract. The year 2019 marked the centenary of the publication of the book *Problems of Cosmogony and Stellar Dynamics* by James Jeans in which he summarized the work on dynamics of stellar systems based on his works published from 1915 onwards. We discuss one important application of his work relevant for contemporary galactic research: we analyze the problem of dark matter in massive early-type galaxies (ellipticals and lenticulars) using various available observational data. We show that in these galaxies dark matter does not dominate in the inner regions, but becomes more important beyond three effective radii.

1. INTRODUCTION

The problem of dark matter (DM) and its contribution to the total dynamical mass of various morphological types of galaxies exists since the 1970s. The existence of DM in spiral galaxies is well documented and the studies of their rotation curves (RCs) provided ample evidence for the existence of DM (see e.g., Bertin 2014). The use of available databases, such as the THINGS (The HI Nearby Galaxy Survey) database (Walter et al. 2008) provides the opportunity to study the DM problem in nearby spirals. For example, Jovanović (2017, and also the contribution by Jovanović et al. in this Book of proceedings) analyzed the spiral galaxy NGC 5055, and also dwarf irregular galaxy DDO 154, using THINGS to examine their RCs. The study of the RCs in both objects shows the significant DM contribution.

The details regarding the study of DM in early-type galaxies (hereafter, ETGs) which include ellipticals and lenticulars are provided in Samurović (2007). It is important to note that ETGs are studied to a lesser degree than their spiral counterparts. The reasons for such a situation include the lack of cool gas (neutral hydrogen HI) in ETGs necessary for obtaining RCs at large galactocentric distances. Another observational fact is that ETGs are faint in their outer parts and thus we need long exposures for obtaining high quality spectra and photometric data at large galactocentric distances (at several effective radii, R_e, where 1 R_e is the radius which encompasses half of the total light of the given galaxy). Last but not least, there is the problem of the lack of knowledge of the shape of orbits in these galaxies and this leads to the well-known mass-anisotropy degeneracy.

The Jeans equations proved to be very useful from the very beginning and remain the main tool of the study of the DM problem in ETGs. There are other, arguably

more sophisticated, but much more computationally demanding, methods for estimating the total dynamical masses of ETGs and they include the method based on orbit superposition (Schwarzschild 1979) and the made-to-measure modeling based on the distribution functions (Syer & Tremaine 1996). Alternative theories of gravitation such as the MOdified Newtonian Dynamics (MOND; Milgrom 1983) have been applied to ETGs with various degrees of success. In the present paper we discuss Newtonian dynamics only and refer the reader to our work where the application of the Jeans equations to ETGs in MOND was discussed (Samurović 2019).

The plan of the paper is as follows. In Chapter 2 historic background and basic details regarding the Jeans equations are presented. In Chapter 3 the application of the Jeans equations using integrated stellar spectra in ETGs is described. In Chapter 4 other tracers of gravitational potential in ETGs such as planetary nebulae (PNe) and globular clusters (GCs) are discussed. Finally, in Chapter 5 the main conclusions are given and some directions of the future investigation of DM in ETGs are outlined.

2. HISTORIC BACKGROUND AND FOUNDATIONS OF THE JEANS EQUATIONS

Sir James Jeans (1877 – 1946) in a series of his papers (Jeans 1915, 1916a, 1916b) and later in his book *Problems of Cosmogony and Stellar Dynamics*[1] (Jeans 1919) introduced equations which are now known as the Jeans equations. He applied for the first time to stellar systems the equations previously derived by James Clerk Maxwell (Maxwell 1867) related to the equilibria of the collisionless systems. On page 229 of his book Jeans says: "It now appears that, for our present universe[2], the problem of stellar dynamics is the same as the problem of the kinetic theory of gases with the collisions left out. This being so, stellar dynamics is naturally very much simpler than gas-dynamics". Maxwell already had a set of equations named after him, so the equations applied by Jeans have become the Jeans equations. However, there were discussions in the literature regarding their name. In 1982 Hénon in his brief paper listed seven possible names and the name Maxwell was conspicuously absent: Liouville equation, Boltzmann equation, collisionless Boltzmann equation, Liouville-Boltzmann equation, Jeans equation, equation of continuity and Vlasov equation (Hénon 1982). He suggested that the proper name would be "collisionless Boltzmann equation". His, as he called it, "plea" to astronomers and physicists was not adopted by the scientific community. Several decades later, Robson et al. (2017) on the 150th anniversary of the Maxwell's 1867 paper reviewed the Maxwell-Boltzmann formalism and called the equations devised by Maxwell: "Maxwell's (other) equations". Thus, Maxwell's fundamental work related to electromagnetism can be distinguished from his contribution in the field of collisionless systems.

Below some most important steps needed for the derivation of the Jeans equations are presented and the reader is referred to the book by Binney & Tremaine (2008) for the detailed description of the procedure.

It can be assumed that an elliptical galaxy is a collisionless system made of several billion stars and one can operate in the six-dimensional phase-space volume $\mathrm{d}^3\mathbf{x}\mathrm{d}^3\mathbf{v}$ around the position determined with $\mathbf{x}$ and velocity $\mathbf{v}$. The distribution function,

[1]The book is available at `https://archive.org/details/problemsofcosmog00jeanrich`.
[2]In modern language this corresponds to our Galaxy.

which is a non-negative function, i.e., $f \geq 0$ is then defined. Using Hamilton's equations, the collisionless Boltzmann equation is obtained which can be written in the following form:

$$\frac{\partial f}{\partial t} + \mathbf{v} \cdot \frac{\partial f}{\partial \mathbf{x}} - \frac{\partial \Phi}{\partial \mathbf{x}} \cdot \frac{\partial f}{\partial \mathbf{v}} = 0, \tag{1}$$

where Φ is the gravitational potential.

Since in a given ETG individual stars cannot be resolved one has to deal with integrated stellar light of the given galaxy which represents the average of the stellar properties of numerous unresolved stars that lie along each line of sight (LOS). We now define line-of-sight velocity distribution (LOSVD, $F(v_{\rm los})$). The fraction of stars contributing to the spectrum of the galaxy which have LOS velocities between $v_{\rm los}$ and $v_{\rm los}+{\rm d}v_{\rm los}$ is given by $F(v_{\rm los}){\rm d}v_{\rm los}$. One can model the LOSVD as a truncated Gauss-Hermite series, i.e., as a Gaussian multiplied by a polynomial (van der Marel & Franx 1993):

$$F_{\rm TGH}(v_{\rm los}) \propto e^{-\frac{1}{2}w^2} \left[1 + \sum_{k=3}^{n} h_k H_k(w)\right], \tag{2}$$

where $w \equiv (v_{\rm los} - \bar{v})/\sigma$. We study h_3 (asymmetric) and h_4 (symmetric) departures from the Gaussian and higher values, h_n with $n > 4$, are also possible. If $h_4 < 0$ then tangential orbits dominate and if $h_4 > 0$ then radial orbits dominate. In dynamical models one can vary $\bar{v}$, σ, h_3 and h_4 until convolution of $F_{\rm TGH}$ and stellar template best reproduces the observed galaxy spectrum and if LOSVD is close to Gaussian then $\bar{v}$ and σ will approximately be equal to $\bar{v}_{\rm los}$ and $\sigma_{\rm los}$.

If we integrate Eq. 1 and take into account that $f(\mathbf{x}, \mathbf{v}, t) = 0$ at sufficiently large $\mathbf{v}$, because there are no stars moving infinitely fast, we obtain:

$$\frac{\partial \nu}{\partial t} + \frac{\partial (\nu \bar{v}_i)}{\partial x_i} = 0, \tag{3}$$

where $\nu(\mathbf{x})$ is the probability per unit volume of finding a given star at the position $\mathbf{x}$, regardless of its velocity $\mathbf{v}$. This is an equation of continuity of probability. The equation analog to the Euler's equation of fluid flow in spherical coordinates can be written as:

$$\frac{{\rm d}\sigma_r^2}{{\rm d}r} + \sigma_r^2 \frac{(2\beta + \alpha)}{r} = a_{N;M} + \frac{v_{\rm rot}^2}{r}, \tag{4}$$

where σ_r is the radial component of the stellar velocity dispersion, the α parameter is defined as $\alpha = {\rm d}\ln\nu/{\rm d}\ln r$ is the slope of tracer density ν, the so called anisotropy parameter β is equivalent to the h_4–parameter and $v_{\rm rot}$ is the rotational velocity. Equations (3) and (4) are the Jeans equations. Eq. 4 is the form of the Jeans equation most frequently used in the analysis of DM in the literature. It can be applied using both Newtonian ("N") and MOND ("M") methodologies where $a_{N;M}$ is an acceleration term calculated separately for each methodology. In the Newtonian approach the acceleration is equal to $a_N = -\frac{GM(r)}{r^2}$, where $M(r)$ is the mass enclosed at radius r.

It took some time for the application of the Jeans equation to ETGs and one of the earliest examples can be found in the work of Duncan & Wheeler (1980) in which the analysis of the central parts of the elliptical galaxy M87 was performed (the term "collisionless Boltzmann equation" was used for the equation which was solved).

3. INTEGRATED STELLAR SPECTRA

3. 1. LONG-SLIT SPECTRA

The contribution of DM in ETGs was studied using the Jeans equation through the investigation of their integrated stellar spectra. Also, the analysis of the total mass profiles based on X-ray observations was performed where possible. An early work by Binney, Davies & Illingworth (1990) introduced the two-integral (2I) Jeans modeling procedure: three ETGs (NGC 720, NGC 1052 and NGC 4697) were modeled using the observed velocity dispersion profiles obtained from their long-slit spectra. Although the study of DM was not in their focus they posed the fundamental question to be addressed in the study of DM in ETGs, "is the mass-to-light ratio constant?". The same technique was later used in van der Marel, Binney & Davies (1990) on other four ETGs (NGC 3379, NGC 4261, NGC 4278 and NGC 4472), to distances at most equal to $\sim 1\ R_e$. It was found that constant mass-to-light ratios can provide successful fits to the observed velocity dispersion profiles. Carollo et al. (1995) obtained the long-slit spectra of several ETGs beyond 1 R_e and found that 3 out of 4 galaxies in their sample must possess a dark halo.

Samurović & Danziger (2005) used long-slit spectra to study 4 ETGs and the DM contribution inside $\sim 1{-}3\ R_e$. ETGs IC 1459, IC 3370, NGC 3379 and NGC 4105 were analyzed using 2I Jeans models taking into account full LOSVD and the comparison with X-ray observations was made (where available). Significant amounts of DM were not detected. IC 1459, an ETG with a counter-rotating core, showed high values of the h_4–parameter in its outer parts which implied the existence of radial anisotropies there; also, it was found that DM in this galaxy is not dominant interior to $\sim 3\ R_e$.

One of the latest applications of the analysis of long-slit spectra on ETGs can be found in Salinas et al. (2012): the kinematics of the NGC 7507 was studied and it was found that the models without DM provide an excellent fit of the observed data.

3. 2. INTEGRAL FIELD SPECTROSCOPY

The integral field spectroscopy (IFS) is a powerful technique which provides the larger spatial coverage of integrated stellar spectra than the long-slit observations. Below, some of the projects and their main results are listed (see the review of the studies of structure and kinematics if ETGs from IFS in Cappellari 2016).

The first generation of IFS surveys included the following projects: SAURON (Spectroscopic Areal Unit for Research on Optical Nebulae), ATLAS^{3D} and CALIFA (Calar Alto Legacy Integral Field Area Survey). They are all completed and the main results important for the present paper are as follows.

SAURON: Emsellem et al. (2004) studied 48 ETGs and estimated velocity, velocity dispersion and the Gauss-Hermite parameters h_3 and h_4 out to $\sim 1\ R_e$. Cappellari et al. (2006) used 2I Jeans and three-integral Schwarzschild dynamical models for a sample of 25 ETGs inside $\sim 1\ R_e$ and discovered that DM contributes to ~ 30 per cent of the total dynamical mass.

ATLAS^{3D}: Cappellari et al. (2013) analyzed the problem of the mass-to-light ratio and DM in their sample, calculated total mass-to-light ratios within $\sim 1\ R_e$ and found median value of DM fraction, $f_{\rm DM} = 13$ per cent.

CALIFA: Approximately 200 galaxies (out of approximately 600 objects) from the CALIFA sample of nearby galaxies belong to the ETG class (Sánchez et al. 2012).

The stellar kinematic maps, which include velocities and velocity dispersions, of approximately 300 galaxies are presented in Falcón-Barroso et al. (2017).

The second generation of IFS which is still producing results includes the following surveys: MUSE (Multi Unit Spectroscopic Explorer), MASSIVE, SAMI (The Sydney AAO Multi Integral Feld) and MaNGA (Mapping Nearby Galaxies at APO).

MUSE: Several ETGs were explored with MUSE. For example, the low-luminosity S0 galaxy NGC 5102 (Mitzkus, Cappellari & Walcher 2017) was analyzed interior to $\sim 1\ R_e$ and a DM fraction of 0.37 ± 0.04 inside $1\ R_e$ was found.

MASSIVE: In Veale et al. (2017) spatially resolved stellar angular momentum, velocity dispersion, and higher moments of the 41 most massive local ETGs were analyzed and it was found that the luminosity-weighted average h_4–parameter, $< h_4 >_e$ is positive, for all 41 ETGs in their sample which is in agreement with the study of Vudragović, Samurović & Jovanović (2016) who found that in the innermost parts of ETGs radial anisotropies with $h_4 > 0$ dominate.

SAMI: In van de Sande et al. (2017) the stellar kinematics on a sample of 315 galaxies, without a morphological selection was measured between 1 and 2 R_e.

MaNGA: The MaNGA survey is part of the SDSS-IV and provides spectral measurements of approximately 10000 nearby galaxies. Rong et al. (2018) used the Jeans dynamical modeling to find that there exists a 1σ significant difference between the acceleration relations of the fast and slow rotators from the MaNGA database.

4. OTHER TRACERS OF GRAVITATIONAL POTENTIAL

For study of DM in ETGs beyond several effective radii ($2 - 3\ R_e$) other methods and approaches are needed. The X-ray approach which does not suffer from the mass-anisotropy degeneracy can be used for this purpose (see e.g., Samurović 2007 and references therein for possible problems). Another possible approach includes the study of stellar shells for the purpose of estimating gravitational fields of ETGs at large galactocentric radii (see e.g., Bílek et al. 2016). Also, tracers such as PNe and GCs in ETGs can be used for establishing the total mass of a given galaxy. Again, it is necessary to solve the Jeans equation (Eq. 4). In Samurović 2019 one can find the description of the necessary steps in such a procedure and more examples of the use of PNe and GCs in the study of DM in ETGs.

4. 1. PLANETARY NEBULAE

PNe are detectable even in moderately distant galaxies through their strong emission lines and proved to be a useful tool in a search for DM in ETGs.

One of the most studied ETGs using the Jeans equation based on both PNe and GCs is the giant elliptical NGC 5128 (Centaurus A). Hui (1993) identified over 400 PNe and applied the spherical Jeans equation to model the observed velocity dispersion profile out to 25 kpc and detected the existence of DM. Hui, Freeman & Dopita (1995) again relied on PNe as tracers and found that the mass-to-light ratio in its central region approximately equal to 3.9 rises to approximately 10 at $5\ R_e$ (in the B-band) which confirmed the existence of the dark halo. Peng, Ford & Freeman (2004) detected 780 spectroscopically confirmed PNe in NGC 5128 and found that DM is necessary to explain the observed stellar kinematics. Samurović (2010) used PNe in NGC 5128 and found that the isotropic Newtonian mass-follows-light models without DM may provide successful fits out to $\sim 6.4\ R_e$ and that to obtain a good fit in the

outermost region ($\sim 10.7\ R_e$) either DM or the existence of tangential anisotropies is needed. The existence of DM in the elliptical galaxy NGC 3379 was studied using PNe in Ciardullo, Jacoby & Dejonghe (1993) who measured radial velocities of 29 PNe (out to $3.8\ R_e$) and found that there is no need for DM. Ten years later, this galaxy was a subject of the study of Romanowsky et al. (2003) who observed PNe in 3 galaxies (NGC 821, NGC 3379 and NGC 4494) and relying on the spherical Jeans models confirmed the lack of DM in NGC 3379 using much larger sample of 109 PNe (out to $\sim 3.5\ R_e$). Samurović & Danziger (2005) analyzed the interior region of NGC 3379 (inside $\sim 1\ R_e$) with long-slit spectra using the Jeans equation and found that DM is not needed there. Douglas et al. (2007) detected 191 PNe of NGC 3379 and using Jeans dynamical models found that inside $5\ R_e$ the mass-to-light ratio in the B-band is $8 < M/L_B < 12$ and that the DM fraction inside this radius is below 40 per cent.

4. 2. GLOBULAR CLUSTERS

One of the earliest examples of usage of GCs in ETGs is the work of Mould et al. (1990) who obtained optical multislit spectra of two giant ellipticals, M49 and M87, from the Virgo cluster and inferred the existence of DM there because of the flat velocity dispersion profiles. Another interesting example of the massive elliptical from the Fornax cluster is NGC 1399. Grillmair et al. (1994) studied the radial velocities of 47 GCs in NGC 1399 and assuming isotropic distribution of the GCs obtained a lower limit on a globally constant mass-to-light ratio of $M/L_B = 79$ which implied strong presence of DM in the outer part of the galaxy. In Samurović & Danziger (2006) it was shown that although the velocity dispersion of NGC 1399 decreases between 4 and $10\ R_e$ there is evidence of DM beyond $\sim 3\ R_e$. This galaxy was re-analyzed using 790 GCs as tracers of the gravitational potential in Samurović (2016) and using the Jeans equation it was shown that a significant amount of DM is needed.

The significant contribution to the study of DM in ETGs has come from the SLUGGS (SAGES Legacy Unifying Galaxies and GlobularS) survey: Pota et al. (2013) analyzed kinematics for over 2500 GCs of 12 ETGs. The SLUGGS sample was used in Samurović (2014): 10 ETGs were studied and in Newtonian approach only one ETG, NGC 2768, could be modeled without DM; three galaxies (NGC 1400, NGC 3377 & NGC 4494) show an increase of the total mass-to-light ratio with radius between the innermost and outermost radii, which suggests the existence of DM in their outer parts and NGC 4486 is the only galaxy that needs significant amount of DM even in its inner region. The remaining 5 galaxies require a significant amount of DM beyond $\sim 2 - 3\ R_e$, and the largest mass-to-light ratio was found in NGC 5846 for which $64.2 < M/L_B < 127.4$ beyond $\sim 6\ R_e$ was established.

Bílek, Samurović & Renaud (2019) studied using the Jeans equation 17 ETGs based on their GCs. For the total sample the median contributions of DM inside $1\ R_e$ and $5\ R_e$ are 20 and 72 per cent, respectively. The DM fractions of the slow rotators are much higher than that of the fast rotators: for the fast rotators the DM fractions are equal to 18 and 69 per cent inside 1 and $5\ R_e$, respectively, whereas for the slow rotators the DM fractions become 40 and 88 per cent at the same radii, respectively.

Samurović & Vudragović (2019) analyzed two massive nearby ETGs, NGC 4473 and NGC 4697, both fast rotators using the data from the SLUGGS database. To calculate the contribution of the visible, stellar, component the 1.40 m "Milanković"

telescope mounted at Vidojevica was used to obtain the deep photometry in the B- and V-bands. NGC 4473 was modeled interior to $\sim 12\ R_e$ and NGC 4697 was modeled interior to $\sim 3\ R_e$ using 3 cases of anisotropies. Newtonian purely baryonic models for both galaxies in most cases could not provide a successful fit of the observed velocity dispersion without the additional, dark component. However, the solutions for both galaxies based on purely baryonic tangentially anisotropic models were found.

5. CONCLUSIONS

The year 2019 marked the centenary of the publication of the James Jeans' book *Problems of Cosmogony and Stellar Dynamics* in which he presented the equations that are now known and used as the Jeans equations.

It was shown that the Jeans equations remain an indispensable tool in the study of galaxies, especially massive ETGs and the problem of DM in them. The application of the usage of the Jeans equations in massive nearby ETGs in case of integrated stellar spectra in galaxies (both long-slit and integrated field spectra), and other tracers of gravitational potential (PNe and GCs) was discussed.

Some future work related to DM in ETGs will include: the study of trends in population and kinematics at radii beyond $\sim 2\ R_e$, studies of the problem of stellar population and the analysis of initial mass functions in ETGs, studies of the trends in total density profiles at large galactocentric distances where DM is expected to dominate and the comparison with spirals.

The new "Milanković" 1.40 m telescope mounted at the Astronomical Station Vidojevica run by the Astronomical Observatory of Belgrade has proven to be a very useful tool in obtaining images of nearby ETGs thus providing the information on the stellar content inside several effective radii.

Acknowledgements

This work was supported by the Ministry of Education, Science and Technological Development of the Republic of Serbia (MESTDRS) through the contract No. 451-03-68/2020-14/200002. Useful discussions with Dr. M. Bílek, Dr. A. Vudragović, M. Jovanović, Dr. O. Vince, Dr. M. Ćirković, Dr. B. Vukotić and Dr. S. Knežević are acknowledged, as well as the work of the technical operators at the Astronomical Station Vidojevica, M. Sekulić and P. Kostić. The financial support by the European Commission through project BELISSIMA (BELgrade Initiative for Space Science, Instrumentation and Modelling in Astrophysics, call FP7-REGPOT-2010-5, contract No. 256772) which was used to procure the 'Milanković' 1.40 m telescope with the support from the MESTDRS is acknowledged as well as the the continued support of the MESTDRS related to the work of the Astronomical Station Vidojevica. The author thanks the referee for useful comments.

References

Bertin, G.: 2014, *Dynamics of Galaxies*, Second Edition, (Cambridge University Press, Cambridge).

Bílek, M., Cuillandre, J.-C., Gwyn, S., Ebrová, I., Bartošková, K., Jungwiert, B., Jílková, L.: 2016, *Astron. Astrophys.*, **588**, A77.

Bílek, M., Samurović, S., Renaud, F.: 2019, *Astron. Astrophys.*, **625**, A32.

Binney, J. J., Tremaine, S.: 2008, *Galactic Dynamics*, Second Edition, (Princeton Univ. Press, Princeton).

Binney, J. J., Davies, R. D., Illingworth, G. D.: 1990, *Astrophys. J.*, **361**, 78.

Cappellari, M.: 2016, *Ann. Rev. of Astron. and Astroph.*, **54**, 597.
Cappellari, M., Bacon, R., Bureau, M. et al.: 2006, *Mon. Not. R. Astron. Soc.*, **366**, 1126.
Cappellari, M., Scott, N., Alatalo, K. et al.: 2013, *Mon. Not. R. Astron. Soc.*, **432**, 1709.
Carollo, C. M., de Zeeuw, P. T., van der Marel, R. P., Danziger, I. J., Qian, E. E.: 1995, *Astrophys. J. Lett.*, **441**, L25.
Ciardullo, R., Jakoby, G. H., Dejonghe, H. G.: 1993, *Astrophys. J.*, **414**, 454.
Douglas, N. G., Napolitano, N. R., Romanowsky, A. J. et al.: 2007, *Astrophys. J.*, **664**, 257.
Duncan, M. J., Wheeler, J. C.: 1980, *Astrophys. J. Lett.*, **237**, L27.
Emsellem, E., Cappellari, M., Peletier, R. F. et al.: 2004, *Mon. Not. R. Astron. Soc.*, **352**, 721.
Falcón-Barroso, J., Lyubenova, M., van de Ven, G. et al.: 2017, *Astron. Astrophys.*, **597**, A48.
Grillmair, C. J., Freeman, K. C., Bicknell, G. V., Carter, D., Couch, W. J., Sommer–Larsen, J., Taylor, K.: 1994, *Astrophys. J.*, **422**, L9.
Hénon, M.: 1982, *Astron. Astrophys.*, **114**, 211.
Hui, X.: 1993, *Publ. Astron. Soc. Pac.*, **105**, 1011.
Hui, X., Ford, H. C., Freeman, K. C., Dopita, M. A.: 1995, *Astrophys. J.*, **449**, 592.
Jeans, J. H.: 1915, *Mon. Not. R. Astron. Soc.*, **76**, 70.
Jeans, J. H.: 1916a, *Mon. Not. R. Astron. Soc.*, **76**, 552.
Jeans, J. H.: 1916b, *Mon. Not. R. Astron. Soc.*, **76**, 567.
Jeans, J. H.: 1919, *Problems of Cosmogony and Stellar Dynamics*, (Cambridge Univ. Press, Cambridge), reprinted in 2009, (Cambridge Univ. Press, Cambridge).
Jovanović, M.: 2017, *Mon. Not. R. Astron. Soc.*, **469**, 3564.
Maxwell, J. C.: 1867, *Philos. Trans. R. Soc. Lond.*, **157**, 49.
Milgrom, M.: 1983, *Astrophys. J.*, **270**, 365.
Mitzkus, M., Cappellari, M., Walcher, C. J.: 2017, *Mon. Not. R. Astron. Soc.*, **464**, 4789.
Mould, J. R., Oke, J. B., de Zeeuw, P. T., Nemec, J. M.: 1990, *Astron. J.*, **99**, 1823.
Peng, E. W., Ford, H. C., Freeman, K. C.: 2004, *Astrophys. J.*, **602**, 685.
Pota, V., Forbes, D. A. Romanowsky, A. J. et al.: 2013, *Mon. Not. R. Astron. Soc.*, **428**, 389.
Robson, R. E., Mehrling, T. J., Osterhoff, J.: 2017, *Eur. J. Phys.*, **38**, 065103.
Romanowsky, A. J., Douglas, N. G., Arnaboldi, M., Kuijken, K., Merrifield, M. R., Napolitano, N. R., Capaccioli, M., Freeman, K. C.: 2003, *Science*, **5640**, 1696.
Rong, Y., Li, H., Wang, J. et al.: 2018, *Mon. Not. R. Astron. Soc.*, **477**, 230.
Salinas, R., Richtler, T., Bassino, L. P., Romanowsky, A. J., Schuberth, Y.: 2012, *Astron. Astrophys.*, **538**, A87.
Samurović, S.: 2007, *Dark Matter in Elliptical Galaxies*, Publications of the Astronomical Observatory of Belgrade, No. 81.
Samurović, S.: 2010, *Astron. Astrophys.*, **514**, A95.
Samurović, S.: 2014, *Astron. Astrophys.*, **570**, A132.
Samurović, S.: 2016, *Astrophys. Space Sci.*, **361**, 199.
Samurović, S.: 2019, *Serb. Astron. J.*, **199**, 1.
Samurović, S., Danziger, I. J.: 2005, *Mon. Not. R. Astron. Soc.*, **363**, 769.
Samurović, S., Danziger, I. J.: 2006, *Astron. Astrophys.*, **458**, 79.
Samurović, S., Vudragović, A.: 2019, *Mon. Not. R. Astron. Soc.*, **482**, 2471.
Sánchez, S. F., Kennicutt, R. C., Gil de Paz, A. et al.: 2012, *Astron. Astrophys.*, **538**, A8.
Schwarzschild, M.: 1979, *Astrophys. J.*, **232**, 236.
Syer, D., Tremaine, S.: 1996, *Mon. Not. R. Astron. Soc.*, **282**, 223.
van der Marel, R. P., Binney, J., Davies, R. L.: 1990, *Mon. Not. R. Astron. Soc.*, **245**, 582.
van der Marel, R. P., Franx, M.: 1993, *Astrophys. J.*, **407**, 525.
van de Sande, J., Bland-Hawthorn, J., Fogarty, L. M. R. et al.: 2017, *Astrophys. J.*, **835**, Issue 1, article id. 104.
Veale, M., Ma, C.-P., Thomas, J. et al.: 2017, *Mon. Not. R. Astron. Soc.*, **464**, 356.
Vudragović, A., Samurović, S., Jovanović, M.: 2016, *Astron. Astrophys.*, **593**, A40.
Walter, F., Brinks, E., de Blok, W. J. G. et al.: 2008, *Astron. J.*, **136**, 2563.

Publ. Astron. Obs. Belgrade No. 100 (2021), 153 - 159 *Invited Lecture*

ZAŠTO JE VAŽNO IZUČAVANJE ASTRONOMIJE U TOKU SREDNJOŠKOLSKOG OBRAZOVANJA?

BILJANA STOJIČIĆ

Zemunska gimnazija, Gradski park 1, 11080 Beograd, Srbija
E–mail: biljanasotjicic963@gmail.com

Abstract. Astronomija je jedna od najstarijih nauka i jedna od nauka koje se danas najbrže razvijaju. Pored Univerziteta, teme iz astronomije se izučavaju i u osnovnoj i srednjoj školi. U ovom radu dat je prikaz nastave astronomije u srednjim školama u Srbiji, kao i pogodnost interdisciplinarnosti astronomije za povezivanje znanja iz više predmeta. Kroz više primera prikazana je mogućnost izvođenja praktične nastave astronomije, koja pored učenja astronomije, pospešuje upoznavanje učenika sa samim istraživačkim procesom.

1. UVOD

Astronomija se u našim školama izučava od XIX veka, a krajem XX veka je ukinuta kao poseban predmet. Od 1991. godine izučava se na prirodno-matematičkom smeru u četvrtom razredu gimnazije sa fondom od 32 časa godišnje, dok se u novom, reformisanom programu predviđa 8 časova. Zanimljivo je da to nije poseban predmet već se izučava u okviru fizike. Izuzetatak su Matematička gimnazija sa jednim časom nedeljno i gimnazija za učenike sa posebnim sposobnostima za fiziku, gde je fond časova duplo veći, a u oba programa predmet je poseban. Nastavu astronomije u našim školama realizuju, pored astronoma, astrofizičara i fizičari. Iskustvo stečeno tokom realizacije nastave astronomije tokom poslednje tri decenije je dragoceno i može poslužiti za kreiranje nastave u budućem periodu.

Svaki nastavnik koji je realizovao program astronomije u gimnaziji je uočio da je astronomija izuzetno zanimljiva učenicima. Neretko se dešava da se i učenik nezainteresovan za učenje pokrene i počne da radi. Razlog tome treba tražiti u samom polju istraživanja astronomije. Upravo je ta zainteresovanost nešto što može biti dobro polazište za ono što se želi postići kroz nastavu astronomije. Program je tako koncipiran da je zapravo moguće, kroz izučavanje sadržaja astronomije ponoviti celokupno gimnazijsko gradivo fizike: mehanika-kretanje nebeskih tela; optika-posmatračka astronomija; nuklearna fizika-energija zvezda... Ne bi trebalo izgubiti iz vida da se astronomija izučava u četvrtom razredu gimnazije, kada su učenici stekli značajna znanja iz matematike (daleko viši nivo u odnosu na prvi razred, kada se izučava mehanika npr.) i kada su mnogo zreliji i sa usvojenim raznim tehnikama učenja. Astronomija pruža široko polje primene znanja iz geometrije, stereometrije, trigonometrije, sferne trigonometrije. Sa razvojem primene solarnih ćelija javile su se

nove potrebe za znanjima iz Solarne geometrije. Sve navedeno omogućava da kroz izučavanje sadržaja iz astronomije razviju i usvoje osnovne koncepte u fizici i primene znanja iz matematike. Na taj način ponavljanje gradiva nije prosta reprodukcija, već se postiže viši kvalitet tog znanja.

Fasciniranost nebeskim svodom prekrivenim zvezdama nije nešto što je svojstveno samo savremenom čoveku. Ta opčinjenost je pokretala stare narode da posmatraju astronomske pojave i tragaju za njihovim objašnjenjima, što je u novije vreme, između ostalog dovelo do formiranja nove oblasti, arheoastronomije. Upravo ta otkrića, učenicima naviknutim na veliku podršku tehničkih sredstava, često deluju neverovatna. Sa druge strane, ona su izvanredni primeri na kojima se demonstrira potreba za pažljivim posmatranjem pojava i njihovog analiziranja, što je duboko vezano za prirodu istraživanja u astronomiji.

Često se može uočiti insistiranje na integrativnoj nastavi u našem obrazovnom sistemu. O važnosti tog pristupa se ne polemiše, ali ono što jeste problem je realizacija. Upravo interdisciplinarnost astronomije daje mogućnost za ovakav pristup u nastavi. Nastava astronomije otvara još jednu mogućnost, a to je projektna nastava. U radu će biti opisane neke od ideja za realizaciju projektne nastave, i to, Eratostenov eksperiment i primena u nastavi u odeljku 3, određivanje lokalnog meridijana u odeljku 4, a određivanje unutrašnjeg meridijana u odeljku 5. Posmatranje prelaska Sunčevog diska preko lokalnog meridijana je opisano u odeljku 6, i simulacija petlji planeta u školskom dvorištu kao što su predložili Bennett J. i saradnici 2004. u odeljku 7.

2. GDE I KAKO SE IZUČAVA ASTRONOMIJA U SREDNJIM ŠKOLAMA U SRBIJI

Osnovna znanja iz astronomije, primereno svom uzrastu učenici u Srbiji stiču još u osnovnoj školi i to kroz predmete Svet oko nas, Geografija i Fizika. Na nivou srednjoškolskog obrazovanja najpotpunija znanja mogu dobiti učenici specijalizovanog odeljenja gimnazije za učenike sa posebnim sposobnostima za fiziku (2 časa nedeljno u četvrtom razredu), potom su to učenici Matematičke gimnazije (1 čas nedeljno u četvrtom razredu). Učenici oba smera imaju poseban predmet i sadržaje astronomije ne izučavaju kroz drugi predmet. Od ostalih učenika najviše sadržaja iz astronomije izučavaju učenici prirodno-matematičkog smera gimnazije (32 časa na godišnjem nivou u okviru nastave fizike u četvrtom razredu), dok ostali mogu steći najelementarnija znanja kroz nastavu fizike i geografije i to kroz daleko manji broj časova. Ovaj model se primenjivao od 1991. godine.

Reformisani plan i program gimnazije predviđa manji broj časova fizike nedeljno u četvrtom razredu (nekada pet sada četiri), što se odrazilo i na smanjenje broja časova posvećenih astronomiji. U školskoj 2021/2022. godini prva generacija će izučavati astronomiju po izmenjenom planu i programu.

Rešenje problema, ko može da realizuje nastavu astronomije u srednjoškolskom obrazovanju u Srbiji je rešen tako što nastavu astronomije realizuju pored astronoma i astrofizičara i nastavnici fizike. Ujedno najčešće rešenje u našim školama je da nastavu realizuju nastavnici fizike. Razlog za takav izbor treba tražiti i u tome što je najčešće mali fond časova astronomije u jednoj školi, što je naročito veliki problem u malim sredinama gde obično postoji jedna gimnazija sa malim brojem odeljenja.

3. ERATOSTENOV EKSPERIMENT

Eratostenov eksperiment je jedan od najinspirativnijih eksperimenata poznatih u istoriji nauke. On pleni svojom jednostavnošću, ali i originalnošću Eratostenove ideje.

Eratosten je svoje merenje zasnivao na činjenici da je u Sieni postojao bunar u kome je na dan letnjeg solsticija u podne bilo moguće videti odraz Sunca u vodi. To je značilo da štap postavljen vertikalno u tom mestu na taj dan ne bi imao senku. Mereći dužinu senke u Aleksandriji, pri čemu je znao udaljenost Aleksandrije od Siene, mogao je da proceni ugao koji grade poluprečnici Zemlje koji povezuju centar Zemlje sa ovim mestima. On je procenio obim Zemlje na osnovu vrednosti tog ugla i poznatog rastojanja od Aleksandrije do Siene. Taj eksperiment se masovno ponavlja širom sveta iz godine u godinu, pri čemu učenici različitog uzrasta učestvuju u njemu, sami ili uz saradnju sa učenicima iz drugih gradova povezujući se kroz platformu http://eratosthenes.ea.gr/. 21.3.2017. godine je sa učenicima Zemunske gimnazije izvršeno merenje obima Zemlje (tj. poluprečnika Zemlje).

Merenja koja vrše učenici širom sveta su simulacija te situacije. Na osnovu lokacije mesta gde se meri može se odredi se lokalno podne koristeći podatke sa sajta https://www.esrl.noaa.gov/gmd/grad/solcalc/. A potom se može odredi rastojanje do ekvatora pomoću sajta *Google Earth*.

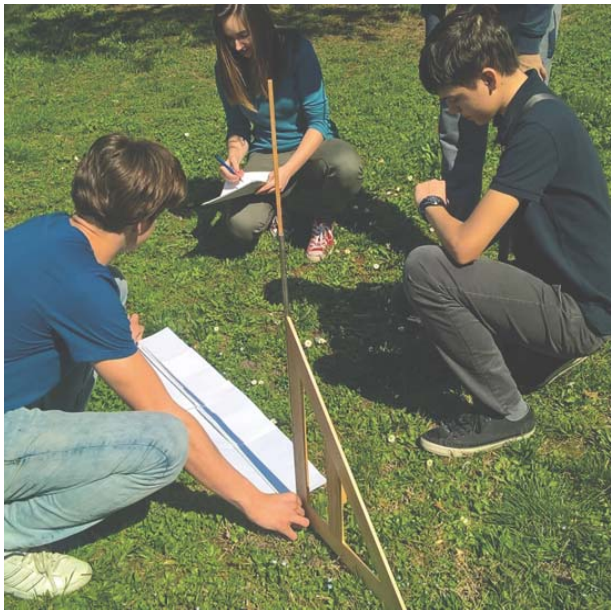

Figure 1: Merenja obavljena u martu 2017. godine.

Rezultat koji je dobijen 2017. godine, korišćenjem podataka za mesto na ekvatoru, koje se nalazi na istom meridijanu kao i Zemun je da je poluprečnik Zemlje 6580 km. Relativna greška je 1,5% u odnosu na uobičajeno korišćeni podatak od 6375 km.

Merenja učenici mogu obaviti i van škole i rad se može koncipirati i na taj način.

4. ODREĐIVANJE LOKALNOG MERIDIJANA

Meridijan u geografiji se definiše kao imaginarna kružnicu na Zemlji koja obuhvata južni i severni pol. Linija označena na horizontalnoj podlozi duž meridijana na Zemlji se naziva meridijan. Sunce pri svom prividnom kretanju nad horizontom opisuje dnevni luk pri čemu dostiže najveću visinu u trenutku lokalnog podneva , kada prolazi kroz ravan meridijana.

Lokalni meridijan se veoma lako može odrediti pomoću vertikalno postavljenog štapa, tj. gnomona, čija se senka posmatra u toku par sati oko lokalnog podneva. U početnom trenutku posmatranja iscrta se ili obeleži na neki drugi način kružnica čiji je centar na mestu gde je postavljen štap u vertikalni položaj. Senka štapa će tokom daljeg posmatranja bivati sve kraća i ona će preseći kružnicu nakon prolaska Sunca kroz ravan lokalnog meridijana. Kada se to dogodi obeleži se taj položaj i odredi simetrala ugla koji grade duži koje spajau početni i krajnji položaj sa štapom. Ta simetrala se poklapa sa lokalnim meridijanom. Kada Sunce prolazi kroz ravan lokalnog meridijana, tj. u trenutku lokalnog podneva, ono se nalazi na jugu, dok senka štapa leži u ravni lokalnog meridijana i usmerena je ka severu.

Figure 2: Lokalni meridijan određen u Zemunskoj gimnaziji 2018. godine.

5. UNUTRAŠNJI MERIDIJAN

Unutrašnji meridijan se obeležava u zatvorenom prostoru i za njegovo određivanje ne koristi se gnomon, već mali otvor na zidu ili krovu zgrade, kroz koji prolazi svetlost. Tokom godine se onda mogu posmatrati položaji lika Sunca pri prolazu kroz ravan lokalnog meridijana.

6. PARALELNI GLOBUSI ILI DING GLOBUS

Iskustvo pokazuje da su za učenje i razumevanje osnovnih pojmova u astronomiji veoma korisni modeli u realnom prostoru koji omogućuju njihovu vizuelizaciju. Dan Noć i Godina Globus (DING), koji se naziva i Paralelni globus (Rossi et al. 2015), omogućuje da posmatrač na Zemlji "vidi" trenutno osunčenje Zemlje onako kako to vidi astronaut iz svog vasionskog broda. Ovo zato što je osa Paralelnog globusa paralelna Zemljinoj osi, a položaj grada u kome je globus je na vrhu globusa. Posmatrač može tokom dana pratiti kretanje terminatora. Tokom godine može da prati promena orijentacije terminatora u odnosu na osu, čime se vizuelizuju posledice kretanja Zemlje duž orbite, a time uzrok smene godišnjih doba na Zemlji.

Prvi takav globus je bilo moguće videti u Srbiji u Parku nauke u Šapcu.

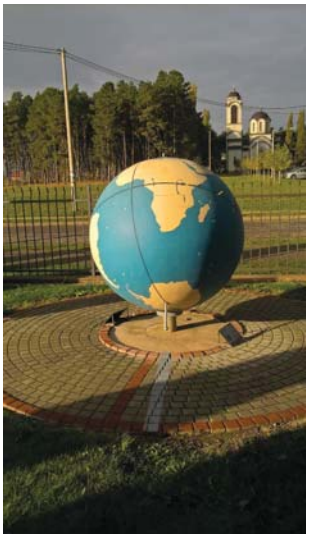

Figure 3: DING u Šapcu.

Model kakav se može videti u Šapcu je dragocen kao inspiracija, i izuzetno demonstraciono sredstvo, ali je i vrlo teško realizovati takav model u svakoj sredini. Međutim identični efekti se mogu postići i sa sredstvima koja su svima dostupna. Jedan takav pokušaj je realizovan u Zemunskoj gimnaziji 2018. godine.

(a) (b) (c)

Figure 4: Prolazak Sunca kroz lokalni meridijan.

Na slici broj 4 može se videti model DING. Za ovaj eksperiment su potrebni geografski globus, plastelin za fiksiranje stubića na globusu i plastične slamčice za izradu stubića. Ovaj materijal dostupan je većini učenika, pa shodno tome moguće je izvesti experiment i u prostoru koji nije u školi (terasa, dvorište ili park). Jedini uslov je da je površina na koju se postavlja globus osunčana tokom dana. Ovo posmatranje može biti organizovano u okviru projekta koji može trajati i više meseci. Tako se na primer može tokom godine posmatrati ugao između terminatora i lokalnog meridijana na Zemlji i videti da se na dan ravnodnevnice terminator i lokalni meridijan poklapaju.

7. SIMULACIJA PETLJI PLANETA

Planetama Sunčevog sistema je potrebno različito vreme da obiđu svoj put oko Sunca, što je u skladu sa III Keplerovim zakonom. Posmatrač sa Zemlje uočava da planete prave pri svom kretanju takozvane petlje u kojima izgleda da te planete počinju da se kreću u suprotnom smeru (retrogradno kretanje). Jasno je da je takva slika posledica položaja posmatrača. Jedan vrlo jednostavnih načina, da se učenicima demonstrira ova pojava, predložili su Bennett J. i saradnici 2004. Oni predlažu da dve grupe učenika idu po obeleženim kružnicama sa zajedničkim centrom. Jedna grupa će predstavljati kretanje Zemlje, a druga neku planetu koja je dalja od Sunca. Uočavanje položaja druge grupe učenika u odnosu na nepokretne elemente (drveće, zgrade) za grupu koja simulira kretanje Zemlje, može simulirati retrogradno kretanje planeta kakvo je uočeno u petljama.

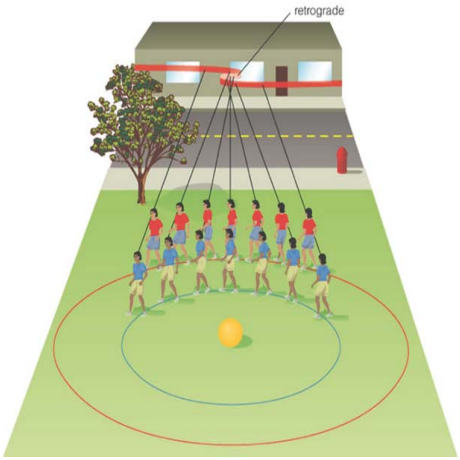

Figure 5: Slika je preuzeta iz knjige J. Bennett, M. Donahue, N. Schneider and M. Voit, *The Cosmic Perspective.*

8. ZAKLJUČAK

Sve do sada izneto, kako iskustva ali i ideje za buduće aktivnosti ukazuje da nastava astronomije pruža izuzetne mogućnosti. Učenicima mogu biti ponuđene prilike za samostalni rad kroz koje će razvijati svoje kompentencije. Pored toga interdisciplinarnost astronomije pruža mogućnost, kako za realizaciju integrativne nastave, tako i za obnavljanje gradiva više školskih predmeta, ali na jedan kvalitativno drugačiji način sa dubljim poimanjem sadržaja.

References

Bennett, J., Donahue M., Schneider, N., Voit, M.: 2004, *The Cosmic Perspective* (San Francisco, CA: Pearson, Addison Wesley).

Rossi, S. et al.: 2015, The parallel globe: a powerful instrument to perform investigations of Earth's illumination, *Phys. Educ.* **50**.

https://www.esrl.noaa.gov/gmd/grad/solcalc/

Publ. Astron. Obs. Belgrade No. 100 (2002), 161 - 168 *Invited Lecture*

NEWS AND FUTURE PLANS IN THE DEVELOPMENT OF THE ASTRONOMICAL STATION VIDOJEVICA

O. VINCE

Astronomical Observatory, Volgina 7, 11000 Belgrade, Serbia
E–mail: ovince@aob.rs

Abstract. Due to the new health situation that affected the whole world, the rhythm of work of the Astronomical Station Vidojevica was disturbed. However, despite this, a lot has been done for the development of the station and they will be presented in this paper. In the first place, it is the construction of the pavilion for the 40cm Meade telescope and its installation and calibration that are still in progress at the time of submission of the paper. In addition to the 40 cm telescope, we will also present news/plans related to the other two telescopes - the 60 cm telescope "Nedeljković" and the 140 cm telescope "Milanković".

1. INTRODUCTION

The Vidojevica Astronomical Station (ASV) is an observation station of the Astronomical Observatory in Belgrade (AOB), which was formed as a result of relocating observation activities from Belgrade to a light-unpolluted place. This relocation was considered as early as in 1980s of the last century, but due to the standard site testings to select the optimal location for the astronomical station and subsequent turbulent historical events, its realization came only in 2003. It was decided that the place for the astronomical station would be on summit of Vidojevica Mountain, which is located in the south of Serbia near the town of Prokuplje.

The station was established in 2003. In the beginning, mostly construction work was done i.e. the construction of a residential building, a telescope pavilion, the introduction of drinking water, internet networking, etc. Since these works are demanding, the station was ready to work only in 2010.

The first instruments procured were a 60cm telescope, several CCD cameras, with several broadband filters for photometric measurements and a portable spectrograph. Also, several auxiliary instruments were provided to aid astronomical observations - a meteorological station, a seeing monitoring camera and an all-sky camera. The 60cm telescope was finally installed at the end of 2010 and the first test measurements began. Although we started with photometric measurements on this telescope, the spectrograph was also installed on the telescope several times, however, due to technical difficulties, it was never systematically used on this telescope. The telescope was later named "Nedeljković" after the first director of the Astronomical Observatory in Belgrade, Milan Nedeljković (e.g. Todorovic & Milić (2019)).

The "Nedeljković" telescope was procured with the idea of testing the site in more detail for observational conditions and with the ultimate goal of procuring a larger telescope if the weather conditions are favorable. Although all the measurement results pointed to a quality sky for astronomical observations (mean seeing 1.5 arcsec with about 180 clear days for observation; see Jovanović et al. (2012)), the procurement of a larger telescope was not so straightforward. Finally, we succeeded in this plan through the BELISSIMA (BELgrade Initiative for Space Science, Instrumentation and Modeling in Astrophysics) FP7 project of the European Commission in 2010. The telescope that was realized through the BELISSIMA project has a diameter of the primary mirror of 1.4m and was finally installed in 2016. It was named "Milanković" after the famous Serbian scientist Milutin Milanković (e.g. Radovanac & Stojanović).

Back in 2004, we purchased a 40cm Meade telescope that had been in operation at AOB for a long time. It was relocated to ASV in 2018. Last year was dedicated to the adoption of this telescope. To that end, we purchased a pavilion with dome from the Polish company ScopeDome. The telescope has not yet been placed in the pavilion and this work, as well as its subsequent calibration, awaits us in the coming period.

In this article, we will describe all three telescopes in more detail. We will point out their current status and future plans. The current functioning of the station as well as the observation projects carried out on our telescopes will be briefly presented.

2. TELESCOPES AND INSTRUMENTS

2. 1. TELESCOPE "MILANKOVIĆ"

The "Milanković" telescope was purchased from the ASA (Astro System Austria) company in Austria. The telescope was temporarily installed in a roll-roof pavilion but was subsequently moved to a new pavilion with a rotating dome that had been built in the meantime. The test phase of the telescope lasted for a year and in that period of time we collimated the optical system, calibrated the telescope and tested the telescope in detail to some of the most important parameters. Due to the large mass of the telescope, it proved to be very stable against wind gasps in the pavilion with a sliding roof. At the same time, one of the greatest qualities of this type of pavilion has been proven, that is, the seeing was below 1 arcsec for most of the time. Figure 1. right is an image of the telescope when it was still in the ASA company.

The mounting of the telescope is AltAz and its optical system is Ritchey-Cretien with 4 ports for placing instruments - two Nasmiths ports on either side of the telescope and two ports that are orthogonal to them. Both Nasmith ports are equipped with an image derotator that compensates for image rotation in the field of view, which is a characteristic of these types of telescope mountings. The effective focal length of the telescope is 11.2m (f/8). One of the Nasmith ports was originally equipped with a corrective lens with the aim of providing the widest possible field of view without aberration (field corrector), so that its effective focal distance was somewhat smaller (about 10.5m). Later, this field corrector was replaced with a 0.64x focal reducer in order to provide the widest possible field of view, so that currently the focal distance at this port is about 7.2m. Table 1. summarizes the main features of our telescopes.

Figure 1: Left,the pavilion for the 140cm telescope. Right, the telescope while it was still in the ASA company.

The telescope is very compact. The entire telescope control system (TCS) is located inside the fork of the telescope, so the telescope is practically a plug-in device with two inputs - one for power and other for ethernet access to the TCS. The telescope mounting is a direct drive motor (DDM), so the telescope is fast and noiseless. Its maximum speed is about 6 degrees per second, but in practical operation it is set to about 4.

The rotating dome of the pavilion for this telescope was purchased from the Italian company Gambato[1]. Originally, it was delivered without automation, so we did the automation of the dome and its synchronization with the telescope later. Likewise the telescope,, the dome is also designed to be fast. Figure 1. left is an image of the the pavilion with the Gambato dome.

One of the Nasmith ports was dedicated to photometric measurements from the very beginning. Currently, the iKonL CCD camera from Andor company[2] is attached to this port in combination with filter-wheel containing standard Johnson-Cousin BVRI filters. In addition to these filters, we provided an L (Luminance) wide-band filter for observation of faint objects (e.g. Müller et al. 2019) and H_α, H_α continuum, and SII narrowband filters of 5nm for studying supernova remnants. Table 2 lists the CCD cameras that are attached to our telescopes and gives their basic characteristics that can be useful for planning observations.

The second Nasmith port with derotator was initially equipped with a SpectraPro spectrograph that was on the telescope for about a year in test function (Vince & Lalović (2005), Vince et al. (2018)). Currently, this port is equipped with a OPTEC Perseus instrument selector[3] that allows the beam to be redirected to four orthogonal outputs in order to use this port for as diverse observation projects as possible. Currently, there are two cameras attached to this port - iXon897 EMCCD from Andor company[4] and SBIG STXL-6303 from Diffraction Limited company[5]. Both CCDs are

[1]https://www.gambato.com/solutions/observatory-domes.html
[2]https://andor.oxinst.com/products/ikon-xl-and-ikon-large-ccd-series/ikon-l-936
[3]https://optecinc.com/astronomy/catalog/perseus/default.htm
[4]https://andor.oxinst.com/products/ixon-emccd-cameras
[5]https://diffractionlimited.com/product/stxl-6303/

Table 1: Main features of our telescopes. Last column lists the CCD cameras that are attached to telescopes at the time of writing the publication.

Tel.	D [mm]	F [mm]	CCD
Milanković PORT A	1400	7168	Andor ikonL
Milanković PORT B	1400	11200	Andor iXon897
Milanković PORT B	1400	11200	SBIG STXL-6303
Nedeljković	600	6000	FLI PL230
Meade LX200	400	4064	SBIG STXL-6303

Table 2: CCD characteristics attached on our telescopes. PS and FOV stands for pixel scale and field of view, respectively. Pixels of all our CCDs are square.

CCD	Resolution	Pixel size [μm]	PS ["/pix]	FOV [']
ikonL @ 140cm tel.	2048x2048	13.5	0.39	13.3x13.5
iXon897 @ 140cm tel.	512x512	16	0.29	2.5x2.5
STXL-6303 @ 140cm tel.	3072x2048	9	0.17	8.5x5.7
Pro230 @ 60cm tel.	2048x2048	15	0.28	9.4x9.4
STXL-6303 @ 40cm tel.	3072x2048	9	0.46	23.4x15.6

used for measuring orbital parameters of visual double systems using "lucky imaging" method (e.g. Pavlović et al. 2013, Cvetković et al. 2019).

We put in a lot of effort to automate the telescope "Milanković". The primary goal of telescope automation is to reduce the need for manpower working at the station but also to extend the observation cycle, which currently stands at 15 nights around the new Moon (more on this in the next chapter). We are currently working on the communication of the TCS with various instruments inside/outside the pavilion in order to protect the telescope and instruments from external (rain, wind, snow) and internal (moisture and dew) conditions. We expect that this level of automation will be completed in 2021. The next step is to automate the observations themselves, which would enable observations completely independent of people. This would fulfill our ultimate goal for this telescope, i.e. telescope robotization.

As mentioned earlier, our telescopes are currently optimized for performing photometric measurements. However, we plan to purchase a spectrophotometer for the "Milanković" telescope, which we hope will enrich the observation program on the telescope. In fact, an improvised polarimeter with Savart Plate has been already installed in 2019. for testing purposes. Testing was performed on dozens od standard polarized stars and several objects known to show a high degree of polarization (e.g. blazar 0716+714) and preliminary results showed that the telescope is suitable for performing polarimetric measurements (polarimetric accuracy 0.01% with ∼40 minutes total integration time for 14mag star).

2. 2. TELESCOPE NEDELJKOVIĆ

The "Nedeljković" telescope was also purchased from the ASA company. The diameter of the primary mirror is 60 cm. The telescops mounting is German equatorial and, unlike the 1.4m telescope, it is powered by two stepper motors. The optical system

Figure 2: Left, the roll-roof pavilion designed to temporarily house a 140cm "Milanković" telescope. Right, the 60cm 'Nedeljković' telescope, which is currently in this pavilion.

is Cassegrain with an effective focal distance 6m. The telescope was delivered with a 0.5x focal reducer, which is not used systematically for astronomical observations due to the relatively large aberrations at the ends of our CCD images. Some of the main features of this telescope is described by Vince & Jurković (2012).

As already mentioned, the telescope was installed in 2010 in a pavilion with a rotating dome made by an Serbian manufacturer. Unfortunately, the dome had malfunctions from the very beginning, due to which we often had suspensions of observation activities. Therefore, in 2018, we moved the telescope to a temporary pavilion, soon after the 1.4m telescope was transferred to the newly built pavilion. Currently, the telescope is equipped with the FLI PL230 CCD camera[6] and BVRIL filters for imaging, photometric and astrometric measurements. Figure 2. shows the telescope and the temporary pavilion in which the telescope is currently housed.

The degree of automation of this telescope (and pavilion) is much lower than with "Milanković". Moreover, due to the unreliable and inaccurate mounting, some more serious automation is not even possible. That is why we decided to replace the old equatorial mounting with a DDM (specifically the DDM200 from ASA company). We hope to accomplish this task and restart observations by the end of 2021.

As for the original pavilion for the 60cm telescope, which is now empty, we plan to replace its dome and then return the 60cm telescope. The main reason is that the 60cm telescope is relatively light and in the roll-roof pavilion it is more sensitive to wind gusts.

2. 3. MEADE 16" TELESCOPE

The Meade 16" LX200 telescope was purchased in 2004 and has been used at AOB for more than ten years. Due to light pollution in the city, the telescope has been limited to observing only very bright objects. With intent to use the full capacity of this telescope, it was transferred to ASV in 2018.

[6]https://www.flicamera.com/proline/

Figure 3: ScopeDome 3M pavilion (left) and the 16" Meade LX200 telescope (right).

The optical design of the telescope is Smith-Cassegrain, i.e. catadioptric telescope that combines a Cassegrain telescope with a Smith correction plate in front of the primary mirror of the telescope which corrects images for spherical aberration. The diameter of the primary mirror and the efective focal length of the telescope are 40 cm and 4064 mm, respectively. The telescope is originally delivered with tripod and is intended to be used as AltAz mounting. However, we will adjust the telescope to the equatorial mounting using a specially made wedge. The main advantage of equatorial mounting is that it avoids the need for a derotator.

We procured a pavilion with rotating dome for the telescope from the Polish company ScopeDome[7] and it was installed at the ASV in 2020 (specifically, "ScopeDome 3M" with a dome 3m in diameter). The pavilion is installed on a concrete pedestal which lifts the pavilion off the ground in case of a large amount of snowfall. The pedestal was built as a small building where electricity and internet were introduced following all standard regulations.

ScopeDome offers several types of domes and we have decided on a variant in which full automation of the dome is possible. Despite the good will, the telescope was not placed in the pavilion and was not put into operation due to complications in the organization of work and workers during the COVID19 pandemic. This job is also postponed for 2021. Figure 3. shows the ScopeDome pavilion (left) and the Meade 16" telescope (right).

3. STATION OPERATION

A total of four people are engaged around the station - a manager, two technical operators and one janitor. Currently, our policy is such that astronomers looking for telescope time to observe are also observers. In this sense, the main task of technical operators is to train new observers and to provide technical support during observations. With this number of technical operators, the station is active for only 15 days in the observation cycle, that is, 15 days around the new Moon. It is for these reasons (lack of technical operators and short observation cycle) that we strive to fully automate our telescopes.

[7]https://www.scopedome.com/

The number of people is certainly insufficient to serve the station. The lack of professional people (electrical engineers, mechanics, etc.) who would perform regular maintenance of telescopes and instruments is most noticeable. Also, there is a lack of staff to maintain our website, which is the main source of information about ASV and a means of communication the public and the observers.

The installation of the "Milanković" telescope in 2016 led to a sharp increase of interest in using our telescopes. This certainly contributed to the need to form a time allocation commission (TAC) in 2018. Application for observation time is done twice a year. The first four months of the semester are scheduled for application submission and the remaining two for the TAC to review applications. Details related to the submission of applications are described in the roolbook on our website http://vidojevica.aob.rs. About 20 applications were submitted for the last open time and they can be classified into the following scientific categories:

- Determination of physical parameters of eclipse binary systems
- Determination of orbital parameters of close binary systems
- Study of active galactic nuclei (reverberation mapping)
- Stydy of Blazars
- Gaia photometric follow-up program
- Study of supernova remnants
- Asteroid photometry.
- Detection of dwarf galaxies and tidal stream effects

In addition to scientific research applications, we regularly have applications for education purposes. The most important one is the application for education of students (astronomers) from the Faculty of Mathematics in Belgrade and the Department of Astronomy at the Faculty of Physics in Novi Sad.

Currently, a number of applications allow us to assign entire evenings for observation to a specific observer. However, as interest in using our telescopes grows from year to year, we will innocently have to change this policy.

4. SUMMARY

In this paper, we describe the current status of ASV. A detailed description of all our telescopes is given, including the Meade 40cm telescope, which we have yet to install and activate for observations. A detailed overview of the instruments currently attached to our telescopes is given, which can help a potential observer to plan observations. Also, for each telescope, we have presented plans that we will implement as soon as the pandemic situation allows.

Unlike the organization of observation work on our telescopes, which is possible via the Internet, the organization of jobs planned for 2019 were hampered by the COVID19 pandemic. Despite that, we managed to implement several larger plans - the installation of the ScopeDome pavilion for the Meade 40cm telescope and the

automation of the 1.4m telescope "Milanković". However, many jobs have been postponed for the next period without a pandemic; first in line are installation/calibration of the 40cm telescope, replacement of the mounting for the 60cm telescope and completion of the automation of the "Milanković" telescope.

Acknowledgements

Oliver Vince is supported by the Ministry of Education, Science and Technological Development of the Republic of Serbia (contract No 451-03-9/2021-14/200002).

References

Cvetković, Z., Pavlović, R., Boeva, S.: 2019, *AJ*, **158**, 215.
Jovanović, M. et, al.: 2012, *Publ.Astron.Obs.Belgrade*, **91**, 83.
Müller, O., Vudragović, A., Bílek, M.: 2019, *A&A*, **632**, 13.
Pavlović, R., Cvetković, Z., Boeva, S., Vince, O., Stojanović, M.: 2013, *AJ*, **146**, 52.
Radovanac, M., Stojanović, M.: 2016, *Publ.Astron.Obs.Belgrade*, **95**, 1.
Todorović, N., Milić-Žitnik, I.: 2019, *RoAJ*, **29**, 167.
Vince, I., Lalović, A.: 2005, *SerAJ*, **171**, 55.
Vince, O., Jovanović, M. D., Vince, I., Janjes, A.: 2018 *Publ.Astron.Obs.Belgrade*, **98**, 341.
Vince, O., Jurković, M.: 2012 *Publ.Astron.Obs.Belgrade*, **91**, 77.

Publ. Astron. Obs. Belgrade No. 100 (2021), 169 - 174 *Invited Lecture*

TESTING THE PERFORMANCE OF THE MILANKOVIĆ TELESCOPE

A. VUDRAGOVIĆ[1], M. BÍLEK[2], O. MÜLLER[2], S. SAMUROVIĆ[1] and M. JOVANOVIĆ[1]

[1] *Astronomical Observatory, Volgina 7, 11060 Belgrade, Serbia*
E–mail: ana@aob.rs

[2] *Université de Strasbourg, CNRS, Observatoire Astronomique de Strasbourg (ObAS), UMR 7550, 67000 Strasbourg, France*

Abstract. We have undertaken a multi-band imaging campaign of several galaxies to study their low surface brightness features such as shells and streams. Using the 1.4-m Milanković telescope, we measured the surface brightness limits in various bands depending on the exposure time. Remarkably, within three to four hours of observations with the L-filter we reached the surface brightness limit of μ_g=28.5-29.0 mag/arcsec^2. We have confirmed the faint stream of the elliptical galaxy NGC 474 discovered with MegaCam. The comparison to other deep photometric surveys has revealed that within few hours of observations we can produce competitive results, showing that the Milanković telescope can be a valuable asset in the study of the low-surface brightness Universe.

1. INTRODUCTION

The low surface brightness Universe received renewed attention in the last decade. Several specially designed and envisioned projects started to collect very deep data (e.g., van Dokkum et al. 2014; Duc et al. 2015; Rich et al. 2020; Bílek et al. 2020). Deep imaging revealed low surface brightness features in the form of stellar streams and shells, and extended optical disks (almost the size of the HI disks) around nearby galaxies.

According to the ΛCDM paradigm, massive galaxies formed hierarchically by consuming surrounding smaller galaxies (Frenk & White 2012). The accretion of dwarf satellites had left stellar streams in the outskirts of their massive hosts that are long lived and memorize past events. Cosmological simulations predict numerous disruption signatures left over from the formation and evolution of massive galaxies (Bullock et al. 2005; Cooper et al. 2010). The detection of such features and, moreover, subsequent analysis involving their quantification, provides a strong test for this hierarchical model of galaxy formation. However, these features are hidden in the low-surface brightness regime well beyond 26 mag/arcsec^2.

Reaching the depth required to study low surface brightness structures, which are around 30 mag/arcsec^2 requires special observation technique and careful background subtraction. The method widely used is a technique called dithering – off-setting the telescope randomly to sample different portions of the sky. This dithering pattern

has to be large enough to make the target galaxy fall on different parts of the CCD chip. The result is a correction that can be used to remove the prevalent systematics in the image, such as residuals from the flat-fielding or the sky background.

The quantification of the observation depth that allows comparison between different surveys is not well defined. There are in principle two ways to measure the surface brightness limit reached by an observation: (1) finding the limiting magnitude of the surface brightness profile of the object itself; or (2) quantifying background fluctuations. The problem with the former is that extrapolations of the profile can easily lead to misinterpretations of the true depth reached. The latter is independent of the modelling of the target galaxy, allowing for a better comparison between observations, which is why we use this approach.

To study the capabilities of the Milanković telescope mounted at the Astronomical Station Vidojevica near Prokuplje (Serbia) and equipped with the IkonL CCD camera, we have imaged two galaxies for several hours – namely NGC 474 and NGC 467 – in four filters (B, V, I and L). In Section 2 of this article, we describe the data acquisition and data reduction. In Section 3 we compare the surface brightness limit reached here to other surveys like the Sloan Digital Sky Survey (SDSS; York et al. 2000), the Beijing Arizona Sky Survey (BASS; Zou et al. 2017) and the Dark Energy Survey (DES; Dey et al. 2019). And finally, in Section 4 we discuss the results.

2. OBSERVATIONS AND DATA REDUCTION

2. 1. NGC 474 GALAXY: L-BAND

We have imaged the elliptical galaxy NGC 474 in the L-band on October 22$^{\rm nd}$ 2019 with the 1.4m Milanković telescope using the IkonL CCD camera. We have applied a randomized dithering pattern with offsets of ∼300 pixels (∼2 arcsin). The individual exposure times were 300 s and the airmass ranged from 1.29 to 1.92. We have taken 33 exposures using the L-filter, resulting in an on-source integral exposure time of 2.75 h. The image quality was on average 1.3 arcsec. An individual frame covers a square box of 13.3 arcmin, utilizing the focal reducer. As a result of the dithering the final co-add has the dimensions of 17.5 × 17.9 arcmin^2 (Figure 1, left). Previously, NGC 474 was observed by Duc et al. (2015) using the 3.6m Canada–France–Hawaii Telescope (CFHT) equipped with the MegaCam camera (Figure 1, right) in the g-band with a total exposure of 0.7h. In both images – the Milanković and the CFHT images – the shell structure is prominent and the stellar stream stretching to the north-east is clearly visible.

The astrometric solution was found using the Astrometry code (Lang et al. 2010). The data reduction was done using the Milanković pipeline (Müller et al. 2019) following standard procedures: bias, dark, and flat field corrections. The creation of the super sky flat was achieved trough stacking individual frames using their native (image) scale. Simply, they were all median combined ignoring their astrometric solution. This super sky flat image was then normalized to the median value of each individual science frame and subtracted from them. Finally, the subtraction of the super sky flat was done on all the individual frames that were previously bias, dark, and flat field corrected. The last step was the co-addition of individual frames using IRAF's `imcombine` task.

Table 1: Surface brightness 3-sigma limits with the errors in the B-, V-, I- and L-band depending on the integral exposure time (in hours).

Time [Hours]	B-limit [mag/arcsec^2]	L-limit [mag/arcsec^2]	Time [Hours]	V-limit [mag/arcsec^2]	I-limit [mag/arcsec^2]
0.25	25.15 ± 0.02	27.27 ± 0.01	0.15	26.12 ± 0.01	26.54 ± 0.03
0.75	25.89 ± 0.03	27.86 ± 0.01	0.45	26.79 ± 0.01	27.33 ± 0.02
1.25	26.22 ± 0.02	–	0.75	27.11 ± 0.02	27.65 ± 0.02
1.75	26.42 ± 0.02	28.27 ± 0.02	1.05	27.22 ± 0.06	27.80 ± 0.03
2.25	26.58 ± 0.04	28.35 ± 0.03	1.35	27.39 ± 0.01	27.89 ± 0.02
2.75	26.68 ± 0.03	28.48 ± 0.03	1.65	27.35 ± 0.02	27.91 ± 0.02
3.25	26.77 ± 0.05	–	1.95	27.40 ± 0.01	27.94 ± 0.04
3.75	26.85 ± 0.03	–	2.25	27.54 ± 0.03	27.96 ± 0.04

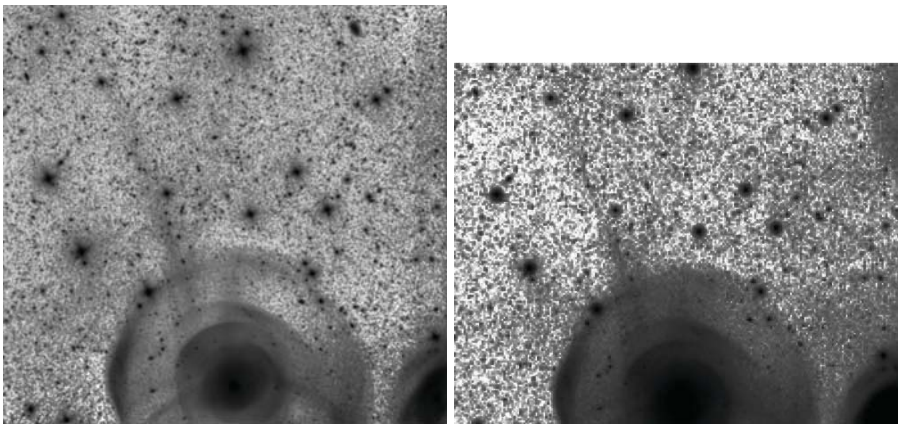

Figure 1: NGC 474: (*left*) L-band image from the Milanković telescope and (*right*) g-band image from the CFHT/MegaCam (Duc et al. 2015).

2. 2. NGC 467 GALAXY: B-, V- AND I-BAND

We have observed galaxy NGC 467 on September 28$^{\text{th}}$ and 29$^{\text{th}}$ 2019. The same equipment was used as with NGC 474. We have employed three filters: B, V and I. The individual exposure times were 300s for the B-band, and 180s for V- and I-band. In total, 47 images were taken in each band equaling to 3.9h in the B-band and 2.35h in the V- and I-bands. Dithering was $\sim$ 200 pix ($\sim$ 1 arcmin) and the seeing 1.3 arcsec. The final co-add image has the size of 16.3 $\times$ 16.6 arcsec^2. The same procedure as before was applied: (1) astrometric solution was obtained with Astrometry code and (2) the Milanković pipeline was applied to reduce the raw data.

3. SURFACE BRIGHTNESS LIMIT

Magnitudes were measured with the standard IRAF package `daophot` in the final co-add images of both galaxies in all filters. The photometric calibration was done using the linear regression formula: $m_f = a_0 + a_1 * m_{\rm cal}$, where the subscript f stands for filters used (B,V,I, and L), a_0, a_1 are the intercept and slope, and $m_{\rm cal}$ is the standard star magnitude from the photometric catalog used for the calibration.

We have calibrated the magnitudes using the TOPCAT software (Taylor 2005). The magnitude zeropoint a_0 and the corresponding slope a_1 inside the whole FOV of each galaxy were inferred from SDSS DR12 photometric catalog using g-band magnitudes (Alam et al. 2016). They are: 32.7 ± 0.2 and 1.01 ± 0.02 (L-band), 29.50 ± 0.2 and 1.01 ± 0.02 (B-band), 30.80 ± 0.3 and 1.03 ± 0.03 (V-band), 31.6 ± 0.9 and 1.1 ± 0.01 (I-band). They are all expressed in the g-band. All stars brighter than the 22$^{\rm nd}$ magnitude and fainter than 14$^{\rm th}$ magnitude in the g-band were selected for measurements.

Our main interest was to determine, apart from the final surface brightness limit, the limit reached throughout the observing run. To estimate how deep the images were in shorter exposures than the integral one, we have created lists of images with integral exposure time starting from 15 minutes up to 3.75 hours increasing with steps of 30 minutes. Lists of individual frames were created to correspond to these shorter exposures and each list was combined with IRAF's `imcombine` task to make a stack. In each stack we measured the standard deviation inside a dozen boxes of 10 arcsec sides in empty regions (without objects). Standard deviations were averaged and their standard deviations were reported as the errors of the surface brightness limit converted to the g-band (Table 1).

The results of the surface brightness limiting magnitudes in various bands were converted to the g-band using linear regression and compared to the commonly used sky surveys SDSS, BASS and DES (Figure 2). It appears that in about an hour and a half the depth of the SDSS has been reached with our observations in all the filters. During the same time the BASS and DES limiting magnitudes are reached with all the filters except for the B-filter. And in the particular case of the L-filter all the limits are exceeded in less than hour. However, using the L-filter in 7.2 hours we have reached the 3-sigma surface brightness limit of 28.4 ± 0.04 mag/arcsec^2 in the g-band (Müller, Vudragović & Bílek 2019). This appears to be the limit of the L-band observations with the given strategy. Here, this limit has been reached in less than 3 hours (Figure 2).

4. DISCUSSION

We have measured the limiting surface brightness in the B-, V-, I- and L-band using observations of the two nearby galaxies imaged with the Milanković telescope, equipped with IkonL CCD camera. The results can be used as a guideline for the exposure time needed for a given target surface brightness.

Comparing to other sky surveys (SDSS, BASS and DES), we have shown that in $\sim$ 1.5h we can reach greater depth. Moreover, our L-band observations exceed the limits of these surveys after only 45 minutes of on-target time. However, with the currently used imaging strategy, even after 7.2h integral exposure time, we couldn't breach the 28.4 mag/arcsec^2 g-band 3-σ limit. A larger dithering pattern, including

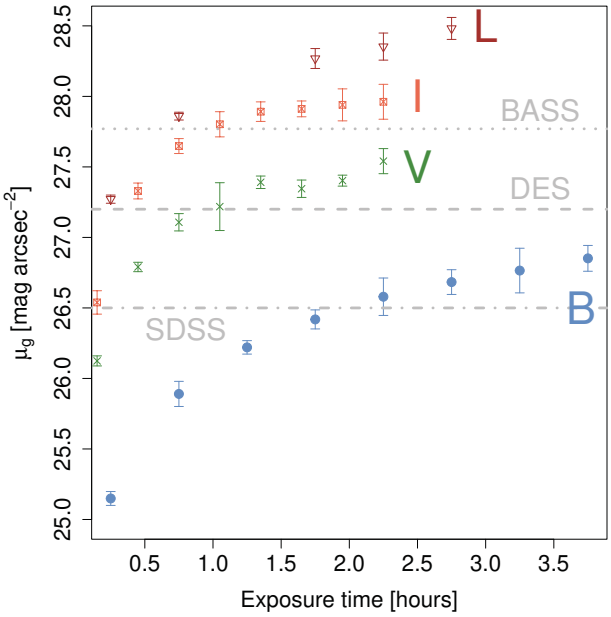

Figure 2: Surface brightness limit (3-sigma) in the B-, V-, I- and L-band variation with exposure time compared to: SDSS, BASS and DES surveys (green dashed lines).

the rotation of the telescope, may overcome this issue. Despite this, our observations show that the Milanković telescope is capable of studying the low-surface brightness Universe and can be used to follow-up structures identified in other surveys, as well as to hunt for hitherto undetected features.

Acknowledgements

We acknowledge the financial support of the Ministry of Education, Science and Technological Development of the Republic of Serbia (MESTDRS) through the contract No 451-03-68/2020-14/200002 and the financial support by the European Commission through project BELISSIMA (BELgrade Initiative for Space Science, Instrumentation and Modelling in Astrophysics, call FP7-REGPOT-2010-5, contract No. 256772), which was used to procure the Milanković 1.4 meter telescope with the support from the MESTDRS. O.M. is grateful to the Swiss National Science Foundation for financial support. M.B. acknowledges the financial support by *Cercle Gutenberg*. The authors are grateful to Pierre-Alain Duc for providing the image of NGC 474 galaxy shown in Figure 1. We thank the technical operators at the Astronomical Station Vidojevica (ASV), Miodrag Sekulić and Petar Kostić for their excellent work.

References

Alam, S., Albareti, F. D., Allende, P. C. et al.: 2016, *VizieR Online Data Catalog*, V/147.
Bertin, E., Arnouts, S.: 1996, *Astron. and Astroph. Supplement S.*, **117**, 393.
Duc, P. A., Cuillandre, J.-C., Karabal, E. et al.: 2015, *Mon. Not. R. Astron. Soc.*, **446**, 120.

Dey, A., Schlegel, David J., Lang, D. et al. : 2019, *Astron. J.*, **157**, 168
Bílek, M., Duc, P.-A., Cuillandre, J.-C. et al.: 2020, *Mon. Not. R. Astron. Soc.*, **498**, 2138.
Bertin, E., Mellier, Y., Radovich, M. et al.: 2002, *Astronomical Data Analysis Software and Systems*, **281**, 228.
Bullock, J. S., Johnston, K. V.: 2005, *Astrophy. J.*, **635**, 931.
Cooper, A. P., Cole, S., Frenk, C. S. et al.: 2010, *Mon. Not. R. Astron. Soc.*, **406**, 744.
Frenk, C. S., White, S. D. M.: 2012, *Annalen der Physik*, **524**, 507.
Lang, D., Hogg, D. W., Jester, S. et al.: 2009, *Astron. J.*, **137**, 4400.
Rich, M. R., Brosch N., Bullock, J. et al.: 2020, DOI: 10.1093/mnras/staa678.
Müller, O., Vudragović, A., Bílek, M.: 2019, *Astron. & Astroph.*, **632**, L13.
Taylor, M. B.: 2005, *Astronomical Society of the Pacific Conference Series*, **347**, 29pp.
van Dokkum, P. G., Abraham, R., Merritt A.: 2014, *Astrophys. J.*, **782**, 2.
York, D. G., Adelman, J., Anderson, John E. J. et al.: 2000, *Astron. J.*, **120**, 1579.
Zou, H., Zhou, X., Fan, X. et al.: 2017, *Publications of the Astronomical Society of the Pacific*, **129:064101**, 9pp.

Publ. Astron. Obs. Belgrade No. 100 (2021), 175 - 182 *Invited Lecture*

GALACTIC HABITABILITY AND STELLAR MOTION

B. VUKOTIĆ
Astronomical Observatory, Volgina 7, 11060 Belgrade, Serbia
E–mail: bvukotic@aob.rs

Abstract. One of the key factors of both, galactic and Galactic habitability, is the movement of stars. Stellar flybys can influence the stability of planetary systems and possible matter exchange between the individual stellar systems. The recent detection of interstellar objects, Oumuamua asteroid and comet 2I/Borisov, leads to estimates that about ten such objects are present in the Solar system at any instant. In addition, the indications of stellar migrations within the Galactic disk imply that individual stellar systems may experience different Galactic environments during their lifetimes. Advanced models of Galactic habitability should appreciate these factors. We consider the potential for capturing the interstellar objects and stellar migrations, given the overall distribution of stars in the Galactic disk and re-assess the recent findings on Galactic habitability.

1. INTRODUCTION

Planet Earth and the Solar system are an integral part of the Milky Way galaxy. It is a well established notion that galaxies interact with each other and evolve and change over time. Even isolated galaxies are subjected to evolutionary changes being the aggregates of evolving stellar populations and gaseous and dust content , together with the evolution of Cold Dark Matter Halo (CDMH) as well. Even in the case of isolated galaxies where most of the CDMH evolution was finished in the very early epochs, some of them could unfold slow enough to have some impact in the later epochs, when the galaxy under consideration is already habitable.

Habitability of a particular planet can not be considered as an isolated phenomena, particularly on timescales that are relevant for galactic processes. On the other end of the scale, the galaxies are the most pronounced constituents (visual) of the Universe and their evolution is conditioned with cosmological parameters.

A life on Earth, or on any other planet, can not be fully comprehend if studied as an isolated phenomena against the rather "empty" vastness of interstellar space and cosmological galaxy-less voids. The traces of microbial activity date back to > 3.7 Gyr ago (Dodd et al. 2017). This establishes biological evolution at time scales of billions of years, similar as the timescales of galactic evolution.

We are yet to find out what life is. So far we know what it is not and we are very good in perceiving the material manifestations of life, its matter dwelling. Because of the constant interaction with its physical environment, manifesting through multiple feedback cycles and influences, life could then be viewed as a part of the overall evolution of matter in the Universe.

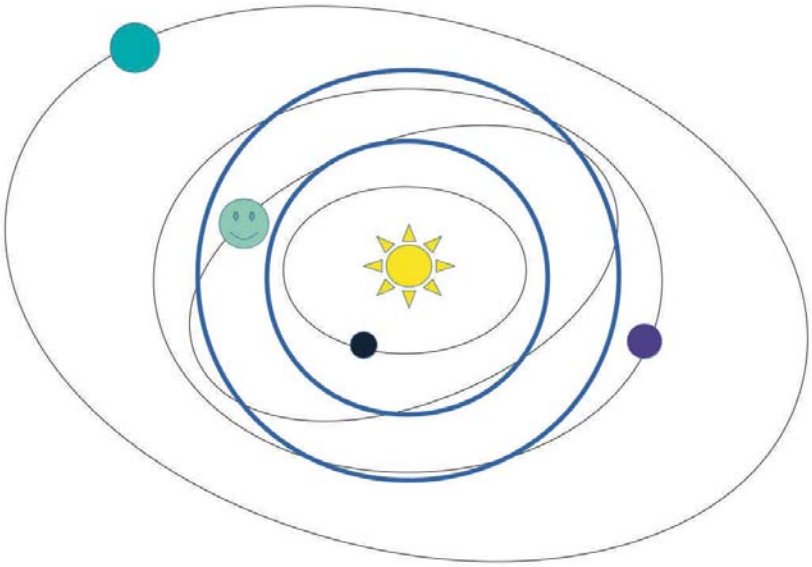

Figure 1: Schematic representation of the Circumstellar Habitable Zone.

The material part, or material foundation of a biosphere dwells in the planetary host. Earlier considerations of life being wide-spread in the Galaxy were significantly boosted by the discovery of exoplanet(s) (Mayor & Queloz 1995) – surely worth the Nobel Prize in physics for 2019. With the increasing number of newly discovered exoplanets, especially thanks to the Kepler space mission, people started to wonder which one of them might be habitable. Because of the importance of Sun for life on Earth creating a lush biosphere, it was a logical step to consider the habitability of exoplanets with a model that highlights the importance of the host star for defining the habitable parts of the planetary system.

First such models of planetary habitability were models of Circumstellar Habitable Zone (CHZ). Simply viewed as the distance from the host star where the radiation field of the star enables the black body approximated planet to attain temperatures indicative of liquid water:

$$\sigma T_{\mathrm{p}}^4 = L_*/(4\pi d^2), \tag{1}$$

where the planet's temperature T_{p}, depends on stellar luminosity L_* and distance d from the star. A simple schematic representation of the CHZ is depicted in Figure 1. In the planar-like shape, that characterizes the planetary systems, such a constraint appear like an annular ring centered on the host star, with the inner edge characteristic of T_{p} values that can efficiently evaporate planetary water content, while at the outer boundary T_{p} drops to water freezing point. We note here that sufficiently small eccentricities (circularized orbits) are assumed. Close stellar passages and major planetary migrations are likely to lead to strong build-ups of eccentricity, which subsequently might take quite a long time to circularize. The later improvements of such concept added the effect of the planetary atmosphere and radiogenic heating.

While this surely moved the position of the boundaries, it did not change the overall shape of the CHZ. It is also evident that even the evolution of stellar luminosity would only also change just the extent but not the shape. In the next section, we describe how the galactic habitability in general and also the habitability of the Milky Way in particular, were introduced starting from similar principles used in CHZ models.

2. GALACTIC HABITABILITY MODELING

In the case of abiogenesis the galactic conditions should be critical for the formation of habitable planets and their respective stellar hosts, in addition to required subsequent continuity in habitable conditions. This might give more weight to galactic "climate"[1] at the immediate environment of the biosphere, but could also be misleading in comprehending abiogenesis and life development in other parts of the galaxy which is very relevant for modern SETI studies. In addition, the panspermia hypothesis assumes slow wide spreading of life which also requires the global consideration of galactic conditions.

The galaxies, as the main constitutional units of matter in the Universe, are focal points for life evolution studies in cosmological context. The evolution of galaxies and related phenomena are thus the key to understand the overall evolution of life. The evolution of galaxies considered in habitability context include the evolution of galaxies in general but also the evolution of Milky Way. This follows essentially from the Copernican principle suggesting that we should treat our Galaxy as a typical kind of habitat for life, unless we have some evidence to the contrary. Of course, such evidence can only be found, in the first place, by looking into what particular properties of galaxies are indeed relevant to life and intelligence, so the problem is not trivially simple as sometimes looks (and is, rather carelessly, dismissed). For instance, it may be the case that star-formation in the Milky Way is somewhat more quiescent than in an average large spiral galaxy (Hammer et al., 2007), although this was before the discovery of Fermi superbubbles, so should be taken with a grain of salt. In any case, we should be on constant watch for anything atypical or "special" as far the Galaxy is concerned.

A robust CHZ model presented in the previous section, greatly influenced the first models of the galactic habitability. By replacing the role of host star radiation gradient with the gradient of galactic metallicity, as the primary parameter that describes the availability of material for the formation of planets (Gonzalez et al., 2001), the Galactic Habitable Zone (GHZ) appeared also as an annular ring-shaped area in the plane of the Milky Way disk that encompass Sun's Galactic orbit.

However, very soon, it became clear that other factors might interfere with such a simplistic initial view of galactic habitability. While certain amount of metals makes the available material for the formation of planets, the metallic content also enables efficient cooling of the proto-planetary disc and hence more gas is available for accretion onto planetary cores and giant planet formation. Migrations of such planets can interfere with the habitability of Earth-like worlds (Lineweaver, 2001).

Another habitability constraint might come from stellar fly-buys, that can disrupt the orbits of planets with life and disable habitable conditions on their surfaces, along

[1] As with the case of the Earth system and our everyday experience, climate both consists of local and short-term (weather) conditions, and is not entirely reducible to such conditions.

the lines of the CHZ modeling approach. In addition, an intense radiation from a nearby stellar explosion could significantly erode atmospheres of planets within distances of up to $\sim 10^3$ pc affecting their potential to accommodate surface life.

Depending on the implementation way of relevant Galactic parameters, their adopted values and habitability relevance, the GHZ models gave diverse predictions. Early conservative approach by Lineweaver, Fenner and Gibson (2004) positioned the GHZ ring between 7 and 9 kpc. According to Gowanlock et al. (2011), central parts of the Galactic disk were hosting the higher numbers of habitable planets and GHZ was more pronounced in the inner parts of the Galactic disk. Prantzos (2008) made a re-assessment of GHZ modeling and the resulting Galactic habitability constraints indicating that it might be likely that the whole Galactic disk might be hospitable to life. For more studies that also include GHZ habitability modeling see also Peña-Cabrera & Durand-Manterola (2004), Spitoni et al. (2014) or Legassick (2015).

Unlike in the case of CHZ models, large number of parameters that are relevant for galactic habitability made no census on the GHZ constraints, which was particularly relevant for SETI studies and possible Fermi Paradox solutions. The main goal of probabilistic based approaches (Đošović et al., 2019; Vukotić & Ćirković 2012) was to examine the available space of astrobiological parameters within a single modeling platform. While the work of Đošović et al. (2019) was focused on the rectifying the values of relevant timescales that fit into our current perception of Galactic life, a Probabilistic Cellular Automata (PCA) approach from Vukotić & Ćirković (2012) included a spatial spreading aspect of possible advanced civilizations in our galaxy.

The PCA was evolved on a 2D grid, with grid cells having one of the four states indicating the astrobiological complexity from 0 – no life to 3 – a civilization with colonization capacity (Figure 2, left). The intrinsic evolution of cells towards the states of higher complexity was constrained by the beamed radiative explosion events (indicative of gamma-ray bursts) and also with omni-directional radiation from events of smaller magnitude (supernovae or even magnetar burst events). Apart from the grid parts with no presence of advanced civilizations, the results also showed a percolated clusters of civilizations spreading which both fits into our current perception of Fermi Paradox (Figure 2, right).

3. STELLAR MOTION AND GALACTIC HABITABILITY

All of the galactic habitability models presented above lack the direct implementation of stellar motion, i.e. stellar dynamics. The mounting evidence of stellar migrations (e.g., Roškar et al. 2012) highlighted that stars can make significant radial migrations during their lifetimes, i.e. change the galactocentric distance of their orbits. Together with the vertical motions of the planetary systems in respect to the plane of the galactic disk, this significantly changes the galactic environment imposed onto the habitable planets. All this clearly puts the question of life into cosmological context and pronounce the need to conduct modern habitability studies including evolution of galaxies and their interactions within the cosmological framework.

One of the best tools to implement stellar dynamics in habitability studies are N-body simulations of individual galaxies and also cosmological simulations of structure evolution on a larger scale. The use of this tool for habitability studies of isolated Milky Way like galaxy was presented in Vukotić et al. (2016). The results indicated that the outward motion of galactic stellar component makes the outer parts of the

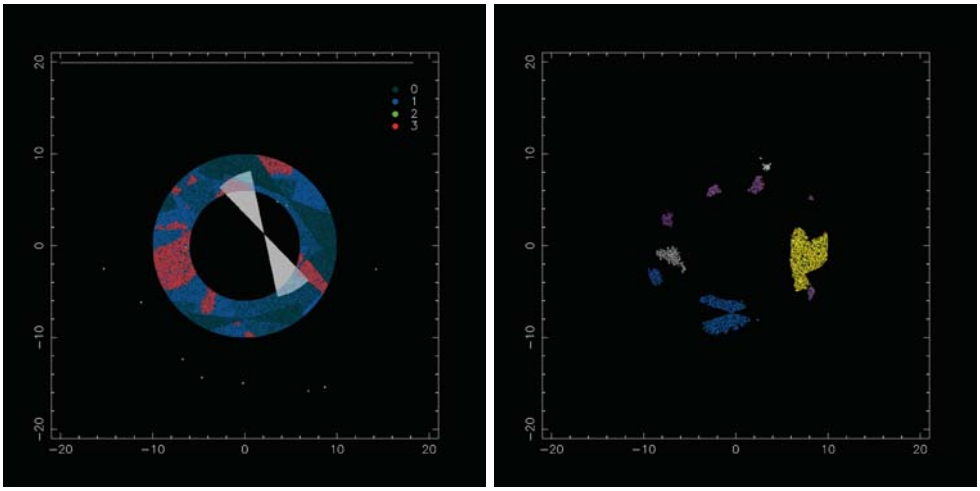

Figure 2: Axis designate the galactic distance in kpc. Left: A late epoch (a white line just below the top axis represent time from the beginning of the run) PCA snapshot from the model described in Vukotić & Ćirković (2012). White areas present radiation events that constrain the evolution of astrobiological sites towards higher complexity. The cell states are coded as 0-no life, 1-simple life, 2-complex life and 3-advanced life. Right: The clusters of advanced civilizations (state 3 of PCA grid cells) at the end of the simulation run. Color coding represents different clusters of state 3.

galactic disk $\sim 10 - 15$ kpc populated with stars that have the highest probability of being habitable. A similar result was reached by Forgan et al. (2017), performing the analysis of cosmological simulation of the Local Group. They also find a significant habitability of dwarf satellite galaxies.

These were much different habitability landscapes when compared with the ones from the first studies of galactic habitability. Also, other prominent works that inspect galactic habitability in the cosmological context were by Dayal et al. (2015), Gobat & Hong (2016), Stanway et al. (2018) and also Stojković et al. (2019ab). This further changed our notions of habitability distribution, e.g. Zackrisson et al. (2016) reported that a typical earth-like planet in a local universe is located in a galaxy that is dominated by a spheroid shape a with a stellar mass comparable to the stellar mass of our Galaxy. Clearly, the introduction of dynamical aspect of galactic evolution and a wider, cosmological perspective, have significantly change our views of galactic habitability than the ones that have emerged from the pioneering studies.

The habitability concerns from nearby stellar encounters were discussed in Jiménez-Torres et al. (2013). Apart from a possibility to disrupt planetary orbits they could also lead to matter exchange between the planetary systems and hazardous small body encounters.

The recent discovery of extrasolar visitors in the Solar system, an asteroid like object Oumuamua (Meech et al. 2017) and a comet 2I/Borisov (Guzik et al. 2019, Guzik et al. 2020), demonstrate that evolution of the habitability of individual planetary systems should account for their galactic environment. A study by Bailer-Jones

et al. (2020) integrated the orbits of stellar neighborhood stars from GAIA DR2 data to argue that 2I/Borisov might have been picked up in the Solar interstellar encounter occurring 910 kyr ago. A similar analysis was performed earlier for Oumuamua (Bailer-Jones et al. 2018a). This approach was also used to predict the 20 stellar nearby passages within 1 pc from the Sun per Myr (Bailer-Jones at el. 2018b).

The possibilities for the exchange of matter during stellar encounters, described above, except their direct relevance for galactic habitability, also raise another aspect that is important for galactic habitability concerning the question of origin of life. The panspermia hypothesis (as reviewed in Vukotić et al. 2021) heavily depends on the possibility of matter exchange. On the other hand, even the abiogenesis might depend on the disturbance of asteroidal belts and volatiles delivery on the rocky planets (for water delivery by asteroids on the planets in TRAPPIST-1 system see Đošović et al. 2020 and references therein). A hypothesis that cycles of hydration and dehydration are crucial for synthesis or encapsulated organic material, possibly occurring near hot springs is presented in Damer & Deamer (2020). It should be also noted here that, in contrast to pure matter transport, panspermia is inherently nonlinear phenomenon: a small cause can cause large consequences. Even the directed panspermia (in the most general sense, which includes colonization of other planetary systems by evolved civilizations) could be included in the wider picture. A very small initial shift in abiogenesis could lead to transformation of the large parts of the Milky Way!

4. A HYBRID APPROACH

The extent of exploiting the dynamical aspect of the habitability modeling clearly depends on the stellar mass resolution that is achieved in the models (simulations). The simulations with mass resolution on a single star level are still not achieved, even for isolated galaxies. The reported masses of stellar component in such N-body simulations are usually at 10^4 $M_\odot$, which is a mass indicative of a stellar cluster.

However, a conceptual aspect, readily found in meteorology, would still be at stake. Even at unrealistically high resolution in mass and time, there would still remain a random component that would make a difference between actual and simulated values. This highlights the need for statistical approach that uses multiple simulation runs which raise the computing requirements even higher. A possibility to achieve higher mass resolutions, with multiple run allowance, might be to make models that use analytic potential in the cosmological framework of numerically generated potential. An analytical approximation might then be used to generate galactic trajectories of individual stars for a given epoch in order to obtain the galactic habitability landscape of higher resolution. As argued in Stojanović (2015), the data from a GAIA mission, on components of stellar motion, can be used to calculate realistic stellar orbits in a given Galactic potential.

There is a significantly more stars in the Milky Way ($\sim 10^{11}$) then the typical number of particles used in an N-body simulation of an isolated galaxy ($\sim 10^7$). Calculation of stellar orbits in an analytic potential might offer the means to bridge this gap in terms of required computation times. According to Stojanović (2015), a highly efficient calculation can be achieved for stars with regular galactic orbits, e.g. nearly circular orbits of thin disk stars from the Solar neighborhood. Another important aspect is that the ambition for GAIA is to ultimately have about 10^9 objects, which is far more representative than the Solar vicinity. Therefore, on its

basis one could precisely calculate how typical our immediate environment is in terms of particular parameters of interest for astrobiology, e.g., the distribution of stellar metallicities, multiplicity, etc.

5. SUMMARY

The studies of galactic and Milky Way habitability have significantly matured in the past two decades. It is now clear that the robust results can be achieved relying on a cosmological framework of evolution of galaxies and not just on a simple circumstellar-like habitability model that was extensively used in the pioneering studies of galactic habitability.

The emerging picture of galactic habitability turn out to be much more complex than previously thought. The motion of stars within a galaxy at timescales of several Gyr is one of the key factors that should be studied to a greater extent in the context of habitability and galactic environments that these stellar systems are subjected to. Also, individual planetary systems should not be considered as an isolated chunks of habitable matter within the rather empty interstellar space. The recent discovery of extrasolar bodies that are passing through our Solar system shows that habitability concerns clearly reach beyond the confinement of Sun's influence.

This lecture proposed that a detailed models of stellar motion that include cosmological effects of galactic evolution and interaction might be computationally realized with the use of hybrid models that mix analytical and numerical approaches. The future studies of galactic habitability should consider this kind of modeling.

Acknowledgements

The author thanks Milan M. Ćirković for constructive and elaborate criticism that have significantly improved the manuscript. Another, anonymous referee, is acknowledged for various text improvements. Richard Gordon and Bojan Novaković helped with many discussions in regard to galactic habitability and origin of life during our long and fruitful collaborations. This work is funded through the contract number 451-03-9/2021-14/200002, between the Ministry of Education, Science and Technological Development of the Republic of Serbia and Astronomical Observatory in Belgrade.

References

Bailer-Jones, C. A. L., Farnocchia, D., Meech, K. J., Brasser, R., Micheli, M., Chakrabarti, S., Buie, M. W., Hainaut, O. R.: 2018a, *The Astronomical Journal*, **156**(5), article id. 205, 11 pp.

Bailer-Jones, C. A. L., Farnocchia, D., Ye, Q., Meech, K. J., Micheli, M.: 2020, *Astronomy & Astrophysics*, **634**, id. A14, 6 pp.

Bailer-Jones, C. A. L., Rybizki, J., Andrae, R., Fouesneau, M.: 2018b, *Astronomy & Astrophysics*, **616**, id. A37, 13 pp.

Dayal, P., Cockell, C., Rice, K., Mazumdar, A.: 2015, *The Astrophysical Journal Letters*, **810**(1), id. L2, 5 pp.

Damer B., Deamer, D.: 2020, *Astrobiology*, **20**(4), 429-452.

Dodd, M. S., Papineau, D., Grenne, T., Slack, J. F., Rittner, M., Pirajno, F., O'Neil, J., Little, C. T. S.: 2017, *Nature*, **543**(7643), 60-64.

Đošović, V., Novaković, B., Vukotić, B., Ćirković, M. M.: 2020, *Monthly Notices of the Royal Astronomical Society*, **499**(4), pp. 4626-4637.

Đošović, Vukotić, B., Ćirković, M. M.: 2019, *Astronomy & Astrophysics*, **625**, id. A98, 8 pp.
Forgan, D., Dayal, P., Cockell, C., Libeskind, N.: 2017, *International Journal of Astrobiology*, **16**(1), 60-73.
Hammer, F., Puech, M., Chemin, L., Flores, H., Lehnert, M. D.: 2007, *The Astrophysical Journal*, **662**(1), 322-334.
Gobat, R., Hong, S. E.: 2016, *Astronomy & Astrophysics*, **592**, A96.
Gonzalez, G., Brownlee, D., Ward, P.: 2001, *Icarus*, **152**(1), 185-200.
Gowanlock, M., Patton, D. R., McConnell, S. M.: 2011, *Astrobiology*, **11**(9), 855-873.
Guzik, P., Drahus, M., Rusek, K., Waniak, W., Cannizzaro, G., Marazuela, I. P.: 2019, *The Astronomer's Telegram*, **13100**, 1.
Guzik, P., Drahus, M., Rusek, K., Waniak, W., Cannizzaro, G., Pastor-Marazuela, I.: 2020, *Nature Astronomy*, **4**, 53-57.
Jiménez-Torres, J. J., Pichardo, B., Lake, G., Segura, A.: 2013, *Astrobiology*, **13**, 491–509.
Legassick, D.: 2015, Master's thesis, University of Exeter, UK. ArXiv e-prints: 1509.02832.
Lineweaver, C. H.: 2001, *Icaarus*, **151**(2), 307-313.
Lineweaver, C., Fenner, Y., Gibson, B. K.: 2004, *Science*, **303**(5654), 59-62.
Mayor, M., Queloz, D.: 1995, *Nature*, **378**(6555), 355-359.
Meech, K. J., Weryk, R., Micheli, M., Kleyna, J. T., Hainaut, O. R., Jedicke, R., Wainscoat, R. J., Chambers, K. C., Keane, J. V., Petric, A., Denneau, L., Magnier, E., Berger, T., Huber, M. E., Flewelling, H., Waters, C., Schunova-Lilly, E., Chastel, S.: 2017, *Nature*, **552**, 378-381.
Peña-Cabrera, G. V. Y., Durand-Manterola, H. J.: 2004, *Advances in Space Research*, **33**, 114–117.
Prantzos, N.: 2008, *Space Science Reviews*, **135**(1-4), 313-322.
Roškar, R., Debattista, V. P., Quinn, T. R., Wadsley, J.: 2012, *Monthly Notices of the Royal Astronomical Society*, **426**(3), 2089-2106.
Spitoni, E., Matteucci, F., Sozzetti, A.: 2014. *Monthly Notices of the Royal Astronomical Society*, **440**, 2588-2598.
Stanway, E. R., Hoskin, M. J., Lane, M. A., Brown, G. C., Childs, H. J. T., Greis, S. M. L., Levan, A. J.: 2018, *Monthly Notices of the Royal Astronomical Society*, **475**(2), 1829-1842.
Stojanović, M.: 2015, *Serbian Astronomical Journal*, **191**, 75-80.
Stojković, N., Vukotić, B., Ćirković, M. M.: 2019a, *Serbian Astronomical Journal*, **198**, 25-43.
Stojković, N., Vukotić, B., Martinović, N., Ćirković, M. M., Micic, M.: 2019b, *Monthly Notices of the Royal Astronomical Society*, **490**(1), 408-416.
Vukotić, B., Ćirković, M. M.: 2012, *Origins of Life and Evolution of Biospheres*, **42**(4), 347-371.
Vukotić, B., Gordon R., Seckbach J. (eds.): 2021, *Planet Formation and Panspermia: New Prospects for the Movement of Life through Space*, Wiley-Scrivener, Beverly Massachusetts, USA, in press.
Vukotić, B., Steinhauser, D., Martinez-Aviles, G., Ćirković, M. M., Micic, M., Schindler, S.: 2016, *Monthly Notices of the Royal Astronomical Society*, **459**(4), 3512-3524.
Zackrisson, E., Calissendorff, P., González, J., Benson, A., Johansen, A., Janson, M.: 2016, *The Astrophysical Journal*, **833**(2), id. 214, 12 pp.

Progress Reports

Publ. Astron. Obs. Belgrade No. 100 (2021), 185 - 191 *Progress Report*

THE FIRST YUGOSLAV NATIONAL COMMITTEE FOR ASTRONOMY

B. ARBUTINA

Department of Astronomy, Faculty of Mathematics, University of Belgrade, Studentski trg 16, 11000 Belgrade, Serbia
E–mail: arbo@matf.bg.ac.rs

Abstract. Although Serbia, as a member of the Allied Powers and a World War I winner, was one of the founding members of the International Research Council in the context of which the International Astronomical Union (IAU) was established in Brussels in the summer of 1919, it joined IAU, within the Kingdom of Yugoslavia, only in 1935. The formal representative of Yugoslavia at this assembly was Prof. Vojislav Mišković, a member of the Serbian Royal Academy and Director of the Astronomical Observatory of Belgrade. Shortly after the assembly, the first Yugoslav National Committee for Astronomy was established. Its president was Prof. Milutin Milanković, a member of the Serbian Royal Academy and one of the greatest Serbian scientists.

1. INTRODUCTION

The story begins by the end of World War I (WWI), when the Allied Powers decided to abandon existing international scientific organizations and form new ones, with the Central Powers banned from joining and neutral countries being accepted only later. In the period of roughly one year, three so-called inter-allied conferences were organized: 1st Inter-allied Conference on International Scientific Organizations, London, 9–11 October 1918; 2nd Inter-allied Conference, Paris, 26 November – 1 December 1918; 3rd Inter-allied Conference, Brussels, 18–28 August 1919. Serbian representatives at the first Conference were Bogdan Popović, Professor of Literature and Rhetoric at the University of Belgrade, and Jovan Žujović, president of the Serbian Royal Academy (SRA) (N/A 1918). At the second Conference Serbia was represented by Mihailo Petrović, Professor of Mathematics at the University of Belgrade and a member of the SRA, and Jovan Žujović, while at the third Conference the delegates were Mihailo Petrović and Jovan Cvijić, the renowned Serbian geographer, Rector of the University of Belgrade, a member and later the President of the SRA (Petrović 1920, Trifunović 1967). The 3rd Inter-allied Conference was also the founding assembly of the International Research Council (IRC) in the context of which numerous scientific unions were established. According to Campbell (1919), the countries and delegates represented at the Conference in Brussels in the summer of 1919 were: Belgium 101, Canada 2, USA 27, France 45, United Kingdom 18, Italy 15, New Zealand 1, Poland 1, Romania 2, Serbia 2. Beside the countries listed, among the founding

members of IRC were also: Brazil, Greece, Japan, Portugal, Australia and South Africa (N/A 1919, Trimble 1997).

The prevailing mood that existed among scientists from the Allied Powers at the time is nicely depicted in a quote by the Serbian-American physicist and professor at Columbia University Mihajlo Pupin, given in Blaauw (1994):

I heartily endorse the sentiments expressed by Monsieur Picard and by Mr. W. W. Campbell in the highest expression of a civilization. Allied Science is, therefore, radically different from Teutonic Science. It is true that the highest aim in Science is to disassociate itself from all its anthropomorphic elements, but we are still very far that ideal goal. ...

In such an atmosphere, still largely influenced by the atrocities of WWI, during the 3rd Inter-alied Conference, on 28 August 1919 in Brussels the International Astronomical Union (IAU) was formed (Blaauw 1994, Andersen et al. 2019). Founding members of the IAU were: Belgium, France, Japan, Canada, Greece, Mexico, Great Britain, Italy and United States (Trimble 1997).

2. YUGOSLAV NCA AND ITS FIRST MEMBERS

Although Serbia, that is the newly-formed Kingdom of Serbs, Croats and Slovenes, as a member of the Allied Powers and a WWI winner was one of the founding members of the IRC, unfortunately it did not participate in the founding of the IAU and it joined this organization only in 1935 (Arbutina and Atanacković 2019). The reason for this probably lies in the fact that there was no Serbian astronomer present in Brussels in 1919. As we have seen, Serbia was represented at the 3rd Inter-allied Conference by a mathematician and a geographer. The formal representative of the Kingdom of Yugoslavia at the 5th General Assembly in Paris, July 9-17, 1935, when it was formally admitted to the IAU, together with China and USSR, was Vojislav Mišković, Professor at the University of Belgrade, a member of the SRA and the Director of the Astronomical Observatory of Belgrade (AOB) (Mišković 1935, Stratton 1936). According to available data, Vojislav Mišković is the first Serbian/Yugoslav member of the IAU. Before Yugoslavia was addmited, the IAU Secretary General F.J.M. Stratton informed the University of Belgrade Rector's Office by a letter dated March 31, 1933 that the Executive Committee had elected V. Mišković as a member of the Commission 20 for Minor Planets (Mišković 1933). Cased on the *IAU Transactions B* from the 1935 General Assembly in Paris (Stratton 1936), the only Yugoslav member was V. Mišković (p. 423) and there is no mention of the Yugoslav National Committee for Astronomy (NCA) (p. 412-414).

After Mišković's return from Paris, activities started to form the NCA. In the period December 17-22, 1935, three meetings were held at which the statute of the NCA was written and submitted to the academies (SRA and Yugoslav Academy of Sciences and Arts (YASA) in Zagreb) for formal consideration and adoption. President, vice-president and secretary of the NCA were elected. This established the Yugoslav NCA, with a 4-year term for the period 1936-1939 (Mišković 1938). Its members were:

1) Milutin Milanković, SRA member, Prof. at Univ. of Belgrade, NCA president (representing the SRA)

2) Vojislav Mišković, correspond. member of the SRA, Prof. at the Univ. of Belgrade, Director of AOB, NCA secretary (representing the the SRA)

3) Stjepan Škreb, Prof. at the Univ. of Zagreb, Director of the Geophysical Institute, NCA vice-president (representing the YASA)
4) Željko Marković, Prof. at the Univ. of Zagreb (representing the YASA)
5) Vjačeslav Žardecki, Associate Prof. at the Univ. of Belgrade (representing his university)
6) Vladimir Vrkljan, Associate Prof. at the Univ. of Zagreb (representing his university)
7) Josip Plemelj, Prof. at the Univ. of Ljubljana (representing his university)

We will include in this contributed paper only a few words about each member.

Milutin Milanković (1879–1958)

Milutin Milanković was born in Dalj, present-day Croatia on May 28, 1879. He enrolled in a grammar school in Osijek in 1889. In 1896, Milanković began studying engineering at the Technical School in Vienna, where in 6 years he obtained the title of a graduate engineer. He defended his doctoral thesis (*Theorie der Druckkurven*) in Vienna in 1924. From 1905 to 1909 he worked as a civil engineer in several Viennese companies, and gained affirmation as a designer of reinforced concrete buildings. Upon the invitation of Jovan Cvijić, Mihailo Petrović and Bogdan Gavrilović, Milanković left his lucrative job in 1907 and accepted the position of associate professor of applied mathematics at the University of Belgrade. He remained at this position until his retirement in 1955. Milanković spent WWI in internment in Budapest. After the war, he returned to Belgrade and continued his university career (becoming full professor in 1919). He was elected corresponding member of the SRA and YASA in 1920, and full member of the SRA in 1924. He published a number of scientific papers, several university textbooks and monographs. He is most famous for his astronomical theory of climate and explanation of ice ages. His capital work *Kanon der Erdbestrahlung und seine Anwendung auf das Eiszeitenproblem* (Canon of Insolation and the Ice-age problem) was published by the SRA in 1941, but the majority of copies were destroyed in fire during the bombing of Belgrade. Nevertheless, the Canon (including its later editions) remains one of the most highly cited works of any Serbian scientist (Dimitrijević 2000). Milutin Milanković died in Belgrade on December 12, 1958. His remains were reburied in the family tomb in Dalj, according to his wish, in 1966 (see Andjelić 1979 for more details).

Vojislav Mišković (1892–1976)

Vojislav Mišković was born in Fužine, Gorski Kotar, present-day Croatia on January 18, 1892. The education of V. Mišković took place in various cities: Belgrade, Čačak, Priboj, Sukovo (near Pirot). Mišković attended high school in Novi Sad (Serbian Gymnasium) and graduated in 1910. He started university studies in Budapest, Göttingen and Vienna. After the outbreak of WWI, he joined the Serbian army, to be released of military duties in Thessaloniki in 1918 and sent to France to complete his studies. He graduated in astronomy at the University of Marseille in 1919 and immediately became an assistant at the local Astronomical Observatory. In 1922 he moved to the Astronomical Observatory in Nice, where he stayed until 1925. In the meantime, in 1924 he obtained the state doctorate at the University of Montpellier (with the thesis *Etudes de statistique stellaire*). At the suggestion of professors Mihailo Petrović, Bogdan Gavrilović and Milutin Milanković, he was invited in 1925 to become an associate professor of theoretical and practical astronomy at the University

of Belgrade. A year later he was entrusted with the duty of the director of AOB. He was elected a corresponding member of the SRA in 1929, and a full member in 1940. During World War II (WWII), he was removed from the University, even detained for a while, remaining however the "acting director" of the AOB. After the war, Mišković continued his fruitful work, staying at helm of the Observatory until 1953 and retiring from the University in 1962. Vojislav V. Mišković died in Belgrade on November 25, 1976. (see Mužijević 1982 for more details).

Stjepan Škreb (1879–1952)

Stjepan Škreb was born on July 13, 1879 in Zagreb. He began his studies in chemistry, mathematics and physics at the University of Zagreb in 1897 and finished them in 1901. He received his doctorate in 1910 with the dissertation "Influence of Earth's Rotation on Atmospheric Movements". He was a director of the Geophysical Institute, a member of the YASA, and a professor of Geophysics at University of Zagreb. He also gave lectures in other subjects (Cosmic Physics, Solar Physics, Spherical Astronomy, Celestial Mechanics, Earth's Atmosphere, etc). In his scientific research, S. Škreb worked in the fields of meteorology, climatology and geophysics in general (Lisac 2000). In astronomy he did some work on earthshine on the Moon, i.e. Earth's albedo (see e.g. Škreb 1935). He died on August 14, 1952 in Zagreb. (see Meštrov 2000 for more details).

Željko Marković (1889–1974)

Željko Marković was born on February 20, 1889 in Slavonska Požega, Croatia. He studied mathematics and astronomy at the Universities of Zagreb, Prague and Göttingen. He received his doctorate in 1915 from the Faculty of Philosophy in Zagreb with the dissertation "Application of Linear Integral Equations for the Solution of Differential Equations". He was professor at University of Zagreb and a member of the YASA. The scientific work of Ž. Marković is dedicated to the theory of differential and integral equations and the history of mathematics (especially the works of Rudjer Bošković; Janković 1975), and he also dealt to some extent with the three-body problem. He died on August 23, 1974 in Opatija. (see Niče 1980 for more details).

Vjačeslav Žardecki (1896–1962)

Vjačeslav Žardecki (Wenceslas Jardetzky) was born on April 16, 1896 in Odessa, present-day Ukraine, in a family of Polish origin. He finished primary and secondary school and the Faculty of Natural Sciences and Mathematics in his hometown. After graduating in 1917, he worked for a short time at the Observatory of Odessa and Pulkovo Observatory in St. Petersburg. In 1920 he left Russia, moved to Serbia and got a job at the AOB. In 1923 he defended his doctoral dissertation "On the Motion of a Solid Body on a Curved Line". In 1925 he became an assistant professor and in 1939 a full professor at the University of Belgrade. He left Belgrade University during WWII. In the post-war period, he resided in Austria, where he taught at the University of Graz. In 1949 he emigrated to the United States and worked as a researcher at the Lamont Geological Observatory at Columbia University in New York. In his scientific research he worked on hydrodynamics, rational mechanics, astronomy and geophysics. He wrote 2 university textbooks and 3 monographs. V. Žardecki died in New York on October 23, 1962. In 1992 his son Oleg established at the Lamont-Doherty Earth Observatory a lectureship that bears his father's name. (see Mušicki 2007, Bloh and Rihun 2015).

Vladimir Vrkljan (1894–1974)

Vladimir Srećko Vrkljan was born on August 26, 1894 in Sv. Petar-Orehovac near Križevci, Croatia. He completed his studies in mathematics and physics in 1917 at the Faculty of Philosophy, University of Zagreb, where in 1924 he received his doctorate with the dissertation "Development of the Quantum Theory of Line Optical Spectra". He was a professor at the University of Zagreb and a corresponding member of the YASA. In his scientific research, he worked on theoretical physics, especially on quantum theory and the theory of relativity. He is considered to be the first Croatian physicist who intensively dealt with quantum mechanics. He died on March 1, 1974 in Zagreb. (see N/A 1952, Janković 1978, Hanžek 2012).

Josip Plemelj (1873–1967)

Josip Plemelj was born on December 11, 1873 in Bled, Slovenia. He finished school in Ljubljana, and then in 1894 enrolled at the University of Vienna, where he studied mathematics, physics and astronomy. In his scientific work, he dealt with differential equations (the field in which he received his PhD). He was a professor at the University of Chernivtsi, Ukraine, a professor and the first rector of the University of Ljubljana in 1919, a corresponding member of the YASA since 1923, the SRA since 1930 and a member of the Slovenian Academy of Sciences and Arts since its establishment in 1938. He died on May 22, 1967 in Ljubljana. (O'Connor and Robertson 2003).

Although 7 members of the NCA have been elected for the period 1936-1939, according to the *IAU Transactions B* from the 1938 General Assembly in Stockholm (Oort 1939, p. 501), the Yugoslav NCA had 6 members:

YUGOSLAVIE

Président: M. Milankovitch.
Vice-Président: M. Škreb.
Secrétaire: M. Michkovitch.
Membres: MM. Jardecky, Terzić, Vrkljan.

The two members from the original NCA were missing and one new was included.

Milorad Terzić (1879–1939)

Milorad Terzić was born on April 6, 1880 in Kragujevac, Serbia. He finished high school in Kragujevac, after which he enrolled in the Lower School of the Military Academy. He completed the geodetic course in Nikolajevska Eng. Academy in St. Petersburg. In the Balkan Wars (1912-1913) and in WWI (1914-1918) he was a topographer in the 2nd Army and in the Topographic Department of the Supreme Command. After the war, he became the head of the Astronomical and Geodetic Department of the Traffic Section of Army Headquarters (1920-1928) and a lecturer at the Lower School of the Military Academy (1920-1921). In the period 1937-1939, as a geodetic general, he was the head of the Military Geographical Institute. He died in Belgrade on May 28, 1939 (see Radojčić 2001, Bjelajac 2004).

3. INSTEAD OF CONCLUSIONS

The work of the Yugoslav NCA, as well as the activities of the IAU, were soon halted by the outbreak of WWII. Although, all the members, excluding M. Terzić who died in 1939, survived WWII, in the *IAU Transactions B* from the 1948 General Assembly held in Zurich (Oort 1950), only two Yugoslav members are listed: M. Milanković (member of Commission 7 for Celestial Mechanics) and V. Mišković (member of Commission 19 for Latitude Variation and Commission 20 for Minor Planets). They were indeed the only members of the NCA that can be regarded as professional astronomers. Closest to this field was V. Žardecki, who emigrated to the US, all the others were primarily mathematicians or (geo)physicists. However, it remains unclear to the author what were the exact reasons for the personnel changes in the NCA during the 1936-1939 period, what the composition of the NCA was like afterwards and especially what happened with it immediately after WWII (its breakup in a divided country during the war was inevitable). Nevertheless, this was the period when the AOB started training its own observers and the University of Belgrade started educating professional astronomers: the first student graduating in Astronomy was Slobodanka Dimitrijević in 1936, and the first PhD in Astronomy was awarded to Zaharije Brkić in 1958 (Arbutina et al. 2020). Thus, in addition to Mišković and Milanković, *IAU Transactions B* from the 1952 General Assembly held in Rome (Oosterhoff 1954), lists as members from Yugoslavia: Pero Djurković (AOB), Milorad Protić (AOB) and Leo Randić (University of Zagreb).

References

Arbutina, B., Atanacković, O.: 2019, *Proceedings of the IAU*, **349**, 248.
Arbutina, B., Atanacković, O., Kovačević, A.: 2020, *Publ. Astron. Obs. Belgrade*, **100**, this Proceedings.
Andersen, J., Baneke, D., Madsen, C.: 2019, *The International Astronomical Union - Uniting the Community for 100 Years*, Springer.
Andjelić, T.: 1979, *Galerija SANU*, **36**, 7
Bjelajac, M.: 2004, *Generali i admirali Kraljevine Jugoslavije 1918-1941*, Institut za noviju istoriju Srbije, Beograd.
Blaauw, A.: 1994, *History of the IAU - The Birth and First Half-Century of the International Astronomical Union*, Springer Science + Business Media, B.V.
Bloh, Yu. I., Rikun, E. Yu.: 2015, *Geofiziki rossiyskogo zarubezh'ya, http://www.russiangrave.ru/assets/files/geofiziki-rossijskogo-zarubezhya-1.2-1.pdf*
Campbell, W. W.: 1919, *Publ. Astron. Soc. Pac.*, **31**, 249.
Dimitrijević, M. M.: 2000, *Publ. Astron. Obs. Belgrade*, **67**, 39.
Hanžek, B.: 2012, *KAJ*, **XLV**, 75.
Janković, Z.: 1975, *Glasnik matematički*, **10**(30), 169.
Janković, Z.: 1978, *Ljetopis JAZU za 1973/74*, **78**, 555.
Lisac, I.: 2000, *Spomenica preminulim akademicima*, **90**, 12.
Meštrov, M. (ed.): 2000, *Spomenica preminulim akademicima*, **90**, HAZU, Zagreb.
Mišković, V. (ed.): 1933, *Godišnjak našeg neba za god. 1934*, **V**, 153.
Mišković, V. (ed.): 1935, *Godišnjak našeg neba za god. 1936*, **VII**, 244.
Mišković, V. (ed.): 1938, *Godišnjak našeg neba za god. 1938*, **IX**, 247.
Mušicki, Dj.: 2007, *http://www.mi.sanu.ac.rs/History/zardecki.htm*
Mužijević, M.: 1982, *Vasiona*, **XXX**(4), 79.
Niče, V. (ed.): 1980, *Spomenica preminulim akademicima*, **7**, JAZU, Zagreb.
N/A: 1918, *The Observatory*, **41**, 414.
N/A: 1919, *The Observatory*, **42**, 94.

N/A: 1952, *Ljetopis JAZU za 1949/50.*, 56, 305.
Oort, J. H. (ed.): 1939, *Transactions of the IAU B*, **VI**, 502.
Oort, J. H. (ed.): 1950, *Transactions of the IAU B*, **VII**, 528.
Oosterhoff, P. Th.: 1956, *Transactions of the IAU B*, **VIII**, 866.
O'Connor, J. J., Robertson, E. F.: 2003, *http://www-history.mcs.st-andrews.ac.uk/Biographies/Plemelj.html*
Petrović, M.: 1920, *Srpski književni glasnik*, **I**(1), 130.
Radojčić, S.: 2001, *Načelnici Vojnogeografskog instituta 1876-2001*, VGI, Beograd.
Trifunović, D.: 1967, *Matematički vesnik*, **4**(19), 94.
Trimble, V.: 1997, *Beam Line*, **27**(4), 43.
Stratton, F. J. M. (ed.): 1936, *Transactions of the IAU B*, **V**, 414.
Škreb, S.: 1935, *Godišnjak našeg neba za god. 1936*, **VII**, 254.

Publ. Astron. Obs. Belgrade No. 100 (2021), 193 - 202 *Progress Report*

DEPARTMENT OF ASTRONOMY AT THE FACULTY OF MATHEMATICS, UNIVERSITY OF BELGRADE IN THE PERIOD 1999-2020

B. ARBUTINA, O. ATANACKOVIĆ and A. KOVAČEVIĆ

Department of Astronomy, Faculty of Mathematics, University of Belgrade, Studentski trg 16, 11000 Belgrade, Serbia
E–mail: arbo@matf.bg.ac.rs

Abstract. This contribution represents an attempt to give a brief overview of the development of the Department of Astronomy, Faculty of Mathematics, University of Belgrade in the period 1999-2020. It is primarily based on the paper in Serbian by Atanacković, Arbutina and Kovačević (2019) that chronologically covered in much more detail the period 1999-2018, and, in a sense, it is also a sequel to a paper by Milogradov-Turin (2003) that covered the history of the teaching of astronomy and Astronomy group at the University of Belgrade, from the beginnings until 2002. We hope that this contribution will serve as a valuable historical source to the future generations of Serbian astronomers.

1. INTRODUCTION

In this contributed paper we give a brief overview of the development of the Department of Astronomy, Faculty of Mathematics (MATF), University of Belgrade in the period 1999-2020. The paper is primarily based on the paper by Atanacković et al. (2019), that chronologically covered in much more detail the period 1999-2018. This 20-year period was chosen since there are reviews of previous periods, published by Simovljević (1980) and Simovljević and Milogradov-Turin (1998) covering topics: Astronomy until 1947, Astronomy Group 1947-1977 and Astronomy Group 1978-1998 (all referring to the activities of the Department of Astronomy) at the University of Belgrade. All the previously mentioned papers are written in Serbian. In a sense, this is also a sequel to a lecture/paper by Milogradov-Turin (2003) that covered the history of the teaching of astronomy and Astronomy group at the University of Belgrade, from the beginnings until 2002 (in English). Many information can also be found in review papers and triennial reports on astronomy education in Serbia (Atanacković 2009, 2012, 2013, 2017, 2018, Atanacković and Arbutina 2021). Years 1999 and 2020 have another interesting common feature. In the 2nd semester of school year 1998/1999 the teaching activities stopped (until June 1999) due to NATO bombing of FR Yugoslavia, while in the 2nd semester of school year 2019/2020 the classes stopped, and then continued online, due to the outbreak of SARS-CoV-2 pandemic.

2. OVERVIEW

Here we briefly recapitulate detailed chronology of the period 1999-2018 published in Atanacković et al (2019) and present recent developments in the years 2019 and 2020.

In the school year 1998/99 the teaching staff at the Department of Astronomy was:
Dr Dragutin M. Djurović, Full Professor,
Dr Trajko D. Angelov, Full Professor,
Dr Mike S. Kuzmanoski, Full Professor,
Dr Jelena S. Milogradov-Turin, Associate Professor,
Dr Ištvan I. Vince, Associate Professor (1/3 working hours),
Dr Nadežda R. Pejović, Associate Professor,
Dr Stevo D. Šegan, Associate Professor,
Dr Olga M. Atanacković-Vukmanović, Assistant Professor,
Dr Zlatko S. Ćatović, Assistant Professor,
Mr Dejan V. Urošević, Teaching Assistant,
Andjelka B. Kovačević, Junior Teaching Assistant,
Jelena I. Petrović, Junior Teaching Assistant.

The study program consisted of two subprograms (majors, moduls) at undergraduate level (4 years): *Astronomy* and *Astrophysics*. At MSc level (2 years of exams + MSc thesis) there were four subprograms (subspecializations) that a student could choose: *Fundamental astronomy*, *Celestial mechanics*, *Stellar astronomy* and *Astrophysics*, while at PhD level a student did not have any courses, only research i.e. work on the thesis. Depending on subspecialization, at the graduate level student would obtain MSc or PhD degree in *Astronomy* or in *Astrophysics*.

In the period after 2006 there were several redefinitions and accreditations of study programs. Starting with school year 2006/2007, undergraduate and master studies have new curricula (4+1 years, according to the Bologna convention). PhD studies last 3 + 3 years (or more if needed), for the exams and work on the thesis, respectively. At all levels there are two modules: *Astronomy* and *Astrophysics*.

School year 2009/2010 brings redefinition and accreditation of three study programs at the Faculty of Mathematics, University of Belgrade: "Mathematics", "Informatics" and "Astronomy and astrophysics". At the "Astronomy and astrophysics" program, at undergraduate level there are three moduls: *Computational mechanics and astrodynamics*, *Astrophysics* and *Astroinformatics* (introduced on initiative of Nadežda Pejović), at master level two modules: *Astronomy* and *Astrophysics*, while at PhD level two earlier modules merged into single modul *Astronomy and astrophysics* (upon defending the thesis, the student acquires a title "PhD in Astronomical Sciences"). At other programs at the Faculty of Mathematics one compulsory and several elective courses in astronomy have been introduced (for the students of mathematics and informatics), while at the Faculty of Physics there is one compulsory course in astrophysics and one elective course in astronomy. Since the Department of Mechanics at MATF practically ceased to exist in this period due to the lack of teaching staff, the Department of Astronomy took over some (elective) courses in mechanics.

New study programs, accredited by the end of 2014, started in the 2015/2016 academic year. The study program "Astronomy and astrophysics" consists of two moduls: *Astroinformatics* and *Astrophysics* at undergraduate and master levels. Within the study program "Mathematics" there is now a modul *Astronomy* at undergraduate, and a modul *Astronomy and mechanics* at master level. At PhD level there is one module *Astronomy and astrophysics*.

The total number of graduated and postgraduated students so far is:

- 309 graduated students,
- 45 master theses (from 2007),
- 69 MSc theses (until 2011), and
- 61 PhD theses defended

For some statistics on students, see Arbutina and Atanacković (2019). There is a general trend of increasing number of graduated students over the years (the first was Slobodanka Dimitrijević in 1936) as well as number of MSc and PhD degrees awarded (the first were Sofija Sadžakov in 1968, and Zaharije Brkić in 1958, respectively). Roughly half of the graduate students are women, while this percentage drops as we go on towards the PhD level. The Department's website contains links to the great majority of astronomical PhD theses which, as well as other publications, were scanned and archived in MATF Virtual library (*http://elibrary.matf.bg.ac.rs/*), largely thanks to the efforts of Nadežda Pejović. Among these publications are magazines *Saturn* and *Vasiona*, *Publications of Astronomical Society "Rudjer Bošković"*, *Publications of Department of Astronomy*, *Nautički godišnjak*, many hundreds digitised books and textbooks, e.g. by Atanasije Stojković, Djordje Stanojević, Milan Andonović and Kosta Stojanović (Pejović and Mijajlović 2011, Pejović et al. 2012). Nadežda Pejović also initiated the creation of Digital Legacy of Milutin Milanković at MATF in 2012 (Pejović at al. 2013, Jovanović et al. 2020). A number of textbooks and monographs were also published by the Department stuff during the 1999-2020 period (all the lists are available at *http://astro.matf.bg.ac.rs/*). In 2008 an interactive website BAZA at *http://alas.matf.bg.ac.rs/~astrobaza/* was launched, with the aim of bringing together, at least virtually, the Belgrade astronomical community, now spread across the globe (Atanacković et al. 2009).

Students at the Department of Astronomy, beside classes, participate in numerous curricular and extracurricular activities. *Student Astronomy Workshops* are conceived as meetings of astronomy students from the University of Belgrade and the University of Novi Sad. They have been organized since 2007 on the initiative of Dragana Ilić and Tijana Prodanović and held in Belgrade and Novi Sad, alternately. The program includes introductory lectures, short presentations of student papers, exchange of experiences, etc. *The Student Summer Internship* has also been held since 2007 at the Ondřejov Observatory, Czech Republic. These students' practices in observations and data reduction started on the initiative of Olga Atanacković and Nikola Vitas. The agreement on the cooperation was signed in 2008 by Prof. Petr Heinzel, the director of the Ondřejov Observatory and Prof. Miodrag Mateljević, the dean of the Faculty of Mathematics. Stevo Šegan gave a significant contribution to its practical realization, as well as Brankica Šurlan, who took care of students at the Ondřejov

Observatory. The internship is attended by third and fourth year students during the summer, for two to three weeks. Students are involved in the scientific work of professional astronomers and astrophysicists in the Department of Solar Physics, Department of Stellar Physics, Department of Interplanetary Matter Studies, and Department of the Study of Galaxies and Planetary Systems of the Ondřejov Observatory. Since 2012 students participate in *Student Training at Astronomical Station Vidojevica* (*http://vidojevica.aob.rs/*). Participants in the internship are students of the University of Belgrade and University of Novi Sad, which are under the expert guidance of teachers and associates of these two institutions and the Astronomical Observatory of Belgrade (AOB). From 2014 until 2017 students themselves organized four *Schools of Astronomy* (twice per week) for high-school pupils and younger people at Belgrade Youth Center. Each year on November 8 the "Prof. Dr. Zaharije Brkić" Award is given to the best graduated student at the Department of Astronomy (provided that certain conditions are met, concerning the grade point average and duration of study). Since 1981, 33 students have received the award.

Members of the Department of Astronomy participated in the scientific projects supported by the Ministry of Science (and Education) of the Republic of Serbia in all project periods: 2002-2005, 2006-2010 and 2011-2019. In the last project period one astronomy project was primarily based at the Faculty of Mathematics: No. 176005 "Emission nebulae: structure and evolution" with PI Dejan Urošević. Through this project several young people were employed at the Faculty of Mathematics as research staff. There were also other domestic and international projects realized, such as FP7 project *Stardust* (coordinator Bojan Novaković), project "Pavle Savić" (2013-2014) between Department of Astronomy (Olga Atanacković, Irena Pirković), AOB (Slobodan Jankov, Ivan Milić) and University of Nice (Marianne Faurobert), projects of interacademies cooperation (Serbian Academy of Sciences and Arts and Bulgarian Academy of Science, 2014-2016, 2017-2019, 2020-2022, PIs Dejan Urošević, Bojan Arbutina and Milica Vučetić, respectively), as well as project *Superast* (2019-2020, PI Andjelka Kovačević), through which a small cluster computer was obtained for the Department.

In year 2000, the first ideas emerged about building a new astronomical station at the Vidojevica mountain near Prokuplje. This project, certainly one of the most important in Serbian astronomy in the last decades, was initiated by the MATF and its professors Stevo Šegan and Žarko Mijajlović, who were immediately joined by Nadežda Pejović, head of the Department of Astronomy at the time. In 2004 MATF withdrew from the project in favor of AOB, since the Ministry of Science demanded to have only one party involved (Mijajlović 2007). The 60 cm "Nedeljković" telescope (2011) and the 1.4 m "Milanković" telescope (2016) were installed on site.

From the school year 2011/2012 the University of Belgrade together with 4 other institutions (Institute of Astro- and Particle Physics, University of Innsbruck, Austria; Department of Astronomy, University of Padua, Italy; Astrophysics Section/Department of Physics, University of Rome "Tor Vergata", Italy; Institute for Astrophysics, Department of Astronomy, University of Göttingen, Germany) participated in the international Erasmus Mundus two-year master program - *Astromundus* (thanks to the initiative of Luka Popović and Dragana Ilić). The teaching staff of the Department involved in the realization of the program were: Luka Popović, Dejan Urošević, Andjelka Kovačević, Dragana Ilić, Bojan Arbutina, Dušan Onić (from the school year

2018/19). Through this program a number of foreign students from countries all around the world had a possibility to live and study in Belgrade for one semester or more. The program officially ended in January 2020.

In 1992 Astronomical Observatory of Belgrade and Faculty of Mathematics started to jointly publish a scientific journal *Bulletin Astronomique de Belgrade*, which changed its name to *Serbian Astronomical Journal* in 1998. In 2003 Dejan Urošević became Editor and Nikola Vitas Assistant Editor of the Serbian Astronomical Journal (SAJ), which also got its electronic edition at *http://saj.matf.bg.ac.rs/*. Editor-in-Chief was Zoran Knežević (AOB). In 2006 Nikola Vitas left Serbia and Bojan Arbutina became the Assistant Editor. In 2013 SAJ got international recognition by appearing in SCI or JCR list (Journal Citation Report) at the position 41/59 in the field Astronomy and Astrophysics, with impact factor IF=1.1 (Knežević et al. 2017). In 2014 Dejan Urošević became Editor-in-Chief, Bojan Arbutina Editor and Milena Jovanović (AOB) Assistant Editor.

In the summer of 2018 Serbia became a member of the Board of Directors of the *Astronomy & Astrophysics* (A&A) journal. Negotiations began in May 2017 at the initiative of the Department of Astronomy. The accession was voted at the meeting of the Board of Directors on May 15, 2018, and the agreement entered into force on July 1 (signed on June 11 by ESO Director Prof. Dr. Xavier Barcons and AOB Director Dr. Gojko Djurašević). Previously, an agreement between AOB and MATF was signed on the representation of Serbia and the payment of membership fees. The annual membership fee is divided between the MATF and the AOB. According to the contract, all astronomers who have an affiliation in Serbia can publish their works in A&A free of charge. The first representative of Serbia in the Board of Directors is Andjelka Kovačević.

All professors of the Department were members of the International Astronomical Union (IAU) and actively participated in its commissions. Serbian representatives (National Liaisons) in the IAU Commission 46 for astronomy education were Jelena Milogradov-Turin (until 2003) and Olga Atanacković (2003-2015). The Office of Astronomy for Education (OAE) founded in January 2020 within the IAU Commission C1 has established a network of NAECs (National Astronomy Education Coordinators). Members of the Serbian NAEC team are: Olga Atanacković (chair), Dragana Ilić (contact person), Jelena Kovačević-Dojčinović and Bojan Arbutina.

In 2002 Jelena Milogradov-Turin initiated Serbian team participation in International Astronomical Olympiads for high-school pupils and became the president of the National Astronomical Olympic Committee (see Vidojević et al. 2018). She was succeeded at this position by Nadežda Pejović (2005-2006), Slobodan Ninković (2006-2014) and Sonja Vidojević (2014-). So far the Serbian teams have participated in three types of International Astronomical Olympiads and won 78 medals and 21 recognitions in total (Vidojević et al. 2018, Vidojević et al. 2021).

In the 20-year period under consideration members of the Department had diverse duties, out of which we will mention here only some:

Head of Department
Mike Kuzmanovski (1998-1999)
Nadežda Pejović (1999-2003)
Trajko Angelov (2003-2005)

Olga Atanacković (2005-2007)
Trajko Angelov (2007)
Dejan Urošević (2007-2013)
Nadežda Pejović (2013-2017)
Andjelka Kovačević (2017-2020)
Bojan Arbutina (2020-)

Vice-dean for finance of MATF
Stevo Šegan (1998-2000)
Dejan Urošević (2004-2007 and 2014-)

President of the Society of Astronomers of Serbia
Jelena Milogradov-Turin (1998-2002)
Stevo Šegan (2014-2017)
Vladimir Djošović (2019-2020)

President of the National Comittee for Astronomy
Olga Atanacković-Vukmanović (2005-2008)
Dragana Ilić (2014-2017)
Bojan Arbutina (2017-2020)

Organization of National astronomical conferences, (co)presidents of SOC or LOC
XIII (2002) - J. Milogradov-Turin and G. Popović (SOC), O. Atanacković-Vukmanović (LOC)
XV (2008) - O. Atanacković-Vukmanović and Z. Cvetković (SOC), D. Ilić (LOC)
XVI (2011) - S. Jankov and N. Pejović (SOC), R. Pavlović (LOC)
XVII (2014) - S. Šegan and S. Ninković (SOC), A. Kovačević and B. Novaković (LOC)
XVIII (2017) - L. Popović and D. Urošević (SOC), R. Pavlović (LOC)
XIX (2020) - A. Kovačević and J. Kovačević Dojčinović (SOC), D. Marčeta and D. Onić (LOC)

Organization of international summer schools, (co)presidents of SOC or LOC
2007 - The 1st Summer School in Astronomy and Geophysics - N. Pejović and M.S. Dimitrijević (SOC), A. Kovačević (LOC)
2008 - The 2nd Summer School in Astronomy - M.S. Dimitrijević and T. Prodanović (SOC), A. Kovačević (LOC)
2010 - The 3rd International School in Astronomy: Astroinformatics - Virtual Observatory - A. Kovačević and M. Dimitrijević (SOC), A. Kovačević (LOC)

The Department of Astronomy initiated a number of activities during the International Year of Astronomy 2009 (IYA2009) and global celebration of 100 years of the International Astronomical Union (IAU100). Within IYA2009 the exhibition on the cooperation between Serbia and France in the field of astronomy *Kosmos na dohvat ruke* was held from 7 to 26 September 2009 in the French Cultural Center. It was organized by J. Milogradov-Turin, O. Atanacković, D. Ilić and Z. Knežević as associates,

and S. Vidojević (MSc) and many students (S.Opsenica, V.Zeković, M. Pavlović, A. Ćiprijanović, R. Vujetić, S. Zdolšek, D. Jevtić, K. Racković, J. Mišić, J. Vukadinović) as assistants. In 2009 D. Ilić was the coordinator of the exhibition "From Earth to the Universe" held in Belgrade, Novi Sad and Valjevo. On the occasion of the IAU100 the Women and Girls in Astronomy Day was marked by a series of lectures (on 8 March 2019) organized by the Department of Astronomy. The conference "Astronomy in Serbia and Serbia in International Astronomical Union", organized by MATF and AOB, was held on the 16 May 2019 in SANU. The exhibition "Above and Beyond", organized by Bojan Arbutina, was held during the manifestation "Researchers Night" in Belgrade. Within "IAU100 NameExoWorlds" project Serbia has voted to name the star WASP-60 Morava and its planet WASP-60b Vlasina.

Actually, during this whole 20-years period the staff members of the Department of Astronomy were very active in promotion and popularization of astronomy, e.g. through public lectures at Ilija M. Kolarac Fondation, Museum of Science and Technology, Belgrade Youth Center, Students' Cultural Center, lectures for talented high-school pupils at the Petnica Science Center, lectures at Seminar for physics teachers, etc. The Department staff also participated in numerous workshops, meetings and conferences in the country and abroad. Since 2000 every second Tuesday during the semester (occasionally more frequently) Seminar of Department of Astronomy has been held with domestic and foreign lecturers presenting their research and new astronomical discoveries. Initiator of the Seminar and coordinator until 2016 was Dejan Urošević, from January 2016 to June 2019 coordinator was Dragana Ilić, and afterward Bojan Arbutina. Until the beginning of school year 2020/2021, in total 249 lectures have been held.

3. INSTEAD OF CONCLUSION

Here we list all the persons who came or left the Department at some point, as well as our deceased professors, in the period 1999-2020.

Came to the Department:
Nikola Vitas (1999/2000)
Tamara Plavšin (1999/2000)
Katarina Kovač (2000/01)
Dragana Ilić (2002/03)
Bojan Arbutina (2006/07)
Dušan Onić (2007/08)
Dušan Marčeta (2009/10)
Bojan Novaković (2009/10)
Milica Vučetić (2010/11, project 176005)
Marko Pavlović (2010/11, project 176005)
Aleksandra Ćiprijanović (2010/11, project 176005)
Slobodan Opsenica (2010/11, project 176005)
Viktor Radović (2012/13)
Vladimir Zeković (2012/13, project 176005)
Luka Popović (2012/13, 2019/20)
Stanislav Milošević (2015/16)
Vladimir Jakovljević(2015/16)
Kristina Racković (2016/17, 2018/19 - project 44002)

Mihailo Martinović (2016/17, project 176002)
Vladimir Djošović (2017/18)
Ivana Bešlić (2017/18)
Dušan Vukadinović (2017/18)
Miljan Kolčić (2018/19)
Sara Savić (2019/20)
Isidora Jankov (2019/20, project 176001)
Marco Fenucci (2019/20, project Stardust-R)

Left the Department:
Zlatko Ćatović (1998/99)
Dragutin Djurović (retired in 2000)
Tamara Plavšin (2000/01)
Jelena Petrović (2000/01)
Jelena Milogradov-Turin (retired in 2002)
Katarina Kovač (2001/02)
Nikola Vitas (2006/07)
Ištvan Vince (2009/10)
Trajko Angelov (retired in 2010)
Mike Kuzmanoski (retired in 2012)
Slobodan Opsenica (2012)
Vladimir Jakovljević (2016)
Stevo Šegan (2017)
Nadežda Pejović (retired in 2017)
Ivana Bešlić (2018)
Dušan Vukadinović (2019)
Miljan Kolčić (2019)
Aleksandra Ćiprijanović (2019)

Deceased professors:
Branislav Ševarlić (2001)
Milivoj Rakić (2001)
Jovan Simovljević (2007)
Jelena Milogradov-Turin (2011)
Dragutin Djurović (2013)
Jovan Lazović (2019)
Ilija Lukačević (2020)
Mirjana Vukićević-Karabin (2020)

In the school year 2019/20 teaching staff at the Department of Astronomy is:
Dr Olga Atanacković, Full Professor,
Dr Dejan Urošević, Full Professor,
Dr Luka Popović, Associate Professor (with 10% engagement),
Dr Andjelka Kovačević, Associate Professor,
Dr Dragana Ilić, Associate Professor,
Dr Bojan Arbutina, Associate Professor,
Dr Bojan Novaković, Assistant Professor,

Figure 1: Department of Astronomy staff in 2019. From left to right, the first raw: Dragana Ilić, Aleksandra Ćiprijanović, Dušan Vukadinović, Stanislav Milošević, Andjelka Kovačević, Olga Atanacković, Vladimir Djošović, Vladimir Zeković and Dejan Urošević; the second raw: Viktor Radović, Dušan Marčeta, Dušan Onić, Bojan Novaković and Bojan Arbutina (photo taken on September 13, 2019).

Dr Dušan Onić, Assistant Professor,
Dr Dušan Marčeta, Assistant Professor,
Dr Viktor Radović, Teaching Assistant,
Stanislav Milošević, Teaching Assistant,
Vladimir Djošović, Teaching Assistant
Sara Savić, Junior Teaching Assistant

Additionally, research staff at the Department of Astronomy is:
Dr Mihailo Martinović, Research Associate (on leave),
Dr Milica Vučetić, Research Associate,
Dr Marko Pavlović, Research Assistant (on leave),
Vladimir Zeković, Research Assistant,
Kristina Racković-Babić, Junior Research Assistant,
Isidora Jankov, Junior Research Assistant,
Marco Fenucci, Early Stage Researcher.

References

Arbutina, B., Atanacković, O.: 2019, Astronomy in Serbia and Serbia in the International Astronomical Union, *Proceedings of the International Astronomical Union*, **349**, 248.

Atanacković, O.: 2009, Astronomy Education in Serbia 2005-2008, *Publ. Astron. Obs. Belgrade*, **86**, 231.

Atanacković, O., Vitas, N., Arbutina, B.: 2009, BAZA - Belgrade Astronomical Community Database, *Publ. Astron. Obs. Belgrade*, **86**, 369.

Atanacković, O.: 2012, Astronomy Education in Serbia 2008-2011, *Publ. Astron. Obs. Belgrade*, **91**, 273.

Atanacković, O.: 2013, Astronomy Education and Popularization in Serbia, *Publ. Astron. Obs. Belgrade*, **92**, 107.

Atanacković, O.: 2017, Astronomy Education in Serbia 2011-2014, *Publ. Astron. Obs. Belgrade*, **96**, 397.

Atanacković, O.: 2018, Astronomy Education in Serbia 2014-2017, *Publ. Astron. Obs. Belgrade*, **98**, 91.

Atanacković, O., Arbutina, B.: 2021, Astronomy Education in Serbia 2017-2020, *Publ. Astron. Obs. Belgrade*, this volume.

Atanacković, O., Arbutina, B., Kovačević, A.: 2019, Department of Astronomy 1999-2018, *Publ. Astron. Soc. "Rudjer Bošković"*, **19**, 197.

Jovanović, B., Mijajlović, Ž., Ninković, S., Eds.: 2020, Collected works of Nadežda Pejović, *Publ. Astron. Soc. "Rudjer Bošković"*, **21**, 1.

Knežević, Z., Urošević, D., Arbutina, B.: 2017, Serbian Astronomical Journal in Science Citation Index and Journal Citation Report, *Publ. Astron. Obs. Belgrade*, **96**, 523.

Mijajlović, Ž: 2007, Astronomska stanica na Vidojevici, *Publ. Astron. Soc. "Rudjer Bošković"*, **7**, 153.

Milogradov-Turin, J.: 2003, Department of Astronomy of the University of Belgrade, *Publ. Astron. Obs. Belgrade*, **75**, 289.

Pejović, N., Mijajlović, Ž.: 2011, Early astronomical heritage in Virtual Library of Faculty of Mathematics in Belgrade, *NCD Review*, **19**, 11.

Pejović, N., Mitić, N., Malkov, S., Mijajlović, Ž,: 2013, Digital legacies and archives, *Zb. radova III simp. "Matematika i primene"*, Faculty of Mathematics, University of Belgrade, p. 1.

Pejović, N., Mijajlović, Ž., Valjarević, A., Damljanović, G.: 2012, Serbian Astronomical Works in the Virtual Library of the Faculty of Mathematics in Belgrade, *Publ. Astron. Soc. "Rudjer Bošković"*, **11**, 311.

Simovljević, J.: 1980, "Astronomija" in *Trideset godina Prirodno-matematičkog fakulteta Univerziteta u Beogradu, s osvrtom na razvitak nastave prirodnih i matematičkih nauka u Beogradu, 1947-1977*, Ed. D. Vitorović, Faculty of Natural Sciences and Mathematics, University of Belgrade, p. 165.

Simovljević, J., Milogradov-Turin, J.: 1998, "Astronomija" in *Spomenica, 125 godina Matematičkog fakulteta*, Ed. N. Bokan, Faculty of Mathematics, University of Belgrade, p. 59.

Vidojević, S., Ninković, S., Simonović B., Bešlić, I.: 2018, Astronomy Competitions and their Role in Astronomy Education in Serbia, *Publ. Astron. Obs. Belgrade*, **98**, 217.

Vidojević, S., Prokić, V., Ninković, S., Simonović B.: 2021, Serbia in astronomical contests between 2017 - 2020, *Publ. Astron. Obs. Belgrade*, this volume.

Publ. Astron. Obs. Belgrade No. 100 (2021), 203 - 210 *Progress Report*

ASTRONOMY EDUCATION IN SERBIA 2017-2020

O. ATANACKOVIĆ and B. ARBUTINA
Department of Astronomy, Faculty of Mathematics, University of Belgrade, Studentski trg 16, 11000 Belgrade, Serbia
E–mail: olga@matf.bg.ac.rs, arbo@matf.bg.ac.rs

Abstract. A review of triennial activities in astronomy education in Serbia at all levels is given with an emphasis put on considerable changes introduced within the reform of the primary and secondary school education, especially regarding the representation of Astronomy within Physics in high school teaching. The nomination and participation of Serbian NAEC team within the IAU Office of Astronomy for Education is described. Astronomy education at the universities in Serbia, and the numerous activities of the Department of Astronomy are considered as well.

1. INTRODUCTION

In this paper we give a brief overview of the news and changes in astronomy education in Serbia that occurred in the period from 1 November 2017 to 1 November 2020. The previous period was covered in triennial reviews of astronomy education in Serbia by Atanacković (2009, 2012, 2013, 2017, 2018), Arbutina and Atanacković (2019), Atanacković-Vukmanović (2006a,b) and Milogradov-Turin (2003), and in the references therein.

Some recent news concerning the founding of the International Astronomical Union (IAU) Office of Astronomy for Education (OAE) and the participation of the Serbian team will be described in Section 2. Sections 3 to 5 are devoted to the primary, secondary and university education, respectively. Public outreach is very briefly reviewed in Section 6.

2. THE OAE AND THE SERBIAN NAEC TEAM

Apart from three offices that already exist within the IAU Commision C1 on Astronomy Education and Development: Office for Young Astronomers (OYA, ISYA), Office for Astronomy Development (OAD) and Office for Astronomy Outreach (OAO), the fourth one - Office of Astronomy for Education (OAE) was founded in January 2020 with the aim to promote astronomy in education at school level all over the world. The OAE established a network of NAECs (National Astronomy Education Coordinators). The National Committee for Astronomy of Serbia nominated Serbian NAEC team: O. Atanacković (chair), D. Ilić (contact person), J. Kovačević-Dojčinović and B. Arbutina. So far 251 individual NAECs from 80 countries have been confirmed.

NAECs have submitted a brief review representing the structure of education in their country with the focus on Astronomy in the curriculum and Astronomy education outside the classroom.

From 6 to 9 October 2020 the OAE organized the IAU 2nd Shaw Workshop on Astronomy Education that was held online due to SARS-CoV-2 pandemic. The document "Big Ideas in Astronomy" was offered as a framework on what should any (18 years old) citizen of planet Earth know about Astronomy. The goal is that everyone should be astronomically literate. This framework is supposed to be further developed with the help of NAECs. All of the material created: textbooks, glossary, diagrams, images (a kind of astroEDU data base) will be available under the licence that allows it to be used universally in teaching.

Serbian NAEC team took part in The Astronomy Day in Schools[1], which in 2020 was on the day of the Total Solar Eclipse of December 14. Any amateur or professional astronomer, scientist or teacher was invited to participate. Although this event was visible only on the southern hemisphere, marking and following this event was a unique opportunity for students around the world to participate together in this beautiful natural phenomenon on that specific day as well as to learn something more about the eclipses. Elementary and high-school teachers in Serbia were invited to work with their students on the topics of Solar eclipse. The materials in Serbian were provided: a short video/lecture about eclipse events "Šta su pomračenja?" posted online at *https://youtu.be/OOnST-49tZs*, and a little game to illustrate the moon phases that can be used in the future. The information on the Great conjunction of Jupiter and Saturn on December 28 was shared as well.

3. PRIMARY SCHOOL EDUCATION

In the primary school curricula astronomy topics are mostly taught as part of the Geography course (5th grade). The pupils learn about the Milky Way, stars, the Sun and Solar system, Earth's rotation and revolution and the consequences, the Moon and lunar phases, Earth's atmosphere and climate changes. Additional topics are taught in astronomy clubs organized by the enthusiastic teachers of physics, mathematics or geography.

In the last triennial report (Atanacković, 2018) we wrote about an initiative and the first activities undertaken by the Department of Astronomy to introduce Astronomy as a separate elective course in primary schools. However, according to the most recent reform there will be no more elective courses in primary schools.

4. SECONDARY SCHOOL EDUCATION

As of recently, according to the decision of the National Education Council and Minister of Education, the number of hours of Physics has been reduced from 5 to 3+1 per week[2]. Accordingly, the number of hours of Astronomy within Physics has also been drastically reduced from 32 to 6+2 per year.

[1]The Astronomy Day in Schools initiative is an IAU100 Global Project with the vision of mobilising the astronomical community to organise activities in schools. This is a special opportunity for students to directly interact and engage with astronomers in their communities, and to learn about the significant role that astronomy plays in ours lives.

[2]3 hours of lectures + 1 hour of laboratory exercise.

In 1990, astronomy topics were incorporated in the 4th year Physics course with 32 class hours per year (one hour per week)[3]. Students were taught about gravity, coordinate systems in astronomy, time, distances to celestial bodies, physical processes, radiation, astronomical instruments, Sun and Solar system, stars, galaxies and cosmology. Today, only a few special schools in Serbia (e.g. Mathematical High School in Belgrade, "Jovan Jovanović Zmaj" in Novi Sad, "Svetozar Marković" in Niš) have astronomy as a separate subject. Despite many attempts made by the Serbian astronomical community to reintroduce Astronomy as a separate and compulsory course in all grammar schools, Astronomy is still taught within Physics. To make things even worse, by the decision of the National Education Council, the number of hours of Astronomy within Physics is reduced. The program is now as follows:

- Introduction to astronomy and its basic terms (2)
- Gravitational effects (1)
- Electromagnetic radiation of celestial bodies and astronomical instruments (1)
- Stars and galaxies (1+1)
- The Sun and the Solar system (1+1)

4. 1. TEACHER TRAINING

The Serbian Physical Society organizes annual meetings of physics and astronomy teachers where teachers are acquainted with the latest discoveries and news in astronomy.[4] International seminars for physics teachers have been organized since 2012 as well. A regular session dedicated to astronomy education is included in the program of triennial Serbian Astronomical Conferences (see, e.g. Stojičić 2021). The Commission for astronomy education within the Society of Astronomers of Serbia intends to apply for the organization of seminars in astronomy to help physics teachers to teach astronomy topics. The call of the Institute for the Advancement of Education and Upbringing is expected to be announced in 2021.

4. 2. PETNICA SCIENCE CENTER (PSC)

Petnica Science Center (founded in 1982) has a very important role in extracurricular (informal) astronomy education of the gifted secondary-school students. The program of astronomy in PSC includes 6-7 seminars per year. The main concept of PSC is learning through research. Research projects realized by the participants in the most advanced group are presented at the annual conferences "A Step into Science" and regularly published in "Petnica Notebooks". The activities of PSC in the past three years are described in more detail in the paper by Vukadinović et al. (2021). Let us mention here only two summer schools for students ("Petnica Summer Institute" - PSI) that were held in the past three years: the 6th Summer School on High Energy Physics (12-21 July 2018) and the 7th Summer School on Astrophysics (25 July - 3 August 2019). In 2020 the 8th Summer School was not organized due to SARS-CoV-2 pandemic.

[3]For 25 years (from 1969 to 1994) astronomy was taught in the 4th year of grammar schools as a separate course with one class hour per week.

[4]A comprehensive review on astronomy in seminars for teachers in Serbia (independent astronomical seminars and astronomy at seminars for physics teachers) in the period 1964-1997 is given by Milogradov-Turin (1997).

4. 3. INTERNATIONAL ASTRONOMY OLYMPIAD

Since 2002 Serbian teams have participated with success in the following International Astronomical Olympiads[5]:

- since 2002 at IAO (International Astronomy Olympiad, founded in Russia in 1996),

- since 2009 at IOAA (International Olympiad on Astronomy and Astrophysics, founded on the initiative of Tailand, Indonesia, Iran, China and Poland in 2007),

- since 2013 in the Saint-Petersburg Astronomical Olympiad, which represents the correspondence type competition.

In 2020 GeCAA (Global e-Competition on Astronomy and Astrophysics), an online astronomy and astrophysics competition was held instead of the IOAA due to SARS-CoV-2 pandemic.

So far Serbian teams have won 78 medals and 21 recognitions in total, out of which 12 medals and 5 recognitions in the past three years. The success of Serbian team in the period 2017-2020 is described in more detail in the paper by Vidojević et al. (2021).

Main coordinators and leaders of Serbian teams in the past years are Dr. Sonja Vidojević and Prof. Slobodan Ninković.

A new book "Astronomski zabavnik: zadaci i vežbe iz astronomije i astrofizike" has been published (Vidojević, 2019). It is a translation by Sonja Vidojević of the Russian book "Astronomicheskij divertisment. Zadachi i uprazhnenija po astronomii i astrofizike".

At the assembly held on 16 April 2019 the Society of Astronomers of Serbia decided by a majority vote to withdraw its candidacy for the organizer of the International Astronomical Olympics 2021 in Serbia, due to the financial difficulties and uncertain funding.[6] The withdrawal was sent to the International Olympic Committee (see Vidojević et al., 2021).

5. UNIVERSITY EDUCATION

Astronomy courses are taught at six state universities (University of Belgrade, University of Novi Sad, University of Niš, University of Kragujevac, University of Priština in Kosovska Mitrovica and State University of Novi Pazar).

The University of Belgrade is the only one with the Department of Astronomy (at the Faculty of Mathematics, MATF) where students can major in astronomy from the first study year. The structure of the last accredited study program at the Department of Astronomy (2014) is described in the paper by Atanacković (2018), along with all the courses in astronomy taught at the Faculty of Mathematics for the students of mathematics and informatics and at other faculties within the University of Belgrade (Faculty of Physics, Faculty of Civil Engineering, Faculty of Geography). Previous study programs (in Serbian) at the Department of Astronomy can be found at the Department's website *http://astro.math.rs*.

[5]Prof. Jelena Milogradov Turin (1935-2011) initiated in 2002 the participation of Serbian team at the IAOs. In 2011 "Jelena Milogradov-Turin" award is introduced.

[6]In 2013, at the 7th IOAA, Serbia was nominated as the host for 15th IOAA in 2021 (see Atanacković, 2018; Vidojević et al., 2018).

So far 307 students have graduated from the Department of Astronomy at the University of Belgrade (since 1936), 45 students received Master degree (since 2007), 69 students received MSc degree (1968-2010), and 61 students - PhD degree (since 1958). In the past three years, 10 students graduated, 9 students received master degrees and 5 students received PhD degrees, which is much fewer than in the previous triennial period (Atanacković, 2018).

The best students in their generation won the "Prof. Zaharije Brkić" award: Ivana Bešlić (2016/2017), Andrija Kostić (2017/2018) and Milica Rakić (2019/2020).

AstroMundus, a 2-year European Erasmus Mundus Joint Master program in astronomy and astrophysics between 5 European universities, formally ended in January 2020 (Ilić, 2020). AstroMundus program is described in more detail in the paper by Atanacković (2018).

The students had summer practice - training in observations and data reduction at the Ondřejov Observatory in 2018 (Nikolina Milanović and Marija Obućina), and in 2019 (Sara Savić and Lazar Živadinović). They worked under the supervision of Czech colleagues (Marčeta, 2020).

Three summer students' practices lasting 3 days have been organized at the Astronomical Station Vidojevica (ASV): in April 2018 (3 students), in April 2019 (9 students) and in May 2020 (10 students). The last one was organized completely virtually. Students were trained to use the reflectors "Nedeljković" ($D = 60$ cm) and "Milanković" ($D = 140$ cm).

Two Student Astronomy Workshops (SAW) were held in the past three years: the 10th SAW on 18 November 2017 in Novi Sad (37 students) and the 11th SAW on 2 November 2019 in Belgrade (38 students).

The first students' practice at the Rozhen Observatory was held from 27 February to 4 March 2020. This student training was conducted within the project SUPERAST (Supercomputing astronomy) led by Andjelka Kovačević (2019-2020). Coordinators of the practice were Nikola Petrov (deputy-director of NAO Rozhen), Bojan Arbutina, Dragana Ilić, Dejan Urošević and Stanislav Milošević (MATF). The students (Sara Savić, Nikolina Milanović, Jana Marković, Isidora Jankov and Teodora Žižak) observed emission nebulae.

In the past three years 33 seminars on different topics in astronomy were held on every second Tuesday throughout the academic year at the Department of Astronomy, whereas 33 seminars were held at the Astronomical Observatory in Belgrade.

In this triennial period two new university textbooks were published: "Evolution of supernova remnants" by Bojan Arbutina and "Odabrani tekstovi iz astronomije" ("Selected texts in astronomy") by Mihailo Martinović and Stevo Šegan (Arbutina, 2017; Martinović and Šegan, 2018).

The activities of the Department of Astronomy at the Faculty of Mathematics in Belgrade in the period 1999-2020 are described in the paper by Arbutina et al. (2021).

At the Department of Physics of the Faculty of Natural Sciences (FNS) at the University of Novi Sad eighteen students enrolled in the bachelor programme in Astronomy and astrophysics in 2017/2018, 8 out of which are still studying astronomy. Two students received the Master degree in 2018.

New accredited studies at this department started in 2018/2019. Eleven optional courses in astronomy and astrophysics are offered at the undergraduate studies in

Physics. "Fundamentals of the Solar System" in the 1st study year was elected by 13 students in 2018/2019, by 10 students in 2019/2020 and 12 students in 2020/2021. Two students in 2019/20 and two students in 2020/21 chose "General astronomy" in the 2nd year, whereas one student of the 3rd year chose "General astrophysics" (Prodanović, 2020).

Master studies have also been newly accredited and are focused on High energy astrophysics.

Astro CEEPUS (Central European Exchange Program for University Studies) program, which initiated basically from the University of Novi Sad resulted in international astronomy student conference. The participants of the first regional students workshop "Multi-messenger Astrophysics in Central Europe (ASTRO.CE)", held in Nova Gorica from 13 to 15 May 2019 were from the universities of Banja Luka, Belgrade, Novi Sad, Rijeka and Skopje. The participants from Serbia were Tijana Prodanović, Dragana Ilić, Dejan Urošević, Dušan Onić, Stanislav Milošević, as well as students from Belgrade (Nikolina Milanović, Debora Pavela, Miljan Kolčić, Damnjan Milić, Milica Rakić, Teodora Žižak, Jana Marković, Milana Vuković) and Novi Sad (Marina Pavlović, Isidora Jankov, Nikola Radulović). All the participants gave lectures.

At the University of Niš astronomy, astrophysics and cosmology are taught at the Department of Physics. "Fundamentals of Astrophysics" is the compulsory course for the students of General Physics (2nd year) and elective for the students of Physics - Informatics (1st year). "Introduction to Cosmology" is elective at the 3rd study year, and "Cosmic plasma" and "Fundamentals of cosmology" are elective at the PhD studies. Astronomy is also taught at the master studies at the Department of Biology ("Fundamentals of astrophysics with astrobiology", elective, 1st year) and at the Department of Geography ("Astronomy", elective, 1st year). Several changes are foreseen in the curricula starting from 2021/2022 (Gajić, 2020).

At the Institute of Physics of the Faculty of Natural Sciences of the University of Kragujevac one-semester (2+2) course "Astrophysics and Astronomy" for the 5th-year (master) students, so far optional, became a compulsory course for the module A1 (General physics) according to the new accreditation, while it remained optional for other modules. Prof. Saša Simić is leading the project "Digitalization of Astronomy Teaching" supported by the Ministry for Education of the Republic of Serbia and intended for the development of university education (Simić, 2020).

At the University of Priština in Kosovska Mitrovica a one-semester (2+0) compulsory course, "Fundamentals of astronomy and astrophysics", is taught in the 3rd semester to the students of physics. According to the new accreditation foreseen to start in October 2021, this course will be optional and it will be taught in the 6th semester with 2+2 hours per week (Gulan, 2021). At the Department of Geography at the FNS in Kosovska Mitrovica, a course "Mathematical geography" (2+2) included a lot of astronomical topics (Valjarević, 2021).

During the past five years a one-semester course in astronomy/astrophysics (2+2) was taught at the Department of Physics, Mathematics and Informatics at the State University of Novi Pazar. From 2014/15 to 2016/17 this course was taught to the third year undergraduate students (Mijajlović, 2021), whereas from 2017/18 to 2018/19 this course was transferred to master degree and taught as "Introduction to Astronomy and Astrophysics" (Šegan, 2021).

6. PUBLIC OUTREACH

Public astronomy education in Serbia was realized through many lectures held in: Ilija Kolarac Foundation, Belgrade Youth Center, Students Cultural Center, Serbian Academy of Sciences and Arts, astronomy seminars in Belgrade and Novi Sad, lectures in Planetaria (Belgrade and Novi Sad) and in public observatories, online videos, podcasts, TV series "Svemir na Zemlji", lectures during special events (Festival of Science, Researchers' Night, International Day of Light, Night of Museums, Book Fair, etc.), on radio programmes, in popular journals and books. Public outreach is also realized through various activities of 24 amateur astronomical societies. A detailed review of their activities is given in the paper by Atanacković (2009). Many activities were organized in 2019 during the global celebration of 100 years of the IAU (IAU100), e.g. mini-exhibitions "Above and Beyond", in Belgrade within the Researchers' Night in September, and in Kruševac in November 2019, as well as the NameExoWorlds contest in which Serbia has voted to name the star WASP-60 Morava and its planet WASP-60b Vlasina.

Carpe Noctem association gathers astronomy, physics and geography students and researchers in a joint effort directed at preserving the night sky. Since 2019 Carpe Noctem has the ongoing project Ecological Supernova funded by the Center for the Promotion of Science with the goal of educating about the light pollution and as a part of that has organized many educational activities in astronomy under the open skies such as Astro Walks and Star Triahtlon. They also have very successful cooperation with and have been recognized by the International Dark-Sky Association (Prodanović, 2021).

In July 2020 Monika Jurković replaced Tijana Prodanović as the IAU OAO National Outreach Coordinator (NOC).

7. CONCLUSIONS

In this paper we gave a brief overview of triennial activities in astronomy education in Serbia at all levels, including also the public outreach. Future prospects and plans for the astronomy education in Serbia should include: a larger representation of astronomical content in other subjects such as physics, mathematics, geography, both in elementary and high school teaching, organization of seminars in astronomy for teachers, an agreement with the authorities on the reintroduction of Astronomy in the curricula as a separate subject, larger presence in media and better coverage of astronomical events.

References

Arbutina, B.: 2017, *Evolution of supernova remnants*, *Publ. Astron. Obs. Belgrade*, **97**, 1–92.

Arbutina, B., Atanacković, O.: 2019, Astronomy in Serbia and Serbia in the International Astronomical Union, *Proceedings of the International Astronomical Union*, **349**, 248.

Arbutina, B., Atanacković, O., Kovačević, A.: 2021, Department of Astronomy at the Faculty of Mathematics University of Belgrade in the period 1999-2020, *Publ. Astron. Obs. Belgrade*, this volume.

Atanacković-Vukmanović, O.: 2006a, Astronomy Education in Serbia and Montenegro 2002-2005, *Publ. Astron. Obs. Belgrade*, **80**, 275–283.

Atanacković-Vukmanović, O.: 2006b, Astronomy in Serbia and in Montenegro, in IAU Spec. Session No.5, Eds. J.B. Hearnshaw and P. Martinez.
Atanacković, O.: 2009, Astronomy Education in Serbia 2005-2008, *Publ. Astron. Obs. Belgrade*, **86**, 231–240.
Atanacković, O.: 2012, Astronomy Education in Serbia 2008-2011, *Publ. Astron. Obs. Belgrade*, **91**, 273–284.
Atanacković, O.: 2013, Astronomy education and popularization in Serbia, *Publ. Astron. Obs. Belgrade*, **92**, 107–112.
Atanacković, O.: 2017, Astronomy Education in Serbia 2011-2014, *Publ. Astron. Obs. Belgrade*, **96**, 397–405.
Atanacković, O.: 2018, Astronomy Education in Serbia 2014-2017, *Publ. Astron. Obs. Belgrade*, **98**, 91–99.
Gajić, D.: 2020, Report on Astronomy Education at the University of Niš.
Gulan, Lj.: 2021, Report on Astronomy Education at the University of Priština in Kosovska Mitrovica.
Ilić, D.: 2020, Report on students practices at AS Vidojevica, Student Astronomy Workshops (SAW) and master program Astromundus.
Marčeta, D.: 2020, Report on students practices at Ondřejov Observatory.
Martinović, M., Šegan, S.: 2018, *Odabrani tekstovi iz astronomije*, Faculty of Mathematics, Belgrade (ISBN 978-86-7589-128-4).
Mijajlović, Ž.: 2021, Report on Astronomy Education at the State University of Novi Pazar.
Milogradov-Turin, J.: 1997, Astronomija na seminarima za nastavnike u Srbiji, *Publ. Astron. Obs. Belgrade*, **56**, 229–247.
Milogradov-Turin, J.: 2003, Astronomy education in FR Yugoslavia 1999-2002, *Publ. Astron. Obs. Belgrade*, **75**, 313–318.
Prodanović, T.: 2020, Report on Astronomy Education at the University of Novi Sad.
Simić, S.: 2020, Report on Astronomy Education at the University of Kragujevac.
Šegan, S.: 2021, Report on Astronomy Education at the State University of Novi Pazar.
Stojičić, B.: 2021, Zašto je važno izučavanje astronomije u toku srednjoškolskog obrazovanja?, *Publ. Astron. Obs. Belgrade*, this volume.
Valjarević, A.: 2021, Report on Astronomy Education at the University of Priština in Kosovska Mitrovica.
Vidojević, S., Ninković, S., Simonović B., Bešlić, I.: 2018, Astronomy Competitions and their Role in Astronomy Education in Serbia, *Publ. Astron. Obs. Belgrade*, **98**, 217.
Vidojević, S.: 2019, *Astronomski zabavnik: zadaci i vežbe iz astronomije i astrofizike*, Beograd, Društvo astronoma Srbije, translation from Russian of the book "Astronomicheskij divertisment. Zadachi i uprazhnenija po astronomii i astrofizike" (Redaction: I. A. Utesheva . - Moskva : OOO "Sam Poligrafist", 2018. - pp. 154 ISBN 978-5-00077-697-1).
Vidojević, S., Prokić, V., Ninković, S., Simonović, B.: 2021, Serbia in astronomical contests between 2017-2020, *Publ. Astron. Obs. Belgrade*, this volume.
Vukadinović, D., Milanović, N., Milošević, S., Bošković, M., Božić, N.: 2021, Department of Astronomy at Petnica Science Center: 2018-2020, *Publ. Astron. Obs. Belgrade*, this volume.

Publ. Astron. Obs. Belgrade No. 100 (2021), 211 - 217 *Progress Report*

THE MATLAS SURVEY OF FAINT OUTSKIRTS OF BRIGHT GALAXIES

M. BÍLEK and P.-A. DUC

Université de Strasbourg, CNRS, Observatoire astronomique de Strasbourg (ObAS), UMR 7550, 67000 Strasbourg, France
E–mail: bilek@astro.unistra.fr

Abstract. Deep imaging, that is imaging capable of capturing very low surface brightness extended objects, is a quickly growing field of extragalactic astronomy. Not only can new types of faint objects be discovered, but deep images of bright galaxies are very valuable, too, since they reveal faint signs of past galaxy collisions, the tidal features. Such "archeological" record can be exploited for investigating how galaxies formed. In the MATLAS survey, we obtained extremely deep images of 177 nearby massive elliptical and lenticular galaxies using the 3.5m Canada-France-Hawaii Telescope. In our contribution, we will present the various types of objects and features seen in our images, for example tidal features, faint star-forming regions in otherwise quenched galaxies, or faint dust clouds in our own Galaxy. Finally, we will introduce the deep-imaging efforts at the Milanković Telescope.

1. DEEP IMAGING IN GENERAL

Much of our knowledge of galaxies comes from their images. Big sky surveys, such as the Sloan Digital Sky Survey (SDSS), took images of a huge number of galaxies. However, for the majority of galaxies, only images of their brightest parts are available. Figure 1 shows an example. The left panel shows the galaxies NGC 474 (left) and NGC 470 (right) as imaged by SDSS. They are relatively bright, both having the apparent V-band magnitude of about 11.5. The image already reveals hints of the rich structure in the outer parts of NGC 474. The structures are seen with much better clarity in the right panel. The image comes from the MATLAS survey, that was optimized for detecting objects with a low surface brightness. This is very advantageous for investigating the formation of galaxies, as we will explain later. The survey was made possible because of the development of a technique called deep imaging.

The so called "deep imaging" technique presented here is a relatively new way of exploring the universe. Just as microscope enabled us to study objects with a small size or telescopes enabled us to explore the objects with a small angular size, deep imaging allowed us to explore the objects with a low surface brightness. But unlike in the previous two cases, the availability of new instruments has not been a request for the development of deep imaging. It could also be enabled because of new observing strategies and data processing techniques. Obviously, the meaning of "low surface brightness" has evolved, but today we mean by that the value of

Figure 1: Illustration of deep imaging. Left panel: Standard image of a relatively bright and nearby galaxies NGC 474 (left) and NGC 470 (right) from SDSS. Right: Deep image of the same pair of galaxies from the MATLAS survey shows the faint structures in the stellar halo with much better clarity.

about 28 mag arcsec^{-2}. Reaching such a limit became routinely possible since about a decade even if the necessary telescopes and CCDs had been there before. Initially, the attempts of taking a deep image of an object were based just on collecting light for a long time at a fixed position or with restricted dithering. Then followed the standard calibration by bias, dark frame and flat field. But such an approach most often fails to reveal extended low-surface-brightness features.

The faintest objects we are able to capture today have a surface brightness that is about 1000 times lower than the surface brightness of the sky at the darkest sites of the world. Separating such a small fraction of the useful signal from the total signal we receive is extremely sensitive to systematic errors. The most important systematic errors are the imperfections of the flat field images and the parasitic light, i.e. the sky light reflected from the mechanical parts of the telescope and camera on the CCD chip. Important are also the errors coming from the variations of the sky brightness during the night and the scattered starlight (the wide wings of the point spread function). The standard calibration typically leaves artifacts that appear as large-scale brightness variations of the background (see the example in Duc et al. 2015). They are not too harmful as long as we are interested in small objects; the artifacts can be modeled by a polynomial, for example, and subtracted. The problem appears when we are interested in structures with a size comparable to the artifacts, such as the stellar halos of nearby galaxies.

The technique to overcome this difficulty is somewhat similar to the nodding technique used in near-infrared astronomy, where virtually all observations of astronomical sources are background dominated. The first key step is to take several images of the object of interest such that it is captured every time at a different location on the detector (we move the telescope by several arcmin between the individual frames). The background is calculated taking the median (in the simplest version) of all the individual frames for every pixel. The resulting image does not show any object because

a given pixel captures only blank sky in most of the images. The median image captures just the inhomogenities of the background caused by the parasitic light and flat fielding errors. The median image is then subtracted from the initial images, which makes their background perfectly flat. The background subtracted images are then stacked in the standard way to produce the final image. Obviously, the shifts between the individual frames should be larger than the object we intend to investigate.

2. THE MATLAS SURVEY

The MATLAS deep-imaging survey targets almost 200 nearby massive elliptical and lenticular galaxies. The images were taken with the MegaCam camera at the 3.6 m Canada-France-Hawaii Telescope. Every galaxy was observed in between two and four photometric bands. The images reach the surface brightness limit of 28.5-29 mag arcsec^2. The galaxies are very well explored since all of them belong to the sample of the ATLAS^{3D} project (Cappellari et al. 2011) that aims to collect as much information about its targets as possible. One of the main questions we wish to know about galaxies is how they were assembled. A galaxy can be assembled through two main channels. The first is the formation of stars directly in the galaxy. The second is merging of pre-existing galaxies. Merging means that two galaxies collide to form one bigger galaxy. The main purpose of MATLAS is to look for signs of past galaxy mergers, the so-called tidal features. Examples of several types of them are shown in Figure 2 (shells, streams, tails, disturbed isophotes). The morphology of tidal features gives indications on the mass ratio and other properties of the galaxies that merged (see Wang et al. 2012 or Bílek et al. 2018 for some of the possible complications). The tidal features can remain visible several billions of years after the two original galaxies have merged, even when hints of the past collision have disappeared in the central merged body. The images in MATLAS are therefore highly useful in answering how a typical elliptical or lenticular galaxy forms. Fortunately, other objects also fall in the FOV of MegaCam such as spiral galaxies, dwarfs or globular clusters, and may be studied thanks to the deep images, leading to unexpected discoveries.

Once the images were taken, they were visually inspected and classified typically by 6 people per galaxy. The participants of our classification had at disposal a dedicated online image viewer. It is now available publicly at `http://obas-matlas.u-strasbg.fr`. In this navigator, we can zoom in the image, change the brightness, contrast, display the maps of the color index, or load the information on the objects from the CDS/SIMBAD database and others. The participants were given a dedicated questionnaire with a list of various morphological structures and were asked to answer, for every galaxy, whether a given structure is present and if so, then how many of them are in the galaxy. More sophisticated annotation tools have also been developed.

Figure 2 shows examples of the most important or interesting structures that we were looking for. **Stellar shells** look like azimuthal sharp-edged glowing features. They form when two galaxies collide nearly radially. Recent observational studies suggested that shells can be formed from colliding galaxies of any mass ratio, but mergers of galaxies of very different masses are preferred (Kado-Fong et al. 2018).

Stellar streams appear as long thin structures. They usually form by disruption of a small galaxy by tidal forces. Stellar streams suggest the mergers of a mass ratio of about 1:4 or less.

Tidal tails which have the same tidal origin as the streams, are often thicker and result from the interaction with a galaxy of a comparable mass or of a higher mass. They are more prominent if at least one of the interacting partners rotates.

But all of these merger signs have a limited lifetime. When they get too old, the whole galaxy relaxes toward an equilibrium taking up a shape of a smooth ellipsoid or disk. Just before that, the signs of old mergers can be recognized by the presence of **disturbed outer isophotes** in the galaxies. Some irregularities in the isophotes can also be induced by distant galaxy flybys. In the galaxy in the figure, both mechanisms probably acted.

The elliptical and lenticular galaxies in the MATLAS sample are characterized by their old stellar population. The deep images however revealed that some of the galaxies are surrounded by very faint disks of young stars. It seems that star formation in these galaxies was renewed after some period of inactivity. The reason for this **peripheral star formation** is still unknown.

Finally, some of our images show **galactic cirrus**. They are dust clouds in our own galaxy and their images are characterized by their filamentary structure. In the context of the main goals of MATLAS they are considered as pollutants because they complicate the identification of the real structures in the galaxy of interest. On the other hand, MATLAS images are useful for investigating the properties of interstellar medium in our own galaxy (Miville-Deschênes et al. 2016). Incidentally, we found that the incidence of cirrus correlates excellently with the maps of extinction. Perhaps these images will help to construct more detailed maps of extinction.

The first results of the completed MATLAS survey have been published in Bílek et al. (2020a). Its main goal was to provide the census of the various morphological structures. In total, we found any signatures of galaxy merging in about 30-40 percent of galaxies. We also found that the frequency of such signs usually increases with the mass of the galaxy and the number of its neighbors. This is expected: galaxies encounter more frequently in denser environments and more massive galaxies are more effective in accreting other galaxies because of their stronger gravitational fields. The comparison of the observations to theoretical expectations is planned. In the future, we also want to make use of our results for investigating the formation of galaxies from a purely observational point of view. It will be possible, for example, to look for the connection of galaxy interactions with various peculiar properties of galaxies (e.g., kinematically distinct cores, active galactic nuclei, etc.).

3. DEEP IMAGING AT MILANKOVIĆ TELESCOPE

We tested the observing methods similar to those used for MATLAS using the new 1.4 m Milanković Telescope in Serbia. We found that it can be used for deep imaging very successfully. For example we found that the tip of the faint stream in the northern part of NGC 474 that is barely visible in the MATLAS image can be captured with Milanković in about 3-4 hours. The broadband L filter has to be used for that (it covers most of the optical part of the spectrum). Ana Vudragović gives more details in this book of proceedings. The downsides of deep imaging with Milanković instead of MegaCam at CFHT are the substantially smaller field of view ($13.3' \times 13.3'$ vs. $60' \times 60'$), higher seeing FWHM (typically $1 - 2''$ vs. $< 1''$), and longer observing times are needed when using filters that are narrower than the L filter (many hours vs. 40 min). Actually these are not serious disadvantages if suitable targets are chosen.

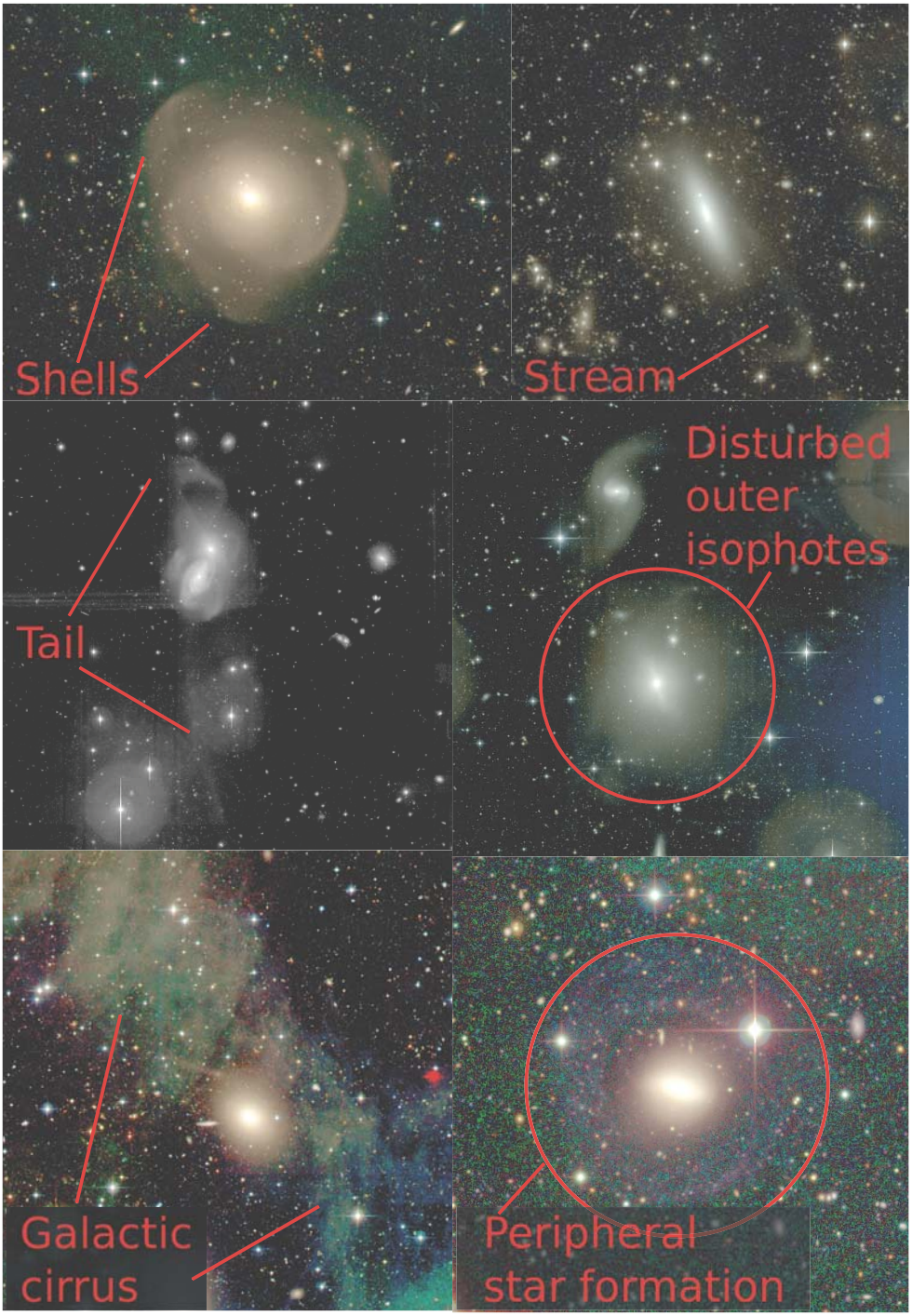

Figure 2: Examples of low-surface-brightness features detected in the MATLAS survey. The names of the galaxies are: NGC 3619 (shells), NGC 4684 (stream), NGC 3226 and NGC 3227 (tidal tail), NGC 3414 (disturbed outer isophotes), NGC 2592 (Galactic cirrus), UGC 09519 (peripheral star formation).

The advantage, compared to MegaCam is a lower scattering of light on the optics of the telescope (less light in the wings of the point spread function) and the point spread function is smoother. This will allow modeling the parasitic glow around bright stars easily and subtracting it to visualize the faint structures (work in progress).

Our first published deep-imaging application of Milanković was the observation of the stellar stream at the galaxy NGC 5907. Initially, amateur astronomers (e.g., Martínez-Delgado et al. 2008) detected repeatedly a stream that forms a double loop wrapping the galaxy. It was a big surprise when professional astronomers equipped by a telescope optimized for deep imaging reported that the stream has a morphology of an arc (van Dokkum et al. 2019). Our deep image agreed with the morphology of the stream seen by the professionals (Müller et al. 2019). The reason why the new observations are different is not clear yet.

We made use of deep imaging also in Bílek et al. (2020b). Here we aimed to reveal more about the nature of an enigmatic "dark cloud" in the Virgo cluster of galaxies. Several of such objects were revealed by a blind HI survey (Taylor et al. 2012). These dark clouds are unique and difficult to interpret because their wide HI lines combine with large distances of the clouds from the nearest neighbor galaxies. The clouds were never captured optically. There is a hypothesis that they are dark matter halos containing gas but little or no stars (Taylor et al., 2016, but other possibilities exist, such as that they are tidal debris, Duc & Bournaud, 2008). We took a very deep image of one of these objects in the hope to detect a faint galaxy. The image did not show it. This allowed us to estimate that the luminosity of the object is below 1.1×10^7 of the solar and that the object contains at least 3 times more mass in gas than in stars. This is another illustration of the potential of deep imaging.

Acknowledgements

We thank the anonymous referee for very useful comments. MB acknowledges the support by Cercle Gutenberg.

References

Bílek, M., Thies, I., Kroupa, P., Famaey, B.: 2018, *Astron. Astrophys.*, **614**, A59.
Bílek, M., Duc, P.-A., Cuillandre, J.-C., Gwyn, S., Cappellari, M., Bekaert, D. V., Bonfini, P. et al.: 2020a, *Mon. Not. R. Astron. Soc.*, **498**, 2138.
Bílek, M., Müller, O., Vudragović, A., Taylor, R.: 2020b, *Astron. Astrophys.*, **642**, L10.
Cappellari, M., Emsellem, E., Krajnović, D. et al.: 2011, *Mon. Not. R. Astron. Soc.*, **413**, 813.
Duc P.-A., Bournaud F.: 2008, *Astrophys. J.*, **673**, 787.
Duc, P.-A., Cuillandre, J.-C., Karabal, E., Cappellari, M., Alatalo, K., Blitz, L., Bournaud, F. et al.: 2015, *Mon. Not. R. Astron. Soc.*, **446**, 120.
Kado-Fong, E., Greene, J. E., Hendel, D., Price-Whelan, A. M., Greco, J. P., Goulding, A. D., Huang, S. et al.: 2018, *Astrophys. J.*, **866**, 103.
Martínez-Delgado, D., Peñarrubia, J., Gabany, R. J., Trujillo, I., Majewski, S. R., Pohlen, M.: 2008, *Astrophys. J.*, **689**, 184.
Miville-Deschênes, M.-A., Duc, P.-A., Marleau, F., Cuillandre, J.-C., Didelon, P., Gwyn, S., Karabal, E.: 2016, *Astron. Astrophys.*, **593**, A4.
Müller, O., Vudragović, A., Bílek M.: 2019, *Astron. Astrophys.*, **632**, L13.
Taylor, R., Davies, J. I., Auld, R., Minchin, R. F.: 2012, *Mon. Not. R. Astron. Soc.*, **423**, 787.

Taylor, R., Davies, J. I., Jáchym, P., Keenan, O., Minchin, R. F., Palouš, J., Smith, R. et al.: 2016, *Mon. Not. R. Astron. Soc.*, **461**, 3001.
van Dokkum, P., Gilhuly, C., Bonaca, A., Merritt, A., Danieli, S., Lokhorst, D., Abraham, R. et al.: 2019, *Astrophys. J.*, **883**, L32.
Wang, J., Hammer, F., Athanassoula, E., Puech, M., Yang, Y., Flores, H.: 2012, *Astron. Astrophys.*, **538**, A121.

Publ. Astron. Obs. Belgrade No. 100 (2021), 219 - 223 *Progress Report*

STATISTICS OF THE LARGEST SAMPLE OF LATE-TYPE CONTACT BINARIES STUDIED SO FAR

ATILA ČEKI, OLIVERA LATKOVIĆ and SANJA LAZAREVIĆ
Astronomical Observatory, Volgina 7, 11000 Belgrade, Serbia
E–mail: atila@aob.rs

Abstract. Late-type contact binaries, also known as W UMa stars, are intriguing objects whose present-day properties, evolutionary history and membership in multiple stellar systems are still not fully understood despite decades of dedicated research. At the same time, they are a favorite target for observations with relatively small, ground-based telescopes because of their short periods, so an entire light curve can often be recorded in a few nights. The last decade has seen a considerable rise in both the number and quality of studies of W UMa stars, and the establishment of de-facto standards in their analysis that help aggregate the results. We have collected new and updated solutions of light curves for 688 W UMa stars, more than half of which have been studied for the first time in the last few years. This is the largest catalog of its sort published to date and it provides ample material for various statistics. We showcase and discuss the most interesting findings.

1. INTRODUCTION

W UMa binaries are the most common class of eclipsing binaries and they account for about 0.2% of all solar-type stars in the Solar system neighborhood (Rucinski 2002). The majority of variable stars in the Catalina Real-Time Transient Survey (CRTS) Variable Star Catalog (Drake et al. 2014) are W UMa binaries.

From the observational standpoint, they are characterized by continuous changes in brightness with periods typically shorter than half a day. Their light curves have minima of similar depth and no clear transitions between eclipse and out-of-eclipse phases, suggesting gravitationally distorted components of nearly equal effective temperatures. At the same time, one star is usually twice or more as massive as the other. This paradoxical property is explained in terms of mass and energy exchange between the components through a co-rotating common envelope (Lucy 1968).

Although W UMa binaries have been studied for decades, our understanding of their evolutionary history and present-day characteristics is still incomplete (see e.g. Webbink 2003). Much of our current knowledge comes from analyzing ensembles of well-studied individual objects (see e.g. Yakut & Eggleton 2005). Yet, to our knowledge, the latest effort to aggregate the results for individual stars from the literature into a comprehensive catalog dates back almost two decades (Pribulla et al. 2003).

We have made such an effort now and compiled the orbital and stellar parameters of 688 W UMa stars by reviewing around 420 relevant papers. Two thirds of this sample (478 stars) are "new" in the sense that they have not been considered in any previous statistical studies. Our catalog is not only the largest to date, but also the most complete in terms of cataloged quantities. Special care was taken to homogenize the results of modeling with different tools; missing quantities were calculated where possible; and additional measurements were included by cross-referencing the Gaia (Gaia Collaboration 2016, 2018) and LAMOST (Qian et al. 2017) archives.

We conducted various analyses of the collected data; the results of this research are being prepared for publication. Here we give a preview of our methods, findings and conclusions.

2. COMPARATIVE STATISTICS

Among the cataloged quantities characterizing W UMa stars, some of the most important ones are categorical rather than numerical. For example: the type of eclipse (partial or total), the A or W subtype (Binnendijk 1979), the presence or absence of spots and third light in the light curve model, the method for finding the mass ratio (photometric or spectroscopic) and so on. To explore and compare the properties of cataloged stars when the full sample is divided according to such groups, we use split violin plots (Figs. 1 and 2).

The split violin plot shows the distribution of a numerical quantity (i.e., the orbital period) when the sample is split according to a categorical quantity (i.e. the A/W subtypes). The distribution is plotted vertically with a split between the groups, making the similarities or differences obvious at a glance. Summary statistics such as mean and median values or the interquartile range can also be included to make the plot more informative. For simplicity, we only include the median, represented by the horizontal line in each distribution.

2. 1. ECLIPSE TYPES AND DETERMINATION OF THE MASS RATIO

Typically, the mass ratio is measured from the radial velocity curves, which are in turn derived from spectroscopic time series. Such observations are difficult to come by, especially for faint targets, and binaries with these measurements are relatively rare (only about 20% of objects in our catalog). However, in contact binaries it is also possible to measure the so-called photometric mass ratio from the light curve alone. Because the components share a common envelope described by the same equipotential surface, their mass ratio is proportional to their size ratio via the relation $R_2/R_1 \approx (M_2/M_1)^{0.46}$ (Kuiper 1941). As the size ratio is readily determined from light curve modeling, so is, in principle, the mass ratio.

This method of measurement is known to be robust when the system is totally eclipsing. But what of partially eclipsing stars with no spectroscopic measurements? In Fig 1 we compare the properties of totally and partially eclipsing stars (panel *a*), and of those with spectroscopic and photometric mass ratios (panel *b*). Objects with partial eclipses have slightly shorter periods, smaller fillouts and lower temperatures than those with total eclipses; most notably, their mass ratios are spread evenly over the range from 0 to 1, whereas the totally eclipsing stars have mass ratios in a much smaller range that tappers off near $q = 0.5$. Stars with photometric and spectroscopic mass ratios have similarly disparate distributions, with more pronounced differences in periods and temperatures, but essentially the same issue with mass ratios.

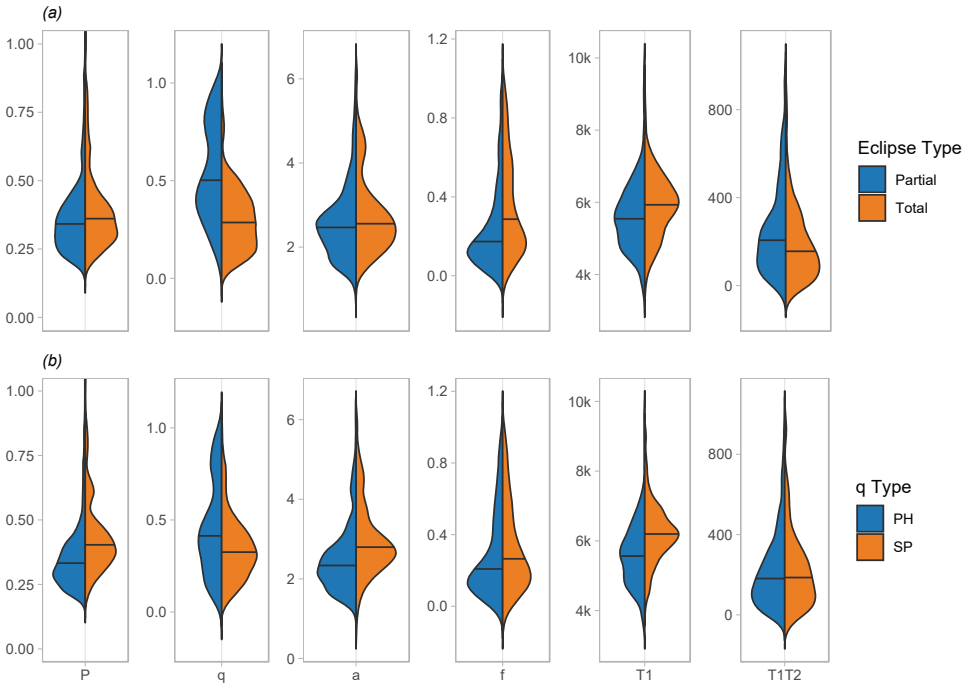

Figure 1: Comparative distributions of selected quantities (from left to right: orbital period, mass ratio, orbital separation, fillout, primary temperature and the temperature difference between the components) for stars with total and partial eclipses (panel *a*) and with mass ratios determined from spectroscopy (SP) and photometry (PH) (panel *b*).

By combining the totally eclipsing systems and those with spectroscopic mass ratios into a "reliable" sample, and the rest into the "unreliable" sample, we could confirm that mass ratios and other parameters obtained from light curve modeling of partially eclipsing W UMa stars without the support of spectroscopic measurements are tentative at best.

2. 2. THE A AND W SUBTYPES AND SPOTS

W UMa binaries are traditionally divided into the A and W subtypes. The original definition came from Binnendijk (1970), who made the classification according to whether the deeper light curve minimum is caused by a transit or an occultation. This translates to a simple criterion by model parameters: in A types, the bigger, more massive star is hotter, and in W types, it is cooler than the companion. Early statistical analyses (see e.g. Maceroni & van't Veer, 1996) showed that members of these two groups have different properties. The A-type systems have longer periods, higher temperatures and larger fillouts.

During data collection, we noticed that many authors use these secondary characteristics for classification of systems under study. As many as 10% of the stars in our sample have subtypes in source publications that conflict with the original definition.

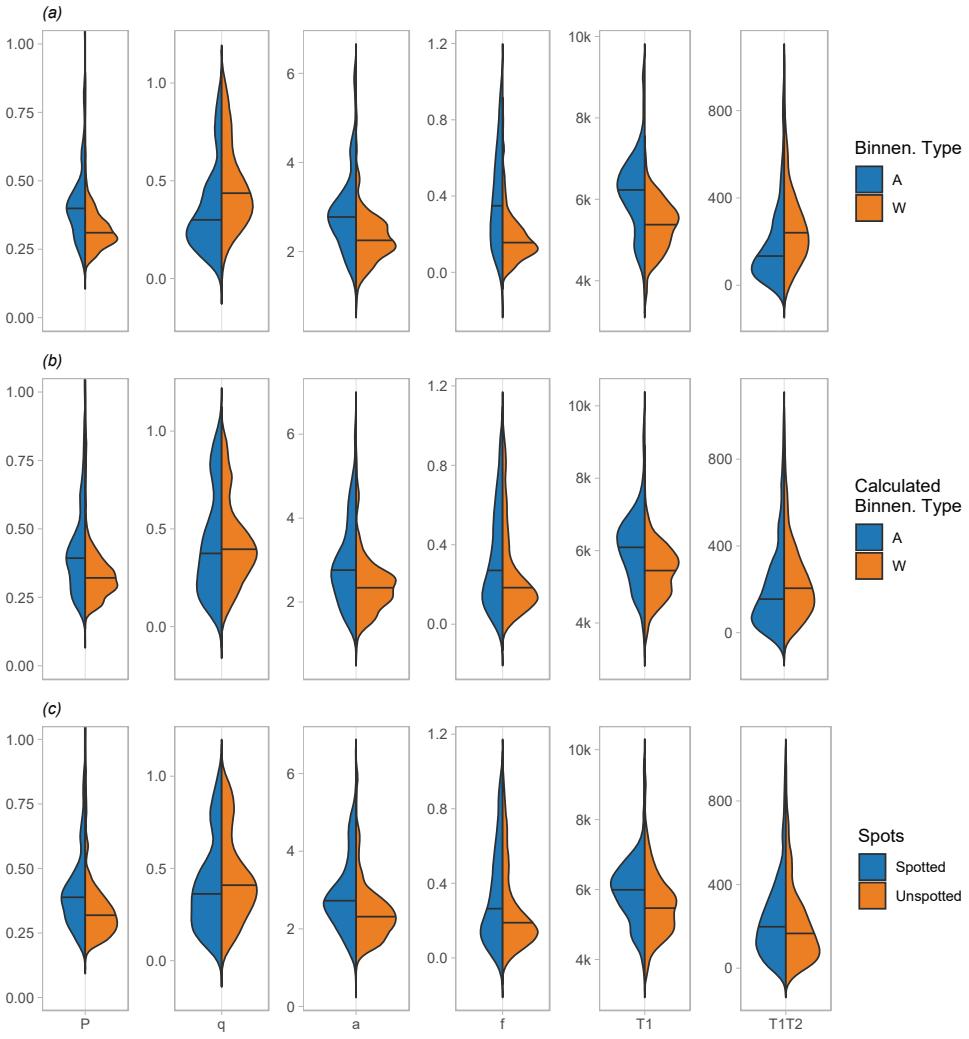

Figure 2: Same as in Fig. 1, but for Binnendijk's A and W types from source publications (panel *a*), those calculated from the original definition (panel *b*), and presence or absence of spots (panel *c*).

Fig. 2 shows the comparative distributions of A and W stars with types adopted from the source papers (panel *a*) and assigned using Binnendijk's definition (panel *b*). We see that the differences in periods, fillouts and temperatures are much less dramatic in the latter case, and the difference in the mass ratios disappears altogether. In a sort of circular argument, the deviations from the definition in the literature have artificially boosted the differences between the subtypes.

This is important because the nature of these subtypes is one of the open questions about W UMa stars. In the most widely accepted evolutionary scenario, they enter contact while still on the main sequence as the orbit shrinks due to the loss of angular

momentum via magnetized winds (Stępień 2011). But that scenario cannot explain the higher temperature of the smaller, less massive components in the W types. It has been suggested that the apparently lower temperature of the larger, more massive companion is the result of spot coverage (Yakut & Eggleton 2005).

Comparing the parameter distributions of the subtypes (Fig. 2*b*) and spotted and unspotted stars in our sample (Fig. 2*c*) shows that indeed, the A-type sample resembles the spotted sample, and the W-type the unspotted. However, when the presence of spots is examined by subtype, it turns out that there are as many spotted as unspotted systems among both the A and W stars, indicating that these groupings are not correlated.

3. SUMMARY

We collected stellar and orbital parameters for 688 late-type contact binaries and conducted a comparative statistical analysis of various groupings within this sample. Among other findings, we show that: 1) parameters derived from light curves with partial eclipses without spectroscopic support should be considered unreliable; and 2) despite markedly similar parameter distributions, there is no correlation between the A/W subtypes and the presence or absence of spots. Other results of our study, including the modeling of parameter distributions and their relationships, are expected to appear in press in 2021.

Acknowledgments

The research presented in this report was funded by the Ministry of Education, Science and Technological Development of the Republic of Serbia (contract No. 451-03-68/2020-14/200002).

References

Binnendijk, L.: 1970, *Vistas in Astronomy*, **12**, 217.
Drake, A. J., Graham, M. J., Djorgovski, S. G. et al.: 2014, *Astrophys. J. Suppl. Series*, **213**, 9.
Gaia Collaboration, Prusti T., de Bruijne, J. H. J. et al.: 2016, *Astron. Astrophys.*, **595**, 1.
Gaia Collaboration, Brown, A. G. A., Vallenari, A. et al.: 2018, *Astron. Astrophys.*, **616**, 1.
Kuiper, G. P.: 1941, *Astrophys. J.*, **93**, 133.
Lucy, L. B.: 1968, *Astrophys. J.*, **153**, 877.
Maceroni, C., van't Veer, F.: 1996, *Astron. Astrophys.*, **311**, 523.
Pribulla, T., Kreiner, J. M., Tremko, J.: 2003, *Contrib. Astron. Obs. Skaln. Pleso*, **33**, 38.
Qian, S.-B., He, J.-J., Zhang, J. et al.: 2017, *Res. Astron. Astrophys.*, **17**, 087.
Rucinski, S. M.: 2002, *Publ. Astron. Soc. Pac.*, **114**, 1124.
Stępień, K.: 2011, *Acta Astron.*, **61**, 139.
Webbink, R. F.: 2003, *3D Stellar Evolution*, , 76.
Yakut, K., Eggleton, P. P.: 2005, *Astrophys. J.*,**629**, 1055.

Publ. Astron. Obs. Belgrade No. 100 (2021), 225 - 232 *Progress Report*

ARCHAEOASTRONOMY AND EXAMPLES OF RESEARCH IN SERBIA

MILAN S. DIMITRIJEVIĆ
Astronomical Observatory, Volgina 7, 11060 Belgrade, Serbia
E–mail: mdimitrijevic@aob.rs

Abstract. In this contribution, the significance, development and importance of archaeoastronomy will be discussed, some examples of research and objects of importance for this topic will be presented and the history and development of archaeoastronomy in Serbia will be briefly reviewed.

1. ARCHAEOASTRONOMY AND ASTRONOMY IN CULTURE

Archaeoastronomy is an interdisciplinary science that investigates and considers how in the past humans observed sky and celestial bodies, understood and recorded what they saw on it and what it meant in their culture, religion, and worldviews. Aveni(1988) defines it as "the study of the practice and use of astronomy among the ancient world cultures based on all accessible forms of evidence, written and unwritten." Ruggles (1991) considers that the word "old" can be freely omitted, from Aveni's definition, to include ethnoastronomy.

The term archaeoastronomy itself was first used by Elizabeth Chesley Baity in 1973 (Sinclair, 2006), although many previous studies may be considered as archaeoastronomic depending on the definition.

Close relations exist between Archaeoastronomy and ethnoastronomy, anthropological studies the sky observations in both earlier and present societies, as well as the history of astronomy, which uses available records to consider the development of astronomy, understanding of the universe and its phenomena and astronomical practice throughout history. It is a relatively new science, developed as a result of exploring the possible astronomical significance of the directions that connect an object, a marker on the horizon and some astronomical phenomenon (sunrise or sunset on solstice, star or constellation rising or setting...). Largely contributed to its developpment and the study of astronomical aspects of the Stonehenge Megalithic Monument in England and astronomical alignments in the architecture of the ancient inhabitants of South America (Aveni, 1986; Urton, 1981, 1990).

Archaeoastronomy uses a number of different methods that include archaeological, anthropological, astronomical, statistical, probabilistic and historical (Iwaniszewski, 2003) and we would add and geodetic ones. It has particularly developed over the last fifty years.

The first international conference that brought together researchers from around the world was held in Oxford in 1981. These were the very beginnings, when, first of all, it was necessary to work on defining and elaborating the research methodology and formulating the terminology of new science. On it, archaeoastronomers from Europe advocated a methodology based on artifacts, facts and statistics. For example, if most of the graves are oriented in one way, or on a possible landmark on the horizon, the sun, moon, individual stars or constellations rise or set on a day associated with an astronomical phenomenon (summer or winter solstice, some holiday ....) it is concluded that such an event had a significant place in the culture, settlement or temple under consideration. American scholars, in view of the much more modest archaeological findings related to Native American tribes, rely much more on the writings of the colonists and ethnographic methods (Zeilik, 1985, 1986), trying to understand the role of astronomy in American civilization, how activities related to heaven and celestial phenomena and bodies looked like, and what it meant for the community under consideration. This enabled them to identify motives and analyze them, which in Europe is generally just a guess. The differences in methodology and topics for research were so great between European and American archaeoastronomers that the Conference Proceedings were printed as two separate volumes (Aveni, 1982; Heggie, 1982). Even today, according to the color of their covers, one speaks colloquially of "green" and "brown" archaeoastronomy. These meetings, with the name Oxford Conference, are still held every four to five years.

Not only did archaeoastronomers disagree on methodology, but discussions were also held on the name of this new scientific discipline. Three major international societies associate archaeoastronomy with cultural research (ISAAC - International Society for Archaeoastronomy and Astronomy in Culture, founded in 1995, which is behind the Oxford Conferences and the journal: *Archaeoastronomy - the Journal of Astronomy in Culture*; SEAC - La Société Européenne pour l'Astronomie dans la Culture, created in 1992, organizes a conference every year and publishes a peer reviewed Proceedings with presented contributions, and, since 2003, SIAC - La Sociedad Interamericana de Astronomía en la Cultura); Ruggles and Saunders (1993) propose the name *Cultural Astronomy*, and, there were and opinion, since it is often a matter of cosmological views, that the more appropriate name is *Cosmovision* (Aveni, 1986b).

For the first time *Cultural Astronomy* as a course on the university has been introduced in 1990 at the University of Leicester by Clives Ruggles, an astronomer and archaeologist, who, after his retirement, became President of the UNESCO Commission on the Protection of Cultural Monuments of Significance for Archaeoastronomy. It was an optional course in the third year of archeology studies, and in 1991 the Chair for Cultural Astronomy was established.

At the Faculty of Mathematics in Belgrade, on Department of Astronomy, from 2009 to the 2014/2015. school year, there was an optional course of *Archaeoastronomy* in doctoral studies, but in the PhD program for 2015/2016. year and later this does not exist. Meanwhile, only Jovan Aleksić passed the exam, and the examiner was author of this paper.

2. SOURCES AND INVESTIGATIONS

The basic sources that provide us with information about how humans interacted with the sky and celestial phenomena are *the significant directions and orientations*

of particular constructions, objects, ethnographic research, calendars, written sources, myths and *cosmologies*.

Significant directions. Basic methods for investigation of significant directions were developed by Alexander Thom during an extensive examination of megalithic monuments and sites in England and such studies are characteristic for "green" archaeoastronomy. He considered that by looking at the horizon and what can be seen on it, one could determine the specific day of an astronomical phenomenon in the year. One has to find a place to see where the Sun is rising or setting on the day of an astronomical phenomenon, such as the summer or winter solstice. To confirm this assumption, he considered a large number of megalithic monuments. Any such individual direction might be a coincidence, but if we have a number of them, it shows that at least one part is intentionally oriented (Thom, 1967).

Figure 1: The first sunrise on the mountain Treskavac on the horizon of Lepenski Vir, 21^{st} of June 2017 (photo Stanko Kostić from the position 44,557142 N 22,026590 E - photo from Bajić and Pavlović (2019)

Particularly impressive is the case when a mountain on the horizon, in a certain day, blocks temporarily the solar disk on its path, so that it appears as if it is rising or setting twice. If the event is seen on the day of an astronomical event, such as the summer or winter solstice, from the place where is the object of importance to the local community, it is a convincing assumption that it was observed for the purpose of determining the date of an important holiday or for setting the calendar.

One of such places is the Mesolithic settlement of the Lepenski Vir and the volcanic rock Treskavac on the Romanian side of the Danube. Their astronomical and calerndrical aspects attracted attention of Živojin Andrejić (2002, 2004a, 2005) who from 1999 to 2005, observed and photographed rising and setting of Sun and Moon on Treskavac and how this could be used for calendrical purposes (Andrejić, 2005). An important study on Lepenski Vir including astronomical aspects is published also by Ljubinka Babović (2006). In 2014, Aleksandra Bajić and Hristivoje Pavlović found that the phenomenon of double sunrise on the Treskavac could be seen from the Lep-

Figure 2: Entrance to Newgrange. Above you can see opening for the entrance of solar rays (https://edition.cnn.com/travel/article/newgrange-ireland-stone-age/index.html)

enski Vir settlement only on the summer solstice. Namely, the Sun first appears in a relatively narrow gap, which lies between the northern slope of the Treskavac and a small solitary pointed rock on it (see Fig. 1). Then it follows Treskavac and rises again on its flattened top. Given the width of this very narrow gap on the horizon, Bajić and Pavlović found (Bajić and Pavlović, 2015, 2018, 2019), taking into account changes in the inclination of the Earth's axis and precession, that this unusual phenomenon can be seen from a specific place in the former position (which is today under the water), uniquely on the summer solstice which makes it possible to determine that day of the year, which is the basis for the solar calendar.

Such special directions to markers on the horizon, which, based on some astronomical phenomenon, helped to determine one special day of the year, were very useful for orienting in time and making calendars. If there was no suitable marker, a special opening could be made in the building, which, for example, allows that the Sun illuminates a certain place once a year. The most famous such object is Newgrange in Ireland, which dates from 3300 to 2900 BC. (Eogan, 1991). Around the winter solstice, the solar rays for several days enter the interior of the building through an opening above the door and, on the day of solstice, fall on the altar. In front of the door is a large stone (see Fig. 2), as if to emphasize that it is not the entrance for the men, but for the Sun God, who should not be disturbed. In Serbia Andreić investigated the illumination by the Sun of specific frescoes in a particular day in the St. Trinity Church in Resava (2011), monasteries Studenica, Žiča and Manasija (2012) and the white church in Karan (2013).

Several astronomically significant directions related to the Sun and the Moon were also determined in England for the Megalithic Monument Stonehenge, built and

rebuilt from 3100 to 1600 BCE. The famous astronomer Fred Hoyle explained how Stonehenge could serve for the prediction of solar and lunar eclipses and determination of solstices, analyzing the resulting cultural implications (Hoyle, 1977).

In Serbia, Andrejić (2009) discussed astronomical directions and orientations in Naisus in addition to Lepenski Vir, Aleksandra Bajić performed an archaeoastronomical analysis of Bogovo Gumno (Bajić, 2012) and the Stone Age Shrine of Pojate-Pojilo near the village of Belica (Bajić, 2016). Moreover, the astronomically significant directions in the palace of the Roman Emperor Galerius, Romuliana Felix in Gamzigrad, have been investigated (Andrejić, 2004b, 2019; Bajić and Dimitrijević, 2019) and the examinations of the archeological site of Sharkamen from the Roman period (Andrejić, 2019) were also carried out. Andor Vince and his associates investigated the orientations of graves and skeletons (Vince et al., 1996; Vince, 1998), what Borislav Jovanović also briefly considered in an overview of some archaeoastronomical examples in the archaeology of the central Balkans (Jovanović, 2007). Živojin Andrejić investigated the orientation of the temples (Andrejić, 2016), and Milutin Tadić, assuming that some proto-masters simply looked where the sun was rising on the day they began construction and took it as east, not only determined the orientation, but also tried to determine time of the beginning of the construction of certain medieval churches in the autonomous region of Kosovo and Metohija (Tadić, 2014).

Objects. Among the most interesting objects of archaeoastronomical significance are the Nebra sky disk from Nebra in Germany, dating from 1600 BC, which is the oldest known pictorial representation of the cosmos. In 2013, it was listed on the UNESCO's Memory of the World and declared for one of the most important archaeological discoveries of the XX century. Of particular importance is also the Antikythera mechanism, an ancient Greek analogous computer with about thirty gears, which was used for astronomical calculations of positions, eclipses and calendar. At the Arts et Métiers Museum in Paris, I saw an entire room dedicated to this marvel of the ancient world. Archaeoastronomical significance have and objects from prehistoric times, with 12 notches indicating the solar cycle or 28 for the lunar one. As an example of such research in Serbia can be cited the book of Milorad Stojić on the archaeological site near the village of Belica (Stojić, 2018). Such items include as well coins with astronomical content (Dimitrijević, 2007).

Some ethnographic studies of interest in the study of astronomy in culture in Serbia are in references Božić (2005) and Vuca (2007).

A common reason for the usefulness of astronomy and the need for it was in earlier times, first and foremost, to develop a sufficiently precise **calendar** for agricultural purposes. In Serbia, this issue, together with time measurement, is considered in Jovanović (2005, 2009), and Babović (2001, 2016, 2018).

Finally, in our country, a larger number of papers (Janković, 1954, 1989; Dimitrijević, 1998; Danezis et al., 2007; Theodossiou etal., 2011abc; [37-42] deal with considerations related to archeoastronomy and astronomy in culture, based on **written sources, myths and cosmology**, what is one of the main forms of "brown" archaeoastronomy

3. BEGINNINGS IN SERBIA

Although particular works that could be classified in this field, existed earlier, the first conference dedicated entirely to the history of astronomy, with a number of contributions that could be included in archaeoastronomy, was the VII National Conference of Astronomers of Yugoslavia, held in 1984, on the 50^{th} anniversary of the founding of the Astronomical Society "Rudjer Bošković". The next was the session "Astronomy in Archaeology, History and Culture", dedicated to archaeoastronomy, organized for the first time on the 4^{th} Yugoslav-Romanian Astronomical Conference in Belgrade (May 5-8, 1998). The study about the astronomical orientations of graves and skeletons in Gomolava and Mokrin, presented at the XI National Conference of Astronomers of Yugoslavia 1996 in Belgrade, by A. Vince, B. Jovanović, I. Vince and O. Vince, was the first archaeoastronomical investigation in Serbia, by a joint team of archaeologists and astronomers. That year, at a meeting held on June 12^{th}, astronomers (M. S. Dimitrijević and Ištvan Vince) and archaeologists (Borislav Jovanović, Milorad Stojić, Andor Vince and Živko Mikić) formed a Group for archaeoastronomy that had been active for about a year. Živojin Andrejić observed and photographed from 1999 to 2005, from Lepenski Vir, rising and setting of Sun and Moon on Treskavac and discussed how this could be used for determination of particular dates (Andrejić, 2005). In 2009, at the Faculty of Mathematics in Belgrade, at the Department of Astronomy, the course of Archaeoastronomy was introduced as an optional course in doctoral studies, which existed until 2014/2015. The archaeoastronomical measurements and observations of the double sunrise with the study how this could be used to determine the beginning of the seasons and to correct the calendar, started by Aleksandra Bajić and Hristivoje Pavlović, in 2014, at Lepenski Vir. That year, the Society for Archaeoastronomical and Ethnoastronomical Research "Vlašići" (http://www.vlasici.org.rs/) was founded in Belgrade.

Archaeoastronomy in Serbia has achieved a number of original and interesting results, but it is not developed like in some of the surrounding countries, such as Greece and Bulgaria in particular.

References

Andrejić, Živojin R.: 2002, Metafizička geometrija i prvo lice Boga sveta kulture Lepenskog Vira, *Razvitak*, **209-210**, Zaječar, 114-123.

Andrejić, Živojin R.: 2004a, Predstava kosmosa Lepenca, *Mitološki zbornik*, **10-11**, Rača, 137-164.

Andrejić, Živojin R.: 2004b, O vremenu i ideologiji rimskih tetrarha, nastanku i značenjima Romuliane, *Razvitak*, **217-218**, Zaječar, 29-46.

Andrejić, Živojin R.: 2005, *Metafizika Lepenskog Vira*, Centar za mitološke studije Srbije, Rača.

Andrejić, Živojin R.: 2009, Rimski imperijalni kult sunca i fundacija i konsekracija Naisa, *Mitološki zbornik*, **22**, Rača, 281-302.

Andrejić, Živojin R.: 2011, Visoka teološka i idejna osmišljenost orijentacije, arhitekture i živopisa Sv. Trojice u Resavi, *Sabornost*, **5**, Požarevac, 181-205.

Andrejić, Živojin R.: 2012, Uslovljenost programa živopisa i arhitekture orijentacijom i svetlom srpskih srednjovekovnih crkava na primeru Studenice, Žiče i Manasije, In: Srednji vek u srpskoj nauci, istoriji, književnosti i umetnosti III, Despotovac, 202-229.

Andrejić, Živojin R.: 2013, Svetlosna orijentacija Bele crkve u Karanu i visoko osmišljena uskladjenost fresko programa, Užički zbornik, **37**, Užice, 29-52.

Andrejić, Živojin R.: 2016, Univerzalna uslovljenost orijentacije hramova u prostoru prema Suncu od mezolita do Hrišćanstva, *Publ. Astr. društva "Rudjer Bošković"*, **16**, 399-431.

Andrejić, Živojin R.: 2019, Uslovljenost orijentacije rimskih carskih palata u Timoku, hramova i konsekrativnih objekata prema suncu, *Publ. Astr. društva "Rudjer Bošković"*, **19**, 477-506.

Aveni, A. F. ed.: 1982, *Archaeoastronomy in the New World: American Primitive Astronomy*, Cambridge: Cambridge University Press.

Aveni, A. F.: 1986, Archaeoastronomy: Past, Present and Future, *Sky and Telescope*, **72**, 456–460.

Aveni, A. F.: 1988, Introduction: whither archaeoastronomy?, in: *World archaeoastronomy*, ed. A. F. Aveni, Cambridge: Cambridge University Press, p. 3.

Babović, Ljubinka: 2001, Prilog proučavanju elemenata kalendarografije i hronometrije bronzanog doba južnog Banata, *Zbornik Narodnog muzeja*, **XVII(1)**, 53-82.

Babović, Ljubinka: 2006, *Svetilišta Lepenskog Vira: Mesto, položaj i funkcija*, Narodni muzej, Beograd.

Babović, Ljubinka: 2016, Komplet "Kapadokijskih idola" - sakralnih kalendara planetarne boginje Meseca iz Kültepe-a, Anadolija (Turska), sa kraja III i početka II milenijuma pre Hrista, *Publ. Astr. društva "Rudjer Bošković"*, **16**, 331-369.

Babović, Ljubinka: 2018, Primeri kalendara, numeričko-simbolički označenih, na pogrebnoj opremi povlašćenih individua iz VI-V veka pre Hr. na prostoru centralnog Balkana (BJR Makedonija i Republika Srbija), *Publ. Astr. društva "Rudjer Bošković"*, **17**, 425-473.

Bajić, Aleksandra: 2012, *Kalendar predaka: vrzino kolo na Bogovom Gumnu*, Beograd: Pešić i sinovi, str. 1-212.

Bajić, A., Pavlović, H.: 2015, *Sunce Lepenskog vira: (arheoastronomska analiza lokaliteta)*, Beograd: Društvo "Vlašići", str. 1-156.

Bajić, Aleksandra: 2016, Moguća astronomska namena kružne formacije na arheološkom lokalitetu Pojate-Pojila u selu Belica, *Publ. Astr. društva "Rudjer Bošković"*, **16**, 371-391.

Bajić, A., Pavlović, H.: 2018, Sunce u Lepenskom Viru (Arheoastronomska analiza lokaliteta), *Publ. Astr. društva "Rudjer Bošković"*, **17**, 475-499.

Bajić, A., Pavlović, H.: 2019, The summer solstice Sun at Lepenski Vir, SEAC 26th, *Harmony and Symmetry: Celestial regularities shaping human culture*, in press.

Bajić, A., Dimitrijević, M. S.: 2019, Feliks Romulijana - Dvorac ni na nebu ni na zemlji, *Publ. Astr. društva "Rudjer Bošković"*, **19**, 507-523.

Božić, Nikola: 2005, Prilog etnoastronomskim istraživanjima u Valjevskom kraju, *Publ. Astr. društva "Rudjer Bošković"*, **5**, 351-353.

Danezis, E., Theodossiou, E., Dimitrijević, M. S.: 2007, Kosmologija u "Besedama na Šestodnev" Vasilija Velikog i uticaj ovog dela kod Srba, *Publ. Astr. društva "Rudjer Bošković"*, **7**, 453-460.

Dimitrijević, M. S.: 1998, Archaeoastronomy and Astronomy in Culture and Relevant Research in Serbia, *Publ. Astron. Obs. Belgrade*, **60**, 157-161.

Dimitrijević, Milan S.: 2007, Kosmički motivi u srpskoj srednjovekovnoj numizmatici, *Publ. Astr. društva "Rudjer Bošković"*, **7**, 461-476.

Eogan, G.: 1991, Prehistoric and Early Historic Cultural Change at Brugh na Bóinne, *Proceedings of the Royal Irish Academy*, **91C**, 105–132.

Heggie, D. C. ed.: 1982, *Archaeoastronomy in the Old World*, Cambridge: Cambridge University Press.

Hoyle, Fred: 1977, *On Stonehenge*, London: Heinemann Educational Books,1-128.

Iwaniszewski, S.: 2003, The erratic ways of studying astronomy in culture, In, *Calendars, Symbols and Orientations: Legacies of Astronomy in Culture (Proceedings of the 9th annual meeting of the European Society from Astronomy in Culture (SEAC), Stockholm, 27–30 August 2001*, eds. Mary Blomberg, Peter E. Blomberg, Göran Henriksson, Uppsala: *Uppsala Astronomical Observatory Report*, **59**, 7–10.

Janković, Nenad Dj.: 1954-1955, Komete u srpskim zapisima i letopisima, *Istoriski časopis*, **5**, 373-386.

Janković, Nenad Dj.: 1989, *Astronomija u starim srpskim rukopisima*, Beograd: Posebna izdanja, Srpska akademija nauka i umetnosti, knj. 590, Odeljenje prirodno-matematičkih nauka, knj. 64, 1-257.

Jovanović, Borislav: 2005, Žrtvena konstrukcija iz kneževske nekropole u Atenici kod Čačka, primer merenja vremena u starijem gvozdenom dobu centralnog Balkana, *Publ. Astr. društva "Rudjer Bošković"*, **5**, 319-327.

Jovanović, Borislav: 2007, Primeri arheoastronomije u arheologiji centralnog Balkana, *Publ. Astr. društva "Rudjer Bošković"*, **7**, 447-452.

Jovanović, Borislav: 2009, Poznavanje kalendarskih elemenata za migraciona kretanja riba familije *Acipenseridae* u kulturi Lepenskog vira, *Publ. Astr. društva "Rudjer Bošković"*, **8**, 417-421.

Ruggles, C. L. N.: 1991, Introduction: Archaeoastronomy - the way ahead, in: *Archaeoastronomy in the 1990s*, ed. Ruggles C. L. N., Loughborough: Group D Publications LTD, p. 1.

Ruggles, C. L. N., Saunders, N. J.: 1993, The Study of Cultural Astronomy, in: *Astronomies and Cultures*,eds. Clive L. N. Ruggles, Saunders Nicholas J., University Press of Colorado, pp. 1–3.

Sinclair, R. M.: 2006, The Nature of Archaeoastronomy, in: *Viewing the Sky Through Past and Present Cultures, Selected Papers from the Oxford VII International Conference on Archaeoastronomy*, Pueblo Grande Museum Anthropological Papers, 15, City of Phoenix Parks and Recreation Department, pp. 13–26

Stojić, Milorad: 2018, *Belica: kultno-astronomsko naselje protostarčevačke kulture : približno 6200-5600. godine pre n.e.*, Beograd: HERAedu, pp. 1-279.

Tadić, Milutin: 2014, Orijentacija najznamenitijih srednjovekovnih crkava u AP Kosovu i Metohiji (Republika Srbija), *Publ. Astr. društva "Rudjer Bošković"*, **13**, 1067-1081.

Theodossiou, E., Manimanis, V. N., Dimitrijević, M. S., Mantarakis, P. Z.: 2011a, Gea, Uran, Helios i Selena tri glavna nebeska tela i nebo u staroj grčkoj kosmogoniji, *Publ. Astr. društva "Rudjer Bošković"*, **10**, 585-603.

Theodossiou, E., Manimanis, V. N., Dimitrijević, M. S., Mantarakis, P. Z.: 2011b, Sirijus u staroj grčkoj i rimskoj literaturi: Od orfičke Argonautike do Astronomskih tablica Georgija Hrizokoke, *Publ. Astr. društva "Rudjer Bošković"*, **10**, 605-628.

Theodossiou, E., Manimanis, V. N., Mantarakis, P. Z., Dimitrijević, M. S.: 2011c, Astronomija i sazveždja u Homerovoj Ilijadi i Odiseji, *Publ. Astr. društva "Rudjer Bošković"*, **10**, 567-584.

Thom, A: 1967, *Megalithic Sites in Britain*, Oxford: Clarendon Press.

Urton, G.: 1981, *At the crossroads of the Earth and sky: An Andean cosmology*, Austin: University of Texas Press.

Urton, G.: 1990, Andean social organization and the maintenance of the Nazca lines, In, *The lines of Nazca*, ed. A F Aveni, Philadelphia: American Philosophical Society, 1990, pp. 175-206.

Vince, A.: 1998, Astronomical Orientation of Skeletons in the Early Eneolithic Necropolis at Podlokanj, *Publ. Astron. Obs. Belgrade*, **60**, 230-233.

Vince, A., Jovanović, B., Vince, I., Vince, O.: 1996, Astronomical orientations of graves and skeletons in Gomolava and Mokrin, *Publ. Astron. Obs. Belgrade*, **54**, 199-202.

Vuca, Petar V.: 2007, Etnoastronomska sećanja u selu Nadanićima opština Gacko, *Publ. Astr. društva "Rudjer Bošković"*, **7**, 495-49776.

Zeilik, M.: 1985, The Ethnoastronomy of the Historic Pueblos, I: Calendrical Sun Watching, *Archaeoastronomy: Supplement to the Journal for the History of Astronomy*, **8(16)**, S1–S24.

Zeilik, M.: 1986, The Ethnoastronomy of the Historic Pueblos, II: Moon Watching, *Archaeoastronomy*, **10(17)**, pp. S1–S22.

Publ. Astron. Obs. Belgrade No. 100 (2021), 233 - 240 *Progress Report*

ELECTRON TRANSPORT, STREAMER PROPAGATION AND LIGHTNING IN THE ATMOSPHERE OF TITAN

S. DUJKO[1], D. BOŠNJAKOVIĆ[1], I. SIMONOVIĆ[1] and C. KÖHN[2]

[1] *Institute of Physics Belgrade, University of Belgrade, Pregrevica 118, 11080 Belgrade, Serbia*
E–mail: sasa.dujko@ipb.bg.ac.rs

[2] *Technical University of Denmark, National Space Institute (DTU Space), Electrovej 328, Kgs Lyngby 2800, Denmark*

Abstract. In this work, we study the transport of electrons, the inception and propagation of streamers and the possibility for lightning in Titan's atmosphere. A multi term theory for solving the Boltzmann equation is used to calculate electron transport coefficients in a N_2-CH_4 mixture that mimics the atmosphere of Titan, over a range of the reduced electric fields. The calculated transport coefficients are then used as input into the classical fluid model to study the transition from an electron avalanche into a negative streamer. We also apply a 2.5 dimensional Particle-in-Cell Monte Carlo Collision (PIC/MCC) code with cylindrical symmetry and photoionization to simulate the inception, propagation and branching of both positive and negative streamers in the ambient electric field between $1.5E_k$ and $3E_k$, where E_k is the breakdown electric field. We found that a successful inception of streamer in Titan's clouds at altitudes of about 20 km, requires a large electric field of 4.2 MV/m, which corresponds to $3E_k$.

1. INTRODUCTION

Lightning is one of the most dramatic phenomena in the Earth's atmosphere, releasing an enormous amount of electromagnetic energy across the wide range of frequencies. Lightning is a signature of atmospheric dynamics and cloud structure, and it plays a vital role in atmospheric chemistry, through the production of numerous chemical compounds. Some of these chemicals are organic molecules and therefore of great significance to biological processes.

Lightning is a phenomenon that is not confined solely to the Earth's atmosphere. Since the time of the Voyager missions in the 1980s, we have clear evidence of lightning in the atmospheres of gas giants, Jupiter and Saturn, and ice giants, Uranus and Neptune (Desch et al. 2002, Yair 2012, Aplin et al. 2020). On the other side, one of the unresolved issues after the Cassini-Huygens mission to the Saturnian system is whether or not lightning occurs in Titan's atmosphere. Titan is the largest of Saturn's satellites and has a massive atmosphere with a surface pressure higher than Earth's by approximately 50%. Titan's atmosphere is made up primarily of N_2 and CH_4 and traces of H_2, HCN and a wide range of hydrocarbons and nitriles (Nixon et al. 2018). Titan's atmospheric chemistry modeling studies suggest the existence of lightning, as

the quantity of HCN and C_2H_2 in the atmosphere cannot be explained in terms of photochemical models (Vuitton et al. 2019).

In this work, we discuss the basic properties of streamer discharges, pre-cursors of lightning, in Titan's atmosphere. Streamers are thin channels of non-equilibrium plasma whose dynamics is controlled by the highly-localized non-linear regions of space charge and steep gradients of the electron number density. Depending on the conditions, they can form complex structures resembling trees or other forms, and can spread over a few centimeters in laboratory experiments or a few kilometers in planetary atmospheres. The first step in studies of streamer discharges is to consider the transport of electrons in a mixture of gases that mimics the atmosphere of Titan. Using the cross section sets for electron scattering in N_2 and CH_4 as input, we solve the non-conservative Boltzmann equation in order to calculate electron transport coefficients. In addition, from the E/N-profiles of the ionization and attachment rates (where E is the electric field while N is the gas number density), we determined the breakdown electric field, which is an important quantity in streamer studies. While electron transport coefficients are required as input data in fluid equation-based models of streamer discharges, sets of cross sections for electron scattering in N_2 and CH_4 are required as input data in the PIC/MCC modeling.

In Section 2, we briefly review the methodology of the present work. First, we present the basic elements of a multi term theory for solving the non-conservative Boltzmann equation which has been used to calculate electron transport coefficients as a function of the electric field. The classical fluid and PIC/MCC models are also briefly outlined and used to study the transition from an electron avalanche into a negative streamer and propagation of streamers in various electric fields and various gas mixtures. The variation of electron transport coefficients with E/N and properties of both negative and positive streamers, are reported in Section 3.

2. METHODS OF CALCULATIONS

2. 1. BOLTZMANN EQUATION ANALYSIS

The behavior of electrons in Titan's atmosphere under the influence of the spatially homogeneous electric field $\mathbf{E}$, is described by the phase-space distribution function $f(\mathbf{r}, \mathbf{c}, t)$ representing the solution of the Boltzmann equation (Dujko et al. 2010, 2011):

$$\frac{\partial f}{\partial t} + \mathbf{c} \cdot \frac{\partial f}{\partial \mathbf{r}} + \frac{e_0}{m} \mathbf{E} \cdot \frac{\partial f}{\partial \mathbf{c}} = -J\left(f, f_0\right), \tag{1}$$

where $\mathbf{r}$ and $\mathbf{c}$ denote the position and velocity coordinates, e_0 and m are the charge and mass of the electrons and t is time. Swarm conditions are assumed to apply and $J\left(f, f_0\right)$ denotes the rate of change of f due to binary collisions between electrons and neutral molecules. The neutral molecules are assumed to remain in thermal equilibrium, characterized by a spatially homogeneous phase-space distribution function f_0.

The angular dependence of $f(\mathbf{r}, \mathbf{c}, t)$ in velocity space, is resolved by expanding the distribution function in terms of spherical harmonics $Y_l^{(m)}\left(\widehat{\mathbf{c}}\right)$, where $\widehat{\mathbf{c}}$ denotes the angles of $\mathbf{c}$. Under hydrodynamic conditions, $f(\mathbf{r}, \mathbf{c}, t)$ is further expanded in terms of the gradients of the electron number density $n\left(\mathbf{r}, t\right)$. Thus, $f(\mathbf{r}, \mathbf{c}, t)$ can be expanded

as

$$f(\mathbf{r},\mathbf{c},t)=\sum_{l=0}^{\infty}\sum_{m=-l}^{l}\sum_{s=0}^{\infty}\sum_{\lambda=0}^{s}\sum_{\mu=-\lambda}^{\lambda}f(lm|s\lambda\mu)Y_l^{(m)}(\widehat{\mathbf{c}})G_\mu^{(s\lambda)}n\left(\mathbf{r},t\right), \tag{2}$$

where $G_\mu^{(s\lambda)}$ is the irreducible gradient tensor operator. The coefficients $f(lm|s\lambda\mu)$ are functions of the speed c, obtained by the expansion

$$f(lm|s\lambda\mu)=\omega\left(T_b,c\right)\sum_{\nu=0}^{\infty}F\left(\nu lm|s\lambda\mu\right)R_{\nu l}\left(T_b,c\right), \tag{3}$$

where $\omega\left(T_b,c\right)$ is a Maxwellian distribution at an adjustable base temperature T_b, and $R_{\nu l}$ is related to a Sonnine polynomial of order (ν,l). The coefficients $F\left(\nu lm|s\lambda\mu\right)$ are called "moments"and they are related to the electron transport quantities.

Substitution of expansions (2)-(3) into the Boltzmann equation (1) leads to a hierarchy of coupled differential equations for the moments $F\left(\nu lm|s\lambda\mu\right)$. These equations are numerically solved and all transport coefficients of interest, including the mean energy, drift velocity and diffusion tensor as well as rate coefficients are expressed in terms of these moments (Dujko et al. 2010, 2011).

2. 2. THE FLUID MODEL

Transition from an electron avalanche into a negative streamer is studied by using the classical fluid model (Dujko et al. 2013). In this model the electron flux is obtained by assuming a steady-state of the momentum balance equation, and that the electron energy of the field-directed motion is much greater than the thermal contribution. The generalized one-dimensional continuity equation for the electron number density is

$$\frac{\partial n_e}{\partial t}=\frac{\partial}{\partial x}\left(W\mathrm{sgn}\left(E\right)n_e+D_L\frac{\partial n_e}{\partial x}\right)+\left(\nu_i-\nu_a\right)n_e, \tag{4}$$

where W and D_L are the electron drift velocity and longitudinal diffusion coefficient, respectively, electric field E is oriented along the x-axis, while ν_i and ν_a are the ionization and electron attachment coefficients, respectively. The drift and diffusion of both positive and negative ions are neglected on the time scales of interest in the present work. Thus,

$$\frac{\partial n_p}{\partial t}=\nu_i n_e,\quad \frac{\partial n_n}{\partial t}=\nu_a n_e, \tag{5}$$

where n_p and n_n are positive and negative ion densities.

The model is realized in a 1.5 dimensional (1.5D) setup. In this model, we assume that the space charge is contained inside a cylinder with radius R_0 and that the charge density varies along the axial direction only. Thus, the total electric field in the system is evaluated as the sum of the uniform external electric field and the electric field due to space charge:

$$E\left(x,t\right)=E_0+\frac{e}{2\varepsilon_0}\int_0^d\left(n_p-n_n-n_e\right)\left(\mathrm{sgn}\left(x-x'\right)-\frac{x-x'}{\sqrt{\left(x-x'\right)^2+R_0^2}}\right)dx', \tag{6}$$

where E_0 and ε_0 are the external (applied) electric field and vacuum permittivity, respectively, and d is the length of the system.

The above fluid equations are closed, assuming the local field approximation. According to this approximation, the input data, including W, D_L, ν_i and ν_a are assumed to be functions of the local instantaneous electric field. In the numerical implementation of our fluid model, the spatial discretization is performed by using the second order central finite difference, while the fourth order Runge–Kutta method is used for the integration in time.

2. 3. PARTICLE-IN-CELL/MONTE CARLO COLLISION SIMULATIONS

In addition to classical fluid model, we also apply a 2.5D PIC/MCC model with a cylindrical symmetry to simulate the development of both positive and negative streamers in the ambient electric field (Chanrion and Neubert 2008, Köhn et al. 2019). In order to simulate positive streamers, the photoionization model initially developed by Zheleznyak et al. (1982) is implemented into the code. In PIC/MCC simulations, we follow the motion of single electrons as they move through a background medium under the influence of the electric field. The Monte Carlo method is used to determine the exact time and the nature of a collision between a single electron and the background molecule. After particle positions have been updated, they are mapped onto the grid for the purpose of computation of the charge density distribution. The space charge profile is then used as a source term for the Poisson equation that determines the electric field for the next time step. As boundary conditions, we use Neumann conditions $\partial\phi/\partial r = 0$ for $r = 0$, L_r, and Dirichlet conditions for the electric potential $\phi(r, 0) = 0$ and $\phi(r, L_z) = \phi_{max} = E_{amb}\, L_z$, where L_r and L_z are dimensions of the simulation domain, while E_{amb} is the ambient electric field.

We initiate all simulations with a charge neutral electron-ion patch at the center of the simulation domain. The initial electron density is given by the Gaussian distribution with a a peak density of $n_{e,0} = 10^{20}$ m^{-3}. For more details on PIC/MCC simulations, the reader is referred to Köhn et al. (2019).

3. RESULTS AND DISCUSSION

On Titan clouds form between 20 and 35 km altitude with the pressure varying between approximately 0.1 bar and 0.6 bar, the ambient temperature varying between 70 and 75 K and the level of CH_4 varying between 1.6% and 2.0%. In our calculation we choose 1.6% of CH_4 while the pressure and temperature are set to 0.3 bar and 75K, respectively. Complete and self-consistent cross section sets for electron scattering in N_2 and CH_4, initially developed by Stojanović and Petrović (1998) and Šašić et al. (2004), are used as an input for solving the Boltzmann equation and performing PIC/MCC simulations.

In figure 1 we show the variation of the drift velocity (a), longitudinal diffusion coefficient (b) and rate coefficients for ionization and electron attachment (c) as a function of E/N. The properties and energy dependence of the cross sections are reflected in the E/N-profiles of the presented transport coefficients. From the E/N-profile of the drift velocity, we observe that there are no signs of a negative differential conductivity (NDC), i.e., the drift velocity is a monotonically increasing function of E/N. We also note that the influence of non-conservative collisions on the electron transport is not apparent until about 100 Td and increases with the electric field. This is consistent with an increase in the ionization rate above this value of E/N.

The attachment rate is negligible for all E/N studied and its explicit influence on the electron transport is minimal. The breakdown field E_k is defined as the electric field when the attachment rate equals the ionization rate. The transition from an avalanche of electrons to a streamer requires the electric field to be at least over the breakdown field. Assuming that Titan's atmosphere is composed of 98.4% of N_2 and 1.6% of CH_4, we find that the breakdown electric field is 50 Td.

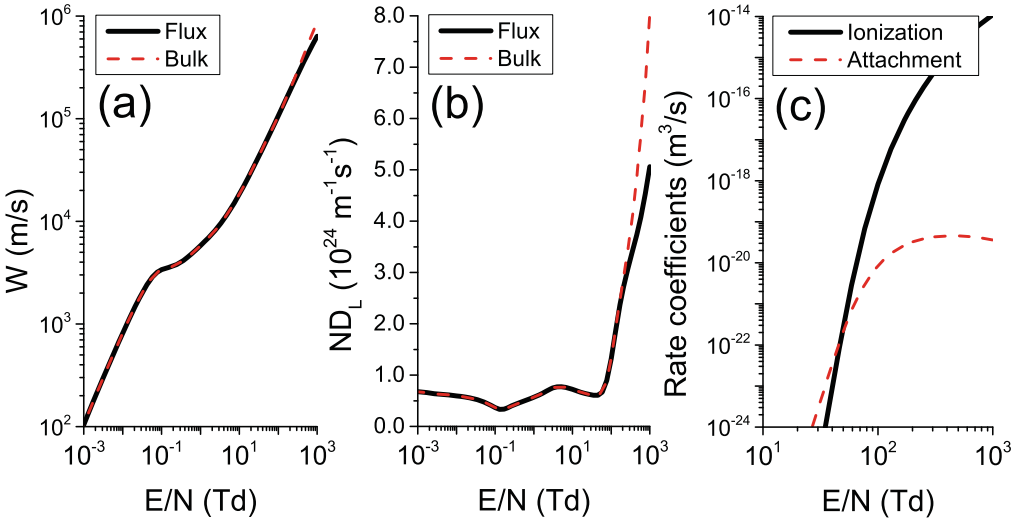

Figure 1: Variation of the drift velocity (a), longitudinal diffusion coefficient (b) and rate coefficients for ionization and attachment (c) with E/N.

Calculated with the 1.5D fluid code, in figure 2 we show the spatial and temporal development of the electron density and the electric field when the externally applied electric field is $4E_k$. The simulation begins with the same initial Gaussian-type distribution of electrons and positive ions reflecting the macroscopic plasma neutrality (panel a). Both flux and bulk transport data are used as an input to solve the system of fluid equations. At the beginning of the evolution, we see that the electron density grows as a result of the electron impact ionization (panel b). The electrons drift in the opposite direction to the electric field while the positive ions drift slowly in the opposite direction. The mobility of positive ions is much lower and therefore the space-charge effects develop (panel c). As the evolution continues, the electric field is enhanced at the front of the streamer, while within the streamer interior is almost entirely shielded. Consequently, ionization processes may not occur in the streamer channel (panel d).

We found that in electric fields $\leq 3E_k$ there is no transition from an avalanche into a streamer. For such electric fields, the initial Gaussian grows due to electron impact-ionization without distorting the external electric field. We also found that the velocity of the streamer considerably exceeds the bulk and flux drift velocities of the electrons. This is expected, as the velocity of a negative streamer is determined by

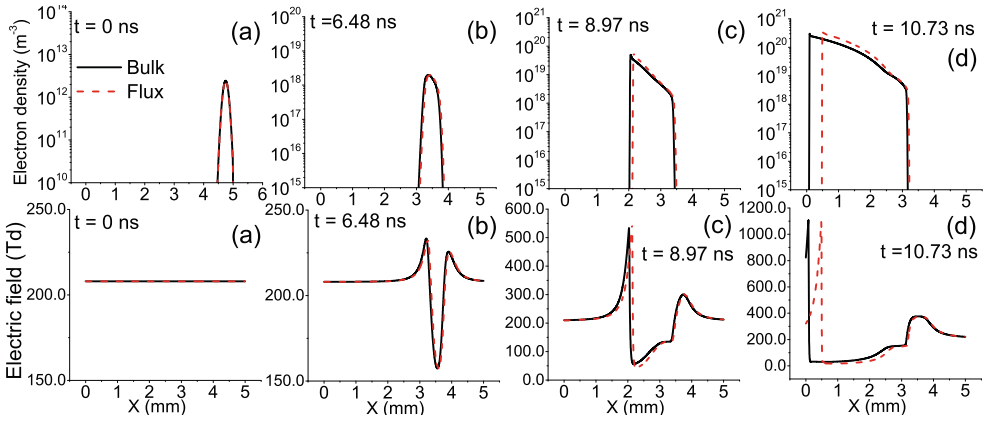

Figure 2: Electron density (first row) and the electric field (second row) in N_2:CH_4=(98.4%):(1.6%) after different time steps. The external electric field is $4E_k$ where E_k is the breakdown electric field.

the combination of the electron velocity and the rate of the electron impact ionization at the front of the streamer, where the electric field is significantly enhanced, as well as by the strong diffusive fluxes in the streamer front. Comparing streamers with bulk and flux input data, we observe that streamers with bulk data are faster.

In figure 3 we show the results of PIC/MCC simulations, including the electron density and the electric field in different spatially homogeneous ambient electric fields. For comparison, the last column shows the electron density and the electric field in N_2:O_2 mixture for the same number density of ambient gas molecules. The set of cross sections for electron scattering are detailed by Dujko et al. (2011). We observe the avalanche-to-streamer transition in N_2-CH_4 mixture mimicking the atmosphere of Titan only for fields above $3E_k$. For electric fields $\leq 3E_k$ there is a distinct motion of electrons towards the positive virtual electrode, while there is no movement of the positive front at all. However, the field enhancement is clearly visible on the positive streamer front as well as the field shielding on the negative upper forehead. This suggests that the avalanche-to-streamer-transition is unlikely to occur at later times.

For electric fields above $3E_k$ we observe an avalanche-to-streamer transition in both N_2-CH_4 and N_2-O_2 mixtures. We observe that the initial electron-ion patch evolves into a bidirectional streamer. The field enhancement is more apparent for the positive front as the positive streamer is narrower and therefore its field enhancement is larger than in the negative streamer. Comparing the evolution on Titan (third column) and in N_2-O_2 mixture (fourth column), we observe that both positive and negative streamer fronts propagate significantly slower in Titan's atmosphere. In addition, the electron density in N_2-CH_4 appears to be smaller and branching is favored.

Using a classical fluid model and PIC/MCC simulations, we have not observed any streamer inception for electric fields below approximately $3E_k$. In the modeling study of cloud dynamics in Titan's atmosphere, it was shown that the generated electrical field could reach 2 MV/m (Tokano et al. 2001). This suggests that the inception of streamers and the appearance of lightning is not possible in Titan's atmosphere.

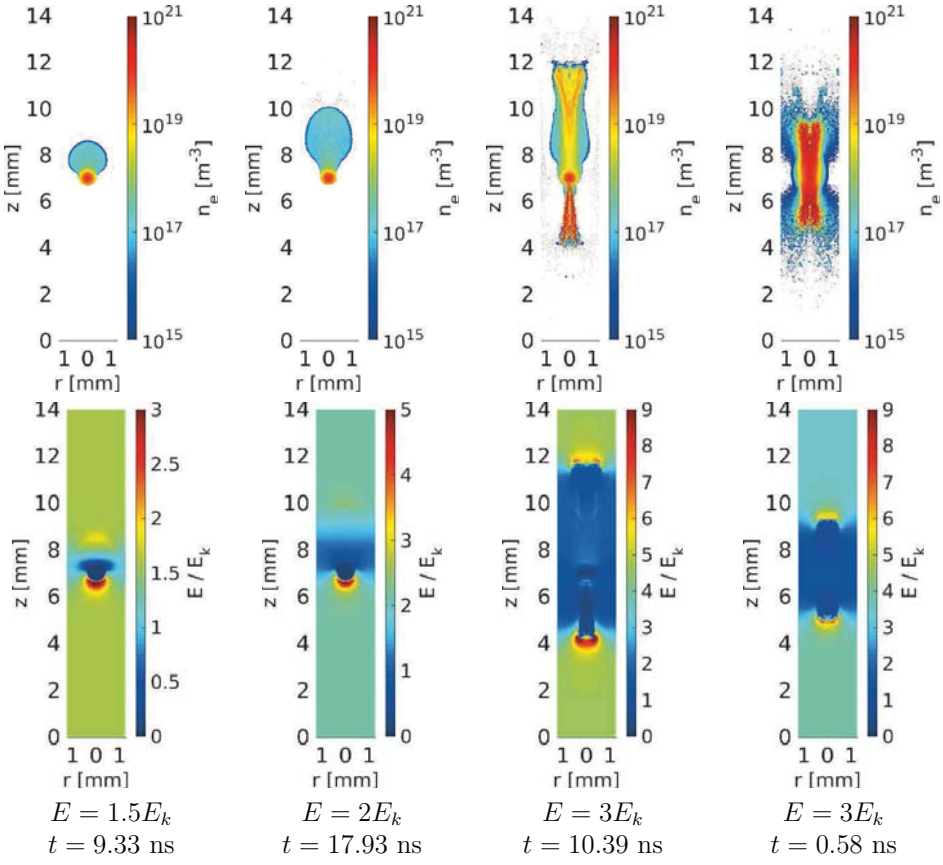

Figure 3: The electron density (first row) and the electric field (second row) in N_2:CH_4=(98.4%):(1.6%) (columns one to three) and in N_2:O_2=(98.4%):(1.6%) (last column) in different ambient electric fields after different time steps. In both mixtures the gas density $N = 2.9 \cdot 10^{25}$ m^{-3}, hence $E_k \approx 1.4$ MVm^{-1} for N_2:CH_4 mixture and $E_k \approx 3.0$ MVm^{-1} for N_2:O_2 mixture (Köhn et al. 2019).

However, this conclusion can be challenged by a comparison of cloud electric fields and breakdown electric fields in the Earth's atmosphere. In numerous independent studies, breakdown electric fields at altitudes between 4 and 20 km have been shown to be significantly higher than cloud electric fields. However, as discussed in the present work, the inception of streamers in Titan's atmosphere strongly depends on the ambient electric field, which is uncertain since it is only provided by models, but not by direct measurements (Köhn et al. 2019). Moreover, the existence of streamer discharges into Titan's atmosphere is still not conclusive proof of lightning. It should also be mentioned that during the 127 flybys of Cassini, and during the descent of a Huygens probe, the traces of lightning were not detected. However, although not observed, it may still mean that lightning exists, but is too weak or too rare for detection. In any case, the existence of lightning in Titan's atmosphere is still an open question, and requires more attention in the near future.

4. CONCLUSION

In this work, we have studied the transport of electrons, the transition from an electron avalanche into a streamer and its propagation, and the possibility for the appearance of lightning in Titan's atmosphere. We have presented the variation of the electron transport coefficients with E/N and we have determined the breakdown electric field in Titan's atmosphere. In this study, ionization collisions were observed to affect electron transport coefficients at high values of E/N, while the insignificant attachment rate had no observable effect. The inception and propagation of streamers were simulated using a fluid equation-based models and PIC/MCC simulations. We have found that the inception of streamers requires the ambient electric field above $3E_k$. We found that streamers that are modeled with bulk data are a little faster than those with flux data. Comparing N_2:CH_4 and N_2:O_2 mixtures, streamers in N_2:O_2 mixtures are much faster. The methodology and mathematical machinery presented in this work can be used as a basis for further studies of streamer discharges and lightning in the atmospheres of other planets in our Solar system, and in the atmospheres of exoplanets.

Acknowledgment

This project has received funding from the European Union's Horizon 2020 research and innovation programme under the Marie Sklodowska-Curie grant agreement 722337. The work of S. Dujko, D. Bošnjaković and I. Simonović is supported by the Ministry of Education, Science and Technological Development of the Republic of Serbia and the Institute of Physics Belgrade.

References

Aplin, K. L., Fischer, G., Nordheim, T. A., Konovalenko, A., Zakharenko, V., Zarka, P.: 2020, *Space Sci. Rev.*, **216**, 26.
Chanrion, O., Neubert, T.: 2008, *J. Comp. Phys.*, **227**, 7222.
Desch, S. J., Borucki, W. J., Russell, C. T., Bar-Nun, A.: 2002, *Rep. Prog. Phys.*, **65**, 955.
Dujko, S., White, R. D., Petrović, Z. Lj., Robson, R. E.: 2010, *Phys. Rev. E*, **81**, 046403.
Dujko, S., White, R. D, Petrović, Z. Lj., Robson, R. E.: 2011, *Plasma Source Sci. Technol.*, **20**, 024013.
Dujko, S., Markosyan, A. H., White, R. D., Ebert, U.: 2013, *J. Phys. D: Appl. Phys.*, **46**, 475202.
Köhn, C., Dujko, S., Chanrion, O., Neubert, T.: 2019, *Icarus*, **333**, 294.
Nixon et al.: 2018, *Planetary and Space Science*, **155**, 50.
Stojanović, V., Petrović, Z. Lj.: 1998, *J. Phys. D: Appl. Phys.*, **31**, 834.
Tokano, T., Molina-Cuberos, G. J., Lammer, H., Stumptner, W.: 2001, *Planetary and Space Sci.*, **49**, 539.
Šašić, O., Malović, G., Strinić, A., Nikitović, Ž., Petrović, Z. Lj.: 2004, *New. J. Phys.*, **6**, 74.
Vuitton, V, Yelle, R. V., Klippenstein, S. J., Hörst, S. M., Lavas, P.: 2019, *Icarus*, **324**, 120.
Yair, Y.: 2012, *Adv. Space Research*, **50**, 293.
Zheleznyak, M. B., Mnatsakanian, A. K., Sizykh, S. V.: 1982 *High Temp.*, **20**, 357.

Publ. Astron. Obs. Belgrade No. 100 (2021), 241 - 246 *Progress Report*

MANIFOLD LEARNING IN THE CONTEXT OF QUASAR SPECTRAL DIVERSITY

I. JANKOV, D. ILIĆ and A. KOVAČEVIĆ

Department of Astronomy, Faculty of Mathematics, University of Belgrade, Studentski trg 16, 11000 Belgrade, Serbia
E–mail: isidora_jankov@matf.bg.ac.rs

Abstract. Here we discuss the interpretation of quasar spectral diversity by subjecting quasars to non-linear treatment using a manifold learning technique called locally linear embedding (LLE). We apply the LLE analysis to a sample of type 1 quasars, for which the spectral features are taken from a Sloan Digital Sky Survey (SDSS) data catalog, which counts a total of ∼14,600 low-redshift objects. When we have a large number of parameters describing objects in question, LLE can be useful because it aims to find a low-dimensional representation of the original data set while preserving the geometry of the local neighborhoods within the data. We have shown that LLE can be used as a contextual tool in the search for essential correlations in the spectral parameters of SDSS quasars.

1. INTRODUCTION

Quasars are extremely bright and compact energy sources located in the central regions of some galaxies. Their extreme brightness is the result of the accretion of the material onto a supermassive black hole (Salpeter 1964, Shakura & Sunyaev 1973). This process creates a complex environment where the emission can be observed over a wide range of frequencies (Netzer 2013). The presence of different relationships between spectral parameters in different quasar populations originating from both physical and orientation effects results in a staggering diversity in their spectra (e.g., Netzer 2015).

In order to study this diversity, we need relatively large number of high quality spectra and appropriate methodology which can assist in finding the main trends in the data. One such method is the principal component analysis (PCA), which belongs to a family of linear dimensionality reduction methods. Identification of eigenvectors, or most dominant relationships, and their association with a fractional contribution to the data set's total variance is an advantageous PCA property. Many authors have utilized PCA to study quasar phenomenology, applying it to the measured spectral parameters (Boroson & Green 1992, Grupe 2004, Grimes et al. 2004, Hamilton et al. 2008, Jankov & Ilić 2020a) or directly on spectra (Francis et al. 1992, Brotherton et al. 1994, Shang et al. 2003, Yip et al. 2004, Ludwig et al. 2009).

One of the pioneering research papers that shed light on the complexity of the quasar parameter space was done by Boroson & Green (1992) where they applied

PCA to a sample of 87 low-redshift quasars from the Palomar–Green Bright Quasar Survey (Schmidt & Green 1983). They have identified an anti-correlation between peak flux of [O III] λ5007 Å and the equivalent width (EW) ratio of Fe II and broad Hβ ($R_{\rm FeII}$) as the main trend in their sample (the first principal component or Eigenvector 1). The full width at half maximum (FWHM) of the broad Hβ was also found to be well correlated with this component. The Eddington ratio was suspected as the driving mechanism behind this trend, but more convincing arguments were provided much later (Marziani et al. 2001, Boroson 2002, Shen & Ho 2014). Expanding further on the PCA analysis of Boroson & Green and also on correlations that emerged from ROSAT (e.g., Wang et al. 1996), Sulentic et al. (2000a) proposed an empirical formalism, analogous to the Hertzsprung-Russell diagram for stars, which allows contextualization of quasar spectral diversity for type 1 sources. They have found that quasars populate an elbow-shaped main sequence in the FWHM Hβ - $R_{\rm FeII}$ plane (E1 optical plane) driven by Eddington ratio convolved with the line of sight orientation. Using the main sequence, two main quasar populations (pop A and pop B) with significantly different physical properties are identified (e.g. Sulentic et al. 2000a,b, Sulentic et al. 2011, Marziani et al. 2018), as well as the highly accreting extreme pop A (Marziani & Sulentic 2014).

All above correlations in quasars were based on PCA results, which is a linear method, and its low dimensional projections cannot account for non-linear relationships that may emerge in the complex real-world data sets, such as quasar spectral data. Therefore, we select to utilize manifold learning (i.e., non-linear dimensionality reduction) and analyze correlations revealed by newly obtained projections. All manifold learning algorithms assume that real-world data sets lie on a low-dimensional manifold embedded in the high-dimensional space. The goal is to unravel the manifold and project it to a low-dimensional space while retaining the geometrical relationships between data points as much as possible. There are several manifold learning algorithms, but here we select to use locally linear embedding or LLE (Roweis & Saul 2000), since it preserves the geometry of the local neighbourhoods within the data, while staying computationally inexpensive and having only two free parameters. It also has a proven record of application in the astronomical context (e.g., Vanderplas & Connolly 2009, Daniel et al. 2011, Matijevič et al. 2012).

Here we give preliminary results of the analysis of the application of the LLE algorithm to a sample of low-redshift quasars. The paper is organized as follows: in Sec.2 we briefly describe the data and the LLE method, in Sec. 3 we give the first results, and in Sec.4 we outline our conclusions.

2. DATA AND METHOD

We use a sample of type 1 low-redshift ($z < 0.35$) quasars taken from the Sloan Digital Sky Survey Data Release 7 quasar catalog with measured optical spectral properties (Liu et al. 2019). The sample comprises of EW, FWHM and line luminosity (L) for broad lines (Hα^b and Hβ^b), EW and L for narrow lines (Hα^n, Hβ^n, [O III]λ5007, [O III]λ6300, [N II]λ6583, [S II]$\lambda\lambda$6716, 6731), continuum luminosity at 5100Å (log L_{5100}), $R_{\rm FeII}$ and luminosity of Fe IIλ4570. During the object selection process, we only included objects with no null values for all previously mentioned spectral parameters. As a result, the sample size was reduced from ∼14,600 down to 6236 objects. As LLE can be sensitive to outliers (Vanderplas & Connolly 2009), we made

a choice to use density distribution in the E1 optical plane (FWHM Hβ - $R_{\rm FeII}$) to locate and remove objects residing in the extremely low density regions. Although, we do have a total of 23 input parameters, we have chosen this particular plane for its proven high contribution to the total variance in quasar samples (Boroson & Green 1992, Sulentic et al. 2000a,b, Shen & Ho 2014). After the outlier removal, we were left with a final sample of 6023 objects. We need also to select the number of nearest neighbors (k) and the number of output dimensions (d) - two free parameters needed by the algorithm, which was done as described in Jankov et al. (2020b).

3. RESULTS AND DISCUSSION

We apply the LLE algorithm (setting $d = 3$ and $k_{opt} = 16$) to 6023 broad line quasars described by 23 spectral parameters using the scikit-learn Python library (Pedregosa et al. 2011), which results in three projections (Figure 1). We focus our attention to the $c_2 - c_3$ projection (*main projection*, further in the text), where the two of three identified branches are clearly distinguished (Figure 1 upper and lower left panel). Locations of objects in the LLE projections are determined by their proximity in the original 23-dimensional parameter space. Objects grouped in the projection have similar spectral parameters and can be potentially described as a distinct quasar population. Evidently, objects with different broad line structure, kinematics, and spectral characteristics described by pop A, B, and xA (e.g. Marziani et al. 2018) are clearly separated in two of three LLE projections, the main projection and $c_1 - c_3$ (see bottom panels in Figure 1). The axes (components) of the projections have no physical meaning (for details see Roweis & Saul, 2000). The main projection identifies object's progression along the N-branch (Narrow line branch) where many parameters associated with narrow emission lines vary. The N-branch is orthogonal to a branch identified as the quasar main sequence (defined as M-branch, Figure 1, bottom left). To study the correlations along this track, bins of the same sizes are created, and mean values of all input parameters are taken for each bin. Bins can be thought of as counterparts to composite spectra. The potentially outlying objects populating low density regions in the projection are eliminated ($\sim$2% of the total sample).

Most prominent trends were spotted, namely the increase of narrow line EW (Figure 2) and narrow line luminosity along the branch, but also the decrease in continuum luminosity at 5100 Å and broad line luminosity (Figure 3). In addition to bin edges, the upper panel of Figure 1 shows the smooth increase in EW of [O III]λ5007, clearly indicating that the trend is indeed real. The N1 bin could contain objects with a range of different luminosities originating from another branch that hides behind our projection (Figure 3). This could produce higher average luminosity in the first bin as some objects would actually be far away in the projected space, and therefore have dissimilar properties in the obtained 3-dimensional LLE projection. That branch is identified as the L-branch (or luminosity branch) and it can be seen on the left side of $c_1 - c_2$ and $c_1 - c_3$ projections in Figure 1 (bottom middle and right panels). Additional analysis of the L-branch is needed to understand the relationships involving luminosities which is out of the scope of this contribution.

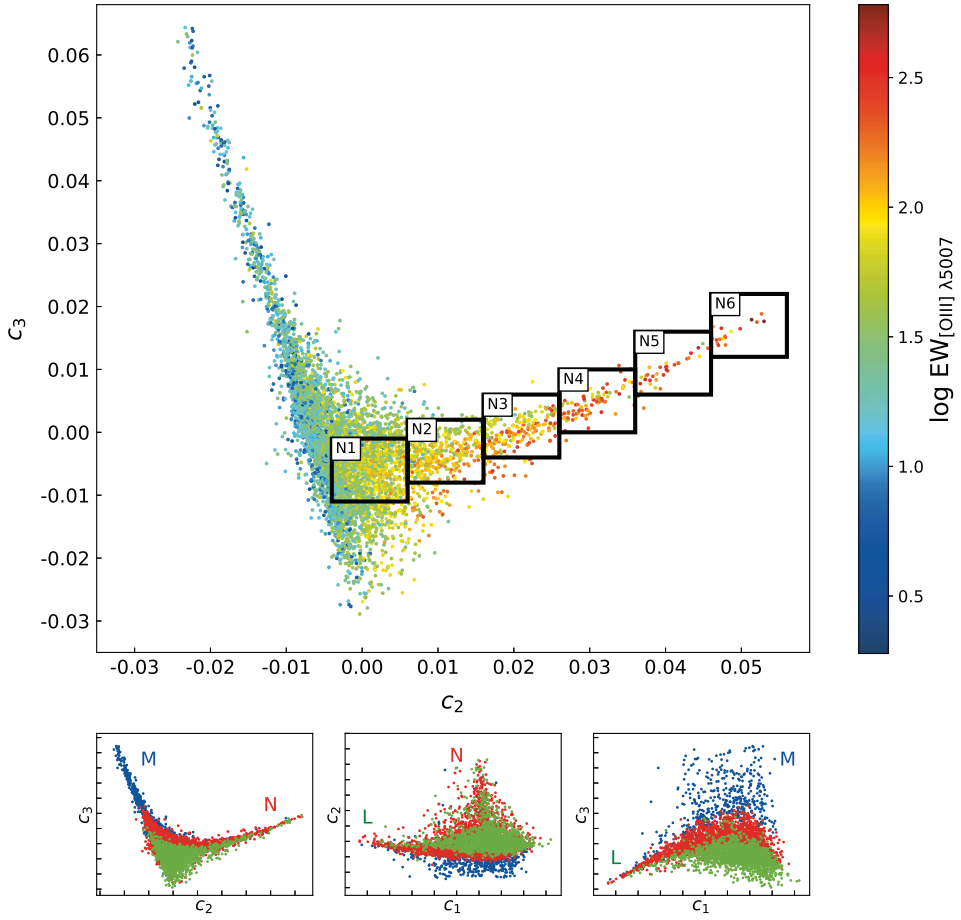

Figure 1: *Upper panel*: The main LLE projection. Number of dimensions is reduced from 23 down to three. This projection was chosen for analysis because of its clear distinction of objects that populate two different branches. The N-branch (Narrow line branch) is sampled by six equally sized bins. Axes are in arbitrary units and correspond to second and third component of LLE decomposition. The colormap indicates the gradient of log EW [O III] λ5007 in the projection. *Bottom panels*: All three LLE projections. Populations xA, A and B are marked with blue, red and green colors, respectively. Different branches are labeled by letters M (Main-sequence branch), N (Narrow line branch) and L (Luminosity branch).

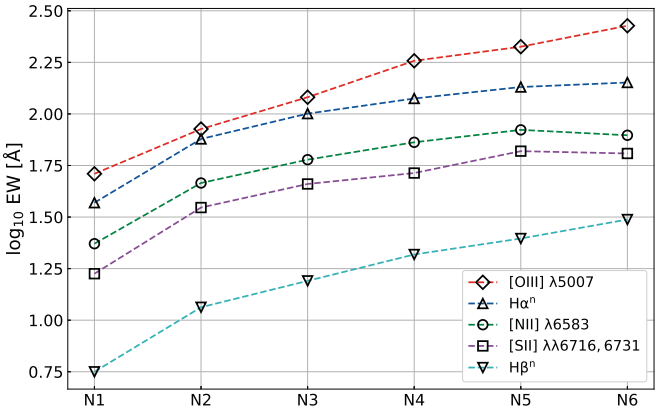

Figure 2: Progression of EW values of [O III] λ5007, narrow Hα, [N II] λ6583, [S II] $\lambda\lambda$6716, 6731 and narrow Hβ indicated by diamonds, triangles, circles, squares and reversed triangles, respectively. Symbols represent the mean values of log EW for each bin. Bins are ordered according to their location on the projection: starting from objects in bin N1 at the core of the projection and going towards the peak of the branch populated by objects from bin N6. Symbols are connected by dashed lines of different colors for clarity.

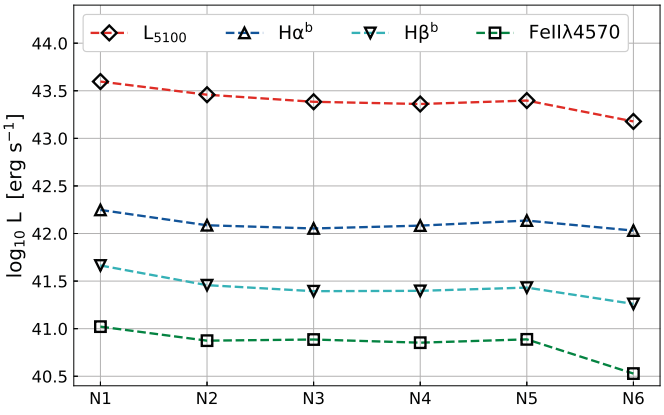

Figure 3: Progression of luminosity of the continuum at 5100 Å (L_{5100}), broad line luminosity (Hα and Hβ) and the luminosity of FeII λ4570. Bins are ordered as described in Figure 2.

4. CONCLUSIONS

We have applied the LLE algorithm to a large sample from SDSS catalogue of quasar spectral properties in order to study the quasar high-dimensional parameter space (23 spectral parameters). We have found a low-dimensional projection which clearly identifies three branches, and we discuss in more details the properties of the objects along the branch of increasing narrow emission lines, i.e., the N-branch. The analysis of bins along the N-branch shows the dominant trend producing the branch itself - the variation of EW of all narrow lines from our sample indicating the presence of a separate quasar population characterized by apparently strong narrow emission lines (e.g., Ludwig et al. 2009). The continuum luminosity appears to decrease along the branch, but this effect must be studied in tandem with other branches because objects from those branches may contaminate the first bin. We conclude that manifold learning techniques, LLE in particular, have proven to be immensely valuable tools for the deep understanding of complex data sets such as quasar spectral data and it may be proven even more useful if applied to ever more complex astronomical data sets of the future.

References

Boroson, T. A.: 2002, *The Astrophysical Journal*, **565**, 78.
Boroson, T. A., Green, R. F.: 1992, *Astrophysical Journal Supplement*, **80**, 109.
Brotherton, M. S. et al.: 1994, *The Astrophysical Journal*, **430**, 495.
Daniel, S. F. et al.: 2011, *The Astronomical Journal*, **142**, 203.
Francis, P. J. et al.: 1992, *The Astrophysical Journal*, **398**, 476.
Grimes, J. A., Rawlings, S., Willott, C. J.: 2004, *MNRAS*, **349**, 503.
Grupe, D.: 2004, *The Astronomical Journal*, **127**, 1799.
Hamilton, T. S., Casertano, S., Turnshek, D. A.: 2008, *The Astrophysical Journal*, **678**, 22.
Jankov, I., Ilić, D.: 2020a, *Contrib. Astron. Obs. Skaln. Pleso*, **50**, 350.
Jankov, I., Ilić, D., Kovačević, A.: 2020b, *Publ. Astron. Obs. Belgrade*, **99**, 291-294.
Liu, H.-Y. et al.: 2019, *Astrophysical Journal Supplement*, **243**, 21.
Ludwig, R. R. et al.: 2009, *The Astrophysical Journal*, **706**, 995–1007.
Marziani, P. et al.: 2001, *The Astrophysical Journal*, **558**, 553.
Marziani, P. et al.: 2018, *Frontiers in Astronomy and Space Sciences*, **5**, 6.
Marziani, P., Sulentic, J.: 2014, *MNRAS*, **442**, 1211-1229.
Matijevič, G. et al.: 2012, *The Astronomical Journal*, **143**, 123.
Netzer, H.: 2013, The Physics and Evolution of Active Galactic Nuclei, by Hagai Netzer, Cambridge, UK: Cambridge University Press, 2013.
Netzer, H.: 2015, *Annu. Rev. Astron. Astrophys.*, **53**, 365-408.
Pedregosa, F. et al.: 2011, *Journal of Machine Learning Research*, **12**, 2825-2830.
Roweis, S. T., Saul, L. K.: 2000, *Science*, **290**, 2323.
Salpeter, E. E.: 1964, *The Astrophysical Journal*, **140**, 796.
Schmidt, M., Green, R. F.: 1983, *The Astrophysical Journal*, **269**, 352-374.
Shakura, N. I., Sunyaev, R. A.: 1973, *Astronomy and Astrophysics*, **500**, 33.
Shang, Z. et al.: 2003, *The Astrophysical Journal*, **586**, 52-71.
Shen, Y., Ho, L. C.: 2014, *Nature*, **513**, 210.
Sulentic, J. W., Marziani, P., Dultzin-Hacyan, D.: 2000a, *Annu. Rev. Astron. Astrophys.*, **38**, 521.
Sulentic, J. W. et al.: 2000b, *The Astrophysical Journal*, **536**, L5-L9.
Sulentic, J. W., Marziani, P., Zamfir, S.: 2011, *Baltic Astronomy*, **20**, 427-434.
Vanderplas, J., Connolly, A.: 2009, *The Astronomical Journal*, **138**, 1365-1379.
Wang, T., Brinkmann, W., Bergeron, J.: 1996, *Astronomy and Astrophysics*, **309**, 81.
Yip, C. W. et al.: 2004, *The Astronomical Journal*, **128**, 2603-2630.

Publ. Astron. Obs. Belgrade No. 100 (2021), 247 - 252 *Progress Report*

DYNAMICAL MODELING OF NEARBY GALAXIES

M. JOVANOVIĆ[1], S. SAMUROVIĆ[1], M. M. ĆIRKOVIĆ[1,2] and A. VUDRAGOVIĆ[1]

[1] *Astronomical Observatory, Volgina 7, 11000 Belgrade, Serbia*
E–mail: milena@aob.rs

[2] *Future of Humanity Institute, Faculty of Philosophy, University of Oxford, Suite 8, Littlegate House, 16/17 St Ebbe's Street, Oxford, OX1 1PT, UK*

Abstract. Here we present the procedure of detailed dynamical modeling applied on a sample of galaxies based on THINGS (The HI Nearby Galaxy Survey). Stellar mass is derived for all galaxies using a free mass-to-light ratio. Where possible, a modeling procedure is also done for a fixed M/L^* based on modern stellar population models. Finally we give the outline of the ongoing work, which is determining the baryon distribution of the Milky Way environment reflected by the Baryonic Mass Function based on the same sample of galaxies.

1. INTRODUCTION

Dynamical modeling of a galaxy recovers the total mass that interacts gravitationally: stellar, gaseous, dark matter. The mass of a galaxy, although not the sole driver of its evolution as it almost is in stars, is still very important for the processes of galaxy formation and evolution; a galaxy's mass probably modulates crucial evolution processes like star formation and quenching (e.g. Courteau et al. 2014). We observe the dynamical mass through the motions of test-particles inside of the gravitational potential of that mass.

In our work, the test-particle or tracer of the gravitational field is HI gas. Therefore, we are interested in galaxies rich with cold neutral gas. Rotationally supported objects are required for this analysis because in that case rotational velocity at a certain radius equals the circular velocity in the disk. Then the virial theorem reduces nicely to the simple expression:

$$V_{\rm circ}^2(r) = r\frac{d\phi}{dr} = G\frac{M(r)}{r} \tag{1}$$

All of this is done within the framework of Newtonian/Einstein gravity.

2. SAMPLE

The sample we used is derived from the THINGS[1] (The HI Nearby Galaxy Survey) survey conducted on the VLA telescope, which is described in Walter et al. (2008) and analyzed in a similar manner in de Blok et al. (2008). The sample covers nearby galaxies ($z < 0.003$, $D < 15$ Mpc) with a large span of morphologies, masses and sizes. Obviously, it was an HI-selected sample and no early-type or lenticular galaxies were represented. From the total of 34 observed objects only (up to) 20 were usable for deriving rotation curves by satisfying the criteria of rotationally-dominated kinematics, not undergoing disruptive interactions and having favorable geometry (inclination between $45 - 70°$).

3. METHOD

3. 1. ROTATION CURVE

The rotation curve for these types of very detailed radio observations can be derived through forming a two-dimensional velocity field. We formed the velocity field from the standard three-dimensional data cube by fitting of a (in most cases) Gauss-Hermite polynomial to the HI line in every spatial point of the observed galaxy disk (see Fig. 1, left). In two cases, for the galaxies NGC 2366 and IC 2574, there were other significant types of motion other than rotation. For them we derived a procedure to extract what we call the 'rotationally dominated velocity field'. The developed procedure is based on the one described in Oh et al. (2008) but simplified, while remaining robust. The schematic of the data cube and determination of the center of the line is shown in Fig. 1 on the left. On the right of the Fig. 1 we show the subsequently constructed velocity field from all the determined line centers in the case of the galaxy NGC 2841 (Samurović, Vudragović & Jovanović 2015).

The rotation curve is derived by tilted-ring fitting to the constructed velocity field through varying parameters in the following expression:

$$V(x, y) = V_{\rm sys} + V_{\rm c}(r) \sin i \cos\theta (+V_{\rm exp}). \tag{2}$$

Here $V(x, y)$ is the resulting velocity on the projected point of the galaxy's disk, $V_{\rm sys}$ is systemic velocity, $V_{\rm c}(r)$ is the circular or rotation velocity at a given radius r, i is the inclination, θ is the phase angle measured in a coordinate system of the galaxy from the receding part of the major axis and $V_{\rm exp}$ is the expansion velocity of the galaxy (should be 0 in most cases).

Fitting is done iteratively with an additional parameter fixed in every new iteration - coordinates of the center (x_0, y_0), systemic velocity ($V_{\rm sys}$), position angle ($P.A.$) and inclination (i). Position angle and inclination were fixed to a series of values, so they would allow for presumed physical changes in these two parameters, for example due to warps. Adopted rotation curve and radial profiles for the position angle and inclination for the galaxy NGC 5055 are shown in Fig. 2 on the left (from Jovanović 2017).

How the rotation curve of the galaxy NGC 2366, based on our rotationally dominated velocity field, compares with ones based on Gauss-Hermite h_3 and mean

[1]available at: `http://www.mpia.de/THINGS`.

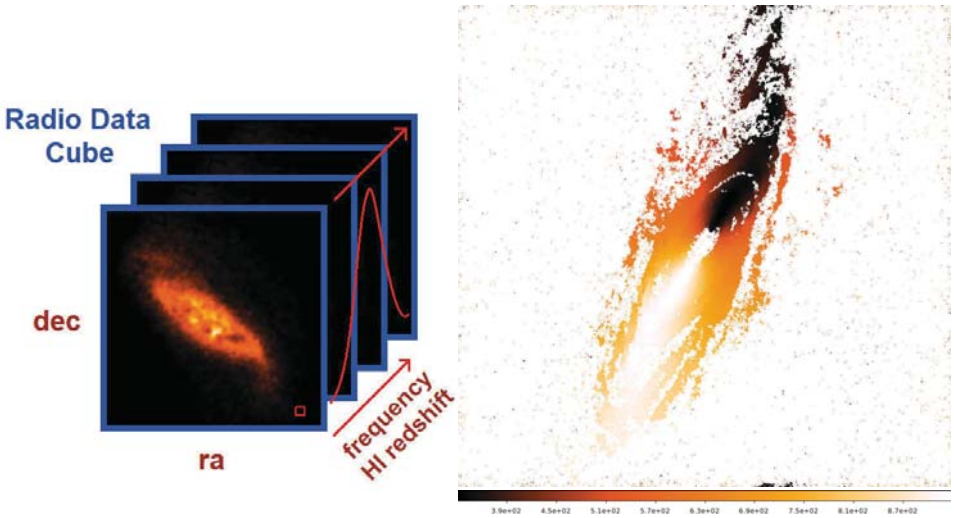

Figure 1: Left: The schematic of the three-dimensional HI observation i.e. data cube. At every pixel we fit the function or use similar procedure to find the center of the line. Right: Velocity field of NGC 2841 derived by using h_3 polynomial.

intensity-weighted velocity (moment 1) is shown in Fig. 2 on the right. All the admitted points in the final rotation curve (blue stars in Fig. 2, right) were present in the observations and not extrapolated. By applying the developed procedure we were able to filter out the profiles that were probably affected by streaming and other non-rotational motions. This provided a rotation curve that is flat to a much larger radius (7.5 compared to 4.5 kpc).

3. 2. DYNAMICAL MODELING

We use the rotation curve to asses the whole enclosed gravitational mass of a galaxy and through dynamical modeling we compare this mass with known contributions from individual galaxy components like stars and gas.

Distances to galaxies in our sample are from the Extragalactic Distance Database[2] and they are mainly based on the Cosmicflows-3 results (Tully et al. 2016).

The gaseous component was also calculated from the THINGS data. Integrated intensity from HI radiation was used, scaled by a factor of 1.36 to account for other species of the cold neutral gas.

Stellar mass was assessed from its radiation by determining the mass-to-light ratio, M/L. This has been done in two different ways - by scaling the observed light with free parameter M/L and by assessing M/L from Stellar Population Synthesis (SPS) models.

For dynamical modeling with free M/L we use the Spitzer 3.6 micron observations to account for stellar light. SINGS[3] products and Spitzer Heritage Archive[4] images were used and then approximated with known models for stellar light like exponential

[2]Available at: `http://edd.ifa.hawaii.edu/`.
[3]Available at: `http://irsa.ipac.caltech.edu/data/SPITZER/SINGS`.
[4]Available at: `https://sha.ipac.caltech.edu/applications/Spitzer/SHA/`.

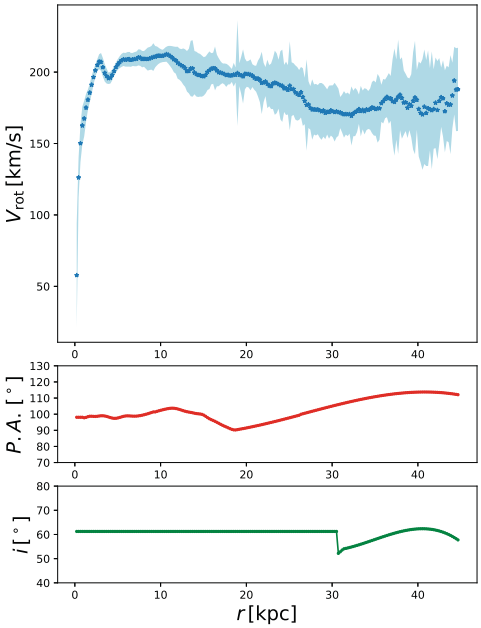

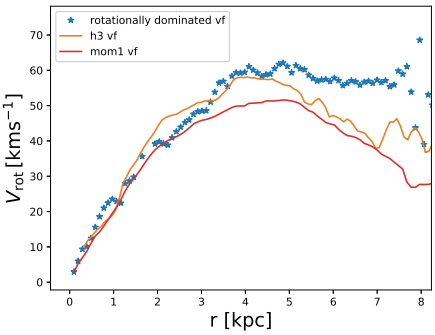

Figure 2: Left: Rotation curve (top panel) with radial profiles for position angle *P.A.* (middle panel) and inclination i (bottom panel) for the galaxy NGC 5055 (from Jovanović 2017). Right: Rotation curve based on different velocity fields for the galaxy NGC 2366. Blue stars mark rotationally dominated, orange line h_3 and red line moment 1 velocity field.

disk or Sérsic bulge. Surface brightness models do not deviate significantly from the observed light distribution, so we can consider this component to be observationally based. The near-infrared 3.6 μm band is thought to trace the old, most massive populations well and is subjected to less extinction. Part of the radiation in this band comes from the dust (Meidt et al. 2014, Querejeta et al. 2015), which is an issue that has not be addressed in our current work.

For SPS models different colors and metallicity (where possible) were used to calculate an M/L ratio using different evolutionary models - based on different initial mass function (IMFs), Star Formation History (SFH), stellar spectra, isochrones, etc. - 13 of them. Calculations of M/L are based on the evolutionary models compiled in Bell & de Jong 2003 and Into & Portinary 2013. It was possible to find a satisfactory dynamical model for 16 galaxies out of 20 (that were used with free models) when fixed M/L was used.

Two classical dark matter profiles were used - isothermal sphere (ISO, Jimenez et al. 2003) and Navarro-Frenk-White (NFW, Navarro, Frenk & White 1997). Originally THINGS data were intended for differentiating between core and cusp dark matter profiles that required sub-kpc scale.

For brevity, here we present an example of the dynamical models with free M/L (see Fig. 3) and isothermal dark mater halo for two galaxies - NGC 5055 and DDO 154 (published in Jovanović 2017).

Both galaxies have satisfactory dynamical models for free M/L and for NGC 5055 SPS models yield the M/L value in the 3.6 micron band that is compatible with the observed rotation curve. For DDO 154 majority of colors are outside the ranges covered with SPS models (which is sometimes the case with dwarf low-metallicity

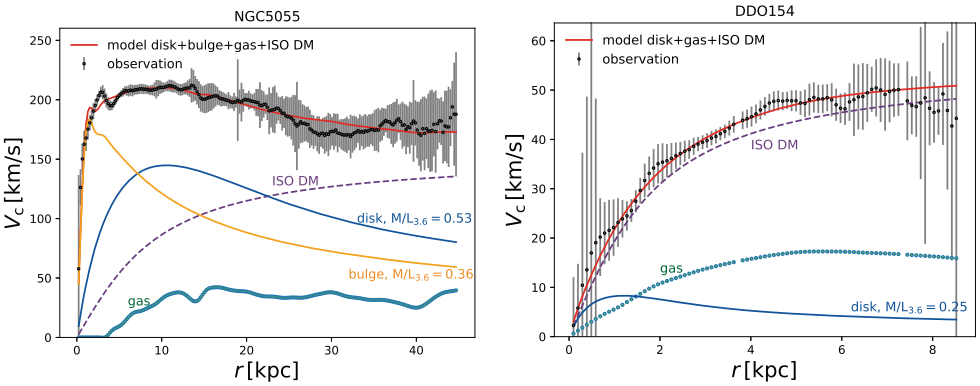

Figure 3: Fitting the observed rotation curves using free M/L and isothermal dark matter profile in case of NGC 5055 (left) and DDO 154 (right).

Table 1: Baryonic mass ($M_{\rm baryon}$) and baryonic fraction ($\frac{M_{\rm baryon}}{M_{\rm total}}$) from dynamical models with free and fixed/SPS mass-to-light ratio and dark matter models (ISO and NFW) is given alongside the morphological type and distance in megaparsecs (from EDD, see footnote 2) for two galaxies from our sample, NGC 5055 and DDO 154.

Galaxy ID	morph. type	D [Mpc]	M/L	dark matter model	$M_{\rm baryon}$ $[10^{10} M_{\odot}]$	$\frac{M_{\rm baryon}}{M_{\rm total}}$
NGC 5055	Sbc	8.99 ± 0.45	free	ISO	13.3 ± 0.6	0.42 ± 0.25
				NFW	12.1 ± 0.7	0.38 ± 0.09
			SPS	ISO	11.2 ± 4.0	0.37 ± 0.80
				NFW	10.9 ± 3.9	0.4 ± 1.7
DDO 154	I	4.04 ± 0.20	free	ISO	0.53 ± 0.02	0.10 ± 0.03
				NFW	0.53 ± 0.01	0.10 ± 0.01
			SPS	ISO	0.52 ± 0.01	0.09 ± 0.01
				NFW	0.52 ± 0.01	0.09 ± 0.01

galaxies). Still, several models do give credible values of M/L that we were able to use in dynamical modeling. Previously observed difficulties of NFW to successfully fit the rotation curves of dwarf galaxies in the center (for example DDO 154) are noted in our work as well.

For all 20 galaxies we calculated the enclosed masses of all the considered components up to the outermost observed radii, and they include the mass of the gas, stellar components, dark matter halo (this is the only component that can actually be extrapolated given that its density profile is theoretical), total mass and baryonic mass. Our primary interest is baryonic mass function (BMF), which is the distribution of baryonic mass (regular mass consisting of protons and neutrons) in our sample. An example of the baryonic mass and fraction calculated from dynamical models for

galaxies NGC 5055 and DDO 154 is given in Table 1. The outline of baryonic mass distribution for models with free M/L and isothermal dark matter is shown in Fig. 4.

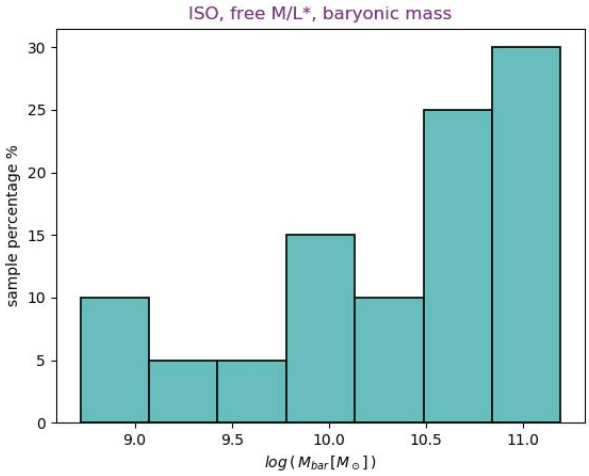

Figure 4: Distribution of the baryonic mass in THINGS galaxies based on dynamical models using free M/L ratio and isothermal dark matter profile.

Detailed analysis of the dynamical models for all the galaxies in the sample along with the discussion are a subject of the PhD thesis of M. Jovanović and a publication in preparation.

Acknowledgements

This work was supported by the Ministry of Education, Science and Technological Development of the Republic of Serbia (MESTDRS) through the contract No. 451-03-68/2020-14/200002. Useful discussions with Dr. M. Bílek and Dr. M. Jurkovic are acknowledged.

References

Bell E. F., de Jong R. S.: 2001, *ApJ*, **550**, 212.
Courteau, S., Cappellari, M., de Jong, R. S.et al.: 2014, *Rev. Mod. Phys.*, **86**, 47.
de Blok, W. J. G., Walter, F., Brinks, E., Trachternach, C., Oh, S.-H., Kennicutt, R. C., Jr: 2008, *AJ*, **136**, 2648.
Into, T., Portinari, L.: 2013, *MNRAS*, **430**, 2715.
Jimenez, R., Verde, L., Treu, T., Stern, D.: 2003, *ApJ*, **593**, 622.
Jovanović, M.: 2017, *MNRAS*, **469**, 3564.
Meidt, S. E., Schinnerer, E., van de Ven, G. et al.: 2014, *ApJ*, **788**, 144.
Navarro, J. F., Frenk, C. S., White, S. D. M.: 1997, *ApJ*, **490**, 493.
Oh, S.-H., de Blok, W. J. G., Brinks, E., Walter, F., Kennicutt, R. C., Jr: 2011, *AJ*, **141**, 193.
Querejeta, M., Meidt, S. E., Schinnerer, E. et al.: 2015, *ApJS*, **219**, 5.
Samurović, S., Vudragović, A., Jovanović, M.: 2015, *MNRAS*, **451**, 4073.
Tully, R. B., Courtois, H. M., Sorce, J. G.: 2016, *AJ*, **152**, 50.
Walter, F., Brinks, E., de Blok, W. J. G., Bigiel, F., Kennicutt, R. C., Jr, Thornley, M. D., Leroy, A.: 2008, *AJ*, **136**, 2563.

Publ. Astron. Obs. Belgrade No. 100 (2021), 253 - 258 *Progress Report*

CONTROL STARS AROUND QUASARS SUITABLE FOR THE ICRF – GAIA CRF LINK

MILJANA D. JOVANOVIĆ[1], GORAN DAMLJANOVIĆ[1] and FRANÇOIS TARIS[2]

[1] *Astronomical Observatory, Volgina 7, 11060 Belgrade 38, Serbia*
E–mail: miljana@aob.rs
E–mail: gdamljanovic@aob.rs

[2] *Observatoire de Paris - SYRTE, 61 av. de l'Observatoire, 75014 Paris, France*
E–mail: francois.taris@obspm.fr

Abstract. Some quasars (QSOs) which were observed by Gaia satellite in optical and by Very Long Baseline Interferometry (VLBI) in radio wavelength will be used to link Gaia CRF and International Celestial Reference Frame. Monitoring photometry stability of candidate sources is of importance for this link. During six years (2013–2019) we observed 47 candidate sources (mostly QSOs), in V and R bands. Their brightness was determined by using differential photometry. In the same manner was obtained the brightness of several control stars around each QSOs. We tested brightness variability of QSOs and stars using F–test. The test shows that most of control stars are suitable for photometry and could be used as comparison stars. The results of five selected objects and their control stars are presented here.

1. INTRODUCTION

The early third Gaia data release (Gaia EDR3) is available since 3 December 2020, the full Gaia DR3 data release will be available in the first half of 2022. The Gaia EDR3 contains data for about 1.8 billion sources and provides full astrometric information (positions, parallaxes, and proper motions) for about 1.5 billion sources (Gaia Collaboration et al. 2020).

The third data realization of the International Celestial Reference Frame (ICRF3) was adopted in August 2018 (Charlot et al. 2020). The ICRF3 is based on data at radio frequencies obtained by very long baseline interferometry (VLBI). The Gaia CRF (based on the observations at optical wavelength) and the ICRF (based on the VLBI observations at radio wavelengths) could be linked using a set of quasars (QSOs) visible in the optical and radio domains. We observed for about six years (2013 – 2019) the 47 candidates sources for this link with high astrometric quality proposed by Bourda et al. (2011). These sources are mostly QSO, the others are BL Lacertae – BL Lac and Seyfert galaxies type 1, they are all subgroup of Active Galactic Nuclei (AGNs). One of the important properties of AGNs, flux variability could be correlated with astrometric possitions of AGNs centroids (Taris et al. 2011). Because of that it is necessary to monitor their brightness changes for the link between

two reference frames over a longer period of time. The brightness was calculated using differential photometry with a few comparison stars from the vicinity of objects. By increasing the number of comparison stars the accuracy of the objects brightness is improved. Therefore we add new control stars, the brightness of which is determined in the same manner. After testing some of these control stars could be used as comparison ones and also for testing the brightness of comparison stars.

The subject of this paper is investigation of brightness variability of control stars of five AGNs which have been the most observed objects. Of these five objects, two are QSOs (1553+231, and 1556+335) and three are BL Lac (1607+604, 1722+119, and 1741+597). They were observed for about 50 nights. For object 1722+119 the first finding chart was given in Smith et al. (1991), but stars are too far from the object and very bright. The second was given in Fiorucci and Tosti (1996), the stars are located near the object, but some stars are very bright in comparison with the object. Because of this we select comparison and control stars for this object from paper Doroshenko et al. (2014). In the paper Jovanović (2019) are presented charts of the fields of the objects and their (comparison and control) stars. In paper Damljanović et al. (2020) are presented analysis of objects brightness variability and calculated amplitudes of their quasiperiods from the similar data sets.

2. OBSERVATIONS AND PHOTOMETRY

The observations were made using eight different telescopes. The most of the data are obtained using two telescopes located at Astronomical Station Vidojevica (ASV) of the Astronomical Observatory of Belgrade, and telescope Joan Oró 80 cm - TJO (robotic one) located at the Montsec Astronomical Observatory, Catalonia, Spain. As for the other five telescopes, three are located at the Rozhen NAO in Bulgaria, one at Belogradchik, Bulgaria and one Leopold Figl at Vienna, Austria. The details about the used telescopes, their mirror diameters and mounted CCD cameras, are presented in Table 1.

Every night CCD images mostly per V and R filters have been obtained. For reduction of CCD images and bad pixels maps were used bias, dark and flat frames obtained for the same nights (dark frames for hot, and flat for dead pixel map). This was performed using Image Reduction and Analysis Facility – the IRAF scripting language (ascl:9911.002) (Tody 1986, 1993). The corrections for cosmic rays was perfomed using Laplacian Cosmic Ray Identification method (Pieter G. van Dokkum 2001).

The brightness of objects and control stars was determined using differential photometry with two comparison stars, with MaxIm DL software. The stars were chosen from the Sloan Digital Sky Survey Data Release 14 (SDSS DR14) catalogue (Abolfathi et al. 2018). The stars of 1722+119 were chosen from paper Doroshenko et al. (2014), because the field of 1722+119 was not covered by SDSS. The comparison and control stars were selected from the object vicinity following several criteria. We chose stars which are not variable, not too bright or faint in comparison with the object, or not very blue or red, etc. The transformation from the SDSS DR14 (PSF g, r, i) magnitudes to the Johnson-Cousins (V and R), was performed using equations (Chonis and Gaskel 2008):

$$V = g - (0.587 \pm 0.022)(g - r) - (0.011 \pm 0.013), \quad (1)$$

$$R = r - (0.272 \pm 0.092)(r - i) - (0.159 \pm 0.022), \quad (2)$$

where $14.5 < g, r, i < 19.5$, $0.08 < r - i < 0.5$ and $0.2 < g - r < 1.4$.

Table 1: Telescopes and cameras.

Telescope with mirror diameter	CCD Camera	CCD resolution	Pixel size (μm)	Pixel scale (arcsec pix^{-1})	Field of view (arcmin)
ASV 60cm	Apogee Alta U42	2048x2048	13.5x13.5	0.466	15.8x15.8
	SBIG ST10 XME	2184x1472	6.8x6.8	0.230	8.4x5.7
	Apogee Alta E47	1024x1024	13.0x13.0	0.450	7.6x7.6
ASV 1.4m	Apogee Alta U42	2048x2048	13.5x13.5	0.243	8.3x8.3
	Andor iKon-L	2048x2048	13.5x13.5	0.244	8.3x8.3
TJO 80cm	FLI PL4240-1-B	2048x2048	13.5x13.5	0.364	12.3x12.3
	Andor iKon-L	2048x2048	13.5x13.5	0.361	12.3x12.3
Rozhen 2m	Andor iKon-L	2048x2048	13.5x13.5	0.176	6.0x6.0
	VersArray 1300B	1340x1300	20.0x20.0	0.261	5.6x5.6
Rozhen 60cm	FLI PL09000	3056x3056	12.0x12.0	0.330	16.8x16.8
Rozhen 50/70cm	FLI PL16803	4096x4096	9.0x9.0	1.080	73.7x73.7
Belogradchik 60cm	FLI PL09000	3056x3056	12.0x12.0	0.335	16.8x16.8
LFOA 1.5m	SBIG ST10 XME	2184x1472	6.8x6.8	0.150	5.6x3.8

In Table 2 are details of objects and their two comparison (A and B) and control stars: coordinates, the V_C and R_C magnitudes of stars (obtained using mentioned equations for stars from SDSS DR14, and those from Doroshenko et al. (2014)), and with V_O and R_O (average magnitudes from our observations). During the six years period of observation, one object 1556+335 had the most stable brightness. The brightness standard deviations of this object in both bands are of the order of about of 0.01, similar to the standard deviations of stars. The standard deviations of other objects are ten times bigger. The differences of extremal magnitudes of objects 1535+231, 1607+604, 1722+119, and 1741+597 are about 1.0, 0.4, 2.0, 1.7 magnitudes in both filters, respectively. Objects with the highest brightness changes have the highest standard deviations. Objects 1535+231, 1607+604, 1722+119, and 1741+597 have standard deviations around 0.2, 0.1, 0.5, and 0.3, respectively.

The V_C and R_C magnitudes of stars (initial values for differential photometry calculated from SDSS DR14) and calculated values V_O and R_O (from our observations) are in good agreement within the limits of errors. The standard deviations of control stars are similar to the ones of comparison.

3. METHODS AND RESULTS

We use the 3σ rule to reject some data and the Shapiro-Wilk test of normality (Razali and Wah 2011) to confirm that tests which require normal data distribution can be applied.

To investigate the brightness variability of objects and control stars we use the F-test described by de Diego (2010). We define three test hypotheses:

1) H_1: $Var(S - A) = Var(S - B)$, alternative H_{a1}: $Var(S - A) > Var(S - B)$,

2) H_2: $Var(S - A) = Var(A - B)$, alternative H_{a2}: $Var(S - A) > Var(A - B)$,

3) H_3: $Var(S - B) = Var(A - B)$, alternative H_{a3}: $Var(S - B) > Var(A - B)$.

Test statistics which correspond to these hypotheses are:

$F_1 = \frac{Var(S-A)}{Var(S-B)}$, $F_2 = \frac{Var(S-A)}{Var(A-B)}$, and $F_3 = \frac{Var(S-B)}{Var(A-B)}$.

Table 2: The coordinates, V and R magnitudes (index C refers to calucalted using SDSS DR14, and O to observed values) with standard errors of objects and their comparison and control stars; period July 2013 — August 2019 using our observations.

Object No.	$\alpha_{J2000.0}(^o)$	$\delta_{J2000.0}(^o)$	$V_C \pm \sigma_{V_C}$(mag)	$R_C \pm \sigma_{R_C}$(mag)	$V_O \pm \sigma_{V_O}$(mag)	$R_O \pm \sigma_{R_O}$(mag)
1535+231	234.31041	23.01126			18.472 ±0.233	18.275 ±0.261
2 (A)	234.31491	23.01831	17.200 ± 0.031	16.658 ± 0.038	17.229 ±0.031	16.750 ±0.067
3	234.30004	23.02486	15.983 ± 0.030	15.633 ± 0.031	16.002 ±0.022	15.707 ±0.059
4 (B)	234.25178	23.01917	16.232 ± 0.024	15.867 ± 0.029	16.225 ±0.012	15.916 ±0.067
7	234.29312	22.96096	16.470 ± 0.027	15.973 ± 0.036	16.451 ±0.026	15.958 ±0.021
8	234.35917	23.01592	15.860 ± 0.035	15.149 ± 0.050	15.841 ±0.024	15.142 ±0.028
1556+335	239.72993	33.38851			17.455 ±0.063	16.988 ±0.052
2 (A)	239.71950	33.39110	17.336 ± 0.030	16.850 ± 0.038	17.352 ±0.032	16.883 ±0.034
3 (B)	239.69035	33.40959	16.381 ± 0.027	16.095 ± 0.030	16.371 ±0.021	16.074 ±0.021
5	239.76798	33.38778	16.271 ± 0.030	15.916 ± 0.031	16.283 ±0.022	15.931 ±0.022
6	239.74562	33.39003	16.198 ± 0.030	15.825 ± 0.031	16.225 ±0.022	15.876 ±0.021
7	239.74317	33.37370	15.552 ± 0.030	15.188 ± 0.031	15.568 ±0.022	15.223 ±0.017
8	239.73398	33.37219	15.743 ± 0.040	14.897 ± 0.064	15.763 ±0.032	14.966 ±0.016
1607+604	242.08560	60.30783			17.400 ±0.126	16.956 ±0.095
2 (A)	242.02882	60.28951	17.068 ± 0.027	16.619 ± 0.031	17.069 ±0.027	16.616 ±0.031
3 (B)	242.02526	60.31162	16.864 ± 0.025	16.423 ± 0.032	16.876 ±0.018	16.441 ±0.025
4	241.97352	60.35552	15.195 ± 0.025	14.781 ± 0.031	15.164 ±0.042	14.729 ±0.041
5	242.09638	60.34816	15.630 ± 0.031	14.965 ± 0.044	15.620 ±0.046	14.938 ±0.036
7	242.16854	60.37746	16.856 ± 0.024	16.467 ± 0.031	16.839 ±0.043	16.424 ±0.061
1722+119	261.26810	11.87096			15.571 ±0.467	15.085 ±0.482
C2	261.27167	11.86997	13.173 ± 0.005	12.570 ± 0.006	13.201 ±0.034	12.623 ±0.024
C3	261.24375	11.86636	14.078 ± 0.012	13.600 ± 0.008	14.095 ±0.025	13.628 ±0.024
1	261.31208	11.89125	13.445 ± 0.009	12.848 ± 0.010	13.466 ±0.037	12.873 ±0.027
2 (A)	261.30458	11.86519	14.823 ± 0.008	14.691 ± 0.012	14.822 ±0.011	14.686 ±0.005
5	261.25667	11.91311	15.873 ± 0.010	15.385 ± 0.016	15.880 ±0.047	15.387 ±0.027
9	261.23333	11.87083	15.809 ± 0.008	15.332 ± 0.014	15.815 ±0.027	15.346 ±0.020
10	261.23875	11.87083	16.142 ± 0.011	15.699 ± 0.019	16.144 ±0.023	15.716 ±0.021
C4 (B)	261.28958	11.85344	15.665 ± 0.009	15.164 ± 0.013	15.667 ±0.024	15.169 ±0.018
1741+597	265.63334	59.75186			18.011 ±0.307	17.549 ±0.305
2	265.62329	59.75176	15.565 ± 0.029	15.204 ± 0.054	15.602 ±0.033	15.268 ±0.044
3 (A)	265.57081	59.75387	16.673 ± 0.029	16.314 ± 0.053	16.674 ±0.019	16.332 ±0.022
4	265.68412	59.76861	16.376 ± 0.034	15.795 ± 0.067	16.407 ±0.042	15.830 ±0.040
5	265.61457	59.79547	16.154 ± 0.031	15.704 ± 0.056	16.187 ±0.034	15.760 ±0.025
6	265.68288	59.71901	16.126 ± 0.038	15.684 ± 0.064	16.125 ±0.033	15.686 ±0.037
7 (B)	265.59766	59.71686	16.633 ± 0.039	16.124 ± 0.074	16.634 ±0.015	16.111 ±0.012

The designations $Var(S-A)$, $Var(S-B)$ and $Var(A-B)$ refer to the variances of magnitude differences between S (control stars or objects) and comparison stars (A or B). The F_i $(i = 1, 2, 3)$ statistics were compared with the critical value (which corresponds to the significance level 0.001 and number of freedom $N-1$, where N is the number of data). The null hypotheses of non variability is discarded when the F_2 and F_3 values are greater than critical. The $F_1 = F_2/F_3$ values should be around 1, because the tested brightness should be variable in the same manner for both comparison stars A and B ($Var(S-A)$ and $Var(S-B)$ should be close to each other). The F_2 and F_3 values, along with number of data points N, and critical

values F_c (for N and $\alpha = 0.001$) are listed in Table 3, for both filters, for objects and their control stars.

The F_1 values are around 1 (for objects and stars) as it is expected, except for control stars of 1535+231, in the R band. The test shows that the brightness of most of the control stars could be considered as non-variable. The F_2 and F_3 exceed the critical values for about 20% stars, which corresponds to data obtained with low quality CCD camera. These data are not rejected because they are close to the average ones within the limits of standard deviations, and they are not excluded after implementing 3σ rule. One object, 1556+335, has the most stable brightness. The other objects have the F_2 and F_3 values significantly greater than critical. It is noticeable that the objects with greater changes in brightness (1722+119 and 1741+597) have higher $F_{2,3}$ values.

Table 3: The F–test results.

Object	N	F_2, F_3	F_c	N	F_2, F_3	F_c
Band		V			R	
1535+231	43	31.00 , 34.50	2.66	48	18.96 , 19.65	2.51
3	43	1.78 , 2.08	2.66	48	4.03 , 1.34	2.51
7	12	1.16 , 1.47	7.76	16	1.05 , 6.16	5.54
8	20	1.14 , 1.53	4.47	24	1.20 , 6.46	3.85
1556+335	41	3.12 , 2.34	2.73	50	1.23 , 1.77	2.46
5	41	1.01 , 1.38	2.73	50	1.06 , 1.71	2.46
6	20	2.53 , 2.01	4.47	27	2.60 , 2.31	3.53
7	20	2.25 , 2.05	4.47	27	2.07 , 3.42	3.53
8	19	1.79 , 1.19	4.68	27	1.98 , 3.85	3.53
1607+604	44	22.26 , 20.29	2.63	48	8.64 , 7.10	2.51
4	39	3.47 , 2.43	2.80	42	1.62 , 1.65	2.69
5	44	3.64 , 3.31	2.63	48	1.81 , 1.50	2.51
7	26	2.57 , 2.38	3.63	27	2.09 , 2.74	3.53
1722+119	36	202.59 , 192.64	2.93	40	1389.46 , 1387.88	2.76
C2	34	1.59 , 2.87	3.04	34	2.70 , 1.82	3.04
C3	36	1.12 , 3.00	2.93	35	1.73 , 1.18	2.98
1	34	1.58 , 1.75	3.04	34	4.22 , 3.43	3.04
5	36	2.23 , 1.37	2.93	40	4.63 , 3.87	2.76
9	36	1.03 , 2.82	2.93	40	2.89 , 1.63	2.76
10	36	1.42 , 1.77	2.93	39	3.25 , 2.28	2.80
1741+597	50	115.13 , 115.12	2.46	56	153.09 , 155.53	2.34
2	50	1.26 , 1.80	2.46	56	2.13 , 3.92	2.34
4	50	1.90 , 1.03	2.46	56	1.05 , 1.07	2.34
5	50	1.31 , 1.69	2.46	56	1.02 , 1.29	2.34
6	50	1.03 , 1.38	2.46	56	1.43 , 2.28	2.34

4. CONCLUSIONS

One of the important properties of AGNs is flux variability. Because of this it is important to monitor flux changes of AGNs which will be used for the link for reference frames Gaia CRF and ICRF. We tested the data (collected for about six years) of some

AGNs which are candidates for the link between the mentioned frames. The test shows that four objects are variable in the V and R bands. The accuracy of photometry will be improved with the higher number of non-variable stars. For that reason we also tested stars from the objects vicinity. The magnitudes of stars which were determined from the observations are in good agreement with the input values for the differential photometry, in line with their standard errors (see Table 2). After implementing the F–test it is concluded that most of the stars (80%) do not have significant changes in brightness, and we consider that they are suitable for photometry. We will continue with observations and investigations of short term changes in brightness of stars and objects. Our plan is also to investigate Intra Day and Long Term object brightness and color variability.

Acknowledgements

During the work on this paper authors were financially supported by the Ministry of Education, Science and Technological Development of the Republic of Serbia through the contract No 451-03-68/2020-14/200002. We gratefully acknowledge the observing grant support from the Institute of Astronomy and Rozhen National Astronomical Observatory, Bulgarian Academy of Sciences, via bilateral joint research projects ″Gaia Celestial Reference Frame (CRF) and fast variable astronomical objects″, and ″Astrometry and photometry of visual double and multiple stars″.

References

Abolfathi, B., Aguado, D. S., Aguilar, G. et al.: 2018, *Astrophys. J., Suppl. Ser.*, **235**, 42.
Bourda, G., Collioud, A., Charlot, P., Porcas, R., Garrington, S.: 2011, *Astron. Astrophys.*, **526**, A102.
Charlot, P., Jacobs, C. S., Gordon, D. et al.: 2020, *Astron. Astrophys.*, **644**, A159.
Chonis, T. S. and Gaskel, M. C.: 2008, *Astron. J.*, **135**, 264.
De Diego, J. A.: 2010, *Astron. J.*, **139**, 1269.
Damljanović, G., Taris, F., Jovanović, M. D.: 2020, *Proceedings of the Journées 2019 "Astrometry, Earth Rotation, and Reference Systems in the GAIA era", Observatoire de Paris, Paris, France, 7-9 October 2019*, Ed. C. Bizouard, pp. 21-26.
Doroshenko, V. T., Efimov, Yu. S., Borman, G. A., Pulatova, N. G.: 2014, *Astrophysics*, **57**, 176.
Fiorucci, M., Tosti, G.: 1996, *Astron. Astrophys., Suppl. Ser.*, **116**, 403.
Gaia Collaboration, Lindegren, L., Klioner, S. A., Hernández, J., et al.: 2020, *Astron. Astrophys.*, **manuscript no. DR3-Astrometry**.
Jovanović M. D.: 2019, *Serb. Astron. J.*, **199**, 55.
Razali, N. M., Wah, Y. B.: 2011, *Journal of Statistical Modeling and Analytics*, **2**, 21.
Taris, F., Souchay, J., Andrei, A. H. et al.: 2011, *Astron. Astrophys.*, **526**, A25.
Smith, P. S., Januzzi, B. T., Elston, R.: 1991, *Astrophys. J., Suppl. Ser.*, **77**, 67.
Tody, D.: 1986, *Proceedings SPIE Instrumentation in Astronomy VI*, ed. D.L. Crawford, **627**, 733.
Tody, D.: 1993, *Astronomical Data Analysis Software and Systems II, A.S.P. Conference Ser.*, eds. R.J. Hanisch, R.J.V. Brissenden and J. Barnes, **52**, 173.
van Dokkum, P. G.: 2001, *PASP*, **113**, 1420.

Publ. Astron. Obs. Belgrade No. 100 (2021), 259 - 266 *Progress Report*

SFC BARYOGENESIS MODEL, INFLATIONARY SCENARIOS AND REHEATING IN THE UNIVERSE

D. KIRILOVA and M. PANAYOTOVA

Institute of Astronomy with NAO Rozhen, Bulgarian Academy of Sciences, 72 Tsarigradsko shose Blvd., Sofia, Bulgaria
E–mail: dani@astro.bas.bg
E–mail: mariana@astro.bas.bg

Abstract. We discuss Scalar Field Baryogenesis Model and its capability to produce the observed baryon asymmetry of the Universe in different inflationary scenarios and for different types of reheating. Interestingly enough among the preferred by SFC baryogenesis models are the Starobinsky inflation model and quintessential inflation model, which are also among the preferred ones by the recent Planck data.

1. INTRODUCTION

Locally, up to galaxy cluster scales our Universe is made of matter. Observational data from cosmic rays and gamma rays point that no significant quantities of antimatter exist up to scales of 10-20 Mpc. (see e.g. Steigman 1976, 2008, Stecker 1985, Ballmoos 2014, Dolgov 2015). It is usually assumed that globally our Universe is also baryon-antibaryon asymmetric. The baryon asymmetry is given by:

$$\beta = (N_b - N_{\bar{b}})/N_\gamma, \tag{1}$$

where N_b is the number of baryons,N_γ - the number of photons. This is to a good approximation $\beta \sim N_b/N_\gamma = \eta$, where η is the baryon-to-photon ratio. η is precisely measured today at two epochs, at BBN and CMB epochs. Namely, η measured by BBN theory and D observations is (see e.g. Pettini, Cooke 2012):

$$\eta_D = 6 \pm 0.3 \times 10^{-10} \text{at } 95\% \text{ C.L.},$$

while η measured by CMB anisotropy data (see e.g. Planck Collab. 2016) is:

$$\eta_{CMB} = 6.11 \pm 0.04 \times 10^{-10} \text{at } 68\% \text{ C.L.}$$

Baryogenesis models have to answer the question how and when in the Universe history this net baryon number has been generated. Alas, at present there are many baryogenesis models, which can successfully produce this number at different epochs in the period after inflation and before BBN. Just to mention the most popular ones: GUT baryogenesis (see e.g. Sakharov 1967, Kuzmin, Rubakov, Shaposhnikov 1985),

SUSY baryogenesis, baryogenesis through leptogenesis (see e.g. Fukugita, Yanagida 1986), Afleck and Dine baryogenesis (see e.g. Affleck, Dine 1985), Scalar Field Condensate baryogenesis (SFC) (see e.g. Dolgov, Kirilova 1990, 1991), etc.

In what follows we discuss SFC baryogenesis model in different inflationary models and for different reheating scenarios. In the next section the SFC baryogenesis model is briefly described. The second section discusses several inflationary models and the popular reheating scenarios. The third section provides the results concerning the baryon asymmetry generation in different inflationary models by SFC baryogenesis and is mainly based on our recent work (Kirilova, Panayotova, 2020b).

2. SFC BARYOGENESIS MODEL

SFC baryogenesis model was first proposed and analytically studied in refs. (see e.g. Dolgov, Kirilova 1990, 1991). The model was appropriate to explain the very large scale structure in the universe and the quasi-periodicity found at very large scales with typical period of 128 h^{-2} Mpc (see the semi-analytical SFC model in e.g. Chizhov, Kirilova 1996, 2000, Kirilova 2003).

Particle creation processes play important role for the determination of the baryon asymmetry produced in that model (see e.g. Dolgov, Kirilova 1990). Precision numerical account for particle creation processes and their role in baryogenesis was provided in refs (see e.g. Kirilova, Panayotova 2014, 2015; Panayotova, Kirilova 2016).

According to the SFC baryogenesis model a complex scalar field φ exists at the inflationary stage, besides the inflaton ψ. Due to quantum fluctuations baryon excess is generated at the inflationary stage and is contained in the condensate of the field $<\varphi>$, namely $B \sim H_I^3$, where B is the baryon charge density and H_I is the value of Hubble parameter at the inflationary stage.

The potential of φ is chosen of the type:

$$U(\varphi) = m^2\varphi^2 + \frac{\lambda_1}{2}|\varphi|^4 + \frac{\lambda_2}{4}(\varphi^4 + \varphi^{*4}) + \frac{\lambda_3}{4}|\varphi|^2(\varphi^2 + \varphi^{*2}). \tag{2}$$

where the mass parameters of the potential $m \ll H_I$, the self-coupling constants λ_i are with values similar to the gauge coupling constant α_{GUT}. The energy density of φ at the inflationary stage is H_I^4, hence

$$\varphi_o^{max} \sim H_I \lambda^{-1/4}, \quad \dot{\varphi_o} = (H_I)^2. \tag{3}$$

As is obvious, this potential contains B-violating terms at large field amplitudes. At later epoch, these terms become negligible, and when φ decays it transfers the B-charge contained in it to the matter particles.

The evolution of $\varphi(t)$ and B(t) from the end of inflation until the decay of $\varphi(t)$ is described by:

$$\ddot{\varphi} + 3H\dot{\varphi} + \frac{1}{4}\Gamma_\varphi\dot{\varphi} + U'_\varphi = 0, \tag{4}$$

$$B = -i(\dot{\varphi}^*\varphi - \dot{\varphi}\varphi^*) \tag{5}$$

where $H = \dot{a}/a$ is the Hubble parameter, $a(t)$ is the scale factor. $\Gamma_\varphi = \alpha\Omega$ is the rate of particle creation, where $\Omega = 2\pi/T$ and T is the period of the field oscillations.

As far as the analytical approach for particle creation process was shown to give up to 2 orders of magnitudes higher values for B in comparison with the exact numerical approach, we have provided numerical account for the particle creation processes. We studied numerically the evolution of $\varphi(t)$ and B(t) in the period after inflation until the B-conservation (BC) epoch developing and executing a computer program in Fortran 77 using Runge-Kutta 4th order method. The system of ordinary differential equations, corresponding to the equation of motion for the real and imaginary part of φ and B contained in it was solved calculating Ω at each step.

We have provided numerical analysis for the evolution of the real and the imaginary components of $\varphi = x + iy$ and for B(t). The parameter range studied was: $H_I = 10^7 - 10^{12}$ GeV, $m = 100 - 1000$ GeV, $\alpha = 10^{-3} - 5 \times 10^{-2}$, $\lambda_1 = 10^{-3} - 5 \times 10^{-2}$, $\lambda_{2,3} = 10^{-4} - 5 \times 10^{-2}$.

In ref.(e.g. Kirilova, Panayotova 2015) we have analyzed over 70 sets of parameters of the model, and for each set we have calculated the final B contained in the condensate $\varphi(t)$ before its decay. The dependence of the produced B on the parameters of the models (namely m, H_I, λ_i and α) were revealed. Namely:

- It was found that B evolution and the final B value decrease with the increase of H_I which is expected since the bigger H_I is, the decrease of β due to particle creation is more efficient.
- The analysis of B dependence on α showed that with increasing α, B evolution becomes shorter and the final B decreases.
- For the dependence on m, we found that B decreases with the increase of the value of m and for big values of H_I this is more clearly expressed.
- B evolution becomes shorter and final B value decreases with increasing λ_1. Possible change of the final B value is within an order of magnitude.
- It was found also that even for small changes of λ_2 and λ_3 the final value of B may differ up to 3 orders of magnitude.

It can be shown that the produced baryon asymmetry in SFC baryogenesis model depends on the baryon excess B, the reheating temperature T_R and the value of the Hubble parameter at the end of inflation H_I. The latter depend on the concrete considered model of inflation and reheating. In the next section we list several popular inflationary models and reheating scenarios.

3. MODELS OF INFLATION AND REHEATING

According to the contemporary cosmological model the universe has experienced a rapid acceleration phase (inflation), followed by reheating, which lead to the standard cosmology radiation dominated phase.

3. 1. INFLATIONARY MODELS

There exist hundreds different models of inflation. Chronologically, the first more semi-realistic inflationary model was proposed by Starobinsky (see e.g. Starobinsky 1980), when he found the solution of Einstein's equations in the presence of curvature

squared terms. In case the curvatures are large, it leads to an effective cosmological constant Λ. The *Starobinsky R^2 inflation model* has a potential as follows:

$$V(\psi) = \Lambda^4 \left(1 - e^{-\sqrt{2/3}\psi/M_{\rm pl}}\right)^2 \tag{6}$$

This model is in agreement with Planck18 data (see e.g. Planck Collab. 2020).

New inflation model or slow-roll inflation model, according to which inflation occurred during the scalar field rolling down a potential energy hill, instead of tunneling out of a false vacuum state, was independently proposed by Linde (see e.g. Linde 1982) and Albrecht and Steinhardt (see e.g. Albrecht, Steinhardt 1982) in 1982.

Chaotic inflationary model was proposed in 1983 (see e.g. Linde 1983, 1985). For its realization neither initial thermal equilibrium nor supercooling and tunneling from the false vacuum is required. This inflationary model is characterized by a single monomial potential

$$V(\psi) = \lambda M_{\rm pl}^4 \left(\frac{\psi}{M_{\rm pl}}\right)^p , \tag{7}$$

where inflation proceeds for $\psi > M_{\rm pl}$. Potentials with $p \geq 2$ are disfavored by the Planck18 data but models with simple linear potentials $p = 1$ or $p = 2/3$ and fractional power monomials are allowed.

One of the most elegant and interesting inflationary models is the model of *quintessential inflation* of Peebles and Vilenkin (see e.g. Peebles, Vilenkin 1999). Using a single scalar field potential:

$$V = \lambda(\psi^4 + M^4), \quad \psi < 0, \tag{8}$$

$$V = \frac{\lambda M^8}{\psi^4 + M^4}, \quad \psi \geq 0. \tag{9}$$

the model provides a unified description for the inflation and the current acceleration stage of the Universe. At $-\psi \gg M$ this is a "chaotic" inflation potential (see e.g. Linde 1983, 1985), at $\psi \gg M$ it is a "quintessence" form, $\lambda = 1 \times 10^{-14}$.

There exist the *hybrid models of inflation* in spontaneously broken supersymmetric (SUSY) grand unified theories described by the potential

$$V(\psi) = \Lambda^4 \left[1 + \alpha_h \log\left(\psi/M_{\rm pl}\right)\right], \tag{10}$$

where $\alpha_h > 0$ is a dimensionless parameter. Planck18 data strongly disfavors these inflationary models.

Here we discuss SFC baryogenesis model in the following inflationary models: new inflation (see e.g. Linde 1982, Albrecht, Steinhardt 1982), chaotic inflation (see e.g. Linde 1983), chaotic inflation in SUGRA (see e.g. Nanopoulos, Olive, Srednicki 1983), Shafi-Vilenkin chaotic inflation (see e.g. Shafi, Vilenkin 1984), Starobinsky inflation (see e.g. Starobinsky 1980) and quintessential inflation (see e.g. Peebles, Vilenkin 1999). Preliminary results, for several of these models, were provided recently in ref. (see e.g. Kirilova, Panayotova 2019, Kirilova, Panayotova 2020). Here we present also the results from ref. (Kirilova, Panayotova 2020b).

3. 2. REHEATING

Different scenarios of reheating process are considered in literature. Historically the first scenario of reheating discussed the perturbative decay of the inflaton ψ to fermions (see e.g. Dolgov, Kirilova 1990, Traschen, Brandenberger 1990).

In case this decay is followed by instantaneous reheating, i.e. an instantaneous conversion of the inflaton energy at the end of inflation into radiation and furthermore efficient thermalization of the decay products, it is easy to estimate the reheating temperature T_R.

$$T_R = (90/32\pi^3 g_*)^{1/4}(M_{Pl}\Gamma)^{1/2}, \tag{11}$$

where $g_* \sim 10^2$, $T_R \sim 0.1(M_{Pl}\Gamma)^{1/2}$. Then for $\Gamma = 2H$, $T_R < 10^9$ GeV (see e.g. Kofman, Linde, Starobinsky 1994, 1997).

It is possible, however, and at present it is commonly accepted, that reheating proceeded more rapidly, usually called *preheating*. In the pioneer works (see e.g. Dolgov, Kirilova 1990, Kofman, Linde, Starobinsky 1994, Boyanovski 1995) it was found that the decay of ψ may proceed non-perturbatively into bosons due to broad resonance. In such case the reached temperatures are much higher, $T_R \sim 10^{12}$ GeV.

However, if thermalization is delayed (due to small ψ couplings $\alpha_\psi \sim 10^{-11}$ and/or big m_ψ) - smaller T_R can result. For detail consideration of the different possibilities for thermalization (see e.g. Mazumdar, Zaldivar 2014, Moghaddam 2017).

We have considered different types of thermalization and scenarios for reheating applicable to the studied inflationary models.

4. BARYON ASYMMETRY GENERATED IN DIFFERENT INFLATIONARY MODELS

As a result of the numerical analysis of several studies (see e.g. Kirilova, Panayotova 2019, Kirilova, Panayotova 2020, Kirilova, Panayotova 2020b) we have found that SFC baryogenesis model produces baryon asymmetry by orders of magnitude bigger than the observed one for $T_R \sim 10^{12}$ GeV for the following inflationary models: new inflation (see e.g. Linde 1982, Albrecht, Steinhardt 1982), new inflation model by Shafi and Vilenkin (see e.g. Shafi, Vilenkin 1984), MSSM inflation (see e.g. Ferrantelli 2017), chaotic inflation (see e.g. Linde, 1985, 1990), simplest Shafi-Vilenkin chaotic inflationary model.

For these models SCF baryogenesis needs strong diluting mechanisms in order to reduce the resultant baryon excess at low energies to its observational value today.

SFC baryogenesis model predicts close to the observational value of the baryon asymmetry in the following inflationary models: Modified Starobinsky inflation (see e.g. Kofman, Linde, Starobinski 1985) for $T_R \sim 10^9$ GeV, Chaotic inflation in SUGRA (see e.g. Nanopoulos, Olive, Srednicki 1983), chaotic inflationary model for $T_R \sim 10^9$ GeV, and Quintessential inflation (see e.g. Salo, Haro 2017) for $T_R \sim 10^5$ GeV, see Table 1.

In the table we present the results for these inflationary models. The second column gives the H_I and T_R parameter values of the considered inflationary models, the next columns provide the parameter sets of the SFC baryogenesis model for which the baryon asymmetry close to the observed one is produced, namely the model parameters - the mass of the scalar field m, α, the self-coupling constants λ_i and the value of the produced baryon asymmetry β.

Table 1: Production of baryon asymmetry value for particular sets of SFC model parameters in different inflationary scenarios

Starobinsky Inflation	$H_I = 10^{11}$ GeV; $T_R = 10^9$ GeV	$\lambda_1 = \alpha = 5 \times 10^{-2}$, $\lambda_2 = \lambda_3 = 10^{-2}$, $m = 100$ GeV, $\beta = 9.3 \times 10^{-10}$	$\lambda_1 = \alpha = 5 \times 10^{-2}$, $\lambda_2 = \lambda_3 = 10^{-2}$, $m = 200$ GeV, $\beta = 1.7 \times 10^{-9}$	$\lambda_1 = \alpha = 5 \times 10^{-2}$, $\lambda_2 = \lambda_3 = 10^{-2}$, $m = 350$ GeV, $\beta = 1.5 \times 10^{-9}$
	$H_I = 10^{12}$ GeV; $T_R = 10^9$ GeV	$\lambda_1 = \alpha = 10^{-2}$, $\lambda_2 = \lambda_3 = 10^{-3}$, $m = 350$ GeV, $\beta = 2.1 \times 10^{-9}$	$\lambda_1 = 5 \times 10^{-2}$, $\alpha = 10^{-2}$, $\lambda_2 = \lambda_3 = 10^{-3}$, $m = 500$ GeV, $\beta = 2.6 \times 10^{-9}$	$\lambda_1 = 5 \times 10^{-2}$, $\alpha = 3 \times 10^{-2}$, $\lambda_2 = \lambda_3 = 10^{-3}$, $m = 350$ GeV, $\beta = 6.6 \times 10^{-10}$
		$\lambda_1 = \alpha = 5 \times 10^{-2}$, $\lambda_2 = \lambda_3 = 10^{-3}$, $m = 350$ GeV, $\beta = 8.0 \times 10^{-10}$	$\lambda_1 = \alpha = 5 \times 10^{-2}$, $\lambda_2 = \lambda_3 = 10^{-2}$, $m = 350$ GeV, $\beta = 1.2 \times 10^{-10}$	
Quintessential Inflation	$H_I = 10^{12}$ GeV; $T_R = 2 \times 10^5$ GeV	$\lambda_1 = \alpha = 10^{-3}$, $\lambda_2 = \lambda_3 = 10^{-4}$, $m = 350$ GeV, $\beta = 4.3 \times 10^{-9}$	$\lambda_1 = 5 \times 10^{-3}$, $\alpha = 10^{-3}$ $\lambda_2 = \lambda_3 = 10^{-4}$, $m = 350$ GeV, $\beta = 4.6 \times 10^{-10}$	$\lambda_1 = 10^{-2}$, $\alpha = 10^{-3}$ $\lambda_2 = \lambda_3 = 10^{-4}$, $m = 350$ GeV, $\beta = 7.8 \times 10^{-10}$
		$\lambda_1 = 10^{-2}$, $\alpha = 10^{-3}$, $\lambda_2 = \lambda_3 = 10^{-3}$, $m = 350$ GeV, $\beta = 1.2 \times 10^{-9}$	$\lambda_1 = 10^{-2}$, $\alpha = 10^{-3}$ $\lambda_2 = \lambda_3 = 5 \times 10^{-3}$, $m = 350$ GeV, $\beta = 1.8 \times 10^{-10}$	$\lambda_1 = 3 \times 10^{-2}$, $\alpha = 10^{-3}$ $\lambda_2 = \lambda_3 = 10^{-4}$, $m = 350$ GeV, $\beta = 7.0 \times 10^{-9}$
		$\lambda_1 = 5 \times 10^{-2}$, $\alpha = 10^{-3}$, $\lambda_2 = \lambda_3 = 10^{-4}$, $m = 350$ GeV, $\beta = 1.1 \times 10^{-9}$		
Chaotic Inflation in SUGRA	$H_I = 10^{11}$ GeV; $T_R = 1.9 \times 10^9$ GeV	$\lambda_1 = \alpha = 5 \times 10^{-2}$, $\lambda_2 = \lambda_3 = 10^{-2}$, $m = 100$ GeV, $\beta = 1.8 \times 10^{-9}$	$\lambda_1 = \alpha = 5 \times 10^{-2}$, $\lambda_2 = \lambda_3 = 10^{-2}$, $m = 200$ GeV, $\beta = 3.3 \times 10^{-9}$	$\lambda_1 = \alpha = 5 \times 10^{-2}$, $\lambda_2 = \lambda_3 = 10^{-2}$, $m = 350$ GeV, $\beta = 2.8 \times 10^{-9}$
Chaotic Inflation, Efficient Thermalization	$H_I = 10^{12}$ GeV; $T_R = 6.2 \times 10^9$ GeV	$\lambda_1 = 5 \times 10^{-2}$, $\alpha = 3 \times 10^{-2}$, $\lambda_2 = \lambda_3 = 10^{-3}$, $m = 350$ GeV, $\beta = 4.1 \times 10^{-9}$	$\lambda_1 = \alpha = 5 \times 10^{-2}$, $\lambda_2 = \lambda_3 = 10^{-3}$, $m = 350$ GeV, $\beta = 5.0 \times 10^{-9}$	$\lambda_1 = \alpha = 5 \times 10^{-2}$, $\lambda_2 = \lambda_3 = 10^{-2}$, $m = 350$ GeV, $\beta = 7.4 \times 10^{-10}$
Chaotic Inflation, Delayed Thermalization	$H_I = 10^{12}$ GeV; $T_R = 4.5 \times 10^8$ GeV	$\lambda_1 = 10^{-2}$, $\alpha = 10^{-2}$, $\lambda_2 = \lambda_3 = 10^{-3}$, $m = 350$ GeV, $\beta = 9.5 \times 10^{-10}$	$\lambda_1 = 5 \times 10^{-2}$, $\alpha = 10^{-2}$ $\lambda_2 = \lambda_3 = 10^{-3}$, $m = 350$ GeV, $\beta = 4.5 \times 10^{-9}$	$\lambda_1 = 5 \times 10^{-2}$, $\alpha = 10^{-2}$ $\lambda_2 = \lambda_3 = 10^{-3}$, $m = 500$ GeV, $\beta = 1.2 \times 10^{-9}$
		$\lambda_1 = 5 \times 10^{-2}$, $\alpha = 3 \times 10^{-2}$, $\lambda_2 = \lambda_3 = 10^{-3}$, $m = 350$ GeV, $\beta = 3.0 \times 10^{-10}$	$\lambda_1 = 5 \times 10^{-2}$, $\alpha = 5 \times 10^{-2}$ $\lambda_2 = \lambda_3 = 10^{-3}$, $m = 350$ GeV, $\beta = 3.6 \times 10^{-10}$	

It is remarkable that from the results for successful production of the baryon asymmetry value in case of Starobinsky, chaotic and SUGRA inflationary scenarios

for $T_R \in [4.5 \times 10^8 - 6.2 \times 10^9]$ GeV and $H_I \in [10^{11}, 10^{12}]$ GeV, the SFC parameters can be determined. Namely they should lie within the following ranges: $m \sim 350$ GeV (with one exception) $\alpha \in [10^{-2}, 5 \times 10^{-2}]$, $\lambda_1 \sim 5.10^{-2}$, $\lambda_{2,3} \in [10^{-3}, 10^{-2}]$. Fixing the inflationary model we can set the parameters of the SFC baryogenesis model, for illustration see Fig. 1 in Kirilova & Panayotova (2020b).

In case of quintessential inflation, however, for $H_I \sim 10^{12}$ GeV and $m \sim 350$ GeV, the reheating temperature and the rest of the SFC parameters - the coupling constants, are much lower $T_R \sim 2.10^5$ GeV, $\alpha \sim 10^{-3}$, $\lambda_1 \in [5.10^{-3}, 10^{-2}]$, $\lambda_{2,3} \in [10^{-4}, 5.10^{-3}]$.

5. CONCLUSIONS

We discuss Scalar Field Condensate Baryogenesis Model and its capability to produce the observed baryon asymmetry of the Universe in different inflationary scenarios and for different types of reheating.

On the basis of the numerical analysis of the evolution of the baryon charge produced in SFC baryogenesis model and the estimation of the produced baryon asymmetry for different sets of models parameters and different reheating temperatures of several inflationary scenarios we have shown that baryon asymmetry close to the observed one is generated in the modified Starobinsky inflation, chaotic inflationary scenario (delayed thermalization), chaotic inflation in SUGRA and Quintessential inflation. In new inflationary scenario, chaotic inflation with high reheating temperatute and MSSM inflation baryon asymmetry is strongly overproduced by several orders of magnitude.

It is noticeable that Starobinsky inflationary scenario and the quintessential inflation are also among the preferred scenarios by the latest Planck CMB data analysis constraints on inflationary models.

Acknowledgments

We thank the unknown referee for the useful comments. We are grateful to the organizers for the nice organization of the conference and the inspiring atmosphere. The authors acknowledge the partial financial support by project DN18/13-12.12.2017 of the Bulgarian National Science Fund of the Bulgarian Ministry of Education and Science.

References

Ade, P., et.al. [Planck Collaboration]: 2016, *Astron. Astrophys.*, **594**, A13.
Affleck, I., Dine, M.: 1985, *Nucl. Phys. B*, **249**, 361.
Aghanim, N. et.al. [Planck Collaboration]: 2020, *Astron. Astrphys.*, **.**641, A6.
Albrecht, A., Steinhardt, P.: 1982, *Phys. Rev. Lett.*, **48**, 1220.
Ballmoos, P.: 2014, *Hyperfine Interact.*, **228**, 91.
Boyanovsky, D. et al.: 1995, *PRD*, **52**, 6805, 1995, *PRD*, **51**, 4419.
Chizhov, M., Kirilova, D.: 1996, *AATr*, **10**, 69.
Dolgov, A.: 2015, *EPJ Web of Conferences*, **95**, 03007.
Dolgov, A., Kirilova, D.: 1990 *Sov. J. Nucl. Phys.*, **51**, 172.
Dolgov, A., Kirilova, D.: 1991, *J. Moscow Phys. Soc.*, **1**, 217.
Ferrantelli, A.: 2017, *Eur. Phys. J. C*, **77**, 716.

Fukugita, M., Yanagida, T.: 1986, *Phys. Lett. B*, **174**, 45.
Haro, J., Amoros, J., Pan, S.: 2019, *Eur. Phys. J. C*, **79**, 505.
Kirilova, D.: 2003, *Nuclear Physics B - Proceedings Supplements*, **122**, 404.
Kirilova, D., Panayotova, M.: 2014, *BAJ*, **20**, 45.
Kirilova, D., Panayotova, M.: 2015, *Advances in Astronomy*, 465.
Kirilova, D., Panayotova, M.: 2019 *AIP Conf. Proc. 2075*, **1**, 090017.
Kirilova, D., Panayotova, M.: 2020, *Proceedings of the XII Serbian-Bulgarian Astronomical Conference, Sokobanja, Serbia, September 25-29, 2020, Publ. Astron. Soc. "Rudjer Boskovic"*, **N20**, 39.
Kirilova, D., Panayotova, M.: 2020b, Scalar Field Condensate Baryogenesis Model in Different Inflationary Scenarios, e-print arXiv:2012.05555, 11 Dec 2020.
Kofman, L., Linde, A., Starobinski, A.: 1985, *Phys. Lett. B*, **157**, 36.
Kofman, L., Linde, A., Starobinski, A.: 1994, *Phys. Rev. Lett.*, **73**, 3195.
Kofman, L., Linde, A., Starobinski, A.: 1997, *Phys. Rev. D*, **56**, 3258.
Kuzmin, V., Rubakov, V., Shaposhnikov, M.: 1985, *Phys. Rev. Lett.* **84**, 3756.
Linde, A.: 1982, *Phys. Lett. B*, **108**, 389.
Linde, A.: 1983, *Phys. Lett. B*, **129**, 177, 1985, *Phys. Lett. B*, **162**, 281.
Linde, A.: 1990, Particle Physics and Inflationary Cosmology.
Mazumdar, A., Zaldivar, B.: 2014, *Nuclear Physics B*, **886**, 312.
Moghaddam, H.: 2017, PhD thesis "Reheating in the Early Universe Cosmology".
Nanopoulos, D., Olive, K., Srednicki, M.: 1983, *Phys.Lett. B*, **127**, 30.
Panayotova, M., Kirilova, D.: 2016, *Bulg. J. Phys.*, **43**, 320.
Peebles, P., Vilenkin, A.: 1999, *Phys.Rev. D*, **59**, 063505.
Pettini, M., Cooke, R.: 2012, *Mon.Not.Roy.Astron.Soc.*, **425**, 2477.
Sakharov, A.: 1967, *JETP*, **5**, 32.
Salo, L., Haro, J.: 2017, *Eur. Phys. J. C*, **77**, 798.
Shafi, O., Vilenkin, A.: 1984, *Phys. Rev. Lett.*, **52**, 691.
Starobinsky, A.: 1980, *Phys. Lett. B*, **91**, 99.
Stecker, F.: 1985, *Nucl. Phys. B*, **252**, 25.
Steigman, G.: 1976, *Ann. Rev. Astron. Astrophys.*, **14**, 339.
Steigman, G.: 2008, *J. Cosmol. Astropart. Phys.*, **0910**, 001.
Traschen, J., Brandenberger, R.: 1990, *PRD*, **42**, 2491.

Publ. Astron. Obs. Belgrade No. 100 (2021), 267 - 273 *Progress Report*

USING BALMER LINES TO UNVEIL THE PRESENCE OF COSMIC RAYS IN THE SUPERNOVA REMNANT SNR 0509-67.5

S. KNEŽEVIĆ[1], G. MORLINO[2], R. BANDIERA[2], S. SCHULZE[3], G. VAN DE VEN[4] and J. C. RAYMOND[5]

[1] *Astronomical Observatory, Volgina 7, 11000 Belgrade, Serbia*
E–mail: sknezevic@aob.rs.

[2] *INAF - Observatorio Astrofisico di Arcetri, Largo E. Fermi 5,I-50125 Firenze, Italy*

[3] *The Oskar Klein Centre, Department of Physics, Stockholm University, AlbaNova, SE-106 91 Stockholm, Sweden*

[4] *Department of Astrophysics, University of Vienna, Türkenschanzstrasse 17, 1180 Vienna, Austria*

[5] *Harvard-Smithsonian Center for Astrophysics, 60 Garden Street, Cambridge, MA, 02138, USA*

Abstract. We present spectroscopic observations of the supernova remnant SNR 0509-67.5 in the Large Magellanic Cloud. We used the integral field-unit MUSE on the Very Large Telescope to spectrally and spatially resolve the fast Balmer shocks around the remnant. We show some preliminary results of the resolved broad Hα-line component, whose width indirectly provides the temperature of the shocked plasma. By coupling this information with the shock speed recently determined by proper motion measurements, we can infer the total amount of energy transformed into cosmic rays in case of their presence. In addition, by comparing monochromatic images of the observed field at various wavelengths, we report a discovery of an object located in the direction of SNR 0509-67.5 that was not observed/reported before.

1. INTRODUCTION

Supernova remnants (SNRs) are widely believed to be the sources of cosmic rays (CRs), the most energetic particles observed on Earth. Direct evidence of CR proton acceleration up to $\sim 10^{15}$ eV energies is still missing, as well as the shock acceleration efficiency, i.e. the amount of energy that SNRs convert into CRs. The acceleration efficiency typically required for SNRs to be the sources of CRs is $\sim 10\%$ (Bykov et al. 2018). In case of efficient acceleration and as a consequence of momentum and energy conservation, the temperature of the plasma behind the shock should be lower than in the case of no acceleration. Moreover, the dynamical reaction of accelerated particles on the background plasma induces the formation of a precursor upstream of the shock (see e.g. Malkov & Drury 2001).

Collisionless shocks propagating through a partially neutral interstellar medium (ISM) have a characteristic spectral signature in the form of Balmer lines among which the Hα line is the brightest. Its characteristic double-component profile reveals

the conditions in the ISM and the shock itself. Post-shock protons interact with pre-shock neutrals overrun by the shock in two ways. In the process of excitation a narrow-line component (width $\sim 10\,\mathrm{km\,s^{-1}}$ reflecting the temperature in front of the shock) is produced, while a broad component (width $\sim 1000\,\mathrm{km\,s^{-1}}$ corresponding to the temperature of immediate post-shock protons[1]) is produced in charge-exchange process (Chevalier & Raymond 1978). The width of the broad component can be used to infer the shock acceleration efficiency, while the width of the narrow component and the narrow-to-broad intensity ratio provide the information on the maximum energy of accelerated particles and the amount of CR heating in the shock precursor (Blasi et al. 2012, Morlino et al. 2012, Morlino et al. 2013).

Some Balmer SNRs seem to be efficient CR accelerators. One of them is SNR 0509-67.5 in the Large Magellanic Cloud (LMC) that shows indication of particle acceleration in the southwestern (SW) region (Smith et al. 1994, Helder et al. 2010). The distance to the LMC is well known and proper motion studies (Hovey et al. 2015) measured the average shock speed of $6500 \pm 200\,\mathrm{km\,s^{-1}}$ (with a peak speed of around $8000\,\mathrm{km\,s^{-1}}$ at some positions). Having an independent shock velocity estimate makes the SNR 0509-67.5 a good candidate for studying CR acceleration, since we know what broad-component widths we can expect in CR absence scenario.

2. DATA ANALYSIS AND RESULTS

2. 1. OBSERVATIONS & DATA REDUCTION

Previous studies (Helder et al. 2010) used long slits to extract profiles from two locations in SNR 0509-67.5. Those observations lack the sensitivity to detect the very faint broad component in the northeastern (NE) region and the spectrum in the SW rim covered the region of multiple shock filaments with different speeds which interpretation cannot unambiguously point towards CR acceleration. Here we present observations with the Multi Unit Spectroscopic Explorer (MUSE) instrument at the ESO Very Large Telescope that we obtained in November and December 2017 and January 2018 (total integration time of 3 hours and good seeing conditions of $1''$). MUSE's large field of view (FOV) of $1' \times 1'$ covers the entire SNR 0509-67.5 (diameter $\approx 30''$). Thanks to its high spatial resolution of $0.2''$/pix, we can trace different shock filaments and resolve the geometric effects. MUSE's high sensitivity enables detection of very faint broad component in the NE rim. The narrow component cannot be resolved with the MUSE spectral resolution power of 3000 at Hα. The spectral range covered was 4750-9350 Å.

The data were reduced using the MUSE pipeline recipes version 2.4.2 and following the standard reduction procedure. We did not take sky exposures, but created a sky model from the region free from remnant (including its interior) and stellar emission. This region was further sampled so that only the faintest parts were used by the pipeline for sky model estimation. The entire FOV is crowded with stars (Figure 1) whose emission affects spectra at some locations on the remnant. To clean the spectral features of the stars on the observed Hα-line profiles, we applied the following stellar subtraction method. We created two off-line stellar images collapsing the

[1]For a gas emitting a thermal, Gaussian-shaped line, the line width relates to the temperature as $W \sim T^{1/2}$. The shock heats up the impacted material to a temperature $T \sim V_{\mathrm{sh}}^2$ (jump conditions). For the assumption of a monoatomic, non-relativistic gas the broad-component width relates to the shock speed as $W \sim V_{\mathrm{sh}}$.

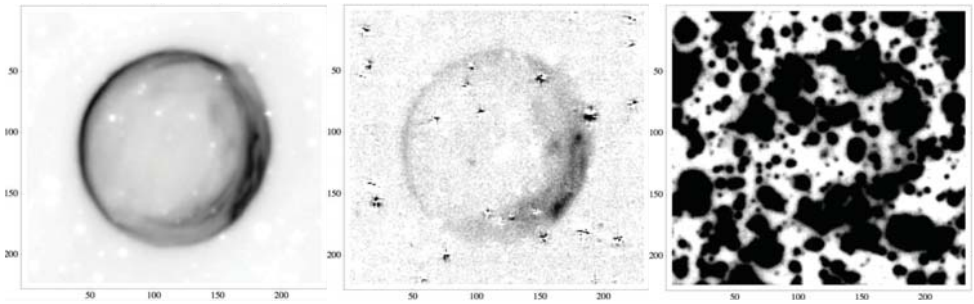

Figure 1: MUSE observations of SNR 0509-67.5: narrow-component map (left), broad-component map (middle) and broad component before stellar subtraction (right).

datacube around certain wavelength (velocity) channels; one from -20 000 km s^{-1} to -8000 km s^{-1} and the other from 8000 km s^{-1} to 20 000 km s^{-1} (the narrow Hα component is centered at zero velocity). The ranges were chosen to avoid the contamination from the broad Hα component. To minimize biases due to the presence of remnant's emission we have masked out all pixels in the area occupied by the SNR. Every datacube channel was then fitted with a linear combination of the two stellar images plus a constant, where χ^2 minimization was done over all unmasked pixels. Coefficients of stellar images contribution were smoothed by a second-order polynomial fits applied to their wavelength trends excluding 20% of the coefficients deviating the most from the fits. The so-created sky- and stellar-subtracted datacube is used further in the analysis.

2. 2. RESULTS ON SNR 0509-67.5

The geometry of the NE rim shows an almost perfect spherical symmetry. We extracted line profiles (Figure 2) from 0.2″ wide circular arcs in the region with position angle in the range (45°, 105°) and distance from the remnant's center in the range (13.6″, 15.7″). We fit double-Gaussian profiles to the Hα profiles and extract surface brightness, width of the broad component, and its offset with respect to the narrow-component centroid. In order to explain the radial profiles of the observables, we have used the following geometric model: the emission is confined to a spherical thin shell located at a radial distance $r_{\rm sh}$ from the remnant's center. The broad-line component is modelled taking into account the thermal velocity dispersion ($\sigma_{\rm vel}$) and the radial bulk velocity ($V_{\rm bulk}$) of the shocked medium. Finally, the model allows for a gradient of the logarithm of the neutral density in the ambient medium. The best fit solution is found for $r_{\rm sh} \approx 15.4''$, $\sigma_{\rm vel} \approx 1500$ km s^{-1}, $V_{\rm bulk} \approx 3000$ km s^{-1} and a density gradient with components $+6.5 r_{\rm sh}^{-1}$ in the projected radial direction and $-0.85 r_{\rm sh}^{-1}$ along the line-of-sight. This suggests that a strong local gradient of neutrals in the NE rim is present. The post-shock bulk velocity is ≈ 3000 km s^{-1} that, following the classical jump relations for a strong shock, would imply a shock velocity ≈ 4000 km s^{-1}, smaller than that derived from proper motions. We need to further investigate whether this smaller speed might be a consequence of the velocity dependence on charge-exchange processes so that the mean velocity of neutrals, the ones created in these processes and responsible for the production of broad component, may be significantly different from that of the ions.

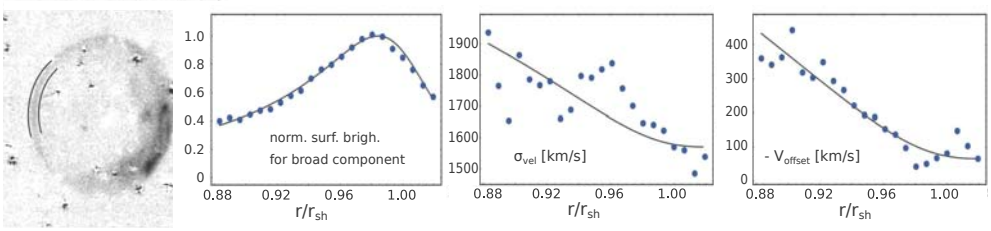

Figure 2: Geometry of the NE rim. Selected region at position angles (45°,105°) and radius (13.6″, 15.7″) from where the line profiles of 0.2″ wide circular arcs were extracted (first panel). Radial profiles of the measured broad-component surface brightness, width and its offset from the narrow-component centroid (second, third and fourth panels). Blue dots are data and black line is the best-fit model.

In addition to profiles in the NE rim, we mapped the Hα profiles all around the remnant at the locations for which the proper motion was measured and presented in the paper Hovey et al. (2015). For the known heliocentric distance of 50 ± 1 kpc to the LMC, these authors estimate a shock velocity of $\approx 6500\,\mathrm{km\,s^{-1}}$ on average all around the remnant. In the left panel of Figure 3 we show a spectrum from nearly the same location in the NE region as observed by Helder et al. (2010) using long slit where the broad component was not resolved. We show that the MUSE data resolved the broad line (FWHM = 3740 ± 210 $\mathrm{km\,s^{-1}}$) successfully even though the broad-to-narrow intensity ratio is 0.06. In the middle panel we show the measured broad-line widths as a function of a position angle. We managed to recover 38 out of 44 Hovey et al. (2015) locations (other segments were significantly affected by a nearby star or signal-to-noise (S/N) was very low to resolve broad component). In the right panel we show measured broad-line widths as a function of a shock velocity and

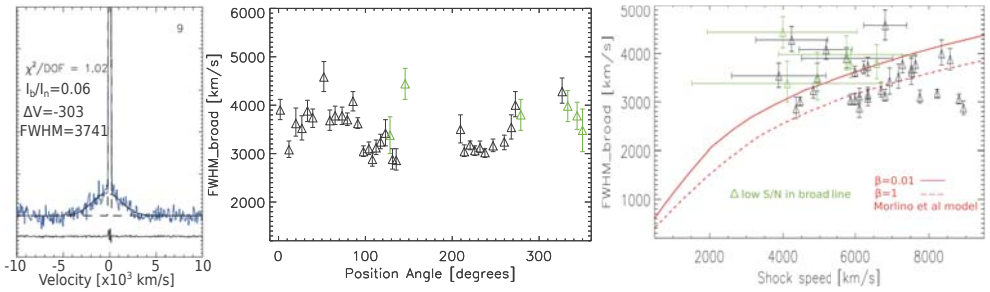

Figure 3: Hα profiles in SNR 0509-67.5. Left panel: spectrum in the NE region (blue line) fitted with double Gaussian (black lines). We measure a broad-to-narrow intensity ratio (I_b/I_n = 0.06 ± 0.01), velocity offset (ΔV = -303 ± 75 $\mathrm{km\,s^{-1}}$) and broad-component width (FWHM = 3740 ± 210 $\mathrm{km\,s^{-1}}$). Middle panel: measured broad-line widths as a function of a position angle. Right panel: measured broad-line widths as a function of a shock velocity together with Morlino et al. (2013) shock model prediction in case of no CRs. Green points are the locations with resolved broad-line component, but with too low S/N to accurately measure parameters.

compare the Morlino et al. (2013) shock model predictions for different electron-to-proton equilibration levels (β), where $\beta = 1$ is full equilibration. The model prediction shown here is without CR acceleration. Any point between the two red lines can be explained without invoking presence of very energetic particles, but the points below the $\beta = 1$ line (dashed line) need some CR physics to be understood. In theory the graph can be populated above the β=0.01 line, but some data points have either uncertain line-parameter estimates or large shock velocity error bars.

2. 3. DETECTION OF A NEW SOURCE

We detected several new sources in the MUSE FOV. One of them is a background object in the SNR field at around RA = 05^{h}:09^{m}:35^{s}.45 and DEC = -67°:31′:15″.02. It is bright at 6333 Å (see Figure 4), but also at 7373 Å, 8258 Å, 8423 Å and 8505 Å (see the spectrum in Figure 5). The object was not previously reported in any catalog. We used Manual and Automatic Redshift Software (Marz; Hinton et al. 2016) to measure the redshift and identify the nature of the object. Before running Marz we cleaned the red part of the spectrum, that is significantly affected by sky residuals, performing principal component analysis with the Zurich Atmosphere Purge (ZAP) code (Soto et al. 2016). Marz uses 12 template spectra: 5 stellar, 6 galactic and 1 AGN template. The best match was found for a high redshift star forming galaxy at redshift 0.69866, where the above mentioned lines 6333 Å, 7373 Å, 8258 Å, 8423 Å, 8505 Å were identified as [OII], Hγ, Hβ, [OIII], [OIII] lines, respectively.

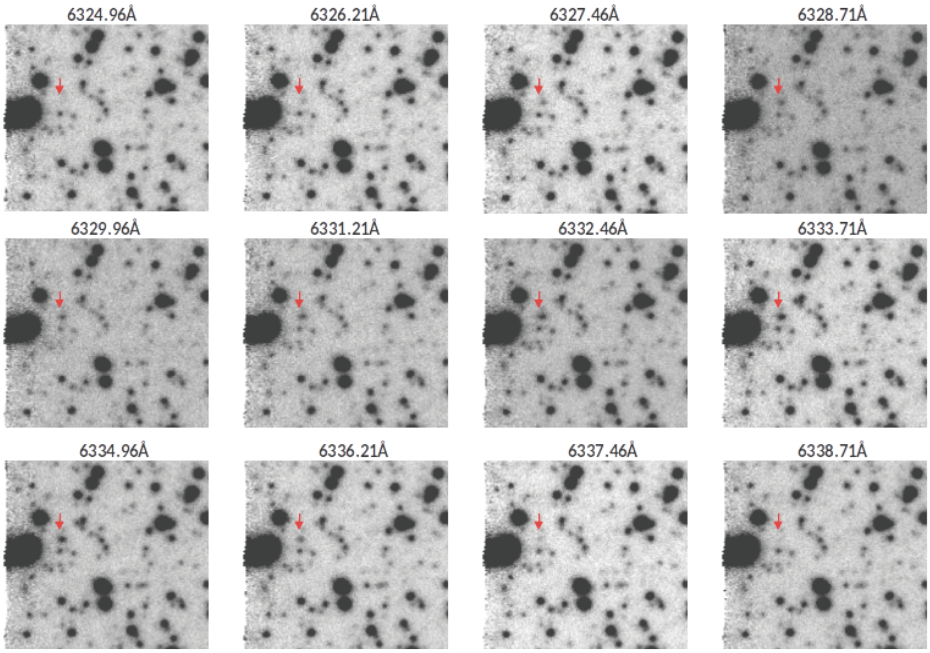

Figure 4: Detected object: Twelve consecutive wavelength-channel images showing the appearance of an object (below the red arrow).

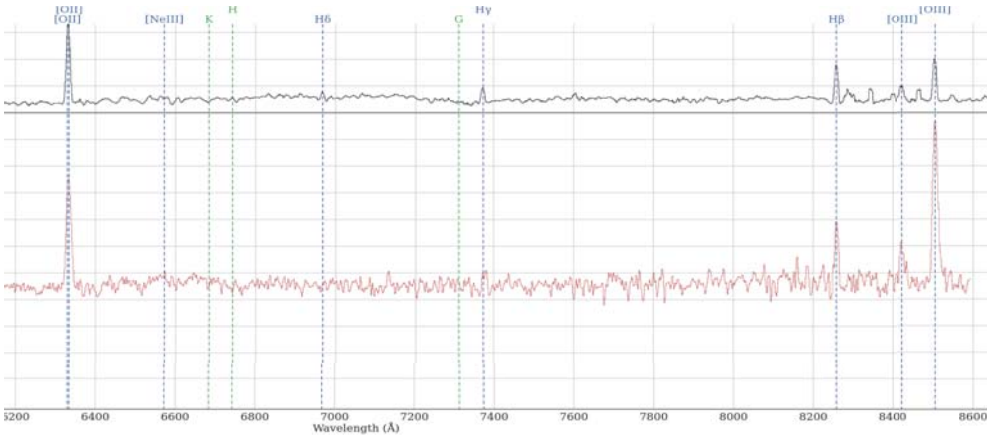

Figure 5: Spectrum of the new source (black line) compared with the template (red line) from Marz software which we used to estimate the redshift and identify the nature of the source. Best match was for high redshift star forming galaxy at z=0.69866.

3. SUMMARY

We presented MUSE observations of the supernova remnant SNR 0509-67.5 in the LMC. Fast Balmer shocks around the remnant were spectrally and spatially resolved due to the instrument's high sensitivity, large FOV and small spatial sampling. We showed the preliminary results of the resolved broad Hα-line component. First results on the shock geometry in the NE region indicate that spherical thin layer model with high neutral density gradients can account for the observed radial trends in the broad-component parameters, but with a lower shock velocity then suggested from proper motions. In addition, we showed that some broad-component widths around the remnant need CR physics to be explained. We are working on combining shock geometry and shock models to interpret the observed line profiles. Finally, we report a discovery of a new object in the FOV that seems to be a galaxy at redshift ≈ 0.7.

Acknowledgements

S. Knežević is supported by the Ministry of Education, Science and Technological Development of the Republic of Serbia through the contract number 451-03-9/2021-14/200002.

References

Blasi, P., Morlino, G., Bandiera, R., Amato, E., Caprioli, D.: 2012, *ApJ*, **755**, 121.
Bykov, A. M., Ellison, D. C., Marcowith, A., Osipov, S. M.: 2018, *Space Sci. Rev.*, **214**, 41.
Chevalier, R. A., Raymond, J. C.: 1978, *ApJ*, **225**, L27.
Helder, E. A., Kosenko, D., Vink, J.: 2010, *ApJ*, **719**, L140.
Hinton, S. R., Davis, T. M., Lidman, C. et al.: 2016, *Astronomy and Computing*, **15**, 61.
Hovey, L., Hughes, J. P., Eriksen, K.: 2015, *ApJ*, **809**, 119.
Malkov, M. A., Drury, L. OC: 2001, *Rep. Prog. Phys.*, **64**, 429.

Morlino, G., Bandiera, R., Blasi, P., Amato, E.: 2012, *ApJ*, **760**, 137.
Morlino, G., Blasi, P., Bandiera, R., Amato, E.: 2013, *ApJ*, **768**, 148.
Smith, R. C., Raymond, J. C., Laming, J. M.: 1994, *ApJ*, **420**, 286.
Soto, K. T., Lilly, S. J., Bacon, R., Richard, J., Conseil, S.: 2016, *MNRAS*, **458**, 3210.

Publ. Astron. Obs. Belgrade No. 100 (2021), 275 - 280 *Progress Report*

COMPUTER VISION AS A TOOL FOR STUDYING CLOSE BINARY STARS

OLIVERA LATKOVIĆ and ATILA ČEKI
Astronomical Observatory, Volgina 7, 11000 Belgrade, Serbia
E–mail: olivia@aob.rs

Abstract. Computer vision is a subfield of artificial intelligence that deals with automated detection and classification of objects from images, used in a variety of advanced applications, from facial recognition to self-driving cars. While other machine learning methods have gained a strong footing in astronomy over the last several years, computer vision is still a relatively rare and novel approach. We have been experimenting with this technique in the context of eclipsing binary stars, with the aim to automate the analysis of photometric time-series data from ground- and space-based surveys. The current and future deluge of such data requires the automation of as many tasks as possible, otherwise much of it will remain unutilized. Computer vision might be used to estimate the stellar and orbital parameters of eclipsing binaries based on the images of their light curves. As proof-of-concept, we have already developed a computer vision system for automated recognition of light curves with total eclipses, and demonstrated that a computer can perform this task as well or better than humans.

1. INTRODUCTION

Close binaries, although well studied, are still at the forefront of astrophysics because they allow us to determine the masses, sizes and temperatures of stars based on relatively simple physics. In eclipsing systems, these parameters are traditionally found by light curve modeling. This involves fitting synthetic light curves, generated from a mathematical model parametrized directly by the orbital parameters of the system and the stellar parameters of the components, to the observations. Several such models are in use. The most popular is the so-called "WD Code" (see e.g. Wilson et al. 2020 and the references within), but a quantity of excellent work has also been done with the model developed within our institute, the "Djurasevic code" (Djurašević 1992, Djurašević et al. 1998) which has recently been modernized for automated applications (see e.g. Djurašević et al. 2016, Latković et al. 2019). This is the model we use for the research reported here.

Finding accurate orbital and stellar parameters of an eclipsing binary from a model is possible because they are encoded in the shape of the light curve. For example, the widths and relative depths of eclipses are indicative of the temperatures and sizes of the components, the amplitude of the light curve is related to the orbital inclination, and so forth. However, a critical parameter, the mass ratio, typically cannot be measured from photometry alone, and requires the construction of radial velocity curves, which are in turn obtained from time-series spectroscopy. In the

case of contact binaries, where the components are immersed in a stable, co-rotating common envelope, spectroscopy can be skipped. The shape of the common envelope is determined by a single equipotential Roche surface, which means the mass ratio is strictly constrained by the size ratio, and the size ratio can be obtained from light curve modeling—but only in the presence of a total eclipse (see the contribution of Čeki et al. in these proceedings for a more substantial discussion).

With the work presented here, we aim to automate the selection of totally eclipsing contact binaries from vast light curve archives of ongoing and future ground- and space-based surveys using a machine learning technique—computer vision. Automation of this and other tasks related to the modeling of close binaries is getting more and more important as the amounts of underutilized observations grow. For example, some 30 000 contact binaries were identified in the Catalina Real-Time Transient Survey (CRTS) Variable Star Catalog (Drake et al. 2014); and more than 70 000 in the ASAS-SN Catalog of Variable Stars (Jayasinghe et al. 2020). These samples are already too large to tackle "manually", by traditional examination of individual objects; and yet even larger ones are sure to follow from Gaia, LSST and so forth.

A human astronomer recognizes a total eclipse as a distinct, flat region inside the light minimum by looking at a plot of the light curve. Computer vision encompasses machine learning algorithms that essentially do the same: recognize objects in images. In what follows, we describe the architecture, training and performance of a computer vision system for detection of total eclipses in the light curves of contact binary stars.

2. COMPUTER VISION MODELS FOR AUTOMATED RECOGNITION OF TOTAL ECLIPSES

Computer vision methods are usually based on convolutional neural networks, or CNNs. A CNN reduces the information contained in a matrix of image pixels to a numeric array that can be processed by an ordinary classification algorithm through a series of convolutions with detection filters—low-dimension matrices trained to select visual features such as vertical or horizontal edges, curves and so on.

Like other supervised machine learning algorithms, CNNs learn by processing large numbers of labeled examples. In our case, that would be the images of light curves with either partial or total eclipses. *Unlike* most other machine learning algorithms, CNNs don't need precalculated features to help them discriminate between objects in images. If we wanted to apply an ordinary neural network to light curves as time series, we would have to engineer the features ourselves. This was done in one of the first applications of machine learning in astronomy, for automatic modeling of thousands of eclipsing binaries observed by Kepler: the light curves were first fitted by chain polynomials, and the coefficients of these polynomials were used as features for the neural network (Prša et al. 2011). A CNN learns the features itself by finding statistical patterns in the data.

The simplest of our CNN models has three convolutional layers that transform input images of 32×32 pixels into 2×2×32 volumes, and eventually feature vectors with 128 elements that are fed to a classification layer that resembles an ordinary neural network. Increasingly complex models, with 4, 5 or 6 convolutions, are trained to process larger images (up to 512×512 pixels), with full light curves or eclipse cutouts.

2. 1. GENERATED TRAINING DATA

For training, we use synthetic light curves created using the Djurasevic code. Some examples are given in Fig. 1. We generate equal numbers of light curves with total and partial eclipses. Labels for the generated images (whether the eclipse is total or not) are assigned automatically based on the light contribution of the eclipsed star. The model parameters for generating these light curves (orbital inclination, mass ratio, the size of the primary star relative to orbit size, its effective temperature and the parameters of a single spot) are drawn randomly from distributions derived using a large sample of individually studied W UMa stars (see the contribution of Čeki et al. in these proceedings).

We generate training images with three levels of noise: noiseless (similar to binned Kepler light curves; see Fig. 1), moderate (representative of what we expect from ground-based observations of individual objects) and noisy (similar to what we have seen in the light curves from ASAS, OGLE and CRTS). The noise is drawn from a normal distribution with the standard deviation approximately equal to 2 and 5% of the light curve amplitude in the latter two cases, respectively.

2. 2. TEST DATA AND HUMAN PERFORMANCE

We also use synthetic light curves to validate the model performance by testing it on labeled data that were not used for training, but we test the model on real observations as well. However, here we face another problem: that of the reliability of human classifications and in general, the availability of ground truth.

With generated data we have access to the fluxes of both stars and can determine the true label beyond doubt. But even simulated total eclipses can be made to look like partial ones in a noisy light curve or if there are too few points in the minimum to make out its shape.

To our knowledge, human ability to recognize total eclipses has never been questioned or measured prior to this work. We measured it on synthetic data (for which we could later look up the ground truth). The two of us (Č.A. and L.O.) looked at randomized sets of 500 generated images in two sizes[1] with all three noise levels, and got the results summarized in Table 1. On average, we achieved 97% balanced accuracy[2] on noiseless examples, down to 85% on noisy examples. Meaning that, in the presence of noise, we misclassified 15% of light curves.

Let us see how this compares to computer vision.

[1]This experiment was done in an early stage of the research and the images used for it are of different sizes (250×250 and 350×175 pixels; see also Table 1) than those we currently use (32×32, 64×64, 128×128 pixels, 256×256 and 512×512 pixels). The 250×250 pixel images are not significantly different from the 256×256 pixel or other square images. The 350×175 pixel images are twice as wide as they are tall, which is helpful (for humans) when trying to determine the nature of the eclipses, but has proven to have no notable effect on the performance of the machine learning method. This is why we discontinued their use. The measurement of human performance with updated image shapes and sizes (and hopefully with more human participants) is part of planned future work.

[2]Balanced accuracy is a performance metric often used instead of the ordinary accuracy (that would be the ratio of correct classifications to the sample size) to account for the "class imbalance" expected in observational data. Namely, there are far more light curves with partial than with total eclipses. In the case of Kepler catalog, out of about 300 contact binary light curves, only around 30 (or 10%) show total eclipses (at least as far as we humans can tell). While not as severe as in many other applications of machine learning, this imbalance can affect the performance of our eclipse recognition system in ways we're yet to quantify.

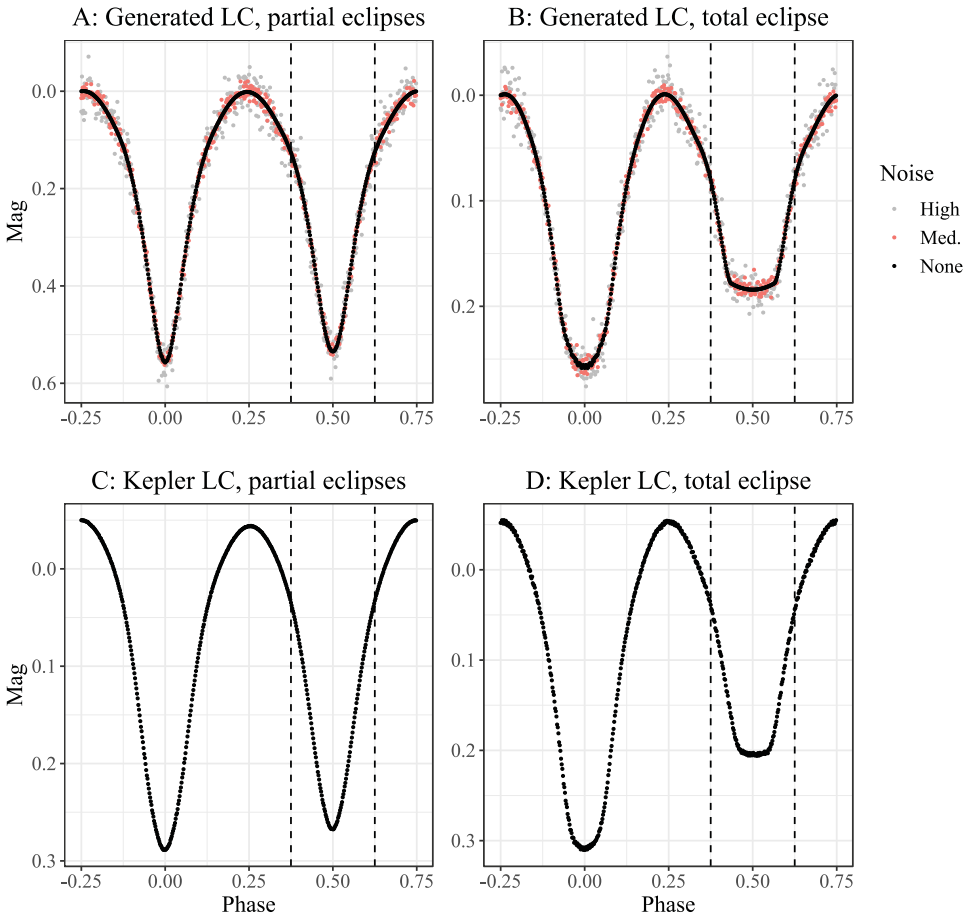

Figure 1: Top – examples of generated light curves with different noise levels and partial (panel A) or total eclipses (panel B). Bottom – examples of binned Kepler light curves, again with partial (panel C, showing data for KIC 10074939) or total eclipses (panel D, showing data for KIC 5022908). These examples are representative of the largest input images (512×512 pixels) used for training and testing of the computer vision algorithm. The vertical dashed lines indicate the phase range for input images with eclipse cutouts (128×128 pixels and smaller).

2. 3. PERFORMANCE OF COMPUTER VISION

Fig. 2A shows how our models fared when evaluated with test data generated the same way as training data. The colors represent different noise levels and the performance obviously declines as the noise increases. The different line types represent images of different sizes; increasing image size moderately improves performance. Finally, from left to right is the size of the training set, starting at 500 and ending at 75 000 training examples. Each set is divided equally between the two classes. The dotted black lines mark the human performance levels from Table 1 for each noise level. Apparently, AI can surpass humans with this task—at least with synthetic light curves.

Table 1: Human performance

Noise level	Image size	Balanced accuracy
	250x250	0.96
	350x175	0.97
0.00		**0.97**
	250x250	0.88
	350x175	0.92
0.02		**0.90**
	250x250	0.84
	350x175	0.85
0.05		**0.85**

In Fig. 2B we see the same plot, but when the models are evaluated using binned Kepler observations instead. The best models, trained with moderate noise, reach just above 90% balanced accuracy and surpass human performance on noisy light curves. The models trained on noisy data perform poorly, but this is expected, because the training light curves generated with high noise are visually very different from smoothed Kepler observations.

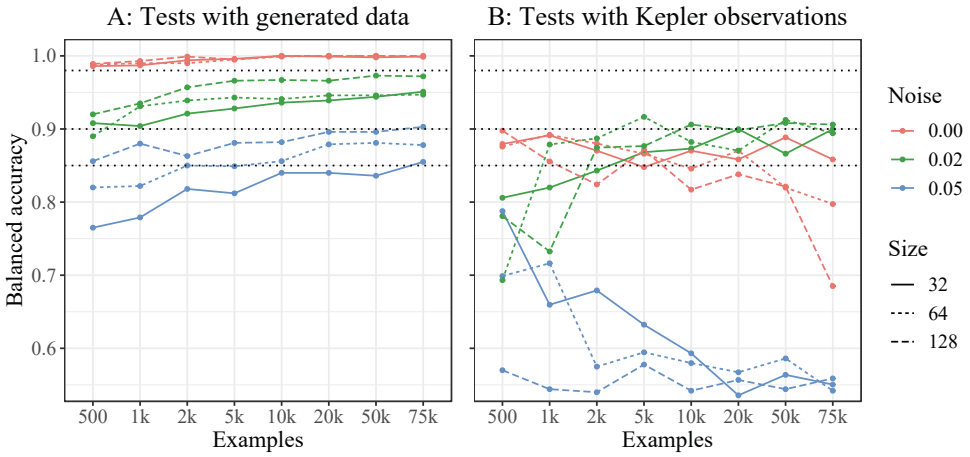

Figure 2: Performance of computer vision in recognition of total and partial eclipses when tested with generated data (panel A) and with binned observations from Kepler (panel B). The horizontal dotted lines mark the human performance at different noise levels (see Table 1).

3. CONCLUSIONS AND FUTURE WORK

The success of training a machine learning algorithm using simulated data depends critically on the ability of the simulation to mimic real-life phenomena the algorithm is intended to work with *after* training. In our case, great performance on generated

light curves but significantly worse on real observations means that there's a "data mismatch". To improve this situation, we might need to re-examine our assumptions about the nature of the noise in the observations, and take into account the factual class imbalance when creating simulated training sets.

There are also other datasets we can test our models on. The application on ASAS data is already a work in progress. Preliminary tests indicate that models trained on noisy generated data perform the best there, but overall, not as well as with Kepler. Another venue is CRTS data, where Sun et al. (2020) have already identified 3000 totally eclipsing systems among the 30 000 light curves of contact binaries.

Once we've established the reliability of our computer vision system, it can be applied to even larger, existing and future datasets, as a first step of a fully automated analysis pipeline.

Acknowledgments

The research presented in this report was funded by the Ministry of Education, Science and Technological Development of the Republic of Serbia (contract No. 451-03-68/2020-14/200002).

References

Djurašević, G.: 1992, *Astrophys. & Sp. Sc.*, **196**, 241.
Djurašević, G., Zakirov, M., Hojaev, A., Arzumanyants, G.: 1998, *Astron. Astrophys. Suppl.*, **131**, 17.
Djurašević, G., Essam, A., Latković, O., Čeki, A., El-Sadek, M. A., Abo-Elala, M. S., Hayman, Z. M.: 2016, *Astron. J.*, **152**, A57.
Drake, A. J., Graham, M. J., Djorgovski, S. G. et al.: 2014, *Astrophys. J. Suppl. Series*, **213**, 9.
Jayasinghe, T., Stanek, K. Z., Kochanek, C. S. et al.: 2020, *Mon. Not. R. Astron. Soc.*, **493**, 4045.
Latković, O., Čeki, A., Djurašević, G., Essam, A,, Hamed, A. S., Youssef, S. M.: 2019, *Astron. J.*, **157**, 3.
Prša, A, Batalha, N, Slawson, R. W. et al.: 2011, *Astron J.*, **141**, 83.
Sun, W., Chen, X., Deng, L., de Grijs, R.: 2020, *Astrophys. J. Suppl. Series*, **247**, 50.
Wilson, R. E., Devinney, E. J., and Van Hamme, W.: 2020, *Astrophysics Source Code Library.*

Publ. Astron. Obs. Belgrade No. 100 (2021), 281 - 286 *Progress Report*

THE INTERMITTENT EXTREME BEHAVIOUR OF BL Lac 1ES 2344+514

M. MANGANARO[1], A. ARBET ENGELS[2], D. DORNER[3], M. CERRUTI[4], J. A. ACOSTA-PULIDO[5], A. V. FILIPPENKO[6,7], T. HOVATTA[8,9], V. M. LARIONOV[†], C. M. RAITERI[10], V. FALLAH RAMAZANI[8,11], M. ŠEGON[1], V. SLIUSAR[12], M. VILLATA[10], and W. ZHENG[6]

on behalf of the MAGIC and FACT collaborations

[1] *University of Rijeka, Department of Physics, 51000 Rijeka*
E–mail: marina.manganaro@uniri.hr
E–mail: segi120@gmail.com
[2] *ETH Zurich, CH-8093 Zurich, Switzerland*
E–mail: aaxel@phys.ethz.ch
[3] *Universität Würzburg, D-97074 Würzburg, Germany*
E–mail: dorner@astro.uni-wuerzburg.de
[4] *Universitat de Barcelona, ICCUB, IEEC-UB, E-08028 Barcelona, Spain*
E–mail: matteo.cerruti@icc.ub..edu
[5] *Inst. de Astrofísica de Canarias, E-38200 La Laguna, and Universidad de La Laguna, Dpto. Astrofísica, E-38206 La Laguna, Tenerife, Spain*
E–mail: jap@iac.es
[6] *Department of Astronomy, University of California, Berkeley, CA 94720-3411, USA*
E–mail: weikang@berkeley.edu
[7] *Miller Senior Fellow, Miller Institute for Basic Research in Science, University of California, Berkeley, CA 94720, USA*
E–mail: afilippenko@berkeley.edu
[8] *Finnish Centre for Astronomy with ESO (FINCA), University of Turku, FI-20014, Turku Finland*
[9] *Aalto University Metsähovi Radio Observatory, Metsähovintie 114, 02540 Kylmälä, Finland*
E–mail: talvikki.hovatta@aalto.fi
[10] *INAF, Osservatorio Astrofisico di Torino, I-10025 Pino Torinese, Italy*
E–mail: claudia.raiteri@inaf.it
E–mail: villata@oato.inaf.it
[11] *Now at Universität Bochum, Fakultät fur Physik und Astronomie, Astronomisches Institut (AIRUB), Universitätsstr. 150, 44801 Bochum*
E–mail: vafar@utu.fi
[12] *University of Geneva, Department of Astronomy, Chemin d'Écogia 16, 1290 Versoix, Switzerland*
E–mail: vitalii.sliusar@unige.ch
[†] *Deceased*

Abstract. The BL Lac object 1ES 2344+514 was one of the first sources to be included in the extreme high-peaked BL Lac (EHBL) family. EHBLs are characterised by a broadband spectral energy distribution featuring the synchrotron peak above ~ 1 keV. 1ES 2344+514 was detected in very-high-energy (VHE) gamma rays for the first time by the Whipple telescope in 1995. The extreme nature of 1ES 2344+514 in the X-ray band was observed in 1996, when Beppo-SAX detected a large 0.1–10 keV flux variability on timescales of a few hours, during another bright outburst in the X-ray band. This extreme behaviour of the source triggered several multiwavelength campaigns in the following years, during which the source appeared to be in a low state. In August 2016, FACT detected the source in a high state, triggering multiwavelength observations. The combination of MAGIC, FACT, and Fermi-LAT spectra provides an unprecedented characterisation of the inverse-Compton peak for this object during a flaring episode. We collected multiwavelength data, and modelled the broadband emission during this peculiar flaring episode using a leptonic and a hadronic model. The source was in an extreme synchrotron state. The peak frequency obtained from the leptonic model corresponds to a synchrotron peak ν_s at 18 keV. The shift of peak frequency with respect to previous observations is ~ 2 orders of magnitude. A harder than usual intrinsic VHE gamma-ray spectrum is observed, with $\Gamma = 2.04 \pm 0.12_{\rm stat} \pm 0.15_{\rm sys}$. The leptonic and hadronic models both describe successfully the data, but require a significantly different magnetisation of the emitting zone. Our conclusion is that 1ES 2344+514 belongs to a subcategory of EHBLs, which reveal to be extreme only in some circumstances.

1. INTRODUCTION

Blazars — active galactic nuclei (AGN) whose relativistic jets are pointed toward the observer — are commonly classified into two main groups: BL Lac objects (BL Lacs, after BL Lacertae) and flat spectrum radio quasars (FSRQ). This categorisation is based on the properties shown by their optical spectra (Urry & Padovani 1995). Blazars which emit in the very-high-energy (VHE, $E > 100$ GeV) γ-ray band belong in the majority of cases to the BL Lac family[1].

The broadband spectral energy distribution (SED) of blazars is characterised by a two-bumped structure (Ghisellini et al. 2017). While the first bump is universally attributed to synchrotron radiation by relativistic electrons, the bump situated at higher energies is often considered to be inverse-Compton (IC) scattering of the synchrotron photons by the same electron population. The simplest interpretation of the broadband SED of a blazar is given by a one-zone synchrotron self-Compton model (SSC). More complex scenarios include the presence of hadronic components (e.g., Cerruti et al. 2015) to describe the high-energy part of the broadband SED. BL Lac objects are divided into three subclasses, depending on the position of their synchrotron peak: low, intermediate, and high-frequency BL Lacs (Padovani & Giommi 1995; Böttcher 2007).

2. EXTREME BL Lacs

Some BL Lacs show a synchrotron peak $\nu_{\rm s}$ at particularly high X-ray energies with $\nu_{\rm s} \geq 10^{17}$ Hz. Because of this extreme characteristic, they were proposed by Costamante et al. (2001) to be a new category of BL Lacs, namely extreme high-frequency BL Lacs (EHBL). EHBL can also have the IC bump peak shifted toward unusually high frequencies in the γ-ray band. In practice, this translates into particularly hard X-ray and VHE γ-ray spectra with a photon index $\Gamma \lesssim 2$.

[1] http://tevcat.uchicago.edu/ (Wackely & Horan 2008)

The archetypal EHBL, 1ES 0229+200 (Aharonian et al. 2007), exhibits these extreme properties in all observations performed so far, while other objects belong to the EHBL category only on some occasions (Ahnen et al. 2018; Foffano et al. 2019). During the observations reported here, we have found that BL Lac 1ES 2344+514 belongs to the latter group.

3. BL LAC 1ES 2344+514

1ES 2344+514 is a BL Lac located at redshift $z = 0.044$ (Perlman et al. 1996). It was discovered by the *Einstein* Slew Survey (Elvis et al. 1992). In 1996, 1ES 2344+514 showed a ν_s significantly above 10^{17} Hz during a flaring state, as reported by Giommi et al. (2000). 1ES 2344+514 was detected in the VHE γ-ray range for the first time in 1995 by the Whipple 10 m telescope, during an intense flare: on that occasion the flux detected by Whipple corresponded to $\sim 60\%$ of the Crab Nebula flux above 350 GeV (Catanese et al. 1998; Schroedter et al. 2005).

In the very bright flare of 1996, 1ES 2344+514 showed a remarkably variable behaviour in the X-ray band (Giommi et al. 2000, Costamante et al. 2001).The variability of the X-ray light curve was ~ 5 ks when the source was at its brightest state, and a large shift of ν_s was observed. At the same time the X-ray spectrum slope underwent very rapid changes. This was the occasion in which the source was marked as an EHBL for the first time.

After those events, several multiwavelength (MWL) campaigns monitored the source in search of simultaneous data which could have allowed a more precise interpretation of the emission scenario, modelling the broadband SED (Godambe et al. 2007; Albert et al. 2007; Acciari et al. 2011; Aleksic et al. 2013). During the course of those campaigns, though, the source was found in a lower state in the X-ray and VHE γ-ray band with respect to the previous observations (Catanese et al. 1998; Giommi et al. 2000). The broadband SEDs obtained in such a low activity state was sufficiently described by a one-zone SSC model.

Concerning the several VHE γ-ray observations by IACT (Imaging Atmospheric Cherenkov Telescopes), the source was found in variable flux states, but in general with integral fluxes lower than 10% of the Crab Nebula flux, excluding two short flares with 60% and 50% of the Crab Nebula flux level already mentioned (Catanese et al. 1998; Acciari et al. 2011). Recently, the temporal properties of 1ES 2344+514 in the VHE γ-ray band on short and long timescales have been investigated (Allen et al. 2017). No significant flaring activity has been observed since 2008.

4. RESULTS

In Acciari et al. (2020a), we reported on the observations of a VHE γ-ray flare of 1ES 2344+514 that happened in August 2016. The high activity in the VHE γ-ray range was first detected by FACT (First G-APD Cherenkov Telescope), which triggered the observations with the MAGIC (Major Atmospheric Gamma Imaging Cherenkov) telescopes. Many instruments, including *Fermi*-LAT (Large Area Telescope), *Swift*-XRT, *Swift*-UVOT (Ultraviolet/Optical Telescope), TCS (Telescope Carlos Sánchez), KAIT (Katzman Automatic Imaging Telescope, at Lick Observatory), KVA (Kungliga Vetenskapsakademien), Stella, LX-200, AZT-8, NOT (Nordic

Optical Telescope), IAC80, and OVRO (Owens Valley Radio Observatory) have observed this enhanced activity of 1ES 2344+514. We collected a dataset from simultaneous and quasi-simultaneous MWL observations which allowed us to study 1ES 2344+514 and for the first time provide the community with an unprecedented characterisation of the IC peak during a flaring state.

MAGIC observations started on MJD 57611 (11 August 2016; UT dates are used throughout this paper) and resulted in a detection with a significance of 13σ in less than one hour and a measured flux of 55% of the Crab Nebula flux above 300 GeV. This value of the flux is comparable to the historical maximum detected from this source in 1995 (Catanese et al. 1998). On the following night (MJD 57612, 12 August 2016) the signal was already fading and the measured flux was 16% of the Crab Nebula flux above 300 GeV. Using the data collected from instruments in the radio, optical, near-infrared, ultraviolet, X-ray, and HE band, we complemented the VHE γ-ray observations and built a broadband SED describing the flaring state with simultaneous data taken on MJD 57613 (13 August 2016). The SED has been modelled within two alternative scenarios: a leptonic SSC, and a proton-synchrotron model.

We have found the source in an extreme state, with a synchrotron peak frequency obtained from the leptonic model $\nu_{\rm s} \approx 4.3 \times 10^{18}$ Hz, corresponding to ~ 18 keV. The shift of $\nu_{\rm s}$ with respect to previous observations (Aleksic et al. 2013; Nilsson et al. 2018) is of about two orders of magnitude.

We also find a harder than usual VHE γ-ray spectrum ($\Gamma = 2.04 \pm 0.12_{\rm stat} \pm 0.15_{\rm sys}$ after extragalactic background light correction). The hardness of the spectrum does not vary between the first and the second night of observation, even though the flux on the second night was a factor of three lower.

The leptonic and hadronic models both successfully describe the data. On the other hand, they imply a significantly different magnetization of the emitting zone; in particular, the hadronic models require a much larger magnetic field, indicating that the emission zone has an equipartition parameter well above 1. The magnetic field energy densities in the case of the hadronic models are a factor of 10^2–10^4 higher than the energy density of the particles in the jet.

We conclude that the BL Lac object 1ES 2344+514 belongs to the subcategory of EHBL which appears extreme only in some circumstances (see Ahnen et al. 2018), and it does not exhibit the typical characteristic of persistent extreme SED as for instance the archetypal EHBL 1ES 0229+200 does (Aharonian et al. 2007).

5. FUTURE PLANS

This "intermittent" extremeness could be studied by acquiring more MWL data in the next few years. Time-dependent modelling to interpret the broadband SED could help to elucidate this peculiarity.

There is still more to discover about the EHBL family (Acciari et al. 2020b), and future MWL campaigns will help to unveil their nature and to move toward a classification of these interesting powerful AGN.

Acknowledgements

We would like to remember our friend and colleague, Dr. Valeri Larionov (1950–2020), who actively contributed to this and many other projects aimed at understanding blazars.

We thank the Instituto de Astrofísica de Canarias for the excellent working conditions at the Observatorio del Roque de los Muchachos in La Palma. Financial support is gratefully acknowledged from the German BMBF, MPG, and HGF; the Italian INFN and INAF; the Swiss National Fund SNF; the ERDF under the Spanish Ministerio de Ciencia e Innovación (MICINN) (FPA2017-87859-P, FPA2017-85668-P, FPA2017-82729-C6-5-R, FPA2017-90566-REDC, PID2019-104114RB-C31, PID2019-104114RB-C32, PID2019-105510GB-C31, PID2019-107847RB-C41, PID2019-107847 RB-C42, PID2019-107988GB-C22); the Indian Department of Atomic Energy; the Japanese ICRR, the University of Tokyo, JSPS, and MEXT; the Bulgarian Ministry of Education and Science, National RI Roadmap Project DO1-268/16.12.2019, and the Academy of Finland grant 320045. This work was also supported by the Spanish Centro de Excelencia "Severo Ochoa" SEV-2016-0588 and CEX2019-000920-S, "María de Maeztu" CEX2019-000918-M, the Unidad de Excelencia "María de Maeztu" MDM-2015-0509-18-2, the "la Caixa" Foundation (fellowship LCF/BQ/PI18/11630012), and the CERCA program of the Generalitat de Catalunya; by the Croatian Science Foundation (HrZZ) Project IP-2016-06-9782 and the University of Rijeka Project 13.12.1.3.02; by the DFG Collaborative Research Centers SFB823/C4 and SFB876/C3; the Polish National Research Centre grant UMO-2016/22/M/ST9/00382; and by the Brazilian MCTIC, CNPq, and FAPERJ.

The FACT collaboration gratefully acknowledges the important contributions from ETH Zurich grants ETH-10.08-2 and ETH-27.12-1, as well as funding by the Swiss SNF and the German BMBF (Verbundforschung Astro- und Astroteilchenphysik) and HAP (Helmoltz Alliance for Astroparticle Physics). Part of this work is supported by Deutsche Forschungsgemeinschaft (DFG) within the Collaborative Research Center SFB 876 "Providing Information by Resource-Constrained Analysis," project C3. We are thankful for very valuable contributions from E. Lorenz, D. Renker, and G. Viertel during the early phase of the project. We acknowledge the Instituto de Astrofísica de Canarias for allowing us to operate the telescope at the Observatorio del Roque de los Muchachos in La Palma, the Max-Planck-Institut für Physik for providing us with the mount of the former HEGRA CT3 telescope, and the MAGIC collaboration for their support. This article is based partly on observations made with the 1.5 m TCS and IAC80 telescopes operated by the IAC in the Spanish Observatorio del Teide. This article is also based partly on data obtained with the STELLA robotic telescopes in Tenerife, an AIP facility jointly operated by AIP and IAC. W.M. acknowledges support from CONICYT project Basal AFB-170002. We acknowledge support from Russian Scientific Foundation grant 17-12-01029. A.V.F. and W.Z. are grateful for support from NASA grant NNX12AF12G, the Christopher R. Redlich Fund, the TABASGO Foundation, and the Miller Institute for Basic Research in Science (U.C. Berkeley). KAIT and its ongoing operation were made possible by donations from Sun Microsystems, Inc., the Hewlett-Packard Company, AutoScope Corporation, Lick Observatory, the US National Science Foundation, the University of California, the Sylvia and Jim Katzman Foundation, and the TABASGO Foundation. Research at Lick Observatory is partially supported by a generous gift from Google.

This research has made use of data and/or software provided by the High Energy Astrophysics Science Archive Research Center (HEASARC), which is a service of the Astrophysics Science Division at NASA/GSFC and the High Energy Astrophysics Division of the Smithsonian Astrophysical Observatory. We acknowledge the use of

public data from the *Swift* data archive. The OVRO 40 m monitoring program is supported in part by NASA grants NNX08AW31G, NNX11A043G, and NNX14AQ89G, and by NSF grants AST-0808050 and AST-1109911. This research has made use the TeVCat online source catalog (http://tevcat.uchicago.edu). Part of this work is based on archival data, software, or online services provided by the Space Science Data Center – ASI.

References

Acciari, V. A. et al.: 2011, *ApJ*, **738**, 169.
Acciari, V. A. et al.: 2020a, *MNRAS*, **496**, 3912.
Acciari, V. A. et al.: 2020b, *ApJS*, **247**, 16.
Aharonian, F. et al.: 2007, *A&A*, **475**, L9.
Ahnen, M. L. et al.: 2018, *A&A*, **620**, A181.
Albert J., et al.: 2007, *ApJ*, **662**, 892.
Aleksic, J. et al.: 2013, *A&A*, **556**, A67.
Allen, C. et al.: 2017, *MNRAS*, **471**, 2117.
Böttcher, M.: 2007, *Ap&SS*, **309**, 95.
Catanese, M. et al.: 1998, *ApJ*, **501**, 616.
Cerruti, M., Zech, A., Boisson, C., Inoue, S.: 2015, *MNRAS*, **448**, 910.
Costamante, L. et al.: 2001, *A&A*, **371**, 512.
Elvis, M., Plummer, D., Schachter, J., Fabbiano, G.: 1992, *ApJS*, **80**, 257.
Foffano, L., Prandini, E., Franceschini, A., Paiano, S.: 2019, *MNRAS*, **486**, 1741.
Ghisellini, G., Righi, C., Costamante, L., Tavecchio, F.: 2017, *MNRAS*, **469**, 255.
Giommi, P., Padovani, P., Perlman, E.: 2000, *MNRAS*, **317**, 743.
Godambe, S. V. et al.: 2007, *Journal of Physics G Nuclear Physics*, **34**, 1683.
Nilsson, K.: et al.: 2018, *A&A*, **620**, A185.
Padovani, P., Giommi, P.: 1995, *ApJ*, **444**, 567.
Perlman, E. S. et al.: 1996, *ApJS*, **104**, 251.
Schroedter, M. et al.: 2005, *ApJ*, **634**, 947.
Urry, C. M., Padovani, P.: 1995, *PASP*, **107**, 803.
Wakely, S. P., Horan, D.: 2008, *International Cosmic Ray Conference*, 3, 1341.

Publ. Astron. Obs. Belgrade No. 100 (2021), 287 - 293 *Progress Report*

A NEW RADIUS-LUMINOSITY RELATION: USING THE NEAR-INFRARED CaII TRIPLET

M. L. MARTÍNEZ-ALDAMA, S. PANDA and B. CZERNY

Center for Theoretical Physics, Polish Academy of Sciences,
Al. Lotników 32/46, 02-668 Warsaw, Poland
E–mail: mmary@cft.edu.pl

Abstract. The Radius-Luminosity (RL) relation has been an excellent option to estimate the black hole mass in single-epoch observations. However, the inclusion of sources radiating close to the Eddington limit show a departure from the standard RL relation, bringing into discussion the validity of this relation for the general AGN population. Since the accretion rate seems to be the main driver behind this scatter, corrections based on it have been suggested to recover the predicted time delay. However, there is a need to search for independent observables that, when incorporated as a correction, can recover the classical result. Particularly, the Eigenvector 1 scheme has found that the intensity of the very low–ionization lines such as the optical Fe II and the Near–Infrared (NIR) Ca II triplet are driven by the Eddington ratio. A correction based on the optical Fe II has recovered the classical RL relation. Combining the aforementioned deductions, this contribution presents a correction based on the NIR Ca II triplet. The correction is computed in two ways: (1) using the linear relation between Fe II and Ca II using 75 objects, and (2) considering independent measurements of Ca II in 13 sources with existing reverberation mapping measurements. The first case provides similar results to one obtained with Fe II. In the second case, the limited sample affects the recovery of a good correction. These results show the relevance and the potential use of the Ca II ion, which should be considered for future observational programs.

1. INTRODUCTION

The distance determination in the Universe is crucial for cosmological studies. Active Galactic Nuclei (AGNs) have been detected in the high-redshift Universe ($z \sim 7.4$, Onoue et al. 2020) enabling their use as potential standard candles. Some observational properties of AGNs have been identified with this purpose (Risaliti & Lusso et al. 2019, Dultzin et al. 2020). However, the uncertainties associated with the cosmological estimations are still high compared to the ones shown by Cepheids, SNIa (Riess et al. 2018) or Cosmic Microwave Radiation (Planck Collaboration et al., 2020). In order to improve the existing measurements using AGNs, we need to perform a better determination of the their properties.

A solid relation between the broad line region (BLR) properties and the Eddington ratio ($L_{\rm bol}/L_{\rm Edd}$) has been revealed by the Eigenvector 1 scheme (Boroson and Green 1992, Marziani et al. 2003, Shen and Ho 2014, Panda et al. 2018). Usually, high

Eddington objects show signatures of outflows and low equivalent widths in high ionization lines (e.g. C IVλ1549 or Si IV λ1397), tiny narrow emission lines (e.g. [O III] $\lambda\lambda 5007, 4959$) and a strong contribution of the very low–emission lines such as the optical Fe II and the NIR Ca II triplet. In addition, highly accreting objects show a small variability in the photometric properties (Sanchez et al. 2017, Zajaček et al. 2021).

In the past, super-Eddington sources were not preferentially monitored by reverberation mapping studies. Since a long monitoring time with decent cadence is required for the reverberation mapping technique, objects with strong [O III] $\lambda\lambda 5007, 4959$ were selected to be observed by small ground-based telescopes in moderate timescales and to ensure correct flux normalizations (Peterson et al. 1998). Thus, the Radius-Luminosity (RL) relation was mostly populated with objects with small Eddington ratios. Recently, the inclusion of highly accreting objects carried out by the Super-Eddington Accreting Massive Black Holes (SEAMBHs) project (Du et al. 2018 and references therein) reveals that these AGN population show a departure from the classic RL relation, which directly affects the black hole mass determination in single-epoch measurements. Since the departure seems to be related to the Eddington ratio, some corrections have been proposed to recover the predicted time delay (Du et al. 2015, Martínez-Aldama et al. 2019, Du & Wang 2019, Dalla Bontà et al 2020, Fonseca-Alvarez et al. 2020, Martínez-Aldama et al. 2020). However, due to the self-dependence between the determination of the Eddington ratio and the time delay, the best option is to select independent observational properties, which in turn are correlated with the Eddington ratio. The most natural parameter is the strength of the optical Fe II expressed as the R_{FeII} (Fe II/Hβ). So, including R_{FeII} in a multilinear fitting with the luminosity and the time delay (τ_{obs}), Du and Wang (2019) and Yu et al. (2019) obtained similar results to the one estimated by the classical the RL relation (Bentz et al. 2013).

On the other hand, the NIR Ca II triplet $\lambda 8498, \lambda 8542, \lambda 8662$ (hereafter CaT) has a linear relation with the optical Fe II (Persson 1988, Joly 1989, Martínez-Aldama et al. 2015, Marinello et al. 2016, Panda et al. 2020). The relation between the two parameters can be expressed as follow (Panda et al. 2020):

$$\log R_{CaT} \approx (0.974 \pm 0.119) \log R_{FeII} - (0.657 \pm 0.041), \quad (1)$$

where R_{CaT} is the flux ratio Ca II/Hβ, which is in turn related to the Eddington ratio (Martínez–Aldama et al. 2021). Contrary to the Fe II, the CaT is a simpler ionic species and the photoionization codes can reproduce its behavior in a better way (Ferland & Persson, 1989; Panda et al. 2020, 2021). However, observing the CaT in AGN at intermediate and high redshifts is a challenge due to the presence of the telluric bands in the near- and mid-infrared. The upcoming generation of space observatories and the improvement in detectors mounted on ground-based telescopes will offer a good possibility to observe the CaT in the future.

In this contribution, we explore a multilinear RL relation where R_{CaT} is included with the purpose to correct the RL relation by the accretion rate effect. The samples and methods are summarized in Sec. 2. The multilinear RL relations are described in Sec. 3. Finally, discussions and conclusions are presented in Sec. 4. Throughout this work we assumed a standard cosmological model with $\Omega_\Lambda = 0.7$, $\Omega_m = 0.3$, and $H_0 = 70\ \mathrm{km\,s^{-1}\ Mpc^{-1}}$.

2. SAMPLES AND METHODS

In order to correct the RL relation by the accretion rate effect, we will perform a multivariate linear regression fitting considering the luminosity at 5100Å (L_{5100}), Hβ time delay ($\tau_{\rm obs}$) and $R_{\rm CaT}$ given by:

$$\tau_{\rm obs} = \alpha + \beta L_{44} + \gamma R_{\rm CaT}, \tag{2}$$

where L_{44} is the L_{5100} in units of 10^{44} erg s^{-1}. The coefficients α, β and γ will be determined using the python packages SKLEARN (Pedregosa et al., 2011) and STATSMODELS (Seabold & Perktold, 2010). We will use two samples which are described below.

- Sample 1. We will consider Du & Wang (2019) sample, which reports the L_{5100}, $R_{\rm FeII}$ and $\tau_{\rm obs}$ for 75 Hβ reverberation mapped objects at $z < 0.2$. Then, using Eq. 1, we will get the $R_{\rm CaT}$ values and obtain the multilinear relation. We expect to find a similar correction to one obtained by Du & Wang (2019).

- Sample 2. We only identified 13 sources with Hβ time lags and independent $R_{\rm CaT}$ measurements, which belong to the CaFe sample with originally 58 sources (Panda et. al. 2020). The CaFe sample includes an up-to-date compilation of observations with both optical Fe II and NIR Ca II measurements. An extensive description of the sample is included in Panda et al. (2020) and Martínez-Aldama et al. (2021). Times delays were collected from the literature. Although the number of sources is smaller with respect to the previous sample, the 13 sources cover a wide range of L_{5100}, $\tau_{\rm obs}$ and $R_{\rm CaT}$, which is suitable for the presented analysis.

Black hole masses were estimated from the classical RL relation (Bentz et al. 2013), and the Eddington ratio throughout the definition $L_{\rm bol}/L_{\rm Edd}$, where $L_{\rm bol}$= $40\left(\frac{L_{5100}}{10^{42}}\right)^{-0.2}$ (Netzer 2019) and $L_{\rm Edd} = 1.5 \times 10^{38}\left(\frac{M_{BH}}{M_\odot}\right)$.

3. RESULTS

In order to justify the inclusion of $R_{\rm FeII}$ and $R_{\rm CaT}$ in a multilinear regression fitting with L_{5100} and $\tau_{\rm obs}$, it is required at first to show the correlation between the Eddington ratio, $R_{\rm FeII}$ and $R_{\rm CaT}$, respectively (Figure 1). For Sample 1 the correlation in both cases is strong considering the Spearman correlation coefficients (ρ) and the $p-$values ($\rho = 0.66$, $p = 2.2 \times 10^{-10}$). Since $R_{\rm CaT}$ was determined from $R_{\rm FeII}$ and their uncertainties are not considered in the estimation of the statistical parameters, ρ and $p-$values are the same in both correlations. On the other hand, due to the small number of sources in Sample 2, the $L_{\rm bol}/L_{\rm Edd}$-$R_{\rm FeII}$ relation is weak ($\rho = 0.32$, $p = 0.28$). However, $R_{\rm FeII}$ values are not used in the presented analysis since the $R_{\rm CaT}$ is estimated independently. We only show them as a reference of the $R_{\rm FeII}$ behavior in Sample 2. The correlation coefficient ($\rho = 0.54$) shows a strong corelation in the $L_{\rm bol}/L_{\rm Edd}$-$R_{\rm CaT}$ relation, although the p-value ($p = 0.058$) indicates a $\sim 5\%$ to reject the correlation. As Martínez-Aldama et al. (2021) pointed out, the correlations with respect to the Eddington ratio are better represented by $R_{\rm CaT}$ than $R_{\rm FeII}$. This result was the motivation to use $R_{\rm CaT}$ instead of $R_{\rm FeII}$ to correct the RL relation by the accretion rate effect.

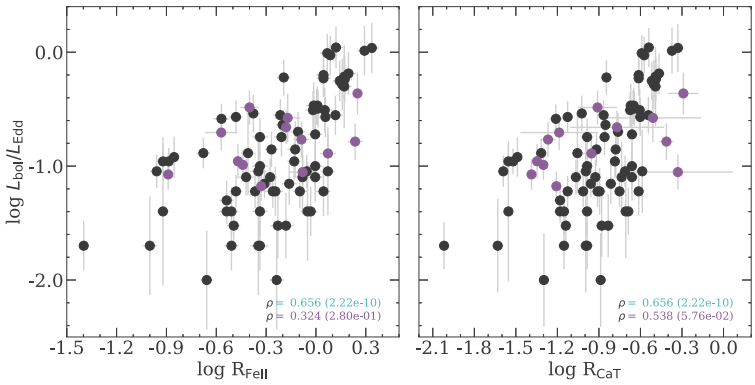

Figure 1: Correlation between the Eddington ratio as a function of R_{FeII} (left panel) and R_{CaT} (right panel), respectively. Cyan and magenta symbols correspond to Sample 1 and 2, respectively (See Sec. 2). The Spearman rank coefficients and the p–values are reported for each case.

The top panels of Figure 2 show the results for the 75 objects from Sample 1. The top-left panel shows the classical RL relation. The color bar represents the R_{CaT} strength, where the strongest R_{CaT} values show the largest departures from the classical RL relation, which is reflected in the large scatter, $\sigma \sim 0.299$ dex. The departure can be estimated by the parameter $\Delta\tau_{obs} = \tau_{obs} - \tau_{RL}$. The inset panel clearly shows the correlation between $\Delta\tau_{obs}$ and R_{CaT} and justifies the inclusion of R_{FeII} in the multilinear relation. Meanwhile, the top-right panel shows the multilinear RL relation including the R_{CaT} where the scatter decreases by almost 1 dex ($\sigma \sim 0.204$). If we compared our relation with the one reported by Du & Wang (2019, $\tau_{obs} = (1.65 \pm 0.06) + (0.45 \pm 0.03)L_{44} + (-0.35 \pm 0.08)R_{FeII}$), both relations are equivalent within uncertainties, since we are using the Eq. 1 to get the values of R_{CaT}. There are small variations in the coefficients and the scatter (0.204 vs. 0.196), however, this does not represent a significant change.

The bottom panels of Figure 2 show the results from the 13 sources with Hβ time delays and independent R_{CaT} estimations (Sample 2). Bottom-left panel shows the classical RL relation with a scatter of $\sigma = 0.289$ dex. The departure parameter $\Delta\tau_{obs}$ from the classical RL relation is not so clear, such as the inset panel with the $\Delta\tau_{obs}$–R_{CaT} relation shows. Although the correlation coefficient ($\rho = 0.44$) shows a moderate correlation between R_{CaT} and $\Delta\tau_{obs}$, the p-value indicates a probability of $\sim 13\%$ to reject the correlation. The bottom-right panel shows the multilinear RL relation with a reduction in the scatter by almost 1 dex, similar to the results for Sample 1. If we compare this correlation with the one obtained from Sample 1 (top-right panel), we find a significant variation in the coefficients. The coefficient associated with L_{5100} is shallower than the one obtained previously (0.39 vs. 0.46). The coefficient associated with the R_{CaT} parameter has a large uncertainty ($\sim 78\%$), which is due to the large uncertainties of R_{CaT} and the weak relation between $\Delta\tau_{obs}$ and R_{CaT}.

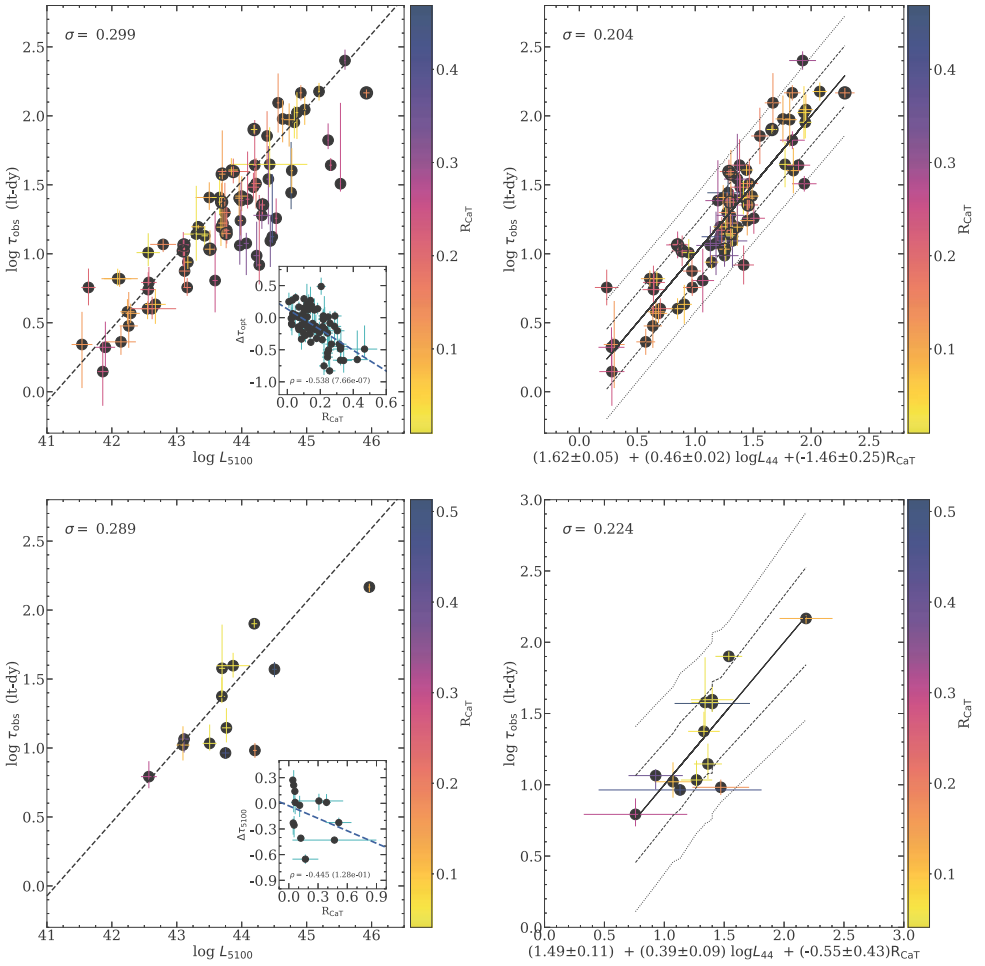

Figure 2: TOP-LEFT PANEL: RL relation using the 75 sources from Du & Wang (2019) sample. TOP-RIGHT PANEL: Multilinear RL relation including the R_{CaT}. Inset plot represents the correlation between $\Delta\tau_{obs}$ and R_{CaT} where the blue dashed lines indicate the best fits. In both panels in the top row, black circles correspond to 10 out of the 13 sources considered in Sample 2 (See Section 2). BOTTOM-LEFT PANEL: RL luminosity relation using the 13 sources from Sample 2. BOTTOM-RIGHT PANEL. Multilinear RL relation including R_{CaT}. In all the panels the color code indicates the R_{CaT} strength. Black dashed lines in the left panels indicate the classical RL relation from Bentz et al. (2013). In the right panels, the black continuous line marks the multidimensional RL relation, while dashed and dotted lines denote the 68% and 95% confidence intervals.

4. DISCUSSIONS AND CONCLUSIONS

We performed a multilinear relation with L_{5100}, τ_{obs} and R_{CaT} in order to recover the classical RL relation (Bentz et al. 2013). Due to the large numbers of sources

in Sample 1, the multilinear RL relation has a better approximation to the classical result (Bentz et al., 2013). Since R_{CaT} measurements were estimated from the R_{FeII}, the relation is so similar to the one obtained from Du & Wang (2019). On the other hand, we could only identify 13 sources with independent measurements of R_{CaT} that are reverberation-mapped. Although the number of sources is small, this second option provides an independent test and will predict better results once the source count increases. In both cases, we achieved to decrease the scatter, however the uncertainties of the coefficients in Eq. 2 are still large for Sample 2. Observing the NIR spectrum in sources already analyzed by the reverberation mapping technique is required in order to improve our results and confirm the Ca II triplet as a proxy of the Eddington ratio with a higher significance.

In results of Sample 1 and 2, the coefficient associated with L_{5100} is shallower than the predicted ($\log \tau_{\rm obs} \propto 0.5 \log L$) by the photoionization theory, theoretical models (e.g. Czerny & Hryniewicz, 2011) and the standard RL relation (Bentz et al. 2013). On the other hand, the independent coefficient in the classical RL relation is given by 1.527 ± 0.31. In our predictions the independent coefficients are in agreement within uncertainties ($\alpha_{S1} = 1.62 \pm 0.05$, $\alpha_{S2} = 1.46 \pm 0.09$). Therefore, we can conclude that the presented multilinear RL relations are in agreement within uncertainties. Some theoretical models have included a shielding effect and a variation in the accretion rate, which shortens the time delay (Naddaf et al. 2021a,b). However, a variation in the slope of L_{5100} is still not included. In the future, these theoretical results will provide the shape of the line profiles and their dependence on the accretion rates. So, it will be a test for the results presented in this paper.

Acknowledgements

The project was partially supported by the Polish Funding Agency National Science Centre, project 2017/26/A/ST9/00756 (MAESTRO 9) and MNiSW grant DIR/WK/2018/12.

References

Bentz, M. C., Denney, K. D., Grier, C. J. et al.: 2013, ApJ, **767**, 149.
Boroson, T. A. and Green, R. F.: 1992, ApJS, **80**, 109.
Czerny, B. and Hryniewicz, K.: 2011, A&A, **525**, L8.
Dalla Bonta, E., Peterson, B. M., Bentz, M. C. et al.: 2020, arXiv:2007.02963.
Du, P. and Wang, J.-M.: 2019, ApJ, **886**, 42.
Du, P., Zhang, Z.-X., Wang, K. et al.: 2018, ApJ, **856**, 6.
Du, P., Hu, C., Lu, K.-X. et al.: 2015, ApJ, **806**, 22.
Ferland, G. J. and Persson, S. E.: 1989, ApJ, **347**, 656.
Fonseca Alvarez, G., Trump, J. R., Homayouni, Y. et al.: 2020, ApJ, **899**, 73.
Dultzin, D., Marziani, P., de Diego, J. A. et al.: 2020, FrASS, **6**, 80.
Joly, M.: 1989, A&A, **208**, 47.
Martínez-Aldama, M. L., Panda, S., Czerny, B. et al.: 2021, submitted to ApJ, arXiv:2101.06999.
Martínez-Aldama, M. L. Zajaček, M., Czerny, B. and Panda, S.: 2020, ApJ, **903**, 2.
Martínez-Aldama, M. L., Czerny, B., Kawka, D. et al.: 2019, ApJ, **883**, 170.
Martínez-Aldama, M. L., Dultzin, D., Marziani, P. et al.: 2015, ApJS, **217**, 3.
Marinello, M., Rodríguez-Ardila, A., García-Rissmann, A. et al.: 2016, ApJ, **820**, 116.
Marziani, P., Zamanov, R. K., Sulentic, J. W. and Calvani, M.: 2003, MNRAS, **345**, 1133.
Naddaf, M.-H., Czerny, B. and Szczerba, R.: 2021a, submitted to ApJ, arXiv:2102.00336.

Naddaf, M.-H., Czerny, B. and Szczerba, R.: 2021b, *XXXIX Polish Astronomical Society Meeting*, **10**, 279.
Netzer, H.: 2019, MNRAS, **488**, 4.
Onoue, M., Banados, E., Mazzucchelli, C. et al.: 2020, ApJ, **898**, 105.
Panda, S., Czerny, B., Adhikari, T. P. et al.: 2018, ApJ, **866**, 115.
Panda, S., Martííez-Aldama, M. L., Marinello, M. et al.: 2020, ApJ, **902**, 76.
Panda, S.: 2021, submitted to A&A, arxiv:2004.13113.
Pedregosa, F., Varoquaux, G., Gramfort, A. et al.: 2011, *Journal of Machine Learning Research*, **12**, 2825.
Persson, S. E.: 1988, ApJ, **330**, 751.
Peterson, B. M., Wanders, I., Bertram, R. et al.: 1998, ApJ, **501**, 82.
Planck Collaboration, Aghanim, N., Akrami, Y. et al.: 2020, A&A, **641**, A6.
Riess, A. G., Casertano, S., Yuan, W. et al.: 2018, ApJ, **861**, 126.
Risaliti, G. and Lusso, E.: 2019, *Nature Astronomy*, **3**, 272.
Sánchez, P., Lira, P., Cartier, R. et al.: 2017, ApJ, **849**, 110.
Seabold, S. and Perktold, J.: 2010, *Proceedings of the 9th Python in Science Conference*, Ed. Stéfan van der Walt and Jarrod Millman, 92–96.
Shen, Y. and Ho, L. C.: 2014, *Nature*, **513**, 210.
Yu, L.-M., Bian, W.-H., Wang, C. et al.: 2019, MNRAS, **488**, 1519.
Zajaček, M., Czerny, B., Martínez-Aldama, M. L. et al.: 2021, submitted to ApJ, arXiv:2012.12409.

Publ. Astron. Obs. Belgrade No. 100 (2021), 295 - 300 *Progress Report – special session "The gravitational-wave Universe" supported by COST Action CA16104*

ALGEBRAIC DEPENDENCIES AND REPRESENTATIONS OF COSMOLOGICAL PARAMETERS

Ž. MIJAJLOVIĆ[1] and D. BRANKOVIĆ[2]

[1] *Faculty of Mathematics, University of Belgrade, Studentski trg 16, 11000 Belgrade, Serbia*
E–mail: zarkom@matf.bg.ac.rs

[2] *School of Electrical Engineering, University of Belgrade, Bulevar kralja Aleksandra 73, 11000 Belgrade, Serbia*
E–mail: danijela@etf.bg.ac.rs

Abstract. Cosmological parameters are taken usually as functions of time. These dependencies are transcendental in general and cannot be represented in the closed form by elementary functions. We show that there are algebraic dependencies between the main cosmological parameters: the scale factor, Hubble parameter, redshift and density parameters related to the cosmological constant, space curvature, radiation and baryonic matter. We exhibit and discuss these dependencies and give several examples of their use in computing certain events in the evolution of the universe.

1. INTRODUCTION

Accurate determination of cosmological parameters is an important task in the study of ΛCDM model, as they enable computing of the main events in the past and prediction of the future evolution of the universe.

Cosmological parameters are taken usually as functions of time t. These dependencies are transcendental in general and cannot be represented in the closed form by elementary functions due to the elliptic integrals which come out as the equivalent solutions of Friedmann equations:

$$t = \frac{1}{H_t}\int_0^1 \frac{s\,ds}{\sqrt{\Omega_{rt}+\Omega_{mt}s+\Omega_{kt}s^2+\Omega_{\Lambda t}s^4}}, \quad \text{or} \tag{1}$$

$$t \equiv \mathcal{J}(a) = \frac{1}{H_0}\int_0^a \frac{s\,ds}{\sqrt{\Omega_{r0}+\Omega_{m0}s+\Omega_{k0}s^2+\Omega_{\Lambda 0}s^4}}. \tag{2}$$

Parameters appearing in these integrals are the scale factor a (taken as an independent variable in (2)), Hubble parameter $H_t = H(t)$ and density parameters $\Omega_{it} = \Omega_i(t)$ at time t related to the cosmological constant Λ, space curvature κ, radiation r and baryonic matter m. We take $H_0 = H(t_0)$, the value of the Hubble parameter at the time moment t_0. The similar convention is applied to the other parameters.

We remind that Friedmann equations, discovered by Alexander Friedmann in 1922, are usually stated as a system consisting of the first and second order differential equations:

$$\begin{aligned} \left(\frac{\dot{a}}{a}\right)^2 &= \frac{8\pi G}{3}\rho - \frac{kc^2}{a^2} + \frac{\Lambda c^2}{3}, && \text{Friedmann equation,} \\ \frac{\ddot{a}}{a} &= -\frac{4\pi G}{3}\left(\rho + \frac{3p}{c^2}\right) + \frac{\Lambda c^2}{3}, && \text{Acceleration equation,} \\ \dot{\rho} &+ 3\frac{\dot{a}}{a}\left(\rho + \frac{p}{c^2}\right) = 0, && \text{Fluid equation.} \end{aligned} \tag{3}$$

These equations represent the core of the ΛCDM model. The function $a(t)$ is the expansion scale factor and it describes the evolution of our universe. Other parameters appearing in Friedmann equations are the pressure $p(t)$ and the energy density $\rho(t)$. Both integrals (1) and (2) can be derived, for example, from the well-known identities

$$H^2/H_0^2 = \Omega_{\Lambda 0} + \Omega_{k0}a^{-2} + \Omega_{m0}a^{-3} + \Omega_{r0}a^{-4}, \quad p = \frac{1}{3}c^2\rho_r. \tag{4}$$

We note that $\mathcal{J}(a)$ is the inverse function of the scale factor $a(t)$, i.e. for any $b > 0$

$$\mathcal{J}(b) = t \text{ if and only if } a(t) = b.$$

Hence, (2) is a parametrization of the cosmic time t in respect to the scale factor a.

2. ALGEBRAIC DEPENDENCIES

We show that there are algebraic dependencies between the main cosmological parameters. Besides discussion of these dependencies, we also exhibit them including those corresponding to the contemporary measurements. Our main motivation was to apply these dependencies in the study of the evolution of the universe.

Two possible applications of found dependencies are presented. The first one is the representation of cosmological parameters in respect to some chosen parameter. The second one is the computation of values of all cosmological parameters at particular points in the evolution of the universe, such as the transition point from radiation dominated to matter dominated era, recombination, or the starting point of the accelerated expansion of the universe.

In order to state precisely these dependencies, we first fix notation. In general relativity first Friedmann equation is

$$H(t)^2 \equiv \left(\frac{\dot{R}(t)}{R(t)}\right)^2 = \frac{8\pi G}{3}\rho(t) - \frac{kc^2}{R(t)^2} + \frac{\Lambda c^2}{3}, \tag{5}$$

where $R = R(t)$ is the curvature radius at time t and $k = 0, 1, -1$ is the curvature index in the FLRW metric. Also, $\rho(t)$ is the mass density which includes rest mass energy and other forms of energy (e.g., energy of photons). Furthermore

$$a(t) = R(t)/R(t_0), \quad H(t) = \dot{R}(t)/R(t) = \dot{a}(t)/a(t), \tag{6}$$

where t_0 is the present time, $H = H(t)$ is the Hubble parameter and $a = a(t)$ is the scale factor, the normalization of $R(t)$.

Let t_0 and τ be two time moments. We take that t_0 is a constant and may stand for the present time. In fact t_0 is a part of the boundary conditions for Friedmann equations.

Let us write $R_0 = R(t_0)$, $R_\tau = R(\tau)$, $H_0 = H(t_0)$, $H_\tau = H(\tau)$, $\Omega_{i\tau} = \Omega_i(\tau)$ and $\Omega_{i0} = \Omega_i(t_0)$. The redshift is denoted by z. Then we have the following algebraic relations between the cosmological parameters.

$$\begin{gathered} a_\tau = 1/x, \qquad R_\tau = R_0/x, \qquad H_\tau = H_0/\sqrt{y}, \qquad z = x - 1, \\ \Omega_{\Lambda\tau} = \Omega_{\Lambda 0} y, \quad \Omega_{k\tau} = \Omega_{k0} x^2 y, \quad \Omega_{m\tau} = \Omega_{m0} x^3 y, \quad \Omega_{r\tau} = \Omega_{r0} x^4 y, \\ y = \frac{1}{\Omega_{\Lambda 0} + \Omega_{k0} x^2 + \Omega_{m0} x^3 + \Omega_{r0} x^4}. \end{gathered} \tag{7}$$

The algebraic dependencies (7) are determined using the standard formulas found in the literature which relate cosmological parameters, for example the defining formulas for density parameters:

$$\begin{aligned} \Omega_\Lambda(t) &= \frac{\Lambda c^2}{3H(t)^2}, \quad \text{cosmological constant density,} \\ \Omega_k(t) &= -\frac{kc^2}{R(t)^2 H(t)^2} = -\frac{\kappa_0 c^2}{a(t)^2 H(t)^2}, \quad \text{curvature density,} \\ \Omega(t) &= \frac{8\pi G}{3H(t)^2}\rho(t), \quad \text{mass density,} \\ \Omega_m(t) &= \frac{8\pi G}{3H(t)^2}\rho_m(t), \quad \text{rest mass density,} \\ \Omega_r(t) &= \frac{8\pi G}{3H(t)^2}\rho_r(t), \quad \text{radiation density.} \end{aligned} \tag{8}$$

In (7) R_0, H_0, Ω_{i0} are constants and they form the boundary condition for Friedmann equations. We may think of them as of the measured values at t_0, while $a_\tau, R_\tau, H_\tau, \Omega_{i\tau}$ are unknowns and x, y are auxiliary variables.

The relations in (7) give an algebraic parameterizations of basic cosmological parameters in respect to x. Obviously, the parameter y is immediately eliminable from this system replacing all appearances of y using the last formula in (7), so the dependencies (7) consist of eight equations and nine unknowns, eight of them representing cosmological parameters. Also, we see that instead of the parameter x we could take the redshift z. But it is also obvious that after these substitutions we would loose the simplicity and easy readability of the algebraic dependencies represented by (7). In fact, instead of x we could take in this system as a free parameter any time-like parameter, i.e. that one which is monotonous in time, either increasing, or decreasing, for example the scale factor a. But all such modifications lead to more complicated set of formulas than (7).

3. APPLICATIONS

The usual approach found in the literature in computing some events in the evolution of the universe, is to locate the epoch at which the event most certainly appear and

then to find an approximation valid for this epoch

$$\tau = G(a, H, \Omega_i) \tag{9}$$

of the solution (1), or its alternative (2). Then using equation (9), time t_0 and the related values of cosmological parameters of the event are computed.

An example of the standard approach is the derivation of Carroll-Press-Turner formula (1992) for pressureless flat universe with cosmological constant. These assumptions correspond to a universe with the curvature $\kappa = 0$ for the period following radiation era, i.e. approximately $\Omega_{r0} = 0$ and $\Omega_{k0} = 0$. Hence

$$\begin{aligned} I &= \int_0^1 \frac{s}{\sqrt{\Omega_{m0} s + \Omega_{\Lambda 0} s^4}}\, ds \\ &= \frac{-\ln(\Omega_{m0}\Omega_{\Lambda 0}) + 2\ln(\Omega_{\Lambda 0} + \sqrt{\Omega_{\Lambda 0}}\sqrt{\Omega_{m0} + \Omega_{\Lambda 0}})}{3\sqrt{\Omega_{\Lambda 0}}}. \end{aligned}$$

Taking $\Omega_{m0} = \Omega_0$ and by $\Sigma_i \Omega_i = 1$, we have $\Omega_0 + \Omega_{\Lambda 0} = 1$, and after some simplifications we obtain the desired formula:

$$H_0 t_0 = \frac{2}{3} \frac{1}{\sqrt{1 - \Omega_0}} \ln\left(\frac{1 + \sqrt{1 - \Omega_0}}{\sqrt{\Omega_0}}\right).$$

Now we give some simple computational examples based on the algebraic dependencies (7). The idea is to find an extra relation which connects the cosmological parameters. With this supplement the system (7) will have nine equations with nine unknowns, what would lead to a solution of the system. For t_0 we take the present time and for values of the parameters at t_0 we take a set of mean currently measured values (Particle Data Group, http://pdg.lbl.gov):

$$\begin{gathered} a_0 = 1, \quad H_0 = 67.4\,(\mathrm{km/s})/\mathrm{Mpc} = 2.1843 \cdot 10^{-18} s^{-1}, \\ \Omega_{\Lambda 0} = 0.685, \quad \Omega_{k0} = 0.0007, \quad \Omega_{m0} = 0.3164, \quad \Omega_{r0} = 0.0000538. \end{gathered}$$

We also take $\Omega_m = \Omega_b + \Omega_c + \Omega_\nu$, where Ω_b, Ω_c and Ω_ν are densities respectively of baryonic mass, cold dark matter and neutrinos.

Before we proceed to examples, we note that the presented method gives theoretically the most accurate calculations of cosmological events. The main part of the method is the numerical computation of the elliptic integral which represents the exact analytical solution (2) of Friedmann equations. No approximation of formulas are assumed as it is usually done in the literature. Hence, the influence of even small values of certain parameters are taken into account which are usually neglected in computations for a chosen cosmological epoch. The other part of computation comes from algebraic dependencies (7) which represent the usual physical laws. Hence, the accuracy of the method, if ΛCDM model is assumed, depends only on the the numerical methods for computing integrals which accuracies are arbitrary high today and the accuracy of the measurements of the contemporary cosmological data which are taken as the input values for the computation.

Age of universe. In this example we take $\tau = t_0$, i.e. we compute the age of the universe. Hence $x = 1$ and we compute

$$t_0 = \frac{1}{H_0} \int_0^1 \frac{s\, ds}{\sqrt{\Omega_{r0} + \Omega_{m0} s + \Omega_{k0} s^2 + \Omega_{\Lambda 0} s^4}} = 13.7815\,\mathrm{Gyr}. \tag{10}$$

Double expansion. In this example we compute time τ when the universe will double its expansion, i.e. $a_\tau = 2$. Then $x = 0.5$, so using (7) we obtain

$$\begin{aligned} y_\tau = 1.3828, \quad H_\tau = 1.8575 \cdot 10^{-18} s^{-1}, \\ \Omega_{\Lambda\tau} = 0.9452, \quad \Omega_{k\tau} = 0, \quad \Omega_{m\tau} = 0.05457, \quad \Omega_{r\tau} = 4.6397 \cdot 10^{-6}, \end{aligned} \tag{11}$$

while the time for this event is computed as

$$\tau = \frac{1}{H_\tau} \int_0^1 \frac{s\, ds}{\sqrt{\Omega_{r\tau} + \Omega_{m\tau} s + \Omega_{k\tau} s^2 + \Omega_{\Lambda\tau} s^4}} = 24.944\,\text{Gyr}. \tag{12}$$

Transition from radiation to matter dominated era. This is more sophisticated example. Radiation dominated epoch covers the period when the expansion of the universe was dominated by radiation. It is usually taken that it started after inflation and lasted until the equalization of matter and radiation. This second event is characterized by

$$\Omega_{m\tau} = \Omega_{r\tau}, \quad \tau \text{ is the equalization time moment.} \tag{13}$$

So we get the ninth equation that supplements the system (7).

In the radiation era, neutrinos were relativistic particles (see Supernova Cosmology Project site), in fact until the recombination which happened far beyond τ. Hence we have to relocate the summand $\Omega_{\nu\tau}$ from $\Omega_{m\tau}$ to $\Omega_{r\tau}$. Therefore, to compute matter density at time τ, instead of

$$\Omega_{m0} = \Omega_{c0} + \Omega_{b0} + \Omega_{\nu 0},$$

we take $\Omega'_{m0} = \Omega_{c0} + \Omega_{b0}$ and $\Omega'_{m\tau} = \Omega'_{m0} x^3 y$ in (7), where $\Omega'_{m\tau} = \Omega_{c\tau} + \Omega_{b\tau}$. Also, as neutrinos at time τ add to the radiation we take $\Omega'_{r\tau} = \Omega_{\gamma\tau} + \Omega_{\nu\tau}$, where $\Omega_{\gamma\tau}$ is the photon density. Hence, instead of the equation (13) we take $\Omega'_{m\tau} = \Omega'_{r\tau}$. Density of neutrinos $\Omega_{\nu\tau}$ at time τ is computed by, see e.g. Gerbino and Lattanzi, Lesgourgues and Pastor:

$$\Omega_{\nu\tau} = \lambda \Omega_{\gamma\tau}, \quad \text{where} \quad \lambda = N_{\text{eff}} \cdot \frac{7}{8} \cdot \left(\frac{4}{11}\right)^{\frac{4}{3}}. \tag{14}$$

Here, $N_{\text{eff}} = 3.046$ is a slightly greater than $N_\nu = 3$, the number of neutrino families. Hence, $\Omega'_{r\tau} = (1+\lambda)\Omega_{\gamma\tau} = (1+\lambda)\Omega_{\gamma 0} x^4 y$. Obviously, we took $\Omega_{r0} = \Omega_{\gamma 0}$, as present neutrinos are non-relativistic, hence they do not add to the radiation. As $\Omega'_{m\tau} = \Omega'_{r\tau}$, we get $\Omega'_{m0} x^3 y = (1+\lambda)\Omega_{\gamma 0} x^4 y$, so

$$x = \frac{1}{1+\lambda} \cdot \frac{\Omega'_{m0}}{\Omega_{\gamma 0}} = \frac{\Omega_{c0} + \Omega_{b0}}{(1+\lambda)\Omega_{\gamma 0}} = \frac{\Omega_{m0} - \Omega_{\nu 0}}{(1+\lambda)\Omega_{\gamma 0}}. \tag{15}$$

As the values of upper and lower bounds and the mean values of the constants Ω_{c0}, Ω_{b0}, $\Omega_{\gamma 0}$ and $\Omega_{\nu 0}$ are known, see the enclosed table, we can solve the system (7) for both values H'_0 and H''_0 (which reflect the Hubble tension). Using the integral (1), or $\mathcal{J}(a)$, we can compute the corresponding times τ. We computed the value $\tau \approx 50\,000$ Yrs which is approximately the same as in Ryden.

Initial data for our computation are displayed in the following table:

Table 1: Values are generated using data from *Particle Data Group*.

Present values of cosmological parameters							
	H_0'	H_0''	$\Omega_{\Lambda 0}$	Ω_{k0}	Ω_{m0}	Ω_{r0}	$\Omega_{\nu 0}$
min	66.9	72.0	0.678	-0.0012	0.3079	$5.23 \cdot 10^{-5}$	0.0012
mean	67.4	73.0	0.685	0.0007	0.3164	$5.38 \cdot 10^{-5}$	0.0021
max	67.9	74.0	0.692	0.0026	0.3249	$5.53 \cdot 10^{-5}$	0.0030

4. CONCLUSION

Algebraic dependencies among the main cosmological parameters are presented. These dependencies can be useful in a uniform approach in computing certain events in the evolution of the universe. We illustrate this usefulness by applying them in computing the age of the universe, the time when the expansion of the universe should be double, and transition moment from radiation to matter dominated era.

References

Carroll, S. M., Press, W. H., Turner, E. L.: 1992, *Ann. Rev. Astron. Astrophis. J.*, **30**, 499.

Friedmann, A.: 1924, Über die Möglichkeit einer Welt mit konstanter negativer Krümmung des Raumes., *Z. Phys.*, **21**(1), 326.

Gerbino, M., Lattanzi, M.: 2018, Status of Neutrino Properties and Future Prospects – Cosmological and Astrophysical Constraints, *Frontiers in Physics*, 06 February 2018.

Lesgourgues, J., Pastor, S.: 2014, Neutrino cosmology and PLANCK, arXiv preprint 1404.1740v1 [hep-ph], 7 Apr 2014.

Ryden, B.: 2006, Introduction to cosmology, Addison Wesley, 2003, 2^{nd} ed. 2006.

Supernova Cosmology Project site, http://supernova.lbl.gov

Particle Data Group, http://pdg.lbl.gov

Publ. Astron. Obs. Belgrade No. 100 (2021), 301 - 305 *Progress Report*

SATURN - A SERBIAN JOURNAL ON ASTRONOMY FROM THE PAST

Ž. MIJAJLOVIĆ and N. PEJOVIĆ

Faculty of Mathematics, University of Belgrade, Studentski trg 16, 11000 Belgrade, Serbia
E–mail: zarkom@matf.bg.ac.rs
E–mail: nada@matf.bg.ac.rs

Abstract. We present astronomical journal *Saturn* which was published in Belgrade in the period 1935 – 1940. The journal was started as a monthly publication of the newly founded Yugoslav astronomical association "Astronomical Society". All 72 volumes of the journal are digitized and deposited in the Virtual library of the Faculty of Mathematics in Belgrade, http://elibrary.matf.bg.ac.rs.

1. INTRODUCTION

There were not so many astronomical publications in Serbia before WWII, in particular periodicals. Overviews on early astronomical books printed in Serbia, or written by scientists of the Serbian origin, one can find in Pejović and Mijajlović (2011), Martocchia and Marchionni (2013) and Milisavljević et al (2011). Also, a lot of valuable historical information are published in proceedings of biannual conferences *Razvoj astronomije kod Srba* (Development of astronomy among Serbs), organized by professor Milan Dimitrijević. The first Serbian astronomical periodicals appeared in the third decade of the XX century. Belgrade observatory started to publish in that time almost in parallel three periodicals in astronomy: *Annuaire de l'Obs. Astr. Belgrade*, *Mémoires de l'Obs. Astr. Belgrade* and *Godišnjak našeg neba* (Almanac). Each of the first two publications was printed for six years, while the last volume of *Godišnjak* (for 1962) was printed in 1961. However, *Nautički Godišnjak* (Nautical Almanac, published by S. Šegan) may be considered as a successor of *Godišnjak našeg neba*. The publication *Saturn* was the first Serbian astronomical periodical oriented to the general public interested in astronomy, geodesy and meteorology and other related sciences. The main purpose of this article is to announce that this journal is completely digitized and made available, as an open access publication, to the general public. Digital copies of the journal are deposited in the Virtual Library of the Faculty of Mathematics in Belgrade.

2. FOUNDATION

The publication of Saturn started in 1935 as a messenger of the Yugoslav *Astronomical Society*, founded in Belgrade a year before. The original title of the Society was *Academic astronomical Society of the Belgrade University*. It changed once more its name in 1939 to *Yugoslav Astronomical Society*. The intention was to stress the Yugoslav nature of the society. The founder of the journal and the society as well was Djordje M. Nikolić (1908-1971), pro-Yugoslav Serbian science historian. Nikolić got Degree and PhD in Astronomy in France, where he acted as a member of the Resistance during WWII. He wrote rather recognized papers on Rudjer Bošković and south-Slav astronomy, as noted by A. Martocchia and S. Marchionni in their paper "Djordje Nikolić' *Yugoslavs in Astronomy*" (2013). The journal was supported by Hypothecary Bank in Belgrade.

This monthly periodical was conceived as a semiprofessional journal with many popular articles intended to astronomy lovers. At the same time the journal was planned to be useful to professional astronomers, surveyors, meteorologists and seismologists, because there were published also scientific articles in these areas. Popular and professional articles were separated into different sections, and there also was a section with short notes and news for people interested in astronomy.

Articles were published in Cyrillic and Latin, reflecting in this way both variants of Serbo-Croatian, following pro-Yugoslav attitude of the founder of the journal, Djordje Nikolić. Slovenian authors published in Slovenian. Some of the leading Yugoslav astronomers and physicists published there, e.g. Serb Milutin Milanković, Croat Stjepan Mohorovičić and Slovenian Lavo Čermelj.

3. EDITORIAL BOARD

The members of the Editorial board were prominent Yugoslav scientists and professionals in astronomy and related sciences. Most of them were from Belgrade, but there were members from Croatia and Slovenia as well. Some of them had very interesting biographies, while the most of them were holding PhD degree in astronomy obtained in then the leading scientific centers in Europe. Djordje Nikolić was the main editor, while the other members were:

General and academician Stevan Bošković (1869-1957), geodesists and professor at Military Academy in Belgrade. He is known for his very extensive geodetic measurements in Serbia in the first decade of XX century and his translation of the famous Tsinger's three volume book on astronomy. Bošković translated these books not by chance. He used Tsinger's method for the purpose of exact time determination needed for measurements the points of all geographic latitudes in Serbia during his very extensive geodetic measurements. Tsinger's book without doubt was his valuable companion during this exploration. He spent some time in the late XIX century studying astronomy and geodesy at the Pulkovo Observatory. Bošković certainly met Tsinger there who was then the leading Russian geodesists and professor in St. Petersburg, see Pejović and Mijajlović (2011).

Vojislav Grujić (1904-1944) who was holding two doctoral dissertations in mathematics related to astronomy, obtained at Strasbourg University in 1933. Before he went to Strasbourg he worked as an associate at the Astronomical observatory in Belgrade. However, due to some social circumstances he was not admitted to the

Observatory upon his return from Strasbourg. Hence, in spite of his very high education and background in astronomy he had no proper chance to work in astronomy professionally. He tragically lost his life in the eve of the very end of WWII.

Fran Dominko (1903-1987), Slovenian physicist and astronomer, got his Degree and PhD in Bologna, Italy. Worked in Belgrade since 1932, first as an astronomer and later as a gymnasium teacher until WWII. He moved to Ljubljana in 1948 for the university professor of astronomy. More details about him one can find for example in Wikipedia, Slovenian edition.

Ladislav S. Mužinić was the member of the first editorial board. We do not know much about him except that he lived in Zagreb before WWII. He published a short note *Breitenbestimmungsversuch von Zagreb* (Attempt to determine the latitude of Zagreb, 1936) in Astronomical notes, the predecessor of Astronomische Nachrichten. He also wrote articles for "Saturn" on astronomy and geodesy.

Nenad Janković (1911-1997) was jurist, but as professor Milan Dimitrijević described him, "his love and passion and his life's commitment was astronomy". He was the great popularizer of astronomy. For more details see Dimitrijević (1998). On the cover page of the first volume of "Saturn" it is written that Janković is the owner of the journal.

4. BROWSING THE JOURNAL

Many interesting, actual and informative articles were published in *Saturn*. They were in agreement with the current knowledge in astronomy and related sciences and obeyed surprisingly high scientific standards. All contributions, including short notes and reviews are meticulously divided into the "Popular part", "Professional part" and "News and notices". On the other side articles are accordingly classified into subjects: astronomy, meteorology, seismology, geodesy, personal news etc. It was not given priority to any particular discipline. For example, in astronomy articles cover many topics, from comets to time measurement and from supernova to cosmology. The used mathematical apparatus was correct and nontrivial. We can freely say that *Saturn* in many senses could compete with other astronomical journals published in that time in Belgrade. Obviously, editors put a lot of effort in preparing each volume of the journal.

As an illustration we give two examples, short notices printed in the journal. The first one is the obituary of Willem de Sitter (1872 - 1934), a prominent Dutch mathematician, physicist, and astronomer. A short biography and his main contribution to science are presented. Djordje Nikolić published in the same volume the article *Da li se vasiona proširuje* (Does the universe expand) where de Sitter views in cosmology are presented.

The second one is the notice on Hans Ertel's formula $gm^2 + mc = \pi he^2\Lambda$ (*Saturn*, year 1935, vol. 3, page 91) which connects fundamental physical constants: the Newton gravitational constant g, electron mass m, the Planck constant h, the electron charge e, speed of light c and the Einstein cosmological constant Λ. Hans Ertel (1904 – 1971) was a German natural scientist and a pioneer in geophysics, meteorology and hydrodynamics. More information on his biography and contribution to cosmology can be found at *Working group history of geophysics and cosmic physics*.

Here is the translation of the content (main articles) of the first volume of the journal. *Introductory part*: Introductory word, Position of astronomy in Yugoslavia

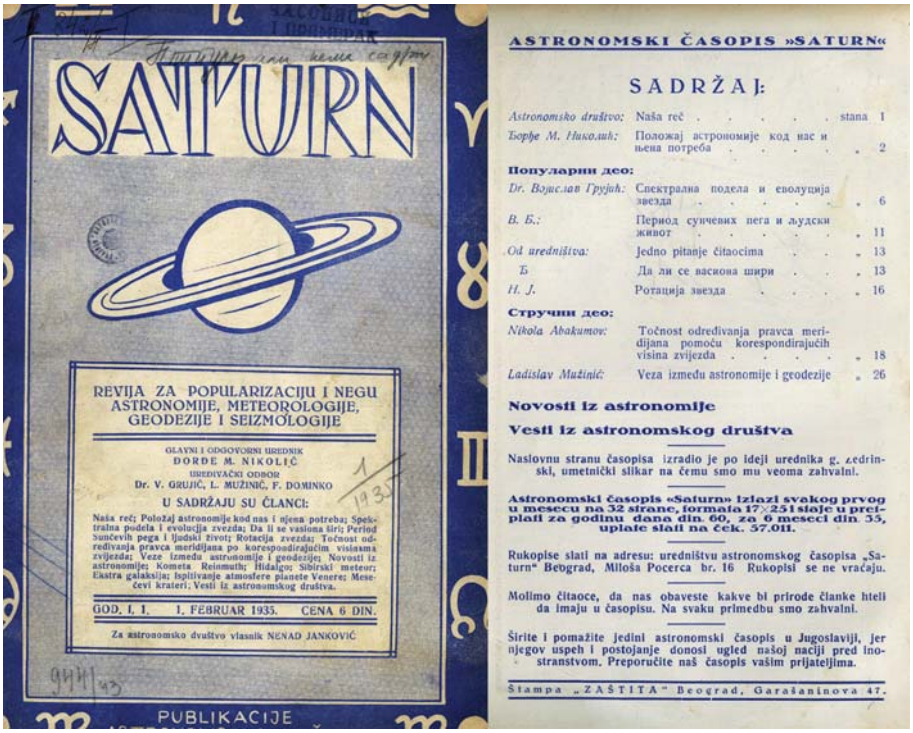

SATURN

REVIJA ZA POPULARIZACIJU I NEGU ASTRONOMIJE, METEOROLOGIJE, GEODEZIJE I SEIZMOLOGIJE

GLAVNI I ODGOVORNI UREDNIK
ĐORĐE M. NIKOLIĆ
UREĐIVAČKI ODBOR
Dr. V. GRUJIĆ, L. MUŽINIĆ, F. DOMINKO

U SADRŽAJU SU ČLANCI:

Naša reč; Položaj astronomije kod nas i njena potreba; Spektralna podela i evolucija zvezda; Da li se vasiona širi; Period Sunčevih pega i ljudski život; Rotacija zvezda; Tačnost određivanja pravca meridijana po korespondirajućim visinama zvijezda; Veze između astronomije i geodezije; Novosti iz astronomije; Kometa Reinmuth; Hidalgo; Sibirski meteor; Ekstra galaksija; Ispitivanje atmosfere planete Venere; Mesečevi krateri; Vesti iz astronomskog društva.

GOD. I. 1. FEBRUAR 1935. CENA 6 DIN.

Za astronomsko društvo vlasnik NENAD JANKOVIĆ

PUBLIKACIJE

ASTRONOMSKI ČASOPIS »SATURN«

SADRŽAJ:

Novosti iz astronomije

Vesti iz astronomskog društva

Naslovnu stranu časopisa izradio je po ideji urednika g. zedrinski, umetnički slikar na čemu smo mu veoma zahvalni.

Astronomski časopis «Saturn» izlazi svakog prvog u mesecu na 32 strane, formata 17×25 i slaje u preplati za godinu dana din. 60, za 6 meseci din. 35, uplate slati na ček. 37.011.

Rukopise slati na adresu: uredništvu astronomskog časopisa „Saturn" Beograd, Miloša Pocerca br. 16 Rukopisi se ne vraćaju.

Molimo čitaoce, da nas obaveste kakve bi prirode članke hteli da imaju u časopisu. Na svaku primedbu smo zahvalni.

Širite i pomažite jedini astronomski časopis u Jugoslaviji, jer njegov uspeh i postojanje donosi ugled našoj naciji pred inostranstvom. Preporučite naš časopis vašim prijateljima.

Štampa „ZAŠTITA" Beograd, Garašaninova 47.

Figure 1: Cover page of the first volume of *Saturn*.

and do we need it. *Popular part*: Spectral division and evolution of stars, Sunspots periods and human life, One question to the readers, Does the Universe expand, Star rotation, *Professional part*: The accuracy in determining the direction of the meridians using the corresponding height of the stars, Connection between astronomy and geodesy.

5. DIGITIZATION

All 72 volumes, about 2100 pages, were digitized during the spring and summer of 2020, and deposited in the Virtual Library of the Faculty of Mathematics in Belgrade. Professor Nadežda Pejović actually initiated this project and organized most of the jobs related to the project. Volumes printed in the period 1935-1937 were digitized by Žarko Mijajlović and in the years 1938 and 1940 by Aleksandar Jovanović, an administrator of the Faculty of Mathematics. Digitization of this periodical for the year 1939 is done by the National Library of Serbia. Mrs Tamara Butigan and Mrs Jasna Majerle from the National Library helped during the realization of this small project and gave us the digital copy of 12 volumes printed in 1939. Milan Jeličić from the *Astronomical Society "Rudjer Bošković"* lent us all hard copies of *Saturn* in possetion of the Society to digitize them and gave us a lot of help and valuable information about this journal. The OCR procedure is utilized on digital copies, so it is easy to search for terms and specific words through all the volumes.

Digital collection of the journal belongs to the division *Periodicals* of the Virtual Library. There are also digital collection of the journal *Godišnjak našeg neba*, see Šegan et al (2009), and digital copies of the significant part of edition of *Vasiona*, the contemporary Serbian popularization astronomical journal.

The National library has all 72 volumes of the journal in the printed form. The *Astronomical Society "Rudjer Bošković"* has all volumes except those printed in 1939.

6. CONCLUSION

The first Serbian and Yugoslav journal *Saturn* on popularization of astronomy and related sciences is presented. We also announced the digital collection of all issues of the journal which are deposited in the Virtual library of the Faculty of mathematics, University of Belgrade. This open access digital collection could be a valuable source for the history of astronomy in Yugoslavia before WWII.

References

Dimitrijević, M. S.: l998, *Serb. Astron. J.*, **158**, 131-145.
Martocchia, A., Marchionni, S.: 2013, *Semantic scholar*, Corpus ID: 219332281.
Milisavljević, S., Samardžija, B., Marčeta, D., Šegan, S.: 2011, *NCD Review*, **18**, 75-82.
Pejović, N., Mijajlović, Ž.: 2011, *NCD Review*, **19**, 11-25.
Protić Benišek, V., Dimitrijević, M.: 2014, *Publ. Astr. Soc "Rudjer Bošković"*, **13**, 625-630.
Šegan, S., Vidojević, S., Racković, K.: 2009, *NCD Review*, **14**, 9-12.
Simovljević, J. L.: 1980, *Trideset godina Prirodno-matematičkog fakulteta Univerziteta u Beogradu, 1947-1977*, PMF, Beograd.
Virtual Library, http://elibrary.matf.bg.ac.rs, Faculy of Mathematics in Belgrade.
Working group history of geophysics and cosmic physics, http://verplant.org/history-geophysics/wdschroeder.htm.

Publ. Astron. Obs. Belgrade No. 100 (2021), 307 - 314 *Progress Report*

COMPLEX OF ASTRONOMICAL OBSERVATORY IN BELGRADE AND ASTRONOMICAL STATION ON VIDOJEVICA

V. MIJATOVIĆ, Z. CVETKOVIĆ and G. DJURAŠEVIĆ
Astronomical Observatory, Volgina 7, 11060 Belgrade, Serbia
E–mail: vesna@aob.rs

Abstract. The Astronomical Observatory in Belgrade (Observatory) is a scientific institution. It consists of a building complex which was proclaimed a cultural monument in 2001 due to its exceptional architectural values. In addition to the unique architectural objects the Observatory possesses a very remarkable and valuable collection of astronomical instruments. Due to chronic lack of finances for the regular maintenance all objects of the Astronomical Observatory were endangered and suffered a rapid perishing. From 2015 the Astronomical Observatory has initiated an integral protection, maintenance and presenting of its both cultural and scientific heritages. The work carried out on conservation and restoration for some objects of the Observatory complex have been finished, whereas for the remaining ones are either still done or foreseen for the future. Concurrently the Observatory has improved the infrastructure at its Astronomical Station Vidojevica, located at the Vidojevica mountain top. During the last five years three new domes were built, the prefabricated pavilion with movable roof, pavilion with rotating dome within which the 1.4 m telescope was mounted and the one for hosting the 40 cm MEADE telescope. Modern radiation detectors have been furnished and the robotisation of observational process is being done.

1. INTRODUCTION

The complex of the Astronomical Observatory in Belgrade (Observatory in further text) was built on its current location in the period between 1929 and 1932, according to the project of Czech architect Jan Dubovy. It is thought that in the beginning of the fourth decade of the XXth century the Observatory complex was the most complicated architectural and urbanistic solution achieved by that time in Belgrade (Mihajlov 2018). Its core is the main building around which the pavilions with telescopes and other objects built for the auxiliary technical staff are distributed (Andonović 2014). The technical staff was in charge of maintaining the instruments and of the entire infrastructure. They had a carpentry and mechanics workshop and an accumulator was hosted in a separate building. The Observatory, as a complex wherein for more than eight decades astronomy has been developed, is among the oldest and most important state institutes of a special significance to scientific, societal and cultural development of Belgrade and Serbia and, as a territory containing special natural, urbanistic and architectural values, it occupies a distinguished place in the Serbian architecture of the XXth century. This was the reason why it became a cultural

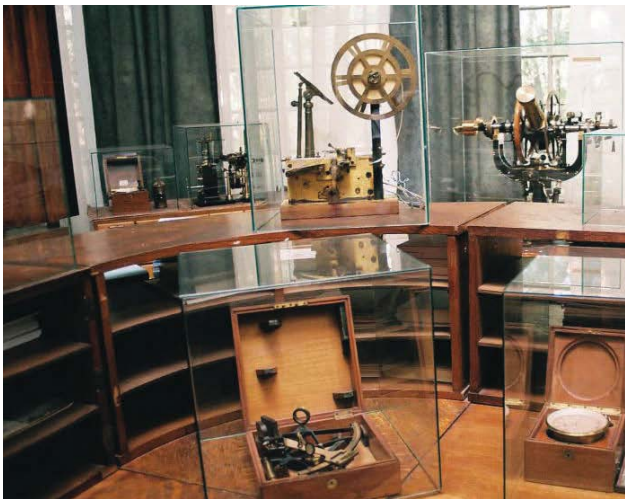

Figure 1: Bust of Milan Nedeljković (left panel) and the Collection of astronomical instruments (right panel).

monument by a decision of the Serbian Government, published in "Službeni glasnik RS" No 32/01 (see N/A 2001).

2. PROTECTION OF THE OBJECTS BELONGING TO THE OBSERVATORY

For a number of years the condition of majority of the Observatory objects was very dilapidated. Due to humidity and leaking very valuable astronomical instruments, which belong to a movable heritage of science, technology and culture, were endangered. In order to preserve the objects (pavilions), but also bearing in mind the necessity of conservation, protection and presentation of the entire astronomical heritage, in 2005 a decision was made to form an Astronomy Museum. The museum would consist of some of the pavilions hosted on the territory of the Observatory at Zvezdara (part of the city where the Observatory is located). The museum area was conceived to incorporate the pavilions no longer used in observational activities. The permanent museum contents would include instruments belonging to astronomical, meteorological, seismic, scientific and cultural heritage of Serbia, from the mere beginning till today.

Therefore, aimed at protecting valuable instruments the Observatory in cooperation with the Museum of Science and Technology in 2015 registered a museum collection of astronomical instruments (Figure 1). This collection contains optical instruments (with complete auxiliary equipment) which once were used in observations. It is important for the history of development of science and technology in Serbia and based on Decision No 176/1-2015 of the Museum of Science and Technology it was established as a cultural heritage of technological culture.

The building complex of Astronomical Observatory in Belgrade is also an ambient entity. Its area is 10 ha, it is situated inside the Zvezdara forest which based on an

official decision became a natural heritage (see N/A 2013). As a unique and specific entity, according to the experience acquired during organising manifestation *Days of Open Doors*, the observatory complex attracts a significant interest of the citizens. The objectives concerning the project of Astronomy Museum were formulated in accordance with this. There are ongoing conservation and protection works of all objects and instruments. The pavilions, which are no longer used for observations, are being adopted and converted into museum rooms. Functional revitalisation of the telescopes for educative purposes, dissemination and promotion of the Serbian astronomical heritage is being carried out. All this work is contributing to the advancement of the cultural and technological heritage in the city of Belgrade.

3. CONSERVATION, RESTORATION AND REDEMPTION INVESTMENT WORKS

In order to improve the protection of its complex the leadership of the Observatory, starting in 2015, has intensified its collaboration with the Cultural Monument Protection Institute of the city of Belgrade. This collaboration resulted in a rapid formation of the technical documentation needed for the restoration projects. On the basis of these projects a complete or partial renovation of individual objects and complex rooms has been done.

With the consent and recommendation of the Cultural Monument Protection Institute of the city of Belgrade the pavilion of the Large Transit instrument was renovated in 2015 (Figure 2). The pavilion hosting the Askania 19/258 cm instrument was brought back to its original condition. In its original form, with a proper illumination, this room was prepared to be presented and used for the museum purposes. The pavilion of the Large Transit Instrument is only one of the rooms foreseen for the permanent museum exhibition.

In 2016 the heating system in the main building was replaced. New heating boilers were mounted and the new fuel, pellet, was started to be used. Its use meets the ecological needs and requirements.

In 2017 and 2018 most of activities of the Observatory on protecting and presenting the cultural-scientific heritage were directed to the formation of projects concerning technical documentation, as well as to the construction and erecting of the bust of Milan Nedeljković, founder of Astronomical Observatory in Belgrade (Figure 1). This bust is located inside the entrance hall of the main building, between the main entrance and that to the library. The author of the bronze bust on a marble pedestal is the sculptor Vladislava Krstić.

One of the completed projects of technical documentation was materialised in 2019. Then conservation-restoration works on the dome, facade and inside the pavilion of the Small Refractor (Figure 3) were carried out. The pavilion hosting the Zeiss 20/302 telescope, that has two photo cameras of 16 cm in diameter, was completely renovated and equipped with internet installations and connections.

Up to now the most comprehensive works which prevented the perishing and collapse of the existing objects of the observatory complex were carried out in 2020. Thanks to the finances provided by the Cultural Monument Protection Institute of the city of Belgrade from the Ministry of Information and Culture the works on the dome, facade and roof terraces of the Large Refractor pavilion (Figure 4) were finished. The documentation needed for the implementation of the project were financed by

Figure 2: Photographs of the Large Transit Instrument: before remediation - left panel; after remediation - right panel.

Figure 3: Photographs of the Small Refractor: before remediation - left panel; after remediation - right panel.

Figure 4: Photographs of the Large Refractor: before remediation - left panel; after remediation - right panel.

Figure 5: Photographs of the School Pavilion: before remediation - left panel; after remediation - right panel.

the Astronomical Observatory in Belgrade. In this way the Zeiss 65/1055 refractor telescope was also protected from perishing. In general, this pavilion has been planned to be the central object of Astronomy Museum. Almost concurrently with the works on the Large Refractor those on the School pavilion were also carried out. Due to the worn out roof and destroyed facade of this object the universal astronomical instrument Askania Bamberwerk was dismounted from the pedestal and because of being endangered was temporarily displaced to the library. In late 2020 the works on the roof and facade of the School pavilion (Figure 5) were completed, whereas the conservation and restoration works inside will be carried out in 2021. During 2020, in the framework of the regular remediation-investment maintenance the offices at the place of the old entrance to the complex were remediated and adapted for the office rooms. The project of technical documentation for the reconstruction and renovation of the Large Vertical Circle pavilion was completed in December of 2020 whereby the prerequisites for carrying out the works on this object were made.

In the main building of the Observatory the library cellar was remediated, whereas the third cellar was adapted to become a cluster hall.

4. ENLARGING INFRASTRUCTURE AT THE ASTRONOMICAL STATION VIDOJEVICA

Because of the necessity of renovation and increasing the scope of observational activities it has been necessary to provide new instruments and radiation detectors which has also required enlarging the infrastructure at the Astronomical Station of Vidojevica (ASV). The subject of this paper part is the construction of objects at ASV and equipment providing from 2015 to 2021.

The main reason for enlarging the infrastructure was the implementation and finishing of project BELISSIMA (BELgrade Initiative for Space Science, Instrumentation and Modelling in Astrophysics), an FP7 infrastructural project of Astronomical Observatory in Belgrade. The project started on July 1, 2010 and was originally foreseen to last three years, but because of problems concerning the providing of the telescope and its mirror was continued two times, by June 30, 2016. The project implementation comprised providing a robotic telescope of 1.4 m main-mirror diameter so that it was necessary to construct a pavilion for it. Because of lack of money in 2015/2016 a prefabricated pavilion with movable roof was built (Figure 6) wherein 1.4 m telescope "Milanković" was mounted in late April 2016.

In 2017/2018 a professional pavilion (Figure 6) for telescope "Milanković" was built, with a rotating dome of 7 m diameter which was purchased from Italian firm Gambato. The complete robotisations of both the telescope and the pavilion became possible, which meant that the presence of observers in the pavilion was no longer required. All observations can be performed remotely, via Internet. In the mid-September of 2018 telescope "Milanković" was moved from the prefabricated pavilion to the one with rotating dome.

A 40 cm MEADE telescope was moved from the Observatory in Belgrade to ASV in 2019. It was for the purpose of observing asteroids at Astronomical Observatory in Belgrade while it was stationed there. A rotating dome pavilion for this telescope was constructed in the first half of 2020. The dome diameter is 3 m, it was purchased from Polish firm Scope Dome (Figure 6). The 40 cm MEADE telescope is planned to be mounted and installed in its final pavilion during the first half of 2021.

Figure 6: Pavilions wherein ASV telescopes are situated: left panel photograph - from left to right: pavilion with 6 m dome, pavilion with movable roof, pavilion with 3 m dome; right panel photograph - pavilion with 7 m dome where is 1.4 m telescope.

Between 2015 and 2020 an Andor iXon 897 Ultra CCD camera was obtained, also three CCD cameras, an Andor iKon-L and two SBIG STXL-8303e ones, as well as a selector instrument, were purchased from the funds of the Observatory via the mediation of the "Jedinica za upravljanje projektom – JUP" of the Serbian government.

The corresponding Ministry, at first that of Science and Technological Development of Serbia, then the one of Education, Science and Technological Development of the Republic of Serbia financed the construction of all objects and gave money for purchasing the 1.4 m telescope.

5. CONCLUSIONS

From the erecting and construction of the Observatory Complex no significant investment in its infrastructure had occurred. Due to this real danger of complete destruction and perishing for all objects with astronomical instruments, telescopes menaced. The period from 2015 till today may be regarded as the time of its complete renovation and revitalisation. Over this period the infrastructure at ASV was significantly enlarged and new instruments and radiation detectors were furnished.

Acknowledgments

We would like to thank to the anonymous reviewer for the careful reading of the paper and the constructive and helpful remarks. The work presented in this paper

was supported by the Ministry of Education, Science and Technological Development of the Republic of Serbia, and these results are parts of the Grant 451-03-9/2021-14/200002 of Astronomical Observatory.

References

Andonović, J.: 2014, Astronomska opservatorija u Beogradu: katalog theničke dokumentacije, Beograd, Zavod za zaštitu spomenika kulture grada Beograda, p. 6.
Mihajlov, S.: 2018, Moderna Beograda: arhitektonska baština prestonice, Beograd, Zavod za zaštitu spomenika kulture grada Beograda, p. 65.
N/A: 2001, Službeni glasnik Republike Srbije, br. 32/01, p. 27.
N/A: 2013, Službeni List grada Beograda, br. 57/I.

Publ. Astron. Obs. Belgrade No. 100 (2021), 315 - 321 *Progress Report*

ACTIVITIES OF THE SERBIAN EUROPLANET GROUP WITHIN EUROPLANET SOCIETY

I. MILIĆ ŽITNIK[1], A. NINA[2], V. A. SREĆKOVIĆ[2], B. P. MARINKOVIĆ[2], Z. MIJIĆ[2]
D. ŠEVIĆ[2], M. BUDIŠA[3], D. MARČETA[4], A. KOVAČEVIĆ[4], J. RADOVIĆ[5]
and A. KOLARSKI[6]

[1] *Astronomical Observatory, Volgina 7, 11000 Belgrade, Serbia*
E–mail: ivana@aob.rs

[2] *Institute of Physics Belgrade, University of Belgrade, Pregrevica 118, 11080 Belgrade, Serbia*

[3] *University of Belgrade School of Electrical Engineering, Bulevar kralja Aleksandra 73, 11000 Belgrade, Serbia*

[4] *Faculty of Mathematics, University of Belgrade, Studentski Trg 10, 11000 Belgrade, Serbia*

[5] *Department of Atmospheric Physics, Faculty of Mathematics and Physics, Charles University, Prague, Czech Republic*

[6] *Technical Faculty Mihajlo Pupin, University of Novi Sad, 23000 Zrenjanin, Serbia*

Abstract. Europlanet society connects many different scientific institutions all over the world. The Serbian Europlanet Group (SEG) was established at 2019. It currently has 20 active scientists from 6 institutions working in Serbia in different fields of planetary science as well as related fields. Here are presented activities of SEG in 2020.

1. INTRODUCTION

The European society promotes the European planetary science as well as related fields. Its aims are to support the development of planetary science at a national and regional level, particularly in countries and areas that are currently under–represented within the community, and early career researchers who established their network within the Europlanet: the Europlanet Early Career (EPEC) network ($https://www.europlanet-society.org/early-careers-network/$). The Europlanet consists of 10 Regional Hubs. More information about organization and activities of this society can be found at the website $https://www.europlanet-society.org/$.

Serbia is one of six countries included in the Southeast European Hub that was established in 2019. The Serbian Europlanet Group (SEG) currently consists of 20 members from 6 institutions. Details of members and activities of SEG can be found at the website $https://www.europlanet-society.org/europlanet-society/regional-hubs/southeast-europe/$. In this paper are described main activities and presented scientific research of SEG members related to the Europlanet fields in 2020.

2. CONFERENCES AND WORKSHOPS OF SEG 2020

2. 1. PARTICIPATION IN THE EUROPLANET SCIENCE CONGRESSES

The Europlanet Science Congress (EPSC) is the annual meeting of the Europlanet Society. In the Europlanet Science Congress 2020, seven scientists from Serbia participated with several lectures. It was first virtual EPSC congress attended by 1168 participants from 49 countries. Here, will be mentioned two of SEG participants.

Dušan Marčeta presented research about population of interstellar asteroids and possibility that one of the observational selection effects, known as Holetschek's effect, could be used for preliminary estimation of the size-frequency distribution of this population. Aleksandra Nina presented research on new methodology for earthquake prediction which was partially realized within the Europlanet workshop in Petnica Science Center in 2019.

2. 2. PARTICIPATION IN THE XII SERBIAN–BULGARIAN ASTRONOMICAL CONFERENCE

Serbian scientists organized a Europlanet session with several lectures during the XII Serbian–Bulgarian Astronomical Conference (SBAC 12). SBAC 12 was held in Sokobanja from September 25 to 29, 2020 (Popović et al. 2020). SEG presented its work (Nina et al. 2020a) and discussed with Bulgarian colleagues and with colleagues from Europlanet Southeast HUB countries about expanding of their cooperation.

2. 3. PARTICIPATION IN THE XIX SERBIAN ASTRONOMICAL CONFERENCE

The work of SEG was presented during the XIX Serbian Astronomical Conference (19 SAC), held at the Serbian Academy of Sciences and Arts in Belgrade from October 13 to 17, 2020 (Kovačević et al. 2020). Aleksandra Nina participated with invited lecture about investigation of the lower ionosphere disturbances as possible earthquake precursors and application of research of the lower ionosphere influences in Earth observations by satellite during influence a solar X-ray flare. Ivana Milić Žitnik gave progress report about asteroid's motion with orbital eccentricity in the range (0, 0.2) across the 2-body mean motion resonances with Jupiter with different strengths due to the Yarkovsky effect (Milić Žitnik & Novaković 2016, Milić Žitnik 2020a).

3. RESEARCHES OF SEG MEMBERS AT 2020

SEG members are scientists in different research fields. Here are a few researches that are in the areas of Europlanet.

3. 1. ASTRONOMY

3.1.1. Model of interstellar asteroids and expected predominance of retrograde object among the discovered objects

Dušan Marčeta and Bojan Novaković examined the model of interstellar asteroids and comets and found analytical expressions for the distributions of their orbital elements (Marčeta & Novaković 2020). They payed special attention to objects which could be detectable by future LSST survey. Also, they found that majority of these objects should move along retrograde orbits resulting in asymmetry of the distribution of

their orbital inclinations. Finally, they found that this asymmetry is a result of the Holetschek effect. Since this effect is size-dependant, its influence is stronger for populations with steeper size-frequency distributions since they are comprised of larger number of smaller objects. This fact could be used for preliminary estimation of the size-frequency distribution of the underlying true population of interstellar objects once when sufficient number of objects become discovered.

3.1.2 The relationship between the 'limiting' Yarkovsky drift speed and asteroid families' Yarkovsky V-shape

Ivana Milić Žitnik examined the relationship between asteroid families' V-shapes and the 'limiting' diameters in the $(a, 1/D)$ plane. Following the recently defined 'limiting' value of the Yarkovsky drift speed at 7×10^{-5} au/Myr (Milić Žitnik 2019), she decided to investigate the relation between the asteroid family Yarkovsky V-shape and the 'limiting' Yarkovsky drift speed of asteroid's semi-major axes. She has used the known scaling formula to calculate the Yarkovsky drift speed in order to determine the inner and outer 'limiting' diameters (for the inner and outer V-shape borders) from the 'limiting' Yarkovsky drift speed. The method was applied to 11 asteroid families of different taxonomic classes, origin type and age, located throughout the Main Belt. Her main conclusion was that the 'breakpoints' in changing V-shape of the very old asteroid families, crossed by relatively strong mean motion resonances on both sides very close to the parent body, are exactly the inverse of 'limiting' diameters in the a versus $1/D$ plane. This result uncovers a novel interesting property of asteroid families' Yarkovsky V-shapes (Milić Žitnik 2020b).

3.1.3 Astrobiology-habitability of exoplanets

Balbi, Hami and Kovačević (2020) present a new investigation of the habitability of the Milky Way bulge, that expands previous studies on the Galactic Habitable Zone. This work discusses existing knowledge on the abundance of planets in the bulge, metallicity and the possible frequency of rocky planets, orbital stability and encounters, and the possibility of planets around the central supermassive black hole. Another concern for habitability is the presence of the supermassive black hole in the Galactic center, but also in nearby Active galactic nuclei, that could have resulted in a substantial flux of ionizing radiation during its past active phase, causing increased planetary atmospheric erosion and potentially harmful effects to surface life as shown by Wislocka, Kovačević, Balbi (2019). This work was featured in famous Forbes Magazine in their section Innovavations. Andjelka Kovačević is a member of Working group of habitability of exoplanets of European astrobiology institute.

3. 2. GEOPHYSICS

3.2.1 Atmospheric aerosol remote sensing and modelling

The EARLINET lidar network was established with the goal of creating a quantitative, comprehensive, and statistically significant database for the horizontal, vertical, and temporal distribution of aerosols on a continental scale. Within the network Belgrade lidar station was involved in initiative for studying the changes in the atmosphere's structure, its dynamics, and its optical properties during the COVID-19 lock-down by comparison to the aerosol climatology in Europe. Near real time de-

livery of the data and fast analysis of the data products proved that aerosol lidars are useful for providing information not only for climatological purposes, but also in emergency situations like detecting airborne hazards for aviation (Papagiannopoulos et al. 2020). The preliminary results indicate that the lock-down did not affected the high troposphere, but for the low troposphere a certain effect can be seen. In addition, ongoing activities are related to the participation in ESA ADM-Aeolus mission (the first high-spectral resolution lidar in space) Cal/Val activity through validation of L2A products of aerosol profiles and studying the relationship between satellite AOD measurements and ground PM concentrations (Mijić & Perišić 2019).

3.2.2 Lower ionosphere

The lower ionosphere research was a continuation of research related to a possible new type of earthquake precursor in the form of signal noise amplitude reduction (Nina et al. 2020b) and examinations of the effects of the D-region which is disturbed by a solar X-ray flare on satellite signals (Nina et al. 2020c). Also, a new model for determining ionospheric parameters in the unperturbed D-region was developed.

3.2.3 Investigation of a possible lithosphere-ionosphere coupling through seismo-ionospheric effect

Possible relationship between amplitude and phase delay characteristics of the NWC/19.8 kHz signal transmitted from H. E. Holt in Australia (φ = 21.8° S, Λ = 114.16° E) towards Belgrade AbsPAL receiver (φ = 44.85° N, Λ = 20.38° E) in Serbia and seismic activity reported by Helmholtz-Zentrum Potsdam - Deutsches GeoForschungsZentrum GFZ in period from December 2005 to June 2007 was investigated with the main result presented in Kolarski and Komatina (2020).

3.2.4 Satellite radar technique for atmospheric water vapor measurement and modelling effects of the ionospheric disturbances

Satellite observation and measurements performed by the Synthetic Aperture Radar (SAR) and the Interferometric Synthetic Aperture Radar (InSAR) technique can be used for acquiring more information about the water vapor present within the atmosphere. The methodology of the SAR instrument and the InSAR technique is described in Radović (2020). Additionally, the focus is set on the four different satellites with SAR instruments working on different frequencies. Apart from that, in Radović (2020) is presented how neglecting the ionospheric perturbations which took place during the satellite measurements can influence modelling of the water vapor parameters derived from such measurements acquired by the SAR instruments carried by the mentioned satellites.

3. 3. ASTROPHYSICS

3.3.1. Atomic Molecular and Optical Physics group of researchers at the Laboratory for Atomic Collision Processes

LACP[1], Institute of Physics Belgrade, University of Belgrade, has been studying several collisional processes that involve electron scattering by atomic particles (e.g. for

[1] *http : //mail.ipb.ac.rs/ centar3/acp.html*

helium Jureta et al. (2014)) and laser interactions with gases (Rabasović et al. 2019), nanopowders (Šević et al. 2020a,b) and single crystal phosphors (Šević et al. 2021). Electron impact cross sections are relevant parameters in modelling of processes that occur in cometary coma (Marinković et al. 2017), collisional processes in AGNs (Dimitrijević et al. 2021) or Earth' s and other planets' atmospheres (Vukalović et al. 2021). Due to the immense importance of having full survey and accurate data of electron cross sections, there are several databases that maintain large sets of electron collisional data and even more, a unique portal for accessing such kind of data have been created through European framework programs (for a recent update of the Virtual Atomic and Molecular Data Centre[2] – VAMDC see e.g. Albert et al. (2020)).

BeamDB (Belgrade electron-atom/molecule DataBase[3]) is a collisional database that is maintained by the researchers of the LACP and it covers interactions of electrons with atoms and molecules in the form of differential (DCS) and integral cross sections for the processes such as elastic scattering, excitation and ionization (Jevremović et al. 2020). At present the output files that come from the search of BeamDB are present in the xml format of specific syntax developed by the International Atomic Energy Agency (IAEA)[4]. These so called "xsams" files contain full record of data sets including bibliographical entities, but the process of extracting values of cross sections is hard for researchers. That is why this group started to develop a converter which will convert xsams file into textual format file with simple columns that list values of impact energy, scattering angle, DSC and corresponding uncertainty. The next step would be adding a graphical presentation to the webpage of the BeamDB database. The graphics should present logarithm of DCS data points with error bars associated to the uncertainty versus impact energy and scattering angle in 3D graph.

Exploiting the fact that BeamDB contains large sets of DCS values obtained both experimentally and theoretically, they are in the process of developing machine learning algorithms for determining extrapolated DCS in the regions which are not accessed by experiments (Ivanović et al. 2020). The primary goal is to determine extrapolated values toward zero scattering angle as well as to large angles, usually from 150° to 180°.

It is envisaged that the BeamDB will contain electron spectroscopy data as well, beside the cross section data. At present, there is only a single threshold photoelectron spectrum of argon curated in the BeamDB, but the plans are to add energy loss spectra, presumably obtained in the LACP. This would allow them to develop tools for spectral classification and particular spectra identification based on data-mining methods. An overview of various data mining methods has been recently presented by Yang et al. (2020).

3.3.2. A&M data for stellar atmosphere modelling

Work on topics of modelling various astrophysical and laboratory plasma which are of interest for Europlanet community is continued. A&M datasets e.g. rate coefficients, Stark broadening parameters, line profiles, etc. are published during this year (see

[2] $https://portal.vamdc.eu/vamdc_portal/$
[3] $http://servo.aob.rs/emol$
[4] $https://www-amdis.iaea.org/xsams/documents/$

some of the papers: Srećković et al. 2020; Majlinger et al. 2020; Dimitrijević et al. 2020). Part of the data are hosted on SerVO at AOB[5].

4. CONCLUSION AND FURTHER WORK

In this paper are presented activities of Serbian scientists within Europlanet society. In the first part of the paper, are described briefly conferences that occurred in 2020 which promoted work of Serbian Europlanet Group. In the second part are presented several studies of SEG important for the Europlanet research fields. Serbian scientists plan to continue work within Europlanet society in the following years and to promote the Europlanet and SEG activities, as well as to expand SEG.

Acknowledgments

This research is supported by the Europlanet. The authors acknowledge funding provided by the Institute of Physics Belgrade, Astronomical Observatory (the contract 451-03-68/2020-14/200002), Faculty of Mathematics University of Belgrade (the contract 451-03-68/2020-14/200104) through the grants by the Ministry of Education, Science, and Technological Development of the Republic of Serbia.

References

Albert, D., Antony, B. K., Ba, Y. A. et al.: 2020, *Atoms*, **8(4)**, 76.
Balbi, A., Hami, M., Kovačević, A.: 2020, *Life*, **10(8)**, 132.
Dimitrijević, M. S., Srećković, V. A., Zalam, A. A., Miculis, K., Efimov, D. K., Bezuglov, N. N., Klyucharev, A. N.: 2020, *Contrib. Astron. Obs. Skaln. Pleso*, **50(1)**, 66.
Dimitrijević, M. S., Srecković, V. A., Ignjatović, Lj. M., Marinković, B. P.: 2021, *New Astronomy*, **84**, 101529.
Ivanović, S., Uskoković, N., Marinković, B. P., Mason, N. J.: 2020, *Publ. Astron. Obs. Belgrade*, **99**, 43.
Jevremović, D., Srećković, V. A., Marinković, B. P., Vujičić, V.: 2020, *Contrib. Astron. Obs. Skalnaté Pleso*, **50(1)**, 44.
Jureta, J. J., Milosavljević, A. R., Marinković, B. P.: 2014, *Int. J. Mass Spectrom.*, **365-366**, 114.
Kolarski, A., Komatina, S.: 2020, *Book of Abstracts*, International Symposium GEOSCIENCE 2020, November 20 - 22 2020, Bucharest, Romania, 81.
Kovačević, A., Kovačević Dojčinović, J., Marčeta, D., Onić, D.: 2020, *Book of Abstracts*, XIX Serbian Astronomical Conference, October 13 - 17, 2020, Belgrade, Serbia.
Majlinger, Z., Dimitrijević, M. S., Srećković, V. A.: 2020, *Mon. Not. R. Astron. Soc.*, **496(4)**, 5584.
Marinković, B. P., Bredehöft, J. H., Vujčić, V., Jevremović, D., Mason, N. J.: 2017, *Atoms*, **5(4)**, 46.
Marčeta, D., Novaković, B.: 2020, *Mon. Not. R. Astron. Soc.*, **498(4)**, 5386.
Mijić, Z., Perišić, M.: 2019, *Book of abstracts*, "Integrations of satellite and ground-based observations and multi-disciplinarity in research and prediction of different types of hazards in Solar system", Petnica Science Center, May 10-13, 2019, Geographical Institute "Jovan Cvijić" SASA, Belgrade, 51.
Milić Žitnik, I., Novaković, B.: 2016, *Aphys. Journ. lett.*, **816**, L31.
Milić Žitnik I.: 2019, *Mon. Not. R. Astron. Soc.*, **486**, 2435.
Milić Žitnik I.: 2020a, *Serb. Astron. Journ.*, **200**, 25.
Milić Žitnik I.: 2020b, *Mon. Not. R. Astron. Soc.*, **498(3)**, 4465.

[5]see e.g. *http : //servo.aob.rs/mold*

Nina, A., Radovanović, M., Popović, L. Č., Černok, A., Marinković, B., Srećković, V., Kovačević, A., Radović, J., Čelebonović, V., Milić Žitnik, I., Mijić, Z., Veselinović, N., Kolarski, A., Zdravković, A.: 2020a, *Proceedings of the XII Serbian-Bulgarian Astronomical Conference (XII SBAC)*, Sokobanja, Serbia, September 25-29, 2020, Eds: L. Č. Popović, V. A. Srećković, M. S. Dimitrijević, A. Kovačević, Publ. Astron. Soc. Rudjer Bošković, **20**, 107.

Nina, A., Pulinets, S., Biagi, P. F., Nico, G., Mitrović, S. Dj., Radovanović, M., Popović, L. Č.: 2020b, *Science of the Total Environment*, 710, 136406.

Nina, A., Nico, G., Odalović, O., Čadež, V. M., Todorović, M. D., Radovanović, M., Popović, L. Č.: 2020c, *IEEE Geoscience and Remote Sensing Letters*, **17(7)**, 1198.

Papagiannopoulos, N., D'Amico, G., Gialitaki, A., Ajtai, N., Alados-Arboledas, L., Amodeo, A., Amiridis, V., Baars, H., Balis, D., Binietoglou, I., Comerón, A., Dionisi, D., Falconieri, A., Fréville, P., Kampouri, A., Mattis, I., Mijić, Z., Molero, F., Papayannis, A., Pappalardo, G., Rodríguez-Gómez, A., Solomos, S., Mona, L.: 2020, *Atmos. Chem. Phys.*, **20**, 10775.

Popović, L. Č., Srećković, V. A., Dimitrijević, M. S., Kovačević, A.: 2020, *Book of Abstracts*, XII Serbian–Bulgarian Astronomical Conference (XII SBAC) September 25 - 29, 2020, Sokobanja, Serbia, Astronomical Observatory, Belgrade, Serbia.

Rabasović, M. S., Rabasović, M. D., Marinković, B. P., Šević, D.: 2019, *Atoms*, **7(1)**, 6.

Radović, J.: 2020, Master thesis, Faculty of Physics, University of Belgrade, Serbia.

Srećković, V. A., Dimitrijević, M. S., Ignjatović, L. M.: 2020, *Contrib. Astron. Obs. Skaln. Pleso*, **50**, 171.

Šević, D., Rabasović, M. S., Križan, J., Savić-Šević, S., Rabasović, M. D., Marinković, B. P., Nikolić, M. G.: 2020a, *Opt. Quant. Electron.* **52**, 232.

Šević, D., Vlasić, A., Rabasović, M. S., Savić-Šević, S., Rabasović, M. D., Nikolić, M. G., Marinković, B. P., Križan, J.: 2020b, *Tehnika*, **75(3)**, 279.

Šević, D., Križan, J., Rabasović, M. S., Marinković, B. P.: 2021, "Temperature sensing using YAG:Dy single crystal phosphor", *Eur. Phys. J. D.*, submitted.

Vukalović, J., Maljković, J. B., Tökési, K., Predojević, B., Marinković, B. P.: 2021, *Int. J. Molec. Sci.* **22(2)**, 647.

Yang, P., Yang, G., Zhang, F., Jiang, B., Wang, M.: 2020, *Arch. Computat. Methods. Eng.*, accepted, $https://doi.org/10.1007/s11831-020-09401-9$.

Wislocka, A. M., Kovačević, A. B., Balbi, A.: 2019, *Astron. Astroph.*, 624, A71.

Publ. Astron. Obs. Belgrade No. 100 (2021), 323 - 328 *Progress Report*

VARIOUS EFFECTS OF GALAXY FLYBYS: DEPENDENCE ON IMPACT PARAMETER

A. MITRAŠINOVIĆ[1,3], M. MIĆIĆ[1], M. SMOLE[1], N. STOJKOVIĆ[1,3], N. MARTINOVIĆ[2] and S. MILOŠEVIĆ[3]

[1] *Astronomical Observatory, Volgina 7, 11060 Belgrade, Serbia*
E–mail: amitrasinovic@aob.rs

[2] *Mathematical Institute of the Serbian Academy of Sciences and Arts, Kneza Mihaila 36, 11000 Belgrade, Serbia*

[3] *Department of Astronomy, Faculty of Mathematics, Studentski trg 16, 11000 Belgrade, Serbia*

Abstract. Galaxy flybys, interactions where two independent halos inter-penetrate but detach at a later time and do not merge, occur frequently at lower redshifts. Due to their violent nature, these interactions can significantly impact evolution of individual galaxies - from mass loss, and shape transformation, to emergence of tidal features, and formation of morphological disc structures (e.g. bar, spiral arms).

Based on N-body simulations of galaxy flybys, these various effects will be discussed briefly in the context of different impact parameters. While there is clear dependence on impact parameter for some effects, results suggest that secular evolution of galaxies should not be neglected.

1. INTRODUCTION

Galaxy flyby, as defined here, is an interaction where two independent halos inter-penetrate but detach at a later time, thus not resulting in a merger. It has to be noted that these interactions should not be mistaken for close galaxy passages where two halos remain separate at all times. Based on the analysis of cosmological N-body simulations, Sinha & Holley-Bockelmann (2012) found that this type of interaction can be as frequent as mergers. The number of flybys is comparable to the number of mergers on high redshift ($z >\sim 14$), while it can even surpass the number of mergers on lower redshifts ($z <\sim 2$) for halo masses $>\sim 10^{11} M_{\odot} h^{-1}$. In the second part of the series (Sinha & Holley-Bockelmann 2015), the authors further explored parameters of flybys and found that, in majority of flybys, secondary halo penetrates deeper than $\sim R_{\rm half}$ with initial relative velocity $\sim 1.6 \times V_{\rm vir}$ of the primary halo. Typical flyby mass ratio was found to be ~ 0.1 at high redshifts, or lower, at the lower redshift end. While major flybys (with mass ratio greater than 0.3 or even close to 1) are still possible, they are extremely rare.

Both frequency and strength of galaxy flybys suggest that these interactions have a potential to significantly impact evolution of individual galaxies. Previous studies, however scarce, explored various effects of galaxy flybys, primarily focusing on pri-

mary, more massive galaxy. Kim et al. (2014) showed that flybys can create warps at the edges of primary galaxy disk, visible in both gaseous and stellar component. Lang et al. (2014) examined the role of galaxy flybys in bar formation. They found that bar forms in both galaxies in flybys with mass ratio 1, and only in secondary with mass ratio 0.1. They also noted that induced changes are significantly stronger in flybys with prograde[1] orbits (as opposed to retrograde orbits). This was later additionally examined in more detail, and confirmed by Łokas (2018). Detailed study accounting for different galaxy models and orbits (flybys with different mass ratios and different strength of interaction) was done by Pettitt & Wadsley (2018). The authors covered a broad range of initial conditions and found that diverse morphological features can emerge - bars of various strengths and lengths and various manifestations of spiral structure. Particularly of interest is new critical condition for strength of interaction: the authors found that morphological features can emerge in much weaker interactions than previously known. Despite the lack of detailed studies examining secondary galaxy, flybys could still be as significant for its evolution. They were discussed briefly as a potential contributor to formation of ultra-diffuse galaxies (Wright et al. 2020).

The main goal of our work is to probe impact parameter and investigate its role in deeper flybys (where secondary halo penetrates deeper than half mass radius of the primary halo, $R_{\rm half}$). This approach aims to answer a question: is there a functional dependence on impact parameter for these various effects, and if so - what does it look like? In the following sections, we will describe our models, methods and simulations and give a brief overview of preliminary results.

2. METHODS

Primary galaxy model, with virial radius $R_{\rm vir} = 197.4$ kpc, was constructed as three-component model consisting of: NFW dark matter halo (600.000 particles with total mass $M_{\rm H} = 9.057 \cdot 10^{11} {\rm M}_{\odot}$), exponential stellar disk (300.000 particles with total mass $M_{\rm D} = 7.604 \cdot 10^{10} {\rm M}_{\odot}$), and Sérsic stellar bulge (100.000 particles with total mass $M_{\rm B} = 2.502 \cdot 10^{10} {\rm M}_{\odot}$). For the sake of simplicity, intruder galaxy, with virial radius $R_{\rm vir} = 91.56$ kpc, was scaled down to be 10 times smaller (in both number of particles and total mass), and consisting only of spherical components: NFW dark matter halo (60.000 particles) with total mass $M_{\rm H} = 9.044 \cdot 10^{10} {\rm M}_{\odot}$), and Sérsic stellar bulge (40.000 particles with total mass $M_{\rm S} = 1.022 \cdot 10^{10} {\rm M}_{\odot}$). Both models were evolved for 5 Gyr in isolation using publicly available code `Gadget2` (Springel 2005). This was done to ensure model stability in isolation, and to provide fiducial (data) points which will help differentiate flyby-induced changes from the ones arising from secular evolution.

Flyby simulations were evolved for 5 Gyr with outputs (snapshots) being saved every 0.01 Gyr. Primary and intruder galaxy were set as almost contact system (initial distance being roughly equal to the sum of their virial radii, $d \simeq 290$ kpc), with primary galaxy remaining static at the center of simulation box. Intruder galaxy was set on prograde parabolic orbit coplanar with primary galaxy disk with initial relative velocity $v_0 = 500$ km s^{-1}. This value, despite being larger than the most common one, falls into the range of realistic relative velocities in galaxy flybys. By

[1] the spin of the galaxy disk and its orbital angular momentum with respect to the perturber are aligned

Table 1: List of flyby simulations where b is pericentre distance (impact parameter), $R_{\mathrm{vir},1}$ virial radius of main galaxy, and v_b pericentre velocity.

Name	b [kpc]	$b/R_{\mathrm{vir},1}$	v_b [km s^{-1}]
B30	22.50	0.114	660.14
B35	26.53	0.135	650.86
B40	30.69	0.156	641.80
B45	35.07	0.178	632.86
B50	39.62	0.201	624.25
B55	44.27	0.224	616.16
B60	48.99	0.248	608.09
B65	53.72	0.272	601.28

slightly varying angles of initial position and intruder velocity vector, we achieved different impact parameters in different simulations while keeping interaction duration constant at 1.08 Gyr. Interaction duration is defined as the time during which halos overlap, i.e. distance between centers of galaxies is smaller than the sum of their virial radii, $d \leq R_{\mathrm{vir},1} + R_{\mathrm{vir},2}$. List of flyby simulations with relevant parameters is given in Table 1.

2. 1. ANALYSIS PROCEDURES

Our method is based on Fourier analysis for detection of morphological structures (bars and two armed spirals) in primary galaxy disk. When disk is decomposed in Fourier modes, these structures contribute the most to second mode C_2. Relative (mass normalized, since zeroth mode C_0 yields total mass) second mode is calculated as:

$$\frac{C_2}{C_0} = \frac{1}{M}\sum_{j=1}^{N} m_j e^{2i\phi_j} = C_{21} + iC_{22} \tag{1}$$

where M is total mass, and summation is performed over all particles with masses m_j and angles ϕ_j in $x-y$ plane. We then calculate amplitude $A_2 = \sqrt{C_{21}^2 + C_{22}^2}$ and phase $\phi_2 = \arctan(C_{22}/C_{21})$. Calculation was performed locally, by slicing the disk in annuli in $x-y$ plane for each simulation snapshot. This results in evolution maps for both amplitude $A_2(t, R/R_{\mathrm{D}})$ and phase $\phi_2(t, R/R_{\mathrm{D}})$ where R is central radius of each annulus, R_{D} disk scale radius, and t time of each snapshot. Detailed analysis is out of scope of this article, yet these maps can provide serviceable insight into structure formation and evolution. Both stellar bars and two armed spiral structure are characterized by high enough amplitude A_2 (most commonly $A_2 > 0.2$) but they differ in behaviour of phase ϕ_2 along radial component - bars have almost constant phase while phase of spiral arms is uniformly changing.

While analyzing intruder galaxy, we used three different mass estimates which we will refer to as: bound, virial and core mass. Bound mass filters particles with negative total energies (sum of kinetic and potential energy), thus gravitationally bound particles. Virial mass filters particles inside virial radius, which was determined by fitting NFW to spherical density profile, for each snapshot. Finally, core mass estimate is based on circular velocity profile. First, we calculate circular velocity

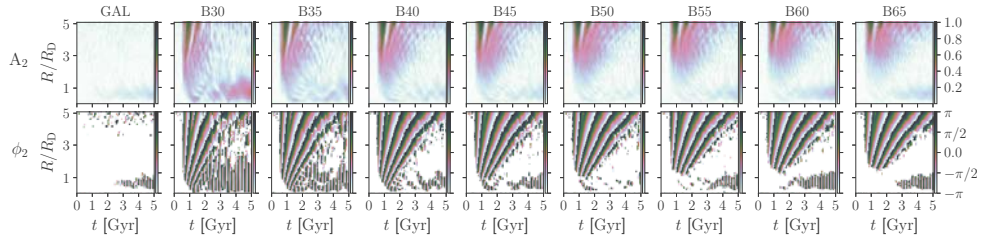

Figure 1: Evolution maps of Fourier second mode: amplitude $A_2(t, R/R_\mathrm{D})$ (upper panels) and phase $\phi_2(t, R/R_\mathrm{D})$ (lower panels). GAL row shows primary galaxy fiducial simulation, while the rest are showing flyby simulations, as defined in Table 1.

profile as $V_\mathrm{circ}(r) = \sqrt{GM(<r)/r}$, where $M(<r)$ is cumulative mass and r spherical radius. Radius r_max where this profile reaches maximum V_max is chosen as cutoff, and $M(<r_\mathrm{max})$ represents core mass.

3. RESULTS

3. 1. PRIMARY GALAXY

Fourier maps described in previous section are shown on Figure 1: amplitude $A_2(t, R/R_\mathrm{D})$ (upper panels) and phase $\phi_2(t, R/R_\mathrm{D})$ (lower panels). GAL row shows primary galaxy fiducial simulation, while the rest are showing flyby simulations, as defined in Table 1.

Two armed spiral structure forms almost immediately after the interaction. Radii of origin appear directly proportional to impact parameter, starting lower than scale radius ($R/R_\mathrm{D} < 1$) in simulation with the lowest impact parameter (B30), and ending with mid-disk origin ($R/R_\mathrm{D} \geq 2$) in simulation with the highest impact parameter (B65). However, these *deeper* spiral arms tend to wind up and dissolve faster suggesting that their lifetimes are inversely proportional to impact parameter.

Early bar formation is observed in two closest simulations (B30, B35). In B30, formed bar quickly evolves to get stronger and longer and remains present until the end of simulation, while its evolution in B35 is slower and chaotic. Bar evolution gets more stable in simulations with larger impact parameters, but their strengths and lengths do not correlate uniformly with impact parameter. One of the simulations (B50) is particularly interesting due to suppression of pre-existing bar instability (i.e. that the bar never fully forms). One possible explanation for chaotic bar evolution (in simulations with lower impact parameters) is co-evolution with winded, dissolving spiral arms. Spiral structure's and bar's regions never overlap in B55, b60, and B65 - allowing independent evolution of these features. This does not explain non-uniform dependence of bar's strength and length with impact parameter - more detailed analysis is needed to tackle that issue.

3. 2. INTRUDER GALAXY

Stellar component of intruder galaxy retains its mass, while significant dark matter mass loss is observed. Evolution of mass estimates is shown on Figure 2. Bound mass

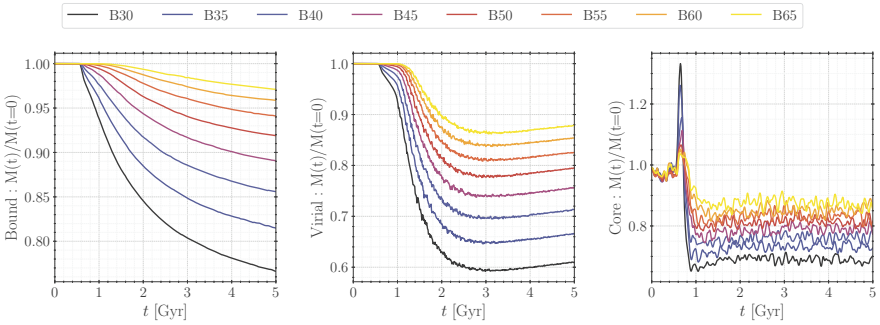

Figure 2: Evolution of mass estimates: bound mass (left), virial mass (middle), and core mass (right panel). Different simulations are represented with different colors. All mass estimates are calculated as a fraction of initial mass.

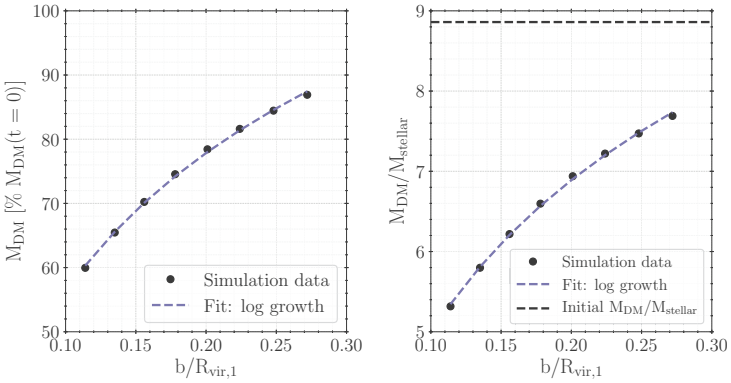

Figure 3: *Left*: Average virial mass of dark matter component after 2.5 Gyr (as a percentage of initial virial mass) as a function of impact parameter (in units of primary galaxy virial radius). Dots represent different simulations, while dashed line shows log growth fit. *Right*: Similarly to left panel, dark-to-stellar mass ratio after 2/5 Gyr as a function of impact parameter. Additional black dashed line represents initial dark-to stellar mass ratio.

continually decays until the end of every simulation. This is due to definition of this estimate - it includes gravitationally bound tidal features which, eventually unbind and detach from intruder galaxy. Core mass stabilizes by the end of interaction, being fairly constant with negligible variations until the end of every simulation. Core mass loss is lower than virial mass loss, implying that the core of intruder is semi-preserved. Following steep decline, virial mass stabilizes after 2.5 Gyr. Due to recapturing of some particles forming tidal feature, virial mass slightly increases near the end. Nevertheless, this mass estimate provides the best insight into total intruder mass. Thus, average virial mass after 2.5 Gyr is used in further analysis. It is shown on Figure 3 as a function of impact parameter, alongside dark-to-stellar mass ratio. Logarithmic growth (with impact parameter) for both of these is evident.

4. SUMMARY

Galaxy flyby is an interaction where two independent halos inter-penetrate but detach at a later time and do not merge. We performed a series of simulations to explore dependence of various effects caused by these interactions on impact parameter.

Both two armed spirals and stellar bars can form in the disk of primary galaxy. Spiral arms show clear dependence on impact parameter - their radii of origin are directly and their lifetimes are inversely proportional to impact parameter. Stellar bars, however, have non-uniform dependence on impact parameter. Strong and long bar forms in simulation with the smallest impact parameter, followed by weaker bar with chaotic evolution as impact parameter increases. Bar evolution gets more stable towards the highest impact parameters, but its strengths and lengths do not correlate with impact parameter. Suppression of pre-existing bar instability is also detected in one of the simulations. All of this raises new questions - did we neglect other possible contributions to chaotic bar evolution, and should we consider co-evolution of stellar bars and spiral arms?

We also found that secondary, intruder galaxy exhibits significant dark matter mass loss, while stellar component remains unaffected. This translates to decrease in dark-to-stellar mass ratio. Dependence of both virial mass and dark-to-stellar mass ratio on impact parameter follows logarithmic growth law. It is unclear whether this logarithmic growth law is universal or sensitive to initial conditions. Most likely, the law itself should remain universal with possible different fitting parameters for different initial conditions. This result is particularly of interest as it suggests that strongest or multiple subsequent flybys have the potential of stripping intruder galaxy of majority of its dark matter. More research is needed to fully explore those possibilities.

Acknowledgements

This work was supported by the Ministry of Education, Science and Technological Development of the Republic of Serbia (MESTDRS) through the contract no. 451-03-68/2020/14/200002 made with Astronomical Observatory of Belgrade, and the contract no. 451-03-68/2020/14/200104 made with Faculty of Mathematics, University of Belgrade.

References

Kim, J. H., Peirani, S., Kim S., Ann, H. B., An, S.-H., Yoon, S.-J.: 2014, *The Astrophysical Journal*, **789**, 90.

Lang, M., Holley-Bockelmann, K., Sinha, M.: 2014, *The Astrophysical Journal Letters*, **790**, L33.

Łokas, E. L.: 2018, *The Astrophysical Journal*, **857**, 6.

Pettitt, A. R., Wadsley, J. W.: 2018, *Monthly Notices of the Royal Astronomical Society*, **474**, 5645.

Sinha, M., Holley-Bockelmann, K.: 2012, *The Astrophysical Journal*, **751**, 17.

Sinha, M., Holley-Bockelmann, K.: 2015, *arXiv e-prints*, arXiv:1505.07910.

Springel, V.: 2005, *Monthly Notices of the Royal Astronomical Society*, **364**, 1105.

Wright, A. C., Tremmel, M., Brooks, A. M., Munshi, F., Nagai, D., Sharma, R. S., Quinn, T. R.: 2020, *arXiv e-prints*, arXiv:2005.07634.

Publ. Astron. Obs. Belgrade No. 100 (2021), 329 - 332 *Progress Report*

ON NEARLY CIRCULAR ORBITS

S. NINKOVIĆ
Astronomical Observatory, Volgina 7, 11060 Belgrade, Serbia
E–mail: sninkovic@aob.rs

Abstract. Nearly circular orbits are characteristic for thin discs of spiral galaxies, the subsystem and the type of galaxies to which the Sun and the Milky Way belong. Such orbits are studied in a way different from the usual one (epicycles). Formulae wherein the total energy and the conserved angular momentum component are expressed in terms of the mean distance and eccentricity are derived. The classical results concerning the sinusoidal dependence of distance on time and the ratio of the circular period to the anomalistic one for the same mean distance are confirmed.However, it is shown that, whereas the dependence on time even for a very low eccentricity begins to deviate from the sinusoidal form noticeably, the period ratio remains practically unaffected for eccentricities almost as high as 0.5.

1. INTRODUCTION

Orbits of stars which belong to the thin discs of spiral galaxies are known to be almost circular. This motion can be decomposed into the motions with respect to the axis of symmetry and with respect to the midplane. The former one is then analogous to the case of spherical symmetry (central motion) because of the conservation of one component (along axis of symmetry) of the angular momentum. Due to the assumption of low eccentricity it has been reduced to the linear harmonic oscillations (epicyclic approximation). On this subject information can be found in many books (e.g. Binney and Tremaine 2008, 3.2.3, p. 162).

More detailed studies of the motion of stars belonging to the thin disc in the solar neighbourhood show that the semi-separability assumption (see next section) is more realistic than the separability one, i.e. the maximum distance from the midplane is affected by the distance to the axis of symmetry, as well as that the dependence of the coordinates on time does not strictly follow simple sinusoidal forms (e.g. Stojanović 2015). In the same paper it is also inferred that, if eccentricity is low enough, assuming a power law dependence of the circular speed on the distance realistic orbital elements are obtained.

This is a short presentation only. The full account is to be published elsewhere.

2. BACKGROUND

The motion of a test particle is studied in an inertial reference frame. The coordinate system $Oxyz$ with origin at the centre of an axially symmetric stellar system (galaxy) is right-handed. Besides, the potential governing the motion is stationary. Because

of the axial symmetry it is convenient to replace the rectangular coordinates x and y with the cylindrical ones R and θ ($x = R\cos\theta$, $y = R\sin\theta$). The motion of the test particle is described by means of the Lagrange equations:

$$\ddot{R} - \frac{J_z^2}{R^3} = \frac{\partial \Pi}{\partial R} \; ; \tag{1}$$

$$\ddot{z} = \frac{\partial \Pi}{\partial z} \; .$$

In these two equations the potential is denoted as Π ($\Pi \geq 0$) and J_z is the designation for the component of the specific (per unit mass) angular momentum which is conserved.

The next assumption is that for the test particle motion it is always valid $z \approx 0$. In such conditions the potential $\Pi(R, |z|)$ is approximately equal to the corresponding potential in the plane $z = 0$ (midplane), $\Pi(R, 0)$ (semi-separability). Then the potential in (1) will be $\Pi(R, 0)$, which is independent of z. As a consequence, the partial derivative may be replaced by the total one and since the state is steady, the following quasi-integral of motion will be valid

$$E_p \approx \text{const}, \quad E_p = \frac{1}{2} V_p^2 - \Pi(R, 0);$$

$$V_p = \sqrt{\dot{R}^2 + \frac{J_z^2}{R^2}} \; .$$

For convenience the two integrals of motion, E_p and J_z, will be here replaced by the mean distance and eccentricity. Both will be defined via the pericentric and apocentric distances, R_p and R_a, respectively. The mean distance is

$$R_m = \frac{R_a + R_p}{2} \; ;$$

and eccentricity e

$$e = \frac{R_a - R_p}{R_a + R_p} \; .$$

In the case of the pure circular motion it will be: $e = 0$ and $R = R_m$ =const. A nearly circular motion ipso facto would be $e \approx 0$ and $R \approx R_m$. By introducing variation of the distance δR, $\delta R = R - R_m$, and the effective potential (subtracting square of tangential velocity component from potential), bearing in mind that the variation is expected to be small equation (1) can be reduced to the form of harmonic oscillations. However, the prerequisite is that in the binomial on e contained in J_z^2 the linear term should be absent. This prerequisite has not been examined. Therefore, in what follows the two integrals E_p and J_z will be expressed in terms of the mean distance and eccentricity.

The energy is expressed in the following way

$$E_p = \frac{1}{2} f u_c^2(R_m) - \Pi(R_m) \; ,$$

where f is dimensionless and u_c is the circular speed. As for J_z, it is borne in mind that at both $R = R_p$ and $R = R_a$ it is valid $\dot{R} = 0$. The energy conservation is used so that the potential at the extremal distances is expanded in series where the terms higher than two are neglected. The quantity J_z^2 is represented twice, once as $J_z^2(R_p)$ and once as $J_z^2(R_a)$. Since they must be equal to each other, one finds the following solutions

$$f = 1 \ ; \tag{2}$$

$$J_z^2 = R_m^2 u_c^2(R_m)[1 - (3 - \gamma_2)e^2] \ . \tag{3}$$

The dimensionless quantity γ_2, more precisely $\gamma_2(R_m)$, is defined via the second derivative of the potential at $R = R_m$ in this way

$$\frac{d^2\Pi(R,0)}{dR^2}(R_m) = \gamma_2(R_m)\frac{u_c^2(R_m)}{R_m^2} \ .$$

However, in addition to (2) and (3) there is another solution. It is based on the fact that the effective potential has the same value at $R = R_p$ and at $R = R_a$. Then one finds that J_z^2 is proportional to $[R_m u_c(R_m)]^2$ multiplied by $(1 - e^2)^2 \approx 1 - 2e^2$. The solutions are

$$f = 1 + [1 - \gamma_2(R_m)]e^2 \ ;$$

$$J_z^2 = R_m^2 u_c^2(R_m)[1 - 2e^2] \ .$$

In order to understand the meaning of these solutions another approximation is introduced, namely that in the surroundings of R_m the behaviour of the circular speed obeys this law

$$u_c(R) \propto R^\delta \ ; -\frac{1}{2} \leq \delta \leq 1$$

Since this is a local approximation only, δ will be in fact $\delta(R_m)$. It is easy to establish a relation between $\gamma_2(R_m)$ and $\delta(R_m)$. Thus one has

$$\delta(R_m) \leq 0, f = 1 \ , J_z^2 = R_m^2 u_c^2(R_m)[1 - 2(1 + \delta)e^2] \ .$$

$$\delta(R_m) \geq 0, f = 1 + 2\delta e^2 \ , J_z^2 = R_m^2 u_c^2(R_m)(1 - 2e^2) \ .$$

It is easy to see that the two solutions are congruent if $\delta(R_m) = 0$. For convenience (R_m) after δ is omitted in the formulae.

In order to obtain the dependence $R(t)$, provided that $e \approx 0$, the classical procedure is used. In other words, since $\dot{R} \equiv dR/dt$, one obtains an integral in R with a function of R in the denominator, then the approximations following from the condition $e \approx 0$ are taken into account and, finally, it is obtained

$$R = R_m \left[1 + e \sin\left(\frac{2\pi}{P_a}t - \frac{\pi}{2}\right)\right] \ . \tag{4}$$

Here P_a is the anomalistic period; for $e \approx 0$ it is given as

$$P_a(R_m) = P_{circ}(R_m)\left[2\left(\delta(R_m)+1\right)\right]^{-\frac{1}{2}} \ , P_{circ}(R_m) = \frac{2\pi R_m}{u_c(R_m)} \ . \tag{5}$$

These results are well known, but when they are obtained following the procedure applied here, then the term in the J_z^2 expression containing e^2 must be taken into account. If it is omitted, in the denominator of the integral we would have a square root from a negative value. In addition, it is seen that in the binomial in e for J_z^2 the linear term is zero, the prerequisite to obtain linear harmonic oscillations in the Lagrange equation.

3. DISCUSSION AND CONCLUSIONS

The behaviour of (4) and (5) will be considered when the eccentricity value is varied. For a test particle (star) satisfying the condition $e \approx 0$ the motion in R is examined numerically for a realistic potential. The general conclusion is that the period relation (5) suffers only minor changes when eccentricity increases, even to as high values as $e = 0.5$. On the other hand, time dependence (4) with increasing eccentricity rather rapidly shows changes, in particular that $R = R_m$ is attained, not after the quarter of period as it follows from (5), but earlier. In other words, if it is assumed $R = R_p$ corresponds to $t = 0$, then the time t_m when $R = R_m$ is shorter than $(1/2)P_a - t_m$. The test particle stays at distances exceeding R_m longer than at those shorter than R_m. As an improvement the following relation may be proposed

$$\frac{R}{R_m} = 1 + e\sin\left(\frac{2\pi}{P_a}t - \frac{\pi}{2}\right) + \frac{e^2}{\sqrt{2(1+\delta)}}\cos^2\left(\frac{2\pi}{P_a}t - \frac{\pi}{2}\right) \ .$$

Of course, it is $\delta = \delta(R_m)$. This relation is proven more realistic because it yields the time interval between $t = t_m$ and $t = (1/2)P_a$ longer than that between $t = 0$ and $t = t_m$ and their ratio increases with increasing eccentricity.

References

Binney, J., Tremaine, S.: 2008, Galactic Dynamics, Second Edition, Princeton University Press.

Stojanović, M.: *Serbian Astronomical Journal*, **191**, pp. 75-80

Publ. Astron. Obs. Belgrade No. 100 (2021), 333 - 338 *Progress Report*

PHYSICAL CONDITIONS IN THE LOW-IONIZATION BROAD-LINE REGION IN ACTIVE GALAXIES

S. PANDA[1,2]

[1] *Center for Theoretical Physics, Polish Academy of Sciences, Al. Lotników 32/46, 02-668 Warsaw, Poland*
E–mail panda@cft.edu.pl.

[2] *Nicolaus Copernicus Astronomical Center, Polish Academy of Sciences, ul. Bartycka 18, 00-716 Warsaw, Poland*

Abstract. Resolving the complexity in FeII species in quasar spectra has been an ongoing work for over 40 years. First identified and reported for the prototypical Narrow-line Seyfert 1 galaxy, I Zw 1 (Phillips 1978), the study has made a niche of its own in the field of AGN research. Seminal works led by Boroson & Green (1992), Verner et al. (1999), Sigut & Pradhan (2003) and others encapsulate the 'yet to be complete' understanding of the physics of the line formation for this first-ionized state of iron (FeII). A major part of the puzzle is lent by the sheer number of spectral lines in FeII that spans across a wide energy range (from UV to NIR). This extended emission seen in the spectra mimics a continuum of sorts, thus the telltale term *pseudo-continuum*. Gaining knowledge from the past studies and of our own, in this study we search for a reliable proxy to FeII. This proxy, CaII, is a much simpler ionic species which is characterized by its triplet in the near-infrared part of an AGN spectrum. The analogous line excitation mechanisms (dominated by the Lyα fluorescence and collisional excitation) for the production of these two species is confirmed by the tight correlation between the respective line strengths that we observe from our up-to-date collection of coincident measurements in the optical and NIR, and re-affirmed by our photoionization models. Additionally, our models constrain the physical parameters, such as the required level of ionization and the density of the medium, i.e. the broad-line region (BLR), that contain these ionic species, hinting also to the cloud's composition and structure (Panda et al. 2020; Panda 2020). This study reveals the utility of the CaII as a proxy for FeII in ways more than one, primarily, establishing a new radius-luminosity relation and in quasar main sequence studies.

1. INTRODUCTION

The complexity of FeII is majorly due to the numerous transition lines this first ionized state of Fe has, spreading across the near infrared (NIR) to ultraviolet (UV) wavelengths (Boroson & Green 1992, Bruhweiler & Verner 2008, Garcia-Rissmann et al. 2012) which makes it quite complicated to be modelled. The difficulty in understanding the FeII emission has led us in search of other reliable, simpler ionic species such as CaII and O I (Martínez-Aldama et al. 2015 and references therein) which would originate from the same part of the BLR and could play a similar role in quasar main sequence studies. Here, the CaII emission refers to the *Ca triplet* (CaT),

i.e., the IR triplet emitting at λ8498Å, λ8542Å and λ8662Å. We refer the readers to Panda et al. (2020) for an overview on the issue of CaT emission in AGNs and its relevance to the FeII emission.

2. METHOD & ANALYSIS

We make use of a subset of the photoionization models executed in Panda (2020) using CLOUDY (v17.02, Ferland et al. 2017) which covers a wide range of parameter space, i.e. varying the cloud particle density, $10^{10.5} \leq n_H \leq 10^{13}$ (cm^{-3}), the ionization parameter, $-4.25 \leq \log U \leq -1.5$, the metallicity, $0.1Z_\odot \leq Z \leq 10Z_\odot$, at a base cloud column density, 10^{24} cm^{-2}. We utilize the spectral energy distribution (SED) for the nearby (z= 0.061) NLS1, I Zw 1[1]. In this paper, we concentrate only on the metallicity case at solar ($Z_\odot$) and at $10Z_\odot$. Furthermore, an additional set of models were performed that included a non-zero microturbulence value, i.e. at 20 $km\,s^{-1}$. This value of microturbulence has been shown in our previous works (Panda et al. 2018, 2019, Panda 2020) to aid in further increase in the optical FeII emission. We focus on the four low-ionization lines (LILs, IP $<$ 20 eV) that are confined in the broad-line clouds, i.e. Hβ, the optical FeII blend[2], O I λ8446[3] and CaT; and extract the information about their line emission by estimating their line equivalent widths (EWs). The EWs are estimated using continua appropriate for the emission lines in consideration obtained from the models, e.g. a continuum luminosity at 4885.36Å for the Hβ and the optical FeII blend, and one at 8329.26Å for the O I λ8446 and CaT.

A vital information to constrain the emitting region of these lines is given by their distance from the ionizing source, the radius of the BLR ($R_{\rm BLR}$) in this case. The $R_{\rm BLR}$ can be inferred using the photoionization theory,

$$R_{BLR}\,[cm] = \sqrt{\frac{Q(H)}{4\pi U n_H c}} \equiv \sqrt{\frac{L_{bol}}{4\pi h\nu\ U n_H c}} \simeq \frac{2.294 \times 10^{22}}{\sqrt{U n_H}} \tag{1}$$

where, $R_{\rm BLR}$ is the distance of the emitting cloud from the ionizing source which has a mean local density n_H and receives an ionizing flux that is quantified by the ionization parameter, U. $Q(H)$ is the number of ionizing photons, which can be equivalently expressed in terms of the bolometric luminosity of the source per unit energy of a single photon, i.e. hν. Here, we consider the average photon energy, hν = 1 Rydberg (Wandel et al. 1999, Marziani et al. 2015). The bolometric luminosity of I Zw 1 is $L_{\rm bol} \sim 4.32 \times 10^{45}$ erg s^{-1}. This is obtained by applying the bolometric correction prescription from Netzer (2019) on I Zw 1's $L_{5100} \sim 3.48 \times 10^{44}$ erg s^{-1} (Persson 1988).

3. RESULTS & DISCUSSIONS

CLOUDY calculates the equivalent width by assuming a 100% covering factor[4]. Baldwin et al. (2004) showed that a covering factor of $\approx$ 20% is a good indicator of a successful

[1]The I Zw 1 ionizing continuum shape is obtained from NASA/IPAC Extragalactic Database.
[2]the optical FeII emission blue-ward of the Hβ emission line within λ4434-4684 Å.
[3]the NIR emitting lines at λ8446.25Å, λ8446.36Å and λ8446.76Å.
[4]Covering factor or CF is defined as the fraction of 4π sr covered by the clouds, as seen from the central black hole. Normally, the CF is expressed as $\Omega/4\pi$, where Ω is the solid angle.

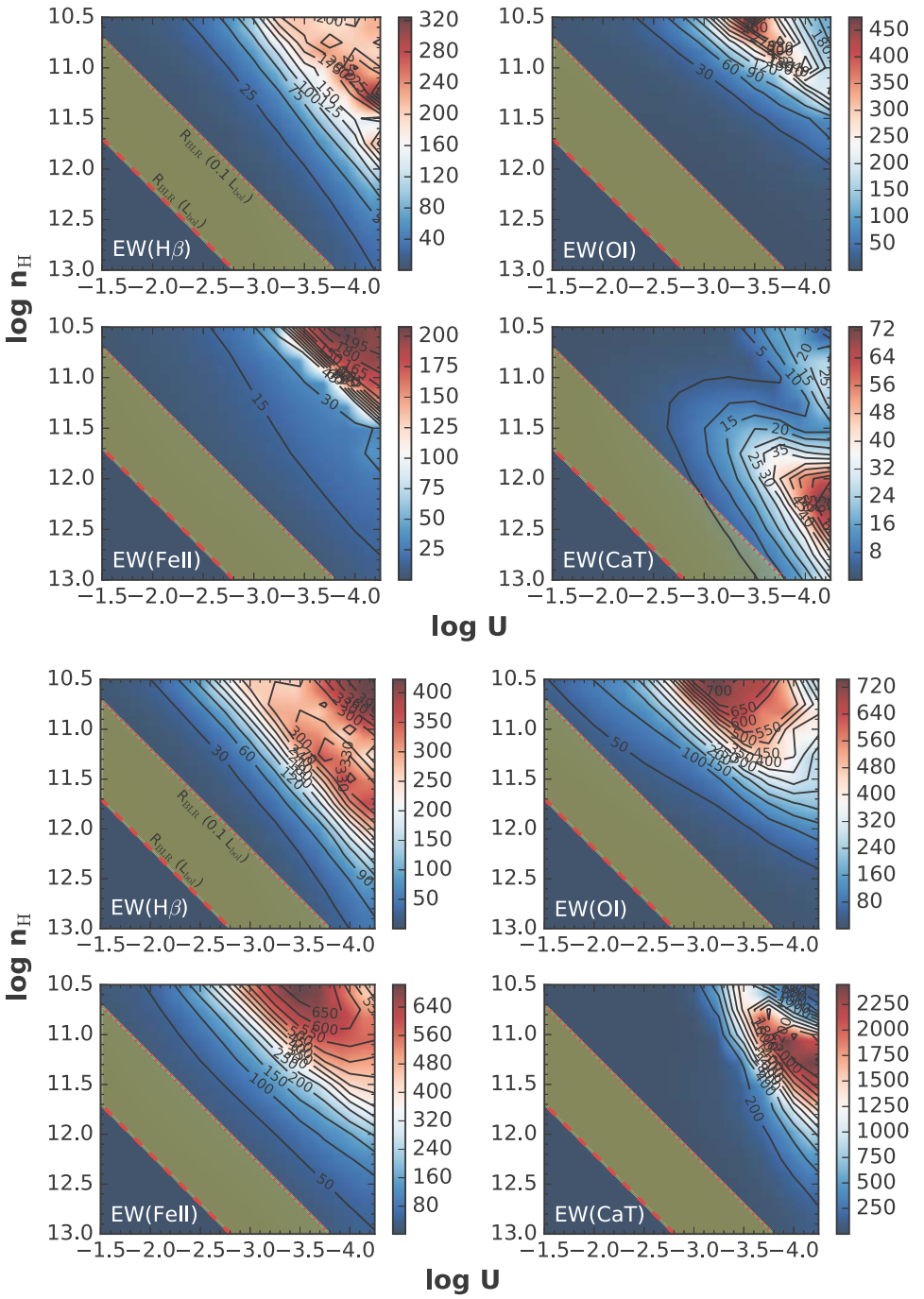

Figure 1: Base model at Z = $Z_\odot$ (*UPPER*) vs at Z = $10Z_\odot$ (*LOWER*) at zero microturbulence. The colorbar and the contours mark the EWs of the respective lines considering a 20% CF. The shaded region depicts the inferred size of the BLR using Equation 1 for $10\%L_{\rm bol}$ and at $L_{\rm bol}$ for `I Zw 1`.

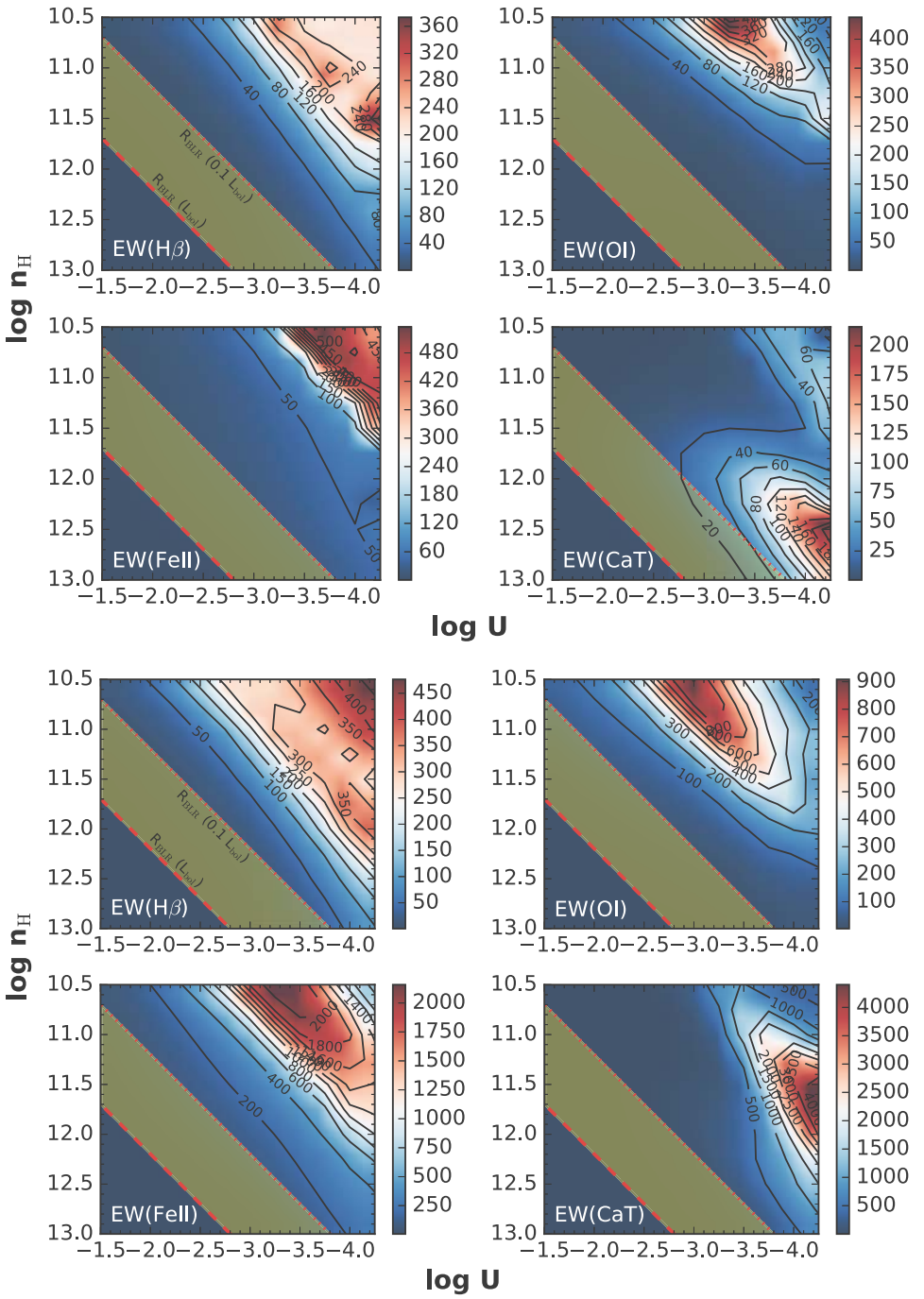

Figure 2: Base model at $Z = Z_\odot$ (*UPPER*) vs at $Z = 10Z_\odot$ (*LOWER*) at 20 km s^{-1}. The colorbar and the contours mark the EWs of the respective lines considering a 20% CF. The shaded region depicts the inferred size of the BLR using Equation 1 for $10\%L_{\rm bol}$ and at $L_{\rm bol}$ for `I Zw 1`.

model. A typical CLOUDY predicted equivalent width of > 400 Å is consistent with the observed value with a $\sim$20% of covering factor. We utilize this value of CF to estimate the EWs for the four LILs in our analysis.

3. 1. NEED FOR HIGHER-THAN-SOLAR METALLICITY IN THE BLR

In Figure 1, we illustrate the distribution of the EWs for the four LILs in the $\log U - \log n_H$ diagram. The two sets of illustration correspond to two selected cases of metal content in the BLR cloud - at solar metallicity ($Z_\odot$) and at $10Z_\odot$. In our earlier studies (Panda et al. 2018, 2019, 2020, Panda 2020), we have found in order to reproduce the required FeII emission for sources with significantly high FeII strength (R_{FeII}[5] $\gtrsim 1$), higher metal content is required in addition to relatively high number density (i.e. $\sim 10^{12}$ cm^{-3}) and cloud sizes that are of the same order (this requires to set a cloud column density $\sim 10^{24}$ cm^{-2}). The shape of the ionizing continuum has also a role to play to provide sufficient number of ionizing photons carrying energies up to 1 Rydberg (Panda et al. 2020). The panels for the solar metallicity case in Figure 1 show a preference of a low-ionization ($-4.25 \leq \log U \leq -3.0$), relatively low density ($10^{10.5} \leq n_H \leq 10^{11.5}$ cm^{-3}) for the Hβ and FeII, while this is slightly shifted to higher ionization values and lower densities for O I λ8446. For CaT, the emission is quite spread out in terms of the EWs recovered, with densities covering the full range assumed in the models, albeit the fact that the ionization levels are similar to the other lines. We have found in Panda (2020) that an optimum metallicity requirement for the FeII and CaT emission for I Zw 1 is $\gtrsim 10Z_\odot$, with CaT emission able to be significant even at lower metal content (but above solar values). Another key to the issue is the location of the BLR cloud from the ionizing source, i.e. the accretion disk. This is illustrated in the panels wherein we use Eq. 1 and assume two cases for the bolometric luminosity - at 10% and 100%. The former case has been tested in our previous work (Panda 2020) that infers perfect agreement of the radial size from photoionization to the reverberation-mapped radius for this source. This implies that the continuum that the BLR *sees* is different from what a distant observer perceives. The inferred EWs within this highlighted zone in Figure 1 suggest EWs < 15Å(in solar case) for Hβ, O I λ8446 and FeII, and ~ 5Å for CaT. This then implies a quite low value for R_{FeII} ($\sim$0.6) and equivalently for R_{CaT} (i.e., ratio of the CaT emission to the Hβ, $\sim$0.4). This issue gets resolved in the $10Z_\odot$ models where the EWs recovered are sufficient to provide strengths of FeII and CaT that are identical to the observed estimates (Persson 1988, Marinello et al. 2016). It is also worth noticing that the increase in the metal content pushes the CaT emission closer to the other three lines.

3. 2. PUSHING THE LIL EMISSION: CHAOTIC MOTIONS WITHIN THE BLR

Local turbulence substantially affects the FeII spectrum in photoionization models by facilitating continuum and line-line fluorescence. Increasing the turbulence can increase the FeII strength and give better agreement between the predicted shape of the FeII blends and observation (Shields et al. 2010). The effect of the microturbulence has been carefully investigated in our previous works (Panda et al. 2018, 2019, Panda 2020) where a systematic rise in the R_{FeII} estimates is obtained by increasing the microturbulence up to 10-20 km s^{-1}. We test this in the context of this work

[5] i.e., the ratio of the integrated FeII emission in the optical blue-wards of the broad Hβ line to the Hβ emission.

and the results are illustrated in Figure 2. The individual lines' EWs rises by up to $\sim$2 times when the turbulence in the medium is raised from 0 to 20 $\mathrm{km\,s^{-1}}$, and the inferred $\mathrm{R_{FeII}}$ values are higher for models with 20 $\mathrm{km\,s^{-1}}$ turbulence. The case with 20 $\mathrm{km\,s^{-1}}$ and $10\mathrm{Z_\odot}$ results in bringing all the four species in agreement in terms of the parameter space occupied by them. Their individual behaviour needs further investigation and will be explored in a future work.

Acknowledgements

The project was partially supported by the Polish Funding Agency National Science Centre, project 2017/26/A/ST9/00756 (MAESTRO 9) and MNiSW grant DIR/WK/2018/12.

Softwares: `CLOUDY` v17.02 (Ferland et al. 2017); `MATPLOTLIB` (Hunter 2007); `NUMPY` (Oliphant 2015)

References

Baldwin, J. A., Ferland, G. J., Korista, K. T. et al.: 2004, *ApJ*, **615**, 610.
Boroson, T. A., Green, R. F.: 1992, *ApJS*, **80**, 109.
Bruhweiler, F., Verner, E.: 2008, *ApJ*, **675**, 83.
Ferland, G. J., Chatzikos, M., Guzmán, F. et al.: 2017, *RMxAA*, **53**, 385.
Garcia-Rissmann, A., Rodríguez-Ardila, A., Sigut, T. A. A., Pradhan, A. K.: 2012, *ApJ*, **751**, 7.
Hunter, J. D.: 2007, *Computing in Science and Engineering*, **9**, 90.
Marinello, M., Rodríguez-Ardila, A., Garcia-Rissmann, A. et al.: 2016, *ApJ*, **820**, 116.
Martínez-Aldama, M. L., Dultzin, D., Marziani, P. et al.: 2015, *ApJS*, **217**, 3.
Marziani, P., Sulentic, J. W., Negrete, C. A. et al.: 2015, *ApSS*, **356**, 339.
Netzer, H.: 2019, *MNRAS*, **488**, 5185.
Oliphant, T.: 2015, *NumPy: A guide to NumPy*, 2nd edn., CreateSpace Independent Publishing Platform, USA, http://www.numpy.org/http://www.numpy.org/
Panda, S., Czerny, B., Adhikari, T. P. et al.: 2018, *ApJ*, **866**, 115.
Panda, S., Czerny, B., Done, C., Kubota, A., 2019, *ApJ*, **875**, 133.
Panda, S., Martínez-Aldama, M. L., Marinello, M. et al.: 2020, *ApJ*, **902**, 76.
Panda, S.: 2020, arXiv e-prints, arXiv:2004.13113.
Persson, S. E.: 1988, *ApJ*, **330**, 751.
Phillips, M. M.: 1978, *ApJ*, **226**, 736.
Shields, G. A., Ludwig, R. R., Salviander, S.: 2010, *ApJ*, **721**, 1835.
Sigut, T. A. A., Pradhan, A. K.: 2003, *ApJS*, **145**, 15.
Verner, E. M., Verner, D. A., Korista, K. T. et al.: 1999, *ApJS*, **120**, 101.
Wandel, A., Peterson, B. M., Malkan, M. A.: 1999, *ApJ*, **526**, 579.

Publ. Astron. Obs. Belgrade No. 100 (2021), 339 - 343 *Progress Report*

LUCKY IMAGING AT VIDOJEVICA

R. PAVLOVIĆ, Z. CVETKOVIĆ, G. DAMLJANOVIĆ and M. D. JOVANOVIĆ
Astronomical Observatory, Volgina 7, 11060 Belgrade, Serbia
E–mail: rpavlovic@aob.rs

Abstract. We use a Lucky Imaging technique to obtain images with much improved angular resolution. We present the first results from a short observational campaign on the 1.4 m telescope "Milanković" at Vidojevica and quantify the performance of our system when astronomical seeing is 1.5 arcseconds or more. Also, we are investigating the limits of our equipment and possible application to other observational programmes.

1. INTRODUCTION

As early as from 2011 researchers of the Astronomical Observatory in Belgrade who study visual double stars have been trying to get the necessary equipment for speckle interferometric technique of observing these objects and/or lucky imaging. Here we present lucky imaging technique which efficiently uses a high number of images in order to freeze the influence caused by atmospheric turbulences. This technique improves the image resolution under the limits imposed by atmospheric seeing.

A fast CCD camera Andor iXon 897 Ultra was obtained in 2017 and it was tested immediately at the 60 cm telescope "Nedeljković" (Pavlović et al. 2018). Due to problems with opening the dome inside which the 60 cm telescope was situated, this CCD camera was transferred to the left port of the 1.4 m telescope "Milanković". Telescope "Milanković" optical configuration is Ritchey-Crétien with "bent" Cassegrain focus which provides users with two available ports where instruments can be mounted. After a short time at the left port of this telescope a focal reducer and a new Andor iKon-L CCD camera were mounted, whereas the Andor iXon 897 Ultra CCD camera was moved to the right port without focal reducer. The left port has a focal reducer which reduces the focal length of the telescope from 11.2 m to 7.1 m. This would be an ideal configuration: at the left port there is a good camera with a large field of view, whereas at the right one an ultrafast camera. For the lucky imaging technique it is necessary to use concurrently two CCD cameras, one capable of obtaining frames of short exposures, of the order of a few milliseconds, and another one which has a wide field of view used in orientation determination, i.e. position angle. Due to its alt-azimuth mount, telescope "Milanković" has derotators for the field of view on both ports and those derotators are not synchronized. This produces a problem in determining the position angle of the components of double stars. To solve this, it was necessary to provide another CCD camera and selector instrument in order to mount both cameras at the same telescope port. Finally, the equipment for lucky

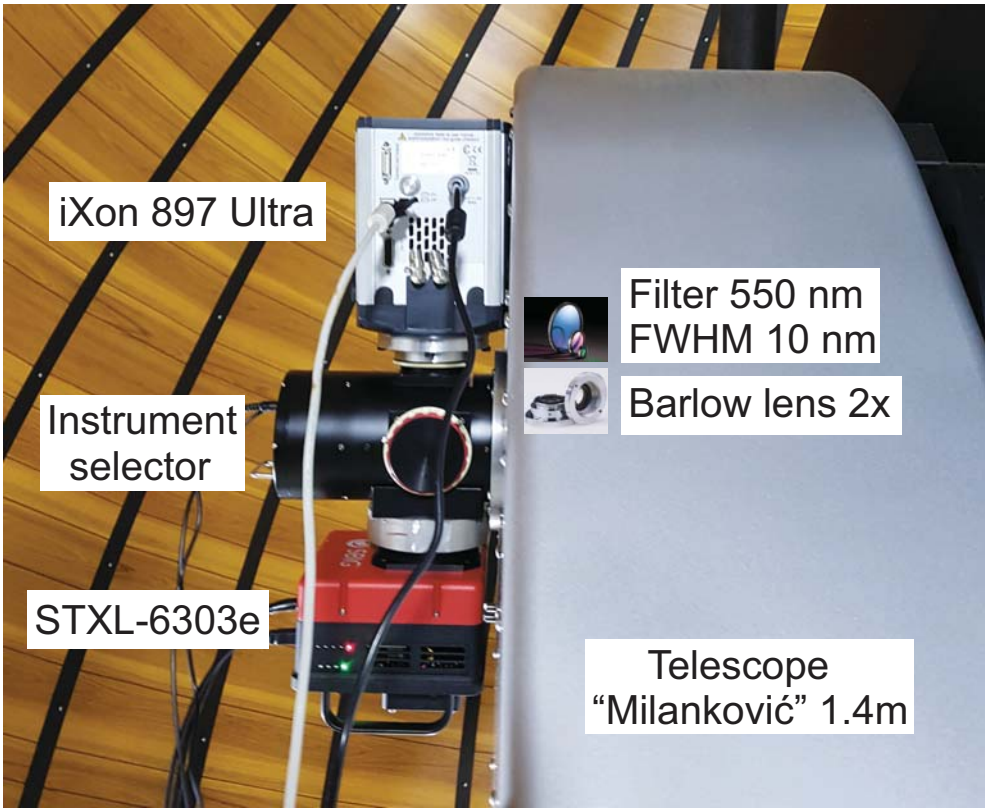

Figure 1: The equipment for lucky imaging attached to telescope “Milanković” at AS Vidojevica.

imaging was completed in early 2020, and in July first observations of double and multiple stars were performed using this technique.

2. LUCKY IMAGING ON “MILANKOVIĆ”

As already mentioned, our equipment for lucky imaging mounted at the right port of “Milanković” telescope consists of two CCD cameras Andor iXon 897 Ultra and SBIG STXL-6303e and an Optec Perseus 4-port Instrument Selector (Figure 1). The properties of these two cameras are given in Table 1. The selector instrument makes it possible to divert a light beam from either camera to the other one. Within the instrument selector and in front of the iXon 897 Ultra camera there are two more components: a single filter with central wavelength at 550 nm and full width-half maximum of 10 nm, and a Barlow lens with 2× magnification.

For the purpose of calibrating his optical system for lucky imaging Kohl (2013) observed binaries with precisely determined orbits. Afterwards he used the orbital elements in order to recalculate the separation and the position angle for the observational epoch. By comparing these quantities with those obtained from the observations he determined the pixel scale and the orientation of the camera. For the

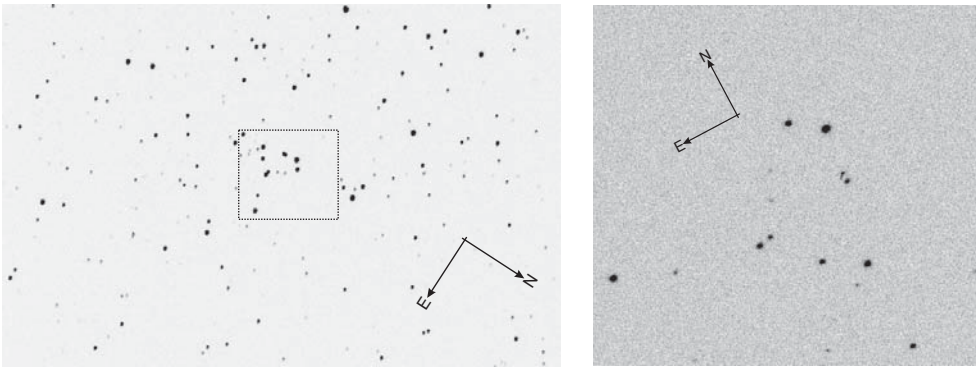

Figure 2: Open cluster M52 recorded by CCD camera SBIG STXL-6303e (left) and Andor iXon 897 Ultra (right). The rectangle on the left panel indicates the part of the sky shown in the right panel.

purpose of determining these parameters we use an alternative approach. In order to have a sufficient number of stars in the field of view of Andor iXon 897 Ultra we start the observation night or session by taking frames of a star cluster. Then we obtain another frame of the same cluster with the other camera. Using a plate solver engine, Astrometry.net[1] or PinPoint[2], we directly obtain the pixel scale, and then the connection between the northwards directions for both cameras. In this way we can determine the position angle during the calibration of frames of double stars. An example of such frames is presented in Figure 2.

During the night of August 13th, 2020, we took 200 frames with the exposition of 0.1 seconds of binary system WDS 22202+2931 = BU 1216, for which there exist orbital elements[3]. In this way we obtained images with high signal-to-noise ratio after processing. From all exposures an average bias and dark frame was subtracted, but flat fielding was not performed because we had a problem to take flat-fields that night. The left panel of Figure 3 shows the result that was obtained by just stacking all short exposures without further image processing whereas the right panel shows the result obtained by lucky imaging i.e. using only 20 % of the best frames according to their FWHM of the PSFs. In the right panel it is seen that the binary components are clearly resolved, whereas in the left panel they are blurred. The parameters for this binary, separation and position angle, determined by using lucky imaging are: $\rho = (0.918 \pm 0.014)$ arcseconds, $\theta = (276.57 \pm 0.57)^\circ$. The ephemerides for the observational epoch 2020.61875 are: $\rho = 0.916$ arcseconds and $\theta = 276.2^\circ$ in a fairly good agreement with our measurements. The seeing for that night was about 1.9 arcseconds, whereas we measured a double star the separation of which is twice as small. Because of this we hope that we shall be able to resolve even closer pairs when we have a better seeing.

[1]https://astrometry.net
[2]http://pinpoint.dc3.com
[3]http://www.usno.navy.mil/USNO/astrometry/optical-IR-prod/wds/orb6

Table 1: CCD cameras used for lucky imaging at AS Vidojevica and its properties. Both cameras are attached at the right port of telescope "Milanković". More details about the telescope can be found on the website http://vidojevica.aob.rs/index.php?option=com_content&view=article&id=40:the-1-4m-telescope&catid=22:teleskopi&Itemid=249

CCD camera	iXon 897 Ultra	SBIG STXL-6303e
Active pixels	512×512	3072×2047
Sensor size (mm)	8.2×8.2	27.7×18.5
Pixel size (μm)	16×16	9×9
Read noise	$< 1e^-$	$15e^-$
Maximum cooling ($^\circ C$)	-100	-40
Pixel scale ($''$/pixel)	0.1488	0.1649
Field of view (arcmin)	1.3×1.3	8.2×5.5
Illumination	back	front

Figure 3: The binary WDS 22202+2931 = BU 1216.

3. CONCLUSIONS

Here we show that using lucky imaging at 1.4 m telescope "Milanković" at AS Vidojevica, with the existing equipment, we can resolve double stars for which the separation is at least twice as small as the seeing value. There is a room for improvement, instead of Barlow lens 2× to use another one with a higher magnification, for instance 3× or even 5×. There is another possibility, in the next period to substitute the existing filter with another one which would have a larger transparency width and to estimate if this will result in an improvement.

Acknowledgments

The results presented in this paper are based on observations with the 1.4 m telescope "Milanković" at AS Vidojevica. We would like to thank to the anonymous reviewer for the careful reading of the paper and the constructive and helpful remarks. The

work presented in this paper was supported by the Ministry of Education, Science and Technological Development of the Republic of Serbia, and these results are parts of the Grant 451-03-9/2021-14/200002 of Astronomical Observatory.

References

Kohl, S.: 2013, *Publ. Astron. Obs. Belgrade*, **92**, 175.
Pavlović, R., Cvetković, Z., Damljanović, G., Vince, O., Jovanović, M. D.: 2018, *Publ. Astron. Obs. Belgrade*, **98**, 321.

Publ. Astron. Obs. Belgrade No. 100 (2021), 345 - 350 *Progress Report – special session "The gravitational-wave Universe" supported by COST Action CA16104*

STATISTICS OF RECOILING SUPERMASSIVE BLACK HOLES FROM COSMOLOGICAL SIMULATION

M. SMOLE[1], M. MIĆIĆ[1], A. MITRAŠINOVIĆ[1], N. STOJKOVIĆ[1], N. MARTINOVIĆ[2] and S. MILOŠEVIĆ[3]

[1] *Astronomical Observatory, Volgina 7, 11000 Belgrade, Serbia*
E–mail: msmole@aob.rs

[2] *Mathematical Institute of the Serbian Academy of Sciences and Arts, Kneza Mihaila 36,*

[3] *Department of Astronomy, Faculty of Mathematics, Studentski trg 16, 11000 Belgrade, Serbia*

Abstract. Black hole (BH) mergers are one of the most powerful sources of gravitational wave emission. During BH mergers asymmetry in the binary system will lead to the asymmetric emission of gravitational radiation and BH recoil. In this process newly formed BH receives a kick, whose magnitude depends on the characteristics of the BH binary system. Those recoiling BHs could be observed as spatially offset active galactic nuclei (AGN).

We compare trajectories of recoiling BHs in analytical and numerical models of galaxy merger remnants. Our results suggest that BH escape velocities in numerical major merger remnant galaxies can be up to 25 per cent lower compared to those in analytical models. Further, we use results from the Illustris cosmological simulation to explore statistics of spatially offset AGN in numerical and analytical models.

1. INTRODUCTION

Hierarchical model of structure formation predicts that massive galaxies experience a large number of mergers throughout their history. Following a galaxy merger, central black holes (BHs) will form a binary system whose further evolution depends on galaxy morphology, gas content, and mass ratio of progenitor galaxies. In gas rich mergers, gas that is fueled to the central regions will lead to efficient binary hardening and final merger, while galaxy mergers with low mass ratio do not necessary lead to BH merger (e.g. Khan et al. 2016 and references therein).

When the separation between BHs becomes $\leq 10^{-3}$ pc, gravitational wave radiation becomes an efficient mechanism for extraction of angular momentum and energy from the binary system, which leads to rapid BH merger (Begelman et al. 1980). Any asymmetry in the binary system, caused by BHs with unequal masses and/or spins, will lead to the asymmetric emission of gravitational radiation and BH recoil. Newly formed BH receives a kick velocity, whose magnitude depends on the mass ratio of BHs, the spin magnitude and orientation with respect to the binary orbital plane, and the eccentricity of the orbit. Distribution of possible kick velocities is wide, ranging from few to several thousands km/s, meaning that BHs can be ejected even from

the most massive elliptical galaxies (Gonz´ales et al. 2007; Campanelli et al. 2007; Lousto & Zlochower 2011).

Recoiling BHs could be observed as spatially or kinematically offset active galactic nuclei (AGN). Numerous candidate offset AGN have been observed, although alternative explanations cannot be ruled out (we refer to Ward et al. 2020 for more detailed summary of offset AGN observations). Smole et al. (2019) investigated trajectories of recoiling BHs in various analytical and numerical models of merger remnant galaxies in order to test how central BH mass distribution and the mass ratio of progenitor galaxies influence escape velocities of recoiling BHs. Our results show that static analytical models of major merger remnant galaxies overestimate the BHs escape velocities. During major mergers violent relaxation leads to the decrease of galaxy mass and lower potential at large remnant radii. This process is not depicted in static analytical potential, making the evolving numerical model a more realistic description of dynamical processes in galaxies with merging BHs. We find that BH escape velocities in numerical major merger remnant galaxies can be up to 25 per cent lower compared to those in analytical models.

Here, we extend the above work and use the results to calculate analytical and numerical escape velocities for major merger remnant galaxies extracted from the Illustris-1 simulation. Then, for a given kick velocity distribution, we are able to estimate number of offset AGN at cosmological scales, and make a statistical comparison between analytical and numerical models. In Section 2 we describe the method. In Section 3 we present our results. We summarize and discuss our results in Section 4.

2. METHOD

In order to compare analytical and numerical models of major merger remnant galaxies, we use publicly available data from the Illustris-1 cosmological simulation (Nelson et al. 2015). The Illustris-1 is a large cosmological simulation which was conducted with the moving-mesh hydrodynamics code AREPO (Springel 2010). The simulation has a periodic simulation cube of side length $L = 106.5h^{-1}$ Mpc, with a dark matter particle mass of $6.26 \times 10^6\,\mathrm{M}_\odot$ and a typical gas cell mass of $1.26 \times 10^6\,\mathrm{M}_\odot$. ΛCDM cosmology used for the Illustris-1 simulation is the following: $\Omega_\mathrm{m} = 0.2726$, $\Omega_\Lambda = 0.7274$, $\Omega_\mathrm{b} = 0.0456$ and $h = 0.704$, where h is the Hubble constant at $z = 0$ in units of 100 km/s/Mpc.

From the Illustris-1 simulation we extracted merger histories of a sample containing all galaxies with masses in range $10^{11} - 10^{13}\,\mathrm{M}_\odot$ at $z = 0$. Next, we search through the merger trees of the sample galaxies selecting major merger events, defined as a mergers of galaxies with the total mass ratio $\geq 1:3$. Additionally, we require that merger remnant galaxies have a minimum total mass of $10^{10}\,\mathrm{M}_\odot$. We do not include low mass galaxy mergers in our analysis since the resulting merger remnants have low potential wells and even low kick velocities can lead to the complete BH ejection. This sample of merging galaxies, containing ~ 6000 major merger remnants, is further populated with BHs, using two different approaches. In the first model BH masses are taken directly from the simulation. In the Illustris-1 simulation a BH particle with a seed mass of $10^5\,\mathrm{M}_\odot$ is placed in each galaxy more massive than $7.1 \times 10^{10}\,\mathrm{M}_\odot$, and then allowed to grow via gas accretion and by mergers. However only ~ 7 per cent of all merging pairs have both pre-merger galaxies more massive then a threshold for a BH seed in the Illustris-1 simulation. This excludes a significant number of mergers

from our analysis. In the second model we explore an alternative approach where we populate merging galaxies with BHs whose masses are estimated using $M_{\rm BH} - M_{\rm HALO}$ local scaling relation (Ferrarese 2002). Since this model does not hold a minimum threshold for BH seeds, in this case all major mergers from the original sample are included in the analysis. BH mass distribution for both models is shown on Fig. 1 and further discussed in the next section.

When major mergers events are extracted from the cosmological simulation and each pre-merger galaxy is seeded with a central BH, the next step is to assign escape velocity to each remnant galaxy. Numerical and analytical escape velocities are estimated for each post-merger galaxy using the results from our previous work (Smole et al. 2019). For the given merger remnant mass, its central BH mass and the mass ratio of the merging galaxies, escape velocities calculated in Smole et al. (2019) are extrapolated and assigned to each galaxy from our the Illustris-1 sample. The next step is to calculate kick velocities for each newly formed BH, adopting the method described by Micic et al. (2011). Kick velocity depends on BH mass ratio and BH spins, both orientation and magnitude. Following Micic et al. (2011), we employ two models for BH spins: in the first model BH spin parameters are taken from a uniform distribution ("random spins" model), while in the second model BH spins are always aligned with the orbital angular moment of the binary ("aligned spins" model), resulting with lower kick velocities. For each merger remnant galaxy BH kick velocities are sampled from one of those distributions 10000 times, in order to employ Monte Carlo method and create a statistical analysis of offset AGN distribution.

The final step is to compare escape and kick velocities for each merger remnant galaxy in order to estimate number of offset AGN. Here we adopt a crude definition for an offset AGN described as a post merger galaxy with escape velocity lower then the kick velocity. We note that kick velocities close to escape velocities may place central BH on a bound orbit outside of the galactic nuclei for a prolonged period of time, however investigation of BH orbits is beyond scope of this work.

3. RESULTS

Fig. 1. shows the distribution of BH masses taken from the scaling relation (filled histogram with dashed borderline) and directly from the Illustris-1 simulation (open histogram with solid borderline). The total number of major merger events where both pre-merger galaxies host a central BH is significantly lower for BHs taken from the Illustris-1. This results from a minimum mass threshold imposed for BH seeds in the Illustris-1 simulation. Further this implies that a majority of major merger events are in fact mergers of galaxies with masses $< 7.1 \times 10^{10}$ (threshold for a BH seed), and can partially explain generally less massive BHs calculated from the scaling relation. Additional difference between BH masses taken from two different models comes from using local scaling relation between host galaxy and the central BH, which might not hold high redshift galaxies. Recent work (Kazuhiro & Takuma 2019) have shown that quasars at $z \sim 6$ have at least one order of magnitude more massive central BHs than their local counterparts with the same mass. However, choosing one relation over the other does not ultimately affect our result regarding offset AGN statistics, since the resulting kick velocity depends only on the mass ratio of the merging BH and not on their total mass.

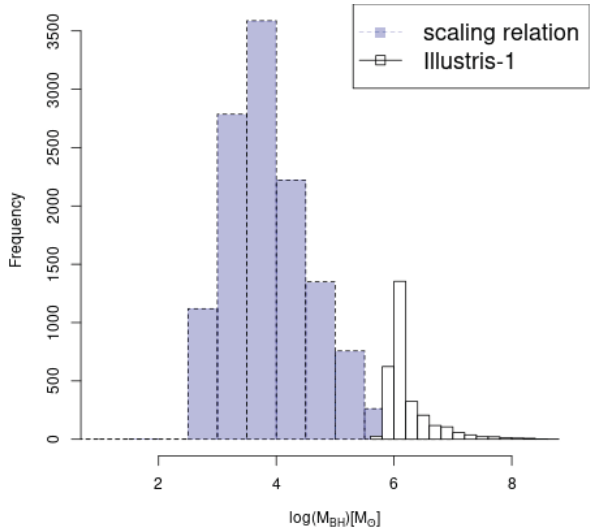

Figure 1: Histogram of BH masses populating pre-merger galaxies taken from the Illustris-1 (open histogram with solid borderline) and from $M_{\rm BH} - M_{\rm halo}$ relation (filled histogram with dashed borderline).

Fig. 2 shows statistics of offset AGN with 2-sigma confidence level as a function of redshift, for different models of kick velocity distribution, i.e. for "random spins" and "aligned spins" models. Left panels show BH masses estimated from the Illustris-1 simulation, while right panels show BH masses from scaling relation. Percentage of offset AGN in analytical and numerical models are represented with circles and triangles, respectively. Fig. 2 shows that each model reveals statistically significant difference between numerical and analytical potential. Evolving numerical potential predicts greater number of offset AGN at both high and low redshifts, and this trend is insensitive to the particular choice of BH mass and/or BH spins distribution. We note that for the Illustris-1 BH mass distribution at $z > 3$ our model predicts no offset AGN in both analytical and numerical models. However, our results in this region are biased since the number of major mergers with progenitor galaxies more massive than the threshold for a BH seed in the Illustris-1 is too low for statistical predictions, resulting with zero to several merger events per redshift bin.

Statistics of offset AGN changes drastically with a particular choice of BH mass distribution. BH masses taken from the simulation predict significantly lower fraction of offset AGN compared to the case where BH masses are taken from the scaling relation. This is a consequence of two combined effects induced by adopting a particular BH mass distribution. When BH masses are estimated using scaling relation, major mergers in lower mass galaxies are included in analysis. Such galaxies tend to have shallow potential wells, making them prone to BH ejections. Second, when BH massed are taken from $M_{\rm BH} - M_{\rm HALO}$ relation, BH mass ratio will always be $\geq 1:3$, which is our major merger definition. Mergers of two BHs with similar masses will always results with higher amplitude of kick velocities (Micic et al. 2011, figure 2), adding to the difference between percentage of offset AGN for different BH mass distributions. On the other hand, BH masses taken from the Illustris-1 show greater

diversity in mass ratios, which also reflects at their kick velocities, however number of merger events for galaxies at $z > 3$ is simply to low to make statistical predictions.

Kick velocity distribution models bring only a lesser influence on offset AGN statistics. "Aligned spins" model yields lower kick velocities, reducing the percentage of offset AGN in both numerical and analytical models.

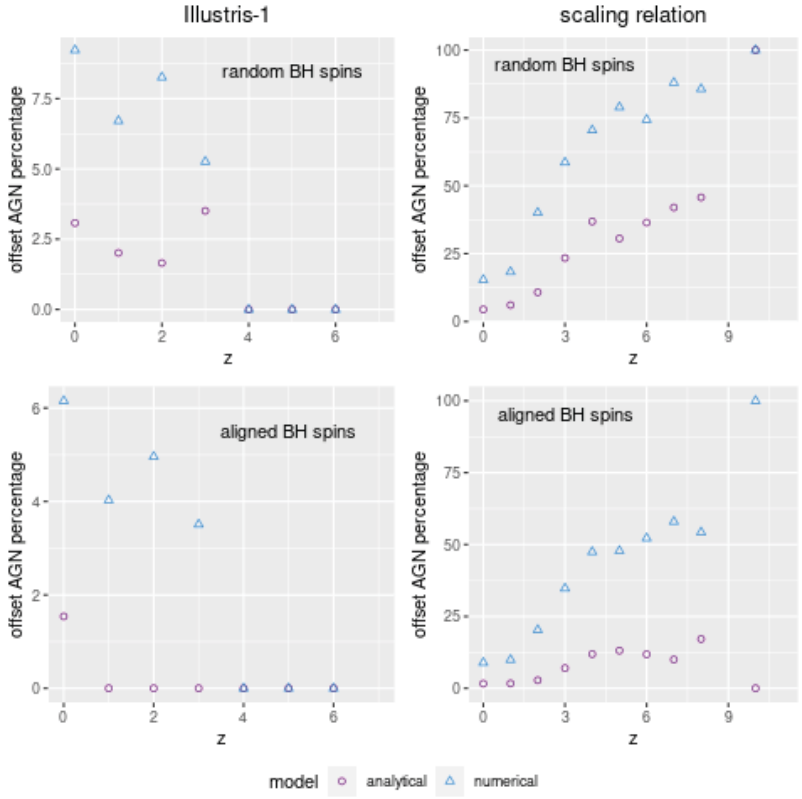

Figure 2: Percentage of offset AGN with 2-sigma confidence level as a function of redshift, for different models of kick velocity distribution, and for analytical (circles) and numerical (triangles) models. Left panels show offset AGN for BH masses taken from the Illustris-1, while right panels show BH masses from $M_{\rm BH} - M_{\rm HALO}$ relation.

4. SUMMARY

We have investigated statistics of offset AGN on cosmological scales with the main goal to compare percentage of offset AGN in analytical and numerical models. Major merger remnants and properties of pre-merger galaxies are extracted from the Illustris-1 simulation and then seeded with central BHs, whose mass is taken either directly from the simulation, or estimated using local $M_{\rm BH} - M_{\rm HALO}$ relation. Here we use a simple definition for offset AGN referring to a recoiling BH whose kick velocity is greater the the escape velocity of the host galaxy. Escape velocities of recoiling

BHs were estimated using the results from Smole et al. (2019), where we calculated analytical and numerical escape velocities for various merger remnants. BH kick velocities are sampled from one of two different distributions (assuming random or aligned BH spins), using Monte Carlo method.

We have shown that numerical models predict a greater number of offset AGN on cosmological scales. Numerical models represent a better description of dynamical processes occurring in galaxies with merging BHs, which are not taken into account in analytical models, leading to overestimation of escape velocities in the later case.

However, the statistics of offset AGN changes severely with a particular choice of BH seed mass model. For BH masses taken directly from the Illustris-1 simulation, the imposed threshold for a BH seed limits the number of BH merger events especially at high redshifts, leaving only massive galaxies with deep potential wells capable to retain recoiling BHs, except for rare high kick velocities. On the other hand, if BH masses are estimated from scaling relation, number of BH merger events is significantly higher, however this approach induce bias toward mergers of BH with equal masses that always result with high kick velocities. Observing recoiling BHs has proven to be a challenging task, however the results from the recent study favor models which predict a low percentage of offset AGN, i.e. BH masses taken from the Illustris-1 and aligned BH spins (Ward et al. 2020).

We note that this work serves as a proof of concept to demonstrate differences between analytical and numerical potential. More appropriate approach, which we are going to employ in the future work, would be to use BH merger catalogs that are written at much higher time resolution than simulation snapshots. Using BH merger catalogs makes it possible to track process of BH mergers between simulation snapshots, providing a more precise model for successive merger events.

Acknowledgements

The authors acknowledge financial support from the Ministry of Education, Science and Technological Development of the Republic of Serbia (MESTDRS) through the project #ON176021 “Visible and invisible matter in nearby galaxies: theory and observations ”. This work was supported by MESTDRS through the contract no. 451-03-9/2021-14/200002 made with the Astronomical Observatory of Belgrade.

References

Begelman, M. C., Blandford, R. D., Rees, M. J.: 1980, *Nature*, **287**, 307.
Campanelli, M., Lousto, C. O., Zlochower, Y., Merritt, D.: 2007, *Phys. Rev. Lett.*, **98**, 231102.
González, J. A., Hannam, M., Sperhake, U., Brugmann, B., Husa, S.: 2007, *Phys. Rev. Lett.*, 98w1101G.
Ferrarese, L.: 2002, *Astrophys. J.*, **578**, 90.
Kazuhiro, S., Takuma, I.: 2019, *Astrophys. J.*, **872**, L29.
Khan, F. M., Fiacconi, D., Mayer, L., Berczik, P., Just, A.: 2016, *Astrophys. J.*, **828**, 73.
Lousto, C. O., Zlochower, Y.: 2011, *Phys. Rev. Lett.*, **107**, 1102 451-03-9/2021-14/200002.
Micic, M., Holley-Bockelmann, K., Sigurdsson, S., 2011, *MNRAS*, **414**, 1127.
Nelson, D. et al.: 2015., *Astronomy and Computing*, **13**, 12.
Smole, M., Micic, M., Mitrasinovic, A.: 2019, *MNRAS*, **488**, 5566.
Springel, V.: 2010, *Mon. Not. R. Astron. Soc.*, **401**, 791.
Ward, C., Gezari, S., Frederick, S.: 2020, *Astrophys. J.*, submitted, arXiv:2011.11656.

Publ. Astron. Obs. Belgrade No. 100 (2021), 351 - 356 *Progress Report*

SOLAR NEIGHBOURHOOD KINEMATICS BASED ON THE GAIA DATA

M. STOJANOVIĆ[1], R. CUBARSI[2], Z. CVETKOVIĆ[1], R. PAVLOVIĆ[1] and S. NINKOVIĆ[1]
[1] *Astronomical Observatory, Volgina 7, 11060 Belgrade, Serbia*
E–mail: mstojanovic@aob.rs
[2] *Departament de Matemàtiques, Universitat Politècnica de Catalunya, Barcelona, Spain*

Abstract. From GAIA catalog we have selected a sample of stars within 100 pc from the Sun. To avoid sample biases a special concern was taken in regard to radial velocities and multiplicities. We have selected those with necessary data − direction, parallax, proper motion and radial velocity. The kinematics of this sample is analysed. The sample size is 62,598 stars. Using an analytic model of Galactic gravitational potential the galactocentric orbits of these stars are calculated. It is shown, as can be expected, that in the Solar neighbourhood stars mostly belong to the thin disc (86.3%). This is followed by the thick disc which has a fraction of 12.4%, whereas the lowest fraction belongs to the halo (1.3%). The kinematical similarity for suspected binaries is also examined.

1. INTRODUCTION

There is now almost a consensus that, at least as stars from the solar neighbourhood are concerned, the following distinction - thin disc, thick disc and halo - is possible. Classification of particular star in such a manner is usually based on kinematics. To this end one could use merely the velocity components, but also study the motion of individual stars with respect to the centre of the Milky Way, which means to calculate its orbit. Orbit calculation requires reliable data, such as parallax, proper motion and radial velocity. After the Hipparcos Catalogue the progress in astrometric data has become evident. At present thanks to the GAIA Catalogue (Gaia Collaboration et al. 2018) proper motions and parallaxes are available for a vast number of neighbouring stars. The radial velocity data are more scarce. Nevertheless, even within rather small volumes it is possible to find many stars possessing necessary data of sufficiently high quality.

The experience concerning detecting objects of similar kinematics in other astronomical fields, say minor planets in the Solar System (Milani et al. 2014), indicates the importance of the approach based on orbit calculation. To be more clear, it is well known that stars of the thin disc are expected to be always sufficiently near the Galactic plane and also not exhibiting significant changes in their distance to the Galactic axis of symmetry.

In this way we can determine the fractions of the three groups within an unbiased sample of stars, as well as the basic kinematical parameters, such as the mean motion,

velocity dispersion, etc. It is also of interest to examine stellar multiplicity for sample member. This offers the possibility of comparing star pairs attributed to either of the two discs to those classified to belong to the halo.

2. SELECTION OF DATA AND METHOD OF ANALYSIS

In this section we describe how we have formed the sample of stars from GAIA DR2 data. At the beginning of 2018, the ESA's Gaia mission produced the second data release Gaia DR2. Gaia DR2 provides position, parallax and proper motions for about 1.3×10^9 stars in the Milky Way (Lindegren et al. 2018), and radial velocity for about 7.2 million stars (Soubiran et al. 2018) measured using a Radial Velocity Spectrograph.

We used two criteria to obtain our sample of stars from the Solar neighbourhood. First we have selected all the stars that have parallax greater than 10 mas. Then, from these sources we have selected those that satisfy the two following conditions: the astrometric parameters are solved and for every source the radial velocity is given. In this way we have obtained a sample of stars, in the solar neighbourhood with distance smaller then 100 pc, consisting of 74,339 stars.

The next step was to remove contamination factors as many as possible. First we considered sources with poor astrometric solutions, but such are expected for Gaia sources that have small parallaxes, so they should not present a potential contamination of our sample. A much more complicated case is with stars that have poorly defined radial velocities. The ESA-Gaia website[1] contains information on a potential radial velocity problem found by Boubert et al. (2019). They cut Gaia DR2 sources with a radial velocity that have a companion in the full Gaia DR2 catalogue within 6.4 arcsec that either itself has a radial velocity or that is brighter in GRP or G magnitudes. The resulting list of 70,365 Gaia DR2 sources with potentially contaminated radial velocities are available in the published paper. The Gaia Radial Velocity Spectrometer team is investigating the issue further in order to improve the Gaia pipeline for future releases. The Gaia team announced that only about 4000 sources have erroneous radial velocities. Among the erroneous ones are e.g. all cases where the Gaia DR2 radial velocity (absolute value) is more than 625 km/s. They also announced that these 4000 erroneous cases will not be copied over to Gaia EDR3, while every other radial velocity entry will be copied from Gaia DR2 to Gaia EDR3. A new set of radial velocities, with improved precission, will be provided as part of Gaia DR3 release.

Then, we clear our sample from multiple stars, because stellar multiplicity can be the case of large errors when calculating orbits. In order to do that, we checked for each star from our sample whether it is contained in the Washington Double Star Catalog, WDS[2]. This process of cross-identification will be explained in more detail in the full account of this research. Our final sample consists of 62,598 stars.

In order to determine galactocentric orbits we used the model of the Milky Way potential proposed by Ninković (1992). This model assumes three contributors to the potential of the Milky Way: the bulge, the disc, and the corona (the subsystem consisting of dark matter). The latter is assumed as spherically symmetric, while

[1]https://www.cosmos.esa.int/web/gaia/dr2-known-issues#RadialVelocitiesCrowdedRegions
[2]http://www.usno.navy.mil/USNO/astrometry/optical-IR-prod/wds

the other ones are assumed to be axisymmetric. The contributions to the Galactic potential of the former two are described by the same formula, that of Miyamoto and Nagai (1975). The only difference concerns the values of the model parameters. The values of model parameters are obtained on the basis of the model constants, which are assumed a priori. The data from Gaia DR2 (five-parameter astrometry solution and radial velocity) are used as input for the model. The integration of the galactocentric orbits for each star is done for 10 Gyr by using a 4th order Runge Kuta method. In this way, the values for various quantities were obtained, but for the purpose of segregation we use only z_{min} and z_{max}; $|z|$ is the distance from the Galactic plane.

Since the input data are given in the equatorial spherical reference system, it is necessary to transform them into the heliocentric Cartesian system in which the coordinate axes are along the Galactic coordinates. Furthermore, the obtained heliocentric Cartesian velocity components should be corrected for the Solar motion. Usual designations are adopted:

U direction towards Galactic centre: $l = 0^\circ$, $b = 0^\circ$;

V direction of Galactic rotation: $l = 90^\circ$, $b = 0^\circ$;

W direction towards the north Galactic pole: $b = 90^\circ$.

Their values are used for the purpose of the segregation in addition to z_{min} and z_{max}.

3. DISCUSSION AND RESULTS

According to the Boubert (2019) we have removed the stars with problematic radial velocities. In our sample of 74,339 stars we found 9,891 stars that should be removed in order to get a better quality of our sample. Top panel in Fig. 1 shows our sample of stars including those stars that have been removed due to radial velocity contamination. The abbreviation LSR means that the velocity components are with respect to the local standard of rest.

We identified 9905 stars from our sample in the WDS catalogue, and then we checked for each of them whether it is possibly a multiple star, by comparing its radial velocity, magnitude and parallax. In total, we found 3200 stars belonging to possible binary systems (1600 pairs), and we found 69 to belong to possible triple systems (23 systems). For the remaining 6636 stars from WDS, we have the required data from Gaia for only one of the system components. Middle panel in Fig. 1 shows these 3269 stars that were removed from our sample. Bottom panel in Fig. 1 indicates the correlation between stellar multiplicity and radial velocity contamination. This is a good indicator showing that multiplicity of stars can potentially make a problem for radial velocity determination.

We found for some well known binaries that the components have significantly different galactocentric orbits. There are examples where for a binary we can find in the Sixth Catalog of Orbits of Visual Binary Stars, ORB6[3] orbital elements of sufficient quality, but nevertheless for the components we obtain different galactocentric orbits. Most likely this is due to unreliable parallax, radial velocity or proper motion measurements. Two examples are shown in Fig. 2: first row - `WDS 06048-4828 = DUN 23` and second row - `WDS 21008-0821 = BU 678`. On the left panels of this figure we can

[3]http://www.usno.navy.mil/USNO/astrometry/optical-IR-prod/wds/orb6

see galactocentric orbits of the primaries, while on the right panels we see the secondaries. Title of each panel is Gaia DR2 source id. In the case of such measurements the motion of mass centre can cause significant errors. Parameters from Gaia DR2 for these four stars are presented in Table 1. These four stars, among others, are removed from our sample.

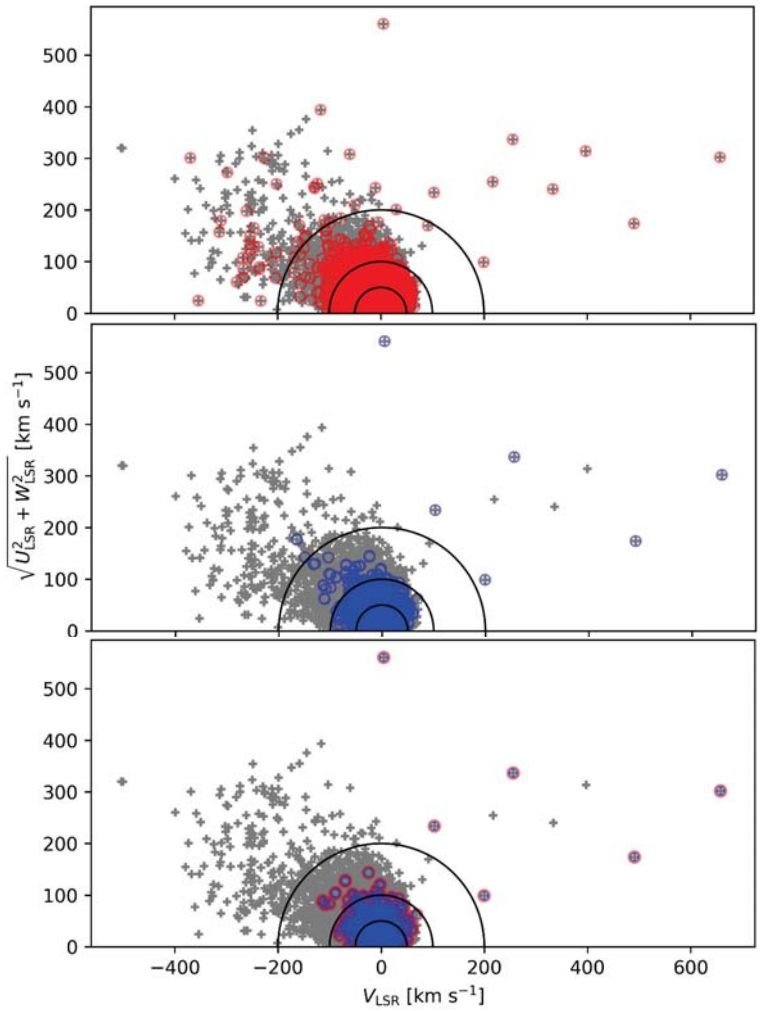

Figure 1: Toomre diagrams showing the stars from our sample (gray cross) and those removed due to: contamination in the radial velocity (top panel), multiplicity (middle panel), both criteria (bottom panel). Semicircles (black lines) represent $|V_{LSR}|$ less than or equal to 50, 100 and 200 km s^{-1}, respectively.

Finally our sample of Gaia DR2 sources consists of 62,598 stars. In our kinematical approach for defining which star belongs to which component of the Galaxy we used the following segregation method. This method originates from our previous studies (Ninković et al. 2012, Stojanović 2015, Cubarsi et al. 2017).

Table 1: Parameters from Gaia DR2 for four stars presented in the Fig 2.

WDS id	l	b	Gaia_source_id	π	err	μ_α	err	μ_δ	err	V_r	err
DUN_23_P	091.19470494847	−48.45883408526	5554191685019290368	32.47	0.02	−117.38	0.05	−39.04	0.04	14.25	0.17
DUN_23_S	091.19383987985	−48.45839608168	5554191685020871424	32.51	0.03	−101.11	0.06	−22.69	0.06	35.24	5.25
BU_678_P	315.20448826514	−08.34289191004	6908757299968653440	29.11	0.04	227.12	0.07	46.77	0.05	−34.26	1.14
BU_678_S	315.20527437965	−08.34275522474	6908757299969652480	29.15	0.04	237.94	0.08	26.74	0.05	−35.96	0.15

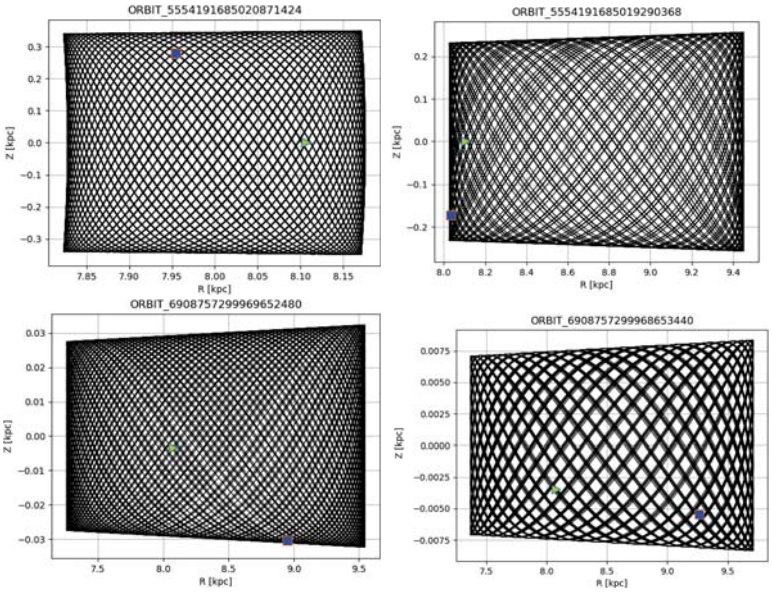

Figure 2: Binary systems: first row - `WDS 06048-4828 = DUN 23` and second row - `WDS 21008-0821 = BU 678`; primary components - left panels, secondary components - right panels. Triangle is starting point of integration which is actually input from Gaia DR2, blue square is end point in integration. Panel titles are Gaia DR2 source ids. Integration time 10 Gyr.

First we select those stars that satisfy the following three conditions:

$$-110 \text{ km s}^{-1} \leq U \leq 90 \text{ km s}^{-1};$$
$$-80 \text{ km s}^{-1} \leq V \leq 40 \text{ km s}^{-1};$$
$$z_{\min} \geq -0.5 \text{ kpc} \quad \& \quad z_{\max} \leq 0.5 \text{ kpc}.$$

These stars should belong to thin disc. The selection is thus based on the speed of a star with respect to LSR and its maximum distance from the Galactic plane. The number of stars for which this condition is satisfied is 54,033 (86.3%). Next, in the case of the halo it is enough that a star fulfils one of the following conditions:

$$U \leq -210 \text{ km s}^{-1} \quad \text{or} \quad U \geq 190 \text{ km s}^{-1};$$
$$V \leq -130 \text{ km s}^{-1} \quad \text{or} \quad V \geq 70 \text{ km s}^{-1};$$
$$z_{\min} \leq -1.5 \text{ kpc} \quad \text{or} \quad z_{\max} \geq 1.5 \text{ kpc}.$$

The number of such stars is 784 (1.3%). At the end of this process the remaining stars should belong to the thick disc. Their number is 7781 (12.4%). The results of

Table 2: Components of our Galaxy with the number of stars, percentage, mean motion ($\overline{U}$, $\overline{V}$, $\overline{W}$) and random velocity matrix for each component.

Component	Number	Percentage	Mean motion		Random velocity matrix		
Thin Disc	54033	86.3	$\overline{U}$	–9.6	1036.13	118.53	6.03
			$\overline{V}$	–18.4	118.53	419.01	5.76
			$\overline{W}$	–6.7	6.03	5.76	158.23
Thick Disc	7781	12.4	$\overline{U}$	–11.47	2758.04	224.45	–69.18
			$\overline{V}$	–33.72	224.45	1428.73	–1.33
			$\overline{W}$	–13.99	–69.18	–1.33	1376.97
Halo	784	1.3	$\overline{U}$	–13.45	11353.33	–640.23	–79.77
			$\overline{V}$	–116.90	–640.23	8101.03	–763.08
			$\overline{W}$	–14.69	–89.77	–763.08	5659.85

this selection of stars according to the defined kinematical properties are presented in Table 2, together with the mean motion ($\overline{U}$, $\overline{V}$, $\overline{W}$) and random velocity matrix for each component.

4. CONCLUSION

Our first objective is to form an unbiased sample of nearby stars. The purpose is to study the local kinematics. We find that the GAIA data still have errors. Inter alia in the case of some already confirmed binaries (inner motion evaluated with high grades) our calculation of galactocentric orbits for each binary component individually, gave unrealistic values! Of course, such a result in our opinion is due to the data errors, in particular, in parallax, radial velocity and proper motion. So we find additional criteria to avoid including stars with doubtful data in the final sample. By comparing the initial sample size with the final one we find that almost 16% of stars had to be excluded. In the final sample following our established segregation criteria we have for the fractions: thin disc 86.3%, thick disc 12.4% and halo 1.3%.

Acknowledgments

We would like to thank to the anonymous reviewer for the careful reading of the paper and the constructive remarks. The work presented in this paper was supported by the Ministry of Education, Science and Technological Development of the Republic of Serbia, Grant number 451-03-9/2021-14/200002 of Astronomical Observatory.

References

Boubert, D.: et al.: 2019, *Monthly Notices of the Royal Astronomical Society*, **486**, pp. 2618.
Cubarsi, R., Stojanović, M., Ninković, S.: 2017, *Serbian Astronomical Journal*, **194**, pp. 33.
Gaia Collaboration, Brown, A. G. A. et al.: 2018, *Astronomy and Astrophysics*, **616**, A1.
Lindegren, L. et al.: 2018, *Astronomy and Astrophysics*, **616**, A2.
Milani, A., Cellino, A., Knežević, Z., Novaković, B., Spoto, F., Paolicchi, P.: 2014, *Icarus*, **239**, pp. 46.
Miyamoto, M., Nagai, R.: 1975, *Publications of the Astronomical Society of Japan*, **27**.
Ninković, S.: 1992, *Astronomische Nachrichten*, **313**, 83.
Ninković, S., Cvetković, Z., Stojanović, M.: 2012, *Publications of the Astronomical Observatory of Belgrade*, **91**, pp. 163.
Soubiran, C. et al.: 2018, *Astronomy and Astrophysics*, **616**, A7.
Stojanović, M.: 2015, *Serbian Astronomical Journal*, **191**, pp. 75.

Publ. Astron. Obs. Belgrade No. 100 (2021), 357 - 362 *Progress Report*

SERBIA IN ASTRONOMICAL CONTESTS BETWEEN 2017 - 2020

S. VIDOJEVIĆ [1], V. PROKIĆ [2], S. NINKOVIĆ[3] and B. SIMONOVIĆ[4]

[1] *State University of Novi Pazar, Department of Mathematical Sciences, Vuka Karadžića bb, 36300 Novi Pazar, Serbia*
E–mail: sonja@matf.bg.ac.rs

[2] *Gymnasium "Svetozar Marković", Branka Radičevića 1, 18000 Niš, Serbia*
E–mail: vera.prokic@gsm-nis.edu.rs

[3] *Astronomical Observatory, Volgina 7, 11000 Belgrade, Serbia*
E–mail: sninkovic@aob.rs

[4] *Astronomical Society "Rudjer Bošković", Kalemegdan, Gornji grad 16, 11000 Belgrade*
E–mail: baltazartodor@yahoo.com

Abstract. The subject concerns contests in astronomy and astrophysics under the supervision of the National Astronomical Olympic Committee of Serbia, both national and international, during $2017-2020$. Included are: contests in Serbia (Regional – 15 1^{st} prizes, 6 2^{nd}, 9 3^{rd}, 16 honorable mentions and National – 9 1^{st} prizes, 5 2^{nd}, 9 3^{rd}, 3 honorable mentions), as well as Serbian participation in contests held abroad, such as International Olympiad in Astronomy and Astrophysics (2 silver medals, 4 bronze, 4 honorable mentions), St-Petersburg Astronomical Olympiad (1 2^{nd} prize, 5 3^{rd}) and Global electronic Competition on Astronomy and Astrophysics (2 2^{nd} prizes, 2 3^{rd} and 2 honorable mentions).

1. INTRODUCTION

The history of attending contests in astronomy for pupils of secondary school in Serbia is quite long. It started in 2002, so that, next year (2022) we will celebrate the 20^{th} anniversary.

Contests in astronomy are organized by the National Astronomical Olympic Committee of Serbia (NAOC) every year. In Serbia there are two levels of contests: Regional (from 2008) and National (from 2002). The selection of the Serbian team for international contests is based on the success in the National Contest. International contests which have been attended by pupils from Serbia are: International Astronomy Olympiad (IAO), International Olympiad on Astronomy and Astrophysics (IOAA) and Sanint-Petersburg Astronomical Olympiad (SPAO). The first IAO was held in 1996 in Russia (Nizhnij Arkhyz), and XXIV IAO took place in 2019 in Romania (Piatra Neamt), in 2020 IAO was not held because of the COVID-19 pandemic. The first IOAA was held in 2007 in Thailand (Chiang Mai) and the last one, XIII IOAA, took place in 2019 in Hungary (Keszthely); in 2020 it was not held because of the pandemic. Instead, an on-line contest was organized, Global electronic Competition

on Astronomy and Astrophysics (GeCAA). SPAO is a correspondence type of competition. The first SPAO was held in school year 1994/95 and XXVI SPAO is for the current school year 2020/21.

Serbia appeared in an international contest in 2002 at VII IAO in Russia (Nizhnij Arkhyz). In the subsequent years participants from Serbia were regularly present in IAO, except 2003 (VIII IAO, lack of funds), the last time Serbia participated in XVI IAO in 2011 in Kazakhstan (Alma-Ata). Serbia participated for the first time in III IOAA in 2009, Iran (Tehran). From that time Serbia was regularly present in IOAA including the last one in 2019. Therefore, in 2009, 2010 and 2011 Serbia attended both IAO and IOAA. GeCAA was also attended by Serbian pupils. The first attendance in SPAO of Serbia was in XX SPAO by only one pupil, Marko Purić (2^{nd} grade, Mathematical Grammar School, Belgrade) in school year 2012/13. He won the first prize! From that time Serbian pupils have been participating in SPAO regularly including the current school year (2020/2021).

Other important details can be found in Vidojević et al. (2018). In the present contribution we will describe the participation of Serbian pupils in national and international astronomical competitions between 2017 and 2020.

2. COMPETITIONS

2. 1. COMPETITIONS WITHIN SERBIA

There are two levels of competitions within Serbia and they are organised on two levels: Regional and National. Regional: only theoretical part (3 questions + 4 tasks). Selection for higher competition level: every participant who achieves 30% of total number of points, or has right of direct participation, if in the previous year a medal at International olympiad was obtained. National: theoretical part (5 tasks) + practical part (data analysis & observations-indoor or outdoor depending on weather) Selection: 5 to 10 best participants become members of the Serbian national team for international competitions. Since the competitions by 2017 are described in Vidojević, et al. (2018) here we give the data concerning the most recent competitions.

In the three Regional Competitions the participants were from the following regions, i.e. schools: in 2018 Mathematical Grammar School and Zemun Gymnasium (City of Belgrade), Gymnasium "Svetozar Marković" (Niš, Nišava District), Gymnasium "Branko Radičević" (Stara Pazova, Srem District), Čačak Gymnasium (Čačak, Moravica District); in 2019 Mathematical Grammar School, Zemun Gymnasium, I Belgrade Gymnasium, IX Belgrade Gymnasium and XIV Belgrade Gymnasium (City of Belgrade), Gymnasium "Svetozar Marković" (Niš, Nišava District), Čačak Gymnasium (Čačak, Moravica District) and Mitrovica Gymnasium (Sremska Mitrovica, Srem District); in 2020 Mathematical Grammar School, IX Belgrade Gymnasium and XIV Belgrade Gymnasium (City of Belgrade), Gymnasium "Svetozar Marković" (Niš, Nišava District), Čačak Gymnasium (Čačak, Moravica District), Mitrovica Gymnasium (Sremska Mitrovica, Srem District) and Gymnasium "Takovski ustanak" (Gornji Milanovac, Moravica District).

In the two National Competitions the participants were from the following regions, i.e. schools: in 2018 Mathematical Grammar School (City of Belgrade), Gymnasium "Svetozar Marković" (Niš, Nišava District), Gymnasium "Branko Radičević" (Stara Pazova, Srem District), and Čačak Gymnasium (Čačak, Moravica District); in 2019

Mathematical Grammar School, (City of Belgrade), Gymnasium "Svetozar Marković" (Niš, Nišava District), Čačak Gymnasium (Čačak, Moravica District) and Mitrovica Gymnasium (Sremska Mitrovica, Srem District). Unfortunately, the National Competition in 2020 had to be cancelled – that was the official instruction from the Ministry of education.

Table 1: Competitions in Serbia $2018-2020$; the last column (special prize + honourable mention).

Year	Level	Participants	Gold	Silver	Bronze	Recognition
2018	Regional	28	5	5	5	$0+5$
2018	National	24	5	2	0	$0+2$
2019	Regional	19	5	0	1	$0+8$
2019	National	13	4	3	1	$0+1$
2020	Regional	14	5	1	3	$0+3$

The lack of literature on astronomy in the Serbian language is evident, and therefore NAOK is making great efforts to alleviate this lack. Collections of problems are translated most often from English and Russian e.g. Vidojević 2019(1), 2019(2).

The best participant at the National competition wins a special prize named after Jelena Milogradov Turin $(1935-2011)$, the founder of the astronomical competitions in Serbia. The winners of this prize are presented in Table 2. It is worth to notice that in 2018 for the first time the award went outside of Belgrade (Mathematical Grammar School) – to Niš Gymnasium "Svetozar Marković", and next year – 2019 – to Gymnasium in Čačak.

Table 2: Jelena Milogradov-Turin award, from 2011 till 2020.

Year	Name (year of birth), school, city
2011	Stefan Andjelković (1992), Mathematical Grammar School, Belgrade
2012	Luka Bojović (1996) & Ivan Tanasijević (1995), both from Mathematical Grammar School, Belgrade
2013	Ivan Tanasijević (1995), Mathematical Grammar School, Belgrade
2014	Ivan Tanasijević (1995, Mathematical Grammar School, Belgrade)
2015	Vuk Radović (1998), Mathematical Grammar School, Belgrade
2016	Vuk Radović (1998), Mathematical Grammar School, Belgrade
2017	Igor Medvedev (1999), Mathematical Grammar School, Belgrade
2018	Bogdan Stanojević (1999), Gymnazium "Svetozar Marković", Niš
2019	Zlatan Vasović (2001) Čačak Gymnazium, Čačak
2020	not awarded because competition was not held (COVOD-19 pandemic).

The National Astronomical Olympic Committee (NAOC) possesses a telescope (Portable Telescope-PT) foreseen to be used for the purpose of extra-teaching only (see Vidojevic et al. 2018 , Telescope 2 – Newton type, 150/750 mm with equatorial mounting EQ3). Interested students should acquire necessary observational skill by using PT without any assistance. PT is to be sent to schools throughout Serbia to be at disposal within an allocated time. For the first time PT was sent to Gymnasium

"Svetozar Marković" in Niš on April 25, 2019. Niš is the city with the highest number of pupils interested in astronomy after Belgrade. The PT testing in Niš indicated the necessity of removing some shortcomings. For this reason PT was sent several times from Niš to Belgrade and vice versa, until these shortcomings were removed.

The pandemic was a hindrance to the accomplishment of the plans. Life regime and school activities were changed (teaching via internet, restricted motion and gathering of groups exceeding 5 persons and the like). The accomplishment of the planned activities has not been possible from March 2020 till the present time (early March 2021 onwards). After suppressing the pandemic and returning to the normal life and school activities PT will continue all its activities from the point where it was stopped. During the pandemic PT is kept by Astronomical Society "Rudjer Bošković" in Belgrade.

2. 2. INTERNATIONAL COMPETITIONS

Serbia has participated in several International Olympiads: IOAA – International Olympiad on Astronomy and Astrophysics (from 2009); Structure of the competition: theoretical part + practical (data analysis + observation) + group competition. IAO – International Astronomy Olympiad (2002 – 2011); Structure: similar to IOAA except group competition. SPAO – Saint Petersburg Astronomical Olympiad (from 2013) correspondence type of competition; structure: theoretical part + data analysis part. For detailed reports from various olympiads see e.g. Eskin et al. 2012, Miler 2009, 2011, Ninković & Milić 2011, 2014, Vidojević & Ninković 2016, Vidojević et al. 2018(2).

In 2020 instead of the regular IOAA an on-line competition – Global electronic Competition on Astronomy and Astrophysics (GeCAA, https://gecaa.ee/) – was organized by an international academic committee where Serbia had a representative, dr Sonja Vidojević. This committee invited/asked all 38 participating countries to submit their proposals for the tasks. One of Serbian proposals was selected–that one for the data analysis. The Serbian team for GeCAA was selected on the basis of the achievements in the Regional Competition, exceptionally only for this competition, due to pandemic (National Competition was not held). The participants who won any of prizes (9 students) acquired right to contest individually and the ones with honorable mention (3 students) to participate in group competition (for achievements see Table 3). The GeCAA was attended by 278 students from 38 countries.

The Society of Astronomers of Serbia at the assembly held on 16 April 2019 decided by a majority vote not to support the organization of the IOAA 2021 in Serbia due to uncertain fundings and insufficient professional staff for this undertaking.[1] The withdrawal of the candidacy was sent to the International Olympic Committee (see Fig. 1).

3. CONCLUSION

The participation of our team was helped and enabled by many people of good will who gave a great contribution with their enthusiasm and volunteer work. There are also certain institutions and companies that have recognized the importance of

[1]In 2013, at the 7th IOAA, Serbia was nominated as the host for 15th IOAA in 2021 (see Atanacković 2018, Vidojević et al. 2018(1)).

The Society of Astronomers of Serbia

Друштво астронома Србије

ДРУШТВО АСТРОНОМА СРБИЈЕ
БЕОГРАД
Број 511/2019
24. 06. 2019. год
БЕОГРАД – Волгина 7

Друштво астронома Србије
Волгина 7
11060 Београд

ПИБ: 100132062
Матични број: 07084650

Dear Dr Stachowski,

As president of the Society of Astronomers of Serbia (SAS), I need to inform You that at the last held assembly of the SAS we made a decision that Serbia and our Society (even with the help of our Government) does not have enough funds, as well as people who will be able to participate in the organization of International Olympiad of Astronomy and Astrophysics in 2021 (IOAA 2021) in Serbia. Thus, with regret, I have to inform you that Serbia has to withdraw from the candidacy to host the IOAA 2021. We are very sorry about this situation and we hope that Serbia will be able to host some of the future IOAA events.

My sincere apologies and I wish You success in your future events.

Best regards,

Vladimir Đošović

President of the Society of Astronomers of Serbia

Department of Astronomy,

Faculty of Mathematics,

University of Belgrade

e-mail: vladimir_djosovic@matf.bg.ac.rs

ДРУШТВО АСТРОНОМА СРБИЈЕ БЕОГРАД

Figure 1: The withdrawal of the candidacy sent to the International Olympic Committee. The presentation of this document is due to courtesy of Vladimir Djošović, President of SAS (Serbian Astronomical Society) 2019–2020.

Table 3: Olympiad achievements. The number of participants (4^{th} column) pertains to senior+junior+automatically qualified (winners from previous Olympiad); the last column (special prize+honorable mention).

Year	Olympiad	Country	Participants	Gold	Silver	Bronze	Recognition
2018	IOAA	China	3	0	0	1	0 + 2
2018	SPAO		3	0	0	1	0 + 0
2019	IOAA	Hungary	5	0	0	1	0 + 1
2019	SPAO		8	0	0	4	0 + 0
2020	GeCAA	On-line	12	0	2	2	0 + 2
2020	SPAO		2	0	1	0	0 + 0
Total				0	3	9	0 + 5

the participation of our talented students in such a great world competition, not only to show their knowledge, but also to gain new acquaintances and experiences in socializing with peers from around the world and in the best way to represent our country by friendliness, cosmopolitanism, selflessness, willingness to help, and many other beautiful qualities that adorn our competitors.

The competitions within Serbia – Regional and National – have been already planned and included in the official Competition Calendar for 2021. IOAA 2021 should be held in Colombia, the country which was originally foreseen as host for 2020, but because of the pandemic (COVID-19) the competition did not take place.

Acknowledgement

The authors would like to thank the co-editors for their patience and generous extension of the manuscript submission deadline.

We would also like to thank the referee for careful reading of our manuscript and valuable comments and suggestions which helped to improve the manuscript.

References

Atanacković, O.: 2018, "Astronomy Education in Serbia 2014-2017", *Publications of the Astronomical Observatory of Belgrade*, **98**, pp. 91-99.

Eskin, B., P. Tarakanov, M. Kostina: 2012, Astronomy olympiads in Russia and their position in astronomy education , *Publications of the Astronomical Observatory of Belgrade*, **91**, 287-292.

Miler, R.: 2009, XII medjunarodna astronomska olimpijada, Zbornik radova konferencije Razvoj astronomije kod Srba V, ur. Milan S. Dimitrijević, *Publikacije Astronomskog društva "Rudjer Bošković"*, **8**, 859-868.

Miler, R.: 2011, XIV medjunarodna astronomska olimpijada, *Zbornik radova konferencije Razvoj astronomije kod Srba VI*, ur. Milan S. Dimitrijević, Publikacije Astronomskog društva "Rudjer Bošković", **10**, 1315-1326.

Ninković, S. i Milić, I.: 2011, Učešće srpskog nacionalnog tima na Trećoj medjunarodnaoj olimpijadi iz astronomije i astrofizike, *Zbornik radova konferencije Razvoj astronomije kod Srba VI*, ur. Milan S. Dimitrijević, Publikacije Astronomskog društva "Rudjer Bošković", **10**, 1327-1330.

Ninković, S. i Milić, I.: 2014, Astronomska takmičenja 2010 i 2011 godine, *Zbornik radova konferencije Razvoj astronomije kod Srba VII*, ur. Milan S. Dimitrijević, Publikacije Astronomskog društva "Rudjer Bošković", **13**, 1407-1411.

Vidojević, S. i S. Ninković, S.: 2016 Učešće Srbije na medjunarodnim olimpijadama iz astronomije i astrofizike 2012. i 2013. godine, *Zbornik radova konferencije Razvoj astronomije kod Srba VIII*, ur. Milan S. Dimitrijević, Publikacije Astronomskog društva "Rudjer Bošković" (tom **16**, str. 177-188).

Vidojević, S. et al.: 2018(1), Astronomy Competitions and their Role in Astronomy Education in Serbia, *Publications of the Astronomical Observatory of Belgrade*, **98**, 217-223.

Vidojević, S. et al.: 2018(2), Uloga i značaj rukovodilaca na MOAA, *P*roceedings of the conference Development of astronomy among Serbs IX, Belgrade, April 18-22, 2017, ed. Milan S. Dimitrijević, **17**, p.283-291.

Vidojević, S.: 2019 (1), Zadaci iz astronomije i astrofizike : Zbirka zadataka sa Medjunarodne olimpijade iz astronomije i astrofizike (2007-2014), Beograd, Društvo Astronoma Srbije, pp. 254, translation from English of A Problem book in Astronomy and Astrophysics, Compilation of problems from IOAA (2007-2014), ed. A. Sule, Universities Press India, Hyderabad, 2015. ISBN 978-973-1768-60-1 Eng. ed., ISBN 978-86-912445-8-3 Ser. ed.

Vidojević, S.: 2019 (2), Astrofizički zabavnik : Zadaci i vežbe iz astronomije i astrofizike, Beograd, Društvo Astronoma Srbije, pp. 161, translation from Russian of I.A.Utešev, Astronomičesky divertisment, "Sampoligrafist", Moskva, 2018. ISBN 978-5-00077-697-1 Russ. ed., ISBN 978-86-912445-7-6 Ser. ed.

Publ. Astron. Obs. Belgrade No. 100 (2021), 363 - 367 *Progress Report*

DEPARTMENT OF ASTRONOMY AT PETNICA SCIENCE CENTER: 2018-2020

D. VUKADINOVIĆ[1], N. MILANOVIĆ[2], S. MILOŠEVIĆ[3], M. BOŠKOVIĆ[4] and N. BOŽIĆ[2]

[1] *Max-Planck-Institute für Sonnersystemforschung, Justus-von-Liebig-Weg 3, 37075 Göettingen, Germany*
E–mail: vukadinovic@mps.mpg.de

[2] *Petnica Science Center, Poštanski fah 14, 14000 Valjevo, Serbia*
E–mail: nikolinamilanovicc@gmail.com
E–mail: bozicn@petnica.rs

[3] *Faculty of Mathematics, University of Belgrade, Studentski trg 16, 11000 Belgrade, Serbia*
E–mail: stanislav@matf.bg.ac.rs

[4] *SISSA - International School for Advanced Studies, Via Bonomea 265, 34136 Trieste, Italy*
E–mail: mboskovi@sissa.it

Abstract. We review the activities of the Department of Astronomy at Petnica Science Center (PSC) within the years 2018-2020. The Department of Astronomy's dominant activities are aimed at high school students. The main educational principle of PSC is "education of students by other students" as high school students are taught and mentored mostly by undergraduate students. The full educational cycle at the Department of Astronomy presumes two years during which participants are introduced to the basics of astronomy and research methodology and, as a result of that, finish a research project. We will outline the present structure of the astronomical educational activities at PSC, topics of the participants' research projects and other activities in the mentioned period and future plans.

1. INTRODUCTION

Petnica Science Center (PSC) is the biggest and one of the oldest (established in 1982) independent nonprofit organization for extracurricular, informal science education in South Eastern Europe for highly motivated high school students. It is located near the village Petnica, close to Valjevo (Serbia). Educational activities are realized by a series of seminars on an annual basis. The organisation of the seminars is done by sixteen departments, one of which being the Department of Astronomy (AST), formed at the beginning of PSC. Besides its primary focus, PSC also organizes seminars and camps for elementary school and undergraduate students, as well as science teachers. This progress report focuses on the present structure of the educational activities at AST, topics of the participants' research projects and other activities during the period between 2018. and 2020. and future plans.

The extensive description of the organization and work of AST at PSC is given in previous publications (see Bošković et al. 2018 and reference therein). In this progress

report, we will outline the difference in the organization of AST seminars and describe high-school student projects done in the previous years. Since this years' projects are in the preparation for publication, we will describe them in a future progress report. Heads of the AST department in the period on which this report focuses were Dušan Vukadinović (2018 and 2019), Nikolina Milanović (end of 2019 and the beginning of 2020) and Stanislav Milošević (2020).

2. RESEARCH PROJECT TOPICS

Topics of most of the high-school student projects done at AST are: planetary science, stellar astrophysics, extragalactic astronomy, astroparticle physics and cosmology and observational astronomy.

Research projects in *extragalactic astronomy* studied galaxy mergers and interactions via N-body simulations. Majority of these projects are using GADGET2 N-body code (Springel 2005) for simulating galaxy mergers. Before using the GADGET2 (or other complex codes) for their projects, students would write a rudimentary N-body code in order to understand basic features of the integrator.

One student project (Ristić 2018) focused on the formation of polar ring galaxies - massive spiral galaxies around which we observe ring in a plane normal to the galaxy disk. The student simulated the process of ring formation through the minor merger of spiral and dwarf galaxies and found that these structures could be transient events. This finding led to the follow-up research (Ristić 2019) where Illustris simulation (Vogelsberger et. al 2014) was used to investigate how often do polar ring galaxies form. Participant found that it is more probable to have a formation of polar ring galaxies in a minor than in a major merger which was in contrast to the previously known formation process of this type of galaxies. Dodović (2018) simulated the formation of bars inside spiral galaxies through galaxy fly-by. It was found that the strongest bar is produced if the two interacting spiral galaxies have the same rotation direction. Question of how the galaxy merger influences formation of elliptical galaxies was investigated in Vrhovac (2019). In this project, the student focused on the merger of galaxies with two different directions of rotation. In the case of the co-rotating galaxies, a boxy elliptical galaxy would form, while in the opposite case, a disky galaxy would form. In Dodović and Despotović (2019) students analyzed the formation of Giant Southern Stream in the Andromeda galaxy. Through the interaction of the simulated Andromeda galaxy with a dwarf galaxy, students managed to reproduce the observed stream structure and obtain a rough estimate of the dwarf galaxy mass.

Projects in *astroparticle physics and cosmology* investigated observational imprints of various dark matter models on different scales using semi-analytical methods. Savić and Jevtović (2019) argued that the rotation of halos, made from ultra-light bosons, could stabilize them against the attractive self-interaction. Angular momentum of dark halos was estimated via cosmological perturbation theory. Projects of Jevtović (2018) and Stepanović and Ćeranić (2019) studied phenomenology of ultra-light dark matter on smaller scales. Stepanović and Ćeranić (2019) investigated orbital properties and in particular occurence and properties of resonances of stars in halos of this kind of dark matter. Jevtovic (2018) modeled the gravitational wave signal from an inspiral of stellar-mass compact object into supermassive black hole mimicker made from particles in the dark sector. Finally, Đurić (2020), in the spirit of effective field theory, tried to understand what aspects of general relativity could have been antic-

ipated in the Newtonian era from the precession of Mercury perihelion, deflection of starlight passing near the Sun and the Shapiro time delay.

Student projects in *planetary sciences* analyzed the dynamics of Solar system small bodies and the planetary structure. Anastasijević (2018) modelled the tidal interaction between Saturn and it's satellite Enceladus. Model was used to calculate internal heating of the Enceladus as a check. Another student project focused on asteroid transport from the asteroid belt to the near Earth region (Ranisović 2020). Here, the student used numerical code Mercury (Chambers 1999) to simulate the ejection of asteroids from the asteroid belt due to mean-motion resonance with Jupiter.

Research in *stellar astrophysics* was focused on the analysis of stellar and the exoplanet atmospheres as well as stellar structure and evolution. One project (Srećković 2020) investigated the difference between theoretical atmosphere models in 1D and empirical models on the example of star HD 209458. Using the limb darkening coefficients obtained from the transit observations, the student derived the temperature, electron pressure and gas pressure profiles. One group of students (Savić, Obradović and Herček 2018) modelled the photometric signal of the exoplanet - cepheid binary. First, they modelled the oscillations in the outer layers of cepheid and then estimated the part of the parameter space of exoplanet radius - orbital semi-major axis in which the Kepler telescope would detect exoplanet around δ Cep star. Another project examined the planet habitability taking into account the thermal properties of the planet's surface and the atmosphere (Bulaja 2018).

In previous years, stellar clusters have been a frequent topic of our students projects and the period that we report on is not an exception. Dakić (2019) estimated the age of the M92 cluster and the distance to it from the luminosity function. Bulaja (2019) used publicly available data from MUSE spectrograph (at the VLT telescopes) to infer the electron temperature and concentration in the central part of Orion nebula.

The majority of students have their first experience with a telescope during astronomy seminars at PSC and naturally, a group of projects done are *observational*. Špegar (2018) used Nedeljković telescope at astronomical observatory Vidojevica to observe the transit of the WASP-69 system and infer the transit parameters by MCMC fitting procedure. Photometric observations are mostly recorded on CCD cameras which have large quantum efficiency and low thermal noise. However, Jevtić (2018) performed a photometric observation of V2455 Cyg using a DSLR camera. He was able to obtain the light curve in the green filter and estimate the period of the star. In the following years, the student wrote a code for reducing the observations and extracting the light curve of the observed variable star with a DSLR camera as a follow-up project (Jevtić 2020).

3. PARTNER PROGRAMS AND COLLABORATIONS

Senior and junior associates from the Department of Astronomy are also involved in other programs as participants and organizers. Petnica Summer Institute (PSI) is organized every summer (from 2013) in PSC and it covers several topics in a four years cycle: cosmology, particle physics, astrophysics, and general relativity. PSI brings together senior undergraduate/master students of astronomy, physics and mathematics from former Yugoslavia and other countries to meet each other and learn about the

novel results in modern science. Lecturers are mostly senior PhD students and post-docs (as well as some senior researchers) in the spirit of Petnica principle - education of students by other students.

One of the oldest groups in Petnica is Petnica Meteor Group (PMG). Like PSI, PMG also gathered many participants from AST but also participants and associates from other departments. PMG organizes meteor observing camps. The largest camp is in August for observing the Perseid meteor shower. Every year the School of Meteor Astronomy is also organized in Petnica and for several years the journal "Perseids" was published.

Our senior and junior associates are students or staff at the Department of Astronomy (Faculty of Mathematics) and Astronomical Observatory in Belgrade. These institutions have been major partners of the AST department for many years. However, some of our student-assistants are studying theoretical physics, electrical engineering and mathematics. Also, some of our senior associates work at the Faculty of Science in Novi Sad, Mathematical Institute of the Serbian Academy of Sciences and Arts, various foreign universities and institutes (e.g. CERN, SISSA in Trieste, Max Planck Institutes in Göttingen and Munich) and for software companies.

4. COVID YEAR AND FUTURE PLANS

In the year 2020, due to the COVID-19 pandemic, there were only two AST seminars on site in Petnica in March and October for high-school students who are in their first year of attendance. All other seminars were organized online in August and October. Three student projects were presented online at the conference "A Step into Science". Although the pandemic interrupted regular activities at PSC we tried to substitute them with online lectures and discussions as much as possible.

During the past several years AST has organized "R&D astronomy workshops" - informal lectures by and for our associates on the topics of interest and relevance for the seminar. In 2018 a workshop was organized on the topic of relativistic astrophysics and cosmology and appropriate "scaled-down" version of these lectures was presented to the participants in the second year of attendance during the Summer seminar of 2019. We plan to continue with these activities in the following period.

The number of observational projects is rising in recent years. New observational equipment has arrived in 2018 - Celestron CGX EQ mount and SBIG STF-8300 monochrome CCD. We have also upgraded our computational facilities with a new computer named "Prometej". This computer is available for our participants if they work on the projects that demand high CPU power as well as to our senior and junior associates.

Acknowledgements

We thank all of the junior and senior associates for their continuing contribution in shaping the AST seminar. We would also like to thank participants, to whom our efforts aimed, who shaped educational activities with their comments. Here we explicitly thank to all project tutors and associates who were most responsible for shaping current educational activities presented in this report - Aleksandra Arsovski, Ivana Bešlić, Jovan Božuta, Teodora Čapko, Matija Dodović, Darko Donevski, Vladimir Đošović, Vladan Đukić, Andrija Kostić, Stevan Golubović, Vladisav Jelisavčić, Luka

Jevtović, Boris Majić, Nemanja Martinović, Ivan Milić, Sanja Mihajlović, Damnjan Milić, Anđelka Milovanović, Andrej Obuljen, Božidar Obradović, Debora Pavela, Dušan Pavlović, Nastasija Petković, Vanja Petković, Jovana Petrović, Milica Rakić, Petar Saulić, Nikola Savić, Ivan Stanković, Marko Simonović, Lazar Živadinović, Miroslav Živanović.

References

Anastasijević, I.: 2018, *Petničke sveske*, **76**, 30-39.

Bošković, M., Obuljen, A., Vukadinović, D., Milošević, S., Milić, I., Božić, N.: 2018, *Publications de l'Observatoire Astronomique de Beograd*, **98**, 101-108.

Bulaja, L.: 2018, *Petničke sveske*, **76**, 44-48.

Bulaja, L.: 2019, *Petničke sveske*, **77**, 66-74.

Chambers, J. E.: 1999, *Monthly Notices of the Royal Astronomical Society*, **304**, 793-799.

Dakić, V.: 2019, *Petničke sveske*, **77**, 35-43.

Dodović, M.: 2018, *Petničke sveske*, **76**, 53-65.

Dodović, M., Despotović, P.: 2019, *Petničke sveske*, **77**, 5-17.

Đurić, J.: 2020, *Petničke sveske*, **78**, 5-12.

Jevtić, S.: 2018, *Petničke sveske*, **76**, 40-43.

Jevtić, S.: 2020, *Petničke sveske*, **78**, 23-28.

Jevtović, L.: 2018, *Petničke sveske*, **76**, 66-73.

Ranisović, T.: 2020, *Petničke sveske*, **78**, 29-35.

Ristić, D.: 2018, *Petničke sveske*, **76**, 22-29.

Ristić, D.: 2019, *Petničke sveske*, **77**, 60-65.

Savić, N., Obradović, B., Herček, F.: 2018, *Petničke sveske*, **76**, 5-21.

Savić, N., Jevtović, L.: 2019, *Petničke sveske*, **77**, 18-34.

Springel, V.: 2005, *Monthly Notices of the Royal Astronomical Society*, **364**, 1105-1134.

Srećković, T.: 2020, *Petničke sveske*, **78**, 13-22.

Stepanović, M., Ćeranić, A.: 2019, *Petničke sveske*, **77**, 44-51.

Špegar, J.: 2018, *Petničke sveske*, **76**, 49-52.

Vogelsberger, M., Genel, S., Springel, V., Torrey, P., Sijacki, D., Xu, D., Snyder, G., Bird, S., Nelson, D., Hernquist, L.: 2014, *Nature*, **509**, 177-182.

Vrhovac, K.: 2019, *Petničke sveske*, **77**, 52-59.

Posters

Publ. Astron. Obs. Belgrade No. 100 (2021), 371 - 374 *Poster*

DEEP PHOTOMETRY OF SPIRAL GALAXY NGC 941

J. HORVAT[1] and A. VUDRAGOVIĆ[2]

[1] *Faculty of Mathematics, Studentski trg 16, 11000 Belgrade, Serbia*
E–mail: jasminahorvat2705@gmail.com

[2] *Astronomical Observatory, Volgina 7, 11060 Belgrade 38, Serbia*
E–mail: ana@aob.rs

Abstract. We have modelled surface brightness profile of the spiral galaxy NGC 941 using SDSS Stripe82 deep images in the r-band. The depth of Stripe82 images reaches the stellar halo brightness level (28.5 mag arcsec^{-2} in the r-band), which was our basic motivation to start the study. We have simultaneously modelled NGC 941 galaxy with multiple components to find that its surface brightness profile could be missclassified as Type II. The "feature" responsible for the apparent downbending of the light profile is the spiral arms structure.

1. INTRODUCTION

The radial surface brightness profiles of spiral galaxies are exponential. However, only minority of spirals show simple exponential decline, while the majority (∼90%) show either up- or down-bending profiles. They are being classified according to the outer shape of their profiles as: Type I galaxies that follow a simple exponential law, Type II galaxies that show a downbending break with a steeper outer exponential (Pohlen et al. 2002; Erwin, Pohlen & Beckman 2008) and Type III galaxies that show an upbending break with a shallower outer exponential (Erwin, Beckman & Pohlen 2005).

Different shapes of surface brightness profiles may indicate different evolutionary paths. This was our motivation to explore in great depth the shape of NGC 941 galaxy surface brightness profile.

2. DATA

We have used SDSS Stripe 82 data[1] for our study, because they are very deep. The SDSS Stripe82 Survey is a wide region (2.5 degree) along the celestial equator. It has been imaged repeatedly 80 times. The images were co-added taking special care of background subtraction. These final co-added images reached 3-sigma surface brightness limit of 28.5 mag/arcsec^2 in the r-band.

[1] SDSS Data Archive Server: http://research.iac.es/proyecto/stripe82/pages/data.php

3. METHODS

Modelling of the surface brightness profile of the galaxy NGC 941 was done following the standard procedure. First, we have used Sextractor (Bertin & Arnouts 1996) to build a catalog of objects in the image to obtain a good mask. Then we modelled light profile of NGC 941 using Galfit code (Peng, Ho & Impey 2010), that creates 3D models. We were working with SDSS Stripe82 data with the exposure map instead of the sigma-image. To create a sigma-image we have masked all the objects except for the target galaxy, and then run Galfit code without sigma-image to get estimate of the RMS (root-mean-square). Then we created the sigma image, using the formula

$$\sigma_{i,j} = I_{i,j} * \mathrm{GAIN}_{\mathrm{eff}} + \mathrm{RMS}^2 * \mathrm{GAIN}_{\mathrm{eff}}^2, ^2 \quad (1)$$

where $I_{i,j}$ is the intensity in each i, j pixel of the image, and $\sigma_{i,j}$ the corresponding uncertainty.

Additionally, we have extracted the surface brightness profile applying isophotal analysis that resulted in a set of concentric ellipses inside which flux intensity was averaged, using Photutils package from the Astropy library.[3] To model properly outer parts of the light distribution, we kept ellipticity and position angle fixed.

4. RESULTS

Galfit results are shown in Figure 1: galaxy image, model and the residuals, respectively.

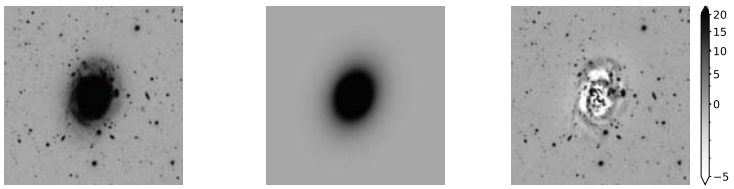

Figure 1: 3D decomposition: galaxy (left) was modelled with multiple components: a point spread function (PSF), inner and outer bar, an exponential disk, and a bar-like structure that successfully modelled spiral arms (center). The residual structure is also shown (right).

To better visualize the results, we have plotted our modelling results obtained with Galfit over the surface brightness points from the isophotal analysis (Figure 3). The most successful fit is the five-component fit with galaxy disk modelled as a pure exponential disk, inner and outer bars modelled as Sersic components with index n = 0.2, and another "bar-like" structure that accounts for the spiral arms contribution (Figure 3). Broken disk model (green dashed line in Figure 2) is not

[2] $\mathrm{GAIN}_{\mathrm{eff}} = 2./3. * \mathrm{GAIN} * \mathrm{weightmap.data}$. Factor of 2/3 comes from the fact that images are median combined.

[3] https://photutils.readthedocs.io/en/stable/

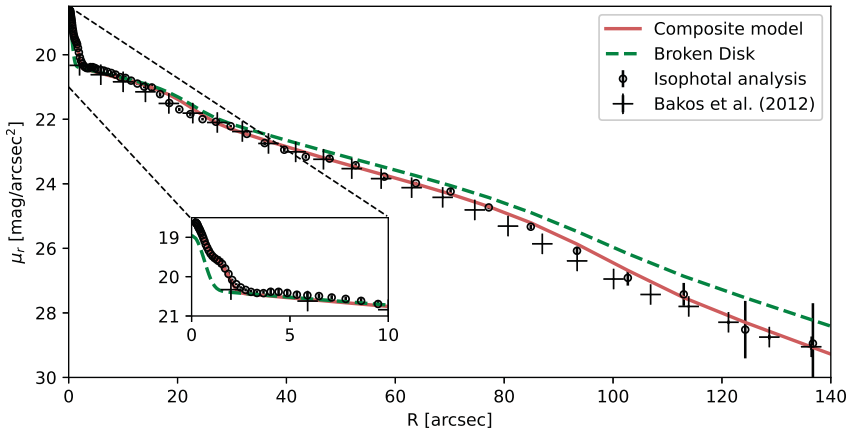

Figure 2: Results of the isophotal analysis (open circles) agree well with Bakos et al. (2012) which are presented with crosses. Three dimensional models from Galfit are shown : Composite model (solid red line; see Fig. 4 for details) with χ^2=1.47, and Broken Disk model (green dashed line) consisting of a PSF, an inner bar, an exponential broken disk, and a bar with χ^2=1.50. Inner most part is shown enlarged as inset figure.

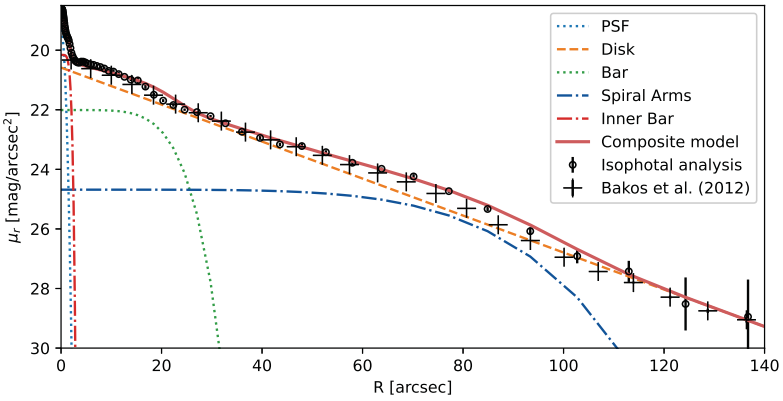

Figure 3: Components of the 3D modelling of the surface brightness profile of NGC 941 galaxy: five-component profile (red line) is decomposed into constituent components – a point spread function (PSF; blue dashed line), a disk (orange dashed line), a bar (green dotted line), inner bar (red dash-dotted line), and spiral arms modelled as a bar structure (blue dash dotted line).

particularly successful in modelling both the inner most part and the outer part of the surface brightness galaxy profile. Bakos et al. (2012) concluded that this galaxy has a downbending disk, but we believe that the presence of the spiral arms resembles the break in their 1D analysis. Residuals from the best fitting model can be seen in the Figure 4: the left image contains the spiral structure, successfully modeled by the "bar-like" component resulting in the residuals given in the middle image. Residuals in the right image come from modeling the structure on the left with the broken disk. The residuals in the middle and in the right image are indistinguishable, but there is a slight difference in the χ^2 value seen more clearly in the Figure 2. "Bar-like" component has a χ^2=1.47 and the broken disk gives χ^2=1.50.

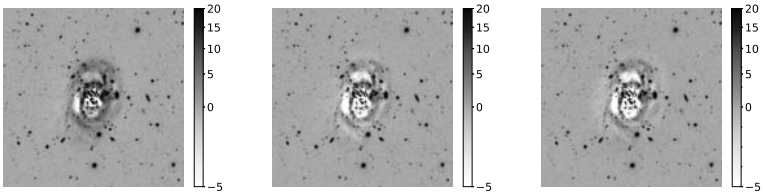

Figure 4: Residuals from the modelling the NGC 941 galaxy surface brightness profile: (left) residual image with spiral arms left (χ^2=1.65); (center) residual image without spiral arms that were modeled as a "bar-like" structure (χ^2=1.47); (right) residual image without spiral arms modelled as a broken disk (χ^2=1.50).

5. DISCUSSION

Using SDSS Stripe82 data we have modelled surface brightness profile of the galaxy NGC 941. We have found that downbending of the light profile of NGC 941 galaxy might be caused by the presence of the spiral arms structure. The analysis was done for a single galaxy, so it is a question if the conclusion holds in general.

Acknowledgements

This work was supported by the Ministry of Education, Science and Technological Development of the Republic of Serbia (MESTDRS) through the contract No 451-03-9/2021-14/200002.

References

Bakos, J., Trujillo, I.: 2012, arXiv:1204.3082.
Bertin, E., Arnouts, S.: 1996, *Astronomy and Astrophysics Supplement Series*, **117**, 393-404.
Erwin, P., Beckman, J. E., Pohlen, M.: 2005, *Astrophy. J.*, **626**, L81.
Erwin, P., Pohlen, M., Beckman, J. E.: 2008, *Astron. J*, **135**, 20.
Peng, C. Y., Ho, L. C., Impey, C. D.: 2010, *Astron. J*, **139**, 2097.
Pohlen, M., Dettmar, R. J., Lütticke, R. et al.: 2002, *Astron. & Astroph.*, **392**, 807.

Publ. Astron. Obs. Belgrade No. 100 (2021), 375 - 386 *Poster*

CORRESPONDENCE BETWEEN MILUTIN MILANKOVIĆ AND ELSE WEGENER–KÖPPEN

NATALIJA JANC[1], MILIVOJ B. GAVRILOV[2], SLOBODAN B. MARKOVIĆ[2,4], VOJISLAVA PROTIĆ BENIŠEK[3], LUKA Č. POPOVIĆ[3] and VLADIMIR BENIŠEK[3]

[1] *Baltimore, Maryland 21212, USA*
E–mail: natalijanc@earthlink.net. Corresponding author

[2] *University of Novi Sad, Faculty of Sciences, Trg Dositeja Obradovića 3, 21000 Novi Sad, Serbia*

[3] *Astronomical Observatory, Volgina 7, P.O.Box 74, 11060 Belgrade, Serbia*

[4] *Serbian Academy of Sciences and Arts, Kneza Mihaila 35, 11000 Belgrade, Serbia*

Abstract. Milutin Milanković (1879–1958) had a very close collaboration with famous climatologist Wladimir Köppen (1846–1940) and genial geophysicist Alfred Wegener (1880–1930). Else Wegener–Köppen (1892–1992) was the daughter of Wladimir Köppen and the wife of Alfred Wegener.

Correspondence between Milutin Milanković and Else Wegener-Köppen is in the legacy of Milutin Milanković, archived in the Serbian Academy of Sciences and Arts in Belgrade.

For the first time, as far as the authors know, in 1930 she addressed Milanković with a request to send her information about the journals she needed while translating the biography of Carl Anton Bjerknes (1825–1903) from Norwegian.

To supplement the biography of Wladimir Köppen, she asked Milanković in 1949 to describe to her how his collaboration with Köppen began on the book *Climates of the Geological Past* and about their correspondence in general. Milanković answered that he presented his personal impressions in the German edition of the book *Through the Universe and Centuries*, and about scientific cooperation in the *Canon*. That scientific cooperation lasted from 1921 until Köppen's death.

The correspondence is short, but the content of the letters is interesting and contributes to the study primarily of Wladimir Köppen, as well as to the participation of other important scholars who assisted Else Wegener in the work on his biography.

1. INTRODUCTION

Milutin Milanković had a very rich correspondence with many scientists, about which he wrote in his *Memories, Experiences, and Knowledge from 1909 to 1944* (Milanković, 1952). Later the content of the letters translated into Serbian was also published (Milanković, 1997). However, one part of the correspondence remained unpublished and unprocessed for a long time. Among them is the long-term correspondence with Vojislav Mišković (1892–1976), the director of the Astronomical Observatory in Belgrade. This significant correspondence between the two academics has recently been processed, presented at conferences and published (Janc et al., 2018a,

2018b, 2019). Milutin Milanković's letters to Vojislav Mišković, Vojislava Protić-Benišek were kindly received from the Mišković family, while Vojislav Mišković's letters to Milutin Milanković are in the Serbian Academy of Sciences and Arts (SASA) in Belgrade. During the processing of this correspondence, in the post scriptum of the letter that Milanković sent to Mišković on November 24, 1930, a letter he received from Elsa Wegener was mentioned. This gave the idea to find the mentioned letter of Else Wegener and to check whether there was more correspondence between Milutin Milanković and Else Wegener. During the review of Milutin Milanković's legacy in SASA, this Elsa Wegener's letter was not found, but it was a pleasant surprise that several other letters of Else Wegener and Milanković's drafts of his responses have been preserved. Correspondence between them was conducted in German, and Milanković's drafts are also in German.

Milutin Milanković had scientific cooperation and family ties with Wladimir Köppen and Alfred Wegener that started in 1921. Because of that, Else Wegener–Köppen in the course of writing the biography of her father, asked Milutin Milanković to help to complete data about their mutual cooperation.

2. ELSE WEGENER–KÖPPEN

Else Wegener–Köppen was the daughter of Wladimir Köppen. Wladimir Köppen was vitally interested in developing physics of the atmosphere. As Else recalled, her father wanted the whole family to share his excitement in development of his "young science" telling them "we need in meteorology these days the kind of minds coming our way from physics; it is now the time to comprehend and explain, from the standpoint of physics, the atmospheric processes we have discovered in the course of our kite and balloon ascents" (Greene, 2015). In this way, under her father's influence, she developed a great interest for the natural sciences.

The triennial meeting of the German Meteorological Society (Deutsche Meteorologische Gesellschaft) was held from 28th to 30th September 1908 in Hamburg. At the meeting, Wegener presented at talk about his research in Greenland, illustrated with slides. Else, then sixteen, got permission to stay away from school to attend Wegener's lecture. She also got an invitation to the official banquet and she was to be Wegener's guest at the table. After the meeting, Köppen invited Wegener for an informal dinner with family and friends at his home (Greene, 2015). That was the beginning of their relationship (Fig. 1).

Because of Alfred's expedition to Greenland, the couple postponed their wedding plans until November 1913 (Wegener–Köppen E. and Thiede J. (Eds), 2018). So, while waiting for him to return, Else traveled to Oslo and lived with the Bjerknes family teaching Bjerknes' children the German language (Fig. 2a) (Wegener–Köppen E. and Thiede J. (Eds), 2018). This way, boys would be ready to move to Germany, where their father Vilhelm Bjerknes[1] had taken up the Leipzig professorship in 1912 (Greene, 2015). That stay enabled Else to develop friendly relationship with the Bjerknes family.

[1]Vilhelm Friman Koren Bjerknes (1862–1951) was a Norwegian meteorologist who did much to found the modern practice of weather forecasting. He formulated the simple (basic) equations that are still in use in numerical weather prediction and climate modeling.

Figure 1: Newlyweds Else and Alfred Wegener, a picture from the late 1913. She was 20 and he was 33 years old. (https://www.pinterest.com/pin/408068416210428586/)

Else Wegener was in 1992 appointed a honorary member of the German Society for Polar Research (Deutsche Gesellschaft für Polarforschung) (Wegener–Köppen E. and Thiede J. (Eds), 2018).

3. CORRESPONDENCE

Else Wegener worked on biographies of Carl Anton Bjerknes, a Norwegian mathematician and physicist, well-known for his studies in hydrodynamics. For the first time, as far as the authors know, in 1930 she addressed Milanković with a request to send her information about the journals she needed while translating Bjerknes' biography from Norwegian (Janc et al., 2018a). That letter is not in SASA, but it is known indirectly from the letter of Milutin Milanković sent November 24, 1930 to Vojislav Mišković (1892–1976), the director of the Astronomical Observatory in Belgrade (Janc et al., 2018b).

Universitet Matematički institut Beograd, 24. XI 1930.

Mathematical Institute of the University, Belgrade, 24 November 1930

Dear Mišković,

(. . . The full text of the letter is here omitted)

Your Milanković

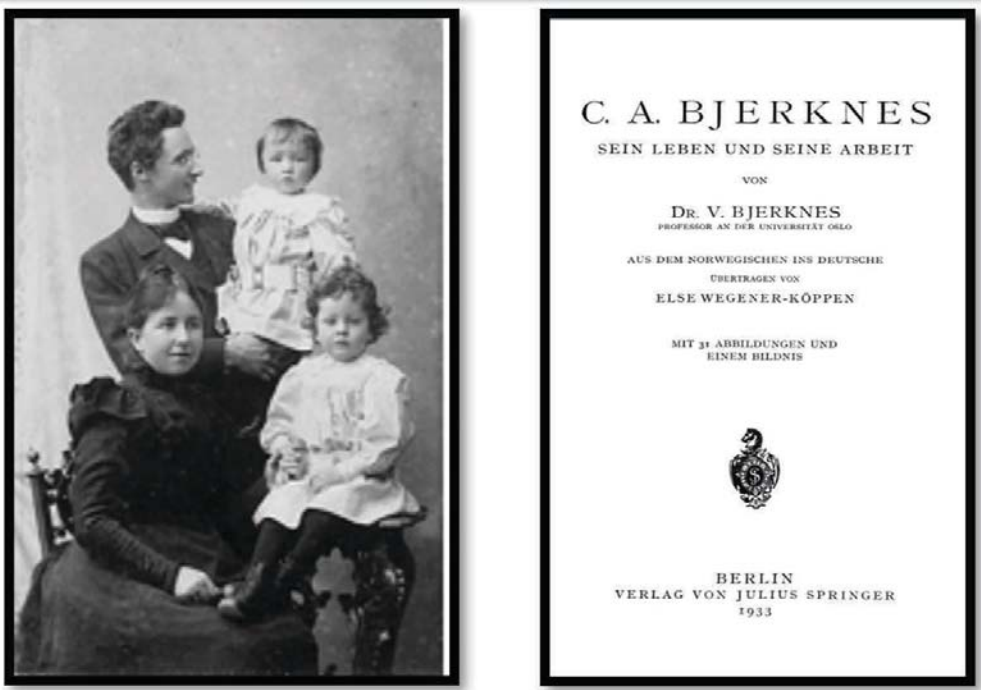

a) b)

Figure 2: a) Vilhelm Bjerknes with his wife Honoria and their first two sons Karl Anton and Jacob Aall Bonnevie, circa 1898. (Wikipedia https://creativecommons.org/licenses/by-sa/4.0/deed.en.) b) C. A. Bjerknes, Sein Leben und seine Arbeit, von Dr. V. Bjerkens, Übertragen von Else Wegener–Köppen, Berlin, Verlag von Julius Springer, 1933.

P.S. Now I just got one letter from Mrs. Wegener. She translates from Norwegian a biography of C. A. Bjerknes, to be supplemented with some quotes from Lagrange, which came out in the journal Lindenau–Bohnenberger, Zeitschrift für Astronomie, somehow around the years 1816–1818. She asks if we have that journal here, because she could only get the volumes 5 and 6; the others are gone. I have no doubt that this journal is not available, but I'm asking you if you don't happen to know more about this journal that came out in just six to eight volumes.

The last letter to Else, Alfred Wegener wrote in September 1930 on his way to the polar station Eismitte. The next communication arrived more than a half year later as a cable from May 1931, informing her what had happened to her husband: "Death on the ice-sheet in the interior" (Voß, 1992). This shows that Milutin Milanković and Else Wegener exchanged letters not having any idea of the tragic destiny of Alfred Wegener at that time.

Else Wegener's translation of the Carl Bjerknes' biography was published in 1933, *C. A. Bjerknes, Sein Leben und Seine Arbeit*, von Dr. V. Bjerknes, Übertragen von Else Wegener–Köppen, Berlin, Verlag von Julius Springer (Fig. 2b).

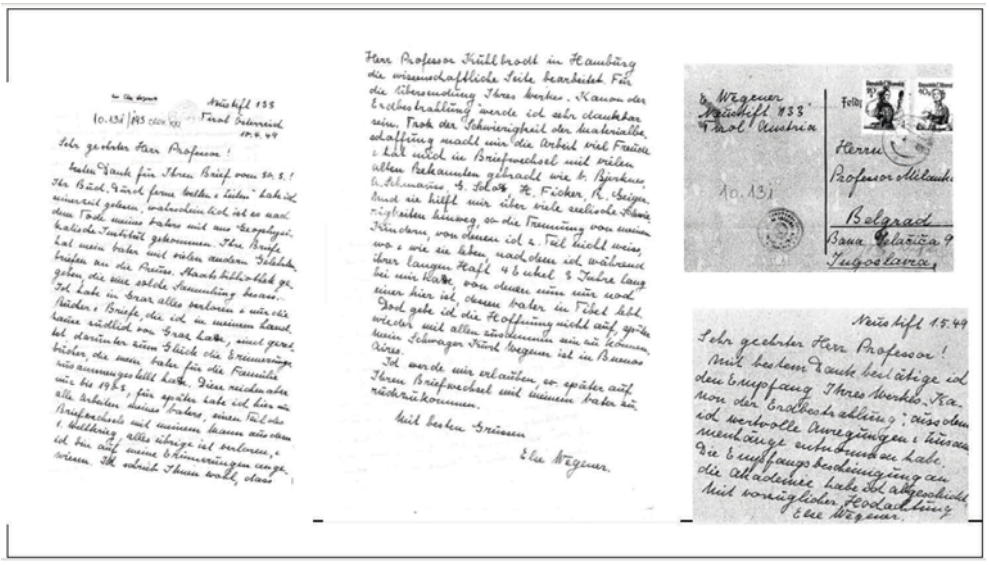

Figure 3: Facsimiles of several letters Else Wegener sent to Milutin Milanković.

About the last days of Wladimir Köppen, Else Wegener wrote to Milanković from Graz on September 28, 1940. In that letter Milanković added "received October 7, 1940."

Graz 28.9.40, (received September 7, 1940, – Milanković's note on the letter)

Dear Mister Professor!

In June I could not send you a death notice because the post office did not accept printed matter at the time. Thank you very much for your letter!

In May Papa was not doing very well after spending the winter so well that we hoped he could spend a few weeks with my sister in the summer, who moved to Graz in April. It then went downhill quickly with his powers. He was no longer able to read the second correction of his additions to the climates of the past, although I asked for it by telegraph to be accelerated and received it very quickly. (. . .)

Warm regards from home to home,

Else Wegener

After the deaths of her husband and father, Else Wegener devoted herself to writing about their lives and accomplishments. That helped her survive the painful separation from her children, as she wrote in a letter to Milanković.

Correspondence between Milutin Milanković and Else Wegener–Köppen is in the legacy of Milutin Milanković in SASA in Belgrade (Fig. 3).

To supplement the biography of Wladimir Köppen, Else Wegener–Köppen asked Milanković in 1949 to explain to her how his collaboration with Köppen on the book *Climates of the Geological Past* began and about their correspondence in general.

Figure 4: Milutin Milanković, *Canon* and the German edition of the book *Through the Universe and Centuries.*

Neustift 133, 6. 3. 1949. (received March 9, 1949 – Milanković's note on the letter)

Dear Mister Professor!

Since autumn I have been working on a biography of my father, which is to appear in a series of "Great naturalists." Up to 1903 I had 7 volumes of memory put together by my father, until 1919 I still had part of the correspondence between my husband and my father, but from then on only my work and my memory. Professor Kuhlbrodt in Hamburg provides me with information and excerpts from the scientific work, which luckily, I have almost all here. But, of course, I'm also interested in the suggestions for this work. May I ask you to tell me something about how you came to work with my father on the book "The Climates of Geological Past." Do you have any letters from my father that I could use for this that you could possibly have made extracts from? Or would you provide me with memories of your being with him in Graz or Belgrade? In what year did he visit you in Belgrade? As far as I remember my parents wanted to fly from Sofia to Belgrade back then, but it didn't work out because the plane didn't come due to bad weather. Is that correct?

You were kind enough to visit my parents in transit several times. Was there still a certain scientific collaboration at the time? I don't remember any of that.

Please forgive me for taking your inquiries, which I am sure, will take up your valuable time. It is important to me to give a well-rounded and truthful picture of his work and personality.

With best regards,

Else Wegener

Milanković answered that he presented his personal impressions in the German edition of the book *Through the Universe and Centuries*, and about scientific cooperation in the *Canon* (Fig. 4). That scientific cooperation lasted from 1921 until Köppen's death. Milanković received altogether 73 letters or postcards from Köppen, but he mostly kept only the drafts of his answers. Part of those contacts were near the end of Köppen's work at the Hamburg German Naval Observatory that dealt with meteorology, oceanography, geophysics, aeronomy, Earth magnetism, time service, instrument gauging, etc.

To Else Wegener, Neustift 133, Tirol, Oesterreich

30-III-1949 (March 30, 1949)

Highly esteemed Mrs. Professor,

I was very pleased with your kind letter, as I did not know where you were or how you have been. Now I know you are in a wonderful area and at work, describing your father's memories, to whom science was so close and whom I also admired as a person. I consider it a personal happiness to have lived and worked with him in friendship.

I described my personal experiences with your father in my book "Through the Universe and Centuries" Leipzig, Koehler & Amelang 1936, our scientific collaboration in my principal work "Canon of Earth Radiation." Of that first book, the second edition of which was destroyed by an air raid on Leipzig, I have not a single copy available, but I sent one to your father at the time; he had received it and read it. The second work was published after the death of your father. You will soon receive a copy of the same from our Academy of Sciences.

We did exchange letters. All letters that your father wrote to me are well preserved.

From 1921 until his death, I had a regular correspondence with your father and during this time I received and kept 73 letters and postcards from him. A part of my replies is a machine copy, the other part only exists as draft. Your father kept the originals of my letters and announced to me that he intended to hand them over to the State Library. I do not know what happened to these letters.

In an emergency, my typewritten copies and drafts are available if it should be for publication and scientific work or this correspondence, as it is of historical interest.

I started about a year ago just by writing down my memoirs. It is my intention in this book to present the friendship and cooperation with your father from my memory and from the correspondence received (that I have given to our Academy of Sciences). However, my work is progressing very slowly. I am still an active professor at our university, Vice President of the Academy of Sciences, and heavily burdened with other duties. Moreover, I am in my seventies; ... so I am with my life memories ... only when I was 18 years old up to the acquaintance with your father, when I was 43 years old.

You cannot, madam, of course wait until the turn of the chapter "Köppen" in my life recollections.

I would therefore like to ask you to read through the material about your father in my two mentioned works and see how I could be of further assistance to you.

I would be very happy to learn more about your personal well-being and if I could hear good news.

With this expectation and my high respect, I remain yours sincerely [. . .] MM

P.S. As I see from my diaries, your father was with me twice in Belgrade, the first time from October 16-19, 1928, after he was not able to take the plane from October 12 [. . .], the second time from October 12–15, 1929. I have myself visited him five times in Graz, as far as I can remember, the first time in July 1925, the last time in September 1936.

Else Wegener thanked Milanković for the letter in which she found information of interest to her. In addition, she informs Milutin Milanković that their family copy of the translation into German of *Through the Universe and Centuries* was sent with the legacy of Wladimir Köppen to the Geophysical Institute of the Prussian State Library in Berlin.

Writing her father's biography had brought Else Wegener in contact with many of her and Wladimir Köppen's old friends and distinguished scientists like Vilhelm Bjerknes, Gerhard Schott[2], August Schmauss[3], Heinrich von Ficker[4], Rudolf Geiger[5], and Erich Kuhlbrodt[6] (Fig. 5).

Else Wegener informed Milanković that Professor Erich Kuhlbrodt in Hamburg was working on the scientific side of her research, and she would be very grateful if Milanković sent her a copy of *Canon of Earth Radiation*.

Neustift 133, Tirol, Österreich, 10. 4. 1949. (October 4, 1949)

Dear Mister Professor!

Thank you for your letter from March 30th! I read your book "Through the Universe and Centuries" at the time, it probably came to the Geophysical Institute after my father's death. My father gave his letters to the Prussian State Library, which had such a collection, along with many other scholarly letters. I lost everything in Graz and only the books and letters that I had in my country house south of Graz have been saved, including luckily the souvenir books that my father had put together for the family. But these only cover the period until 1903, for later I only have all my father's work here, part of the correspondence with my husband from the First World War, everything else is lost, and I am dependent on my memories. I am writing to you that Professor Kuhlbrodt is working on the scientific side in Hamburg. I will be very

[2]Gerhard Schott (1866–1961) was a German geographer and oceanographer. He was the best-known ocean researcher in the world in his field. During an expedition when he was still a student, he discovered the relationship between the barometric pressure and the length of ocean waves.

[3]August Schmauß (1877–1954) was a German physicist, meteorologist, and climatologist. In the 1920s he introduced the notion of singularity in the research of regular meteorological phenomena.

[4]Heinrich von Ficker (1881–1957) was a German-Austrian meteorologist and geophysicist. He is known for his treatise *Foehn and Foehn Effects* in the Alpine regions and important research of cold fronts and heat waves that occur in Russia and northern Asia.

[5]Rudolf Geiger (1894–1981) was a German meteorologist, one of the leading pioneers in microclimatology. He researched and collected extensive measurement data through systematic experiments in Bavarian forests and about changes in the existing climate depending on exposure and about the influence of soil vegetation on the local climate.

[6]Erich Walter Gotthard Kuhlbrodt (1891–1972) was a German meteorologist with fundamental results in maritime aerology, maritime weather observations, and maritime climatology. He earned his PhD with the topic of meteorology and climatology of Macedonia (Kuhlbrodt, 1920).

Figure 5: Photos of August Schmauss, Erich Kuhlbrodt, Heinrich von Ficker, Rudolf Geiger and Gerhard Schott.

grateful for the submission of your work "Canon of Earth Radiation." Despite the difficulty of obtaining materials, I enjoy my work and it has brought me in contact with many old friends like V. Bjerkness, A. Schmauss, G. Schott, H. Ficker, R. Geiger. (...)

I will take the liberty of coming back to your correspondence with my father later.

Best regards,

Else Wegener

Milanković immediately sent the *Canon* through the Serbian Academy of Sciences. Else Wegener received the book and thanked Milanković and the Academy.

[Postcard] 10.131, [date and seal not readable...Republic of Serbia]

From: Else Wegener, Neustift 133, Tirol, Oesterreich

To: Herrn Professor Milanković, Belgrad, Bana Jelačića 9, Jugoslavia

Neustift 1.5.49 (May 1, 1949)

Very esteemed mister Professor,

With best thanks I confirm the receipt of your work "Canon of Earth Radiation," from which I have taken valuable suggestions and contexts. I sent the acknowledgement receipt to the Academy.

With great respect

Else Wegener

4. ABOUT COLLABORATION OF WLADIMIR KÖPPEN AND MILUTIN MILANKOVIĆ IN THE BOOK "WLADIMIR KÖPPEN — SCHOLAR FOR LIFE"

The first edition of the Köppen's biography that was written by his daughter Else Wegener–Köppen, was published in 1955 as "Wladimir Köppen, Ein Gelehrtenleben für die Meteorologie" in edition *Grosse Naturforscher*, edited by Hans Walter Frickhinger, published by Wissenschaftliche Verlagsgesellschaft in Stuttgart. The second, revised and augmented bilingual edition, in English and German, appeared in 2018 with editors Else Wegener–Köppen and Jörn Thiede[7] *Wladimir Köppen – Scholar for life / Ein Gelehrtenleben für die Meteorologie* with 313 pages and 54 illustrations; the publisher is Borntraeger Science Publishers, Berlin (Fig. 6). In the introductory part of the book, a paragraph 4. "Köppen, Wegener and Milankovich – a 'winning team' in paleoclimatology," was written about their collaboration on the book "The climates of the geological past" (Wegener–Köppen E. and Thiede J. (Eds), 2018). About that trinity Milanković wrote that "Köppen is a worldwide know climatologist, Wegener genius geophysicist and expert in everything connected to that science. And I realized: it was not a pure random event, but the causality of events that brought the three of us together" (Mijajlović 2013)[8].

When Else Wegener mentioned Milanković for the first time in this book, she explained in a footnote: "Milankovitch, Milutin, geb. 1879, jugoslawischer Mathematiker." (Milankovitch, Milutin, born 1879, Yugoslav mathematician.) (Wegener–Köppen E. and Thiede J. (Eds), 2018). In the book she does not mention explicitly her correspondence with Milanković, but knowing the content of the correspondence, there are parts clearly indicating that she was relying on it.

In 1920 Wladimir Köppen got acquainted with the work of Milanković *Théorie mathematique des phénomènes thermiques produits par la radiation Solaire* and later, Milanković provided Wladimir Köppen and Alfred Wegener with the mathematical means to review the glaciations and contribute to the basics of his calculations of solar radiation in the Quaternary and its results and table plus a diagram for their book *The climates of the geological past* published in 1924 (Wegener–Köppen and E. and Thiede J. (Eds), 2018). According to Else Wegener (2018):

"On this, a lovely correspondence ensued, which Milankovitch reports on in his book *Canon of the Earth's irradiation*.

"*Before I could get to work on this problem, a preliminary question had to be answered, namely, what meteorological element and what season was this ice age*?"

After an exhaustive discussion of all relevant boundary condition, Köppen answered Milankovitch's question in such a way, that the decrease of temperatures during the summer half of the year is decisive for glaciations."

Families Milanković, Köppen and Wegener became over time close friends that were visiting each other. For example, on their trip from Varna to Graz in 1930, Wladimir Köppen and his wife Marie, paid a visit to the Milanković family (Wegener–Köppen E. and Thiede J. (Eds), 2018).

[7]Jörn Thiede (1941–), geologist, paleontologist and university professor, a foreign member of the Russian and Norwegian academies of science. From 1997 until 2007 he was the director of the Alfred Wegener Institute.

[8]See http://legati.matf.bg.ac.rs/milankovic/paper.wafl?paper=saradnja_kepen_vegener

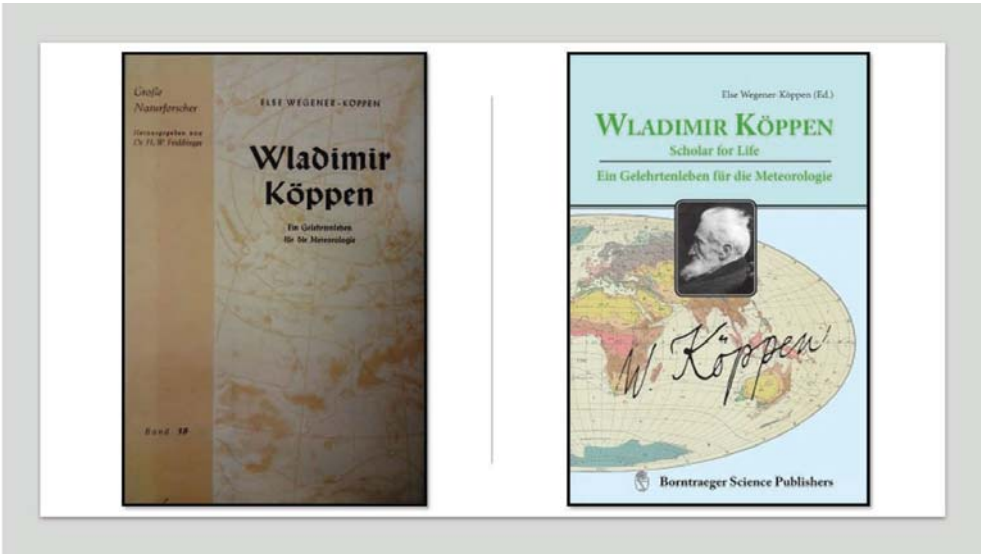

Figure 6: a) Else Wegener Köppen (1955): "Wladimir Köppen, Ein Gelehrtenleben für die Meteorologie" in edition Grosse Naturforscher, edited by Hans Walter Frickhinger, published by Wissenschaftliche Verlagsgesellschaft in Stuttgart. b) Else Wegener Köppen (Editor), Jörn Thiede (Editor), (2018): "Wladimir Köppen. Scholar for life / Ein Gelehrtenleben für die Meteorologie," edition by Borntraeger Science Publishers, Stuttgart.

5. CONCLUSION

The correspondence is short, but the content of the letters is interesting and contributes to the study primarily of Wladimir Köppen, as well as the participation of other important scholars who assisted Else Wegener–Köppen in the work on his biography, like Vilhelm Bjerknes, Gerhard Schott, August Schmauß, Heinrich von Ficker, Erich Kuhlbrodt, and Rudolf Geiger.

Despite the difficulties in obtaining materials, she was enjoying her work. Else Wegener–Köppen authored Wladimir Köppen's biography *Wladimir Köppen - Scholar for life*.

Wladimir Köppen was a well-established climatologist keen to support two young revolutionary researchers, Milutin Milanković and Alfred Wegener, who both significantly advanced geosciences. Köppen's authority played a crucial role in a long-term process of acceptance of these two "heretic" scientific approaches developed by Milanković and Wegener. Else Wegener–Köppen in her biographic works authentically preserved the memory of this important period in the development of earth sciences.

Acknowledgements

The authors thank Mirko Janc, PhD (mathematics) for the precious help in translating the correspondence between Milutin Milanković and Else Wegener and compiling and translating several resources from German language.

References

Greene, M. T.: 2015, Alfred Wegener, Science, Exploration, and the Theory of Continental Drift. *Johns Hopkins University Press, Baltimore*, 696.

Janc, N., Protić-Benišek, V., Benišek, V., Gavrilov, M. B., Popović, L. Č., Marković, C. B.: 2018a, Academicians Milutin Milanković and Vojislav Mišković: Correspondence about Alfred Wegener and Wladimir Köppen, *Astronomical and Astrophysical Transactions (AApTr): Journal of the Eurasian Astronomical Society*, **30** (4), 505–510.

Janc, N., Protić-Benišek, V., Benišek, V., Popović, L. Č., Gavrilov, M. B., Marković, S. B.: 2018b, Correspondence of Vojislav V. Mišković about his doctorate with Milutin Milanković, Miodrag Ibrovac and Oton Kučera, *Publications of the Astronomical Observatory of Belgrade*, **98**, 371–377.

Janc, N., Gavrilov, M. B., Marković, S. B., Protić-Benišek, V., Benišek, V., Popović, L. Č., Tomić, N.: 2019, Ice age theory: correspondence between Milutin Milanković and Vojislav Mišković, *Open Geosciences*, **11** (1), 263–272.

Kuhlbrodt, E.: 1920, Klimatologie u. Meteorologie von Mazedonien, Ein Beitrag zur Klimakunde d. Balkanhalbinsel. (Under Berücksichtigung d. Windverhältnisse in d. Höhe), Hamburg, 4. M. 45 tab. 61 OBr. (in German).

Mijajlović, Ž., Malkov, S., Mitić, N.: 2013, Digital legacies, NCD Review 148–152, 22 (see http://legati.matf.bg.ac.rs/milankovic/paper.wafl?paper=saradnja_kepen_vegener).

Milanković, M.: 1952, Reminiscences, Experiences and Knowledge 1909 to 1944, *Serbian Academy of Sciences, Special Editions, Book CXCV, Department of Natural and Mathematical Sciences, Book 6*, Belgrade, 229, (in Serbian, Cyrillic script).

Milanković, M.: 1997, Articles, speeches, correspondence, Correspondence with the Great Scientists, translation from the German language: Dr Milan Ćirić, translation from the French language: Dragan Mraović, *Institute for Textbooks and Teaching Aids*, Belgrade, (in Serbian, Cyrillic script).

Voß, J.: 1992, In Memoriam Else Wegener, 1 February 1892 – 27. August 1992. *Polarforschung* **61** (2/3): 183–184.1991 (published in 1992), (in German).

Wegener–Köppen, and Thiede, J. (Eds): 2018, Wladimir Köppen. Scholar for life / Ein Gelehrtenleben für die Meteorologie, *Borntraeger Science Publishers*, Berlin, 52 illustrations, 313, (English and German).

Publ. Astron. Obs. Belgrade No. 100 (2021), 387 - 390 *Poster*

MONITORING VLF SIGNAL PERTURBATIONS INDUCED BY SOLAR ACTIVITY DURING JANUARY 2005

A. KOLARSKI[1] and D. GRUBOR[2]

[1] *Technical Faculty Mihajlo Pupin, University of Novi Sad, Djure Djakovića bb, 23000 Zrenjanin, Serbia, E–mail: aleksandrakolarski@gmail.com*

[2] *Faculty of Mining and Geology, University of Belgrade, Djušina 7, 11000 Belgrade, Serbia E–mail: davorka.grubor@rgf.rs*

Abstract. Simultaneous monitoring of VLF (3-30 kHz) radio signals, transmitted within Earth-Ionosphere waveguide, from USA (NAA/24.0 kHz), GB (GQD/22.1 kHz) and Australia (NWC/19.8 kHz) towards Serbia and registered by narrowband AbsPAL receiving system, stationed at Institute of Physics in Belgrade (44.85N, 20.38E), was carried out. Series of Solar events during January 2005 were surveyed and analyzed. Modeling of related perturbed D region (50-90 km) ionospheric conditions, by means of LWPC program routine, was conducted. Based on the Wait′s model of the lower Ionosphere, electron density height profiles were estimated. Inspected Solar events revealed different effects as observed on monitored VLF signal traces. Main results are presented in this paper.

1. INTRODUCTION

Solar flare events, through emitted X-ray flux during period of solar flare activity, are well known as major source of additional ionization within region of the lower ionosphere (50 - 90 km). Incident radiation changes electron density height profile in this region and affects Very Low Frequency (VLF, 3 - 30 kHz) radio signal propagation within the Earth-ionosphere waveguide (Mitra 1974). Consequently, phase delay and amplitude of VLF signals undergo changes, as well. Absolute Phase and Amplitude Logger (AbsPAL) narrowband system stationed at Institute of Physiscs (44.85N, 20.38E), University of Belgrade, Belgrade, Serbia, was used for monitoring of VLF radio signals analyzed in this paper. VLF signals propagating within transmitted Earth-Ionosphere waveguide, transmitted from Maine (44.63N; 67.28W) USA (NAA/24.0 kHz), Skelton (54.72N; 2.88W) GB (GQD/22.1 kHz) and E. H. Holt (21.8S, 114.16E) Australia (NWC/19.8 kHz) towards Serbia, were simultaneously monitored for period of intense solar flare activity during January 2005. VLF signal propagation parameters changes related to such solar flare activity were studied and related amplitude and phase delay perturbations of observed VLF signals were presented in this paper, for case of NAA/24.0 kHz signal trace, during perturbed day of January 20th, 2005. Some of the recent results of ionospheric D-region monitoring

Table 1: Propagation parameters of monitored VLF signals.

VLF signal code and frequency (kHz)	Transmitter location	Emitted power (kW)	GCP distance to Belgrade (km)
NAA/24.0	Maine, USA	1000	6547
GQD/22.1	Skelton, UK	500	1982
NWC/19.8	E. H. Holt, Australia	1000	11980

by VLF/LF technique by Belgrade VLF group can be found in Srećković et al. 2017, Ilić et al. 2018 and Nina et al. 2019.

2. RESULTS AND DISCUSSION

Main characteristics of monitored VLF signals are given in Table 1. GQD/22.1 kHz signal propagates along WNW-ESE mostly overland path long $\approx$ 2 Mm, NAA/24.0 kHz signal propagates along W-E mostly oversea path long $\approx$ 6.5 Mm while NWC/19.8 kHz signal propagates along SE-NW both overland and oversea path long $\approx$ 12 Mm. Possible GCPs for monitored VLF signals were calculated by Long Wavelength Propagation Capability computer program LWPCv21 (Ferguson J. A. 1998), based on Long Wave Propagation Model developed from Wait's theory (Wait J. R. 1962). Electro-conductivity maps incorporated within prvwPlot subroutine are based on real electro-conductivity data globally measured. In model of Earth-ionosphere waveguide for VLF waves propagation, electron density height profile in the lower ionosphere is characterized by two parameters:β (1/km) - sharpness and H' (km) - reflection height (Wait J. R. and Spies K. P. 1964).

Observed propagation parameters of analyzed NAA/24.0 kHz signal trace during perturbed day of January 20th, 2005 are given in Figure 1. X-ray irradiance diurnal variation on perturbed day January 20th, 2005 is given in black, according to GOES12 one-minute satellite data listings of the X-ray (0.1-0.8 nm) irradiance. NAA signal amplitude variations during perturbed day January 20th, 2005 are given in red, while during quiet day of January 20th, 2007 are given in blue. The dominant feature during perturbed day is X7.1 class flare event recorded at 07:01 UT, which severely affected NAA signal propagation during the entire day, by raising the amplitude signal level during daytime for up to 10 dB as compared to quiet conditions.

The Earth-ionosphere waveguide for monitored VLF signals propagation conditions during perturbed day January 20th, 2005, was modeled for few characteristic times during the flare event duration. Electron density height profile Ne(z)(m^{-3}) for altitude z (km) was calculated, for given pairs of parameters β (1/km) - sharpness and H' - reflection height, using the equation (Wait J. R. and Spies K. P. 1964):

$$N_e(z, H', \beta) = 1.43 \cdot 10^{13} e^{-0.15H'} e^{(\beta - 0.15)(z - H')} \tag{1}$$

Propagation paths of monitored VLF signals were simulated by LWPCv21 code for few characteristic states, with goal of obtaining the best fitting pairs of parameters (β/H') estimated to be the closest possible values to real measured VLF signals phase delay and amplitude, at the site of Belgrade receiver. Vertical electron density height profiles through ionospheric D-region were calculated using (1).

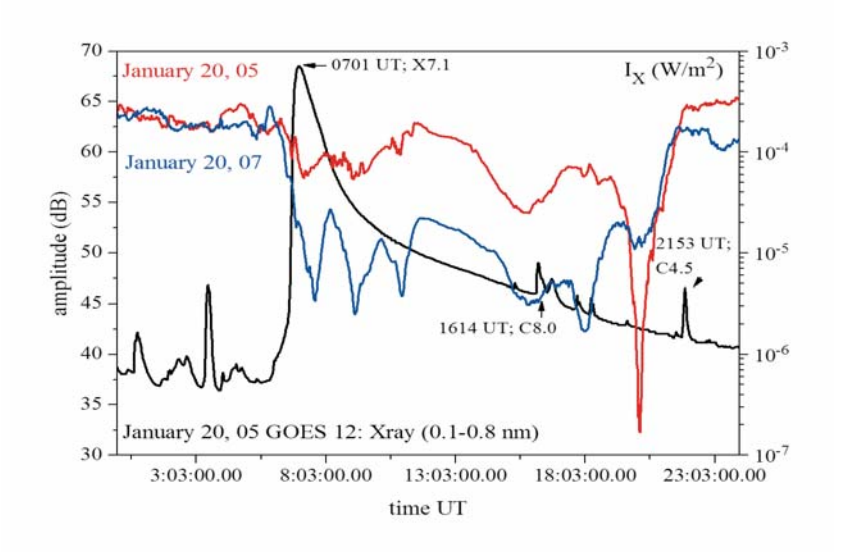

Figure 1: NAA/24.0 kHz signal perturbation

Electron density height profiles Ne(z) in 60 - 90 km altitude range for NAA/24.0 kHz transmitter to receiver distance D (km) along GCP, at midday max time 11:28 UT, during perturbed day of January 20th, 2005 (red) and quiet day of January 20th, 2007 (blue) are given in Figure 2. Solid red and blue lines represent Ne(z) profiles at the place of receiver in Belgrade (Serbia), for perturbed and quiet conditions, respectively. In case of receiver site in Belgrade (Serbia), Ne(z) profiles obtained by modeling vary in several orders of magnitude depending on observed altitude: the differences in calculated Ne(z) vary between about half order of magnitude at the lower boundary of observed altitude range, up to about two orders of magnitude at the upper boundary of observed altitude range, with about one and half orders of magnitude at the 74 km altitude. It should be noted, that results obtained in cases at the altitude boundaries should be taken with caution, due to uncertainties related by calculation method used.

3. CONCLUSIONS

Simultaneous monitoring of NAA/24.0 kHz, GQD/22.1 kHz and NWC/19.8 kHz VLF signals transmitted towards Belgrade AbsPAL receiver (44.85N, 20.38E) was carried out for series of solar X-flare events during January 2005, and inspected Solar events revealed different effects as observed on monitored VLF signal traces. Case of NAA/24.0 kHz signal trace behavior was analyzed and presented in this paper. Perturbations in ionospheric D-region induced by Solar flare activity that took place during perturbed day of January 20th, 2005, severely affected propagation conditions within Earth-ionosphere waveguide of NAA/24.0 kHz signal trace, in way that NAA/24.0 kHz signal amplitude stayed raised during the entire day for up to 10 dB, as compared to quiet conditions. Based on applied modeling method and conducted

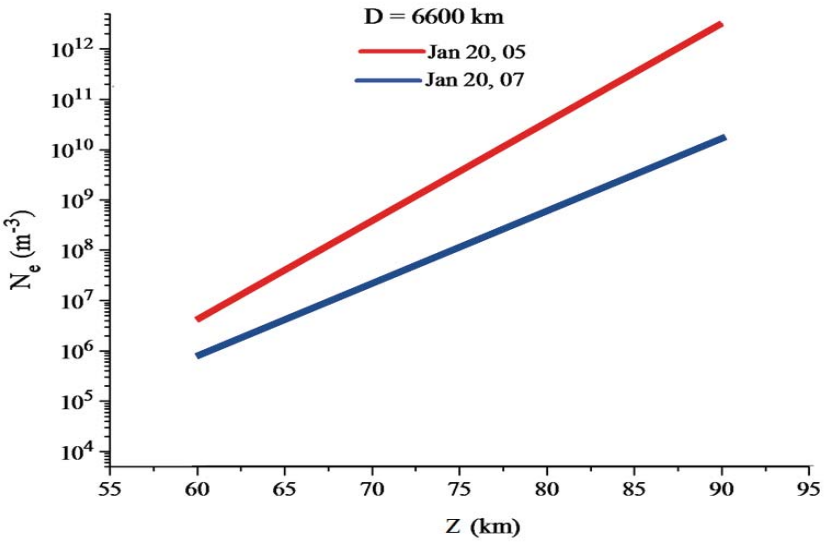

Figure 2: Electron density height profiles Ne(z) in 60 - 90 km altitude range for NAA transmitter to receiver distance D (km) along GCP, at midday max time 11:28 UT

calculations, at the place of Belgrade receiver site, at the altitude of 74 km, registered Solar flare activity induced increase in electron density of about one and half orders of magnitude compared to unperturbed conditions.

Acknowledgments

The thanks are due to Ministry of Education, Science and Technological Development of Republic of Serbia. Authors thank Institute of Physics, University of Belgrade, Belgrade, Serbia for VLF data provided and D. Šulić for instrumental set-up.

References

Ferguson, J. A.: 1998, *Computer Program for Assessment of Long-Wavelength Radio Communications*, Version 2.0, Technical document 3030, Space and Naval Warfare Systems Center, San Diego CA, USA.

Ilić, L., Kuzmanoski, M., Kolarž P., Nina, A., Srećković, V., Mijić, Z., Bajčetić, J., Andrić, M.: 2018, *J. Atmos. Sol.-Terr. Phys.*, **171**, 250.

Mitra, A. P.: 1974, *Ionospheric Effects of Solar Flares, Astrophysics and space science library*, **46**, D. Reidel publishing Company, Boston, USA.

Nina, A., Srećković, V. A., Radovanović, M.: 2019, *Sustainability*, **11**(4), 974.

Srećković, V. A., Nina, A.: 2019, *Data*, **4**(1), 21.

Wait, J. R.: 1970, *Electromagnetic waves in stratified media*, Pergamon Press, Oxford, England.

Wait, J. R., Spies, K. P.: 1964, *Characteristics of the Earth-ionosphere waveguide for VLF radio waves*, Technical Note 30, National Bureau Standards, Boulder, CO, USA.

Publ. Astron. Obs. Belgrade No. 100 (2021), 391 - 394 *Poster*

STARK BROADENING OF Co II SPECTRAL LINES FOR STELLAR SPECTRA INVESTIGATIONS

ZLATKO MAJLINGER[1], MILAN S. DIMITRIJEVIĆ[1,2] and VLADIMIR A. SREĆKOVIĆ[3]

[1] *Astronomical Observatory, Volgina 7, 11060 Belgrade, Serbia*
E–mail: zlatko.majlinger@gmail.com
E–mail: mdimitrijevic@aob.rs

[2] *LERMA, Observatoire de Paris, PSL Research University, CNRS, Sorbonne Universities, UPMC Univ. Paris 06, 5 Place Jules Janssen, 92195 Meudon Cedex, France*
E–mail: milan.dimitrijevic@obspm.fr

[3] *Institute of Physics Belgrade, University of Belgrade, P.O. Box 57, 11001 Belgrade, Serbia*
E–mail: vlada@ipb.ac.rs

Abstract. Stark Full Widths at Half Maximum for 46 Co II multiplets have been calculated in Majlinger et al. (2018) by modified semiempirical method described in Dimitrijević and Konjević (1980). The calculated results have been used to investigate the importance of Stark broadening mechanism for Co II lines in A type star and DA and DB white dwarf atmospheres (Majlinger et al., 2020). Stark broadening parameters from this paper will enter in the STARK-B database (http://stark-b.obspm.fr/). Here, as an example of obtained results, the influence of Stark broadening on two multiplets of ionized cobalt in atmospheres of DA and DB white dwarfs has been shown. It has been demonstrated that Stark broadening is more significant for DB white dwarfs and for larger wavelengths.

1. INTRODUCTION

Important applications of Stark broadening data are for research, analysis and synthesis of stellar spectra (see e.g. Dimitrijević and Sahal-Bréchot, 2014). One such element without the convenient Stark broadening parameters in literature is Co II. Its spectral lines have been observed in many stars as for example in so-called Cobalt Ap stars (Co-stars), where anomalous excess of cobalt abundance is observed as HD 200311 (Adelman, 1974) and HD 203932 (Gelbmann et al., 1997).

In order to provide Stark broadening parameters of Co II spectral lines for stellar plasma analysis, we have calculated Stark widths for 46 Co II multiplets using the modified semiempirical method (Dimitrijević and Konjević, 1980), and published them elsewhere (Majlinger et al., 2018, 2020b). Using these data we also investigated the influence of Stark broadening in atmospheres of A-type stars and DA and DB white dwarfs (Majlinger et al., 2020a).

In order to demonstrate the importance of obtained data for Co II Stark broadening parameters for investigation of Co II lines in stellar spectra we compare here as an example, using the obtained results, Stark and Doppler widths as functions of

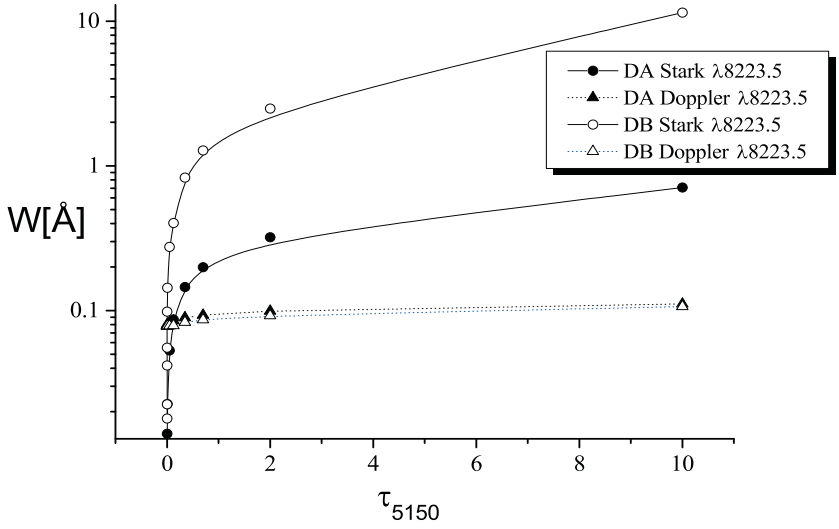

Figure 1: Comparison of Stark and Doppler broadening influence on Co II line λ8223.5 in the atmosphere of DA and DB white dwarf respectively, as a function of optical depth. Model parameters $T_{eff} = 15000$ K and $\log g = 8$ are used (Wickramasinghe, 1972)

optical depth and temperature of atmospheric layers in the case of DA and DB white dwarfs.

2. RESULTS AND DISCUSSION

In Figs. 1-4 the comparisons of Stark and Doppler widths for Co II(^{4}P)4s b^{3}P - (^{4}P)4p z^{3}S^o, $\lambda = 2613.4$ Å and Co II (^{4}F)5s e^{5}F - (^{4}F)5p ^{5}G^o, $\lambda = 8223.5$ Å is shown for DA and DB white dwarf model atmospheres of Wickramasinghe (1972), with the effective temperature $T_{eff} = 15000$ K and the surface gravity $\log g = 8$. In Figs. 1 and 2, the comparisons of Stark and Doppler widths for Co II $\lambda = 8223.5$ Å is given for the mentioned DA and DB white dwarf models as a function of the optical depth τ_{5150} for 5150 Å (Fig. 1) and as a function of layer temperature (Fig. 2). The same comparisons but for Co II $\lambda = 2613.4$ Å are shown in Figs. 3 and 4.

Co II $\lambda = 2613.4$ Å is in the ultraviolet part of the spectrum, while Co II $\lambda = 8223.5$ Å is in the infrared part of the spectrum. We can see that the influence of Stark broadening in comparison with Doppler broadening is larger for λ8223.5 in the infrared than for λ2613.4 in the UV part of the spectrum. This is the consequence of the fact that the larger wavelength means that the corresponding atomic energy levels are closer, so that the perturbation of the emitter during a collision is larger, since the probability for such transition is higher, and the resulting spectral line is broader. Additionally, Stark widths are proportional to λ^2 and Doppler ones to λ (see e.g. Majlinger et al., 2020ab).

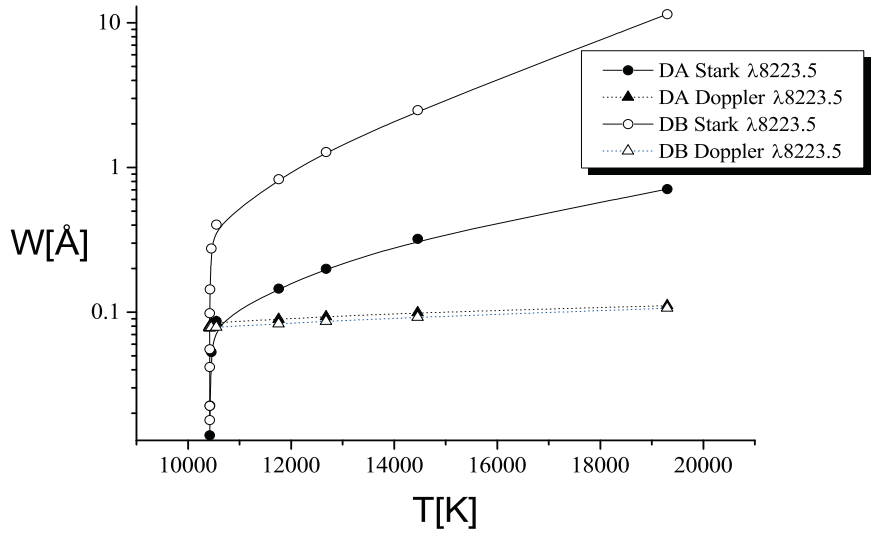

Figure 2: Same as in Fig. 1, but as a function of atmospheric layer temperature instead of optical depth, with the same model parameters.

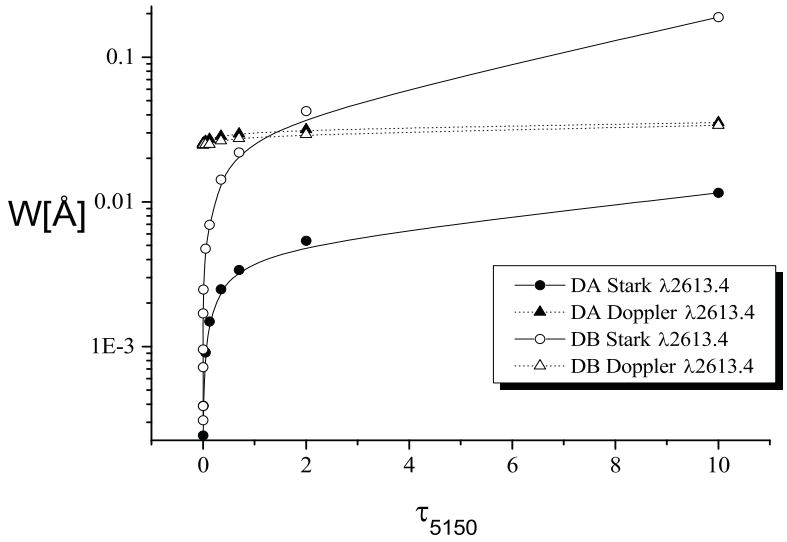

Figure 3: Comparison of Stark and Doppler broadening influence on Co II line λ2613.4 in the atmosphere of DA and DB white dwarf respectively, as a function of optical depth. Same model parameters are used as for Fig.1 and Fig. 2.

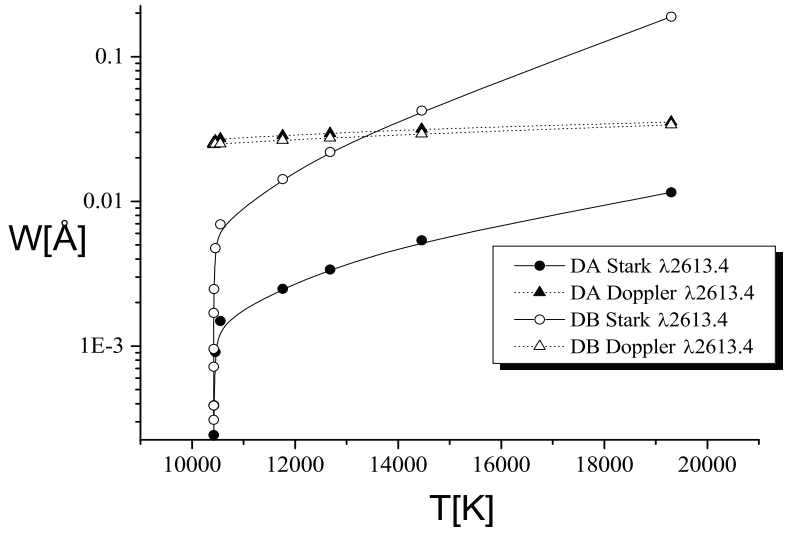

Figure 4: Same as in Fig. 3, but as a function of atmospheric layer temperature instead of optical depth, with the same model parameters.

We can see in Figs. 1-4 that Stark broadening is more important for helium-rich DB white dwarfs than for hydrogen-rich DA white dwarfs. This difference between the importance of Stark broadening in comparison with thermal Doppler broadening is due to the fact that a helium-rich DB white dwarf can generate more free electrons when helium atoms are mostly ionized, than hydrogen-rich DA white dwarf, causing higher perturber density (Majlinger et al., 2020b).

The Stark widths of 46 Co II multiplets obtained in Majlinger et al. (2018, 2020b) will be implemented in the STARK-B database (Sahal-Bréchot et al., 2015), which enter in the Virtual Atomic and Molecular Data Center - VAMDC (Dubernet et al., 2016, Albert et al., 2020).

References

Adelman, S. J.: 1974, *Astrophys. J. Suppl. Series*, **254**, 51.
Albert, D. et al.: 2020, *Atoms*, **8(4)**, 76.
Dimitrijević, M. S., Konjević, N.: 1980, *J. Quant. Spectrosc. Radiat. Transfer*, **24**, 451.
Dimitrijević, M. S., Sahal-Bréchot, S.: 2014, *Atoms*, **2**, 357.
Dubernet, M. L. et al.: 2016, *J. Phys. B*, **49(7)**, 074003.
Gelbmann, M., Kupka F., Weiss W. W., Mathys G.: 1997, *Astron. Astrophys.*, **319**, 630.
Majlinger, Z., Dimitrijević, M. S., Simić, Z.: 2018, *Astron. Astrophys. Trans.*, **30(3)**, 323.
Majlinger, Z., Dimitrijević, M. S., Srećković, V. A.: 2020a, *Data*, **5**, 74.
Majlinger, Z., Dimitrijević, M. S., Srećković, V. A.: 2020b, *Mon. Not. R. Astron. Soc.*, **496**, 5584.
Sahal-Bréchot, S., Dimitrijević, M. S., Moreau, N., Ben Nessib, N.: 2015, *Phys. Scripta*, **50**, 054008.
Wickramasinghe, D. T.: 1972, *Mem. R. Astron. Soc.*, **76**, 129.

Publ. Astron. Obs. Belgrade No. 100 (2021), 395 - 399 *Poster*

COMPARISON OF GROUND-BASED AND GAIA PHOTOMETRY OF ASTROMETRIC RADIO SOURCES

Z. MALKIN[1,2]

[1] *Pulkovo Observatory, Pulkovskoe shosse 65, St. Petersburg 196140, Russia*
E–mail: malkin@gaoran.ru

[2] *Kazan Federal University, Kremlyovskaya street 18, Kazan 420008, Russia*

Abstract. A comparison was made between *Gaia* magnitudes and magnitudes obtained from ground-based observations for astrometric radio sources . The comparison showed that these magnitudes often not agree well. There may be several reasons for this disagreement. Nevertheless, such an analysis can serve as an additional filter for verification of the object cross-identification. On the other hand, it can help to detect possible errors in optical magnitudes of astrometric radio sources coming from unreliable or inconsistent data sources.

1. INTRODUCTION

Comparison of the VLBI and *Gaia* positions of astrometric radio sources gives us an opportunity to investigate both systematic errors of both catalogs and the physical structure and evolution of objects observed by optical and radio techniques. However, the reliability of the results of such studies depends on the reliability of cross-identification between objects in VLBI and *Gaia* catalogs. Although for most sources the cross-identification looks straightforward, this is is not always the case. Errors in cross-identification introduce additional noise and outliers in the position difference statistics, which may impact the result and conclusions of these studies.

Different authors use different strategies for cross-identification between the objects in radio and optical catalogs (Mignard et al. 2016, Petrov and Kovalev 2017, Lindegren et al. 2018, Malkin 2018, Makarov et al. 2019, Liu et al. 2020). They all are based on analysis of the differences between VLBI and *Gaia* source position, sometimes along with other criteria, such as quality of the *Gaia* astrometric solution (Mignard et al. 2016, Lindegren et al. 2018) or object density in the vicinity of the source (Petrov and Kovalev 2017). Some of these supplement criteria may be disputable, but a comparison and discussion of cross-identification methods described in the literature is beyond the scope of this paper.

The present study is aimed at an investigation of a possibility of using *Gaia* and ground-based photometry as a supplement criterium to verify the cross-identification based on an analysis of the difference between radio and optics positions.

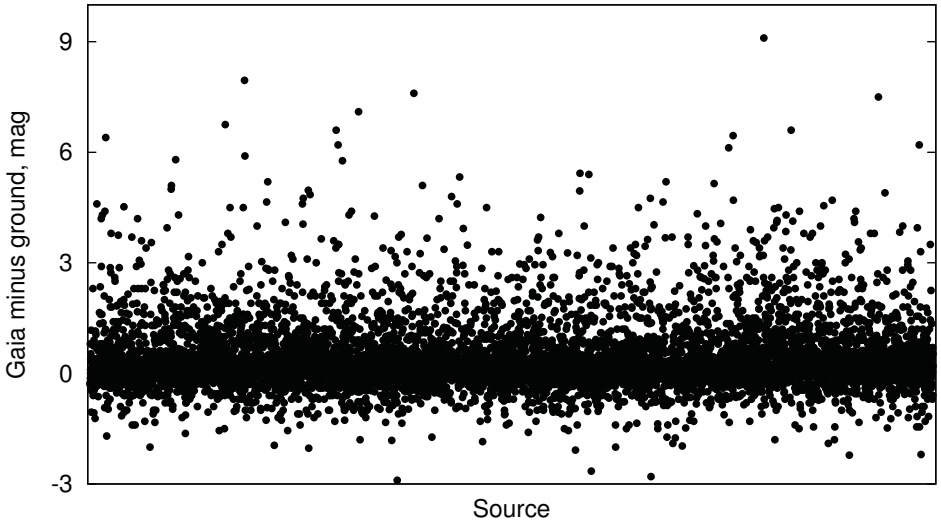

Figure 1: Differences between *Gaia G* and ground-based magnitudes for 7179 common sources between the *Gaia* DR2 and OCARS catalogs.

2. COMPARISON OF GROUND-BASED AND GAIA PHOTOMETRY

In this study, the G magnitudes given in the *Gaia* DR2 release were compared to ground-based magnitudes provided in the OCARS catalog[1] (Malkin 2018). There are 8197 sources in common between the *Gaia* DR2 and OCARS. 7179 of them have photometry data in OCARS in at least one of four bands: V, r, R, and i, close to *Gaia G* band. The latter sources were used in this work.

OCARS magnitudes are taken from different data sources: Sloan Digital Sky Survey[2] (SDSS), NASA/IPAC Extragalactic Database[3] (NED), SIMBAD[4] database managed by the Centre de Donnees astronomiques de Strasbourg (CDS), the Million Quasars (Milliquas) catalog[5], and Large Quasar Astrometric Catalogue[6] (LQAC), in the order of preference. The contribution of two latter catalogs is small. The data in these catalogs and data bases are not always consistent and reliable. To mitigate this impact, the average magnitude of V, r, R, and i was used in this work. The magnitude differences *Gaia G* minus OCARS for all 7179 common sources are shown in Fig. 1. One can see that they can be both positive and negative in the interval from about -3^m to about 9^m.

The positive magnitude differences can generally be explained by the fact that corresponding objects are extended galaxies hosting AGN observed by VLBI. Their ground-based (OCARS) magnitudes are related to the integrated flux from the entire

[1] http://www.gaoran.ru/english/as/ac_vlbi/ocars_m.txt
[2] http://www.sdss.org
[3] http://ned.ipac.caltech.edu
[4] http://simbad.u-strasbg.fr/simbad/
[5] https://heasarc.gsfc.nasa.gov/W3Browse/all/milliquas.html
[6] https://cdsarc.unistra.fr/viz-bin/cat/J/A%2bA/624/A145

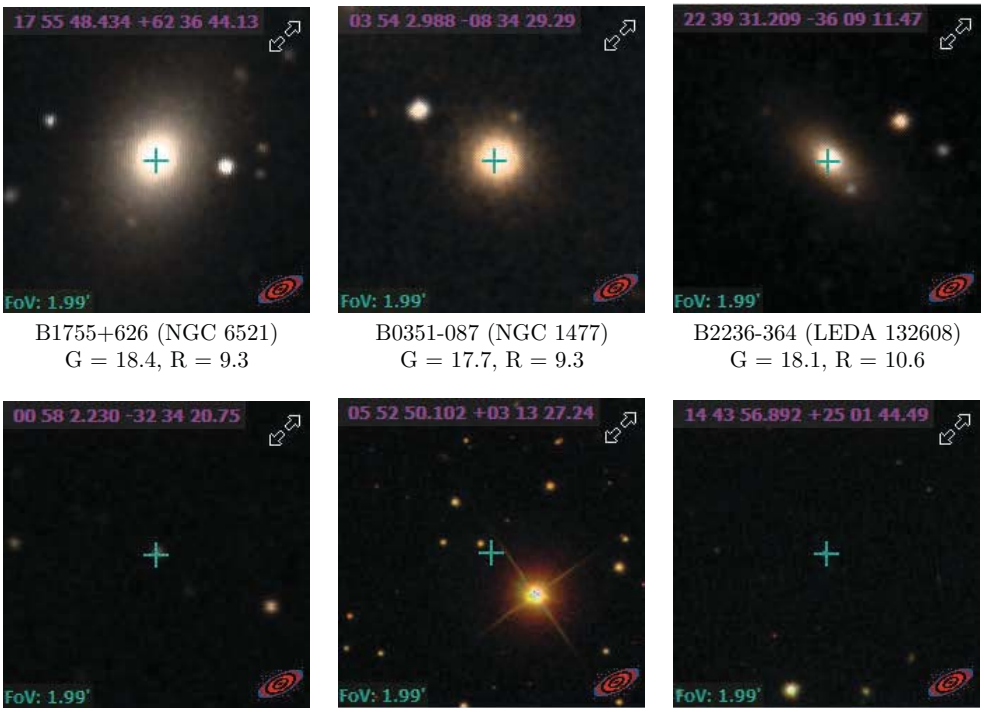

B1755+626 (NGC 6521) G = 18.4, R = 9.3 | B0351-087 (NGC 1477) G = 17.7, R = 9.3 | B2236-364 (LEDA 132608) G = 18.1, R = 10.6

ICRF J005802.2-323420 G = 17.1, R = 20.0 | ICRF J055250.1+031327 G = 19.9, R = 22.8 | ICRF J144356.8+250144 G = 17.5, R = 19.7

Figure 2: Top row: three objects with large negative *Gaia* minus OCARS optical magnitude difference. They all are large galaxies. Bottom row: three faint objects with large positive G–R difference. The images are provided by the Aladin Sky Atlas (https://aladin.u-strasbg.fr/).

galaxy or its wide central region, whereas *Gaia* most probably observes the brightest point-like center of the galaxy. Three typical objects of this type are shown in Fig. 2. Therefore, positive magnitude difference is mostly a trivial case.

To check this conclusion, the same data were re-organized and depicted in Fig 3, where the magnitude difference G–R is shown as a function of R. One can see that optically faint objects show relatively small magnitude difference *Gaia* minus OCARS, while bright objects show much large differences. Most probably, this is a consequence of the *Gaia* observing mode for which the faint galaxies are observed as a single object, unlike large (extended) galaxies. Detailed discussion of observation of galaxies with *Gaia* is given by de Souza et al. 2014.

More interesting is a case of negative magnitude difference, which is the subject of a special investigation for each source that shows such a feature. There may be various reasons for this:

- The observed magnitude difference may be a result of wrong cross-identification of the astrometric radio source with *Gaia* object.

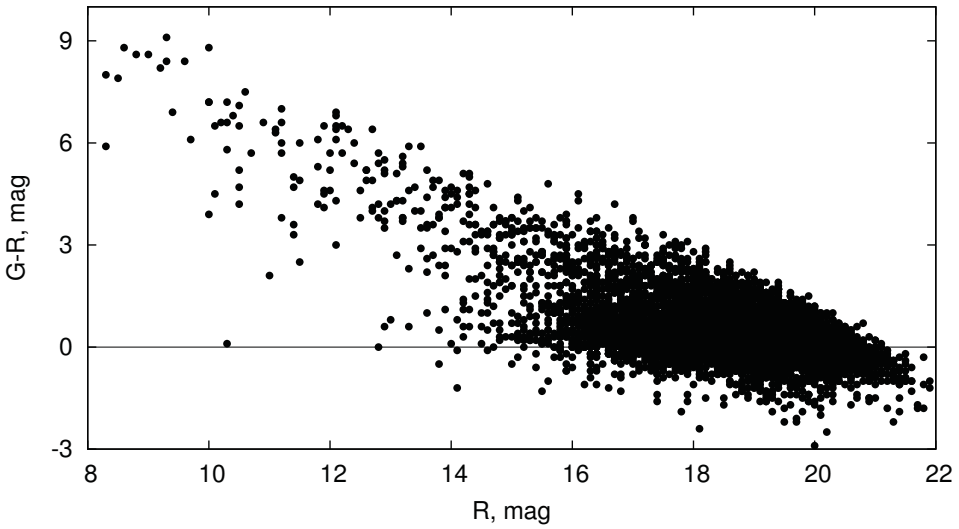

Figure 3: Differences between *Gaia* G and ground-based R magnitudes as function of R.

- The observed magnitude difference may be a result of a source optical variability. The photometry data in *Gaia* and OCARS were generally made at different epochs as discussed by Damljanović et al. 2017. Results of optical monitoring of ICRF sources made by, e.g., Taris et al. 2016, showed the spread of the brightness variations may exceeds two magnitudes.
- The observed magnitude difference may be a result of wrong cross-identification of the radio source with an optical object in one of the catalogs contributed to OCARS. In the course of the present work about a half of dozen of such cases was found.

Of course, the same considerations can be applied to positive *Gaia* minus OCARS magnitude differences.

3. CONCLUSION

The goal of this work was to investigate whether a comparison of the optical magnitudes of astrometric radio sources with the magnitudes obtained from ground-based (or other wide-field) observations can be useful to improve the reliability of cross-identification of *Gaia* objects with radio sources included in VLBI astrometric catalogs. It was found that the direct comparison of *Gaia* and ground-based magnitudes can hardly be practical for this purpose. A typical case is a bright galaxy for which VLBI and *Gaia* positions are measured for the optically and radio strong central point-like area (AGN), whereas the ground-based magnitudes are related to the integral galaxy flux.

Therefore, comparison of the *Gaia* and OCARS magnitudes cannot be used straightforward for check of object cross-identification in *Gaia* and VLBI catalogs. However,

in some cases, this may be useful to detect a wrong cross-identification, especially in case of negative *Gaia* minus OCARS magnitude differences. Besides, this comparison allows us to identify possible inconsistencies or even errors in a ground-based photometry data taken from different, not always reliable, catalogs and data bases. In particular, in the course of this work, several OCARS sources with erroneous magnitudes were detected and corrected or flagged in OCARS.

In any case, a further deeper investigations in this direction may be useful to improve the reliability of the object cross-identification in VLBI and *Gaia* catalogs.

Acknowledgments

This work has made use of data from the European Space Agency (ESA) mission *Gaia*[7], processed by the *Gaia* Data Processing and Analysis Consortium[8] (DPAC). Funding for the DPAC has been provided by national institutions, in particular the institutions participating in the *Gaia* Multilateral Agreement.

This research has made use of the SIMBAD database and Aladin Sky Atlas operated at at the Centre de Données Astronomiques[9] (CDS), Strasbourg, France, and the SAO/NASA Astrophysics Data System[10] (ADS).

This work was partly supported by the Russian Government program of Competitive Growth of Kazan Federal University.

The author is grateful to Sergey Klioner for useful discussion and to the anonymous referee for suggestions on improving the manuscript.

References

Damljanović, G, Taris, F., Andrei, A.: 2017, *Astrometry and Astrophysics in the Gaia sky, Proc. IAU*, **330**, 88.

de Souza, R. E., Krone-Martins, A., dos Anjos, S., Ducourant, C., Teixeira, R.: 2014, *Astron. Astrophys.*, **568**, A124.

Lindegren, L., Hernández, J., Bombrun, A. et al.: 2018, *Astron. Astrophys.*, **616**, A2.

Liu, N., Lambert, S. B., Zhu, Z., Liu, J. C.: 2020, *Astron. Astrophys.*, **634**, A28.

Makarov, V. V., Berghea, C. T., Frouard, J., Fey, A., Schmitt, H. R.: 2019, *Astrophys. J.*, **873**, 132.

Malkin, Z.: 2018, *Astrophys. J. Suppl. Series*, **239**, 20.

Mignard, F., Klioner, S., Lindegren, L. et al.: 2016, *Astron. Astrophys.*, **595**, A5.

Petrov, L., Kovalev, Y. Y.: 2017, *Mon. Not. R. Astron. Soc.*, **467**, L71.

Taris, F., Andrei, A., Roland, J., Klotz, A., Vachier, F., Souchay, J.: 2016, *Astron. Astrophys.*, **587**, A112.

[7]https://www.cosmos.esa.int/gaia

[8]https://www.cosmos.esa.int/web/gaia/dpac/consortium

[9]https://cds.u-strasbg.fr/

[10]https://ui.adsabs.harvard.edu/

Publ. Astron. Obs. Belgrade No. 100 (2021), 401 - 404 *Poster*

RYDBERG ATOMIC COMPLEXES IN ASTROPHYSICAL PLASMAS

V. A. SREĆKOVIĆ[1], LJ. M. IGNJATOVIĆ[1], M. S. DIMITRIJEVIĆ[2] and V. VUJČIĆ[2]
[1]*Institute of Physics Belgrade, UB, PO Box 57, 11000 Belgrade, Serbia*
[2]*Astronomical Observatory, Volgina 7, 11060 Belgrade 38, Serbia*

Abstract. In this contribution, we further investigate processes which include Rydberg atomic complexes important for the different astrophysical environments. The range of the used physical parameters covers the area important for plasma modeling from astrophysical standpoint (white dwarfs, central stars of planetary nebulae, etc). Naturally, these results can be of interest and use in investigation of different laboratory plasmas. Also, we present overview of future developments and needs in the areas of Rydberg collisional processes.

1. INTRODUCTION

Elementary processes which involve highly excited i.e. Rydberg atoms (RA) with principal quantum number $n \gg 1$ in different environments still attract attention of scientists as they may be connected with the characteristics of many types of laboratory and astrophysical plasmas (see e.g., Gnedin et al. 2009; Mihajlov et al. 2016, Marinković et al. 2017; Dimitrijević et al. 2020). Recently in the laboratory Rydberg atoms with n close to 10^2 are being explored (especially experiments with so-called Rydberg-atom matter (RM), i.e., clusters of Rydberg atoms), whilst the astrophysicists now observe the RA with n close to 10^3 and RM in space connected with low-density condensed dark matter (Badiei & Holmlid 2002).

The aim of this paper is consideration of atom-Rydberg atom ($A + RA$) collision processes which simultaneously occur i.e. collisional ionization/ recombination processes and excitation-deexcitation processes. In this contribution we studied two types of collisional ionisation/recombination processes: the non-symmetric processes

$$A^*(n) + X \Leftrightarrow e + \begin{cases} AX^+, & \text{(1a)} \\ A + X^+, & \text{(1b)} \end{cases}$$

and the symmetric-processes

$$A^*(n) + A \Leftrightarrow e + \begin{cases} A_2^+, & \text{(2a)} \\ A + A^+, & \text{(2b)} \end{cases}$$

where A, X, A^+ and X^+ are atoms and their atomic ions in the ground states, $A^*(n)$ is the atom in a highly excited (Rydberg) state, A_2^+ and AX^+ are the molecular ions in ground electronic states. The investigated excitation-deexcitation processes are

$$A^*(n, l) + A \Leftrightarrow A + A^*(n', l). \quad (3)$$

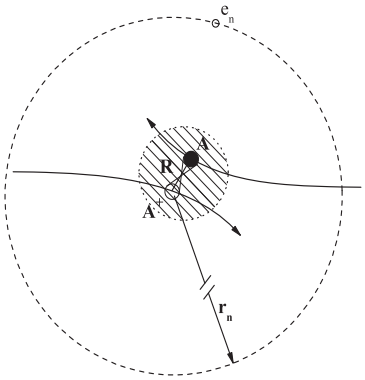

Figure 1: Schematic presentation of $RA+A$ collision (the region of R where the outer electron is collectivized is shaded; Gnedin et al. 2009).

The theory and mechanism of the processes Eqs. (1)-(3) as well as the respective numerous literature have been recently presented in details in Mihajlov et al. (2012) and Srećković et al. (2020). Here we will describe shortly its main features.

2. THEORY

Here will be analyzed the current state of the research of ionisation/ recombination processes and excitation and de-excitation processes in $A + RA$ collisional reaction. Since these processes are treated already for some time on the bases of the so-called dipole resonant mechanism (DRM), we will describe shortly its main features. In this description of the collisional ionisation and excitation events, it is envisaged that processes are induced by the dipole part of the electrostatic interaction between the outer Rydberg electron and the inner ion-atom system. Here R is the internuclear distance in the considered collision system, and $r_n \sim n^2$ the mean radius of e.g. atom $A^*(n)$. The resonant mechanism works in that part of the region $R \ll r_n$, where the ion-atom sub-system $A^+ + A$ of the system $A^*(n) + A$ can be treated as a quasi-molecular complex. Fig. 1 illustrates the mentioned DRM as a resonant energy exchange within the electronic component of the collision system $A^*(n, l) + A$: the transition of the subsystem $A + A^+$, from excited electronic state with the energy $U_2(R)$ in the ground electronic state with the energy $U_1(R)$ is followed by the simultaneous transition of the Rydberg electron from the initial bound state.

3. ASTROPHYSICAL PLASMAS

The solar atmosphere modeling: The influence of collision processes with Rydberg atoms (1)-(3), on hydrogen atom excited-state populations in solar photosphere has been examined. It has been concluded that the considered collision processes dominate over the relevant concurrent electron-atom and electron-ion processes in almost whole solar photosphere (Mihajlov et al. 2016; Srećković et al. 2020). It is shown that these processes are important for the non-local thermodynamic equilibrium modeling. In

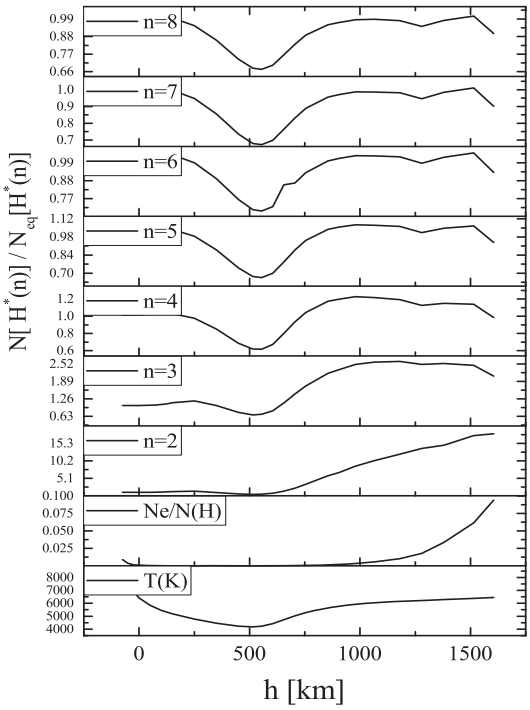

Figure 2: The ratio $N(\mathrm{H}^*)(n)/N(\mathrm{H}^*_{eq})(n)$, as a function of height h. The *eq* stand for excited atom densities corresponding to thermodynamical equilibrium conditions for given T.

Fig. 2, deviations of non-LTE populations of excited hydrogen atom states with $2 \leq n \leq 8$, in solar photosphere are illustrated.

The atmospheres of late type (M) stars: The examined processes (1)-(3) with *RA* and Rydberg complexes influence to the populations of all hydrogen atom excited states. This suggest that these processes, due to their influence on the excited state populations and the free electron density, also should influence on the atomic spectral line shapes in late type (M) stars. The line profiles are synthesized with PHOENIX code, and line shape analysed with and without inclusion of processes (1) and (2).

AGN BLR clouds: The possibility that the $A + RA$ collisions, may be useful for the diagnostics, modelling and confirmation of existence or non existence of very dense weakly ionised domains in clouds in BLR and NLR regions of AGN has been investigated recently (Srećković et al. 2018). Also the importance of processes (3) for H*(n)+H(1s) collisions, for the principal quantum number $n \geq 4$, in AGN BLR clouds has been investigated too (Srećković et al. 2020). The results (e.g. see data and python scripts for data analysis on https://github.com/sambolino/hexocin) show that the corresponding processes must have influence on the populations of hydrogen highly excited atoms in moderately ionized layers of dense parts of the BLR clouds.

Geo-cosmical plasmas: The $A + RA$ collisions, for the case of alkali metals potentially important for modeling of geo-cosmic weakly ionized plasma have been in-

vestigated recently (Ignjatović et al. 2019). The results indicate that the considered processes are factors which influence on the ionization degree and atom excited-state populations in geo-cosmical plasmas. Fig 3 shows $A + RA$ collisions rate coefficient for cases $\mathrm{Li}^*(n) + \mathrm{Na}$, $\mathrm{Li}^*(n) + \mathrm{Li}$ and $\mathrm{Na}^*(n) + \mathrm{Na}$ for modeled atmospheres of Io.

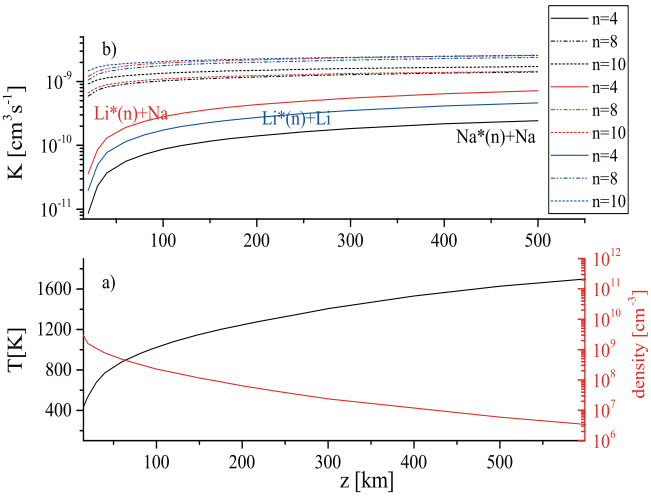

Figure 3: a) Temperature and density altitude profiles for low-density Io model atmosphere; b) Total rate coefficient in $A + RA$ collisions for the low density model atmosphere of Io.

White dwarfs modeling: The influence of considered $A + RA$ processes in the reference to the other ionization and excitation processes was examined in the photospheres of the DB white dwarfs with 12000 K $\leq T_{eff} \leq$ 20000 K. On the basis of the data from model it was established that in the parts of photosphere (8000 K $\leq T \leq$ 20000 K) these processes dominate over concurrent electron-RA impact processes.

References

Badiei, S., Holmlid, L.: 2002, *Mon. Not. R. Astron. Soc.*, **333**, 2, 360.
Dimitrijević, M. S., Srećković, V. A., Zalam, A. A., Miculis, K., Efimov, D. K., Bezuglov, N. N., Klyucharev, A. N.: 2020, *Contrib. Astron. Obs. Skaln. Pleso*, **50**, 1, 66.
Gnedin, Yu N. et al.: 2009, *New Astron. Rev.* **53**, 7-10, 259.
Ignjatović, L. M., Srećković, V. A., Dimitrijević, M. S.: 2019, *Mon. Not. R. Astron. Soc.*, **483**, 3, 4202.
Marinković, B. P., Jevremović, D., Srećkovic, V. A. et al.: 2017, *Eur. Phys. J. D*, **71**, 158.
Mihajlov, A. A., Srećković, V. A., Ignjatović, L. M., Dimitrijević, M. S.: 2016, *Mon. Not. R. Astron. Soc.*, **458**, 2, 2215.
Mihajlov, A. A., Srećković, V. A., Ignjatović, L. M., Klyucharev, A. N.: 2012, *J. Clust. Sci.*, **23**, 1, 47.
Srećković, V. A., Dimitrijević, M. S., Ignjatović, L. M.: 2018, *Mon. Not. R. Astron. Soc.*, **480**, 4, 5078.
Srećković, V. A., Dimitrijević, M. S., Ignjatović, L. M.: 2020, *Contrib. Astron. Obs. Skaln. Pleso*, **50**, 171.

Publ. Astron. Obs. Belgrade No. 100 (2021), 405 - 409 *Poster*

RESEARCH OF THE IMPACT OF STRONG SOLAR FLARES ON THE LOWER IONOSPHERE BY VLF/LF RADIO WAVES AND SATELLITE OBSERVATIONS

V. A. SREĆKOVIĆ[1] and D. M. ŠULIĆ[2]

[1] *Institute of Physics Belgrade, BU, PO Box 57, 11000 Belgrade, Serbia*
E–mail: vlada@bg.ac.rs

[2] *University Union - Nikola Tesla, 11000 Belgrade, Serbia*

Abstract. Solar flare X-ray energy can cause strong enhancements in the electron density in the Earth's atmosphere. This intense solar radiation and activity can cause sudden ionospheric disturbances and further create potential natural disasters. The focus of this work is on the study of these changes induced by strong solar X-ray flares using Very Low Frequency (VLF, 3-30 kHz) and Low Frequency (LF, 30-300 kHz) radio signal. All data were recorded by Belgrade stations system. The model computation is applied to obtain the ionosphere parameters induced by intense solar radiation.

1. INTRODUCTION

Methods of investigation of the Earth's atmosphere are diverse and numerous. Depending on the ionospheric composition, ionospheric altitudes, preferred technics, geographical locations, for its investigation scientists usually use rockets, satellites, balloons, digisonde, GPS, different ground based measurements such as radars, radio measurements, optical instruments, etc. (see Mitra, 1974; Nina et al., 2011; Šulić & Srećković, 2014 and references therein). At the altitude region 60–90 km called D-region measurements are mostly based on radio wave propagation technique (Šulić et al., 2016). The monitoring of the lower ionosphere layers by the mean of the VLF/LF technique can play an important role for a better understanding of Space Weather under these extreme conditions (Srećković et al., 2017, Ilić et al. 2018; Nina et al. 2015, 2019). The intense solar radiation and activity can cause sudden ionospheric disturbances (SIDs) and further create ground telecommunication interferences, blackouts as well as natural disasters like forest fires (see e.g. Radovanović et al. 2017).

2. RESULTS AND DISCUSSION

In this research we focus our attention to the analysis of amplitude and phase data, acquired by monitored VLF/LF radio signals emitted by worldwide distributed transmitters and satellite data during SIDs.

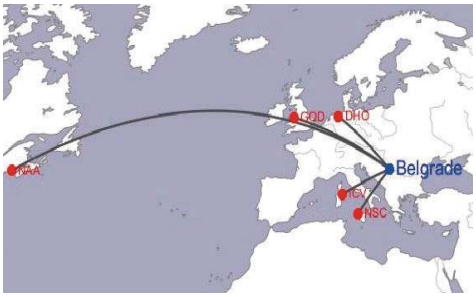

Figure 1: The geographic position of Belgrade system of VLF/LF receivers and the surrounding transmitters.

2. 1. MONITORING

All the data were recorded at a Belgrade site (44.85^0 N, 20.38^0 E) by two receiver systems: Absolute Phase and Amplitude Logger (AbsPAL) system (Šulić et al., 2016) and Atmospheric Weather Electromagnetic System for Observation Modeling and Education (AWESOME) [1]. The details and description of the Belgrade site are provided in Šulić & Srećković (2014). Locations of some transmitters and the receiving site are presented in Fig.1. The analysis and comparison of VLF/LF data has been carried out together with the examination of the corresponding solar X-ray fluxes. The intensity of solar X-ray flux is recorded by the GOES satellites [2]. The GOES satellites record the X-ray fluxes in two wavelength bands: 0.1-0.8 nm, referred to as "long" or "XL" and 0.05-0.4 nm, referred to as "short" or "XS". The most important data in our work are data of intensity of X-ray flux in the band 0.1-0.8 nm. Solar flares are destructive explosions in the solar chromosphere which release radiation across entire electromagnetic spectrum accompanied by the energetic particles (Srećković & Nina 2019). Fig. 2 shows an image of the 10 solar flares that occurred on 8 March 2011. As presented in Fig. 3, the phase (φ) and amplitude (A) variations of the

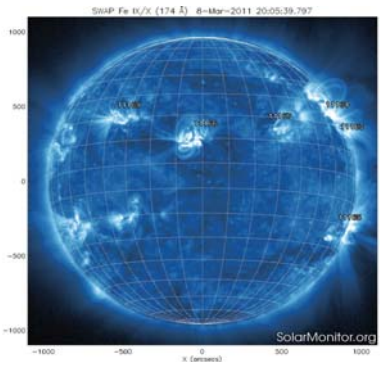

Figure 2: The solar corona in extreme ultraviolet light (17.1-nm band) at 20:08 UTC on 8 March 2011 (https://solarmonitor.org).

[1] http://solar-center.stanford.edu/SID/AWESOME/
[2] https://www.ngdc.noaa.gov/stp/satellite/goes/dataaccess.html

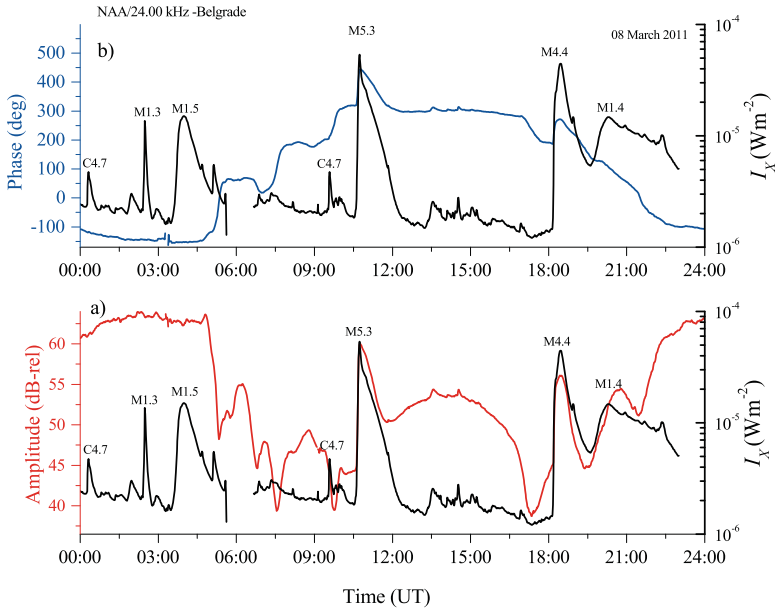

Figure 3: Amplitude a) and phase b) of NAA/24.00 kHz radio signal recorded at Belgrade against universal time on 08 March 2011. X-ray flux is presented on right axes of panel a) and b).

NAA/24.00 kHz radio signal on 8 March 2011 follow the intensity of X-ray flux quite closely at daytime during development of these solar flares (C4.7 to M5.3).

2. 2. STATISTICAL RESULTS

Simultaneous observations of amplitude and phase of VLF/LF radio signals during solar flares could be applied for calculation of ionospheric parameters. Therefore, the perturbation of amplitude and phase was estimated as a difference between values of the perturbed amplitude induced by flare and amplitude in the normal ionospheric condition. During the occurrence of solar flares, classified as a minor and small flare up to the C3 class, the amplitude of the signal does not have significant perturbations. A solar flare in the range from C3 to X classes induced a noticeable increase of the amplitude (see Fig. 3 and Fig. 4). In the presence of ionospheric disturbances, a standard numerical procedure for the calculation of electron density is based on comparison of the recorded changes of amplitude and phase with the corresponding values obtained in simulations using the Long-Wave Propagation Capability (LWPC) numerical software package (Ferguson, 1998) as explained in Nina et al. (2012).

On the base of statistical analysis of events (ranging from C3.6 to X2.2 class) we present results (ionospheric parameters) of simulations on Fig. 4 together with changes of amplitude, phase and X-ray flux. Changes of amplitude and phase are proportional to the increase of the X-ray irradiance. Using Fig. 4 we can approximately estimate the values of electron density and ionospheric parameters for larger solar X-ray flares just knowing the class of solar flare.

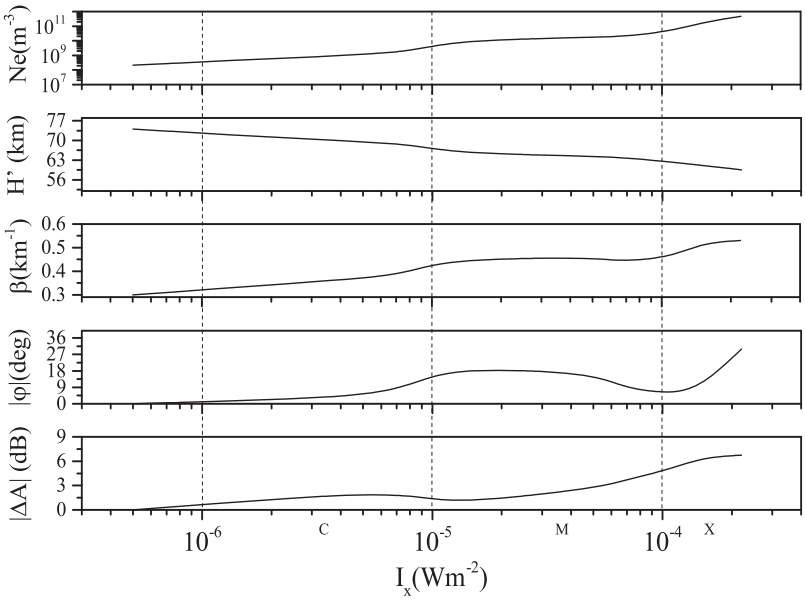

Figure 4: SID VLF signatures and calculated data by LWPC code as a function of intensity of X-ray flux during solar flare events, ranging from class C3 to X2, observed at Belgrade.

3. CONCLUSIONS

In this paper we present our study of effect during the enhancements of X-ray flux due to the solar flares, on the propagating VLF and LF radio signals. The model computation is applied to determine structures of the perturbed D-region, during occurrences of solar flares. It can be concluded that the solar explosive events lead to an increased rate of electrons production and electron density can increase depending on flare intensity up to few orders of magnitude. The results confirmed the successful utilization of used technique for detecting/analysing space weather phenomena such as solar explosive events.

References

Ferguson, A. J.: 1998, in "Computer Programs for Assessment of Long-Wavelength Radio Communications, V2.0, Tech.doc.3030", Space and NavalWarfare Syst. Cent., San Diego.

Ilić, L., Kuzmanoski, M., Kolarž, P., Nina, A., Srećković, V., Mijić, Z., ..., Andrić, M.: 2018, *J. Atmos. Sol.-Terr. Phys.*, **171**, 250-259.

Mitra, A. P.: 1974, *in "Ionospheric Effects of Solar Flares." eds. D.Reidel, Holland.*

Nina, A., Čadež, V., Srećković, V. A., Šulić, D.: 2012, *Nucl. Instrum. Methods Phys. Res. B*, **279**, 110-113.

Nina, A., Čadež, V. M., Srećković, V. A., Šulić, D.: 2011, *Balt. Astron.*, **20**, 609.

Nina, A., Srećković, V. A., Radovanović, M.: 2019, *Sustainability*, **11** 974.

Nina, A., Simić, S., Srećković, V. A., Popović, L. Č.: 2015, *Geophys. Res. Lett.*, **42(19)**, 8250-8261.

Radovanović, M., Gomes, J. F. P., Yamashkin, A. A., Milenković, M., Stevančević, M.: 2017, *Journal of the Geographical Institute" Jovan Cvijic", SASA*, **67(2)**, 213-218.
Srećković, V. A., Šulić, D. M., Vujčić, V., Jevremović, D., Vyklyuk, Y.: 2017, *Journal of the Geographical Institute" Jovan Cvijic", SASA*, **67(3)**, 221-233.
Srećković, V. A., Nina, A.: 2019, *Data*, **4(1)** 21.
Šulić, D. M, Srećković, V. A.: 2014, *Serb. Astron. J.*, **188**, 45-54.
Šulić, D. M, Srećković, V. A., Mihajlov, A. A.: 2016, *Adv. Space Res.*, **57**, 1029-1043.

AUTHORS' INDEX


Isidora Jankov
Monika Jurkovic
Sasa Dujko
Marko Simonovic
Danielakirilova
Stanislav Milosevic
Dusan Marceta
Zarko
NatasaTodorovic
Abbas Askar
Milena Jovanović
MiroslavMicic
Tijana Prodanovic
bora
Aleksandr...prijanovic
Olga Atanackovic
MiljanaJovanovic
ZarijaLukić
BojanArbutina
Istvan Vince
Ana Mitrasinovic
VladimirĐošović
Nemanja Martinovic
Dusan Keres
Edi Bon
Srdjan Samurovic
Conference photo
19th SAC
VIRTUAL 19th SAC 2020| October 2020

CIP- Каталогизација у публикацији
Народна библиотека Србије

52-355.3(082)
533.92:537.228.5(082)
520/524:376(082)

SERBIAN Astronomical Conference (19 ; 2020 ; Beograd)
Proceedings of the XIX Serbian Astronomical Conference Belgrade, October 13 - 17, 2020 = Зборник радова XIX Српске астрономске конференције Београд, 13 - 17. oktobar 2020. / [organized by Astronomical Observatory of Belgrade together with Department of Astronomy, Faculty of Mathematics, Belgrade University] ; edited by Anđelka Kovačević ... [et al.]. - Belgrade : Astronomical Observatory, 2021 (Grocka : DonatGraf). - 414 str. : ilustr. ; 24 cm. - (Публикације Астрономске опсерваторије у Београду = Publications of the Astronomical Observatory of Belgrade, ISSN 0373-3742 ; св. 100)

Tiraž 150. - Bibliografija uz svaki rad. - Registar.

ISBN 978-86-80019-96-3

1. Astronomska opservatorija (Beograd) 2. Matematički fakultet (Beograd). Katedra za astronomiju

a) Астрофизика - Зборници b) Плазма - Спектрална анализа - Зборници c) Астрономија - Образовање - Зборници

COBISS.SR-ID 40848905

УНИВЕРЗИТЕТ У БЕОГРАДУ
ИНСТИТУТ ЗА ФИЗИКУ | БЕОГРАД
ИНСТИТУТ ОД НАЦИОНАЛНОГ ЗНАЧАЈА ЗА РЕПУБЛИКУ СРБИЈУ

cost
EUROPEAN COOPERATION IN SCIENCE & TECHNOLOGY

Република Србија

Министарство просвете, науке и технолошког развоја

Од 13. до 17. октобра 2020. у САНУ одржана је 19. Конференција астронома Србије на чијем програму је била специјална сесија посвећене гравитационим таласима, а под покровитељством COST акције за гравитационе таласе и црне рупе, GWverse, при чему је гост на отварању био руководилац COST акције проф. др Vitor Cardoso. Копредседнице Научног организационог комитета су проф. др Анђелка Ковачевић са Математичког факултета Универзитета у Београду и др Јелена Ковачевић Дојчиновић са Астрономске опсерваторије у Београду. Конференција је и медијски пропраћена на порталу PTC.

CA16104 - Gravitational waves, black holes and fundamental physics (GWverse)

News and events from COST Actions

In the press - The XIX Conference of Astronomers of Serbia

COST Action, Gravitational waves, black holes and fundamental physics, GWverse (CA16104), held a special session "The gravitational-wave Universe" at the Serbian Astronomical Conference. PTC news covered the story, Read more...

PTC VESTI KOVID19 MOJA ŠKOLA OKO SPORT MAGAZIN TV RADIO EMISIJE RTS Ostalo

FILM I TV MUZIKA TEHNOLOGIJA PUTUJEMO STIL SVET POZNATIH ZDRAVLJE ZANIMLJIVOSTI NAUKA PI
GLEDAOCI REPORTERI KULTURNO ARHIVA RUBRIKA

Čitaj mi! ▶ 0:00 / 2:27

SREDA, 14. OKT 2020, 18:46 -> 23:42 | IZVOR: RTS | AUTOR: LAZAR JANOVIĆ

XIX Konferencija astronoma Srbije okupila preko 120 učesnika širom sveta

Zvezdana i fizika međuzvezdanog prostora, galaktički i zvezdani sistemi, kosmologija... samo su neke od tema Devetnaeste konferencije astronoma Srbije koja se od 13. do 17. oktobra, zbog epidemiološke situacije, održava onlajn.